METHODS IN MOLECULAR BIOLOGY™ 463

The Nucleus

Volume 1: Nuclei and Subnuclear Components

Edited by

Ronald Hancock

Humana Press

The Nucleus

Volume 1

For other titles published in this series, go to
www.springer.com/series/7651

The Nucleus

Volume 1: Nuclei and Subnuclear Components

Ronald Hancock
Editor

Laval University Cancer Research Centre, Hôtel-Dieu Hospital,
Québec, Canada

Humana Press

Editor
Ronald Hancock
Laval University Cancer Research Centre
Hôtel-Dieu Hospital
Québec, Canada

Series Editor
John M. Walker
University of Hertfordshire
Hatfield, Herts., UK

ISBN: 978-1-58829-977-2 e-ISBN: 978-1-59745-406-3
ISSN: 1064-3745 e-ISSN: 1940-6029
DOI:10.1007/978-1-59745-406-3

Library of Congress Control Number: 2008929443

Cover illustration: Figure 5, Chapter 15, "Multicolor 3D Fluorescence In Situ Hybridization for Imaging Interphase Chromosomes," Marion Cremer, Florian Grasser, Christian Lanctôt, Stefan Müller, Michaela Neusser, Roman Zinner, Irina Solovei, and Thomas Cremer.

Printed on acid-free paper

9 8 7 6 5 4 3 2 1

springer.com

Preface

It was a pleasure to have the efficient and generous collaboration of the contributors to the two volumes of *The Nucleus*. For many of them, the good personal and scientific contacts that facilitated this project owe much to Wilhelm Bernhard's ideals of life and science and to the atmosphere of the "Wilhelm Bernhard Nuclear Workshop" that perpetuates them. Numerous other protocols of interest to those who work with nuclei are available in previous volumes of the Methods in Molecular Biology and other series, as well as online. The present volumes attempt to draw attention to and foster interest in less well-explored and emerging areas, and to offer a more global perspective on nuclear biology. While the subjects presented inevitably reflect to some extent the interests of the editor, the emphasis on imaging methods in *Volume 2: Chromatin, Transcription, Envelope, Proteins, Dynamics and Imaging* can be justified plausibly by the major contributions that imaging has made in recent years to our understanding of the nucleus. The help of Joe Gall, Peter Hemmerich, and Dominic Ploton in identifying contributors to this volume, of Joanna for congenial working conditions, and of David Casey of Humana Press, who produced these volumes with meticulous expertise, are gratefully acknowledged.

Québec
December 2007

Ronald Hancock

Contents

Part V Interphase Chromosomes

Contributors

Nicole Angelier
Nuclei and Cell Cycle Laboratory, Institut Jacques Monod, CNRS, University Paris VI and Paris VII, Paris, France

Jacob A. Aten
Center for Microscopical Research, Department of Cell Biology and Histology, University of Amsterdam, Amsterdam, The Netherlands

Sandrine Augui
Mammalian Developmental Epigenetics Group, CNRS UMR 218, Curie Institute, Paris, France

Adrien Beorchia
DTI, UMR 6107, UFR de Sciences, Reims, France

Hélène Bobichon
Unité MEDyC, CNRS UMR 6237, IFR 53, Université de Reims-Champagne Ardenne, Reims, France

Brian T. Chait
Laboratory of Mass Spectrometry and Gaseous Ion Chemistry, The Rockefeller University, New York, NY, USA

Julie Chaumeil
Mammalian Developmental Epigenetics Group, CNRS UMR 218, Curie Institute, Paris, France

Min Chen
Institut für Umweltmedizinische Forschung at Heinrich-Heine-University Düsseldorf, Düsseldorf, Germany

Jennifer C. Chow
Mammalian Developmental Epigenetics Group, CNRS UMR 218, Curie Institute, Paris, France

Marion Cremer
Department of Biology II, Ludwig-Maximilians-University Biozentrum, Planegg-Martinsried, Germany

Thomas Cremer
Department of Biology II, Ludwig-Maximilians-University Biozentrum, Planegg-Martinsried, Germany

Jeffrey A. DeGrasse
Laboratory of Mass Spectrometry and Gaseous Ion Chemistry, The Rockefeller University, New York, NY, USA

Martina Dvořáčková
Laboratory of DNA-Molecular Complexes, Institute of Biophysics, Academy of Sciences of the Czech Republic, Brno, Czech Republic

Jiři Fajkus
Department of Functional Genomics and Proteomics, Faculty of Science, Masaryk University, Brno, and Laboratory of DNA-Molecular Complexes, Institute of Biophysics, Academy of Sciences of the Czech Republic, Brno, Czech Republic

Mark C. Field
Department of Pathology, University of Cambridge, Cambridge, UK

Florian Grasser
Department of Biology II, Ludwig-Maximilians-University Biozentrum, Planegg-Martinsried, Germany

Paul J. Hagerman
Department of Biochemistry and Molecular Medicine, UC Davis School of Medicine, Davis, CA, USA

Ronald Hancock
Laval University Cancer Research Centre, Hôtel-Dieu Hospital, Québec, Canada

Edith Heard
Mammalian Developmental Epigenetics Group, CNRS UMR 218, Curie Institute, Paris, France

Danièle Hernandez-Verdun
Nuclei and Cell Cycle Laboratory, Institut Jacques Monod, CNRS, University Paris VI and Paris VII, Paris, France

Ron A. Hoebe
Center for Microscopical Research, Department of Cell Biology and Histology, University of Amsterdam, Amsterdam, The Netherlands

Sui Huang
Department of Cell and Molecular Biology, Northwestern University Feinberg School of Medicine, Chicago, IL, USA

Bruno Huettel
Gregor Mendel Institute of Molecular Plant Biology, Austrian Academy of Sciences, Vienna, Austria

Christine Iwahashi
Department of Biochemistry and Molecular Medicine, UC Davis School of Medicine, Davis, CA, USA

Roland Kanaar
Department of Cell Biology and Genetics and Department of Radiation Oncology, Erasmus MC, Rotterdam, The Netherlands

Hervé Kaplan
IFR53, Reims, France

Przemek M. Krawczyk
Center for Microscopical Research, Department of Cell Biology and Histology, University of Amsterdam, Amsterdam, The Netherlands

Nathalie Lalun
Unité MEDyC, CNRS UMR 6237, IFR 53, Université de Reims-Champagne Ardenne, Reims, France

Christian Lanctôt
Department of Biology II, Ludwig-Maximilians-University Biozentrum, Planegg-Martinsried, Germany

Emilie Louvet
Nuclei and Cell Cycle Laboratory, Institut Jacques Monod, CNRS, University Paris VI and Paris VII, Paris, France

Antonius J.M. Matzke
Gregor Mendel Institute of Molecular Plant Biology, Austrian Academy of Sciences, Vienna, Austria

Marjori Matzke
Gregor Mendel Institute of Molecular Plant Biology, Austrian Academy of Sciences, Vienna, Austria

Peter McKeown
Department of Cell and Developmental Biology, John Innes Centre, Colney, Norwich, UK

Anna von Mikecz
Institut für Umweltmedizinische Forschung at Heinrich-Heine-University Düsseldorf, Düsseldorf, Germany

Garry T. Morgan
Institute of Genetics, School of Biology, University of Nottingham, Queens Medical Centre, Nottingham, UK

Stefan Müller
Department of Biology II, Ludwig-Maximilians-University Biozentrum, Planegg-Martinsried, Germany

Michaela Neusser
Department of Biology II, Ludwig-Maximilians-University Biozentrum, Planegg-Martinsried, Germany

Marie-Françoise O'Donohue
UMR CNRS 5099, IFR 109, Université Paul Sabatier Toulouse III, F 31062 Toulouse, France

Carel H. van Oven
Center for Microscopical Research, Department of Cell Biology and Histology, University of Amsterdam, Amsterdam, The Netherlands

Alison F. Pendle
Department of Cell and Developmental Biology, John Innes Centre Colney, Norwich, UK

Dominique Ploton
Unité MEDyC, CNRS UMR 6237, IFR 53, Université de Reims-Champagne Ardenne, Reims, France

Andrei N. Prusov
A.N. Belozersky Institute of Physico-Chemical Biology, Lomonosov Moscow State University, Moscow, Russia

Joseph C. Reese
Department of Biochemistry and Molecular Biology, Pennsylvania State University, University Park, PA, USA

Thomas Rockel
Institut für Umweltmedizinische Forschung at Heinrich-Heine-University Düsseldorf, Düsseldorf, Germany

Michael P. Rout
Laboratory of Cellular and Structural Biology, The Rockefeller University, New York, NY, USA

Andrea Scharf
Institut für Umweltmedizinische Forschung at Heinrich-Heine-University Düsseldorf, Düsseldorf, Germany

Eric C. Schirmer
Wellcome Trust Centre for Cell Biology, University of Edinburgh, Edinburgh, UK

Santiago Schnell
Indiana University School of Informatics and Biocomplexity Institute, Bloomington, IN, USA

Peter J. Shaw
Department of Cell and Developmental Biology, John Innes Centre, Colney, Norwich, UK

Alicja Slusarczyk
Department of Cell and Molecular Biology, Northwestern University Feinberg School of Medicine, Chicago, IL, USA

Irina Solovei
Department of Biology II, Ludwig-Maximilians-University Biozentrum, Planegg-Martinsried, Germany

Marie-Odile Soyer-Gobillard
Biologie Cellulaire et Intégrée, UMR CNRS 7628, Observatoire Océanologique Laboratoire Arago, Université Pierre et Marie Curie Paris 6, Banyuls-sur-mer, France

Jan Stap
Center for Microscopical Research, Department of Cell Biology and Histology, University of Amsterdam, Amsterdam, The Netherlands

Eva Sýkorová
Department of Functional Genomics and Proteomics, Faculty of Science, Masaryk University, Brno, and Laboratory of DNA-Molecular Complexes, Institute of Biophysics, Academy of Sciences of the Czech Republic, Brno, Czech Republic

Pavel Tchelidze
Department of Morphology, Institute of Biology, Tbilisi State University, Tbilisi, Georgia, and Unité MEDyC, CNRS UMR 6237, IFR 53, Université de Reims-Champagne Ardenne, Reims, France

Marc Thiry
Laboratory of Cell and Tissue Biology, Department of Life Sciences, University of Liège, Liège, Belgium

Marc Tramier
Macromolecular Complexes in Live Cells, Institut Jacques Monod, CNRS, University Paris VI and Paris VII, Paris, France

Gavin S. Wilkie
Wellcome Trust Centre for Cell Biology, University of Edinburgh, Edinburgh, UK

Johannes van der Winden
Gregor Mendel Institute of Molecular Plant Biology, Austrian Academy of Sciences, Vienna, Austria

Laurence Wortham
INSERM ERM 0203, Laboratoire de Microscopie Électronique, Reims, France

Olga V. Zatsepina
A.N. Belozersky Institute of Physico-Chemical Biology, Lomonosov Moscow State University, Moscow, and Shemyakin-Ovchinnikov Institute of Bioorganic Chemistry, Russian Academy of Sciences, Moscow, Russia

Hesheng Zhang
Department of Biochemistry and Molecular Biology, Pennsylvania State University, University Park, PA, USA

Zhengjian Zhang
Department of Biochemistry and Molecular Biology, Pennsylvania State University, University Park, PA, USA

Oxana O. Zharskaya
A.N. Belozersky Institute of Physico-Chemical Biology, Lomonosov Moscow State University, Moscow, and Shemyakin-Ovchinnikov Institute of Bioorganic Chemistry, Russian Academy of Sciences, Moscow, Russia

Roman Zinner
Department of Biology II, Ludwig-Maximilians-University Biozentrum, Planegg-Martinsried, Germany

List of Color Plates

The images listed below appear in the color insert.

Color Plate 1 *Fig. 3, Chapter 4*. Fixed and immunostained GV spread from an axolotl oocyte. *See* complete caption on p. 63.

Color Plate 2 *Fig. 3, Chapter 9*. Nop52 and B23 interact in the nucleolus of living cells. *See* complete caption on p. 132.

Color Plate 3 *Fig. 2, Chapter 12*. General views of an isolated nucleus. *See* complete caption on p. 171.

Color Plate 4 *Fig. 2, Chapter 13*. Immunofluorescence staining of inclusions at various steps in their isolation and purification. *See* complete caption on p. 189.

Color Plate 5 *Fig. 2, Chapter 14*. Induction of protein aggregation by silica nanoparticles. *See* complete caption on p. 199.

Color Plate 6 *Fig. 1, Chapter 15*. Three-color 3D-FISH on nuclei of normal diploid human fibroblasts. *See* complete caption on p. 217.

Color Plate 7 *Fig. 2, Chapter 15*. Six-color 3D-FISH on nuclei of human fibroblasts. *See* complete caption on p. 227.

Color Plate 8 *Fig. 3, Chapter 15*. Four-color 3D Immuno-FISH on single optical sections of human fibroblast nuclei. *See* complete caption on p. 228.

Color Plate 9 *Fig. 4, Chapter 15*. FISH on sections of paraffin-embedded tissues. *See* complete caption on p. 230.

Color Plate 10 *Fig. 5, Chapter 15*. FISH on vibratome sections. *See* complete caption on p. 230.

Color Plate 11 *Fig. 6, Chapter 15*. FISH on cryosections. *See* complete caption on p. 231.

Color Plate 12 *Fig. 7, Chapter 16*. *Top row*, examples of images of YFP fluorescent dots in nuclei of ovules in carpels (hemizygous plant, *left*; homozygous plant, *right*). *See* complete caption on p. 258.

Color Plate 13 *Fig. 1, Chapter 17*. Fluorescence in situ hybridization on mouse MEF chromosome spreads. *See* complete caption on p. 281.

Chapter 1
The Intranuclear Environment

Santiago Schnell and Ronald Hancock

Keywords Cell nucleus; Macromolecular crowding; Reaction kinetics; Stochastic nature of reactions; Entropic forces; Phase separation; Ionic environment; Diffusion

Abstract Many of the chapters in this volume are concerned with processes or structures inside the nucleus, and it is relevant to consider the properties of their environment, or rather of the multiple different and specific environments that must exist in local regions of the highly heterogeneous intranuclear space. Relatively little is known about the fundamental physical properties of these environments, and theoretical treatments of phenomena in such concentrated mixtures of charged macromolecules are complex and as yet poorly developed. Some of the phenomena that occur at the molecular level are unexpected and counterintuitive for biologists, although well known to colloid and polymer scientists; for example, the existence of short-range attractive forces between macromolecules or structures with like charges. As a background for the chapters that follow, we consider here some of the particular features of intranuclear environments, how they may influence processes and structures in the nucleus, and their implications for working with nuclei.

1 The Macromolecular Environment

The particular properties of the macromolecular environment within the nucleus are only now becoming recognised ***(1–5)***, and we believe that they are central to understanding molecular interactions, the formation of structures, and processes in the nucleus. Values for the global concentration of macromolecules within the nucleus, measured by several different approaches, range from 65 to 220 mg/mL (Table 1.1). At these concentrations, phenomena termed "macromolecular crowding" are observed (**refs.** ***(6–9)*** and references therein) that arise basically because the thermodynamic activities of macromolecules greatly exceed their concentrations, and that have important implications for processes within the nucleus.

R. Hancock (ed.) *The Nucleus: Volume 1: Nuclei and Subnuclear Components*,

Table 1.1 Concentration of macromolecules in the nucleus

	Concentration (mg/mL)	Method
Nuclei		
Hepatocytes, rat	100[a]	Chemical assays
HeLa cells	96	Interference microscopy
Hepatocytes, human	165	Interference microscopy
Spermatocytes, *Schistocerca gregaria*	220	Interference microscopy
Salivary gland cells (polytene), *Drosophila*	65	Interference microscopy
Glial cells, human	150–180	Interference microscopy
Nucleoplasm		
Oocytes, *Xenopus*	106[b]	Interference microscopy
Chromatin		
Interphase chromosomes, human	75	Calculation
Nucleosomes (HeLa cells)	30–60	Fluorescence correlation spectroscopy
Heterochromatin, *Euglena* sp.	400	Quantitative scanning transmission electron microscopy
Nucleoli		
Hepatocytes, rat	270[a]	Chemical assays
Mesothelial cells, newt	220	Interference microscopy
HeLa cells	200	Interference microscopy
Oocytes, *Xenopus* (dense fibrillar region)	215[b]	Interference microscopy

Reproduced with permission from **ref.** ***(5)***, where complete references are given
[a]Isolated nuclei and nucleoli
[b]As protein, all other values are totals

1.1 Reaction Kinetics

Macromolecular crowding has important consequences for the thermodynamics of the cell ***(6–9)***, strongly affecting reaction kinetics ***(8, 9)*** and diffusion processes ***(10)***. The thermodynamics of solutions with a high macromolecular content is specifically affected by entropic effects termed "depletion forces" ***(11)***. These occur in a mixture of molecules of different sizes because contact between larger molecules (or particles) is favoured since it causes the excluded volumes that surround them to overlap, thus, increasing the volume accessible to smaller molecules and increasing the system's entropy ***(12, 13)***. Particular local entropic environments may surround different macromolecules and structures ***(14)***.

Crowding results in quantitative effects on both the rates and the equilibrium of reactions involving macromolecules ***(7–9, 12, 13, 15)***; the changes depend on the sizes of the molecules, on the crowding agents, and on the milieu ***(13, 14)***. Enzymes that catalyze sequential reactions such as replication, repair, and transcription in the

nucleus form macromolecular complexes, so that the product of one enzyme does not have to diffuse to reach another enzyme, thus, increasing metabolic efficiency ***(16)***.

Relatively little is known about the fundamental physical properties of the intranuclear environment ***(17)***. In particular, how biochemical reactions in the nucleus and in other intracellular compartments differ from those in the test tube remains inadequately understood ***(9, 18)***. The rate laws for chemical reactions occurring in intracellular environments with macromolecular crowding like the nucleus, characterized by heterogeneity and confinement, which make chemicals diffuse anomalously, have been studied previously ***(9, 19, 20)***. Here we consider the validity of two central concepts of classic chemical kinetics in the cell nucleus: chemical equilibrium and the law of mass action.

1.2 Chemical Equilibrium and the Law of Mass Action

In ligand-receptor dynamics, the ligand (L) and receptor (R) associate and dissociate reversibly following the reaction scheme:

$$L + R \underset{k_{-1}}{\overset{k_1}{\Leftrightarrow}} C, \qquad \text{(Eq. 1.1)}$$

where k_1 and k_{-1} are the forward and backward rate constants, respectively.

A *chemical equilibrium* is achieved in any closed reaction system such as Eq. 1.1 as $t \to \infty$. In this state, there is no net activity, which means that the chemical concentrations are not changing in time. From the thermodynamic point of view, the chemical equilibrium is reached when the forces driving the reaction in Eq. 1.1 are equal and opposite. According to the zeroth principle of thermodynamics, the change in the net Gibbs free energy of the ligand and receptor reaction is null ***(21)***. In physicochemistry, thermodynamics studies changes in states and their stability and is only concerned with the initial and final states of chemical species in reactions.

Chemical equilibrium can be understood from a different perspective, that of chemical kinetics, which focuses on understanding reaction mechanisms and the timescales of changes of chemical concentrations. In the domain of chemical kinetics, chemical equilibrium is achieved when the rates of the forward and backward reactions are equal and opposite. The rate of reaction in classic chemical kinetics obeys *the law of mass action*, which says that the rate of a reaction is proportional to the product of the concentrations of the reactants. Applying the law of mass action, the equilibrium concentrations for Eq. 1.1 obey the following conservation expression:

$$-k_1[L](t \to \infty)[R](t \to \infty) + \kappa_{-1}[C](t \to \infty) = 0, \qquad \text{(Eq. 1.2)}$$

where the square brackets denote concentrations and ($t \to \infty$) their value at equilibrium.

We can now derive an expression for the equilibrium constant, K_{eq}:

$$K_{eq} = \frac{k_{-1}}{k_1} = \frac{[L](t \to \infty)[R](t \to \infty)}{[C](t \to \infty)}, \qquad \text{(Eq. 1.3)}$$

which depends only on the thermodynamics properties of the reacting system in Eq. 1.1 (22). It is important to emphasize that the forward and backward elementary reactions continue at chemical equilibrium, although at this stage there is no measurable change in the reaction because the forward and backward rates are equal.

These principles are valid for most experimental conditions in standard laboratory practice, that is closed, constant-volume systems maintained at constant temperature and pressure. The reactions occur in a homogeneous environments, typically that of an ideal gas or a well-mixed liquid phase. Unfortunately, biochemical reactions rarely occur in these conditions in vivo, particularly in the nucleus. Therefore, what are the principles of reactions in the nucleus?

1.3 Chemical Equilibria

During the 1960s and early 1970s, A.G. Ogston and T.C. Laurent carried out pioneering investigations on protein thermodynamics in polymer solutions with properties similar to those found in the nucleus ***(23, 24)***, where, as in other intracellular compartments ***(25)***, macromolecules occupy a significant fraction of the total volume. As a consequence, they are spatially constrained on the microscopic level by force fields such as steric repulsion and attractive interactions that occur between them. These forces can be either specific, if they depend on the structure of the interacting molecules, or nonspecific, if they depend on the global properties of the solvent or reaction medium. If the molecules are considered part of a mixture of hard spheres, the total free energy of interaction between a specific molecule and all the other molecules in the crowded environment is inversely proportional to the probability of placing the specific molecule at a random location within the crowded medium ***(26)***. The total free energy depends then upon the numbers, sizes, and shapes of the other molecules present in the reaction compartment ***(7, 27)***. The effect of steric-repulsive forces on the volume available to a given molecule depends on the centre of mass of the molecule and the molecules already present in the solution or "background" molecules. If the molecule to be introduced into the reaction is much smaller than the background molecules, the available reaction volume is large because small molecules can diffuse between the large molecules. However, if the molecule introduced into the reaction has a similar size to the background molecules, the available volume is substantially smaller, because the centre of a molecule can approach the centre of another only to the distance at which the surfaces of the molecules contact each other. This phenomenon is known as the volume exclusion ***(8)*** or depletion effect ***(11)***.

Allen P. Minton has systematically analysed the effects of background macromolecules on biochemical equilibria ***(13, 27, 28)***. By analogy, Minton treated the interstitial elements of free volume due to background molecules as pores. When the size of a pore is not much larger than that of an enclosed molecule, steric-repulsive interactions between the molecule and the pore boundaries result in a reduction of the volume available to it. Therefore, free energy is required to transfer the molecule from an element of unbounded solution into a pore of equal volume ***(29)***. In this case, the magnitude of excess work depends strongly upon the relative sizes and shapes of both the confined molecules and pores ***(30)***; this phenomenon is known as macromolecular confinement ***(7, 30)***. Macromolecular crowding can also cause a different type of phenomenon: if the molecule bears a net charge opposite to that of the background molecules, then the molecule can be reversibly and non-specifically adsorbed onto the surface ***(31)***. This is known as macromolecular adsorption ***(7)***. When the absorption is spontaneous, the free energy change is negative and its magnitude depends on factors that vary with the size and shape of the molecule ***(32)***.

The influence of macromolecular crowding on a chemical equilibrium is represented by an apparent equilibrium constant:

$$\tilde{K}_{eq} = \Gamma K_{eq}, \qquad \text{(Eq. 1.4)}$$

where K_{eq} is the equilibrium constant measured in an ideal solution (in the case of the reaction in Eq. 1.1, this is Eq. 1.3) and Γ is a nonideal correction factor. The activity coefficient is equal to unity if the equilibrium occurs in an ideal solution. Otherwise, the correction factor can take constant values, different from unity. The value of the correction factor can be calculated theoretically from the hard spherical particle model in porous media, which assumes that the law of mass action is valid and the rate of the reaction is also subject to a non-ideal correction. The value of the correction factor depends on the sizes, shapes, and concentrations of the reacting and background molecules ***(13)***. This model is valid under a restricted set of conditions: the rate of encounter between the ligand and receptor is larger than the rate of dissociation. In this case, macromolecular crowding does not occupy a significant fraction of the total volume and reactions are not subject to limited diffusion.

If macromolecular crowding occupies a significant fraction of the total volume, reactions will be subject to a limited and anomalous diffusion ***(10, 33)***. The rate of encounter of reactants generally varies relative to the rate with which their intermediates break down. Under this condition, the law of mass action is invalid ***(9, 19)*** and the classic picture of thermodynamic equilibrium also breaks down ***(34, 35)***. The chemical equilibrium is not generally a true thermodynamic equilibrium, but rather a non-equilibrium steady state as $t \rightarrow \infty$. The exact value of this non-equilibrium steady state has to be calculated using kinetics approaches taking into account dynamics effects. The overall Gibbs free energy principle cannot be postulated a priori to determine the chemical equilibrium.

1.4 The Law of Mass Action in the Nucleus

The structural organisation of the nucleus is far from the homogeneous, well mixed solution typical of an in vitro experiment. The consequences of the complexities of the rates of reactions are only now becoming more generally understood ***(9, 19, 20, 36)*** with the aid of various computational frameworks to extract rate laws or empirical rate equations from simulation experiments. Among these, simulations based on Monte-Carlo approaches are the most popular and widely used.

A systematic computational investigation of reactions in environments with a fraction of the total volume occupied by obstacles has revealed that there are at least two reaction rate laws governing reactions in heterogeneous media ***(19)***. For the bimolecular irreversible reaction scheme:

$$A + B \xrightarrow{f} C, \qquad \text{(Eq. 1.5)}$$

the rate of product formation, v, is governed by the following expression:

$$v = f\, a(t) b(t), \qquad \text{(Eq. 1.6)}$$

where f is a rate function, and $a(t)$ and $b(t)$ are the reactant concentrations at time t. Note that if the law of mass action is valid, f is a rate constant.

The reaction kinetics of Eq. 1.5 are not determined by the nature of the background molecules, but by the value of the reaction probability between A and B and their initial concentrations. The computational analysis of reaction Eq. 1.5 has shown that the law of mass action is valid if the reaction probability between A and B is small and one of these chemical species is at a low concentration relative to the other ***(19)***.

In agreement with theoretical and experimental evidence of reactions occurring in heterogeneous media, the computational analysis of the elementary reaction in Eq. 1.5 shows that the rate law always follows time-dependent power-law behaviour as $t \to \infty$, known as fractal-like kinetics ***(37)***, in confined environments with high macromolecular content. Hence, the rate function follows:

$$f = k(t = 1)\, t^{-h} \quad t \geq 1, \qquad \text{(Eq. 1.7)}$$

where k is a rate constant and h is a constant measuring the dimensionally of the confined system. This constant is bounded between 0 and 1 ($0 \leq h \leq 1$). The results of computational investigations show that physically dissimilar structures of the cell exhibit the same type of rate laws. However, it is possible that complex covalent interactions of molecules with the molecular background can affect the rate laws. The replacement of the rate constants by a time-dependent rate coefficient has unexpected consequences. Experiments with reaction mechanisms known to be elementary are easy to follow in time and have been used to test fractal-like kinetics ***(37)***. However, the more complex reaction mechanisms of biochemical reactions

are more difficult to follow in time ***(38)***. There is an alternative rate law for diffusion-limited reactions, where the reaction rate is equal to the encounter rate between reacting species ***(13)***. The rate of encounter decreases exponentially with increasing concentrations of background molecules, and not due to specific interactions between the reacting and background molecules. Under these conditions, theory ***(39)*** suggests that the rate function is:

$$f = k_0 \exp(-g\ m), \qquad \text{(Eq. 1.8)}$$

where k_0 is the rate of the reaction (encounter rate) in ideal conditions, g is a function of the relative sizes and shapes of the reacting molecules, and m is the concentration of the background molecules.

1.5 Experimental Observations and Relevance to Biochemistry in the Nucleus

Thermodynamic and reaction kinetic models to study the effects of macromolecular crowding upon reactions have been developed during the last 20 years ***(9, 13, 19, 30, 32, 36)***. These are based on mesoscopic-level models that take simplified representations of the reacting molecules, their interactions, and the effects of the background non-reacting molecules ***(36)***. These models provide simplifications for quantitative study of the chemical equilibrium of reactions in environments as complex and intrinsically variable as the nucleus. To date, these models have been successfully employed to predict and study effects of background molecules upon the chemical equilibrium and reaction rates of diverse molecules in vitro ***(6–8, 28, 40)***. These in vitro studies are a useful starting point to further our understanding of the reaction kinetics in the nucleus and other intracellular compartments. However, there has not been any application to reactions in vivo.

The intracellular environment is more complex and dynamic than a test tube experiment with high a macromolecular content. The nucleus is a complex structure formed of multiple compartments with different microenvironments. For example, reacting molecules can encounter a region of extremely high concentration of DNA, or an area of high concentration of lipids and proteins in the nuclear membrane, or a region crowded with soluble macromolecules. It is possible that differences in the nature of the macromolecular crowding agents, the hydrodynamics of molecules, and the geometry of the microenvironment can affect the reaction dynamics. These effects are under investigation in theoretical and experimental studies.

In conclusion, the chemical equilibria and reaction kinetics in the nucleus are expected to be governed by anomalous rate laws due to macromolecular crowding in reaction environments. Reactants are spatially constrained in crowded

environments on the microscopic level by force fields such as steric repulsion, and by non-specific attractive interactions that can occur between reacting and background molecules. Theory shows that the free energy of a reaction changes with the number, size, and shapes of other molecules present in the reaction environments and that reaction kinetics are affected by the limited diffusion of reacting molecules. We have considered how biochemical reactions within the nucleus could differ from those in the test tube. We must acknowledge that the current theory represents a simplified picture of the nuclear environment, but, during the last 20 years, systematic in vitro experimental work where the composition of the reaction environment is changed has begun to emulate the in vivo environment and experimental techniques are currently being developed for monitoring reacting concentrations in time within individual cells ***(41)***. These methods, together with the theory discussed here, will help quantitative understanding of how much biochemical reactions within the nucleus differ from those in test tubes.

2 Effects of Macromolecular Crowding in the Nucleus

2.1 Enhanced Intermolecular Association

In crowded media, macromolecular association constants are predicted to be as much as several orders of magnitude greater than in the dilute solutions commonly employed for studies in vitro ***(6)***. Figure 1.1a illustrates such an effect observed experimentally for the association of two 70S ribosomal particles of *Escherichia coli* to form a 100S particle. The short-range attractive forces that occur between macromolecules or structures with like charges are also enhanced in crowded media ***(42–44)***.

These effects may contribute to the self-organisation of the macromolecular complexes that form intranuclear structures and compartments, such as the nucleolus and the different types of intranuclear bodies ***(1)***. Exogenous macromolecules introduced into the nucleus may also form regions of high local concentration or "foci" (reviewed in **ref. *(1)***). The possible significance of crowding for the formation of nuclear aggregates of macromolecules in pathological conditions (*see* **Chapter 14** by von Mikecz et al. and **Chapter 13** by Iwahashi and Hagerman in this volume) remains to be examined.

2.2 Modified Reaction Conditions

Crowding can greatly modify or extend the range of conditions under which enzymes or proteins are functional ***(6)***. For example, in the presence of the crowding agent poly(ethylene glycol) (PEG), DNA polymerase I shows a different optimum concentration of KCl for nick translation ***(45)*** (Fig. 1.1b) and the requirement for

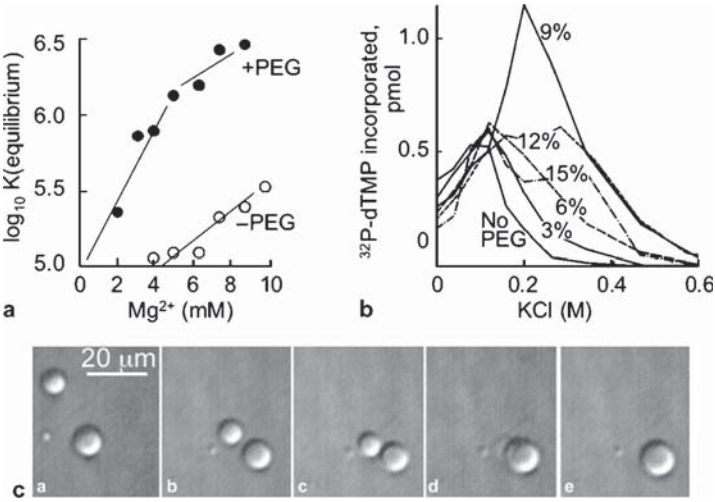

Fig. 1.1 Examples of effects of macromolecular crowding on macromolecular interactions. **a** The influence of crowding by poly(ethylene glycol) (PEG) (8 kDa, 4% w/v) on the equilibrium constant for the association of two *E. coli* 70S ribosome subunits to form a 100S particle. Note that in the presence of PEG, association proceeds in the absence of Mg^{2+} ions (reproduced from **ref.** ***(46)*** by permission of Oxford University Press). **b** The influence of PEG (8 kDa) at different concentrations (w/v) on the response of the nick translation reaction of *E. coli* DNA polymerase l to the concentration of KCl ***(45)*** (Copyright 1987, National Academy of Sciences, USA, reproduced with permission). **c** Phase separation in a solution of deoxyhaemoglobin (Hb) and PEG (8 kDa, 1% w/v) in 0.15 *M* K phosphate buffer, pH 7.35. The dense spheres contain Hb at a concentration ~12 times higher than the solution, and were formed at 300 mg Hb/mL at 42°C; similar phase separation was seen at 96 mg Hb/mL and 35°C. The sequence shows droplets of the dense phase coalescing during a 55-sec period ***(51)*** (Copyright 2002, National Academy of Sciences, USA, reproduced with permission)

Mg^{2+} ions for self-association of *E. coli* 70S ribosomal subunits is no longer seen ***(46)*** (Fig. 1.1a). The binding of *lac* repressor and RNA polymerase of *E. coli* to DNA in vitro is strongly dependent on salt concentration, whereas, in the crowded intracellular environment in vivo, their binding to specific sites is insensitive to the intracellular K^+ level ***(47)***. When determining the optimum conditions for a nuclear enzyme or reaction in vitro, the use of crowded conditions may therefore give a better indication of the characteristics of the reaction in vivo.

2.3 Compaction of Extended Polymers

Depletion forces in a crowded environment cause extended or linear polymers to collapse to more compact conformations (reviewed in **ref.** ***(5)***). This effect could contribute to the compaction of extended macromolecular complexes in the nucleus, including the polynucleosome chains of interphase chromosomes.

2.4 Phase Separation

In a solution of macromolecules or particles of different sizes and shapes, specific components may demix and form separate phases (e.g. **ref.** ***(48, 49)***). Phase separation can also be induced by the addition of counterions to a solution of macroions ***(50)***. In a concentrated solution of a single protein, phase separation can occur, forming spherical regions containing the protein at a high concentration (e.g. **ref.** ***(51)***) (Fig. 1.1c).

2.5 Effects on Intrinsically Unstructured Proteins

Many nuclear proteins, including transcription factors and High Mobility Group (HMG) proteins, contain regions of intrinsically disordered structure in solution ***(52)***. Disordered regions can become structured in crowded media ***(53, 54)***, raising the possibility that in the nuclear environment these proteins may be more structured than predicted.

2.6 Stochastic Nature of Reactions

There is growing evidence that at least some reactions are stochastic in the nucleus. At the molecular level, random fluctuations are inevitable when molecules are at low numbers per cell or collide with background molecules ***(18)***. In recent years, random fluctuations in the regulation of gene expression have been observed where small numbers of regulatory proteins interact with DNA binding sites in the gene's promoter region. These intrinsic noise effects have been measured recently using fluorescent probes (e.g. **refs.** ***(55, 56)***). Low copy numbers of expressed RNAs may be significant for the regulation of downstream pathways ***(57)***. In this and other cases when there are only small numbers of molecules in the reaction volume, a stochastic modelling approach is required (**refs.** ***(18, 36)*** and references therein). This means that experimentalists needs to shift from the deterministic kinetics of molecular concentration in a traditional reaction kinetics assay to a stochastic model, based on the probability that a molecule will be at a particular state.

3 The Ionic Environment

3.1 Cations

The concentrations of ions within the nucleus are often deduced from their measured global content in nuclei and used as a basis for preparing buffers for isolating

and handling nuclei. However, these ions are unlikely to be distributed homogeneously in the intranuclear space because the surfaces of charged macromolecules and structures create particular local ionic environments, and theory predicts that their distributions in different regions are highly heterogeneous (e.g. **refs.** ***(58, 59)***). Simulation of the "interplay of electrostatics, dispersion forces, thermal motion, polarization, fluctuations, hydration, ion size effects and the impact of interfacial water structure makes it hard to identify a universal law" ***(60)***. The concept that concentrations of ions within the nucleus can be defined is therefore questionable.

The concentrations of ions within the nucleus may not be reflected by those in buffers commonly employed to stabilise isolated nuclei because, in vivo, the nucleus is stabilised by a further factor, the crowding effect exerted on it by the high concentration of macromolecules in the cytoplasm ***(10)***, which is relaxed when the cell membrane is removed. When this effect is replaced by a crowding agent such as PEG or dextran included in the cell lysis buffer, cations are no longer required in buffers to prepare stable nuclei (***(5)***; R. Hancock, unpublished data). The use of buffers containing a crowding agent for isolation of nuclei and intranuclear structures such as nucleoli, instead of conventional cation-containing media, may therefore reproduce more closely the conditions in vivo.

3.2 Hydrogen Ions

The concentration of hydrogen ions measured by pH-sensitive dyes in the nucleus of a number of cell types is ~7.3, and higher by 0.3–0.5 pH units than that in the cytoplasm ***(61, 62)***. The local concentration of hydrogen ions, like that of other cations, is expected to vary considerably near the surfaces of macromolecules and structures; for example, localised regions of pH 4.5 are predicted to occur in the minor groove of DNA in a buffer at pH 7.5 ***(58)***.

Spitzer and Poolman ***(63)***, considering the cytoplasm, drew attention to the possibility that electrochemical gradients resulting from heterogeneous microenvironments caused by the charged surfaces of macromolecules could be involved in the transport of charged low molecular weight molecules.

4 The Redox Environment

Nuclei contain glutathione (GSH) at an estimated concentration in the millimolar range ***(64, 65)***; newer methods yield somewhat lower values (reviewed in **ref.** ***(66)***). GSH is one of two systems that reduce protein thiols in the nucleus, the second being based on thioredoxin 1 (Trx1) ***(67, 68)***. The maintenance of a reducing environment appears to be important for many nuclear activities; depletion of GSH impairs the transcriptional activation of heat shock genes ***(69)***, cysteine residues in several transcription factors must be reduced for activity (reviewed in **ref.** ***(70)***), and

reducing conditions are required for maximal activity of telomerase ***(71)***. Redox-sensitive motifs occur in the majority of cell cycle-associated proteins that function in the nucleus in the G1 phase ***(70)***. The reducing environment may also contribute to promoting repair of oxidative damage to DNA and to protecting oxidant-sensitive proteins from oxidation ***(72)***. During the isolation of nuclei, disulphide crosslinks may be formed between nuclear proteins (e.g. **ref.** ***(73)***), probably as a result of vigorous aeration during homogenisation of tissues.

The nuclear GSH pool escapes from nuclei in aqueous buffers ***(74)***, and there is therefore a case for including a reducing agent such as glutathione or dithiothreitol ***(75)*** in solutions for isolating nuclei and their components to reproduce the redox conditions in vivo.

5 Diffusion in the Nucleus

The observed diffusion constants of macromolecules in the nucleus are, at first view, unexpectedly high. Compared with those in aqueous solution, they are similar for oligodeoxynucleotides ***(76)***, three to five times lower for dextrans of 500–750 kDa ***(77, 78)***, and approximately two to three times lower for enhanced green fluorescent protein (EGFP) and rod-shaped oligomers of EGFP ***(79)***. Within the nucleolus, however, the latter probes diffuse ~20-fold more slowly than elsewhere in the nucleus ***(79)***. The relatively unhindered diffusion of macromolecules within the nucleus contrasts with the much more restricted diffusion of intranuclear compartments and chromosomes ***(80, 81)***.

Crowding imposes constraints to diffusion that vary with the size, shape, and chemical properties of the diffusing molecules ***(77, 82)*** and anomalous diffusion is observed in crowded environments ***(83, 84)***. Diffusion rates may be higher than predicted, because depletion effects at the surface of a moving macromolecule produce a low-viscosity layer around it, which strongly reduces the friction that it experiences ***(85, 86)***.

6 Perspectives

The view of the nucleus as a crowded and confined mixture of charged macromolecules provides new perspectives for both experimental and theoretical approaches. In experimental studies, an oversimplified approximation to conditions in vivo would be provided by using buffers that are crowded by addition of PEG, dextran, or Ficoll (e.g. **ref.** ***(46)***). These crowded solutions are presently the best systems to study nuclear enzymes, enzyme systems, and intranuclear structures such as the nucleolus in vitro. Limits on the salt content of buffers that will reproduce the environment in vivo are imposed by the exquisite sensitivity to salts of clustering and phase separation of proteins in concentrated solutions (e.g. **refs.** ***(87, 88)***).

Theoretical approaches of a new and more quantitative nature are needed to understand the entropic and depletion effects. These forces are likely to be major contributors to the formation of structures, and are also crucial for modelling complex sequential processes such as replication and transcription ***(3)*** and for signalling and control networks. It should be noted that analogous problems arise in physical chemistry (colloid and interface sciences) and are currently investigated using both theoretical and experimental methods. Some of these studies can provide interesting clues to understand biophysical–chemical processes in the nucleus; for example, they bring new perspectives on the forces that may determine the conformation of interphase chromosomes ***(5)***. Interdisciplinary approaches associating nuclear biologists with mathematicians, colloid, surface, and interface scientists are likely to be essential to understand the nucleus and the effects of macromolecular crowding in intracellular environments.

Acknowledgments Santiago Schnell thanks Edward Flach (University of Oxford) for his comments. Santiago Schnell's work is based upon research supported by the National Science Foundation under Grant No. 0513701, and the National Institutes of Health under Grant No. R01GM076692. Any opinions, findings, and conclusions or recommendations expressed in this material do not necessarily reflect the views of the National Science Foundation or the National Institutes of Health. Ronald Hancock is supported partly by funds from the Medical Faculty and the Cancer Research Centre of Laval University.

References

1. Hancock, R. (2004) A role for macromolecular crowding effects in the assembly and function of compartments in the nucleus. *J. Struct. Biol*. **146**, 281–290.
2. Misteli, T. (2005) Concepts in nuclear architecture. *Bioessays* **27**, 477–487.
3. Marenduzzo, D., Micheletti, C., and Cook, P.R. (2006) Entropy-driven genome organization. *Biophys. J*. **90**, 3712–3721.
4. Iborra, F.J. (2007) Can visco-elastic phase separation, macromolecular crowding and colloidal physics explain nuclear organisation? *Theor. Biol. Med. Model*. **4**, 15.
5. Hancock, R. (2007) Packing of the polynucleosome chain in interphase chromosomes: Evidence for a contribution of macromolecular crowding. *Semin. Cell Dev. Biol*. **18**, 668–675.
6. Zimmerman, S.B. and Minton, A.P. (1993) Macromolecular crowding: Biochemical, biophysical and physiological consequences. *Annu. Rev. Biophys. Biomol. Struct*. **22**, 27–65.
7. Minton, A.P. (2006) How can biochemical reactions within cells differ from those in test tubes? *J Cell Sci*. **119**, 2863–2869.
8. Minton, A.P. (2001) The influence of macromolecular crowding and macromolecular confinement on biochemical reactions in physiological media. *J. Biol. Chem*. **276**, 10577–10580.
9. Schnell, S. and Turner, T.E. (2004) Reaction kinetics in intracellular environments with macromolecular crowding: simulations and rate laws. *Prog. Biophys Mol. Biol*. **85**, 235–260.
10. Luby-Phelps, K. (2000) Cytoarchitecture and physical properties of cytoplasm: Volume, viscosity, diffusion, intracellular surface area. *Int. Rev. Cytol*. **192**, 189–221.
11. Asakura, S. and Oosawa, F. (1958) Interaction between particles suspended in solutions of macromolecules. *J. Polymer Sci*. **33**, 183–192.
12. Minton, A.P. (1997) Influence of excluded volume upon macromolecular structure and associations in 'crowded' media. *Curr. Opin. Biotechnol*. **8**, 65–69.

13. Minton, A.P. (1981) Excluded volume as a determinant of macromolecular structure and reactivity. *Biopolymers* **20**, 2093–2120.
14. Lago, S., Cuetos, A., Martinez-Haya, B., and Rull, L.F. (2004) Crowding effects in binary mixtures of rod-like and spherical particles. *J. Mol. Recognit*. **17**, 417–425.
15. Ellis, R.J. (2001) Macromolecular crowding: obvious but underappreciated. *Trends Biochem. Sci*. **26**, 597–604.
16. Cavalier-Smith, T. (1987) The origin of eukaryote and archaebacterial cells. *Ann. NY Acad. Sci*. **503**, 17–54.
17. Handwerger, K.E. and Gall, J.G. (2006) Subnuclear organelles: new insights into form and function. *Trends Cell Biol*. **16**, 19–26.
18. Turner, T.E., Schnell, S., and Burrage, K. (2004) Stochastic approaches for modelling in vivo reactions. *Comput. Biol. Chem*. **28**, 165–178.
19. Grima, R. and Schnell, S. (2006) A systematic investigation of the rate laws valid in intracellular environments. *Biophys. Chem*. **124**, 1–10.
20. Grima, R. and Schnell, S. (2006) How reaction kinetics with time-dependent rate coefficients differs from generalized mass action. *Chem. Phys. Chem*. **7**, 1422–1424.
21. Hammes, G.G. (2000) *Thermodynamics and kinetics for the biological sciences*. Wiley-Interscience, New York.
22. Chandler, D. (1987) *Introduction to modern statistical mechanics*. Oxford University Press, New York.
23. Laurent, T.C. and Ogston, A.G. (1963) Interaction between polysaccharides and other macromolecules. 4. Osmotic pressure of mixtures of serum albumin and hyaluronic acid. *Biochem. J*. **89**, 249–253.
24. Laurent, T.C. (1995) An early look at macromolecular crowding. *Biophys. Chem*. **57**, 7–14.
25. Fulton, A.B. (1982) How crowded is the cytoplasm? *Cell* **30**, 345–347.
26. Lebowitz, J.L., Helfand, E., and Praestga.E. (1965) Scaled particle theory of fluid mixtures. *J. Chem. Phys*. **43**, 774–779.
27. Minton, A.P. (1998) Molecular crowding: Analysis of effects of high concentrations of inert cosolutes on biochemical equilibria and rates in terms of volume exclusion. *Methods Enzymol*. **295**, 127–149.
28. Minton, A.P. (1983) The effect of volume occupancy upon the thermodynamic activity of proteins: some biochemical consequences. *Mol. Cell. Biochem*. **55**, 119–140.
29. Giddings, J.C., Kucera, E., Russell, C.P., and Myers, M.N. (1968) Statistical theory for equilibrium distribution of rigid molecules in inert porous networks. Exclusion chromatography. *J. Phys. Chem*. **72**, 4397–4408.
30. Minton, A.P. (1992) Confinement as a determinant of macromolecular structure and reactivity. *Biophys. J*. **63**, 1090–1100.
31. Lakatos, S. and Minton, A.P. (1991) Interactions between globular proteins and F-actin in isotonic saline solution. *J. Biol. Chem*. **266**, 18707–18713.
32. Minton, A.P. (1995) Confinement as a determinant of macromolecular structure and reactivity. II. Effects of weakly attractive interactions between confined macrosolutes and confining structures. *Biophys. J*. **68**, 1311–1322.
33. Saxton, M.J. (1994) Anomalous diffusion due to obstacles: A Monte Carlo study. *Biophys. J*. **66**, 394–401.
34. Voituriez, R., Moreau, M., and Oshanin, G. (2005) Reversible diffusion-limited reactions: "Chemical Equilibrium" state and the Law of Mass Action revisited. *Europhys. Lett*. **69**, 177–183.
35. Voituriez, R., Moreau, M., and Oshanin, G. (2005) Corrections to the law of mass action and properties of the asymptotic $t=\infty$ state for reversible diffusion-limited reactions. *J. Chem. Phys*. **122**, 84103.
36. Grima, R. and Schnell, S. (2007) A mesoscopic simulation approach for modeling intracellular reactions. *J. Stat. Phys*. **128**, 139–164.
37. Kopelman, R. (1988) Fractal reaction kinetics. *Science* **241**, 1620–1626.
38. Schnell, S. and Maini, P.K. (2003) A century of enzyme kinetics: Reliability of the K_M and v_{max} estimates. *Comm. on Theor. Biol*. **8**, 169–187.

39. Minton, A.P. and Ross, P.D. (1978) Concentration dependence of the diffusion coefficient of hemoglobin. *J. Phys. Chem*. **82**, 1934–1938.
40. Hall, D. and Minton, A.P. (2003) Macromolecular crowding: qualitative and semiquantitative successes, quantitative challenges. *Biochim. Biophys. Acta* **1649**, 127–139.
41. Srividhya, J., Schnell, S., Crampin, E.J., and McSharry, P.E. (2007) Reconstructing biochemical pathways from time course data. *Proteomics* **7**, 828–838.
42. Bhuiyan, L.B., Vlachy, V., and Outhwaite, C.W. (2002) Understanding polyelectrolyte solutions: macroion condensation with emphasis on the presence of neutral co-solutes. *Int. Rev. Phys. Chem*. **21**, 1–36.
43. Rescic, J., Vlachy, V., Outhwaite, C.W., Bhuiyan, L.B., and Mukherjee, A. K. (1999) A Monte Carlo simulation and symmetric Poisson–Boltzmann study of a four-component electrolyte mixture. *J. Chem. Phys*, **111**, 5514–5521.
44. Deserno, M., Arnold, A., and Holm, C. (2003) Attraction and ionic correlations between charged stiff polyelectrolytes. *Macromolecules* **36**, 249–259.
45. Zimmerman, S.B. and Harrison, B. (1987) Macromolecular crowding increases binding of DNA polymerase to DNA: An adaptive effect. *Proc. Natl. Acad. Sci. USA* **84**, 1871–1875.
46. Zimmerman, S.B. and Trach, S.O. (1988) Effects of macromolecular crowding on the association of E. coli ribosomal particles. *Nucleic Acids Res*. **16**, 6309–6326.
47. Richey, B., Cayley, D.S., Mossing, M.C., Kolka, C., Anderson, C.F., Farrar, T.C., and Record, M.T Jr. (1987) Variability of the intracellular ionic environment of Escherichia coli. Differences between in vitro and in vivo effects of ion concentrations on protein–DNA interactions and gene expression. *J. Biol. Chem*. **262**, 7157–7164.
48. Buitenhuis, J., Donselaar, L.N., Buining, P.A., Stroobants, A., and Lekkerkerker, H.N.W. (1995) Phase-separation of mixtures of colloidal boehmite rods and flexible polymer. *J. Coll. Interface Sci*. **175**, 46–56.
49. Frenkel, D. (1999) Entropy-driven phase transitions. *Physica A* 263, 26–38.
50. Linse, P. (2001) Structure and phase separation in solutions of like-charged colloidal particles. *Phil. Trans. Roy. Soc. Lond. A* **359**, 853–866.
51. Galkin, O., Chen, K., Nagel, R.L., Hirsch, E., and Vekilov, P.G. (2002) Liquid-liquid separation in solutions of normal and sickle cell hemoglobin. *Proc. Natl. Acad. Sci. USA* **99**, 8479–8483.
52. Xie, X., Vucetic, S., Iakoucheva, L.M., Oldfield, C.J., Dunker, A.K., Uversky, V.N., and Obradovic, Z. (2007) Functional anthology of intrinsic disorder. 1. Biological processes and functions of proteins with long disordered regions. *J. Proteome Res*. **6**, 1882–1898.
53. Dedmon, M.M., Patel, C.N., Young, G.B., and Pielak, G.J. (2002) FlgM gains structure in living cells. *Proc. Natl. Acad. Sci. USA* **99**, 12681–12684.
54. Morar, A.S., Olteanu, A., Young, G.B., and Pielak, G.J. (2001) Solvent-induced collapse of alpha-synuclein and acid-denatured cytochrome c. *Protein Sci*. **10**, 2195–2199.
55. Elowitz, M.B., Levine, A.J., Siggia, E.D., and Swain, P.S. (2002) Stochastic gene expression in a single cell. *Science* **297**, 1183–1186.
56. Blake, W.J., Kærn, M., Cantor, C.R., and Collins, J.J. (2003) Noise in eukaryotic gene expression. *Nature* **422**, 633–637.
57. McAdams, H.H. and Arkin, A.P. (1997) Stochastic mechanisms in gene expression. *Proc. Natl. Acad. Sci. USA* 94, 814–819.
58. Lamm, G. and Pack, G.R. (1990) Acidic domains around nucleic acids. *Proc. Natl. Acad. Sci. USA* **87**, 9033–9036.
59. Beard, D.A. and Schlick, T. (2001) Modeling salt-mediated electrostatics of macromolecules: The discrete surface charge optimization algorithm and its application to the nucleosome. *Biopolymers* **58**, 106–115.
60. Koelsch, P., Viswanath, P., Motschmann, H., Shapovalov, V.L., Brezesinski, G., Mohwald, H., Horinek, D., Netz, R.R., Giewekemeyer, K., Salditt, T., Schollmeyer, H., von Klitzing, R., Daillant, J., and Guenoun, P. (2007) Specific ion effects in physicochemical and biological systems: Simulations, theory and experiments. *Coll. Surf. A* **303**, 110–136.
61. Dubbin, P.N., Cody, S.H., and Williams, D.A. (1993) Intracellular pH mapping with SNARF-1 and confocal microscopy. II: pH gradients within single cultured cells. *Micron* **24**, 581–586.

62. Seksek, O. and Bolard, J. (1996) Nuclear pH gradient in mammalian cells revealed by laser microspectrofluorimetry. *J. Cell Sci*. **109**, 257–262.
63. Spitzer, J. and Poolman, B. (2005) Electrochemical structure of the crowded cytoplasm. *Trends Biochem. Sci*. **30**, 536–541.
64. Soboll, S., Grundel, S., Harris, J., Kolb-Bachofen, V., Ketterer, B., and Sies, H. (1995) The content of glutathione and glutathione S-transferases and the glutathione peroxidase activity in rat liver nuclei determined by a non-aqueous technique of cell fractionation. *Biochem. J*. **311**, 889–894.
65. Bellomo, G., Palladini, G., and Vairetti, M. (1998) Intranuclear distribution, function and fate of glutathione and glutathione-S-conjugate in living rat hepatocytes studied by fluorescence microscopy. *Microsc. Res. Tech*. **36**, 243–252.
66. Hansen, J.M., Go, Y-M., and Jones, D.P. (2006) Nuclear and mitochondrial compartmentation of oxidative stress and redox signaling. *Annu. Rev. Pharmacol. Toxicol*. **46**, 215–234.
67. Watson, W.H. and Jones, D.P. (2003) Oxidation of nuclear thioredoxin during oxidative stress. *FEBS Lett*. **543**, 144–147.
68. Halvey, P.J., Hansen, J.M., Johnson, J.M., Go, Y-M., Samali, A., and Jones, D.P. (2007) Selective oxidative stress in cell nuclei by nuclear-targeted D-amino acid oxidase. *Antioxid. Redox Signal*. **9**, 807–816.
69. Rokutan, K., Hirakawa, T., Teshima, S., Honda, S., and Kishi, K. (1996) Glutathione depletion impairs transcriptional activation of heat shock genes in primary cultures of guinea pig gastric mucosal cells. *J. Clin. Invest*. **97**, 2242–2250.
70. Conour, J.E., Graham, W.V., and Gaskins, H.R. (2004) A combined in vitro/bioinformatic investigation of redox regulatory mechanisms governing cell cycle progression. *Physiol. Genomics* **18**, 196–205.
71. Borrás, C., Esteve, J.M., Viña, J.R., Sastre, J., Viña, J., and Pallardó, F.V. (2004) Glutathione regulates telomerase activity in 3T3 fibroblasts. *J. Biol. Chem*. **279**, 34332–34335.
72. Green, R.M., Graham, M., O'Donovan, M.R., Chipman, J.K., and Hodges, N.J. (2006) Subcellular compartmentalization of glutathione: Correlations with parameters of oxidative stress related to genotoxicity. *Mutagenesis* **21**, 383–390.
73. Kaufmann, S.H., Okret, S., Wikstrom, A.C., Gustafsson, J.A., and Shaper, J.H. (1986) Binding of the glucocorticoid receptor to the rat liver nuclear matrix. The role of disulfide bond formation. *J. Biol. Chem*. **261**, 11962–11967.
74. Loh, S.N., Dethlefsen, L.A., Newton, G.L., Aguilera, J.A., and Fahey, R.C. (1990) Nuclear thiols: Technical limitations on the determination of endogenous nuclear glutathione and the potential importance of sulfhydryl proteins. *Radiat. Res*. **121**, 98–106.
75. Jackson, D.A., Yuan, J., and Cook, P.R. (1988) A gentle method for preparing cyto- and nucleo-skeletons and associated chromatin. *J. Cell Sci*. **90**, 365–378.
76. Politz, J.C., Browne, E.S., Wolf, D.E., and Pederson, T. (1998) Intranuclear diffusion and hybridization state of oligonucleotides measured by fluorescence correlation spectroscopy in living cells. *Proc. Natl. Acad. Sci. USA* **95**, 6043–6048.
77. Seksek, O., Biwersi, J., and Verkman, A.S. (1997) Translational diffusion of macromolecule-sized solutes in cytoplasm and nucleus. *J. Cell Biol*. **138**, 131–142.
78. Verkman, A. S. (2002) Solute and macromolecule diffusion in cellular aqueous compartments. *Trends Biochem. Sci*. **27**, 27–33.
79. Pack, C., Saito, K., Tamura, M., and Kinjo, M. (2006) Microenvironment and effect of energy depletion in the nucleus analyzed by multiple oligomeric EGFPs. *Biophys. J*. **91**, 3921–3936.
80. Tseng, Y., Lee, J.S.H., Kole, T.P., Jiang, I., and Wirtz, D. (2004) Micro-organization and visco-elasticity of the interphase nucleus revealed by particle nanotracking. *J. Cell Sci*. **117**, 2159–2167.
81. Görisch, S. M., Lichter, P., and Rippe, K. (2005) Mobility of multi-subunit complexes in the nucleus: accessibility and dynamics of chromatin subcompartments. *Histochem. Cell Biol*. **123**, 217–228.
82. Lukacs, G.L., Haggie, P., Seksek, O., Lechardeur, D., Freedman, N., and Verkman, A.S. (2000) Size-dependent DNA mobility in cytoplasm and nucleus. *J. Biol. Chem*. **275**, 1625–1629.

83. Weiss, M., Elsne, M., Kartberg, F., and Nilsson, T. (2004) Anomalous subdiffusion is a measure for cytoplasmic crowding in living cells. *Biophys. J*. **87**, 3518–3524.
84. Banks, D.S. and Fradin, C. (2005) Anomalous diffusion of proteins due to molecular crowding. *Biophys. J*. **89**, 2960–2971.
85. Koenderink G.H., Sacanna S., Aarts D.G.A.L., and Philipse A.P. (2004) Rotational and translational diffusion of fluorocarbon tracer spheres in semidilute xanthan solutions. *Phys. Rev. E* 69021804.
86. Tuinier, R., Dhont, J.K.G., and Fan, T.H. (2006) How depletion affects sphere motion through solutions containing macromolecules. *Europhys. Lett*. **75**, 929–935.
87. Broide, M.L., Tominc, T.M., and Saxowsky, M.D. (1996) Using phase transitions to investigate the effect of salts on protein interactions. *Phys. Rev. E* **53**, 6325–6335.
88. Stradner, A., Sedgwick, H., Cardinaux, F., Poon, W.C., Egelhaaf, S.U., and Schurtenberger, P. (2004) Equilibrium cluster formation in concentrated protein solutions and colloids. *Nature* **432**, 492–495.

Chapter 2
Purification of Nuclei and Preparation of Nuclear Envelopes from Skeletal Muscle

Gavin S. Wilkie and Eric C. Schirmer

Keywords Muscle nuclei; Myonuclei; Skeletal muscle; Nuclear envelope; Sarcoplasmic reticulum; Integral membrane protein; Nuclear lamina

Abstract The nuclear envelope is a complex membrane–protein system that is notoriously difficult to purify because it has many connections to both nuclear and cytoplasmic components. This difficulty is compounded by the fact that the nature of these connections vary in different cell types, and so methods must be significantly adapted according to the cell type from which nuclear envelopes are being purified. Here we present a detailed method for purification of nuclear envelopes from one of the most intransigent tissues: skeletal muscle. We further note in the procedure how this method differs from that for other tissues. Identification of nuclear envelope-specific proteins is principally encumbered by endoplasmic reticulum contamination; therefore, we also present a method to purify sarcoplasmic reticulum from muscle.

1 Introduction

The nuclear envelope (NE) is a double membrane system that includes a number of integral membrane proteins, nuclear pore complexes, and the intermediate filament lamin polymer ***(1–3)***. Recently, several inherited diseases, especially muscular dystrophies, have been associated with mutations in NE proteins ***(2, 4)***, sparking renewed interest in the muscle NE ***(5)***. Purification of NEs from cell lines and tissues in general is encumbered with problems due to the high degree of connectivity between the nuclear membrane and other cellular structures on both sides. At the cytoplasmic face, the outer nuclear membrane is continuous with the endoplasmic reticulum and contains unique transmembrane proteins that connect it to the cytoskeleton ***(6–8)***. Inside the nucleus, the inner nuclear membrane proteins connect to lamins, and both lamins and integral membrane proteins bind directly to chromatin proteins and DNA ***(9, 10)***. These connections vary in different cell types; so the tricks used to separate NEs from other cellular structures must be modified according to each tissue from whence the envelopes are being prepared.

R. Hancock (ed.) *The Nucleus: Volume 1: Nuclei and Subnuclear Components*,

In general, the first step in NE preparation is to isolate intact nuclei, taking advantage of their large mass relative to other organelles, either following homogenization of tissue in buffers lacking detergent or hypotonic lysis of cells ***(11)***. Subsequent Dounce homogenization followed by pelleting through dense sucrose may reduce the amount of endoplasmic reticulum connected to the nuclei, but cannot fully eliminate it because the outer nuclear membrane, studded with ribosomes, is itself part of the endoplasmic reticulum. Treatment with enzymes to digest nucleic acids followed by salt washes and pelleting through sucrose cushions reduces the relative abundance of chromatin proteins ***(12–14)***.

We have previously elaborated procedures specific to purification of NEs from liver and from blood cells ***(15, 16)***. These and other established procedures for the isolation of nuclei from soft tissues such as liver, kidney, and brain cannot be successfully applied to skeletal muscle. Several methods for the purification of nuclei from skeletal muscle have been published previously (reviewed in ref. ***(17)***). However, they require Triton X-100 for the efficient release of nuclei from muscle fibers during homogenization: in the absence of detergent, the yield drops by a factor of ten ***(18)***. These procedures cannot be used for isolation of NEs, because the detergent removes the nuclear membranes. The preparation of nuclei from skeletal muscle presents several problems unique to this tissue. Firstly, the number of nuclei in skeletal muscle is very low compared with that of other tissues, meaning that yields are comparatively low per gram of starting material. The DNA content of muscle is 17% that of liver and only 9% compared with kidney ***(17)***. Secondly, muscle fibers are extremely tough and homogenization procedures must be chosen with care to balance maximum disruption of the tissue with a minimum of damage to nuclei. Thirdly, the purification of nuclei from muscle homogenates on sucrose gradients often yields unsatisfactory results due to the presence of dense myofibrillar material derived from sarcomeres that tends to copurify with nuclei.

To carry out a proteomic analysis of the NE of muscle nuclei, we have developed a procedure for preparing muscle NEs on a relatively large scale. Muscle tissue is initially broken down by mincing, and is then gently homogenized using a motorized Dounce homogenizer (such as a Potter-Elvehjem). The resulting homogenate is filtered to remove the bulk of the fibrous material and poorly disrupted tissue pieces, and a crude nuclear pellet is obtained by low-speed centrifugation. Nuclei are initially purified from the dense myofibrillar material by isopycnic banding in Percoll gradients ***(19)***. Ultracentrifugation through discontinuous sucrose gradients is then used to further purify the nuclei from other cytoplasmic components. However, we found that a three-step gradient in which the muscle nuclei are floated on a 2.8 M sucrose cushion instead of just being pelleted through 2 M sucrose improved purity, because it separates dense contaminants such as any remaining myofibrils to the pellet ***(20)***. Finally, the nucleoplasmic contents are removed by enzymatic digestion of chromatin and salt washes, yielding a NE fraction highly enriched in lamins and integral NE proteins.

It is important to note that because of the large number of connections that NEs have to chromatin, the endoplasmic reticulum (sarcoplasmic reticulum in muscle), and cytoskeletal components, no method can truly “purify” NEs to homogeneity.

However, subsequent purification steps may be employed to remove contaminants. Some further purification procedures are based on the biochemical properties of the nuclear lamina, which, as an intermediate filament system, remains insoluble in the presence of relatively high concentrations of salt and detergent ***(10)***. Other procedures rely on the solubility properties of membrane proteins ***(16, 21, 22)***, though with the possible loss of true NE proteins. Therefore, we also describe a method to purify sarcoplasmic reticulum membranes from the nuclear and mitochondrial-depleted muscle homogenate. This fraction can be used for a comparative analysis to subtract proteins that are not unique to the NE in silico ***(23)***.

2 Materials

2.1 Preparation of Tissue (Rodent Leg Muscle)

1. This procedure has been developed using the hind leg muscles of 6- to 10-week-old rats (e.g., Sprague-Dawley or equivalent). However, it could easily be adapted to use some skeletal muscle types other than leg muscle, or different organisms, such as mice.
2. Volumes in the protocol are given based on grams of muscle or millions of nuclei. To estimate how many animals to use: 20–30 g of muscle can be obtained from the hind limbs of one rat. We generally produce 10–20 million nuclei from 150 g of muscle obtained from six rats, although yields may vary a further two-fold in either direction (*see* **Note 1**).
3. Guillotine or equivalent local method for euthanizing animals.
4. Dissection scissors, forceps/ tweezers, scalpels, single-sided razor blades and bone scissors (kitchen scissors that will cut chicken bones are adequate).
5. Two beakers on ice, one containing phosphate-buffered saline (PBS) and one containing homogenization buffer.
6. Appropriate materials for covering surfaces during the procedure and for cleaning and waste disposal.
7. PBS: 4.3 m*M* sodium phosphate, 137 m*M* sodium chloride, 2.7 m*M* potassium chloride, and 1.4 m*M* potassium phosphate, adjusted to pH 7.4 with HCl. Store at room temperature. Two hundred and fifty milliliters of PBS is sufficient for washing and collecting leg muscles from six rats.

2.2 Purification of Nuclei from Skeletal Muscle

2.2.1 Hardware

1. Standard meat mincer, as can be purchased in local grocery or hardware stores.
2. Potter-Elvehjem homogenizer with a motor-driven Teflon pestle providing 0.1- to 0.15-mm clearance and a drive motor capable of 1,000 rpm (e.g., Potter S

homogenizer motor 853 3032, 60 mL homogenizer cylinder 854 2600, and PFTE Plunger 854 3003 from Sartorius or equivalent).
3. Loose fitting (Wheaton type B pestle) glass Dounce homogenizer with a clearance of between ~0.1 and 0.15 mm.
4. Swinging-bucket floor-model centrifuge and rotor capable of spinning 50-mL clear tubes to speeds of 27,000×*g* for Percoll gradients (e.g., Beckman J-25 centrifuge with a JS 13.1 rotor and Nalgene 3110-9500 50-mL centrifuge tubes, *see* **Note 2**).
5. Swinging-bucket ultracentrifuge and rotor capable of 82,000×*g* (e.g., Beckman Coulter SW28 rotor with Beckman Coulter 344058 Ultra-Clear 25×89-mm centrifuge tubes) for sucrose gradients.
6. Standard light microscope, with phase contrast if possible; and glass slides and coverslips.
7. Assorted 500–1,000 mL beakers, two funnels, twenty-five 50-mL centrifuge tubes, and several spatulas.
8. Two large ice buckets with ice for keeping all solutions and tubes cold.
9. Sterile cheesecloth for filtering homogenate (*see* **Note 3**). Two pieces of cheesecloth 50×20 cm are required for 500 mL of muscle homogenate.
10. Large-bore Luer-lock stainless steel needles (e.g., 14 gauge) of length greater than the centrifuge tubes, and glass Luer-lock syringes to dispense dense sucrose solutions.

2.2.2 Solutions

Many of the solution names include the initials for the primary components: S for sucrose, H for Hepes, K for KCl, and M for $MgCl_2$ (*see* **Note 4**).

1. Protease inhibitor cocktail, e.g., Sigma P8340 (*see* **Note 5**), should be freshly added to all solutions at a 1:250 dilution (*see* **Note 6**). If general protease cocktails are used, make certain that they do not contain ethylene-diamine tetraacetic acid (EDTA) because this interferes with steps of NE preparation (e.g., Mg^{2+} ions are required to stabilize chromatin and as a cofactor for DNase I).
2. Percoll (Sigma) should be diluted to a working stock of 81% (v/v) in 10 m*M* Hepes pH 7.4, 60 m*M* KCl, 0.1 m*M* EDTA, 0.1 m*M* EGTA, and 300 m*M* sucrose (*see* **Note 7**). Store at 4°C. Each Percoll gradient requires 13.3 mL of this buffered 81% Percoll solution and is sufficient for 100–200 g of starting material.
3. Homogenization buffer: 10 m*M* Hepes pH 7.4, 60 m*M* KCl, 0.5 m*M* spermidine, 0.15 m*M* spermine, 2 m*M* EDTA (*see* **Note 8**), 0.5 m*M* EGTA, and 300 m*M* sucrose. Store at 4°C. Add protease inhibitors and 2 m*M* dithiothreitol (DTT; from a 1 *M* solution in H_2O) immediately before use. For every gram of muscle, 2.5–5 mL of homogenization buffer is required (e.g., 100–200 g of minced muscle should be suspended in 500 mL of buffer).
4. Percoll gradient buffer: 10 m*M* Hepes pH 7.4, 60 m*M* KCl, 0.5 m*M* spermidine, 0.15 m*M* spermine, 0.1 m*M* EDTA, 0.1 m*M* EGTA, and 300 m*M* sucrose. Store at 4°C. Add 2 m*M* DTT and protease inhibitors before use. For 100–200 g of starting material, 150 mL of Percoll gradient buffer is required.

5. HKM: 50 m*M* Hepes pH 7.4, 25 m*M* KCl, and 5 m*M* $MgCl_2$. Store at 4°C. Add 2 m*M* DTT and protease inhibitors before use. For 100–200 g of starting material, 100 mL of HKM is required.
6. 0.25 *M* SHKM: 250 m*M* sucrose, 50 m*M* Hepes pH 7.4, 25 m*M* KCl, and 5 m*M* $MgCl_2$. Store at 4°C. Add 2 m*M* DTT and protease inhibitors before use. For 100–200 g of starting material, 150 mL of 0.25 *M* SHKM is required.
7. 2.15 *M* SHKM: 2.15 *M* sucrose (from a 2.5 *M* sucrose stock, *see* **Note 9**), 50 m*M* Hepes pH 7.4, 25 m*M* KCl, and 5 m*M* $MgCl_2$. Store at 4°C. Add 2 m*M* DTT and protease inhibitors before use. For 100–200 g of starting material, 20 mL of 2.15 *M* SHKM is required.
8. 2.3 *M* SHKM: 2.3 *M* sucrose (from a 2.5 *M* sucrose stock, *see* **Note 9**), 50 m*M* Hepes, pH 7.4, 25 m*M* KCl, and 5 m*M* $MgCl_2$. Store at 4°C. Add 2 m*M* DTT and protease inhibitors before use. For 100–200 g of starting material, 100 mL of 2.3 *M* SHKM is required.
9. 2.5 *M* sucrose: Dissolve 855.75 g of sucrose in a total volume of 1 L of distilled water by stirring and heating. Store at 4°C. This stock can be used to make all working solutions that contain sucrose, except the 2.8 *M* SHKM.
10. 2.8 *M* SHKM: 2.8 *M* sucrose (*see* **Note 10**), 50 m*M* Hepes pH 7.4, 25 m*M* KCl, and 5 m*M* $MgCl_2$. Store at room temperature. Add 2 m*M* DTT and protease inhibitors and chill on ice immediately before use. For 100–200 g of starting material, 20 mL of 2.8 *M* SHKM is required.

2.3 Preparation of Nuclear Envelopes

1. The same hardware is required as for preparation of nuclei, *see* **Section 2.2.1.**
2. DNase I (e.g., Sigma cat. D4527) at 10 U/μL in H_2O. Store at −20°C.
3. RNase A (e.g., Sigma cat. R4875) in H_2O at 10 mg/mL, boiled for 20 min. Store at −20°C.
4. 10% SHM buffer: 0.3 *M* sucrose, 10 m*M* Hepes pH 7.4, 2 m*M* $MgCl_2$, and 0.5 m*M* $CaCl_2$ (*see* **Note 4**). Store at 4°C. Add 2 m*M* DTT and protease inhibitors before use. For 20 million nuclei, 50 mL of 10% SHM buffer is required.
5. 30% SHKM buffer: 0.9 *M* sucrose, 10 m*M* Hepes pH 7.4, 25 m*M* KCl, and 2.5 m*M* $MgCl_2$. Store at 4°C. Add 2 m*M* DTT and protease inhibitors before use. Two milliliters of 30% SHKM buffer is required for 20 million nuclei to underlay the 10% SHM and form a sucrose cushion during centrifugation.

2.4 Preparation of Sarcoplasmic Reticulum Membranes

1. The same hardware is required as for preparation of nuclei.
2. A Type 45 Ti fixed-angle ultracentrifuge rotor or equivalent that can provide 150,000 × *g*, and matching tubes.

3. The same sucrose solutions used for preparation of nuclear envelopes can be used in preparing microsomes. In particular, 2.8 *M* SHKM and 0.25 *M* SHKM will be required.

2.5 Determining the Purity/Quality of Fractions

2.5.1 Fluorescent Staining of Chromatin

1. Hoechst 33342 or 4,6-diamidino-2-phenylindole (DAPI) (e.g., Molecular Probes) for fluorescent labeling of chromatin.
2. An epifluorescence microscope capable of at least ×400 magnification. Excitation and emission filters suitable for viewing DAPI or Hoechst 33342 fluorescence will be required (the excitation and emission spectra of these dyes are very similar).
3. Standard microscope slides and coverslips.

2.5.2 Western Analysis of Fractions

1. Standard labware for sodium dodecylsulfate (SDS) polyacrylamide gel electrophoresis (PAGE) and Western blotting.
2. Antibodies to lamins, characterized integral NE proteins, and endoplasmic reticulum proteins. Among the best lamin antibodies are 119D5-F1 against lamin B1 (MAB3213; Chemicon Europe, Chandlers Ford, UK) and 131C3 against lamin A/C (MAB3538; Chemicon). For endoplasmic reticulum proteins, a number of companies sell antibodies to calnexin or calreticulin, but we do not have personal experience with these antibodies.
3. An assay system for estimating protein concentration in purified fractions (e.g., Bradford reagent and a spectrophotometer capable of measuring absorbance at 595 nm).

3 Methods

If NEs are being prepared from muscle, the entire procedure can take 8 or 9 hours to complete. If several preparations of nuclei are required to generate sufficient material for NEs, it may be more practical to freeze the purified muscle nuclei and to prepare NEs from the accumulated nuclei at a later time.

3.1 Preparation of Tissue (Rodent Leg Muscle)

Most of the NE preparation procedure can be efficiently performed with one individual; however killing and dissecting the animals should be done quickly, and it is very helpful to have assistance at this point.

1. Kill the rats according to local animal protocols.
2. Pull up the skin in the dorsal posterior area and cut through the skin and fur with scissors perpendicular to the length of the body. Make another incision along the backbone down the length of the body. Peel the skin back to remove the fur and expose the hind legs.
3. Pull off extraneous fat and then cut along the muscle line delineating the hip with a razor blade. Likewise, in the anterior aspect, cut underneath the pelvis so that the larger muscle mass is disconnected around the connection between the femur and hip bone.
4. Remove the hind legs by cutting through the hip joint with bone scissors.
5. Rinse legs in ice-cold PBS to wash off hair and blood.
6. Remove the muscle tissue from the bone using a single-sided razor blade. Grasp the tissue with tweezers to avoid injury to hands. Cut up muscle tissue into small chunks of up to 5-mm square and collect in a small volume (e.g., 50 mL) of ice-cold PBS. If possible, have several people working at this point so that one can begin processing the material while the other deals with disposal and cleanup.

3.2 Purification of Muscle Nuclei

The first step in NE enrichment is the isolation of nuclei. Although release of nuclei can be achieved in cell suspensions by hypotonic lysis and with soft tissue by Dounce homogenization, the fibrous nature of muscle and associated connective tissue requires that the tissue be broken down by mincing, followed by extensive Douncing using a motorized Potter-Elvehjem homogenizer to release the nuclei. An extra Percoll gradient step is required to remove contaminating muscle fibers from the homogenate. Finally, the nuclei are spun through a three-step sucrose gradient in the ultracentrifuge (in contrast to the two-step sucrose gradients used in most other nuclear purification protocols). This floats microsomal membranes and pellets any dense contaminants, while allowing purified nuclei to collect on a 2.8 *M* sucrose cushion.

1. Drain the PBS from the muscle tissue and weigh the material.
2. Use a meat mincer (e.g., a domestic hand mincer) to finely mince the muscle tissue. Pass the tissue through the mincer at least three times, using 50 mL of ice-cold homogenization buffer to wash all the tissue through. Collect the minced muscle in a tray cooled on ice.

3. Add additional ice-cold homogenization buffer to minced muscle to achieve a final volume of between 2.5 and 5 mL for every gram of muscle (e.g., 100–200 g of muscle should be suspended in 500 mL of homogenization buffer) and mix thoroughly. Pour into a 55-mL Potter-Elvehjem homogenizer and homogenize at 900–1,000 rpm on ice, bringing the pestle to the bottom at least eight times (*see* **Note 11**). If the total volume exceeds 55 mL, homogenize in batches and collect the homogenate on ice. Rinse the homogenizer with buffer when finished and add to the homogenate. This combination of mincing and Douncing releases a significant proportion of the nuclei.
4. In a 4°C room, fold cheesecloth into four layers and place in a funnel. Pour 100–200 mL of crude homogenate through the cheesecloth and collect the filtrate in beaker. As the flow slows, fold the cheesecloth over and roll a sterile pipette (or similar clean cylindrical tool) from top to bottom, to squeeze the remaining fluid out (Fig. 2.1; *see* **Note 12**). Pour 25 mL of ice-cold homogenization buffer through the cheesecloth after the homogenate has drained to wash out any trapped nuclei. A large amount of solid material should remain in the cheesecloth (Fig. 2.1). This is rich with collagen, connective tissue, and large contractile filaments.
5. Transfer the filtrate to centrifuge tubes (e.g., Falcon conical centrifuge tubes, 50-mL capacity) and pellet nuclei at 1,000 × *g* in a swinging bucket rotor (e.g., 2,000 rpm in a Beckman Coulter J6MI floor model centrifuge) for 10 min at 4°C.
6. Remove the supernatant carefully because the pellets are very soft. Keep this supernatant if sarcoplasmic reticulum membranes (*see* **Section 3.4**) are to be prepared at the same time, because they are contained in this fraction (*see* **Note 13**).
7. Resuspend the crude nuclear pellets in ice-cold Percoll gradient buffer. Reduce the volume of the original homogenate fivefold (e.g., from 500 mL of muscle homogenate, resuspend the nuclear pellets in 100 mL of Percoll gradient buffer).
8. Pellet nuclei again at 1,000×*g* in a swinging bucket rotor for 10 min at 4°C. Remove the supernatant carefully, because the pellets are soft. This step concentrates nuclei away from much of the mitochondria and vesiculated cell membranes that pellet at higher speeds, and washes away additional collagen. However, the nuclei are still heavily contaminated with these structures and with myofibrils.
9. Resuspend crude nuclear pellets in 26.7 mL of ice-cold Percoll gradient buffer. Add Percoll to a final concentration of 27% v/v (e.g., add 13.3 mL of 81% Percoll in gradient buffer).
10. Transfer to a clear round-bottomed centrifuge tube with a capacity of greater than 40 mL. Centrifuge at 27,000×*g* for 30 min at 4°C, preferably in a swinging bucket rotor (*see* **Note 2**). The Percoll gradient is self-forming under these conditions.
11. Myofibrils will form a layer at the top of the tube (Fig. 2.2a), which can be aspirated away with a pipette. Nuclei should band near the bottom of

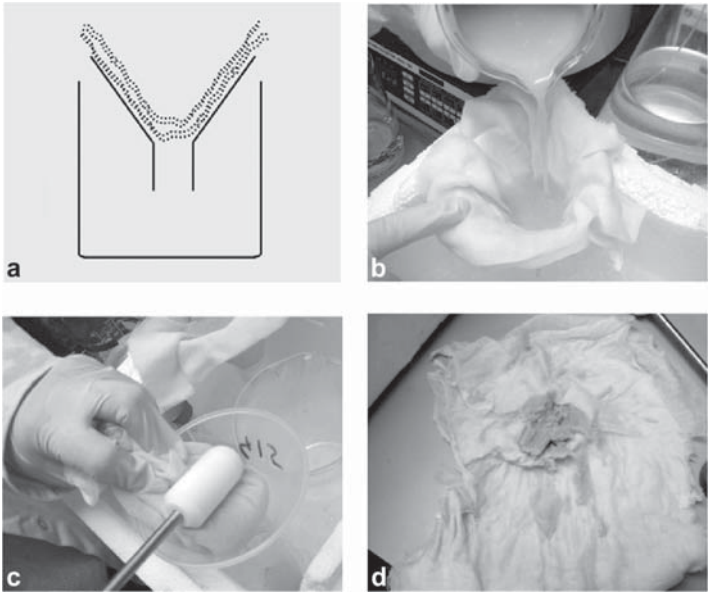

Fig. 2.1 Filtration of muscle homogenate. **a** In a cold room, arrange four layers of cheesecloth in a funnel suspended in a beaker. **b** 100–250 mL of homogenate is poured into the cheesecloth and allowed to drain into a beaker. **c** The cheesecloth is squeezed to recover remaining homogenate, using a pipette or similar tool to roll toward the bottom of the funnel. **d** A large amount of fibrous material should remain in the cheesecloth after all liquid has been recovered

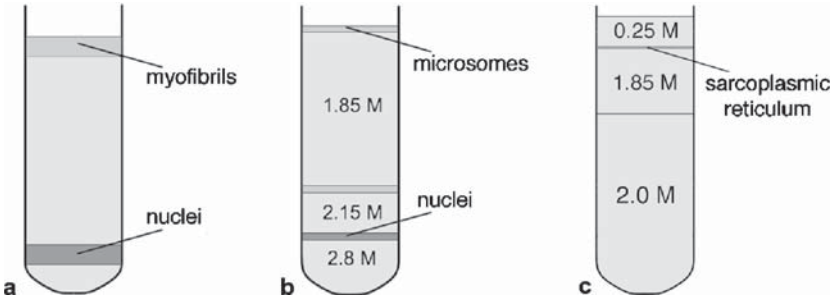

Fig. 2.2 Position of fractions in Percoll and sucrose gradients. **a** After centrifugation at 27,000 × *g*, the Percoll gradient separates nuclei and myofibrils. Nuclei form a layer at or near the bottom of the tube. **b** After centrifugation of the discontinuous sucrose gradient at 82,000×*g*, purified nuclei will form a layer at the interface between 2.8 *M* and 2.15 *M* sucrose. Other cellular components are separated by the gradient; microsomes float on top of the 1.85 *M* sucrose, cytoplasmic contaminants form a layer at the 1.85/2.15 *M* sucrose interface, and any remaining dense myofibrils pellet to the bottom of the 2.8 *M* sucrose. **c** After centrifugation at 57,000 × *g*, microsomal membranes derived from sarcoplasmic reticulum collect at the interface of the 0.25 *M* and 1.85 *M* sucrose layers

the tube and can be collected with a clean pipette. Check under the microscope that the fraction collected is enriched in muscle nuclei, and ensure that any nuclei pelleted at the bottom of the tube are collected. This step is necessary because many of the myofibrils broken off from the muscle tissue during homogenization have a similar mass or size to nuclei, but a different density (19). The isopycnic gradient floats the less dense myofibrillar material.

12. Dilute nuclei tenfold with ice-cold 0.25 M SHKM and centrifuge in 50-mL conical tubes at 4,000 × g for 20 min at 4°C in a swinging bucket rotor. Remove the supernatant with care. The pink-colored pellet contains nuclei, microsomal membranes, and other cytoplasmic contaminants.
13. Resuspend the pelleted nuclei in 11 mL of ice-cold 0.25 M SHKM. Use a Dounce homogenizer with a loose-fitting pestle to break up any aggregated nuclei (*see* **Note 14**). Bring the volume to 50 mL by adding 39 mL of ice-cold 2.3 M SHKM, thus, adjusting the sucrose concentration to 1.85 M.
14. Pipette 25 mL of nuclei in 1.85 M SHKM into each of two SW28 ultracentrifuge tubes on ice. Underlay the nuclear suspension with 5 mL of ice-cold 2.15 M SHKM and then underlay this with 5 mL of ice-cold 2.8 M SHKM, using a Luer-lock syringe with a 14-gauge needle (*see* **Note 15**). Handle the tubes with care to avoid mixing the layers.
15. Balance the tubes and centrifuge in a SW28 swinging bucket ultracentrifuge rotor for 60 min at 82,000×g (25,000 rpm) at 4°C (*see* **Note 16**).
16. The pink layer at the top of the tube (Fig. 2.2b) contains microsomal membranes derived from sarcoplasmic reticulum, and should be aspirated away with a pipette. Muscle nuclei should be visible as a grey band at the interface of the 2.8 M and 2.15 M sucrose layers (Fig. 2.2b). Nuclei can be collected using a Luer-lock syringe with a 14-gauge needle by inserting the needle through the upper sucrose layers and aspirating the nuclei from the 2.15 M/2.8 M interface. It is important to use a microscope to determine the content of different fractions at this stage (*see* **Note 17**).
17. Dilute the nuclei tenfold in ice-cold HKM buffer and centrifuge at 4,000×g for 20 min at 4°C in a swinging bucket rotor.
18. The grey pellet (if visible) contains purified muscle nuclei. Aspirate the supernatant carefully, because the pellet may be soft. Resuspend the purified nuclei in 10 mL of ice-cold 0.25 M SHKM and use a hemocytometer and a phase contrast microscope to estimate the number of nuclei and to check their relative purity. The nuclei should be free of contaminants and should display the characteristic elongated shape of muscle nuclei (Fig. 2.3).
19. If required, purified nuclei can be stored at this stage by freezing in SHKM buffer containing at least 1 M sucrose as a cryoprotectant. Pellet the nuclei at 4,000 × g for 20 min at 4°C in a swinging bucket rotor, and resuspend in 0.5 mL of ice-cold 0.25 M SHKM. Add 0.5 mL of 2.15 M SHKM, mix well and snap-freeze in liquid nitrogen. Store at −80°C.

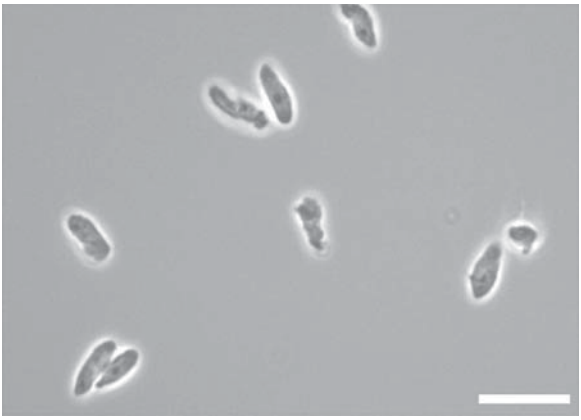

Fig. 2.3 Light micrograph showing purified muscle nuclei viewed with phase contrast at ×400 magnification. Scale bar, 20 μm

3.3 Preparation of Nuclear Envelopes

The critical step in the preparation of NEs is the removal of nucleoplasmic contents from the purified nuclei. This is achieved by enzymatic digestion of DNA and RNA to break chromatin up into pieces small enough to be washed out of nuclei. This is more difficult to achieve for muscle nuclei compared with nuclei from soft tissues, at least in part because muscle nuclei do not swell appreciably in hypotonic buffer. Salt washes are an absolute requirement to wash digested chromatin from muscle nuclei, and care should be taken to ensure efficient chromatin removal using a fluorescent stain such as Hoechst 33342 or DAPI (*see* **Section 3.5.1**). From this point in the procedure, amounts are based on millions of nuclei rather than on grams of tissue.

1. Resuspend purified muscle nuclei in ice-cold 10% SHM (*see* **Note 18**) at a concentration of 1–2 million nuclei/mL. Use a Dounce homogenizer with a loose-fitting pestle to break up any aggregated nuclei.
2. Withdraw a small sample of nuclei that will not be digested, for comparison with the digested material after salt washes.
3. Add DNase I to 10 U/mL and RNase A to 1.4 μg/mL (*see* **Note 19**). Incubate on ice for 20 min to begin chromatin digestion (*see* **Note 20**).
4. Centrifuge at 4,000 × g for 20 min at 4°C in a swinging bucket rotor to pellet the nuclei. Discard the supernatant.
5. Resuspend the nuclei in ice-cold 10% SHM at a concentration of 2–4 million nuclei/mL. Do a second digestion of chromatin, but now with 50 U DNase I/mL and 5 μg RNase A/mL for 20 min on ice (*see* **Note 21**). In contrast to nuclei from other cell types, chromatin removal cannot be monitored by phase contrast microscopy (*see* **Note 22**).
6. Centrifuge at 4,000×g for 20 min at 4°C in a swinging bucket rotor to pellet the nuclei. Discard the supernatant and resuspend nuclei in 10 mL of ice-cold 10% SHM supplemented with 300 m*M* NaCl to wash out digested chromatin (*see* **Note 23**).

7. Transfer NEs in 10% SHM/300 m*M* NaCl to a clear round-bottomed centrifuge tube (e.g., a 15-mL glass Corex tube) and underlay with 0.15 volumes of 30% SHKM using a Luer-lock syringe with a 14-gauge needle. Handle tubes with care to avoid mixing layers. Centrifuge in a swinging bucket rotor (*see* **Note 24**) at 6,000×*g* for 30 min at 4°C (e.g., 6,200 rpm in a Beckman JS 13.1 rotor or 5,000 rpm in a Beckman-Coulter floor model J6MI centrifuge). This step floats digested chromatin away from the NEs, which pellet through the 30% sucrose cushion.
8. The supernatant may be cloudy, because it contains histones and chromatin (*see* **Note 25**). Aspirate the supernatant very carefully (do not decant by pouring) because the NE pellet is very soft.
9. Because, unlike in nuclei from most other tissues, no clear phase-dark to phase-lucent transition occurs in muscle nuclei during chromatin digestion, it is important to set aside a small sample to test for chromatin digestion by staining with a fluorescent chromatin marker such as Hoechst 33342 or DAPI (*see* **Section 3.5.1**). After washing in 300 mM NaCl, chromatin should be almost completely removed leaving only a small amount of staining closely associated with the NE (Fig. 2.4). The fluorescence intensity should also be greatly diminished in the digested sample compared with undigested nuclei. If a large amount of chromatin remains, pellet the nuclei and repeat the digestion (go back to Step 4).
10. Centrifuge at 4,000×g for 20 min at 4°C in a swinging bucket rotor to pellet nuclei. Discard supernatant and resuspend nuclei in 10 mL of ice-cold 10% SHM supplemented with 400 mM KCl. This step washes away any remaining digested chromatin.
11. Centrifuge at 4,000×g for 20 min at 4°C in a swinging bucket rotor to pellet nuclei. Resuspend purified NEs in a small volume of ice-cold 10% SHM and aliquot to tubes suitable for storage (e.g., 1.5-mL Eppendorf tubes). Centrifuge at 6,000×g for 30 min at 4°C.
12. Carefully aspirate the supernatant and freeze the NE pellets immediately in liquid nitrogen. Store at −80°C.

3.4 Preparation of Microsomes Derived from Sarcoplasmic Reticulum Membranes

1. Take the supernatant after pelleting of nuclei from the muscle homogenate (step 6 in **Section 3.2**, Purification of Muscle Nuclei) and add EDTA to a final concentration of 0.5 m*M* to inhibit metalloproteases. Centrifuge at 10,000×*g* at 4°C for 20 min (e.g., 8,000 rpm in a Beckman JA14 centrifuge rotor) to pellet mitochondria.
2. Transfer the post-mitochondrial supernatant to ultracentrifuge tubes and centrifuge at 100,000 × *g* for 45 min at 4°C (e.g., 36,000 rpm in a Beckman Type 45 Ti fixed angle ultracentrifuge rotor, *see* **Note 26**). This step pellets the microsomes derived from sarcoplasmic reticulum membranes, reducing the soluble protein

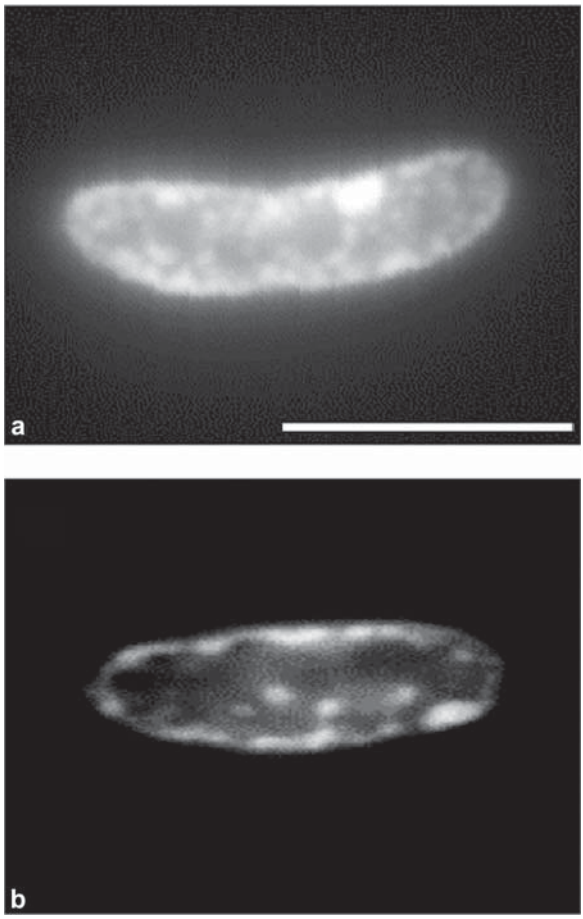

Fig. 2.4 Removal of chromatin from purified muscle nuclei. **a** Nucleus stained with Hoechst 33342 and imaged with an epifluorescence microscope at ×1,000 magnification. Scale bar, 10 µm. **b** Muscle nucleus imaged exactly as in (**a**) but after digestion with DNase I and RNase A and washing in 300 m*M* NaCl. The majority of chromatin has been removed, except that which is tightly associated with the nuclear envelope

content and lowering the volume required for subsequent fractionation in sucrose gradients.

3. Resuspend each crude microsomal pellet in a small volume (e.g., 5 mL) of ice-cold 0.25 *M* SHKM by pipetting. Make the sucrose concentration up to 2 *M* by adding 2.7 volumes of ice-cold 2.8 *M* SHKM (e.g., add 13.5 mL of 2.8 *M* SHKM to 5 mL of resuspended microsomes) and mix thoroughly. Alternatively, freeze the crude microsomal pellet at −80°C at this stage.
4. Aliquot 28 mL of microsomal extract in 2 *M* SHKM to SW28 ultracentrifuge tubes on ice. Overlay each tube with 7 mL of ice-cold 1.85 *M* SHKM and 3 mL of 0.25 *M* SHKM. Centrifuge at 57,000 × *g* for 4 h at 4°C (e.g., 21,000 rpm in a SW28 swinging bucket ultracentrifuge rotor). This step forces the microsomes to float upward into the less dense sucrose, while pelleting other contaminants derived from muscle cell cytoplasm.

5. The microsomes will be found at the interphase between the 1.85 *M* sucrose layer and the uppermost 0.25 *M* sucrose layer (Fig. 2.2c) and have a fluffy yellow-brown appearance, if visible. The microsomal band can be recovered by aspiration with a syringe, either by puncturing the tube with a needle or by inserting the needle through the upper phase.
6. Dilute the purified microsomes with four volumes of 0.25 M SHKM and pellet them at 152,000 × *g* in an ultracentrifuge (e.g., 44,000 rpm in a type 45 Ti, 48,000 rpm in a type 50 Ti, or 60,000 rpm in a TLA100.3 rotor) for 75 min.
7. Discard the supernatant and scrape the microsomal pellet out of the ultracentrifuge tube using a clean spatula. The microsomal pellets should have an orange/brown, toffee-like appearance. Aliquot the microsomal pellets into preweighed tubes suitable for freezing (e.g., 1.5-mL Eppendorf tubes) and calculate the additional mass due to the microsomes by weighing.
8. Freeze the microsomes in liquid nitrogen, and store at −80°C.

3.5 Determining the Purity/Quality of Fractions

3.5.1 Fluorescent Staining of Chromatin

Staining of chromatin with fluorescent dyes allows the efficiency of chromatin removal during NE preparation to be monitored with high sensitivity using an epifluorescence microscope.

1. Take a small sample of nuclei before chromatin digestion (step 2 in **Section 3.3**), and a second sample after chromatin digestion and washing with 300 m*M* NaCl (step 9 in **Section 3.3**). Place the samples in suitable small tubes (e.g., 1.5-mL Eppendorf tubes) and pellet at 5,000 × *g* for 10 min at 4°C in a microcentrifuge.
2. Resuspend the nuclei in a small volume (e.g., 50–100 µL) of 10% SHM containing DAPI or Hoechst 33342 (25 µg/mL). Mix well, pipette 5–10 µL of each sample onto a glass slide, and place a coverslip on top. Seal the edges with nail varnish.
3. View samples on an epifluorescence microscope, using a filter set appropriate for DAPI excitation and emission (this is also suitable for Hoechst 33342). The fluorescence intensity of the sample should be much fainter after chromatin digestion, with only a few areas of chromatin evident around the nuclear rim and little fluorescence remaining in the nucleoplasm (Fig. 2.4).

3.5.2 Western Blot Analysis of Fractions

Western blotting can be used to track the partitioning of known NE or microsomal membrane proteins during fractionation of muscle nuclei and in subsequent extraction of NEs. Nuclear lamins and NE transmembrane proteins should become significantly enriched during the procedure (Fig. 2.5).

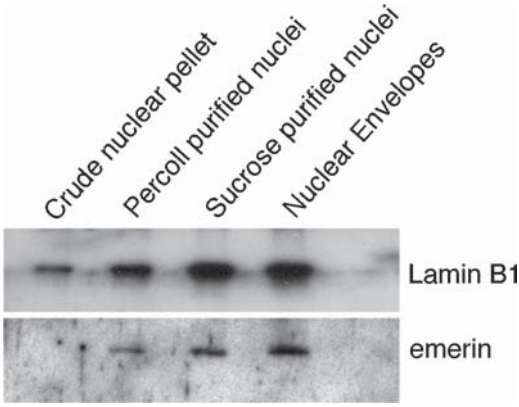

Fig. 2.5 Western blot of purified fractions. An equal amount of protein was loaded in each lane and subjected to SDS-PAGE and Western blot analysis. Lamin B1 (a component of the nuclear lamina) and emerin (an integral inner nuclear membrane protein) are both enriched during the purification of muscle nuclear envelopes. Lanes show from left to right: crude nuclear pellet (1,000×*g* pellet of muscle homogenate); purified nuclei after the Percoll gradient; purified nuclei after the sucrose gradient; and purified nuclear envelopes after chromatin removal

1. Take small samples of material from throughout the purification procedure, for example, of raw homogenate, crude nuclear pellet, nuclei after Percoll gradient, nuclei after sucrose gradient, and purified NEs. Place samples into suitable small tubes (e.g., 1.5-mL Eppendorf tubes).
2. Pellet samples at 6,000 × *g* for 10 min at 4°C in a microcentrifuge. Discard the supernatant containing soluble proteins.
3. Nuclear lamins and transmembrane proteins tend to be insoluble. Resuspend the pellets in a small volume (e.g., 50 µL) of PBS + 0.1% (v/v) Triton X-100 by pipetting. Then add 1.3 volumes of 8 *M* urea, bringing the final urea concentration to 6 *M* (e.g., add 66 µL of 8 *M* urea to 50 µL of sample in PBS + 0.1% Triton X-100). Mix thoroughly by pipetting.
4. Pellet insoluble material by centrifugation at 6,000×*g* for 2 min. Transfer the supernatant to a new tube.
5. Estimate the protein concentration of each sample (e.g., by Bradford assay), and normalize the samples to contain equal amounts of total protein.
6. Resolve proteins by electrophoresis on a 10% SDS-PAGE gel, loading an equal amount of protein in each lane.
7. Carry out a Western blot (24) of the gel with antibodies against nuclear lamins and integral NE proteins. These should show significant enrichment during the purification procedure (Fig. 2.5).

4 Notes

1. As with most protocols, there is an optimal middle ground, with too little or too much starting material resulting in lower yields. In our hands, six rats produce optimal yields without saturating two sucrose gradients in a Beckman-Coulter SW28 rotor.
2. The original protocol for Percoll gradient centrifugation (19) uses a fixed angle rotor (e.g., Beckman JA20). We have found that a swinging bucket rotor (e.g., Beckman JS13.1) gives superior separation of myofibrils and nuclei.
3. Muslin can be used in place of cheesecloth if not chemically treated: make certain to ask the supplier.
4. The $MgCl_2$ concentration in the original NE purification procedure was 5 m*M* throughout (11, 25). However, if NEs are being prepared for viewing by electron microscopy, reducing the concentration through most of the procedure to 0.1 m*M* will yield better structure. During DNase I digestion, it is important to increase the $MgCl_2$ concentration back to 2 m*M*, supplemented with 0.5 m*M* $CaCl_2$ for the enzyme to function efficiently.
5. Protease inhibitors should be tailored to individual tissues according to their most abundant proteases.
6. Phenylmethylsulfonyl fluoride (PMSF) or 4-(2-aminoethyl)benzenesulfonyl fluoride hydrochloride (AEBSF) (both from Sigma-Aldrich), a protease inhibitor with similar activity to PMSF but water soluble and less toxic, may be used to inhibit proteases in the initial homogenization step to reduce costs, because the volume is likely to be high.
7. Do not add spermine or spermidine to the 81% Percoll solution, because this tends to encourage the formation of a precipitate. The spermine and spermidine contained in the homogenization and gradient buffers are sufficient to stabilize the chromatin.
8. EDTA and EGTA in the homogenization buffer and Percoll gradient buffer are essential to remove the endogenous Ca^{2+} released during homogenization of muscle tissue, which can cause the contraction of sarcomeres. Contraction leads to a broader distribution of myofibrils in the Percoll gradient, thus contaminating the band of nuclei (19). During this step, the absence of Mg^{2+} ions is not detrimental because chromatin is stabilized with spermine/spermidine.
9. The 2.3 *M* SHKM can be prepared by adding 230 mL of a 2.5 *M* sucrose stock to 12.5 mL of 1 *M* Hepes, 6.25 mL of 1 *M* KCl, and 1 mL of 1 *M* $MgCl_2$, and freshly added 2 m*M* DTT and protease inhibitors. The 2.3 *M* SHKM can be stored at 4°C. Lesser concentrations of sucrose can be obtained by mixing the 2.3 *M* SHKM with HKM, if required.
10. The 2.8 *M* SHKM can be prepared by dissolving 240 g of sucrose in a total volume of 250 mL of distilled water containing 5 mL of 1 *M* Hepes pH 7.4, 6.25 mL of 1 *M* KCl, and 1.25 mL of 1 *M* $MgCl_2$. Vigorous stirring and heating are required to dissolve the sucrose. This stock solution tends to deteriorate rapidly due to precipitation of sucrose, which can be minimized by storage at room

temperature or even at 37°C. However, it is best not to use the 2.8 *M* SHKM for preparing 2.3 *M* or 2.15 *M* SHKM stocks by dilution with HKM. A working 2.8 *M* SHKM solution can be prepared by mixing DTT and protease inhibitors and chilling on ice immediately before use.

11. This requires a reasonable amount of physical strength and one must take care to keep the homogenizer parallel with the direction of the pestle, or the homogenizer can break. Only start the motor when the pestle is at least partly inserted into the homogenizer tube. Never stop the pestle rotation while it is inserted inside the homogenizer with liquid, or this also can become stuck or break due to the vacuum produced during homogenization.
12. It is important to let most of the liquid drain through the cheesecloth before beginning squeezing, because the homogenate can easily spray out or spill into the filtrate when pressure is applied. Alternatively, if gloves are sterile and powder-free, it is possible to lift the cheesecloth and twist it to produce squeezing.
13. If the intent is to prepare sarcoplasmic reticulum membranes at a later time, the postnuclear supernatant (*see* **Section 3.4.1**) can be frozen at −80°C after a high-speed spin to pellet mitochondria. It is important to remove mitochondria because they might otherwise fragment, contaminating the sarcoplasmic reticulum fraction with mitochondrial membranes.
14. Use of a Dounce homogenizer at this step is important to reduce traces of sarcoplasmic reticulum membrane still adhering to the nuclei.
15. Due to the high viscosity of the 2.8 M sucrose solution, it takes several minutes to underlay each tube if an 18-gauge needle is used. In contrast, with the wide bore size of the 14-gauge needle, this procedure can be performed in 30 sec. It is important to use a Luer-lock syringe because the viscosity of the solution can produce a high pressure on the connection.
16. Nuclei from different tissues have distinct densities; thus the concentration of sucrose in buffers may need to be altered or centrifugation steps lengthened if nuclei are to be isolated from muscles other than leg muscles, or species other than rats.
17. The nuclei collected from the interface of the 2.15 *M*/2.8 *M* sucrose layer should be examined under a microscope to check their purity. Any material that pellets through the 2.8 *M* sucrose cushion should be resuspended in a small volume of 0.25 *M* SHKM and examined under the microscope to ensure that it does not contain significant numbers of nuclei. Similarly, material from the 1.85 *M*/2.15 *M* sucrose interface should be checked for absence of nuclei. Sucrose concentrations may need to be modified to efficiently purify nuclei from different muscle types or from organisms other than rats.
18. The 10% SHM is hypotonic, which helps to wash nucleoplasmic contents out of nuclei. However, muscle nuclei do not appear to swell appreciably in this buffer, in contrast to muscle or blood nuclei for those familiar with these procedures.

19. Micrococcal (S7) nuclease (e.g., Worthington cat. LS004797) can be used in place of DNase I/RNase A for chromatin digestion. Micrococcal nuclease digests both DNA and RNA, and requires a buffer containing Ca^{2+} and slightly higher pH for optimum activity. We found that a buffer containing 0.3 *M* sucrose, 10 m*M* Hepes pH 8.2, 1.5 m*M* $CaCl_2$, 2.5 m*M* $MgCl_2$, 2 m*M* DTT, and protease inhibitors worked well for chromatin removal using two subsequent digestions with micrococcal nuclease at 5 µg/mL and 20 µg/mL, respectively.
20. Chromatin digestion continues during centrifugation steps. Therefore, the centrifugation step should proceed even in the absence of any evident chromatin removal.
21. Two subsequent digestions appear to be necessary to break chromatin into small enough pieces to be readily removed through the still-intact NEs.
22. In contrast to liver or lymphocyte nuclei, the grey appearance of muscle nuclei under phase contrast microscopy does not change, because chromatin appears to remain in myonuclei after nuclease digestion (*see* **Note 23**).
23. The 300 m*M* NaCl wash is essential to wash chromatin out of nuclei. However, do not add stock 5 *M* NaCl directly to nuclei in 10% SHM because the concentrated salt can locally affect the stability of the nuclear lamina, thus damaging NEs. Chromatin removal can be monitored using a fluorescent stain such as Hoechst 33342 or DAPI after the 300 m*M* NaCl wash step (Fig. 2.4).
24. It is important to use a swinging bucket rotor when spinning the NEs through the sucrose cushion at this point to float any chromatin that is released away from the NEs.
25. The supernatant may appear cloudy, but this is mostly chromatin that should give a dark, worm-like appearance under the microscope.
26. The type 45 Ti rotor tubes must be filled near to the top or they can collapse.

Acknowledgments We thank Juliet Ellis for useful discussions, and Nadia Korfali and Poonam Malik for assistance in developing this procedure. This work was supported by a Senior Research Fellowship to Eric Schirmer from the Wellcome Trust.

References

1. Hetzer, M. W., Walther, T. C., and Mattaj, I. W. (2005) Pushing the envelope: structure, function, and dynamics of the nuclear periphery. *Annu. Rev. Cell Dev. Biol*. **21**, 347–380.
2. Mattout, A., Dechat, T., Adam, S. A., Goldman, R. D., and Gruenbaum, Y. (2006) Nuclear lamins, diseases and aging. *Curr. Opin. Cell Biol*. **18**, 335–341.
3. Schirmer, E. C. and Gerace, L. (2005) The nuclear membrane proteome: extending the envelope. *Trends Biochem. Sci*. **30**, 551–558.
4. Roux, K. J. and Burke, B. (2007) Nuclear envelope defects in muscular dystrophy. *Biochim. Biophys. Acta*. **1772**, 118–127.
5. Wilkie, G. S. and Schirmer, E. C. (2006) Guilt by association: the nuclear envelope proteome and disease. *Mol. Cell Proteomics* **5**, 1865–1875.
6. Starr, D. A. and Han, M. (2002) Role of ANC-1 in tethering nuclei to the actin cytoskeleton. *Science* **298**, 406–409.

7. Crisp, M., Liu, Q., Roux, K., Rattner, J. B., Shanahan, C., Burke, B., Stahl, P. D., and Hodzic, D. (2006) Coupling of the nucleus and cytoplasm: role of the LINC complex. *J. Cell Biol*. **172**, 41–53
8. Houben, F., Ramaekers, F. C., Snoeckx, L. H., and Broers, J. L. (2007) Role of nuclear lamina-cytoskeleton interactions in the maintenance of cellular strength. *Biochim. Biophys. Acta* **1773**, 675–686.
9. Mattout-Drubezki, A. and Gruenbaum, Y. (2003) Dynamic interactions of nuclear lamina proteins with chromatin and transcriptional machinery. *Cell Mol. Life Sci*. **60**, 2053–2063.
10. Stuurman, N., Heins, S., and Aebi, U. (1998) Nuclear lamins: their structure, assembly, and interactions. *J. Struct. Biol*. **122**, 42–66.
11. Blobel, G. and Potter, V. R. (1966) Nuclei from rat liver: isolation method that combines purity with high yield. *Science* **154**, 1662–1665.
12. Aaronson, R. P. and Blobel, G. (1975) Isolation of nuclear pore complexes in association with a lamina. *Proc. Natl. Acad. Sci. USA* **72**, 1007–1011.
13. Dwyer, N. and Blobel, G. (1976) A modified procedure for the isolation of a pore complex-lamina fraction from rat liver nuclei. *J. Cell Biol*. **70**, 581–591.
14. Gerace, L., Ottaviano, Y., and Kondor-Koch, C. (1982) Identification of a major polypeptide of the nuclear pore complex. *J. Cell Biol*. **95**, 826–837.
15. Florens, L., Korfali, N., and Schirmer, E. C. (2008) Subcellular fractionation and proteomics of nuclear envelopes, in *Methods in Molecular Biology*. Humana, Totowa, NJ, **432,** 117–137.
16. Korfali, N., Fairley, E. A., Swanson, S. K., Florens, L., and Schirmer, E. C. (2009) Use of sequential chemical extractions to purify nuclear membrane proteins for proteomics identification, in *Methods in Molecular Biology*. Humana, Totowa, NJ, pp (in press).
17. Kuehl, L. (1977) Isolation of skeletal muscle nuclei. *Methods Cell Biol*. **15**, 79–88.
18. Kuehl, L. (1975) Isolation of skeletal muscle nuclei. *Exp. Cell Res*. **91**, 441–448.
19. Hahn, C. G. and Covault, J. (1990) Isolation of transcriptionally active nuclei from striated muscle using Percoll density gradients. *Anal. Biochem*. **190**, 193–197.
20. Liew, C. C., Jackowski, G., Ma, T., and Sole, M. J. (1983) Nonenzymatic separation of myocardial cell nuclei from whole heart tissue. *Am. J. Physiol*. **244**, C3–10.
21. Dreger, M., Bengtsson, L., Schoneberg, T., Otto, H., and Hucho, F. (2001) Nuclear envelope proteomics: novel integral membrane proteins of the inner nuclear membrane. *Proc. Natl. Acad. Sci. USA* **98**, 11943–11948.
22. Cronshaw, J., Krutchinsky, A., Zhang, W., Chait, B., and Matunis, M. (2002) Proteomic analysis of the mammalian nuclear pore complex. *J. Cell Biol*. **158**, 915–927.
23. Schirmer, E. C., Florens, L., Guan, T., Yates, J. R., and Gerace, L. (2003) Nuclear membrane proteins with potential disease links found by subtractive proteomics. *Science* **301**, 1380–1382.
24. Sambrook, J., Fritsch, E. F., and Maniatis, T. (1989) *Molecular cloning: a laboratory manual*. Cold Spring Harbor Laboratory Press, New York.
25. Aaronson, R. P. and Blobel, G. (1974) On the attachment of the nuclear pore complex. *J. Cell Biol*. **62**, 746–754.

Chapter 3
Isolation of Highly Purified Yeast Nuclei for Nuclease Mapping of Chromatin Structure

Joseph C. Reese, Hesheng Zhang, and Zhengjian Zhang

Keywords *Saccharomyces cerevisiae* nuclei; Nucleosome mapping; Yeast chromatin structure; Micrococcal nuclease

Abstract Probing chromatin structure with nucleases is a well-established method for determining the accessibility of DNA to gene regulatory proteins and measuring competency for transcription. A hallmark of many silent genes is the presence of translationally positioned nucleosomes over their promoter regions, which can be inferred by the sensitivity of the underlying DNA to nucleases, particularly micrococcal nuclease. The quality of this data is highly dependent upon the nuclear preparation, especially if the digestion products are analyzed by high-resolution detection methods such as reiterative primer extension. Here we describe a method to isolate highly purified nuclei from the budding yeast *Saccharomyces cerevisiae* and the use of micrococcal nuclease to map the positions of nucleosomes at the *RNR3* gene. Nuclei isolated by this procedure are competent for many of the commonly used chromatin mapping and detection procedures.

1 Introduction

The inevitable consequence of packaging DNA into chromatin is that it restricts the access to essential cellular machineries. Thus, the regulation of chromatin structure plays a pivotal role in transcription regulation and the other DNA related processes ***(1, 2)***. One metric of chromatin structure is nucleosome positioning, the preferred translational positioning of a nucleosome over a certain region of DNA. A variety of methods have been developed to study nucleosome positioning in vivo ***(3–7)***. Chromatin is probed with reagents that preferentially attack nucleosome-free DNA such as DNase I, micrococcal nuclease (MNase), or restriction endonucleases. Most procedures require either the isolation of nuclei or the permeabilization of cells to allow access of enzymes to the chromatin. Each method has its advantages and disadvantages. For example, the procedure for isolating highly purified nuclei is more time consuming than procedures that use detergents

R. Hancock (ed.) *The Nucleus: Volume 1: Nuclei and Subnuclear Components*,

to permeabilize spheroplasts, but the former usually provides higher-quality mapping data. Chromatin prepared from nuclei of lower purity generally contains more nicks in the DNA, which confound the analysis when reiterative primer extension is used to detect the digestion products ***(8)***. After purification of genomic DNA, the digestion products are detected by either indirect end-labeling (Southern blotting) or by a reiterative primer extension method using thermostable DNA polymerases ***(6–8)***. The indirect end-labeling procedure is useful for analyzing chromatin structure over a relatively large area, up to 2 kilobases, but its resolution limit is approximately 20–50 base pairs. On the other hand, primer extension is considered "high resolution" because it can detect changes at the resolution level of a single base pair, but it is more fastidious and is prone to artifacts caused by nicking of DNA during chromatin isolation.

In this chapter, we describe a procedure for isolating nuclei from yeast and probing chromatin structure using micrococcal nuclease and the indirect end-labeling method for detection of the products. Nuclei prepared by this method can be used to probe chromatin structure using DNase I and restriction endonucleases as well, and are of high enough quality to use the reiterative primer extension detection method ***(9)***. The *RNR3* gene is an excellent model for studying chromatin structure because its nucleosomes are well positioned when the gene is repressed and it undergoes dramatic remodeling upon activation ***(10, 11)***.

2 Materials

2.1 Isolation of Nuclei and MNase Digestion

1. Sorbitol buffer (SB): 1.4 ***M*** sorbitol, 40 m*M* HEPES pH 7.5, and 0.5 m*M* $MgCl_2$. Filter sterilize and store at 4°C.
2. Sorbitol wash buffer: sorbitol buffer supplemented immediately before use with phenylmethylsulfonyl fluoride (PMSF) and beta-mercaptoethanol (BME) at 1 m*M* and 10 m*M*, respectively.
3. Sorbitol digestion buffer: sorbitol buffer supplemented immediately before use with PMSF and BME at 1 m*M* and 2 m*M*, respectively.
4. Ficoll buffer (FB): 18% (w/v) Ficoll 400 (GE Biosciences Corporation, Piscataway NJ, USA), 20 m*M* PIPES pH 6.5, and 0.5 m*M* $MgCl_2$. Filter sterilize and store at 4°C.
5. Glycerol–Ficoll buffer: 7% (w/v) Ficoll 400, 20% (v/v) glycerol, 20 m*M* PIPES–Na pH 6.5, and 0.5 m*M* $MgCl_2$. Filter sterilize and store at 4°C.
6. Digestion buffer: 10 m*M* HEPES pH 7.5, 0.5 m*M* $MgCl_2$, and 0.05 m*M* $CaCl_2$. Autoclave and store at 4°C.
7. Beta-mercaptoethanol (BME): 14.25 ***M*** stock solution, store at 4°C.
8. Phenylmethylsulfonyl fluoride (PMSF): 200 m*M* PMSF dissolved in ethanol, store at 4°C.

9. Zymolyase: 10 mg/mL of zymolyase 100T (Associates of Cape Cod, East Falmouth, MA, USA) in sorbitol buffer (SB), stored in small aliquots at −80°C. Avoid freeze–thaw cycles.
10. Micrococcal nuclease: 10 U micrococcal nuclease/μL (Worthington Biochemical Corporation, Lakewood, NJ, USA) in water, stored in small aliquots at −20°C. Do not freeze–thaw.

2.2 Genomic DNA Isolation

1. 0.5 *M* Na–ethylene-diamine tetra-acetic acid (Na-EDTA) pH 8.0: autoclave and store at room temperature.
2. DNase-free RNase A: 5 mg/mL (e.g., Sigma-Aldrich, St. Louis, MO, USA; or prepared as described in ref. (12)), store in aliquots at −20°C.
3. 20% (w/v) Sarkosyl: dissolve *N*-lauryl sarcosine (free acid) in water, adjust to pH 7.5 with NaOH, and sterilize by filtration. Store at room temperature.
4. 5 *M* $NaClO_4$: dissolve in water and store at room temperature.
5. Protease K: 10 mg protease K/mL (e.g., Invitrogen cat. 25530-015; Invitrogen, Carlsbad, CA, USA) in water, stored at −20°C.
6. Phenol–chloroform–isoamyl alcohol: buffer-saturated phenol (e.g., Invitrogen; cat. 15513-047) plus chloroform plus isoamyl alcohol mixed at a ratio of 25:24:1 (v/v) and stored at 4°C.
7. Chloroform–isoamyl alcohol: chloroform plus isoamyl alcohol mixed at a ratio of 24:1 (v/v) and stored at 4°C.
8. 3 *M* sodium acetate: dissolved in water, adjusted to pH 5.2 with glacial acetic acid. Autoclave and store at room temperature.
9. Absolute ethanol: prechilled at −20°C.
10. 0.1× TE: 1 m*M* Tris-HCl pH 8.0, and 0.1 m*M* EDTA, autoclaved.

2.3 Detection of MNase Digestion Products by Indirect End-labeling

1. 5× TBE: (per liter) 54 g Tris-base, 27.5 g boric acid, and 20 mL of 0.5 *M* EDTA pH 8.0. Filter through a 0.45-μm membrane to retard precipitation.
2. 0.2 *M* HCl: dilute 20 mL of concentrated HCl (38%) into 980 mL of water.
3. Denaturing buffer: 1.5 *M* NaCl and 0.5 *M* NaOH.
4. Renaturing buffer: 1.5 *M* NaCl and 1 *M* Tris-HCl pH 7.4
5. 20× SSC: dissolve 175.3 g NaCl and 88.2 g sodium citrate in 800 mL of distilled water, bring the volume to 1 L with water, and adjust the pH to 7.0 with NaOH.
6. Prehybridization buffer: 6× SSC, 5× Denhardt's reagent, 0.5% sodium dodecylsulfate (SDS), 100 μg/mL sheared salmon sperm DNA (from a 10 mg/mL stock solution in water denatured by heating at 95–100°C) added to the prehybridization

solution prewarmed to 60°C. Denhardt's reagent and denatured salmon sperm DNA are available commercially (e.g., Boston BioProducts, Worcester, MA, USA) or may be prepared as described in **ref.** ***(12)***.
7. Blot washing buffer: 1× SSC and 0.1% SDS.

3 Methods

3.1 Yeast Cell Culture and Harvesting

1. Inoculate a 5-mL culture of the appropriate medium at 30°C with one to two colonies and grow overnight on a roller wheel or shaker.
2. The next morning, seed the saturated culture into a 500-mL flask containing 100 mL of fresh medium. Dilute the culture to an appropriate starting density to achieve log phase growth (OD_{600} of ~1.0) by the evening.
3. Reseed a portion of the 100-mL starter culture into two 2-L flasks containing 500 mL of culture medium to achieve a final OD_{600} between 0.8 and 1.2 the next morning. Grow overnight at 30°C with shaking. The inoculation volume needs to be empirically determined and depends on the growth rate of the strain, temperature, and medium (*see* **Note 1**).
4. The cells are collected by centrifugation for 5 min at 4,500×*g* using a Sorvall SLC-6000 rotor (Kendro Laboratory Products, Newtown, CT, USA). Centrifugation can be carried out at 4°C or room temperature. Pour off the culture medium and immediately place the cells on ice.
5. Prepare a sufficient quantity of sorbitol wash buffer for washing all the samples, and prechill the sorbitol wash buffer on ice.
6. Resuspend the cell pellet in 30 mL of freshly prepared sorbitol wash buffer using a pipet and transfer to a round-bottom 50-mL centrifugation tube (Nalgene Nunc International, Rochester, NY). Collect the cells by centrifugation for 5 min at 4,500×*g* in a Sorvall HB-6 rotor at 4°C. Remove as much supernatant as possible by aspiration, and keep on ice.
7. Repeat the wash step once more as described in **step 6.**

3.2 Preparation of Spheroplasts

1. Prepare a fresh aliquot of sorbitol digestion buffer and store on ice.
2. Weigh the cell pellet (it should be ~1 g/L of culture when the OD_{600} is equal to 1) and, with a pipet, resuspend it in 4 mL sorbitol digestion buffer per gram (wet weight) of cells.
3. Gently shake the cell suspension in the centrifuge tube for 10 min in a water bath at 30°C. During this incubation, thaw the zymolyase in your hand.

4. Add 1/5 of a volume of 10 mg zymolyase/mL stock solution per gram of cell pellet (final enzyme concentration is 0.5 mg/mL), and continue the incubation at 30°C with gentle shaking for 20 min.
5. After 20 min, examine the cell suspension to monitor the extent of digestion by placing 1–2 µL on a glass slide, placing a cover slip over the sample, and examining it at ×200 magnification under a phase contrast microscope. Sufficient zymolyase treatment should convert almost all the cells into spheroplasts. Spheroplast formation is confirmed by hypotonic lysis or by squeezing the cover slip against the glass slide (*see* **Note 2**).
6. Cold sorbitol digestion buffer is slowly added to the suspension to bring the total volume of buffer up to 30 mL. For example, if the cell pellet was resuspended in 4 mL in step 2, add 26 mL of sorbitol digestion buffer. Centrifuge at 4,500×*g* for 5 min at 4°C in a Sorvall HB-6 rotor.
7. During the centrifugation step, prepare an aliquot of sorbitol buffer supplemented with 1 m*M* PMSF and place on ice. Completely but gently resuspend the pellet in 30 mL of ice-cold sorbitol buffer with 1 m*M* PMSF (*see* **Note 3**). Centrifuge at 4,500×*g* for 5 min at 4°C in an HB-6 rotor. Remove as much buffer as possible by aspiration, and keep on ice.
8. Wash the pellet once more by repeating **step 7.**

3.3 Purification of Nuclei

1. Gently resuspend the pellet in 20 mL ice-cold Ficoll buffer (FB) and transfer to a prechilled 55 mL glass homogenizer (e.g., Thomas Scientific, Swedesboro, NJ, USA; cat. 3431E25). Homogenize on ice using a Teflon pestle attached to an electric drill revolving at top speed for six to eight even strokes.
2. Gently layer the homogenate onto a 20-mL cushion of ice-cold glycerol–Ficoll buffer supplemented with 1 m*M* PMSF in a round-bottom 50-mL tube. The two phases should be clearly separated.
3. Pellet the nuclei through the glycerol–Ficoll cushion by centrifugation at 21,500×*g* for 30 min at 4°C using an HB-6 rotor or equivalent (a swinging bucket rotor must be used at this step). Aspirate the supernatant completely.
4. Resuspend the pellet in 20 mL Ficoll buffer using a pipet (*see* **Note 4**). Next, cap the tube tightly and vortex at top speed for 2.5 min, chill on ice for 5 min, and vortex for another 2.5 min for a total of 5 min of vortexing.
5. Pellet the debris and intact cells by centrifugation at 3,300×*g* for 15 min at 4°C in a Sorvall HB-6 rotor. Gently remove the tubes from the rotor and carefully transfer the supernatant to a fresh 50-mL round-bottom tube using a 10-mL pipet. Avoid the pellet, which will be loose. It is better to leave a small fraction behind than to risk transferring some of the pelleted material. The nuclei remain in the supernatant.
6. Centrifuge the supernatant from step 5 at 21,500×*g* for 30 min at 4°C in an HB-6 rotor to collect the nuclei. Aspirate the supernatant thoroughly and place the tube on ice.

7. Resuspend the nuclear pellet in 10 mL of digestion buffer by pipetting (*see* **Note 5**).
8. To estimate the amount of nuclei recovered, dilute 100 µL of the suspension (**step 7**) in 900 µL digestion buffer and measure the OD_{600}. This should be ~0.2 for the nuclei from 1 g of wild-type cells (*see* **Note 5**).
9. Recover the nuclei by centrifuging at 21,500×*g* for 15 min at 4°C. Aspirate the supernatant, place the tube on ice.
10. Resuspend the pellet in 2.4 mL of digestion buffer, making minor adjustments based upon the estimated nuclear density measured in step 8 (*see* **Notes 5** and **6**).

3.4 Micrococcal Nuclease (MNase) Digestion

1. Thaw the MNase stock solution (10 U/µL) on ice, and prepare serial dilutions of 0.8, 0.4, 0.2, and 0.1 U/µL in digestion buffer.
2. Divide the nuclear suspension into six 400-µL aliquots in 1.5-mL tubes and prewarm in a water bath at 37°C for 10 min.
3. Add 4 µL of each concentration of MNase to each of the four aliquots of nuclei to achieve final enzyme concentrations of 8, 4, 2, and 1 U/mL, respectively. Mix by gently vortexing and incubate at 37°C for 10 min. One of the remaining aliquots of nuclei will be used as an undigested control, and the other for preparing genomic DNA that will be digested with MNase after purification (naked DNA digestion) (**step 3.5.8**).
4. Stop the digestion by adding 8 µL of 0.5 *M* EDTA (final concentration is 10 m*M*), and mix by vortexing.

3.5 Purification of Genomic DNA

1. Add 8 µL of 5 mg/mL RNase A to each tube, vortex, and incubate at 37°C for 2 h. The final concentration of RNase is 100 µg/mL.
2. Add 66 µL of 20% Sarkosyl (2.5% final), 20 µL of 5 *M* $NaClO_4$ (200 m*M* final), and 2.5 µL of 10 mg/mL protease K (50 µg/mL final). Mix by vortexing, and incubate overnight at 55°C.
3. Add 500 µL of phenol–chloroform–isoamyl alcohol, mix by vortexing for 2 min, and spin at full speed in a microcentrifuge for 10 min.
4. Carefully transfer the supernatant to fresh tubes, add 8 µL of 5 mg/mL RNase A, mix well, and incubate at 37°C for 30 min.
5. Repeat the phenol–chloroform–isoamyl alcohol extraction once more (step 3.5.3), and then extract once with chloroform–isoamyl alcohol.
6. Carefully transfer a fixed amount of the supernatant (300–400 µL) to new tubes, and add 1/10 volume of 3 *M* sodium acetate and two volumes of cold absolute ethanol. Mix and place on dry ice for 30 min. Precipitate the DNA by centrifugation in a microcentrifuge at maximum speed, aspirate the supernatant, wash the pellet with 1 mL of 70% ethanol, and air dry.

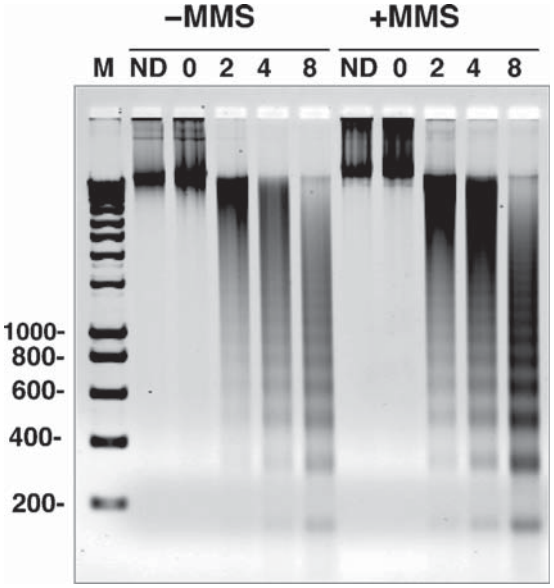

Fig. 3.1 Agarose gel electrophoresis of micrococcal nuclease (MNase) digestion products. Lane 1 (*M*) contains markers with the corresponding length of some bands labeled on the left (in base pairs). Nuclei isolated from wild-type yeast (strain BY4741) were digested with 0, 2, 4, and 8 U/mL MNase respectively (lanes 3–6 and 7–10). Naked DNA (*ND*, lanes 2 and 7) is purified genomic DNA. The DNA was separated on a 1.6% agarose gel and stained with 0.5 μg/mL ethidium bromide. Samples were analyzed from untreated and cells treated with the DNA-damaging agent, methyl methanesulfonate (*MMS*)

7. Dissolve the DNA pellet in 100 μL of 0.1× TE, except for the naked DNA sample (*see* **below**). Expect to recover approximately 50 μg of DNA from each sample.
8. To prepare the sample for digestion of naked DNA, dissolve the DNA pellet in 400 μL of digestion buffer, split into two 200-μL aliquots, and digest with 1 and 2 U/mL MNase for 10 min at 37°C (*see* **Note 7**). Add 3 μL of 0.5 *M* EDTA to stop the reaction, and isolate the DNA as described in steps 3.5.5 and 3.5.6. Dissolve the pellet in 50 μL 0.1× TE.
9. Analyze 2 μL of each DNA sample (both nuclei and naked DNA) by electrophoresis on a 1.6% agarose gel. A successful nuclei preparation and digestion should allow the visualization of >5 nucleosomal repeat lengths (bands). *See* Fig. 3.1 for an example.

3.6 Detection of Digestion Products By Indirect End-labeling

1. Digest 10 μL of each DNA sample (~5 μg of DNA) with the appropriate restriction enzyme overnight at 37°C (*see* **Notes 8** and **9**). We typically perform our restriction endonuclease digestions in a 100 μL volume using 20–25 U of enzyme.

2. Precipitate the DNA by adding 1/10 of a volume of 3 *M* sodium acetate and two volumes of ethanol, incubating on dry ice for 20 min, and centrifuging the samples in a microcentrifuge at high speed. Air dry the sample and dissolve the DNA in 25 µL of 0.1× TE. Add 5 µL of 6× agarose gel loading buffer containing bromophenol blue dye ***(12)***. Load onto a 1.4% agarose gel prepared in 1× TBE. A 27-cm-long gel is recommended for good resolution.

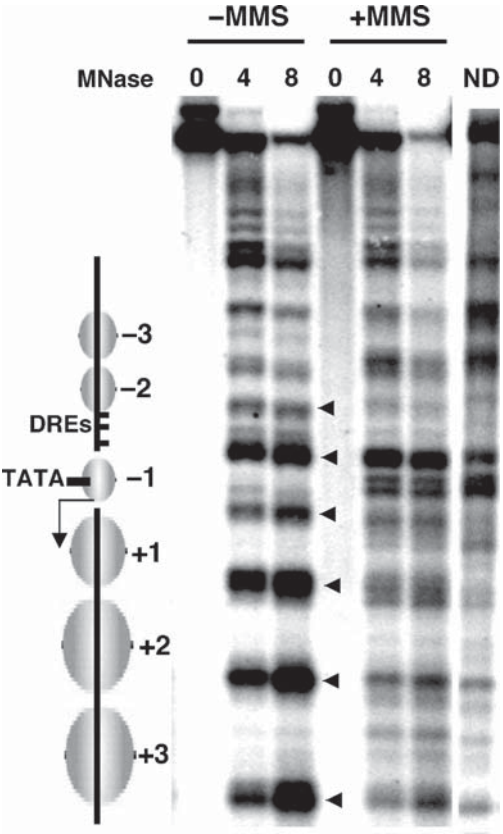

Fig. 3.2 Chromatin mapping of the promoter region of *RNR3* using micrococcal nuclease (MNase). Yeast cells (BY4741) were grown in YPD and treated with (+*MMS*) or without (–*MMS*) 0.03% methyl methanesulfonate for 2 h. MMS is a DNA-damaging agent that strongly induces *RNR3* expression (9). Nuclei were isolated as described in the text, and digested with 0, 4, and 8 U/mL of micrococcal nuclease (MNase) for 10 min at 37°C. Naked DNA (*ND*) was digested with 0.5 U/mL of MNase. The DNA was purified and digested to completion with *Pst*I restriction endonuclease, which cuts at +731 (translation start site as +1) of the *RNR3* gene. The products were separated on a 1.4% agarose gel prepared in 1× TBE buffer, and transferred to a nylon membrane. A radioactively labeled probe corresponding to +486 to +725 of *RNR3* was used. Lanes 1 to 6 are chromatin samples digested with the concentration of MNase indicated above the panel. Lane 7 is digested naked DNA (*ND*). The *filled triangles* represent the internucleosomal hypersensitive sites in wild-type chromatin in the repressed state (–*MMS*). A scheme of the *RNR3* gene and the locations of the DNA damage responsive elements (*DREs*) and the TATA box are also indicated on the left

3. Run the gel in 1× TBE buffer for 4 h at 5.5 V/cm at room temperature.
4. Remove the gel and trim by cutting approximately 2 cm below the bromophenol blue dye and 2 cm below the loading wells.
5. Soak the gel in 0.2 *M* HCl in a glass tray for 10 min at room temperature with gentle shaking to aid the transfer of larger DNA fragments.
6. Rinse the gel twice in high-purity water, place in denaturing buffer (enough to cover the gel and allow it to move freely during shaking), and incubate for 45 min with gentle shaking at room temperature.
7. Rinse the gel twice with high-purity water, transfer to renaturing buffer and incubate for 20 min with gentle shaking. Replace the renaturing buffer and continue shaking for an additional 25 min.
8. Transfer DNA to a charged nylon membrane, with the capillary transfer method in 10× SSC ***(12).***
9. Rinse the gel briefly in 1× SSC and UV cross-link the DNA to the membrane using a Stratalinker (Strategene, La Jolla, CA, USA) or an equivalent apparatus at 1,200 mJ/cm^2. The membrane can be dried and stored, or processed immediately, as described below.
10. Wash the membrane in blot-washing buffer (1× SSC, 0.1% SDS) at 65°C for about 30 min to remove the loading dye(s) and small pieces of agarose from the gel. The membrane is ready for prehybridization.
11. Transfer the membrane from blot washing buffer to prehybridization buffer prewarmed to 60–65°C. Prehybridize for at least 4 h with gentle shaking. Prehybridization and hybridization can be carried out in sealable dishes, bags, or glass hybridization tubes.
12. Add a body-labeled probe prepared by random-primed labeling to a specific radioactivity of at least 100,000 cpm/mL, and continue the incubation at 60–65°C overnight (*see* **Notes 9** and **10**).
13. Remove the membrane from the hybridization solution and wash it in copious amounts of blot washing buffer, 2×15 min at 60–65°C and 2×15 min at room temperature. Mount the membrane on a smooth and clean surface, such as a used X-ray film, cover with plastic wrap, and expose to X-ray film or to a phosphorimager screen (GE Biosciences, Piscataway, NJ, USA or equivalent). An example of an MNase map of the promoter region of *RNR3* is shown in Fig. 3.2.

4 Notes

1. The growth rate of each strain should be calculated ahead of time. For some strains with a severe slow-growth phenotype, it might be necessary to grow the 100-mL starter culture overnight to get enough cells for inoculation of the 500 mL preparative cultures at step 3.1.3. Because certain mutant strains have delayed, and variable, recovery times from stationary phase, we have more consistent results when seeding from a starter culture that is in log phase rather than seeding directly from a saturated culture.

2. The spheroplasts are mostly oval in shape and display different light diffraction properties in phase contrast microscopy compared with intact cells. To verify the extent of spheroplast formation, squeeze the spheroplasts by pushing the cover glass against the slide and move back and forth several times. After squeezing, the oval spheroplasts will become thin rods, but intact cells will retain their shape. Alternatively, add a drop of water to the edge of the cover glass and look for the rupture of the spheroplasts into "ghosts." Too long an incubation with zymolyase at 30°C should be avoided. The time required for digestion will vary between different lots of enzyme and yeast strains.
3. Spheroplasts are fragile and care should be taken during pipetting and resuspending to avoid breakage. We recommend that the pellet be resuspended gently in 5 mL of buffer first. Begin the resuspension process by gently stirring with the pipet tip to break up the larger aggregates, slowly pipetting up and down, then slowly add the remaining 25 mL of buffer. Mix the suspension by inverting the capped centrifuge tube several times gently.
4. It is important to completely resuspend the pellet at this step. We recommend first resuspending the pellet in 5 mL of buffer using a pipet, then adding the remaining 15 mL of buffer. Mix thoroughly by vortexing.
5. It is important that the concentration of nuclei, and hence the amount of DNA, be as similar as possible among all samples. A convenient way to achieve this is to measure the optical density (OD_{600}) of each sample of nuclei at step 7. Using this value, resuspend each of the nuclear pellets in the appropriate volume in step 10 to achieve an equal concentration of nuclei in all samples in the final digestion reaction. Estimating nuclear concentration by this method is effective in most cases. However, for some mutants or growth conditions, additional adjustments in the amount of nuclei or MNase concentrations should be determined empirically based upon previous experience. Nuclear preparations from some mutants or from stressed cells (temperature-sensitive mutants exposed to 37°C or cells treated with DNA-damaging agents) can yield approximately half as much DNA per OD_{600} of cell culture compared with untreated wild-type cells.
6. The digestion buffer described in this protocol works well for DNAse I and MNase mapping. If chromatin structure is being probed by the restriction endonuclease accessibility assay ***(6),*** resuspend the final nuclear pellet (**step 3.3.10**) in 10 m*M* Tris-HCl pH 7.4, 50 m*M* NaCl, 10 m*M* $MgCl_2$, 0.5 m*M* spermidine, 0.15 m*M* spermine, 0.2 m*M* EDTA, 0.2 m*M* EGTA, and 5 m*M* BME.
7. The efficiency of MNase digestion may vary significantly among different naked DNA samples. It is highly recommended to perform test digestions at a range of concentrations to find the proper amount required for each template.
8. The total amount of DNA digested in each sample should be as similar as possible. Adjusting the quantity of DNA can be achieved by using gel scanning software to quantify the amount of DNA in the undigested (no MNase) sample, which appears as a thick band in the gel of **Section 3.5, step 9.**
9. Indirect end-labeling requires that the probe be designed immediately upstream of a restriction endonuclease site. Usually the restriction site should be about

300–2,000 base pairs away from the region of interest. Probes of approximately 200 base pairs in length are prepared by PCR amplification and are purified by agarose gel electrophoresis.

10. Body-labeled probes are prepared using any commercially available random-primed labeling system.

Acknowledgments The assistance of our late colleague Dr. Robert T. Simpson is acknowledged for training us how to map chromatin structure in yeast. Portions of the protocol described above originated from his laboratory. This work was supported by funds provided by the National Institutes of Health (GM58672) and by an Established Investigator Grant from the American Heart Association to J.C.R.

References

1. Kornberg, R. D. and Lorch Y. (1999) Twenty-five years of the nucleosome, fundamental particle of the eukaryote chromosome. *Cell* **98**, 285–294.
2. Wu, J. and Grunstein, M. (2000) 25 years after the nucleosome model: chromatin modifications. *Trends Biochem. Sci*. **25**, 619–623.
3. Hull, M. W., Thomas, G., Huibregtse, J. M., and Engelke, D. R. (1991) Protein–DNA interactions in vivo—examining genes in *Saccharomyces cerevisiae* and *Drosophila melanogaster* by chromatin footprinting. *Methods Cell Biol*. **35**, 383–415.
4. Simpson, R. T. (1998) Chromatin structure and analysis of mechanisms of activators and repressors. *Methods* **15**, 283–294.
5. Simpson, R. T. (1999) In vivo methods to analyze chromatin structure. *Curr. Opin. Genet. Dev*. **9**, 225–229.
6. Gregory, P. and Horz, W. (1999) Mapping chromatin structure in yeast. *Methods Enzymol*. **304**, 365–376.
7. Ryan, M. P., Stafford, G. A., Yu, L., Cummings, K. B., and Morse, R. H. (1999) Assays for nucleosome positioning in yeast. *Methods Enzymol*. **304**, 376–399.
8. Shimizu, M., Roth, S. Y., Szent-Gyorgyi, C., and Simpson, R. T. (1991) Nucleosomes are positioned with base pair precision adjacent to the alpha 2 operator in *Saccharomyces cerevisiae. EMBO J*. **10**, 3033–3341.
9. Li, B. and Reese, J. C. (2001) Ssn6-Tup1 regulates *RNR3* by positioning nucleosomes and affecting the chromatin structure at the upstream repression sequence. *J. Biol. Chem*. **276**, 33788–33797.
10. Sharma, V. M., Li, B., and Reese, J. C. (2003) SWI/SNF-dependent chromatin remodeling of *RNR3* requires TAF(II)s and the general transcription machinery. *Genes Dev*. **17**, 502–515.
11. Zhang, Z. and Reese, J. C. (2004) Ssn6-Tup1 requires ISW2 complex to position nucleosomes in *Saccharomyces cerevisiae. EMBO J*. **23**, 2246–2257.
12. Sambrook, J., Fritsch, E. F., and Maniatis, T. (ed.) (1989) *Molecular cloning, a laboratory manual*. Cold Spring Harbor Laboratory Press, New York, NY.

Chapter 4
Working with Oocyte Nuclei: Cytological Preparations of Active Chromatin and Nuclear Bodies from Amphibian Germinal Vesicles

Garry T. Morgan

Keywords Axolotl; *Xenopus*; Lampbrush chromosome; Cajal body; Nucleolus; Immunofluorescence

Abstract The giant nucleus or germinal vesicle (GV) of amphibian oocytes presents a remarkable opportunity to examine nuclear structures in unprecedented levels of detail. By making use of spread preparations of GVs, it is possible to investigate the structure and function of transcription units in active chromatin and a variety of nuclear bodies, all within the limits of resolution of the light microscope. The basic method for producing GV spreads that is described here is based on simple manual dissection and, therefore, it permits the preparation of nuclear components that have suffered a minimum of experimental manipulation. The particular method described is based on the use of oocytes from a salamander, the axolotl, although the approach is robust and applicable with minor modification to two other model amphibian species, *Xenopus laevis* and *X. tropicalis*. One common approach to investigating the molecular organisation of oocyte nuclear structures by immunofluorescent staining of endogenous or exogenous polypeptides is also described.

1 Introduction

A combination of factors, such as its large size (up to 1 mm diameter), a massive rate of gene activity, and the ease with which its contents can be prepared in a spread-out form has meant that the giant nucleus or germinal vesicle (GV) of the amphibian oocyte can provide exceptionally favourable material for cytological studies of nuclear structure and function, particularly in relation to the control of gene expression. The basic procedure for making spread preparations for light microscopy that is described in this chapter has remained fundamentally the same for many years, and such preparations continue to be the most commonly used approach for studying GV contents. Historically, however, conventional sectioning of oocytes and the preparation of GV contents for electron microscopy in the manner described by Ann Beyer's group (Chapter 4 in Vol. 2) have also contributed important discoveries (reviewed in

R. Hancock (ed.) *The Nucleus: Volume 1: Nuclei and Subnuclear Components*,

ref. ***(1)***), while, in the future, nondisrupted GV whole mounts made in oil will undoubtedly be valuable for live cell approaches ***(2, 3)***.

The key attribute of GV spread preparations is the presence of a range of nuclear structures with extraordinary levels of morphological detail. The best known of these are the giant lampbrush chromosomes (reviewed in **ref.** ***(4)***), which possess extended chromatin loops that are transcribed by RNA polymerase II (pol II) at far greater rates than are most genes in somatic nuclei. Individual transcription units can extend up to several hundred microns in length and their transcriptional polarity can be deduced by phase contrast microscopy simply from the asymmetrical distribution of the large mass of nascent ribonucleoprotein (RNP) associated with the transcribed DNA. This remarkable form of chromatin therefore permits the analysis of transcription sites with a clearly defined structure and provides in situ access to the processes operating during the elongation stage of transcription, all within the limits of spatial resolution of the light microscope. For example, recent studies of lampbrush transcription units have used immunofluorescence microscopy to detect either endogenous or epitope-tagged, exogenous polypeptides in injected oocytes to investigate the composition of nascent RNPs and the disposition of pol II phosphoisomers in highly active chromatin (reviewed in **ref.** ***(4)***). Active chromatin of another type is found in amphibian GVs in the form of numerous extrachromosomal amplified nucleoli, and these structures have long been useful for the study not only of pol I transcription but also of the processing of ribosomal RNAs and other aspects of nucleolar function (see, for example, **refs.** ***(5, 6)***). Other structural components of the amphibian GV have recently been studied in detail by J.G. Gall and collaborators (reviewed in **ref.** ***(7)***). Most notable are B-snurposomes, which are thought to be homologous to splicing speckles/interchromatin granule clusters, and a second type of GV body that is the counterpart of the somatic cell Cajal body (CB). Both of these nuclear bodies are especially amenable to study in GVs because they are larger and more numerous than the somatic equivalents (reviewed in **refs.** ***(8, 9)***).

Preparation of GV spreads comprises just three basic steps: first, a GV is isolated by hand from an oocyte into an isotonic saline. Second, the nuclear envelope is removed, also manually, in a lower ionic strength saline and the gelatinous GV "sap" encouraged to disperse in a small chamber formed on a microscope slide. Finally, the larger macromolecular components of the dispersed GV contents are attached to the slide by centrifugation in preparation for subsequent manipulations such as fixation and immunostaining. Significantly, soluble nucleoplasmic components are rinsed off during the latter manipulations. Detailed and subtle variations on this basic technique have been introduced over the years as oocytes from different amphibian (and nonamphibian, e.g., **ref.** ***(10)***) species have been studied. The physical and chemical principles underlying many of the elements of the basic technique and its variants have been described authoritatively several times ***(1, 11, 12)***) and will not be repeated in detail here. Many of the variations were introduced to allow the dispersal of GV saps that are notably more viscous than others, a property that can be species specific or oocyte stage dependent. Low concentrations of formaldehyde and of calcium in the dispersal media are key ingredients that permit the dispersal of the

more viscous GVs. Recently it has become clear that a major determinant of GV sap viscosity, namely the unusually high concentration of nuclear actin, results from the absence of cognate nuclear export receptors (***(13)***; reviewed in **ref.** ***(14)***).

Although GV spread preparations have been made successfully from many animals, the best material for studies of lampbrush chromosomes is provided by the oocytes of tailed amphibians (urodeles), particularly the newts *Triturus spp*, *Notophthalmus viridescens*, and *Pleurodeles waltl*. These species have dominated research using GV spreads for two main reasons: first, compared with the other main group of amphibians, the frogs and toads (anurans), urodele oocytes possess lampbrush chromosomes in which the transcriptionally active loops are more highly extended. Moreover, unlike anurans and even other urodeles, GVs from those stages of oocyte development in which the chromosomes have well-developed loops are also relatively easy to disperse in newts, contributing to technically superb preparations. However, recently, two problems with the use of newt material have become significant impediments and have lead to the increasing use of other amphibian species. First, newts are increasingly difficult to collect from the wild; indeed, many species are now protected and they are not easily bred in the laboratory. Secondly, related molecular reagents and bioinformatics resources are extremely limited.

Neither of these shortcomings applies to the amphibian model organism that has been studied in countless investigations in molecular, cell and developmental biology, namely, the South African clawed frog, *Xenopus laevis*. Although the more viscous *Xenopus* GV sap has long presented a challenge to the preparation of spreads, recent efforts by J.G. Gall and colleagues have led to the refinement of the spreading procedure to overcome the difficulties in its dispersal ***(15)***. However, it still remains the case that the underdevelopment of the transcriptionally active loops in *Xenopus* lampbrush chromosomes makes them less than ideal for studying active chromatin in situ, although the nuclear bodies of the *Xenopus* GV are currently the best characterised both in spreads and in "live" nuclei (***2, 3***). Fortunately, as described here in detail, the improved approach detailed by Gall ***(15)*** for dispersing the stiff GV sap of *Xenopus* can also be applied essentially unchanged to the preparation of spreads from a species of salamander that has similarly viscous GV sap but that, as a urodele, possesses superbly developed lampbrush chromosomes. Moreover, because of its emergence as the model urodele species for embryological and regeneration studies, this salamander, *Ambystoma mexicanum*—also known as the axolotl —does not exhibit the problems of supply and resources noted above for newts.

Although not often used for studying GVs, *Ambystoma* has made occasional but distinguished appearances in the history of such research; lampbrush chromosomes were first described in sections of *A. mexicanum* oocytes by Flemming in 1882 ***(16)***, and *A. tigrinum* oocytes were among those used by Gall ***(17)*** in his reinvention of lampbrush studies in 1954. Fortunately, axolotl lampbrush chromosomes and nucleoli were also the subject of a later, definitive study by Callan ***(18)***, and the GVs of *A. macrodactylum* have received similar attention from Kezer and colleagues ***(19)***. Hence, there is a small but authoritative body of work on *Ambystoma* GV structures that, particularly with regard to the identification of individual lampbrush chromosomes, is very helpful. The re-introduction of axolotls for preparing

GV spreads is however mainly driven by this species' emergence as a model organism; in effect, it is the urodele equivalent of *Xenopus* with regard to 1) the availability of stocks and ease of establishment of laboratory colonies ***(20)***, and 2) the development of extensive EST sequencing projects and bioinformatics resources (***21, 22***). A final point is that, as noted below, essentially the same approach described here can be applied to prepare active chromatin and nuclear bodies from oocytes of *Xenopus (Silurana) tropicalis*, a species that is becoming of increasing interest because of the potential application of genetic approaches and, uniquely among amphibians, an ongoing genome sequencing project ***(23)***.

2 Materials

2.1 GV Isolation and Dispersal

1. OR2 medium: 82.5 m*M* NaCl, 2.5 m*M* KCl, 1.0 m*M* $CaCl_2$, 1.0 m*M* $MgCl_2$, 1.0 m*M* Na_2HPO_4, and 5.0 m*M* HEPES (from a 0.5 *M* stock, pH 8.3). Final pH 7.4–7.8. Store at 4°C.
2. GV isolation medium: 83 m*M* KCl, 17 m*M* NaCl, 6.5 m*M* Na_2HPO_4, 3.5 m*M* KH_2PO_4, and 1 m*M* $MgCl_2$, stored at 4°C. Just before use, add dithiothreitol (DTT) to 1 m*M* from a 1.0 *M* frozen stock, and filter through a 0.45-µm nitrocellulose filter. Final pH 7.0–7.2.
3. GV dispersal medium: GV isolation medium stock diluted to 25% (final concentrations 20.8 m*M* KCl, 4.3 m*M* NaCl, 1.6 m*M* Na_2HPO_4, and 0.9 m*M* KH_2PO_4) with $MgCl_2$ adjusted to 1.0 m*M*, 0.01 m*M* $CaCl_2$, 0.1% (w/v) paraformaldehyde (from a 20% stock; *see* **Section 2.2.3**; handle in a fume hood). Final pH 7.0–7.2, adjusted with 100 m*M* Na_2HPO_4 if necessary. Stored at 4°C. Just before use add DTT to 1 m*M* from a 1.0 *M* frozen stock, and filter through a 0.45-µm nitrocellulose filter.
4. Dispersal chambers: chambers based on standard microscope slides consist of a gelatin-treated (subbed) slide onto which is fixed a square of Perspex (Plexiglas; 24×24×1.5-mm thick) that has a 6-mm-diameter hole drilled in its centre. The plastic square is stuck temporarily to the centre of the slide using a few drops of a 1:1 mixture of Vaseline (petroleum jelly) and paraffin wax (solidification point 51–53°C). To sub microscope slides, immerse clean, dry slides in a freshly prepared and filtered (#1 paper, Whatman, Maidstone, UK) solution of 0.1% (w/v) gelatin, 0.01% (w/v) $CrK(SO_4)_2$ and drain them before drying overnight at 65°C. If equipment allowing the centrifugation of microscope slides is not available, chambers based on round coverslips can be used (*see* **Note 1**).
5. Instruments for GV manipulation and dissection: three or four pairs of Dumont #5 watchmakers' forceps, preferably not stainless steel, so that their points can be finely sharpened by hand. A sharp tungsten needle mounted in a pencil-sized piece of glass tubing provides a convenient tool for dissecting the GV envelope. Moving the GV between solutions requires Pasteur pipettes (150 mm) that have been stretched in a Bunsen flame from just above the shank, such that the

stretched section can be broken to produce a capillary about 6-cm long with a diameter of about 0.8–0.9 mm at the tip. The broken tip should be polished in a small flame to remove sharp edges that would damage the GV envelope. Use 2-mL rubber teats to aspirate solutions and GVs.
6. Coverslips: 18×18 mm, no. 1½.
7. Petri dishes: 100-mm and 35-mm diameter.

2.2 Attachment and Fixation of GV Contents

1. Carriers for centrifugation of dispersal chambers. These can be either custom-made slide holders as described by Gall et al. ***(12)*** that are designed to fit the swing-out rotor of a high-speed centrifuge (e.g., the HS-4 rotor for a Sorvall RC-5C), or any swing-out centrifuge bucket or plate holder that is large enough to accommodate a microscope slide and is rated for an RCF of 5,000. If either option is unavailable, disc-shaped dispersal chambers can be used that are accommodated by a variety of centrifuge tube and rotor combinations (*see* **Note 1**).
2. Phosphate-buffered saline (PBS): 137 m*M* NaCl, 2.7 m*M* KCl, 4.3 m*M* Na_2HPO_4, and 1.5 m*M* KH_2PO_4; prepared and autoclaved as a 20× stock solution. After dilution, add $MgCl_2$ to 1 m*M*.
3. Paraformaldehyde: 20% (w/v) paraformaldehyde (Sigma-Aldrich, Gillingham, UK) stock solution made up in 4 m*M* Na_2CO_3. In a fume hood, carefully heat on a stirring hot plate to 60°C to dissolve and after cooling filter through Whatman #1 filter paper. Store at 4°C. Prepare fixative by diluting to 2% (v/v) in PBS.

2.3 Immunostaining Fixed GV Spreads

1. Immunoblocking and antibody dilution buffer: 5% (w/v) normal goat serum (NGS) (Jackson Immunoresearch Laboratories, Newmarket, UK) in PBS.
2. DNA stain: 4,6-diamidino-2-phenylindole (DAPI), 1 mg/mL stock stored at 4°C and diluted to 0.5 µg/mL in PBS.
3. Mounting medium: 50% (v/v) glycerol diluted with PBS.

3 Methods

The technique described below is one that I have used successfully to prepare GV spreads from axolotl oocytes. It is directly derived from, and differs in only minor ways from, the latest technique developed by Gall for *Xenopus laevis* oocytes ***(15)***; the variations applicable to the latter are described in the Notes section. Indeed, this robust technique can probably be successfully applied to the preparation of GV spreads from almost any amphibian oocyte, particularly those with a more gelatinous GV sap. For instance, the procedure described is equally applicable to making GV spreads from *Xenopus tropicalis*.

3.1 GV Isolation and Dispersal

1. Ovaries freshly removed from an anaesthetised axolotl are placed in OR2 medium at 18–22°C in a 10-cm diameter Petri dish and, using watchmakers' forceps, are divided into fragments consisting of clumps of 50 to 100 oocytes. Once divided, any damaged oocytes are removed and the ovary fragments transferred to fresh OR2, with only five to six clumps per dish. Oocytes can be used immediately for GV spread preparations, or they can be stored at 18–22°C for several days, provided unhealthy oocytes or their contents are regularly removed from the medium (*see* **Note 2**).
2. Solutions required for GV isolation, washing, and dispersal are allowed to come to room temperature and are made ready on or close to the stage of a dissecting microscope. Isolation and washing are performed in prefilled 35-mm plastic Petri dishes that are clean but have been "seasoned" by multiple uses in this procedure. A dispersal chamber is filled with about 50 µL of medium such that a slight convex meniscus forms. The stretched Pasteur pipettes for handling GVs are charged with isolation or dispersal media that should be completely free of any air bubbles.
3. Transfer to a dish of isolation medium a small clump of oocytes containing some in the optimal size range for lampbrush chromosome preparation (usually 1.3–1.7 mm diameter, i.e., equivalent to stage V ***(24)***; *see* **Note 3**). Using two pairs of sharp watchmakers' forceps, a suitable oocyte is torn apart from the vegetal toward the animal pole. The spherical GV will often be seen as a partial clearing in the continuous film of yolk and should immediately be sucked into a pipette containing isolation medium. The GV should then be transferred swiftly (within 10–20 sec), and with as little yolk as possible in the time frame, into a dish containing the dispersal medium. In all GV transfers, it is crucial to avoid the presence of air bubbles and sharp or broken edges on the pipette, to prevent premature rupture of the GV.
4. Using a second pipette filled this time with dispersal medium, the GV should be transferred in a small volume and with minimal yolk platelets to a prefilled dispersal chamber. In addition to allowing yolk removal, the wash step enables transfer of the GV into the dispersal chamber without an increase in the low salt concentration of the dispersal medium. Again, washing and transfer steps should be completed quickly because this obviates swelling of the GV, which makes subsequent handling difficult. Immediately after transferring the GV to the chamber, pick it up with a pair of watchmakers' forceps to create a firm grip but not puncture the nuclear envelope (lateral illumination from a cold light source and a black background provide the best conditions for observing the GV in the chamber). Holding the GV just above the surface of the chamber, the envelope should be torn open over a third to a half of its circumference using either the finely sharpened point of a tungsten needle or a second pair of forceps. The aim is just to tear the envelope, but not to penetrate beyond the envelope and disrupt the underlying GV contents. The forceps holding the punctured GV should be held perfectly still for as

long as it takes the GV contents to spill out of the envelope; depending on the oocyte, this may take from a few seconds to about a minute. When the last of the GV sap has been released (which may occur quite suddenly as if a physical connection has given way), withdraw the remnants of the envelope, leaving the GV contents as an undisturbed gelatinous mass that will become more liquid and flatter as dispersal continues. As the forceps are taken through the surface of the medium, the remnants of the envelope that they hold will disintegrate (*see* **Note 4**).

5. Place a coverslip over the observation chamber and seal the edges with molten Vaseline (petroleum jelly). Observe the extent of dispersal and flattening of GV contents under an inverted microscope fitted with a low-power phase contrast objective (e.g., ×16). It may take between 20 min and 1 h for the lampbrush chromosomes and GV bodies all to lie in the same plane on the surface of the slide. *See* Fig. 4.1 for the typical appearance of an axolotl lampbrush chromosome at this stage of preparation, i.e., after dispersal but prior to centrifugation and fixation.

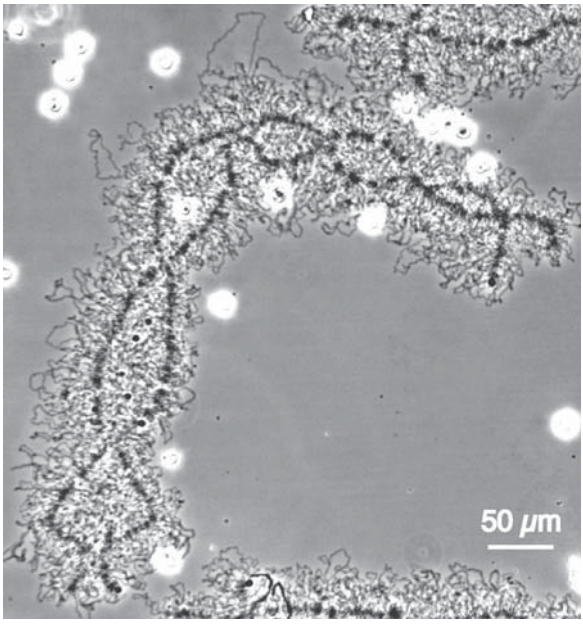

Fig. 4.1 A medium-sized lampbrush chromosome freshly isolated from an axolotl oocyte and observed at low magnification by phase contrast microscopy. The nuclear gel has fully dispersed and the chromosome is lying on the surface of a dispersal chamber awaiting the subsequent centrifugation and fixation steps necessary to permanently attach and preserve the spread chromatin. Prior to their attachment to the chamber surface, the numerous transcriptionally active lateral loops projecting from the axes of this meiotic bivalent are in constant Brownian motion. The rather globular, refractile objects are extrachromosomal, amplified nucleoli

3.2 Attachment and Fixation of GV Contents

1. Once lying flat on the bottom of the slide chamber, the GV structures must be centrifuged to attach them firmly. Transfer the dispersal chambers to an appropriate carrier for centrifugation (*see* **Note 1**) and, using a slow-start setting, centrifuge at 5,000×*g* for 45 min at 4°C. After centrifugation, preparations can be monitored under an inverted microscope prior to fixation.
2. In a fume hood, place the slides vertically into a staining dish containing 2% paraformaldehyde in PBS and, using forceps, gently push to one side the coverslip covering the dispersal chamber (**Note 5**). Leave the preparations to fix for 1–16 h (or less where appropriate for certain antibodies) and then prise off the bored Perspex square from the slide with a razor blade.
3. Remove the slides from the staining dish and rinse in PBS. Preparations can then be immunostained immediately or stored in PBS at 4°C for several weeks for later immunostaining if necessary; alternatively, they could be processed for other purposes such as in situ hybridisation at this stage (**Note 6**).

3.3 Immunostaining Fixed GV Spreads

Because GV spreads comprise simply the chromatin and nuclear bodies from only a single nucleus, the absence of nucleoplasmic and cytoplasmic components contributes to very low background levels even when small volumes of reagents are used for immunostaining. Moreover, the presence of a dam of paraffin wax surrounding each spread also allows for economy of solutions used; it is feasible to use volumes of primary antibody of less than 10 µL. Incubation of slides should then be carried out in a closed chamber moistened with PBS to prevent the preparation drying out.

1. Incubate the preparation in 100 µL of 5% NGS for 15 min and then add primary antibody diluted in the same for 1 h.
2. Wash 3× in 100 µL of 5% NGS and add secondary antibody diluted in PBS for 1 h.
3. Wash 3× in PBS with the penultimate wash containing DAPI at 0.5 µg/mL if desired. The intense DAPI staining of lampbrush chromosome axes makes it simpler to identify and follow individual bivalents than in preparations viewed only by phase contrast or differential interference contrast (DIC) microscopy (Fig. 4.2).
4. Cover the preparation in 20 µL of 50% glycerol/PBS, use a razor blade to scrape away any paraffin wax from around the spread, and mount with an 18-mm square coverslip. An immunostained GV spread from an axolotl oocyte is shown in Fig. 4.3.

Fig. 4.3 (continued) fluorescent images are merged, one comprising the preparation immunostained for RNA polymerase II (pol II *green*), and the other the results of DAPI staining (*blue*) Immunostaining utilised the monoclonal antibody H14, which detects a specific RNA polymerase phosphoisomer; staining is apparent throughout the length of the lateral loops and is particularly intense in Cajal bodies and suspended granules, although in the other nuclear bodies it is undetectable. To view this figure in color, see COLOR PLATE 1

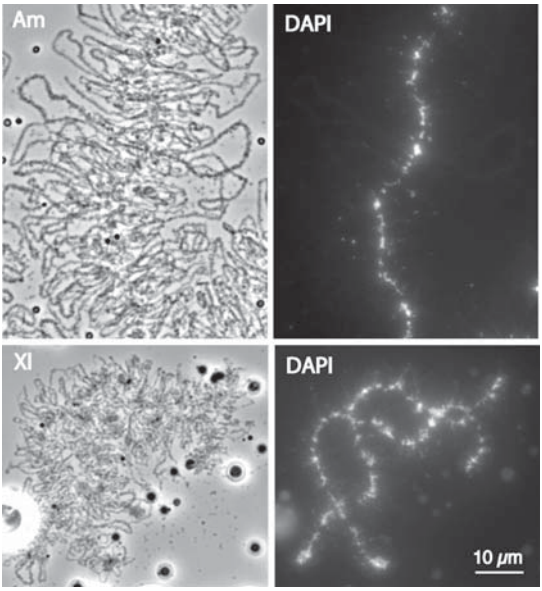

Fig. 4.2 Lampbrush chromosome spread preparations after fixation and DAPI staining viewed at high magnification by phase contrast (*left panels*) and fluorescence (*right panels*) microscopy. In the *top panels*, a small portion of a lampbrush chromosome from an axolotl (*Ambystoma mexicanum* (*Am*)) is shown to the same scale as an entire lampbrush bivalent from a frog (*Xenopus laevis* (*Xl*)) in the bottom panels. As in these examples, when made from oocytes in which the loops are highly extended, the large mass of loop material makes it difficult to discern the chromosome axes without the aid of DAPI staining. As well as the lampbrush chromosomes, GV bodies such as a nucleolus and many B-snurposomes (or interchromatin granule clusters) are visible in the *Xenopus* image

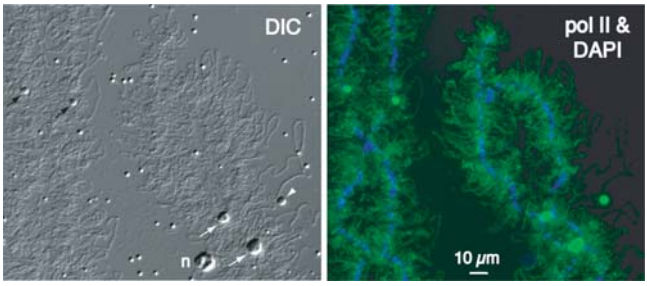

Fig. 4.3 Fixed and immunostained GV spread from an axolotl oocyte. The *left panel* shows portions of two lampbrush bivalents observed by differential interference contrast (DIC) microscopy, which is better suited than phase contrast microscopy for observation of nuclear bodies. As well as the actively transcribed chromosomal loops, two types of body that are regularly attached to axolotl lampbrush chromosomes can also be seen. The *white arrows* indicate Cajal bodies at the two loci on chromosome 13 described by Callan ***(18)***, and the *black arrows* indicate structures that he termed "suspended granules" that are found at homologous positions on many of the chromosomes. Free nuclear bodies are also visible including a Cajal body (*white arrowhead*), a nucleolus (*n*), and many smaller bodies equivalent to the B-snurposomes shown in Fig. 4.2. In the *right panel* two

4 Notes

1. Spread preparations can be made in disc-shaped dispersal chambers that do not require access to the more specialised centrifugation carriers needed for slide-based chambers. Discs 24-mm in diameter are made from 1.5-mm thick Perspex and a 6-mm hole is drilled in the centre. Again use wax to fix a 22-mm diameter, no. 1 1/2 coverslip to the plastic disc and, because the coverslip will form the base of the chamber, prior subbing of its surface (as described above for slides) will enhance the retention of GV material. Once a GV has begun dispersal in the chamber, it is covered with a 19-mm round coverslip for observation and centrifugation. These disc-shaped chambers should be compatible with many standard tube and carrier combinations for swing-out rotors (e.g., 50-mL polycarbonate tubes for the 00480 carriers of the Sorvall HS-4 rotor). Make a flat bed for the disc chamber by putting an appropriately sized rubber stopper into the bottom of the tube or by casting a similarly sized plug of epoxy resin; a hole drilled in the bottom of the tube will allow the insertion of a metal rod in order to lift or lower the stopper or resin plug and thereby facilitate loading and unloading the disc chamber. Although undoubtedly more demanding to handle than slide-based preparations, especially when prising apart the chamber, coverslip-based GV spreads offer the advantage to those experienced in working with cells cultured on coverslips of being amenable to the same containers and techniques for immunostaining, etc.
2. When using *Xenopus* oocytes, allow an overnight period (18–24 h) of recovery after ovary removal before attempting to make GV spreads ***(15)***. This period allows for the maximal extension of lampbrush loops. Incidentally, when preparing defolliculated oocytes for microinjection, it is often useful to incubate them overnight prior to injection in order to identify any oocytes damaged by the defolliculation procedure. Obviously this incubation period, as well as any involved in an injection protocol, will also constitute the recovery period for GV spread preparations that are made from injected oocytes.
3. In particular when studying lampbrush chromosomes, selection of the optimal stage of oocyte development from which to prepare GV spreads is a compromise. On the one hand, the levels of synthetic activity and hence the extent of chromatin decondensation and loop extension are more marked in earlier stages, but on the other, rapid and complete GV dispersal and production of untangled, unbroken chromosomes are difficult in early stages.

   The optimal stage and size of oocyte is also a characteristic of the particular amphibian material to be used. For *Xenopus laevis*, pick oocytes in late stage IV ***(25)*** to early stage V (i.e., ~0.8 to 1.1 mm in diameter), while for the smaller frog *X. tropicalis*, I have found that oocytes of 0.5 to 0.6 mm are optimal for GV spreads.
4. The rapidity of the response of *X. laevis* GVs to gelling in aqueous solutions, coupled with the shorter lampbrush chromosomes, means that a slight modification

of the procedure described above is recommended ***(15)***. The difference is that the GV envelope is removed in the dish of dispersal solution used for washing and *then* the isolated sap is transferred to the dispersal chamber. This aids rapid dissolution of the GV sap and spreading of the nuclear contents. The utmost speed in nuclear isolation, GV envelope removal, and transfer to the dispersal chamber are still of the essence in achieving satisfactory spreading of the GV contents, although the resultant dispersal periods can be much shorter than those for axolotl GVs (just a few minutes). However, in axolotls the characteristics of the GV sap, particularly its initial apparent physical connection to the envelope, and the presence of longer and more delicate chromosomes occupying more of the GV volume, both mean that this adaptation is not helpful for axolotl GV spreads (nor for *X. tropicalis*, in my experience).

5. In some individual axolotls, the GV sap may be less viscous than in others, and the concentration of formaldehyde in the dispersal solutions can be reduced to 0.01%, which may help in ensuring firm attachment of the GV material to the dispersal chamber.
6. Residual paraffin wax will normally mark the position of the well in the observation chamber and surround the attached GV contents. This dam of wax allows the preparation to be temporarily mounted in PBS and the coverslip later removed without damaging the spread. It is useful when initially developing the procedure to check preparations at this stage by phase contrast or DIC microscopy in order to assess the efficacy of spreading, attachment, and preservation prior to immunostaining. The coverslip is then simply floated off in PBS before subjecting the preparation to further processing.

Acknowledgments I am grateful to Joe Gall for numerous helpful tips on making and handling *Xenopus* GV spread preparations and to Andrew Johnson and David Reffin for axolotls.

References

1. Callan, H. G. (1986) *Lampbrush Chromosomes*, Springer-Verlag, Berlin.
2. Handwerger, K. E., Murphy, C., and Gall, J. G. (2003) Steady-state dynamics of Cajal body components in the *Xenopus* germinal vesicle. *J. Cell Biol*. **160,** 495–504.
3. Handwerger, K. E., Cordero, J. A., and Gall, J. G. (2005) Cajal bodies, nucleoli, and speckles in the *Xenopus* oocyte nucleus have a low-density, sponge-like structure. *Mol. Biol. Cell* **16,** 202–211.
4. Morgan, G. T. (2002) Lampbrush chromosomes and associated bodies: new insights into principles of nuclear structure and function. *Chromosome Res*. **10,** 177–200.
5. Mais, C., and Scheer, U. (2001) Molecular architecture of the amplified nucleoli of *Xenopus* oocytes. *J. Cell Sci*. **114,** 709–718.
6. Sommerville, J., Brumwell, C. L., Politz, J. C., and Pederson, T. (2005) Signal recognition particle assembly in relation to the function of amplified nucleoli of *Xenopus* oocytes. *J. Cell Sci*. **118,** 1299–1307.
7. Gall, J. G. (1992) Organelle assembly and function in the amphibian germinal vesicle. *Adv. Devel. Biochem*. **1,** 1–29.
8. Gall, J. G. (2000) Cajal bodies: the first 100 years. *Ann. Rev. Cell Dev. Biol*. **16,** 273–300.

9. Gall, J. G., Wu, Z., Murphy, C., and Gao, H. (2004) Structure in the amphibian germinal vesicle. *Exp. Cell Res*. **296,** 28–34.
10. Solovei, I., Gaginskaya, E., Hutchison, N., and Macgregor, H. (1993) Avian sex chromosomes in the lampbrush form: the ZW lampbrush bivalents from six species of bird. *Chromosome Res*. **1,** 153–166.
11. Macgregor, H. C., and Varley, J. M. (1988) *Working with animal chromosomes. 2nd edn*, John Wiley, Chichester, New York, Brisbane, Toronto, Singapore.
12. Gall, J. G., Murphy, C., Callan, H. G., and Wu, Z. A. (1991) Lampbrush chromosomes. *Methods Cell Biol*. **36,** 149–166.
13. Bohnsack, M. T., Stuven, T., Kuhn, C., Cordes, V. C., and Gorlich, D. (2006) A selective block of nuclear actin export stabilizes the giant nuclei of *Xenopus* oocytes. *Nat. Cell Biol*. **8,** 257–263.
14. Gall, J. G. (2006) Exporting actin. *Nat. Cell Biol*. **8,** 205–207.
15. Gall, J. (1998) Spread preparation of *Xenopus* germinal vesicle contents. In: *Cells. A laboratory manual, Vol. 1* (Spector, D., Goldman, R., and Leinwand, L., eds.), Cold Spring Harbor Laboratory Press, Cold Spring Harbor, pp. 52.51–52.54.
16. Flemming, W. (1882) *Zellsubstanz, Kern und Zelltheilung*, F.C.W. Vogel, Leipzig.
17. Gall, J. G. (1954) Lampbrush chromosomes from oocyte nuclei of the newt. *J. Morphol*. **94,** 283–351.
18. Callan, H. G. (1966) Chromosomes and nucleoli of the axolotl, *Ambystoma mexicanum. J. Cell Sci*. **1,** 85–108.
19. Kezer, J., León, P. E., and Sessions, S. K. (1980) Structural differentiation of the meiotic and mitotic chromosomes of the salamander *Ambystoma macrodactylum. Chromosoma* **81,** 177–197.
20. http://bigapple.uky.edu/~axolotl/.
21. Putta, S., Smith, J. J., Walker, J. A., Rondet, M., Weisrock, D. W., Monaghan, J., Samuels, A. K., Kump, K., King, D. C., Maness, N. J., Habermann, B., Tanaka, E., Bryant, S. V., Gardiner, D. M., Parichy, D. M., and Voss, S. R. (2004) From biomedicine to natural history research: EST resources for ambystomatid salamanders. *BMC Genomics* **5,** 54.
22. Habermann, B., Bebin, A. G., Herklotz, S., Volkmer, M., Eckelt, K., Pehlke, K., Epperlein, H. H., Schackert, H. K., Wiebe, G., and Tanaka, E. M. (2004) An Ambystoma mexicanum EST sequencing project: analysis of 17,352 expressed sequence tags from embryonic and regenerating blastema cDNA libraries. *Genome Biol*. **5,** R67.
23. http://genome.jgi-psf.org/Xentr4/Xentr4.home.html.
24. Beetschen, J.-C., and Gautier, J. (1989) Oogenesis. In: *Developmental biology of the axolotl* (Armstrong, J. B., and Malacinski, G. M., eds.), Oxford University Press, New York, Oxford, pp. 25–35.
25. Dumont, J. N. (1972) Oogenesis in *Xenopus laevis* (Daudin). I. Stages of oocyte development in laboratory maintained animals. *J. Morphol*. **136,** 153–179.

Chapter 5
Preparation of *Arabidopsis* Nuclei and Nucleoli

Peter McKeown, Alison F. Pendle, and Peter J. Shaw

Keywords Arabidopsis thaliana; Plants; Nucleus; Nucleolus; Proteomics; Isolation; Purification

Abstract We describe a method for isolating nuclei from cultured Arabidopsis cells. The same method can be used to further isolate nucleoli. Cell walls are first digested to yield protoplasts, which are purified by flotation on a Percoll gradient. Mechanical homogenisation is used to release nuclei, or with more homogenisation, nucleoli. These fractions are most easily purified by gentle centrifugation. The method has been used for proteomic analysis of nucleoli, as well as for biochemical studies. We also describe a method for immunological labelling of isolated nuclei.

1 Introduction

The nucleus is usually the most easily identifiable membrane-bound organelle in eukaryotic cells. Its composition gives it a substantially higher refractive index than the surrounding cytoplasm, and nuclei are therefore easily visible by phase contrast optical microscopy, which is an essential technique for monitoring their isolation. Nuclei are also easily identified by the use of fluorescent DNA dyes such as DAPI (4′,6-diamidino-2-phenyl-indole) coupled with epifluorescence microscopy. Nuclei contain a number of characteristic internal substructures, of which the most prominent is the nucleolus ***(1, 2)***, but which also include smaller bodies such as Cajal bodies and spliceosomal speckles ***(3)***.

Nuclei from many different species have been purified, both for functional studies in isolation from the rest of the cell contents and for biochemical analysis of their constituent macromolecules. A particularly important current use is for proteomic analysis. Although the protein composition of nuclei is complex, it is not as complex as that of the entire cell, which is still a very difficult target for direct proteomic analysis. The protein composition of sub-nuclear bodies such as nucleoli is of more moderate complexity, and its analysis by current proteomic methods is feasible. Furthermore, the proteomic analysis of such

R. Hancock (ed.) *The Nucleus: Volume 1: Nuclei and Subnuclear Components*,

substructures gives data on cellular localisation. However, it should be remembered that the nucleus is a highly dynamic entity and is integrally linked to the rest of the cell physically by endomembrane and cytoskeleton systems and biochemically by many transport pathways. Thus, isolation of nuclei from the cell is likely to cause many changes, and purified nuclei may differ in many ways from the in vivo organelles. These changes are likely to include loss of mobile proteins and other molecules, changes in membranes and membrane-associated components, cessation of biochemical processes, and changes in chromatin and other components arising from alterations in the ions and other solutes comprising the nuclear microenvironment. On the other hand, the fact remains that nuclei can be purified that retain the characteristic ultrastructure seen in situ and that, in many cases, also retain specific nuclear functions such as gene transcription. The same considerations apply to the isolation of sub-nuclear structures, such as nucleoli. The safest course is to regard any results derived from isolated nuclei and sub-nuclear structures as tentative and suggestive, and to confirm them by whole cell studies.

As with many biochemical studies of plants, the cell wall provides some difficulties; it must either be mechanically broken open or dissolved by cell wall-degrading enzymes before the nuclei can be released. In the protocol we describe here, cultured *Arabidopsis* cells are protoplasted by cell wall-degrading enzymes. Other investigators have used mechanical maceration of frozen plant tissue (*see* Calikowski and Meier ***(4)*** for an excellent review of other methods). The method described here is based on that described by Saxena et al. ***(5)***, and in particular uses low pH buffers, which we have found to be helpful. Many protocols use small concentrations of a non-ionic detergent such as Triton X-100. This helps to separate the nuclei from other cellular contaminants and dissolves chloroplasts and mitochondria. However, it also risks removing nuclear components, particularly the nuclear membrane. For proteomic analyses, we have avoided the inclusion of detergent ***(6)***, although we previously used it in studies of the nuclear matrix ***(7)***. Thiodiglycol (1% v/v) and hexylene glycol (1 *M*) are added to improve the stability of nuclei in some protocols, although not in this one ***(4)***; however they do affect nuclear membrane activity. Thiodiglycol can be difficult to obtain because it is a restricted chemical in some countries. The addition of protease inhibitors is essential if intact protein fractions are required.

Chromatin contains Mg^{2+} bound to the negatively charged phosphates in the DNA. However, this can cause problems in nuclear isolation; some chromatin is inevitably released by nuclear damage during isolation, and this can then be precipitated by interaction with Mg^{2+} to form an unworkable matrix from which intact nuclei cannot be purified. Cook and colleagues recommend encapsulating nuclei in agarose beads, before dissolving the cytoplasm to leave encapsulated nuclei ***(8)*** (*see* **Chap. 9** in **Vol. 2** by D. Jackson). Although this is a very gentle method that is good for retaining nuclear activity, the resulting degree of purification is not as great as more stringent methods. An alternative strategy, adopted in most plant nuclear

isolation protocols, is to remove Mg^{2+} from the isolation buffers, and stabilize the chromatin with the polyamines, spermine and spermidine.

2 Materials

2.1 Plant Growth

1. AT medium: 4.4% (w/v) Murashige and Skoog medium including vitamins (Duchefa Biochemie; available from Melford Laboratories Ltd., Chelsworth, Ipswich, UK) ***(9)***, 3% (w/v) sucrose, 0.05 mg kinetin/L (Sigma-Aldrich, Gillingham, Dorset, UK), and 0.5 mg naphthalene-acetic acid (NAA)/L (Sigma-Aldrich), pH 5.8.
2. ATN medium: 4.4 % (w/v) Murashige and Skoog medium including vitamins (Duchefa Biochemie), Gamborg B5 vitamins and salts (Duchefa Biochemie) ***(10)***, 3% (w/v) sucrose, and 1 µg/mL of 2,4-dichlorophenoxyacetic acid (2,4-D) (Sigma-Aldrich), pH 5.7.

2.2 Nuclear and Nucleolar Isolation

1. Protoplast buffer: 0.5 *M* sorbitol, 10 m*M* 2-*N*-morpholino-ethane-sulphonic acid (MES) adjusted to pH 5.5 with KOH (MES/KOH), and 1 m*M* $CaCl_2$.
2. Flotation buffer: 60% Percoll (v/v), 0.5 *M* sorbitol, 10 m*M* MES/KOH (pH 5.5), 1 m*M* $CaCl_2$.
3. Nuclear isolation buffer: 10 m*M* MES/KOH (pH 5.5), 0.2 *M* sucrose, 2.5 m*M* ethylene-diamine tetra-acetic acid (EDTA), 2.5 m*M* dithiothreitol (DTT), 0.1 m*M* spermine, 0.5 m*M* spermidine, 10 m*M* NaCl, and 10 m*M* KCl. Protease Inhibitor Cocktail Tablets (EDTA-free, containing benzamidine HCl, phenanthroline, aprotinin, leupeptin, pepstatin A, and phenyl methyl sulphonyl fluoride; Roche Diagnostics, Burgess Hill, West Sussex, UK) are added at 1 tablet/50 mL according to the manufacturer's instructions.
4. Nucleolar storage buffer: 0.35 *M* sucrose and 0.5 m*M* $MgCl_2$.
5. Protoplasting enzymes: Cellulase R-10 (Onozuka, Tokyo, Japan); Pectolyase Y-23 (Seishin Corp, Tokyo, Japan).
6. Stainless steel homogeniser: we use a plunger-type homogeniser, with a spherical ball plunger 25 mm in diameter in a cylindrical container. The clearance between the plunger and the container walls is about 25 µm.
7. Phase contrast microscope. This should be convenient, easy to use, and easily accessible, because it is important to monitor the stages by microscopy at frequent intervals. We use a Zeiss Axiovert 25, with non-immersion ×5, ×10, ×20, and ×40 objectives.

8. Haemocytometer (Neubauer, Weber Scientific Instruments, Sussex, UK).
9. Centrifuge: it is important to use a swing-out cooled (bench-top) centrifuge for all stages of this preparation.

2.3 Immunofluorescence Labeling

1. Tris-buffered saline (TBS): 10 m*M* Tris-HCl and 140 m*M* NaCl, pH 7.4.
2. Formaldehyde fixative: make an 8% (w/v) solution by adding 4 g of paraformaldehyde to 50 mL water. Heat with stirring to 60°C in a fume hood, add 1–2 drops of 1 *M* NaOH. The paraformaldehyde should dissolve quickly to give a clear solution. If it does not, or requires more NaOH, a new stock of paraformaldehyde solid should be obtained. Add 50 mL of 2× TBS and leave to cool to room temperature (HCl should never be added to formaldehyde solutions because this can form carcinogenic products; use sulphuric or phosphoric acid, according to the buffer to be used, to acidify solutions containing formaldehyde). *Use all formaldehyde-containing solutions in a fume hood, because formaldehyde is carcinogenic, very toxic, and a skin irritant* (*see* **Note 12**)
3. PAP pen (Electron Microscopy Sciences, Hatfield, PA, USA), used for marking a water-repellant circle on the slide around the specimen. This simplifies incubation and washing during on-slide immunolabelling procedures, preventing the solutions from spreading out on the slide.
4. DAPI: 4′,6-diamidino-2-phenyl-indole (DAPI; Sigma-Aldrich, Gillingham, Dorset, UK) made up as a stock solution in water at 100 µg/mL and diluted to 1 µg/mL prior to use.
5. Vectashield H-1000 anti-fade mounting medium for fluorescence microscopy (Vector Laboratories, Burlingame, CA, USA).
6. Shandon Cytospin cytocentrifuge (Thermo Electron Corporation, www.thermo.com/shandon). This allows small volumes of suspensions to be gently spun down on to glass slides. It works particularly well for crude nuclear preparations.

3 Methods

3.1 Isolation of Nuclei

1. Plant material and growth conditions: *Arabidopsis* Colombia-0 cell culture lines are grown in the dark on an orbital incubator at 150 rpm at 25°C in ATN medium with 50 mL of culture per 250 mL conical flask. Cells are sub-cultured weekly, 15 mL of culture being diluted into 35 mL of fresh ATN medium. *Arabidopsis* Landsberg cell culture lines are grown in full light at 150 rpm and 25°C in AT medium, 100 mL of culture per 250 mL conical flask. Weekly, 6–7 mL are sub-cultured into 100 mL fresh AT medium.

2. Harvest the cells from a 3–4 day old *Arabidopsis* cell culture by centrifuging at 134×*g* for 5 min at room temperature.
3. Gently resuspend the pellet in half the original cell culture volume containing 2% cellulase R-10 and 0.04% pectolyase Y-23 dissolved in protoplast buffer. The cell suspension is gently shaken at 25°C until most cells are judged by optical microscopy to have formed separated, smooth, round protoplasts, typically 1.5 to 2 h. (*see* **Notes 1** and **2**).
4. Harvest the protoplasts by gently centrifuging at 134×*g* for 5 min.
5. Resuspend the protoplasts in flotation buffer using 20 mL per 50 mL of initial cell culture.
6. Overlay the protoplast suspension with a Percoll step gradient. Each 20 mL aliquot of protoplasts in flotation buffer is overlaid with 5 mL of 45%, 5 mL of 35%, and 5 mL of 0% Percoll (Percoll solutions are made by diluting flotation buffer with protoplast buffer to maintain the same osmolarity) (*see* **Note 3**).
7. Centrifuge at 134×*g* for 5 min and the intact protoplasts will float to the 35%/0% Percoll interface.
8. Remove the protoplasts with a Pasteur pipette. This and all subsequent stages and centrifugation steps are carried out on ice or at 4°C.
9. Wash the protoplasts by resuspending in 20 mL of protoplast buffer and centrifuging again.
10. Resuspend the protoplasts in 20 mL of protoplast buffer and count by microscopy using a haemocytometer.
11. Spin down the protoplasts and resuspend in nuclear isolation buffer (NIB) to give no more than 1×10^6 protoplasts/mL of NIB (*see* **Note 4**).
12. Leave for 5–10 min, then homogenise once in a stainless steel homogenizer. Check by microscopy that the majority of protoplasts have been ruptured to release nuclei. If necessary, use more strokes in the homogeniser. Spin nuclei down at 209×*g* for 5 min and resuspend in NIB (*see* **Note 5**).

3.2 Isolation of Nucleoli

1. With still more homogenisation, the nuclei are ruptured to release nucleoli.
2. When most nuclei have been ruptured as judged by phase contrast microscopy, gently spin the nucleoli to a pellet at 209×*g*, resuspend in Nucleolar Storage Buffer, and freeze in aliquots at −80°C. (*see* **Notes 6–10;** Fig. 5.1).

3.3 Immunofluorescence Labeling of Nuclei

1. Centrifuge 50–100 µL of nuclear suspension/slide in a Cytospin at 500 rpm (27×*g*) for 3 min with low acceleration (*see* **Note 11**).

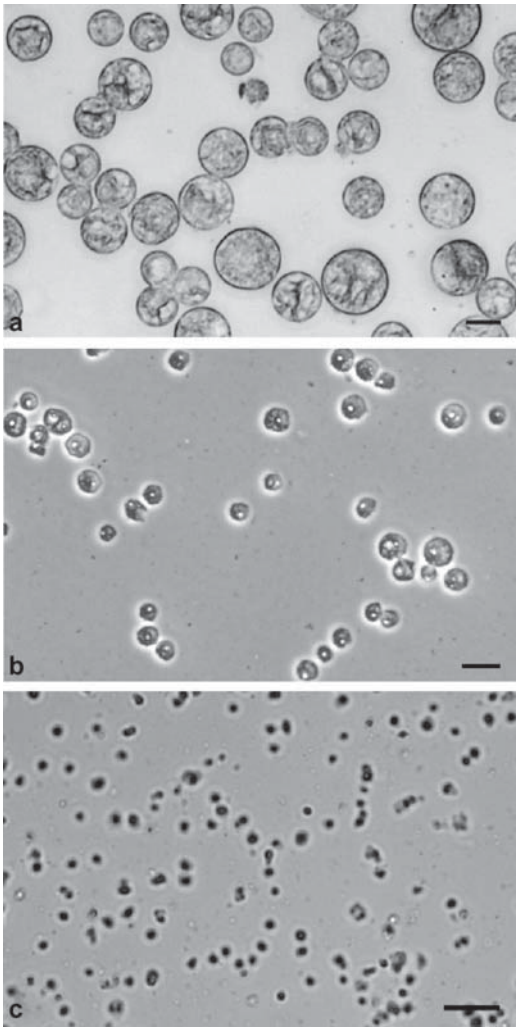

Fig. 5.1 a Purified protoplasts from *Arabidopsis* culture cells. Bright-field micrograph. Bar, 10 µm. **b** Isolated nuclei. Phase contrast micrograph. Bar, 5 µm. **c** Isolated nucleoli. Phase contrast micrograph. Bar, 5 µm

2. Circle the nuclei with a PAP pen and place a few drops of 4% formaldehyde, freshly made from paraformaldehyde (*see* **Note 12**), on the circled area and leave for 30 min.
3. Wash in TBS for 10 min.
4. Wash in H_2O for 10 min.
5. Dehydrate through an ethanol series: 70% (v/v ethanol:water), 90%, and 100% ethanol, 5 min in each.
6. Allow to air dry.
7. Block in 3% w/v bovine serum albumin (BSA) in TBS for 30 min.
8. Incubate in primary antibody diluted in 3% BSA in TBS for a minimum of 90 min.
9. Wash 3× 10 min in TBS.

10. Incubate in secondary antibody diluted in 3% BSA in TBS for a minimum of 90 min.
11. Wash 3× 10 min in TBS.
12. Incubate in DAPI (1 µg/mL in water) for 10 min.
13. Wash 2× 2 min in H_2O.
14. Mount in Vectashield or other anti-fade mountant.

4 Notes

1. Harvested cells are resuspended in solutions of wall-degrading enzymes and gently shaken until most cells are visible as round protoplasts detached from the cells around them. Ensuring good quality protoplasts at this stage is vital for the purification procedure. The protoplasting stage is sensitive to changes in temperature, and excessive enzyme treatment tends to lead to highly unstable protoplasts.
2. *Arabidopsis* culture cells are rather more amenable to protoplasting than some species, but seem to have a strong requirement for pectolyase. Indeed, the concentration and condition of this enzyme appear to be rate-determining, because the use of a different stock from the same supplier produced unstable protoplasts. Pectolyase is responsible for cleaving the pectin oligosaccharides that "cement" the cellulose fibrils into the wall structure, suggesting that digestion of the wall with cellulase alone is not very effective if the pectin matrix is still holding the fragments in place.
3. The cell culture protoplasts are purified on a discontinuous Percoll gradient. This is necessary to remove contamination from protoplasts that have lysed during enzymatic treatment, or the remains of dead cells from the original culture. The use of Percoll gradients can lead to problems, however, because the exact conditions used can prove sensitive. For example, extraction of nucleoli from cells grown and extracted not in the usual AT medium and resuspension buffers, but in a sucrose-free minimal medium, altered the osmolarity of the original protoplast suspension so as to cause the protoplasts to simply pellet, along with other cellular material. Hence, only a partial purification is achieved, and the sample requires additional centrifugal purifications. On the other hand, protoplasts grown in sucrose were observed to migrate on the Percoll gradient much more cleanly, suggesting that a small increase in osmolarity can aid extraction.
4. Once further cleaned by centrifugation, the harvested protoplasts are used for the extraction of nuclei. Our nuclear extraction protocol is based on that of Saxena et al. ***(5)***. These studies used hypertonic disruption of protoplasts in NIB. The various elements of this mixture were empirically determined to improve stability and yield. The polyamines spermine and spermidine and DTT stabilise chromatin; EDTA disrupts chromatin, but inhibits phenol oxidases and DNAses; and polyamines prevent EDTA-mediated chromatin disruption.
5. Protoplasts are disrupted by a stainless steel homogeniser, releasing nuclei. Other protocols subsequently purify these by filtering through layers of

Miracloth and mesh filters, but we do not find this necessary. If required, suitable filters are available from Millipore (Nylon Net Filters with 11 µm, 20 µm, 30 µm, 40 µm, 60 µm, etc. pore size; Millipore, Hatters Lane, Watford, UK). Start with a coarse filter (e.g. 30 µm), finish with an 11-µm filter.

6. Control of the Mg^{2+} concentration is important in isolating nucleoli; if Mg^{2+} is added to the NIB, the nucleoli cannot be separated from the network of nuclear chromatin fibers, whereas without Mg^{2+} in the buffer, the nucleoli begin to show signs of disintegration after 1–2 h. Therefore Mg^{2+} is added to the storage buffer within 30 min of nuclear breakage. The nucleoli isolated by this method are able to incorporate BrUTP, indicating that they retain biological activity (P. McKeown, unpublished data).
7. The numbers of nuclei and nucleoli extracted varies with the age of the cells used. Cultures have been used between 18 h and 10 days after sub-culturing, although most have been 3–4 days old, or 7 days old in the case of SILAC-treated cells (*see* **below**). Typically, 5×10^6–5×10^7 nucleoli are extracted from 100 mL of initial culture. In a published study using this method, 1 L of cell culture generated 4.8×10^8 nuclei and subsequently 3.2×10^8 nucleoli ***(6)***.
8. The protocol has also been used to extract nucleoli from cells starved in a nutrient-free minimal medium, or in the presence of 0.5 *M* sucrose or 75 m*M* LiCl/200 m*M* NaCl. As noted above, different osmolarities caused some differences during extraction on the Percoll gradient, but otherwise followed the same protocol. Salt-treated nuclei were more stable than normal, and needed vigorous additional homogenization to disrupt them.
9. The cell cultures used have mostly been derived from the Landsberg ecotype, but nucleoli have also been extracted from culture cells derived from a Columbia 0 (Col-0) line without modification. The protocol has also been used to extract nuclei and nucleoli from Col-0 cells transformed with agrobacteria. The agrobacteria were separated from the cells by an initial wash and additional centrifugation in ATN, and at the Percoll gradient stage, although some bacterial contamination remained.
10. Stable isotope labeling with amino acids in cell culture (SILAC) experiments: Landsberg culture cells were labelled for MS detection by incorporation of amino acids containing stable isotopes (SILAC) according to the protocols used by Anderson et al. ***(11)*** for human nucleoli and similar to those used by Gruhler et al. ***(12)*** to label *Arabidopsis* culture cells. Landsberg cells were grown as described, but in AT media augmented with either normal lysine and arginine (K0R0); (4,4,5,5-D_4)-lysine and ($^{13}C_6$)-arginine (K4R6); or ($^{13}C_6$)-($^{15}N_2$)-lysine and ($^{13}C_6$)-($^{15}N_4$)-arginine (K8R10). In each case, lysine was supplied at 80 µg/mL and arginine at 150 µg/mL. Combinations were suggested by courtesy of the Lamond Lab, University of Dundee ***(11)***. All amino acids were supplied by Cambridge Isotope Laboratories, Andover, MA, USA. Cells were grown in small volumes of unlabelled or labelled amino acid-supplemented AT medium (typically 25 mL) for 1 week, then sub-cultured into 100 mL of the same medium and grown for a further week. All media were filter-sterilised and autoclaved prior to addition of filter-sterilized isotope-labelled amino acid.

11. The most effective method for producing small quantities of nuclei for microscopy from plant tissue is simply to chop up the tissue in nuclear isolation buffer with a sharp razor blade. The nuclei are filtered in a Pasteur pipette through nylon membranes (Millipore Nylon Net Filters; 30 µm then 11 µm). The nuclei are either left to settle onto slides, or may be spun down onto the slides with a Cytospin. This has the advantage of greatly increasing the number of nuclei adhering to the slide but causes flattening of the nuclei, which is a disadvantage for some studies and an advantage for others.
12. Formaldehyde fixative is best made freshly in small quantities (~100 mL) from paraformaldehyde, because formaldehyde solutions undergo chemical changes on storage. Paraformaldehyde is a relatively stable, solid polymer of formaldehyde. Care should be taken to keep stocks of paraformaldehyde dry, and they should not be stored for more than a year or two. *Always use all formaldehyde-containing solutions in a fume hood because formaldehyde is carcinogenic, very toxic, and a skin irritant*.

References

1. Raska, I., Shaw, P. J., and Cmarko, D. (2006) Structure and function of the nucleolus in the spotlight. *Curr. Opin. Cell Biol*. **18**, 325–334.
2. Raska, I., Shaw, P. J., and Cmarko, D. (2006) New insights into nucleolar architecture and activity. *Int. Rev. Cytol*. **255**, 177–235.
3. Shaw, P. J., and Brown, J. W. (2004) Plant nuclear bodies. *Curr. Opin. Plant Biol*. **7**, 614–620.
4. Calikowski, T. T., and Meier, I. (2006) Isolation of nuclear proteins. *Methods Mol. Biol*. **323**, 393–402.
5. Saxena, P. K., Fowke, L. C., and King, J. (1985) An efficient procedure for isolation of nuclei from plant protoplasts. *Protoplasma* **128**, 184–189.
6. Pendle, A. F., Clark, G. P., Boon, R., Lewandowska, D., Lam, Y. W., Andersen, J., Mann, M., Lamond, A. I., Brown, J. W., and Shaw, P. J. (2005) Proteomic analysis of the *Arabidopsis* nucleolus suggests novel nucleolar functions. *Mol. Biol. Cell* **16**, 260–269.
7. Beven, A., Guan, Y. H., Peart, J., Cooper, C., and Shaw, P. (1991) Monoclonal antibodies to plant nuclear matrix reveal intermediate filament-related components within the nucleus. *J. Cell Sci*. **98**, 293–302.
8. Jackson, D. A., and Cook, P. R. (1985) A general method for preparing chromatin containing intact DNA. *EMBO J*. **4**, 913–918.
9. Murashige, T., and Skong, F. (1962) A revised medium for rapid growth and bioassays with tobacco tissue cultures. *Physiol. Plant* **15**, 473–597.
10. Gamborg, O. L., Miller, R. A., and Ojima, K. (1968) Nutrient requirements of suspension cultures of soybean root cells. *Exp. Cell Res*. **50**, 151–158.
11. Andersen, J. S., Lam, Y. W., Leung, A. K., Ong, S. E., Lyon, C. E., Lamond, A. I., and Mann, M. (2005) Nucleolar proteome dynamics. *Nature* **433**, 77–83.
12. Gruhler, A., Schulze, W. X., Matthiesen, R., Mann, M., and Jensen, O. N. (2005) Stable isotope labeling of *Arabidopsis* thaliana cells and quantitative proteomics by mass spectrometry. *Mol. Cell. Proteomics* **4**, 1697–1709.

Chapter 6
High-Yield Isolation and Subcellular Proteomic Characterization of Nuclear and Subnuclear Structures from Trypanosomes

Jeffrey A. DeGrasse, Brian T. Chait, Mark C. Field, and Michael P. Rout

Keywords Nuclear isolation; *Trypanosoma brucei*; Subcellular fractionation; Proteomics; Sucrose density gradient centrifugation; Nuclear envelope; Nucleolus; Nuclear pore complex

Abstract The vast evolutionary distance between the Opisthokonta (animals and yeast) and the excavata (a major group of protists, including *Giardia* and *Trypanosoma*) presents a significant challenge to in silico functional genomics and ortholog identification. Subcellular proteomic identification of the constituents of highly enriched organelles can alleviate this problem by both providing localization evidence and yielding a manageably sized proteome for detailed in silico functional assignment. We describe a method for the high-yield isolation of nuclei from the kinetoplastid *Trypanosoma brucei*. We also describe the subsequent purification of subnuclear compartments, including the nuclear envelope and nucleolus. Finally, using several proteomic strategies, we survey the proteome of a subcellular structure or organelle, using the nuclear pore complex as an example.

1 Introduction

The excavate euglenozoid *Trypanosoma brucei*, a member of the class Kinetoplastida, is the etiologic agent of the African sleeping sickness (trypanosomiasis), a disease that is invariably fatal if untreated ***(1)***. African trypanosomiasis is endemic to the most rural and undeveloped regions within 36 sub-Saharan African countries, and the emergence of drug resistant strains represents a considerable public health and economic problem ***(2)***. Beyond world health concerns, the evolutionary distance of the trypanosomes from the major model systems amongst the higher eukaryotes is of great interest to comparative and evolutionary biology ***(3)***. Unfortunately, vast evolutionary distance impedes in silico functional assignment and, thus, only partial gene annotation can be achieved ***(4, 5)***. For example, approximately 40% of the open reading frames (ORFs) in the trypanosome genome are considered to be

R. Hancock (ed.) *The Nucleus: Volume 1: Nuclei and Subnuclear Components*,

unique to the kinetoplastida, but there are indications that this number is a considerable overestimate due to limitations of BLAST algorithms ***(6)***.

T. brucei, in particular, has proven to be an excellent distal model system for evolutionary biology ***(7)***. First, trypanosomes are highly divergent from the Opisthokonts ***(8)***. Second, *T. brucei* is amenable to laboratory investigation, with major life stages available to in vitro culture, multiple expression systems available for genetic manipulation, and, significantly, a robust RNA interference (RNAi) system ***(9, 10)***. Third, the genome of *T. brucei* has been sequenced, and comparative data indicate a very high degree of similarity to the related parasites *Leishmania major* and the American trypanosome *T. cruzi*: hence, work in *T. brucei* is directly applicable to these additional pathogens ***(11)***. Here, several of these advantages are exploited in order to produce, in high yield, purified nuclei and then to survey the subnuclear structures to identify novel components ***(12)***.

The first step to producing subnuclear fractions is the isolation of nuclei away from the remainder of the cellular compartments. Once accomplished, these enriched nuclei may be further subfractionated to yield nucleoli, nuclear envelopes, or lipid-stripped nuclear envelopes (termed pore complex–lamina fraction (PCLF)). The subnuclear components are of high quality and suitable for further biochemistry and mass spectrometry. Nuclei from either the vector (procyclic) or the host (blood stream form) life stage may be isolated, providing access to life stage-dependent aspects. However, the procyclic stage is somewhat more convenient because these cells can be grown to higher density in in vitro culture.

2 Materials

2.1 The Isolation of Trypanosoma brucei Nuclei

1. PVP solution: 8% polyvinylpyrrolidone (PVP-40, Sigma-Aldrich, St. Louis, MO, USA), 11.5 m*M* KH_2PO_4, 8.5 m*M* K_2HPO_4, and 750 μ*M* $MgCl_2$. Adjust to pH 6.53 with concentrated H_3PO_4 (~15 μL for 1 L solution). Store at 4°C. (*See* **Note 1**).
2. Sucrose solutions (sucrose/PVP): store in sterile tubes at −20°C. (*See* **Note 2**).
   (a) 2.01 *M*: to 183.3 g sucrose, add PVP solution to a final weight of 338 g. Refractive Index (RI) = 1.4370.
   (b) 2.10 *M*: to 193 g sucrose, add PVP solution to a final weight of 340 g. RI = 1.4420.
   (c) 2.30 *M*: to 216 g sucrose, add PVP solution to a final weight of 340 g. RI = 1.4540.
3. Phosphate-buffered saline (PBS; PBS Tablets, Sigma-Aldrich). Chilled to 4°C.

4. 1 *M* dithiothreitol (DTT). Store at −20°C in 200 µL aliquots.
5. 10% Triton X-100 (Sigma-Aldrich).
6. Protease inhibitor cocktail (PIC) (P8340, Sigma-Aldrich). Store at −20°C.
7. Solution P: 0.04% (w/v) pepstatin A and 1.8% phenylmethanesulfonyl fluoride (PMSF) (both from Sigma-Aldrich) in absolute (anhydrous) ethanol. Store at −20°C (*See* **Note 3**).
8. 0.3 *M* sucrose/PVP: dilute stock sucrose/PVP with PVP solution.
9. Lysis buffer (prepare fresh): 0.05% Triton X-100, 5 m*M* DTT, 1:100 solution P and 1:200 PIC in PVP solution. Twenty milliliters of lysis buffer is equivalent to 1 volume (*See* **Note 4**).
10. Underlay buffer (prepare fresh): 5 m*M* DTT, 1:100 solution P and 1:200 PIC in 0.3 *M* sucrose/PVP. Ten milliliters of underlay buffer is equivalent to 1 volume.
11. Resuspension buffer (prepare fresh): 5 m*M* DTT, 1:100 solution P and 1:200 PIC in 2.1 *M* sucrose/PVP. Eight milliliters of resuspension buffer is equivalent to 1 volume.

2.2 Subnuclear Fractionation

2.2.1 The Nuclear Envelope

1. 0.1 *M* bis-Tris-Cl, pH 6.50.
2. BT/Mg buffer: 0.01 *M* bis-Tris-Cl pH 6.50, 0.1 m*M* $MgCl_2$.
3. Shearing buffer (prepare fresh): 1 m*M* DTT, 1.0 mg/mL heparin, 20 µg/mL DNase I (Sigma-Aldrich, store stock at −20°C), 2 µg/mL RNase A (Sigma-Aldrich, store stock at −20°C), 1:100 solution P, and 1:200 PIC in BT/Mg buffer.
4. 2.10 *M* sucrose in 20% Accudenz (Accurate Chemical & Scientific Corporation, Westbury, NY, USA) in BT/Mg buffer. Store at −20°C.
5. 2.50 *M* sucrose in BT/Mg buffer. The final refractive index should be 1.4533. All sucrose BT/Mg solutions should be stored at −20°C.
6. 2.25 *M* sucrose BT/Mg, by stock dilution.
7. 1.50 *M* sucrose BT/Mg, by stock dilution.

2.2.2 The Pore Complex–Lamina

1. Extraction buffer (prepare fresh): 1.5% Triton X-100, 1.5% sodium taurodeoxycholate, 1:100 solution P, and 1:200 PIC in BT/Mg buffer.
2. 2.50 *M* sucrose BT/Mg.
3. 1.75 *M* sucrose BT/Mg, by stock dilution.

2.2.3 The Nucleolus

1. Disruption buffer (prepare fresh): 10 m*M* bis-Tris-Cl pH 6.50, 0.6 m*M* $MgCl_2$, 0.5 m*M* DTT, 0.34 *M* sucrose/BT, 0.05% Tween 20 (Pierce, Rockford, IL, USA), 1:100 solution P, and 1:200 PIC.
2. 2.50 *M* sucrose BT/Mg.
3. 2.25 *M* sucrose BT/Mg.
4. 1.75 *M* sucrose BT/Mg.

2.3 Biochemistry and Mass Spectrometry

2.3.1 Protein Precipitation

1. HPLC-grade methanol.

2.3.2 Sodium Dodecyl Sulfate (SDS)–Polyacrylamide Gel Electrophoresis (PAGE)–Mass Spectrometry (MS)

1. 1 *M* iodoacetamide. Store at −20°C in 100 μL aliquots.
2. NuPAGE Sample Reducing Agent (Invitrogen, Carlsbad, CA, USA).
3. NuPAGE lithium dodecyl sulfate (LDS) Sample Buffer (Invitrogen).
4. NuPAGE 3-(N-morpholino)propanesulfonic acid (MOPS) SDS Running Buffer (Invitrogen).
5. NuPAGE 10% and 4–12% bis-Tris gels (Invitrogen).
6. Novex 8% Tris-glycine gels (Invitrogen).
7. GelCode Blue Stain Reagent (Pierce, Rockford, IL, USA).
8. 15- or 30-degree Feather MicroScalpel (Electron Microscopy Sciences, Hatfield, PA, USA).
9. Fine Point Diamond Tweezers (Electron Microscopy Sciences).
10. Destain solution: 25 mM ammonium bicarbonate in 50% acetonitrile.
11. Trypsin (bovine, modified, sequencing grade; Roche Applied Science, Indianapolis, IN, USA). Resuspend lyophilized trypsin to 1 μg/μL in 1 mM HCl. Store 1μg aliquots at −20°C.
12. Digestion buffer: 50 mM ammonium bicarbonate.
13. Poros R2 beads (Applied Biosystems, Foster City, CA, USA) (*See* **Note 5**).
14. Poros dilution buffer: 2% (v/v) trifluoroacetic acid, 5% (v/v) formic acid in water.
15. 0.1% trifluoroacetic acid.
16. Elution solution: 20% acetonitrile, 50% methanol, and 0.1% trifluoroacetic acid (aq).
17. ZipTips C18, size P10 (Millipore, Billerica, MA, USA). Prior to use, the ZipTips are washed and conditioned as follows:

(a) Wash twice with 10 µL 0.1% trifluoroacetic acid.
(b) Wash four times with 10 µL elution solution.
(c) Wash four times with 10 µL 0.1% trifluoroacetic acid.
(d) Retain 10 µL of 0.1% trifluoroacetic acid to wet the resin.

18. 2,5-dihydroxybenzoic acid (DHB; Lancaster, Pelham, NH, USA). Prepare a saturated solution in elution solution at room temperature. The saturated solution is diluted to 40% (v/v) saturated DHB just prior to use. Saturated DHB may be stored at 4°C. However, DHB may partially precipitate in storage to form an insoluble pellet. Prior to use, allow the solution to warm to room temperature and add more solid DHB to saturation before diluting.

2.3.3 High-Performance Liquid Chromatography (HPLC)–Mass Spectrometry

1. Digestion buffer: 50 m*M* ammonium bicarbonate.
2. Trypsin: *see* **Section 2.3.2**.
3. Quench solution: 10% trifluoroacetic acid.
4. Mobile phase A: 5% acetonitrile, 0.1% trifluoroacetic acid.
5. Mobile phase B: 95% acetonitrile, 0.1% trifluoroacetic acid.

2.3.4 Hydroxyapatite Chromatography

1. Macro-Prep ceramic hydroxyapatite (HA) type I, 40 µm (Bio-Rad Laboratories, Hercules, CA, USA).
2. 10% SDS.
3. Wash buffer: 200 m*M* Na_2HPO_4. Do not adjust pH.
4. HA sample buffer: 10 m*M* Tris, 10 m*M* DTT, and 2% SDS. Store at 4°C.
5. HA loading buffer: 10 m*M* NaH_2PO_4 pH 6.8, and 0.1 m*M* $CaCl_2$.
6. Mobile phase A: 1 m*M* DTT, and 0.1 m*M* $CaCl_2$. Store at 4°C.
7. Mobile phase B: 1 *M* NaH_2PO_4 pH 6.8, and 1 m*M* DTT. Store at 4°C.
8. Poly-Prep chromatography columns (Bio-Rad).

2.3.5 Chemical Extraction

1. Solution P: *see* **Section 2.1.7**.
2. Salt and detergent extraction buffer: 400 m*M* NaCl and 1% (w/v) β-octylglucoside in 25 m*M* Hepes, pH 7.5.
3. Base extraction buffer: 100 m*M* NaOH.
4. Heparin extraction buffer: 10 mg/mL heparin in BT/Mg buffer.
5. 1 *M* sucrose BT/Mg.

3 Methods

Either the blood stream form (BSF) or procyclic life stage may be used with the following protocol, with similar yields. Procyclic cells are generally easier to culture because they do not require infection of animals to achieve the requisite number of cells for the isolation. At least 4×10^{10} cells are needed, which allows for two separate gradients with 2×10^{10} cells in each. One must be careful not to exceed 2×10^{10} cells in each gradient to maximize efficiency. Unless otherwise noted, cells and lysates must be kept on ice and pelleted in a refrigerated centrifuge at 4°C. The entire protocol is represented as a flow diagram in Fig. 6.1. If desired, the enrichment of the nucleus and subnuclear components may be monitored by Western blotting and thin section electron microscopy (EM) ***(12)***.

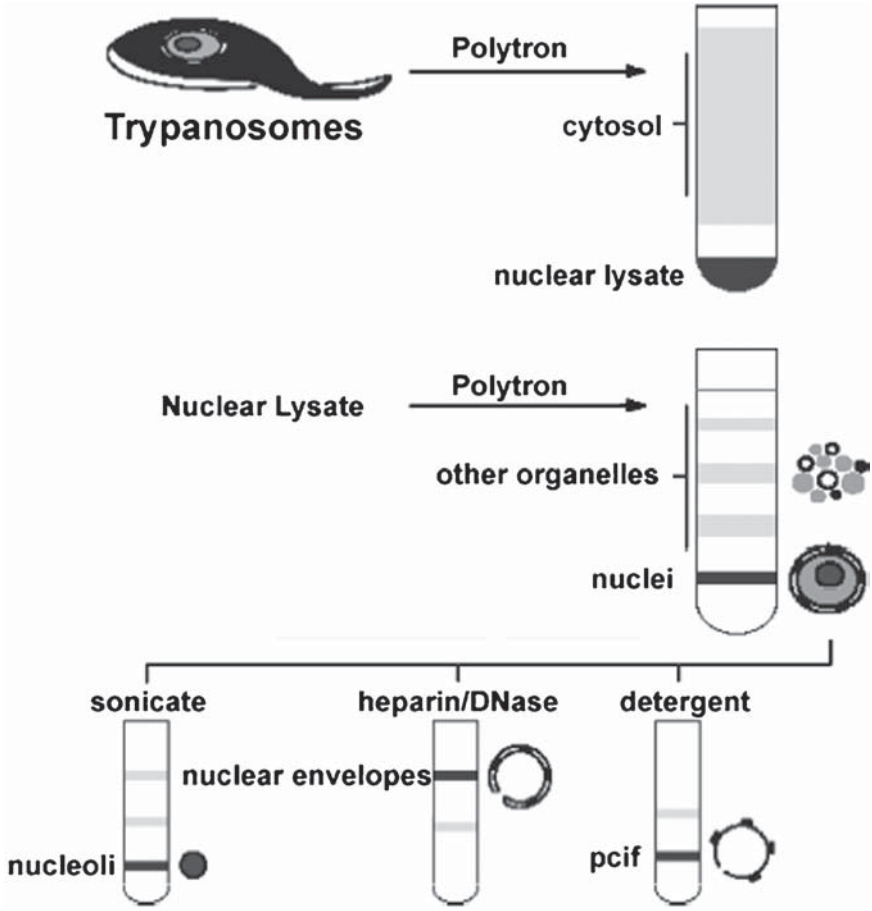

Fig. 6.1 Generalized flow diagram of nuclear isolation protocol. Regions containing isolated nuclear and subnuclear components are shaded *dark gray*

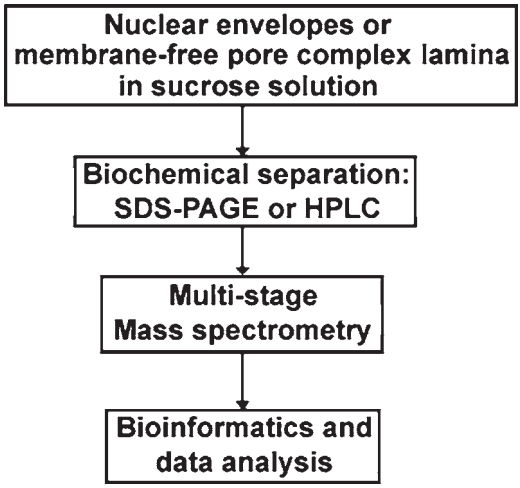

Fig. 6.2 Flow chart for post-isolation biochemistry, proteomics, and analysis

Subcellular proteomics is a robust tool to identify proteins that co-enrich with a particular organelle ***(13)***. In organisms such as *T. brucei*, whose evolutionary distance challenges functional genomics, localization information provides compelling additional functional evidence ***(14)***. Although subcellular proteomics significantly surmounts the many difficulties observed with whole cell proteomics, analysis of subcellular structures remains hindered by complexity (several hundred distinct proteins) and their dynamic range (several orders of magnitude). To overcome these challenges, we have employed a multipronged approach using separation and chemical extraction techniques and multistage mass spectrometry to identify more than 300 proteins that co-enrich with the nuclear envelope (Fig. 6.2). There is an array of bioinformatic algorithms that can be employed to predict which proteins colocalize to the nuclear envelope in vivo; however, a description of their use is beyond the scope of this chapter.

3.1 Nuclear Isolation

1. Gently pellet the cells at 1,700×*g* for 10 min. Discard the supernatant and resuspend the pellet with roughly 25 mL of prechilled PBS. After a second centrifugation, resuspend the pellet in 25 mL of prechilled PBS and transfer the cells to a Sorvall HB-4 tube. Pellet by centrifugation once again (1,800×g, 15 min, Sorvall HB-4 rotor) and discard the supernatant. (*See* **Note 6**).

2. To lyse the cells, add 1 volume per 2×10^{10} cells of lysis buffer to the pellet and immediately disrupt the cells with a Polytron homogenizer (PTA-10, GlenMills, Clifton, NJ, USA) with 1 min bursts. Because the appropriate speed setting may vary between homogenizer models, start with setting #4 and increase in increments of 0.5 until cell lysis is achieved. The lysis should be conducted in a cold room to keep the homogenizer probe and cellular material cooled. Five minutes total homogenization time at the final setting is usually sufficient for an acceptable 70–90% cell lysis, with progress being monitored by phase contrast microscopy. (*See* **Note 4**).
3. Once acceptable cell lysis has been achieved, underlay the equivalent of 2×10^{10} cells with 1 volume of underlay buffer and centrifuge for 20 min at 10,500×g in a Sorvall HB-4 rotor. Decant the supernatant (which contains the crude cytosol) and store at −80°C.
4. The pellet should then be immediately resuspended by homogenization. Add 1 volume of resuspension buffer and homogenize with the Polytron (setting 4.5–5) in 1 min bursts. Monitor the progress with phase contrast light microscopy; all cells should now be lysed (a significant proportion of the total cell lysis can actually occur at this stage), and the nuclei will be visible in the field as many small gray spheres and ovoids. Usually, 4 min is sufficient to achieve full dispersion.
5. Prepare the gradient. Into a Beckman SW-28 centrifuge tube, add the following: 8 mL of 2.30 *M* sucrose/PVP, 8 mL of 2.10 *M* sucrose/PVP, and 8 mL of 2.01 *M* sucrose/PVP (*see* **Note 7**).
6. Carefully add the crude nuclear material on top of the gradient (the portion of the gradient that contains the crude material is designated as "S"). Afterwards, fill to within 5 mm of the brim with PVP solution to prevent collapse. In a Beckman ultracentrifuge and SW-28 rotor, spin the gradient at 141,000×g for 3 h.
7. Subcellular material may be found at the interfaces. Each interface (PVP/S, S/2.01, 2.01/2.1, and 2.1/2.3) should be collected and stored at −80°C for possible future study. Most of the nuclei settle at the 2.10/2.30 interface. The quality of the nuclei can be checked by phase contrast light microscopy. (*See* **Note 8**).
8. The concentration of the nuclei is measured by optical density: 1 OD_{260} is equivalent to about 10^8 nuclei. (*See* **Note 9**).

3.2 Subnuclear Fractionation

3.2.1 Nuclear Envelope

1. To a measured volume of 300 ODs of purified nuclei, add the equivalent of 0.2 volumes of PVP solution and vortex for 1–2 min until the solution is homogenous.

2. In a Beckman Ty50.2Ti rotor, pellet the nuclei by centrifugation at 193,000×g for 1 h. Decant the supernatant.
3. Resuspend the pellet in 3 mL of shearing buffer and shear the nuclear envelopes by vigorous vortexing for 1 full minute after the last traces of the pellet disappear.
4. After shearing, let the tube stand for 5 min at room temperature.
5. Add 10 mL of 2.10 *M* sucrose in 20% Accudenz in BT/Mg buffer and mix well by vortexing.
6. Transfer the mixture to an SW-28 centrifuge tube and overlay with 12 mL of 2.25 *M* sucrose in BT/Mg and 10 mL of 1.50 *M* sucrose in BT/Mg. Top with BT/Mg to within 5 mm of the brim.
7. Spin the gradient at 141,000×g for 4 h.
8. Collect all interfaces. The nuclear envelopes float up to the 1.50 *M*/2.25 *M* interface. Their quality can be checked by microscopy; they appear as faint "C" structures by phase contrast light microscopy.

3.2.2 Nuclear Pore Complex–Lamina

1. To 1 volume of nuclear envelopes add the equivalent of 2 volumes of extraction buffer, and vortex for 5 min at room temperature. Allow the mixture to then incubate at room temperature for 25 min.
2. Prepare the gradient. In a Beckman SW-55 centrifuge tube, add 1 mL of 2.50 *M* sucrose in BT/Mg and then 1 mL of 1.75 *M* sucrose in BT/Mg.
3. Carefully overlay the extracted nuclear envelope mixture on the top of the gradient. Spin the gradient at 240,000×g for 30 min in a SW55Ti rotor.
4. Collect each interface fraction. The pore complex–lamina settles at the 1.75 *M*/2.50 *M* interface.

3.2.3 Isolation of the Nucleolus

1. To one volume of 50 OD_{260} of purified nuclei, add 0.2 volumes of PVP solution and vortex for 1–2 min until the solution is homogenous.
2. The nuclei are then pelleted in a type 80 rotor at 170,000×g for 1 h. Decant the supernatant.
3. 1 mL of disruption buffer is added to the pellet and the nuclei are disrupted by sonication with a microprobe in 6 sec bursts in the cold room. Progress between bursts is monitored by phase contrast microscopy (1,000×). Generally, six bursts is sufficient to achieve >99% disruption, releasing the small dark gray nucleoli.
4. The disrupted nuclei are then thoroughly mixed 1:1 (v/v) with 1.75 *M* sucrose in BT/Mg.
5. The mixture is then layered on top of the following gradient in a Beckman SW-55 centrifuge tube: 1 mL 2.50 *M* sucrose in BT/Mg buffer, 1.5 mL of 2.25 *M* sucrose in BT/Mg buffer, and 1.5 mL of 1.75 *M* sucrose in BT/Mg buffer.

6. The gradient is then centrifuged at 240,000×*g* for 2 h in a SW55Ti rotor. Collect all interface fractions. Nucleoli collect at the 2.00 *M*/2.50 *M* interface.

3.3 Biochemistry and Mass Spectrometry

Sections 3.3.2 and **3.3.3** are general methodologies and may be used in conjunction with either hydroxyapatite chromatography or chemical extraction.

3.3.1 Protein Precipitation

1. Prior to biochemistry and mass spectrometry, the proteins need to be recovered from the sucrose solutions. To one volume of nuclear or subnuclear material, add 5 volumes of HPLC-grade methanol and incubate for 4 h at 4°C. (*See* **Note 10**).
2. Spin at 3,300×*g* in a Beckman GH-3.8 for 15 min at 4°C.
3. Remove and discard the supernatant. Resuspend the pellet with 500 µL of 90% methanol and transfer to a microcentrifuge tube, if necessary, then incubate for 1 h at 4°C.
4. Spin the suspension one final time in a microcentrifuge (16,000×*g*, 15 min, 4°C). Discard the supernatant.

3.3.2 SDS-PAGE-MS

1. Resuspend the pellet in 20 µL of LDS sample buffer, 8 µL of sample reducing agent, and 52 µL of water. After mixing, heat to 70°C for 10 min and allow to cool to room temperature.
2. To alkylate the reduced cysteines, add iodoacetamide to a final concentration of 100 m*M* and allow the reaction to proceed, in the dark, for 30 min.
3. Prepare gel, MOPS running buffer, and gel assembly following the manufacturer's instructions. By using several different gradients, one can increase resolution in specific mass ranges. For example, a Novex 8% Tris-glycine gel offers high mass resolution whereas NuPAGE 10% bis-Tris gels offer superior low mass resolution.
4. Load 20 µL of alkylated sample onto each gel and run at a constant 125 V for 5 min followed by a constant 200 V for 45 min.
5. Fix the gel in 50% methanol and 7% acetic acid for 15 min and wash extensively. Stain with GelCode Blue stain and document by photography or digital flatbed scanning.
6. On a white shallow plate or glass pane, use a MicroScalpel to excise 2 mm-wide bands running down the entire gel lane; roughly 35 bands can be excised from a 10 cm gel. Using the fine point tweezers or MicroScapel, dice the excised gel bands into 1 mm cubes. Transfer the cubes to a microcentrifuge tube. (*See* **Note 11**).

7. Completely destain the gel pieces to remove all traces of stain and detergent. To the gel pieces, add 500 µL of destain solution and agitate (medium setting) at 4°C with a vertical vortexer (Tomy Mixer; Tomy Seiko Co., Tokyo, Japan). Replace the solution every 30 min for up to 4 h.
8. Add 100 µL acetonitrile. The gel pieces will dehydrate and turn white. Aspirate the acetonitrile after 10 min and leave the tubes open for several minutes to allow the last traces to evaporate.
9. Resuspend a trypsin aliquot in digestion buffer to a final concentration of 50 ng/µL. Add ≥100 ng trypsin to dehydrated gel pieces. Allow the pieces to swell and become translucent (~10 min) and then add 40 µL of digestion buffer. Incubate at 37°C for 4 h.
10. To 1 volume of Poros R2 bead slurry, add 9 volumes of Poros dilution buffer. Add 40 µL of these diluted Poros beads to the gel pieces. In a vertical vortexer, agitate (medium setting) at 4°C for 4 h. The beads will extract the peptides from the gel pieces and digestion buffer.
11. Transfer the 80 µL peptide/bead mixture into a washed and conditioned ZipTip from the top and, using a syringe, discard the supernatant (*See* **Note 12**). Add 20 µL of 0.1% trifluoroacetic acid to the gel pieces. Transfer the wash solution to the ZipTip from the top and expel wash the solution using a syringe.
12. Wash the Poros Beads twice more using 20 µL of 0.1% trifluoroacetic acid.
13. Slowly elute peptides onto a matrix-assisted laser desorption ionization (MALDI) plate with 2.5 µL 40% DHB in elution solution. When the spot is completely dry (less than 30 min), analyze by mass spectrometry ***(15, 16)***.

3.3.3 HPLC-MS

1. Resuspend the protein sample pellet in 50 µL of 50 m*M* ammonium bicarbonate. Sonication may be required to fully dissolve the pellet.
2. Add 250 ng of trypsin. Incubate at 37°C for 12 h.
3. Add another 250 ng of trypsin. Incubate at 37°C for 12 h.
4. Quench the reaction by the addition of 0.1% trifluoroacetic acid (final concentration).
5. Load an appropriate volume of the peptide solution onto a C-18 reversed phase column and elute under the following conditions: 25% B (95% acetonitrile, 0.1% trifluoroacetic acid) for 5 min, 25–100% B in 40 min. (*See* **Note 13**)
6. Analyze the eluate by online electrospray ionization–MS/MS (Finnigan LCQ series, ThermoElectron Corp., San Jose, CA, USA).

3.3.4 Hydroxyapatite Chromatography

1. In a 50-mL centrifuge tube, wash 7.5 mL of hydroxyapatite (HA) with 20 mL of wash buffer. Allow the hydroxyapatite to settle and aspirate the wash solution and suspended fine particles. Continue to wash 3 times with 20 mL loading

buffer, aspirating the loading buffer and suspended fine particles after each wash. To the final volume of hydroxyapatite, add 4 volumes of loading buffer supplemented with 0.1% SDS.
2. After methanol precipitation (*see* **Section 3.3.1**), resuspend the pellet in HA sample buffer and heat at 60°C for 10 min. Store unused sample solution at −20°C.
3. Dilute 1 volume of sample with 19 volumes of HA loading buffer.
4. Add conditioned HA beads to diluted sample. Roughly 2 mL of bead slurry is required for less than 0.5 mL of sample. Incubate mixture for 30 min, keeping the hydroxyapatite suspended by mechanical rotation or rocking.
5. Pour the mixture into a Poly-Prep chromatography column and collect the flow through. Wash the beads with 4 mL of 0.1% SDS in loading buffer. Collect the wash to monitor protein binding.
6. Elute proteins from the hydroxyapatite. All elution buffers are prepared from appropriate volumes of mobile phase A and mobile phase B, and SDS is added just before use at a final concentration of 0.1%. Add in successive order to the column: 300, 325, 350, 375, 400, and 500 m*M* NaH_2PO_4. Four milliliters of elution buffer is sufficient. (*See* **Note 14**).
7. Adjust the final volume of eluate to 10 mL and precipitate with sodium deoxycholic acid/trichloroacetic acid. (*See* **Note 15**).
8. The proteins may be analyzed by SDS-PAGE-MS or HPLC-MS, as described. An example of hydroxyapatite chromatography coupled to SDS-PAGE is shown in Fig. 6.3.

3.3.5 Chemical Extraction

Perform all extractions in Beckman TLA-55 centrifuge tubes.

1. Salt and detergent extraction:

   To one volume of nuclear envelopes (in sucrose solution) add 9 volumes of salt and detergent extraction buffer with solution P (1:100) and mix completely by vortexing.

2. Base extraction:

   To one volume of nuclear envelopes (in sucrose solution) add 9 volumes of base extraction buffer with solution P (1:100) and mix completely by vortexing.

3. Heparin extraction:

   To one volume of nuclear envelopes (in sucrose solution) add 9 volumes of heparin extraction buffer with solution P (1:100) and mix completely by vortexing.

4. Incubate the extractions on ice for 1 h.

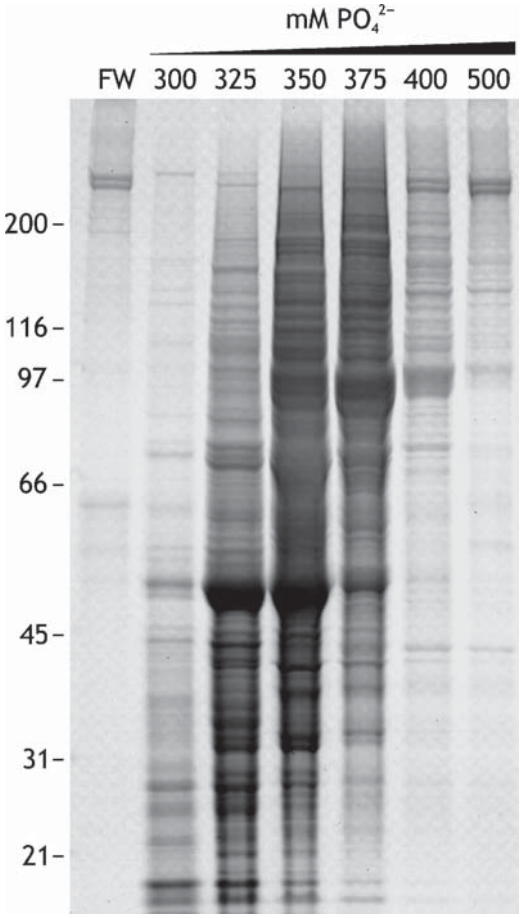

Fig. 6.3 Separation by SDS-PAGE of proteins in the nuclear envelope fraction. Each lane represents a protein fraction eluted from the hydroxyapatite column; the concentration of the elution buffer is indicated above each lane. Molecular weight markers are indicated to the left of the gel. *FW*, combined flow through and wash

5. Underlay the mixtures with 1 *M* sucrose in BT/Mg buffer with solution P (1:100).
6. Pellet by centrifugation at 103,000×*g* for 35 min.
7. Extracted proteins are retained in the supernatant. Carefully transfer the supernatant to a fresh tube and precipitate the proteins (*See* **Note 15**).
8. Wash the non-extracted pellet in 1 mL acetone and transfer the suspension to a microcentrifuge tube, if necessary, and incubate overnight at −20°C. Recover the pellet by centrifugation (16,000×g, 4°C, 1 h).
9. Both the extracted proteins and the pellet can be analyzed by either SDS-PAGE-MS or HPLC-MS, as above.

4 Notes

1. To minimize the risk of contamination when preparing reagents, it is imperative to use the highest reagent quality available. With the exception of polymeric, high density, acidic or basic solutions, aqueous buffers should be filtered with a 0.22-μm-pore syringe or bottle filter. These precautions are especially important when this protocol is coupled to mass spectrometry in order to avoid exogenous protein and dust contamination. All aqueous solutions are made with high-quality filtered water with a measured resistivity of 18.2 MΩ-cm.
2. In a large dish of hot water atop a stirring hot plate, the appropriate amount of sucrose is dissolved into PVP solution in a 500 mL beaker by constant stirring. Once the sucrose has completely dissolved, remove from heat, cover, and allow to cool to room temperature. While continuously stirring the solution, adjust the RI to within 0.0003 by slowly adding PVP solution.
3. For best results, slowly dissolve each peptide inhibitor sequentially into room temperature ethanol.
4. Protease inhibitors become unstable at room temperature at working concentrations. On the bench, solution P must be kept on ice whereas the PIC may be left thawed. We recommend the addition of the protease inhibitors to the working solutions at the last possible moment.
5. A working Poros R2 bead slurry is made as follows:
   (a) 500 mg of Poros R2 beads are washed sequentially with 10 mL of 1) methanol, 2) 80% acetonitrile, and then 3) 20% ethanol.
   (b) Resuspend the washed beads in 20% ethanol at a final concentration of 50 mg/mL.
6. The rotors and centrifuge tube described herein may be replaced by others of similar capacities and rotational velocity. Conversion formulas are widely available.
7. To reduce the viscosity of the sucrose solutions, allow the solutions to completely warm to room temperature. Wide-bore pipets and pipette tips (made by cutting off ~3 mm from the point of the tip) also facilitate handling sucrose solutions. Before use, all sucrose solutions should be supplemented with solution P (1:100) and PIC (1:200).
8. Unloading the gradient will be easier if the interfaces are marked with a permanent marker before centrifugation. Collect the topmost fill layer and halfway through the first sucrose layer. Then, starting from the top, collect from halfway through the upper sucrose layer, through the interface, and continue to collect until halfway through the lower sucrose layer. The material at the interface may be gently dislodged with a pipette tip, if necessary.
9. Add 10 μL of nuclei to 1 mL of 1% SDS. Measure the absorbance at 260 nm against a blank of 1% SDS. Multiply the value by 100 to obtain the OD.
10. It is recommended to precipitate a 1 mL aliquot of the subnuclear fraction and determine the protein concentration using a suitable assay such as Bradford or bicinchoninic acid.

11. To avoid contamination from dust, clean all tools and surfaces with Windex cleaner. As an alternative to manual slicing, one can use a Mickle gel slicer (Brinkman Instruments, Westbury, NY, USA) which can mechanically slice the gel lane at 1 mm intervals.
12. After conditioning, the ZipTips are always loaded from the top. By doing so, the Poros beads settle behind the ZipTip resin, which acts as a frit. The supernatant can be easily expelled from the tip by air using a 1mL syringe fitted with a cut P200 pipette tip such that the ZipTip can form a seal around the pipette tip adaptor. When washing or eluting from the beads, it is imperative that solutions are loaded from the top.
13. For our work, we used an Ultimate HPLC system (LC Packings-Dionex, Sunnyvale, CA, USA) with a C18 column (0.18×250 mm, 1.8 µL/min).
14. The elution can be hastened by use of air pressure, although this is not necessary. After a fraction has been collected, allow the fine particles to settle and pour the eluate to a fresh tube to avoid contamination from proteins still bound to the fine particulates. It is essential to add SDS just before use, otherwise it may begin to precipitate.
15. When the proteins are present at relatively dilute concentrations, we recommend precipitation by sodium deoxycholic acid/trichloroacetic acid. Dilute the protein suspension with water to 1 mL (small scale) or 10 mL (large scale). Add 100 µL or 1 mL, respectively, of 0.3% sodium deoxycholic acid, mix well, and add an equivalent volume of 72% trichloroacetic acid. Incubate at 4°C for 1 h and then spin at maximum rotor speed (1 h, 4°C). Wash the pellet in 1 mL of acetone and transfer to a microcentrifuge tube, if necessary, and incubate overnight at −20°C. Recover the pellet by centrifugation in a microcentrifuge (16,000×*g*, 4°C, 1 h).

Acknowledgments This work was supported by the Tri-Institutional Training Program in Chemical Biology (JAD). Work on the trypanosome isolation procedure was supported in part by a Wellcome Trust International Traveling Fellowship (MCF). This work was also supported by an Irma T. Hirschl Career Scientist Award, a Sinsheimer Scholar Award, and a grant from the Rita Allen Foundation to M.P. Rout, and grants from the National Institutes of Health to M.P. Rout (GM062427, GM071329) and B.T. Chait (RR00862), and to both (RR022220).

References

1. Barrett, M. P., Burchmore, R. J. S., Stich, A., Lazzari, J. O., Frasch, A. C., Cazzulo, J. J., and Krishna, S. (2003) The trypanosomiases. *Lancet* **362,** 1469–1480.
2. The World Health Report 2004—Changing History. (2004) World Health Organization, Geneva.
3. Simpson, A. G., Stevens, J. R., and Lukes, J. (2006) The evolution and diversity of kinetoplastid flagellates. *Trends Parasitol*. **22,** 168–174.
4. Bapteste, E., Charlebois, R. L., Macleod, D., and Brochier, C. (2005) The two tempos of nuclear pore complex evolution: highly adapting proteins in an ancient frozen structure. *Genome Biol*. **6**, R85.

5. Mans, B. J., Anantharaman, V., Aravind, L., and Koonin, E. V. (2004) Comparative genomics, evolution and origins of the nuclear envelope and nuclear pore complex. *Cell Cycle* **3,** 1612–1637.
6. El-Sayed, N. M., Myler, P. J., Blandin, G., Berriman, M., Crabtree, J., Aggarwal, G., Caler, E., Renauld, H., Worthey, E. A., Hertz-Fowler, C., Ghedin, E., Peacock, C., Bartholomeu, D. C., Haas, B. J., Tran, A. N., Wortman, J. R., Alsmark, U. C. M., Angiuoli, S., Anupama, A., Badger, J., Bringaud, F., Cadag, E., Carlton, J. M., Cerqueira, G. C., Creasy, T., Delcher, A. L., Djikeng, A., Embley, T. M., Hauser, C., Ivens, A. C., Kummerfeld, S. K., Pereira-Leal, J. B., Nilsson, D., Peterson, J., Salzberg, S. L., Shallom, J., Silva, J. C., Sundaram, J., Westenberger, S., White, O., Metville, S. E., Donelson, J. E., Andersson, B., Stuart, K. D., and Hall, N. (2005) Comparative genomics of trypanosomatid parasitic protozoa. *Science* **309,** 404–409.
7. Subramaniam, C., Veazey, P., Seth, R., Hayes-Sinclair, J., Chambers, E., Carrington, M., Gull, K., Matthews, K., Horn, D., and Field, M. C. (2006) Chromosome-wide analysis of gene function by RNA interference in the African trypanosome. *Eukaryot. Cell* **5,** 1539–1549.
8. Clayton, C. E. (2002) Life without transcriptional control? From fly to man and back again. *EMBO J*. **21,** 1881–1888.
9. Field, M. C., Horn, D., and Carrington, M. (2008) Analysis of small GTPase function in trypanosomes. In: *Small GTPases in disease* (Balch, W., Der, C., Hall A., eds.). Academic Press, San Diego, CA.
10. Ullu, E., Tschudi, C., and Chakraborty, T. (2004) RNA interference in protozoan parasites. *Cell. Microbiol*. **6,** 509–519.
11. Berriman, M., Ghedin, E., Hertz-Fowler, C., Blandin, G., Renauld, H., Bartholomeu, D. C., Lennard, N. J., Caler, E., Hamlin, N. E., Haas, B., Bohme, W., Hannick, L., Aslett, M. A., Shallom, J., Marcello, L., Hou, L. H., Wickstead, B., Alsmark, U. C. M., Arrowsmith, C., Atkin, R. J., Barron, A. J., Bringaud, F., Brooks, K., Carrington, M., Cherevach, I., Chillingworth, T. J., Churcher, C., Clark, L. N., Corton, C. H., Cronin, A., Davies, R. M., Doggett, J., Djikeng, A., Feldblyum, T., Field, M. C., Fraser, A., Goodhead, I., Hance, Z., Harper, D., Harris, B. R., Hauser, H., Hostetter, J., Ivens, A., Jagels, K., Johnson, D., Johnson, J., Jones, K., Kerhornou, A. X., Koo, H., Larke, N., Landfear, S., Larkin, C., Leech, V., Line, A., Lord, A., MacLeod, A., Mooney, P. J., Moule, S., Martin, D. M. A., Morgan, G. W., Mungall, K., Norbertczak, H., Ormond, D., Pai, G., Peacock, C. S., Peterson, J., Quail, M. A., Rabbinowitsch, E., Rajandream, M. A., Reitter, C., Salzberg, S. L., Sanders, M., Schobel, S., Sharp, S., Simmonds, M., Simpson, A. J., Talton, L., Turner, C. M. R., Tait, A., Tivey, A. R., Van Aken, S., Walker, D., Wanless, D., Wang, S. L., White, B., White, O., Whitehead, S., Woodward, J., Wortman, J., Adams, M. D., Embley, T. M., Gull, K., Ullu, E., Barry, J. D., Fairlamb, A. H., Opperdoes, F., Barret, B. G., Donelson, J. E., Hall, N., Fraser, C. M., Melville, S. E., and El-Sayed, N. M. (2005) The genome of the African trypanosome Trypanosoma brucei. *Science* **309,** 416–422.
12. Rout, M. P., and Field, M. C. (2001) Isolation and characterization of subnuclear compartments from Trypanosoma brucei—Identification of a major repetitive nuclear lamina component. *J. Biol. Chem*. **276,** 38261–38271.
13. Dreger, M., Bengtsson, L., Schoneberg, T., Otto, H., and Hucho, F. (2001) Nuclear envelope proteomics: Novel integral membrane proteins of the inner nuclear membrane. *Proc. Natl. Acad. Sci. USA* **98,** 11943–11948.
14. Dreger, M. (2003) Proteome analysis at the level of subcellular structures. *Eur. J. Biochem*. **270,** 589–599.
15. Tackett, A. J., Dilworth, D. J., Davey, M. J., O'Donnell, M., Aitchison, J. D., Rout, M. P., and Chait, B. T. (2005) Proteomic and genomic characterization of chromatin complexes at a boundary. *J. Cell Biol*. **169,** 35–47.
16. Archambault, V., Li, C. H. X., Tackett, A. J., Wasch, R., Chait, B. T., Rout, M. P., and Cross, F. R. (2003) Genetic and biochemical evaluation of the importance of Cdc6 in regulating mitotic exit. *Mol. Biol. Cell* **14,** 4592–4604.

Chapter 7
Methods for Studying the Nuclei and Chromosomes of Dinoflagellates

Marie-Odile Soyer-Gobillard

Keywords Dinoflagellates; Nuclei; Chromosome architecture; Squashes; Electron microscopy; Whole-mount preparations; B- and Z-DNA immunolocalization; Fast-freeze fixation

Abstract Dinoflagellates are unicellular eukaryotic organisms whose nuclear structure, chromosome architecture, chromatin organization, DNA composition, and mitosis show original features. It has been necessary to adapt techniques and to create innovative methods for growing cells, isolating nuclei, and studies of their chromosomes by transmission electron microscope (TEM). Among these are innovative squash and whole-mount preparations for light and TEM observations of chromosome architecture and the spatial organization of nucleofilaments. Particular attention was given to adapt high-pressure freezing (fast-freeze fixation) techniques for the best preservation of delicate antigenic sites, and good immunodetection. The study of DNA replication with or without incorporation of bromodeoxyuridine (BrdU) was also refined to use confocal laser scanning microscopy. In this chapter, we describe methods that we have invented and/or improved from existing techniques in order to better understand this fragile chromosome architecture and the mechanisms intervening during mitosis and the cell cycle. These methods allowed us to detect specific DNA-binding proteins and the distribution of B-and Z-DNA in chromosomes during the cell cycle and mitosis, and to focus on the indissoluble link between chromosome structure and function.

1 Introduction

The Dinoflagellates are unicellular eukaryotic microorganisms among the Protoctista, widely distributed in marine and fresh waters and constituting a phylum showing great diversity and playing an important role in the trophic chain. They are true eukaryotes with a G1–S–G2–M cell cycle, but their nuclear structure, their chromosome architecture, and their mitotic and cell cycles are distinctive and original features ***(1–4).*** Most show a high DNA content, from 7.0 pg/cell in *Crypthecodinium*

R. Hancock (ed.) *The Nucleus: Volume 1: Nuclei and Subnuclear Components*,

cohnii to 200 pg/cell in *Gonyaulax polyedra* Stein. They are devoid of histone proteins ***(5, 6)*** and thus of nucleosomes, and are characterised by the presence of specific basic proteins and of DNA with a high G+C content and a high proportion of the base hydroxymethyluracil ***(7).*** Surrounded by a persistent nuclear envelope, the chromosomes, ranging from 4 to 200 depending on the species, are quasi-permanently condensed. These features raise interesting questions concerning the replication and transcription of their genome. The work of Sigee ***(8)*** showed that these occur in the periphery of chromosomes by means of delicate DNA loops. It has been necessary to modify and/or improve existing techniques and to create innovative methods for growing cells, isolating nuclei, and studying their chromosomes by optical microscopy and transmission electron microscopy (TEM). In this chapter, we describe some of the methods that we have devised in order to better understand this fragile chromosome architecture and the mechanisms intervening during mitosis (termed dinomitosis, ***(9)***) and the cell cycle. Two species were mainly used for our studies, the autotrophic *Prorocentrum micans* Ehrenberg and the heterotrophic *Crypthecodinium cohnii* Biecheler.

2 Materials

2.1 Growth Media

1. Erd-Schreiber medium for *P. micans*, for 1 L:
   (a) Soil extract: mix 1 L of garden soil, 1 L of distilled water (dH_2O), and 3 g of NaOH, and autoclave at 120°C for 60 min. Centrifuge at 5,000×*g* for 10 min, filter the supernatant, and sterilise it at 120°C for 25 min.
   (b) Vitamin cocktail: 0.1 mg of biotin, 0.1 mg of vitamin B12, and 20 mg of vitamin B1 in 100 mL of dH_2O, filter sterilise.
   (c) Mix 1 mL of sterile 10% $NaNO_3$, 1 mL of sterile 2% w/v Na_2HPO_4, and 5 mL of soil extract, add sea water filtered on a Whatman CFC filter to 950 mL and autoclave at 120°C for 25 min, make to 1 L, add 1 mL of vitamin cocktail.
2. F/2 medium, for 1 L (*see* **Note 1**):
   (a) To ~950 mL of non-sterilised seawater, add components to give these final concentrations while stirring:

   Salts: 880 µ*M* $NaNO_3$, 36 µ*M* NaH_2PO_4, 107 µ*M* Na_2SiO_3
   Trace metals: 11.7 µ*M* $FeCl_3$, 0.04 µ*M* $CuSO_4$, 0.08 µ*M* $ZnSO_4$, 0.05 µ*M* $CaCl_2$, 0.9 µ*M* $MnCl_2$, 11.7 µ*M* Na_2EDTA.

   (b) Bring to 1 L with non-sterilised seawater, cover and autoclave, cool.
   (c) Add sterile vitamin solutions to give these final concentrations: 0.32 m*M* vitamin B1, 10 µ*M* biotin, and 1 µ*M* vitamin B12, store at 4°C.
3. MLH medium ***(10)***:

(a) Salts: 342 m*M* NaCl, 28 m*M* $MgSO_4$, 7.5 m*M* $CaCl_2$, 9 m*M* KCl, 0.79 m*M* Na_2 glycerophosphate, 1.5 m*M* $(NH_4)_2SO_4$, 15 m*M* Na acetate, 0.8 m*M* histidine-HCl, 22 m*M* glucose, 9.7 m*M* betain-HCl
(b) Vitamins: 8.2 n*M* biotin, 2.96 µ*M* thiamine-HCl, 0.75 n*M* vitamin B12
(c) Trace metals: 6 mM nitriloacetic acid, 0.08 m*M* 5-sulphosalicylic acid, 0.18 m*M* $Fe(NH_4)_2(SO_4)_2$, adjust to pH 6.6 with 10 N NaOH.

2.2 Isolation of Nuclei

1. Nuclear isolation buffer: 10 m*M* Tris-HCl pH 7.4, 10 m*M* $CaCl_2$, 5 m*M* $MgCl_2$, 0.35 *M* sucrose, 10% w/v dextran T40, with 5 m*M* $NaHSO_3$ and 0.5 m*M* phenylmethylsulfonyl fluoride (PMSF) as protease inhibitors.
2. 5% v/v Triton X-100 in dH_2O.
3. Gradient solution A: 2.4 *M* sucrose, 10% (w/v) dextran T10 in 10 m*M* Tris-HCl pH 7.4, 10 m*M* $CaCl_2$, 5 m*M* $MgCl_2$, 5 m*M* $NaHSO_3$ and 0.5 m*M* PMSF.
4. Gradient solution B: 2.4 *M* sucrose in 10 m*M* Tris-HCl pH 7.4, 10 m*M* $CaCl_2$, 5 m*M* $MgCl_2$, 5 m*M* $NaHSO_3$, and 0.5 m*M* PMSF.
5. Gradient solution C: 2.2 *M* sucrose, 0.1% (v/v) Triton X-100 in 10 m*M* Tris-HCl pH 7.4, 10 m*M* $CaCl_2$, 5 m*M* $MgCl_2$, 5 m*M* $NaHSO_3$, and 0.5 m*M* PMSF.
6. Methyl green-pyronin stain (Sigma-Aldrich, Saint-Quentin Fallavier, France).

2.3 Squash Procedure for Optical Microscopy

1. Phosphate-buffered saline (PBS): 140 m*M* NaCl, 2.7 m*M* KCl, 8.1 m*M* Na_2HPO_4, and 1.5 m*M* KH_2PO_4, adjust pH to 7.4.
2. Siliconised microscope slides and coverslips (Sigma-Aldrich).
3. Formaldehyde solution (2%): 2 g of paraformaldehyde in 100 mL of PBS, heat (avoid boiling) and stir to dissolve, adjust pH to 7.4. Keep at −20°C.
4. Ethidium bromide: 0.5 µg/mL in dH_2O.
5. Ethanol/acetic acid mixture, 3/1 (v/v).
6. Ethanol 45% v/v.
7. 0.7 *M* NaOH, 4 *M* urea, pH 7.5.
8. 4′,6-diamidino-2-phenylindole (DAPI) (Sigma-Aldrich): 0.1 µg/mL in dH_2O.
9. Propidium iodide (PI) (Sigma-Aldrich): 0.1 µg/mL in dH_2O.

2.4 Spreading Chromosomes for TEM

1. 0.6 *M* sucrose containing 1% w/v paraformaldehyde, pH 7.4.
2. Carbon-coated 300-mesh grids, positively charged by glow discharge in the presence of amylamine vapour ***(11)*** (*see* **Note 2**).

3. Uranyl acetate: 0.5% w/v in dH_2O.
4. Photo-Flo solution: 0.06% (v/v) Photo-Flo 200 (Eastman Kodak, Rochester, NY, USA) in dH_2O, adjust to pH 8.8 and filter. Make fresh daily.

2.5 Whole-Mount Chromosome Preparations for TEM

1. Honda medium ***(12)***: 2.5% w/v Ficoll, 5% w/v dextran (40 kDa), 0.25 *M* sucrose, 25 m*M* Tris-HCl, 10 m*M* $MgCl_2$, pH 7.8 (all from Sigma-Aldrich).
2. Mica (SPI, West Chester, PA, USA), freshly-cleaved; this supplier describes the method for cleaving at http://www.2spi.com/catalog/submat/mica-disk.html.
3. Carbon-coated electron microscopy (EM) grids (*see* **Note 2**).
4. Uranyl acetate: 2% w/v in 50% v/v ethanol.

2.6 Visualising Chromosomes in Thin Sections by TEM

1. BSA solution: 22% w/v in dH_2O, sterile-filtered.
2. Piperazine-1,4-bis(2-ethanesulfonic acid) (PIPES) buffer: 0.2 *M*, adjust pH to 7.0 with 1 N NaOH. Prepare fresh.
3. Prefixing solution: 12.5 mL of 8% w/v paraformaldehyde, 5 mL of 12.5% glutaraldehyde, 25 mL of PIPES buffer, 7.5 mL of dH_2O.
4. Osmium tetroxide (OsO_4) solution: 4% w/v diluted 1/1 with PIPES buffer. Light sensitive and *toxic*. Stable for several months.
5. Dehydrating solutions: 30%, 50%, 70%, 96%, and 100% ethanol in water.
6. Embedding medium: Epoxy embedding kit (e.g. Sigma-Aldrich) (*see* **Note 4**). *Epoxy compounds are toxic and should be handled with care*.
7. Uranyl acetate staining solution: 2% w/v uranyl acetate in dH_2O. Light sensitive, store at 4°C in a stoppered brown bottle; stable for up to 1 year. *Uranyl acetate is radioactive and should be handled with care*.
8. Lead citrate staining solution: in glassware, dissolve 1.33 g of $Pb(NO_3)_2$ in 30 mL of dH_2O, and add 1.76 g of $Na_3C_6H_5O_7.2H_2O$. Shake vigorously for 1 min and intermittently for 30 min. Add 8 mL of freshly made 1 N NaOH and invert slowly, the cloudy solution should clear. Adjust to 50 mL with water. Solution is stable for several months at 4°C in the dark.
9. Saturated solution of uranyl acetate in ethanol.

2.7 Immunolocalization of B- and Z-DNA by TEM

1. Formaldehyde solution: 3% in PBS.
2. PBS, 0.01% v/v Tween 20.
3. PBS, 0.1% Tween 20, 1% bovine serum albumin (BSA).

4. Primary antibodies.
5. Fluorochrome-labelled secondary antibodies.
6. Antifading solution, e.g. Vectashield (Vector Laboratories, Burlingame, CA, USA).

2.8 Fast-Freeze and Freeze Substitution Fixation TEM

1. Cryovacublock (Reichert-Jung, Nussloch, Germany).
2. Molecular sieves (0.4 nm Perlform; Merck, Rahway, NJ, USA).
3. Cryocool apparatus (CRYO Industries, Manchester, NH, USA).

2.9 Equipment

1. Homogeniser: Virtis 45 (Virtis, Gardiner, NY, USA).
2. Glass beads: 0.17 mm (Braun, Melsungen, German).
3. Nylon cloth: 25-µm and 10-µm mesh.
4. Sonicator.
5. Fluorescence microscope: we use a Polyvar (Reichert) with filters for common fluorochromes.
6. OsO_4 solution: 2% w/v in acetone.
7. Molecular sieves (Perlform 0.4 nm; Merck, Darmstadt, Germany).
8. Cryocool apparatus (CRYO Industries).
9. Ultramicrotome: Cryonova (LKB, Stockholm, Sweden).
10. Transmission electron microscope: we use a Hitachi H600 (Hitachi, Pleasanton, CA, USA).
11. Vacuum evaporator for shadowing with platinum.

3 Methods

3.1 Growth of P. micans (see Note 3)

1. Grow at 18°C either in Erd-Schreiber medium with constant illumination at 4,000 lux and gentle bubbling of filtered air (0.45 µm; Millipore) ***(12)***, or in F/2 medium under 12 h cycles of dark/2,000 lux light ***(13)***.
2. For experiments, cultures are initiated at 1,000 cells/mL of medium and exponential growth is reached after about 20 days.

3.2 Growth of C. cohnii (see Note 3)

1. Conserve on MLH medium, 2.3% agar and grow in MLH in the dark at 27°C. The cell cycle lasts for 8 h under these conditions ***(10)***.
2. To obtain high-density liquid cultures (5×10^5 cells/mL), cells are grown in liquid MLH.
3. *C. cohnii* can be partially synchronised ***(14, 15)***:
   (a) Spread 100 µL of an exponential-stage culture on MLH agar medium.
   (b) After 3 days in the dark at 27°C, pour 20 mL of MLH liquid medium on the surface of the agar.
   (c) When swimming cells, which are flagellated and in interphase, begin to emerge from the cysts, wash the surface carefully with fresh MLH and add 20 mL of fresh medium.
   (d) After 10 min, take and culture the newly emerged swimming cells. Only a few cells are harvested, but they possess a high degree (>80%) of synchrony (*see* **Note 4**).

3.3 Isolation of Nuclei

Nuclei can be purified by a modification ***(6)*** of the procedure of Rizzo ***(16)***. Disruption and purification should be carefully monitored with the light microscope after staining with methyl green–pyronin.

1. Harvest cells at the end of the log phase of growth (~2.3×10^4 cells/mL) by centrifugation at 800×*g* for 20 min.
2. Wash the cells 4× with sea water filtered through a 0.45-µm-pore filter and 1× in nuclear isolation buffer.
3. Homogenise the cells in nuclear isolation buffer at 4°C in a Virtis homogeniser in the presence of 0.17-mm glass beads to disrupt the thick cellulosic thecae.
4. Filter the crude homogenate through 25-µm and then 10-µm mesh nylon cloth at 4°C.
5. Stir the filtered extract slowly at 4°C and add Triton X-100 solution to give a final concentration of 0.5% v/v. Stir slowly for 10–15 min to remove adhering cytoplasm.
6. Pellet the nuclei at 400×*g* for 10 min through a cushion of 1.6 *M* sucrose and wash them once with nuclear isolation buffer.
7. Prepare a three-layer gradient in a tube for the Spinco SW 25.2 rotor, consisting of a bottom layer of 7 mL of gradient solution A, a middle layer of 21 mL of gradient solution B, and a top layer of 16 mL of gradient solution C. Layer 10 mL of nuclear suspension on top and centrifuge at 10,000×*g* for 20 min.
8. Wash the pelleted nuclei twice with nuclear isolation buffer and finally centrifuge at 300×*g* for 10 min.

9. Aliquots can be stored in liquid N_2 for studies of chromosomes by TEM (*see* **Section 3.5**).

3.4 Squash Preparations for Optical Microscopy

We have used squash preparations to visualise chromosomes in intact cells, to detect BrdU incorporated into DNA ***(17)***, and to detect B- and Z-DNA ***(18)***. They allow chromosomes to be visualised simply by adding ethidium bromide (0.5 µg/mL) to a drop of culture medium placed on a microscope slide, pressing with a coverslip, and observing immediately with a fluorescence microscope (Figs. 7.1 and 7.2a).

1. Centrifuge *P. micans* cells at 146×*g* for 10 min.
2. Resuspend and fix in 2% paraformaldehyde in PBS for 30 min.
3. Wash the cells for 10 min in PBS.
4. (Optional) If detecting incorporated BrdU, keep the cells in PBS overnight at 4°C to fragilise them, centrifuge, and resuspend them in 0.7 *M* NaOH, 4 *M* urea, pH 7.5 at 4°C for 1 h to denature DNA (*see* **Note 5**).
5. Place the cells on a microscope slide, squash between a coverslip and the slide, and remove the coverslip.
6. Rinse with PBS. Slides can be examined by staining with ethidium bromide, DAPI, or PI (Fig. 7.2a).

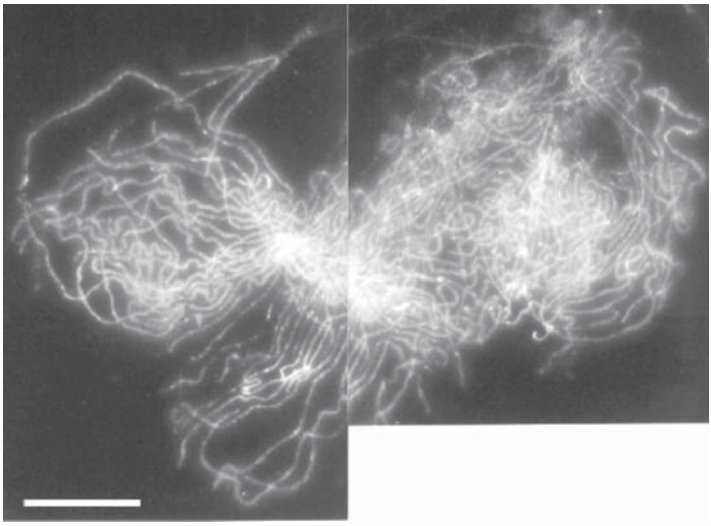

Fig. 7.1 Chromosomes of *Prorocentrum micans* prepared by squashing and stained with ethidium bromide (**Section 3.4**). Preparation and unpublished image by the author. Bar, 1 µm

7. Freeze the slides for 1 h on a block of dry ice and store at −20°C.
8. Process for immunocytochemistry after a rapid wash with PBS.

3.5 Spreading Chromosomes for TEM

This method of spreading was derived from **ref.** ***(19)*** and is described in detail in Chap. 4, Vol. 2 by Osheim et al. We have used this method to examine the effects of divalent cations and RNase on chromosomes ***(20, 21)*** (Figs. 7.2 and 7.3).

1. Thaw a 20-µL aliquot of frozen nuclei at 20°C.
2. Centrifuge through a cushion of 0.6*M* sucrose, 1% w/v paraformaldehyde at 2,000×*g* for 30 min onto positively charged carbon-coated grids ***(22)*** (*see* **Note 2**).
3. Stain the grids in uranyl acetate for 2 min, wash for 1 min in dH_2O.
4. Rinse rapidly in 0.5% v/v Photoflo solution and air dry.
5. Enhance contrast by rotary shadowing with platinum at an angle of 7 to 10 degrees.

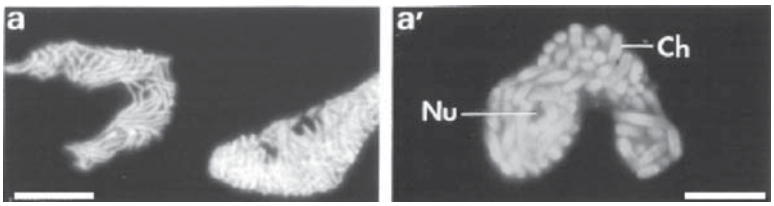

Fig. 7.2 Nuclei of *P. micans* as seen **(a)** after squashing and staining with DAPI **(Section 3.3)** (bar, 5 µm); **(a′)** in a thick section of epoxy-embedded cells and staining with acridine orange **(Section 3.7)** (bar, 2 µm). Ch chromosomes, Nu nucleolus. Reproduced with permission from ***(18),*** copyright 1990, The Rockefeller University Press

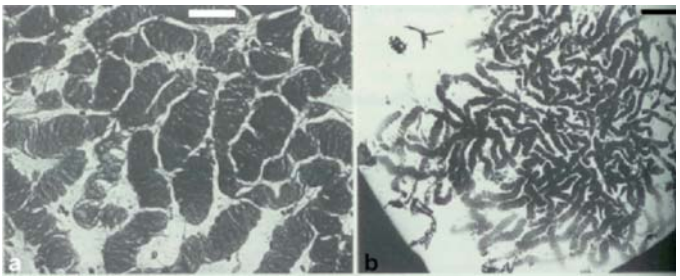

Fig. 7.3 *P. micans* chromosomes. **a** Native chromosomes spread by centrifugation onto an EM grid **(Section 3.5.)** (bar, 2 µm). **b** Low magnification showing that chromosomes prepared as in (**a**) are concentrated in a small area (bar, 10 µm). Reproduced from ***(21)*** with permission of the publishers

3.6 Whole-Mount Chromosome Preparations for TEM

Spreading chromosomes on a water surface for observation by TEM revealed their double-twisted helix organization ***(11, 23–26)***, later confirmed by other authors ***(27–29)***. We have used this method to examine the effects of pronase and RNase on chromosomes ***(30)*** (Figs. 7.3 and 7.4).

1. Collect cells by centrifugation and break them by sonication in Honda medium at 4°C. Breakage should be monitored with the light microscope after staining with methyl green–pyronin.
2. Using freshly cleaved mica as a ramp, allow one drop of this material to run onto a clean water surface.

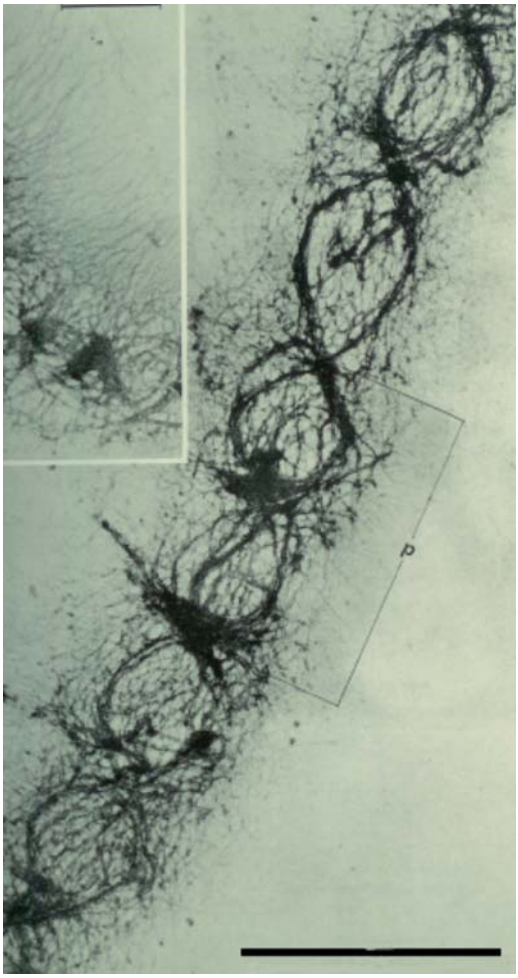

Fig. 7.4 A chromosome of *P. micans* prepared by whole mounting (**Section 3.6**). The completely opened and flattened chromosome shows a figure-eight conformation of chromatid bundles. Bar, 2 µm. Reproduced from ***(26)*** (journal no longer published)

3. Pick up an area of the film formed by ruptured cells and nuclei on carbon-coated EM grids.
4. Stain with 2% uranyl acetate in 50% ethanol for 10–30 min.

3.7 Visualising Chromosomes in Ultrathin Sections by TEM

This method was devised to give optimal preservation of nuclear structures of *P. micans* ***(31, 32)***. In ultrathin sections, chromosomes show an arrangement of the nucleofilaments in a series of regular arches, described for the first time in **ref.** ***(3)*** (Figs. 7.2b, 7.5, and 7.6).

1. Incubate *P. micans* cells in culture medium with 1% BSA for 20 min.
2. Wash the cells 2× in culture medium.
3. Incubate in freshly prepared prefixing solution for 60 min at room temperature.
4. Wash in PIPES buffer for 60 min.
5. Postfix in 4% osmium tetroxide/PIPES buffer (1/1) at room temperature for 60 min.
6. Wash in PIPES buffer and then in dH_2O.
7. Dehydrate in 30%, 50%, and 96% ethanol and then in absolute ethanol (twice) (30 min each).
8. Embed in Epoxy resin, following the supplier's instructions (*see* **Note 6**).
9. Cut ultrathin sections.
10. Contrast the sections with uranyl acetate (2–5 min) and lead citrate (30 sec).

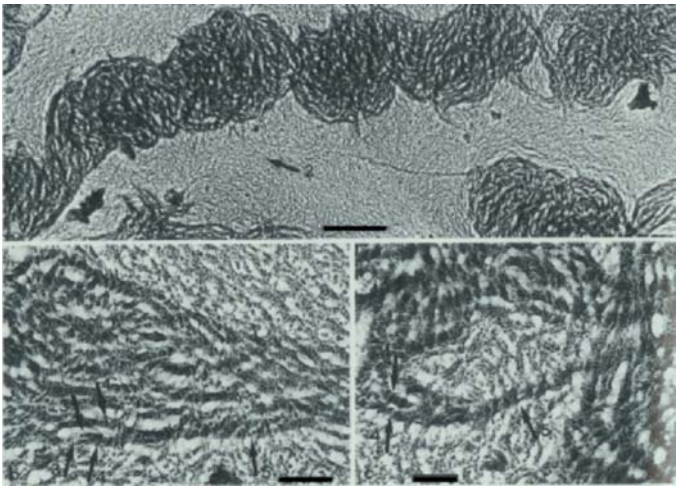

Fig. 7.5 Details of chromosome fibers showing the different organizational levels of nucleofilaments (**Section 3.6**). bar (**a**) 1 µm; (**b**) and (**c**) 0.2 µm. Reproduced from ***(21)*** with permission of the publishers

Fig. 7.6 A prophase nucleus of *P. micans* pretreated with BSA and then fixed according to Karnovsky–Soyer (**Section 3.7**), showing the well-preserved fibrillar structure of the chromosomes. Bar, 1 µm. Reproduced from **ref.** ***(32)*** (journal no longer published)

3.8 Immunolocalization of B- and Z-DNA by TEM

Using anti-B- and anti-Z-DNA antibodies and immunofluorescence or immunoelectron microscopy with gold-labelled secondary antibodies, we demonstrated the presence in nuclei of *P. micans* of regions of Z-DNA mainly localised in the periphery of the chromosomes, themselves essentially composed of B-DNA ***(18)***. Here the protocol for immunogold-labelling of TEM sections is described; an analogous method can be used for immunofluorescence on squashes ***(18)*** (*see* **Note 7**) (Fig. 7.7).

1. Incubate pelleted *P. micans* cells in prefixing solution for 1 h.
2. Wash in 0.2 *M* PIPES buffer.
3. Postfix in 2% OsO_4 for 1 h at room temperature.
4. Embed in Epoxy resin.
5. Cut ultrathin sections and deposit on 300-mesh nickel grids.
6. Slightly etch the samples by incubation in 10% v/v H_20_2 for 10 min at room temperature ***(33)***, wash 2× with dH_2O (all incubations are performed in a humid chamber).
7. Block nonspecific epitopes by incubation for 15 min at room temperature with normal goat serum (1/10 in PBS).
8. Primary and secondary antibodies are diluted in PBS, 0.1% BSA.
9. Incubate with the first antibody for 1 h at 37°C; we used a mixture of a human anti-B-DNA and a polyclonal rabbit anti-Z-DNA antibody ***(18)***.
10. Wash with PBS.
11. Incubate with the secondary antibody; we used a mixture of goat antirabbit and goat antihuman (1/25) coupled respectively with 5 or 7 nm colloidal gold particles ***(18)***.
12. Wash with PBS and dH_2O.
13. Stain in saturated uranyl acetate in ethanol solution for 15 min.

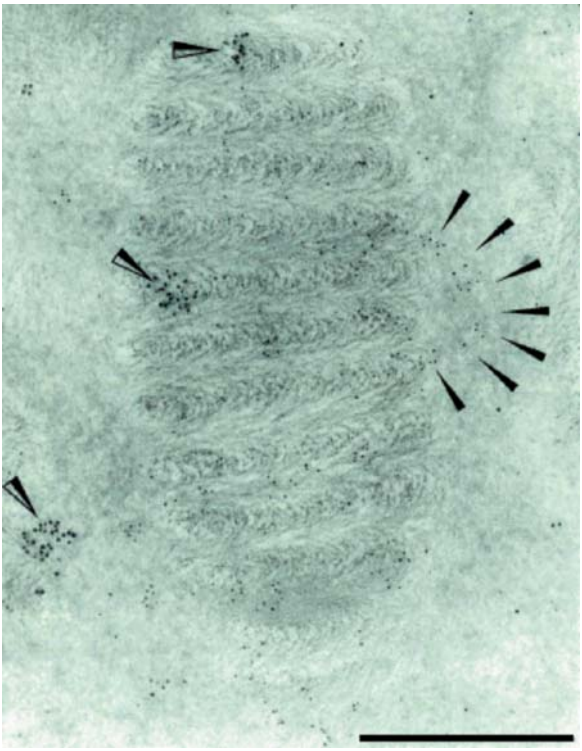

Fig. 7.7 Region of a nucleus of *P. micans* double-immunolabelled with antibodies against B- and Z-DNA. B-DNA was detected with a polyclonal human anti-B-DNA antibody followed by goat anti-human coupled to 5-nm gold particles, and Z-DNA with a rabbit polyclonal anti-Z-DNA antibody followed by goat anti-rabbit coupled to 7-nm gold particles. B-DNA is visible in the chromosome and the nucleoplasm, in which an extrachromosomal loop is visible (*black arrows*). Z-DNA is visible in clumps in the chromosome, typically located in peripheral regions (*black* and *white arrows*) (**Section 3.8**). Bar, 0.5 µm. Reproduced with permission from ***(18)***, copyright 1990 The Rockefeller University Press

3.9 Fast-Freezing (Slam Freezing) and Freeze-Substitution for TEM

This method ***(34, 35)*** preserves the structure of nucleoli of *P. Micans* ***(31)*** and the antigenicity of proteins better than conventional preparation methods due to the rapidity of the freeze-fixation. We employed it to immunolocalise the major basic nuclear DNA-binding protein histone-like *C. cohnii* (HCc) of this dinoflagellate ***(36)*** (Figs. 7.8 and 7.9).

1. A drop (20 µL) of a pellet of *P. micans* cells on filter paper (10 mm^2) is mounted on the specimen holder of a cryovacublock device (Reichert-Jung, Leica) and slammed against a polished copper block precooled with liquid helium at −269°C, then transferred into liquid N_2 prior to freeze substitution.

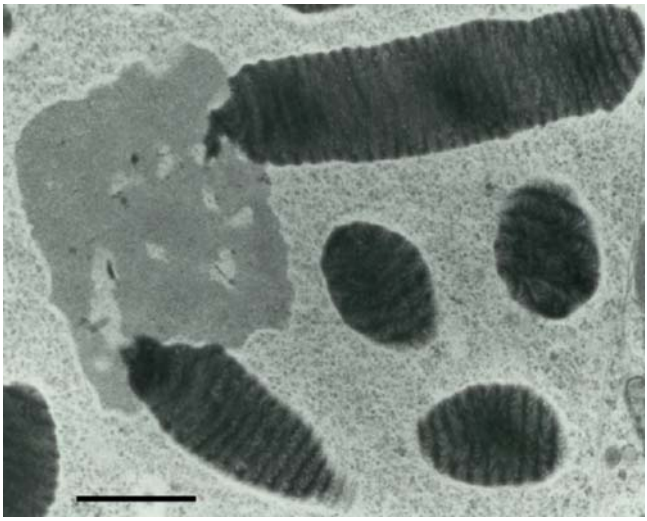

Fig. 7.8 A *P.micans* cell prepared by fast-freeze fixation and freeze-substitution (**Section 3.9**), showing two chromosomes with their unwound telomeric region generating a nucleolus that comprises only fibrillar and fibrillo–granular regions. Bar, 1 µm. Reproduced from ***(29)*** with permission of the Company of Biologists

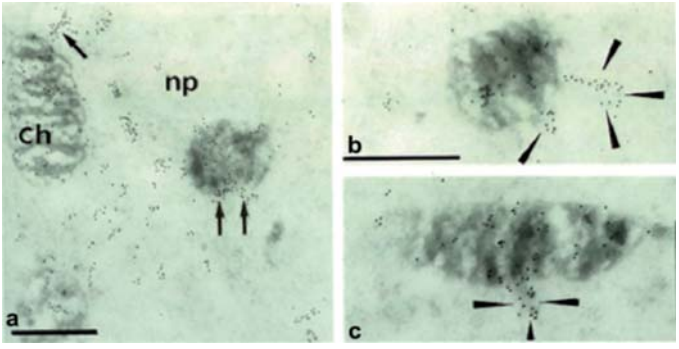

Fig. 7.9 Nuclei of *Crypthecodinium cohnii* immunolabelled with an antibody against the histone-like protein HCc followed by a secondary antibody coupled to 10-nm gold particles (**Section 3.9**). **a** Immunolabelling is detected in the nucleoplasm (*np*) and in the chromosomes (*Ch*), especially in their periphery (*arrows*) (bar, 0.5 µm). In cross (**b**) and longitudinal (**c**) sections, the labelling is located on peripheral loops of the chromosomes (*arrowheads*) (bar, 1 µm). Reproduced from **ref.** ***(32)*** (journal no longer published)

2. Freeze-substitution is in 2% OsO_4 in acetone at −80°C for 3 days using a Cryocool apparatus, in the presence of a molecular sieve to absorb the water extracted from the sample. Gradually raise the temperature to −30°C and kept at −30°C for 2 h.
3. Thaw the samples at room temperature for 1 h and wash successively in pure acetone, absolute ethanol, then propylene oxide, and embed in Epoxy resin.

4. Cut ultrathin sections and label with primary antibody (in our case an affinity-purified polyclonal antibody against the protein HCc ***(36)***) followed by a gold-labelled secondary antibody (*see* **Section 3.8**).
5. Contrast the sections with 2% aqueous uranyl acetate and lead citrate (*see* **Section 3.7**).

4 Notes

1. F/2 medium is available from Aquatic Eco-Systems, Apopka, FL, USA.
2. Protocols to prepare carbon films on EM grids and to charge them positively are beyond the scope of this chapter. Carbon-covered grids are available commercially (e.g. SPI, or Electron Microscopy Sciences, Hatfield, PA, USA).
3. *P. micans* can be obtained from the Botany School, Cambridge University, UK and *C. cohnii* from the ATCC (strain 50050).
4. Because the S phase is short, S phase cells are contaminated with late G1 and/or G2/early M cells. This problem can be overcome by adding aphidicolin at 30 μ*M* to the culture to block cells in early S-phase ***(15)***.
5. Incubation in 2 N HCl for 30 min at room temperature may also be used to denature DNA.
6. We used Epon for embedding in our published work, but this is no longer available.
7. This description is taken from **ref.** ***(18)***, where secondary antibodies from goat were used. When different primary and secondary antibodies are used, the blocking conditions and antibody dilutions should be reevaluated.

Acknowledgments The author thanks previous students (especially Drs. O.K. Haapala and M. Herzog), the research engineer Dr. M. L.Géraud, and the technicians (especially Mrs. M. Albert and D. Saint-Hilaire) for their important participation during her whole scientific career. Without teamwork using the specific competence of each member, scientific work is quasi-impossible.

References

1. Soyer-Gobillard, M.O. and Moreau, H. (2000) Dinoflagellates, in *Encyclopedia of microbiology* (Alexander, M., Bloom, B. R., Hopwood. D. A., Hull, R., Iglewski, B. H., Laskin, A. I., Oliver, S. G., Schaechter, M., Summers, W. C., and Lederberg, J., eds.), Vol 2, Academic Press, San Diego, CA. pp. 42–54.
2. Spector, D. L. (1984) Dinoflagellate nuclei. In: *Dinoflagellates* (Spector, D. L., ed.), Academic Press, New York, pp 107–147.
3. Grassé, P. P. and Dragesco, J. (1957) L'ultrastructure du chromosome des Péridiniens et ses conséquences génétiques. *C. R. Acad. Sci. Paris* **245b**, 2447–2452.
4. Bhaud, Y. and Soyer-Gobillard, M. O. (1986) DNA Synthesis and cell cycle of a primitive dinoflagellate *Prorocentrum micans* Ehr. *Protistologica* **22**, 23–30.
5. Bodansky. S., Mintz, L. B., and Holmes, D. S. (1979) The mesocaryote *Gyrodinium cohnii* lacks nucleosomes. *Biochem. Biophys. Res. Comm*. **88**, 1329–1336.

6. Herzog, M. and Soyer, M. O. (1981) Distinctive features of dinoflagellate chromatin. Absence of nucleosomes in a primitive species *Prorocentrum micans* E. *Eur. J. Cell Biol*. **23**, 295–302.
7. Herzog, M., de Marcillac, G. D., and Soyer, M. O. (1982) A high level of thymine replacement by 5-hydroxymethyluracil in nuclear DNA of the primitive dinoflagellate *Prorocentrum micans* E. *Eur. J. Cell Biol*. **27**, 151–155.
8. Sigee, D. C. (1983) Structural DNA in genetically active DNA in dinoflagellate chromosomes. *Biosystems* **16**, 203–210.
9. Barbier, M., Leighfield, T. A., Soyer-Gobillard, M. O., and Van Dolah, F. M. (2003) Permanent expression of a cyclin B homologue in the cell cycle of the dinoflagellate Karenia brevis. *J. Eukaryot. Microbiol*. **50**, 123–131.
10. Tuttle, R. C. and Loeblich, A. R. (1975) An optimal growth medium for the Dinoflagellate Crypthecodinium cohnii. *Phycologia* **14**, 1–8.
11. Haapala, O. K. and Soyer, M. O. (1973) Structure of Dinoflagellate chromosomes. *Nature* **244**, 195–197.
12. Honda, S. I, Hongladarom, T., and Laties, G. G. (1966) A new isolation medium for plant organelles. *J. Exp. Bot*. **17**, 460–472.
13. Bhaud, Y., Soyer-Gobillard, M. O., and Salmon, J. M. (1988) Transmission of gametic nuclei through a fertilization tube during mating in a primitive dinoflagellate, *Prorocentrum micans* Ehr. *J. Cell Sci*. **89**, 197–206.
14. Bhaud, Y., Salmon, J. M., and Soyer-Gobillard, M. O. (1991) The complex cell cycle of the dinoflagellate protoctist *Crypthecodinium cohnii* as studied in vivo and by cytofluorometry. *J. Cell Sci*. **100**, 675–682.
15. Bhaud. Y., Guillebault, D., Lennon, J. F., Defacque, H., Soyer-Gobillard, M. O., and Moreau, H. (2000) Morphology and behaviour of dinoflagellate chromosomes during the cell cycle and mitosis. *J. Cell Sci*. **113**, 1231–1239.
16. Rizzo, P. J. (1991) The enigma of the dinoflagellate chromosome. *J. Protozool*. **38**, 246–252.
17. Soyer-Gobillard, M. O., Gillet, B., Géraud, M. L., and Bhaud, Y. (1999) Dinoflagellate chromosome behavior during stage of replication. *Internatl. Microbiol*. **2**, 93–102.
18. Soyer-Gobillard, M. O., Géraud, M. L., Coulaud, D., Barray, M., Théveny, B., Révet B., and Delain, E. (1990) Location of B- and Z-DNA in the chromosomes of a primitive eukaryote dinoflagellate. *J. Cell Biol*. **111**, 293–308.
19. Miller, O. L. and Bakken, A. H. (1972) Morphological studies of transcription. *Acta Endocrinol. (suppl.)* **168**, 155–177.
20. Soyer, M. O. and Herzog, M. (1985) The native structure of dinoflagellate chromosomes. Involvement of structural RNA. *Eur. J. Cell Biol*. **36**, 334–342.
21. Herzog, M. and Soyer, M. O. (1983) The native structure of dinoflagellate chromosomes and their stabilization by Ca^{2+} and Mg^{2+} cations. *Eur. J. Cell Biol*. **30**, 33–41.
22. Dubochet, J., Ducommun, M., Zollinger, M., and Kellenberger, E. (1971) A new preparation for dark-field electron microscopy of biomacromolecules. *J. Ultrastruct. Res*. **35**, 147–167.
23. Haapala, O. K. and Soyer, M. O. (1974) Electron microscopy of whole-mounted chromosomes of the Dinoflagellate *Gyrodinium cohnii. Hereditas* **78**, 146–150.
24. Soyer, M. O. and Haapala, O. K. (1974) Electron microscopy of RNA in Dinoflagellate chromosomes. *Histochemistry* **42**, 239–246.
25. Soyer, M. O. and Haapala, O. K. (1973) Filaments extra-chromosomiens: variations et relations avec l'enveloppe nucléaire pendant la division chez les dinoflagellés. *J. Microsc*. **19**, 267–270.
26. Soyer, M. O. and Haapala, O. K. (1974) Division and function of dinoflagellate chromosomes. *J. Microsc*. **19**, 137–146.
27. Livolant, F. and Bouligand, Y. (1978) New observations on the twisted arrangement of Dinoflagellate chromosomes. *Chromosoma* **68**, 21–44.
28. Livolant, F. and Bouligand, Y. (1980) Double helical arrangement of spread Dinoflagellate chromosomes. *Chromosoma* **80**, 97–118.
29. Oakley, B. and Dodge, J. (1979) Evidence for a double helically coiled toroidal chromonema in the dinoflagellate chromosome. *Chromosoma* 70, 277–291.

30. Soyer, M. O. and Haapala, O. K. (1974) Structural changes of dinoflagellate chromosomes by pronase and ribonuclease. *Chromosoma* **50**, 179–192.
31. Soyer-Gobillard, M. O. and Géraud, M. L. (1992) Nucleolus behaviour during the cell cycle of a primitive dinoflagellate eukaryote, *Prorocentrum micans* Ehr., seen by light microscopy and electron microscopy. *J. Cell Sci*. **102**, 475–485.
32. Soyer, M. O. (1977) Une modification de la technique de Karnovsky pour la préservation optimale des structures nucléaires chez les Dinoflagellés. *Biol. Cell*. **30**, 297–300.
33. Zollinger, M. and Bendayan, M. (1983) Ultrastructural localization of antigenic sites on osmium-fixed tissues: applying the protein A gold technique. *J. Histochem. Cytochem*. **31**, 101–109.
34. Escaig, J., Geraud, G., and Nicolas, G. (1977) Rapid freezing of biologic tissue. Measurement of temperature and rate of freezing by thin-layer thermocouple. *C. R. Acad. Sci. Hebd. Seances Acad. Sci. D*. **284**, 2289–2292.
35. Nicolas, G. (1991) Advantage of fast freezing fixation followed by freeze-substitution for the preservation of cell integrity. *J. Electron Microsc. Techn*. **18**, 395–405.
36. Géraud, M. L., Sala-Rovira, M., Herzog, M., and Soyer-Gobillard, M. O. (1991) Immunocytochemical localization of the DNA-binding protein HCc during the cell cycle of the histone-less dinoflagellate protoctista *Crypthecodinium cohnii* B. *Biol. Cell*. **71**, 123–134.

Chapter 8
Isolation of Nucleoli from Ehrlich Ascites Tumor Cells and Dynamics of Nascent RNA within Isolated Nucleoli

Marc Thiry and Dominique Ploton

Keywords Nucleolus; Isolation procedure; BrUTP incorporation; Nascent rRNA; Ehrlich tumor cells; Electron microscopy

Abstract Here we describe a new, rapid method for isolating nucleoli from Ehrlich tumor cells that preserves their morphological integrity and high transcriptional activity. Until now, methods for isolation of nucleoli were generally assumed to empty one of their three main compartments, the fibrillar center, of its contents. This new method consists of sonicating cells in an isotonic medium containing $MgSO_4$, spermidine, and spermine, followed by separation of nucleoli through a Percoll density gradient. Using the nonisotopic approach of labelling with BrUTP, we have further investigated the dynamics of nascent ribosomal RNAs (rRNAs) within morphologically intact isolated nucleoli at the electron microscope level. We show that ribosomal transcripts are elongated in the cortex of the fibrillar center and then enter the surrounding dense fibrillar component.

1 Introduction

The nucleolus is a highly visible structure under the optical microscope in the nucleus of eukaryotic cells, and is essentially specialised in ribosome biogenesis. Synthesis of rRNA and 18S, 5.8S, and 28S RNAs, as well as maturation and assembly of preribosomal particles occur in this nuclear compartment ***(1)***. At the ultrastructural level, the nucleolus consists of three main substructures, the fibrillar center, the dense fibrillar component, and the granular component. It is not delimited by a membrane, but is generally surrounded by a discontinuous layer of condensed chromatin termed the perinucleolar chromatin, which at some places penetrates inside the nucleolar body and comes into contact with the fibrillar center, where it is termed the intranucleolar chromatin ***(2)***.

However, the relationships between the structure and the functions of the nucleolus are, as yet, unclear. In particular, it is generally accepted that transcription occurs in the fibrillar regions, but whether this is within the dense fibrillar component or at

R. Hancock (ed.) *The Nucleus: Volume 1: Nuclei and Subnuclear Components*,

the border of the dense fibrillar component and the fibrillar center, or even within the fibrillar centers, remains a matter of much debate ***(3–12)***. In this regard, a few years ago we reported a new method for incorporation of BrUTP within optimally preserved cells that allowed us to follow the kinetics of rRNA synthesis and maturation ***(13)***. The results of this work showed that rRNAs that had incorporated BrUTP were initially localised both within the fibrillar center and in the inner part of the dense fibrillar component. However, the speed of rRNA synthesis in vivo is so high (25–50 nucleotides per second, ***(14)***) that this localization of incorporated BrUTP could represent both sites of incorporation and of accumulation. To resolve this problem, we used isolated nucleoli, a system in which transcription is slowed down ***(14, 15)***.

Classic methods for isolating nucleoli from mammalian cells involve either one or two steps. The two-step techniques consist of first producing a pure nuclear fraction and then isolating nucleoli from this fraction ***(16, 17)***. One-step procedures, on the other hand, avoid isolating nuclei and involve direct sonication of cells in a hypotonic medium ***(18, 19)***. However, the methods currently in use fail to yield morphologically intact nucleoli; specifically, the fibrillar centers of nucleoli isolated by these procedures are frequently largely empty, possibly due to loss of protein during isolation ***(18, 20)***.

To overcome these drawbacks, we developed a new, rapid method for isolating nucleoli from Ehrlich ascites tumor (ELT) cells ***(21)***. This procedure involves the sonication of cells in an isotonic buffer containing $MgSO_4$, spermidine, and spermine and centrifuging the crude nucleolar fraction through a Percoll/isotonic buffer density gradient. Under these conditions, the ultrastructure of isolated nucleoli is very well preserved (Fig. 8.1).

Moreover, we have shown that nucleoli isolated by this procedure exhibit the same staining pattern of argyrophilic nucleolar organiser regions (AgNORs) as that observed in situ. In addition to preserving the morphological integrity of nucleoli, in vitro transcription experiments using tritiated GTP demonstrated that the isolated nucleoli preserve a high transcriptional activity. These results highlight the reliability of our isolation procedure as a tool for the biochemical and ultrastructural study of the nucleolus. Nucleoli isolated in this way should provide good material for investigating and purifying nucleolar proteins and enzymes, especially, but not only, those of the fibrillar centers. In this regard, a new AgNOR protein was identified on Western blots of proteins extracted from ELT nucleoli isolated by our procedure ***(22)***. The integrity of the isolated nucleoli and their ability to incorporate tritiated GTP at a high rate for a considerable period further highlight the prospects they offer for studying rDNA transcription. In this way, an immunocytological approach for detecting nascent RNA within isolated nucleoli was developed ***(11)*** that involves incubation of isolated nucleoli in medium containing BrUTP and immunocytological detection of BrUTP incorporated into nascent RNA. Using pulse–chase experiments with BrUTP and an elongation inhibitor, cordycepin, it was possible to precisely localise the initial sites of BrUTP incorporation in isolated nucleoli (Fig. 8.2). Our data showed that BrUTP incorporation initially takes place in the fibrillar centers and that elongating rRNAs rapidly enter the surrounding dense fibrillar component.

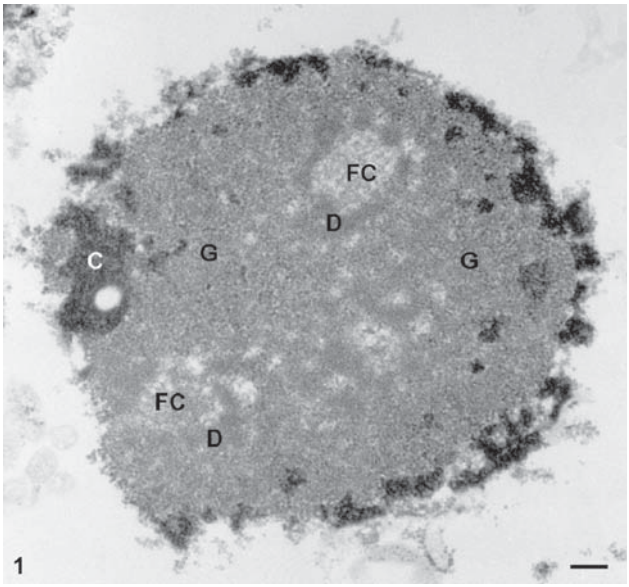

Fig. 8.1 A nucleolus of an Ehrlich tumor cell isolated by the procedure described here. The three major components are very well seen: the fibrillar center (*FC*), the dense fibrillar component (*D*) and the granular component (*G*). The perinucleolar and intranucleolar clumps of condensed chromatin (*C*) are also obvious. Bar, 0.2 µm

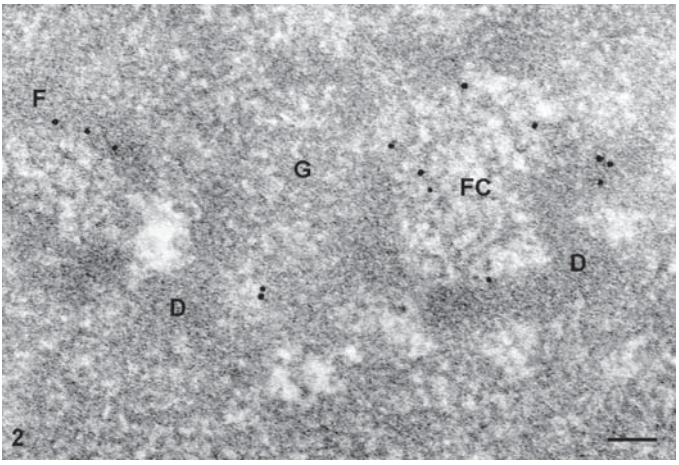

Fig. 8.2 Ultrastructural localization of nascent rRNA molecules within the nucleolus. Ehrlich tumor cells were pulse-labelled with BrUTP for 15 min and BrUTP-labelled rRNAs were detected by immunogold labelling of ultrathin sections of isolated nucleoli. Gold particles are preferentially located in the cortex of the fibrillar center (*FC*) and in the dense fibrillar component (*D*). No label occurs in the granular component (*G*). Bar, 0.1 µm

2 Materials

2.1 Isolation of Nucleoli

1. Hypertetraploid Ehrlich ascites tumor (ELT) cells are cultured at 37°C in medium composed of 45% (v/v) NCTC 109 (Difco Laboratories, Detroit, MI, USA), 45% Hanks' balanced salt solution (Gibco-BRL; Invitrogen, Merelbeke, Belgium) and 10% fetal bovine serum (Gibco-BRL) with 100 U/mL penicillin (Gibco-BRL).
2. Phosphate-buffered saline 1 (PBS1): 150 m*M* NaCl, 3 m*M* Na_2HPO_4, 1 m*M* KH_2PO_4, adjust pH to 7.2. Store at 4°C, stable for up to 1 year (*see* **Note 1**).
3. Isolation buffer: prepare a 10× stock solution with 1.427 *M* NaCl, 45 m*M* KCl, and 20 m*M* 3-(*N*-morpholino)propane-sulphonic acid (Mops; Janssen Chimica, Geel, Belgium), 25 m*M* $MgSO_4$, and adjust the pH to 7.4. Store at 4°C, stable for up to 1 year.
4. Polyamines: stock solutions of 200 m*M* spermidine (Sigma-Aldrich, St. Louis, USA) and 200 m*M* spermine (Sigma-Aldrich) in bidistilled water. Store at −30°C in aliquots.
5. Cocktail of protease inhibitors:
   (a) Stock solution of 0.1 *M* phenylmethylsulfonylfluoride (PMSF; Fluka Biochemika, Buchs, Switzerland) in isopropanol, store at room temperature, stable for 15 days.
   (b) Stock solution with 0.7 mg/mL of pepstatin, 0.7 mg/mL of leupeptin, and 1 mg/mL of aprotinin (all from Sigma-Aldrich) in 1× isolation buffer, store at −30°C in aliquots.
6. B buffer: 1× isolation buffer containing 0.2 m*M* spermidine, 0.4 m*M* spermine, 0.1 m*M* PMSF, 0.7 µg/mL pepstatin, 0.7 µg/mL leupeptin, and 1 µg/mL aprotonin. Prepare just before use.
7. Percoll density gradient: dilute 9 mL of Percoll (Sigma-Aldrich) in 1 mL of 10× isolation buffer. Take 4.4 mL of this solution, dilute in 5.6 mL of 1× isolation buffer, and add 0.1 m*M* PMSF, 0.7 µg/mL pepstatin, 0.7 µg/mL leupeptin, and 1 µg/mL aprotinin. Prepare fresh in a sterile hood just before use.

2.2 In Vitro Transcription Reactions

1. TS buffer: 25% (v/v) glycerol, 100 m*M* KCl, 50 m*M* Tris-HCl pH 7.0, 2 m*M* $MgCl_2$, and 0.5 m*M* EGTA. Store at 4°C, stable for up to 1 year.
2. Polyamines: *see* **Section 2.1.4.**
3. RNase inhibitor 40 U/µL (Roche, Meylan, France). Store at −30°C.
4. Cocktail of protease inhibitors:
   (a) Set of protease inhibitors (Roche): 30 µg/mL antipain, 2 µg/mL aprotinin, 100 µg/mL EDTA, 0.5 µg/mL leupeptin, 200 µg/mL Pefabloc, 30 µg/mL

phosphoramidon, 5 µg/mL bestatin, 0.7 µg/mL pestatin, 10 µg/mL E-64, and 10 µg/mL chymostatin. Store at −30°C in small aliquots.

(b) Prepare a stock solution with 0.1 *M* PMSF (Fluka Biochemika) in isopropanol, store at room temperature, stable for 15 days.

5. Nucleotides:

   (a) Prepare a stock solution with 20 m*M* ATP, CTP, and GTP (Roche) in 50 m*M* Tris-HCl. Store at −30°C in small aliquots.

   (b) Prepare a stock solution of 20 m*M* 5-bromouridine 5-triphosphate sodium salt (Roche) in 50 m*M* Tris-HCl. Store at −30°C in small aliquots.

6. TSC buffer: TS buffer containing 0.2 m*M* spermidine, 0.4 m*M* spermine, 25 U/mL RNase inhibitor, 1 m*M* PMSF, a set of protease inhibitors diluted 1/30, 0.2 m*M* ATP, GTP, and CTP, and 0.4 m*M* BrUTP. Prepare just before use.

2.3 Preparation of Isolated Nucleoli for Electron Microscopy

1. Sörensen's buffer: 0.1 *M* Na_2HPO_4/NaH_2PO_4, pH 7.4, store at 4°C, stable for up to 1 year.
2. Fixative: 4% (w/v) formaldehyde (from a 5-mL ampule of 20%; Ladd Research, Holly Court, VT, USA) and 0.1% (w/v) glutaraldehyde (from a 2-mL ampule of 70%; Ladd Research) in Sörensen's buffer, store at 4°C, stable for 15 to 21 days.
3. A series of ethanol solutions: 70% and 90% (v/v) in bidistilled H_2O, and absolute ethanol.
4. Embedding resin: in a 25-mL Erlenmeyer flask mix 5 g of dodecenyl succinic anhydride (DDSA; Ladd Research) with 5 g of methyl nadic anhydride (MNA; Ladd Research), 0.3 g of 2,4,6-dimethylaminomethyl phenol (DMP-30; Ladd Research), and 10 g of epikote 812 (Fluka Biochemika), close the flask, stir until the appearance of bubbles, and let the mixture rest until the complete disappearance of bubbles. Store at room temperature, stable for 2 to 5 days.
5. Gelatin capsules for embedding for electron microscopy (Ladd Research).
6. Ultramicrotome (Reichert Ultracut S; Leica) with diamond knife (Drukker, Element Six B.V., The Netherlands).
7. 200- to 400-mesh nickel grids with a collodion film for electron microscopy (Ladd Research).
8. Anticapillary forceps (Ladd Research).

2.4 Immunolabelling Procedure

1. Phosphate-buffered saline 2 (PBS-2): 0.14 *M* NaCl, 6 m*M* Na_2HPO_4, 4 m*M* KH_2PO_4, stable at 4°C for up to 1 year.

2. PBSA buffer: PBS 2, add 0.2% (w/v) bovine serum albumin (BSA, fraction V, Sigma-Aldrich) and adjust the pH to 7.2 or 8.2.
3. PBSB buffer: PBS 2, add 1% BSA and adjust the pH to 7.2 or 8.2.
4. Mouse monoclonal anti-bromodeoxyuridine antibody (100 µg/ mL, Roche), store at −20°C in aliquots.
5. Goat anti-mouse IgG coupled to 10-nm-diameter gold particles (Roche), stable at 4°C for up to 3 years.

2.5 Staining of Sections

1. 50% ethanolic uranyl acetate: 0.5 g of uranyl acetate, 12.5 mL of boiled H_2O, 12.5 mL of ethanol, store at 4°C in a brown glass container or otherwise protected from direct light. Stable at 4°C for up to 1 year, filter (0.22-µm pore size) before use.
2. Aqueous lead citrate: 4.2% (w/v) sodium citrate, 2.6% (w/v) lead nitrate, add concentrated NaOH until clearing of the mixture. Stable at 4°C for up to 1 year, filter (0.22-µm pore size) before use.

3 Methods

3.1 Isolation of Nucleoli

1. Scrape off ELT cells from their dishes (*see* **Note 2**).
2. Harvest the cells at 4°C by centrifuging for 5 min at 375×*g* (*see* **Note 3**).
3. Wash the cell pellet at 4°C in PBS1.
4. Harvest cells at 4°C by centrifuging for 4 min at 375×*g*.
5. Wash the cells (~10^8 cells) by resuspending at 4°C in 3 mL of B buffer (*see* **Notes 4** and **5**).
6. Harvest the cells at 4°C by centrifuging for 4 min at 375×*g*.
7. Resuspend the cell pellet at 4°C in 3 mL of B buffer.
8. Sonicate the cells for 15–20 sec at 4°C using the half-duty cycle mode and one-third of the power of a 375 W 20 KHz sonicator (Sonics and Materials, Danbury, UK) (*see* **Note 6**).
9. Spin the crude nucleolar fraction at 4°C through 3 mL of 44% Percoll/B buffer by centrifuging for 10 min at 3,840×*g* (*see* **Note 7**).
10. Wash the pellet twice at 4°C in 3 mL of B buffer by centrifuging for 5 min at 665×*g*.
11. Keep the pellet containing nucleoli on ice.

3.2 In Vitro Transcription Reactions

1. Suspend 50 µL of isolated nucleoli in 250 µL of TSC buffer (*see* **Note 8**).
2. After incubation for 1 to 30 min at 37°C, harvest the nucleoli at room temperature by centrifuging for 2 min at 665×*g*.

3.3 Preparation of Isolated Nucleoli for Electron Microscopy

1. Fix the samples with fixative for 60 min at 4°C.
2. Eliminate the fixative with a pipette and wash the samples three times in Sörensen's buffer (the pellet remains intact).
3. Eliminate the buffer with a pipette and dehydrate the samples in a graded series of ethanol solutions: 15 min in 70% ethanol at 4°C, 5 min in 95% ethanol at room temperature, 3× 20 min in 100% ethanol at room temperature.
4. Eliminate the ethanol with a pipette and infiltrate the samples at room temperature in a graded series of Epon solutions: 60 min in ethanol/Epon 2/1 (v/v), 60 min in ethanol/Epon 1/1(v/v), 60 min in ethanol/Epon 1/2 (v/v), and overnight in pure Epon.
5. Transfer the samples to gelatin capsules by pipette and fill the capsules with fresh resin.
6. Polymerise the resin for 3 to 4 days at 42°C.
7. Cut ultrathin sections (60–90 nm) of the Epon-embedded samples with a diamond knife.
8. Mount the sections on 200- to 400-mesh nickel grids with a collodion film.

3.4 Immunolabelling Procedure

1. Incubate grids for 30 min at room temperature on a drop of PBSB buffer (pH 7.2) containing normal goat serum diluted 1/30, with the face of sections in contact with the drop (*see* **Note 9**).
2. Transfer grids onto a drop of monoclonal anti-bromodeoxyuridine antibody diluted 1/50 in PBSA buffer (pH 7.2) containing normal goat serum diluted 1/50, incubate for 4 h at room temperature.
3. Rinse grids successively in four 15-mL beakers filled with PBSB buffer (pH 7.2).
4. Rinse grids in a 15-mL beaker filled with PBSA buffer (pH 8.2).
5. Incubate grids for 60 min at room temperature with goat anti-mouse IgG coupled to 10-nm-diameter gold particles, diluted 1/40 in PBSA buffer (pH 8.2).
6. Rinse grids successively in four 15-mL beakers filled with PBSB buffer (pH 8.2).
7. Rinse grids successively in four 15-mL beakers filled with bidistilled water.
8. Blot and dry the grids.

3.5 Staining of Sections

1. Transfer grids into a Petri dish with a reduced CO_2 concentration (place NaOH pellets in the dish). Incubate for 5 min at room temperature in darkness on a drop of 50% ethanolic uranyl acetate.
2. Rinse grids successively in three 25-mL beakers filled with boiled bidistilled water.
3. Dry the grids on filter paper.
4. Transfer the grids into a Petri dish with reduced CO_2 concentration (place NaOH pellets in the dish) for 5 min at room temperature on a drop of aqueous lead citrate.
5. Rinse grids successively in three 25-mL beakers filled with boiled bidistilled water.
6. Dry the grids on filter paper.
7. Examine the sections in a transmission electron microscope at 60–80 KV (*see* **Note 10**).

4 Notes

1. Sterilise glassware, tools, and H_2O to be used in this procedure.
2. We describe the method that we use for isolating nucleoli from ELT cells. However, this procedure has also been applied successfully to other cell lines (HeLa and Sf9).
3. When ELT cells are taken directly from the peritoneal cavity of mice, they are washed several times in PBS buffer at 4°C by centrifuging for 4 min at 375×*g*.
4. When ELT cells are incubated for 10 min in a hypotonic medium, the fibrillar centers of their nucleoli are already altered. Specifically, we observe partially reticulated nucleoli where the fibrillar centers are markedly shrunken and/or appear as a hole partially surrounded by the dense fibrillar component and/or have disappeared, the dense fibrillar component forming disorganised strands. To overcome this drawback, we use an isotonic buffer matching physiological conditions as closely as possible (~280 mOsm/kg, ***(23)***).
5. It has been amply shown that Mg^{2+} and Ca^{2+} ions added to the isolation buffer, at concentrations between certain critical values, stabilise both isolated nuclei and nucleoli ***(16, 18, 24, 25)***. In our hands, unfortunately, Ca^{2+} ions even at a low concentration (0.7 m*M*) seem to cause the fibrillar centers to shrink, whereas Mg^{2+} ions at a high concentration give rise to isolated nucleoli that appear extremely compact in electron micrographs ***(26)***. To overcome these drawbacks, we choose to include $MgSO_4$, spermidine and spermine in the isolation buffer; the two polyamines are known to prevent degradation of nucleoli by binding to both DNA and RNA and thereby stabilizing them ***(27)***. By including these two polyamines in the buffer, we could avoid using high concentrations of Mg^{2+} ions. In fact, spermidine alone is sufficient to preserve most of the

nucleolar structure, except for the peripheral part of the fibrillar centers, which is frequently surrounded by a halo. Increasing the spermidine concentration to 0.4–1 m*M* does not prevent this damage, but further addition of spermine prevented the appearance of the halo without modifying the nucleolar morphology. A good combination of additives that protects the nucleoli while avoiding excessive compaction thus appears to be 2.5 m*M* $MgSO_4$, 0.2 m*M* spermidine, and 0.4 m*M* spermine.

6. To check the efficiency of the sonication step, 20 µL of the crude nucleolar fraction is examined under a phase contrast microscope. If the proportion of nucleoli to intact nuclei is low, sonication is continued until the disappearance of the majority of intact nuclei.
7. To avoid osmotic shock during subsequent washing, we prefer to make the density gradients with a compound that does not significantly alter the osmolarity even at high concentration ***(28)***. We therefore spin the crude nucleolar fraction through a density gradient of Percoll instead of sucrose in isolation buffer, and when freed of Percoll, the nucleoli exhibit an ultrastructural morphology resembling that observed in situ ***(21)***.
8. To determine whether pre-rRNAs enter new compartments during the elongation process, the distribution of label can be analysed in nucleoli submitted to pulse-labelling with BrUTP followed by a chase with UTP ***(11)***. Nucleoli are pulse-labelled for 5 to 10 min at 37°C, centrifuged for 1 min at 665×*g*, washed in 8 mL of TS buffer containing 0.4 m*M* UTP, and resuspended in 500 µL of TS buffer containing 0.4 m*M* UTP instead of BrUTP for 15 or 20 min at 37°C, before fixation as described above.

   To identify the initial sites of rRNA elongation, nucleoli are incubated with BrUTP after a transient inhibition of elongation by cordycepin ***(11)***, which leads to premature termination of transcription and release of incomplete transcripts from their templates ***(29, 30)***. In practice, isolated nucleoli are suspended in TS buffer containing 0.4 m*M* cordycepin–5′-triphosphate (Sigma-Aldrich) at 37°C for 15 min, centrifuged for 1 min at 665×*g*, washed in 8 mL of TS buffer containing 0.4 m*M* UTP, and resuspended in 500 µL of TS buffer containing 0.4 m*M* BrUTP for 15 min at 37°C. Fixation and embedding are performed as described above. Control experiments are carried out by suspending nucleoli in TS buffer containing 0.2 m*M* ATP instead of 0.4 m*M* cordycepin–5′-triphosphate and by incubating nucleoli in TS buffer containing BrUTP in the presence of cordycepin–5′-triphosphate.
9. Each step is performed on a drop of solution placed on Parafilm in a moist Petri dish; the face of the grid with the ultrathin sections is floated on the drop. The washing procedure is performed in beakers by agitation the grids for 10 sec using anticapillary forceps. Before each incubation of a grid on a drop, its edge and the face devoid of sections must be blotted on filter paper to ensure that it floats on the surface of the subsequent solution.
10. To verify the specificity of in vitro transcription, the following controls are recommended:

    (a) Substitution of BrUTP with UTP in the transcription mix.

(b) Addition of 0.2 µg/mL of the nucleolar transcription inhibitor actinomycin D (Sigma-Aldrich) to the transcription mix, which should strongly reduce labelling. In contrast, addition of 100 µg/mL of α-amanitin, an inhibitor of extranucleolar transcription (Roche), should not affect labelling.
(c) Omission of the primary antibody.
(d) Substitution of the secondary colloidal gold-coupled antibody with a solution of gold lacking the antibody tag.

Acknowledgments The authors acknowledge the skilful technical assistance provided by F. Skivée. This work received financial support from the Fonds National de la Recherche Scientifique Belge (grant n° 3.4540.06) to M.T., and from the Ligue Régionale de l'Aube and the Association pour la Recherche sur le Cancer (grant N° 4497) to D.P.

References

1. Thiry M and Lafontaine DL. (2005) Birth of a nucleolus: the evolution of nucleolar compartments. *Trends Cell. Biol*. **15**, 194–199.
2. Derenzini M, Pasquinelli G, O'Donohue MF, Ploton D, and Thiry M. (2006) Structural and functional organization of ribosomal genes within the mammalian cell nucleolus. *J. Histochem. Cytochem*. **54**, 131–145.
3. Goessens G. (1976) High resolution autoradiographic studies of ehrlich tumour cell nucleoli. Nucleolar labelling after (3H]actinomycin D binding to DNA or after [3H]TdR or [3H]uridine incorporation in nucleic acids. *Exp. Cell Res*. **100**, 88–94.
4. Fakan S. (1978) High resolution autoradiographic studies on chromatin functions, in *The Cell Nucleus* (Busch H, ed). Academic Press: New York, pp. 3–53.
5. Scheer U and Rose KM. (1984) Localization of RNA polymerase I in interphase cells and mitotic chromosomes by light and electron microscopic immunocytochemistry. *Proc. Natl. Acad. Sci. USA* **81**, 1431–1435.
6. Thiry M, Lepoint A, and Goessens G. (1985) Re-evaluation of the site of transcription in Ehrlich tumour cell nucleoli. *Biol. Cell*. **54**, 57–64.
7. Thiry M and Goessens G. (1991) Distinguishing the sites of pre-rRNA synthesis and accumulation in Ehrlich tumor cell nucleoli. *J. Cell Sci*. **99**, 759–767.
8. Hozak P, Cook PR, Schofer C, Mosgoller W, and Wachtler F. (1994) Site of transcription of ribosomal RNA and intranucleolar structure in HeLa cells. *J. Cell Sci*. **107**, 639–648.
9. Cmarko D, Verschure PJ, Rothblum LI, Hernandez-Verdun D, Amalric F, van Driel R, and Fakan S. (2000) Ultrastructural analysis of nucleolar transcription in cells microinjected with 5-bromo-UTP. *Histochem. Cell Biol*. **113**, 181–187.
10. Biggiogera M, Malatesta M, Abolhassani-Dadras S, Amalric F, Rothblum LI, and Fakan S. (2001) Revealing the unseen: the organizer region of the nucleolus. *J. Cell Sci*. **114**, 3199–3205.
11. Cheutin T, O'Donohue MF, Beorchia A, Vandelaer M, Kaplan H, Defever B, Ploton D, and Thiry, M. (2002) Three-dimensional organization of active rRNA genes within the nucleolus. *J. Cell Sci*. **115**, 3297–3307.
12. Koberna K, Malinsky J, Pliss A, Masata M, Vecerova J, Fialova M, Bednar J, and Raska I. (2002) Ribosomal genes in focus: new transcripts label the dense fibrillar components and form clusters indicative of "Christmas trees" in situ. *J. Cell Biol*. **157**, 743–748.
13. Thiry M, Cheutin T, O'Donohue MF, Kaplan H, and Ploton D. (2000) Dynamics and three-dimensional localization of ribosomal RNA within the nucleolus. *RNA* **6**, 1750–1761.
14. Grummt I. (1978) In vitro synthesis of pre-rRNA in isolated nucleoli, in *The Cell Nucleus* (Busch H, ed). Academic Press: New York, pp. 373–414.

15. Hadjiolov AA. (1985) The nucleolus and ribosome biogenesis. Springer-Verlag, Wien, New York.
16. Zalta J, Zalta JP, and Simard R. (1971) Isolation of nucleoli. A method that combines high yield, structural integrity, and biochemical preservation. *J. Cell Biol*. **51**, 563–568.
17. Muramatsu M, Hayashi Y, Onishi T, Sakai M, and Takai K. (1974) Rapid isolation of nucleoli from detergent-purified nuclei of various tumor and tissue culture cells. *Exp. Cell Res*. **88**, 245–251.
18. Busch H and Smetana K. (1970) The nucleolus. Academic Press: New York, London.
19. Olson MO, Wallace MO, Herrera AH, Marshall-Carlson L, and Hunt RC. (1986) Preribosomal ribonucleoprotein particles are a major component of a nucleolar matrix fraction. *Biochemistry* **25**, 484–491.
20. Olson MO. (1990) The role of proteins in nucleolar structure and function, in *The eukaryotic nucleus, Vol. 2* (Strauss PR, Wilson SH, eds). Telford Press, Caldwell, NJ, pp. 519–559.
21. Vandelaer M, Thiry M, and Goessens G. (1996) Isolation of nucleoli from ELT cells: a quick new method that preserves morphological integrity and high transcriptional activity. *Exp. Cell Res*. **228**, 125–131.
22. Vandelaer M, Thiry M, and Goessens G. (1999) AgNOR proteins from morphologically intact isolated nucleoli. *Life Sci*. **64**, 2039–2047.
23. Delpire E, Duchene C, Goessens G, and Gilles R. (1985) Effects of osmotic shock on the ultrastructure of different tissues and cell types. *Exp. Cell Res*. **160**, 106–116.
24. Higashinakagawa T, Muramatsu M, and Sugano H. (1972) Isolation of nucleoli from rat liver in the presence of magnesium ions. *Exp. Cell Res*. **71**, 65–74.
25. Bachellerie JP, Nicoloso M, and Zalta JP. (1977) Nucleolar chromatin in Chinese hamster ovary cells. Topographical distribution of ribosomal DNA sequences and isolation of ribosomal transcription complexes. *Eur. J. Biochem*. **79**, 23–32.
26. Gfeller E, Stern DN, Russell DH, Levy CC, and Taylor RL. (1972) Ultrastructural changes in vitro of rat liver nucleoli in response to polyamines. *Z. Zellforsch. Mikrosk. Anat*. **129**, 447–454.
27. Busch H, Narayan KS, and Hamilton J. (1967) Isolation of nucleoli in a medium containing spermine and magnesium acetate. *Exp. Cell Res*. **47**, 329–336.
28. Pertoft H and Laurent TC. (1982) Isopycnic separation of cells by centrifugation in percoll gradients. *Prog. Clin. Biol. Res*. **102A,** 95–104.
29. Siev M, Weinberg R, and Penman S. (1969) The selective interruption of nucleolar RNA synthesis in HeLa cells by cordycepin. *J. Cell Biol*. **41**, 510–520.
30. Suhadolnik RJ. (1979) Naturally occurring nucleoside and nucleotide antibodies. *Prog. Nucl. Acids Res. Mol. Biol*. **22**, 193–291.

Chapter 9
Time-lapse Microscopy and Fluorescence Resonance Energy Transfer to Analyze the Dynamics and Interactions of Nucleolar Proteins in Living Cells

Emilie Louvet, Marc Tramier, Nicole Angelier, and Danièle Hernandez-Verdun

Keywords Live cell imaging and dynamics; Fluorescence lifetime imaging microscopy; FLIM; Fluorescence resonance energy transfer; FRET; nucleolus; Prenucleolar bodies; PNB

Abstract The dynamics of proteins play a key role in the organization and control of nuclear functions. Techniques were developed recently to observe the movement and interactions of proteins in living cells; time-lapse microscopy using fluorescent-tagged proteins gives access to observations of nuclear protein trafficking over time, and fluorescence resonance energy transfer (FRET) is used to investigate protein interactions in the time-lapse mode. In this chapter, we describe the application of these two approaches to follow the recruitment of nucleolar processing proteins at the time of nucleolar assembly. We question the role of prenucleolar bodies (PNB) during migration of the processing proteins from the chromosome periphery to sites of ribosomal genes (rDNA) transcription. The order of recruitment of different processing proteins into nucleoli is the consequence of differential sorting from the same PNBs. The dynamics of the interactions between processing proteins in PNBs suggest that PNBs are preassembly platforms for ribosomal RNA (rRNA) processing complexes.

1 Introduction

The analysis of dynamics in living cells is made possible using fluorescent fusion proteins ***(1)***. Time-lapse microscopy can track the movement of large fluorescent complexes in the cell, and the concentration of these complexes can be recorded and quantified in space and with time. In addition, time-lapse analysis of fluorescence resonance energy transfer (FRET) makes it possible to detect interactions between molecules in complexes in living cells. These techniques have been essential for the discovery that the functional organization of nuclei depends on the dynamics of the nuclear machineries, and they are particularly useful to analyze the assembly or disassembly of nuclear domains and the mechanisms controlling these processes ***(2–6)***.

R. Hancock (ed.) *The Nucleus: Volume 1: Nuclei and Subnuclear Components*,

Time-lapse microscopy is based on the recording of signals emitted by fluorescent tags, for example, green fluorescent protein (GFP), coupled to proteins. The sequence of the protein of interest is coupled to the sequence of GFP, and consequently translation of the recombinant protein produces a green signal permitting localization of the overexpressed protein. It is necessary to verify that the recombinant protein is functional in the cell without major disturbances of the endogenous proteins, and that the signal can be recorded in the cell volume with good resolution. Time-lapse FRET analysis is based on the recording of the fluorescence lifetime of a GFP-tagged protein (donor) in the presence of an acceptor ***(7)***. In the presence of a red fluorescent protein (DsRed)-fused acceptor, the lifetime of GFP decreases when FRET occurs, indicating the distance between the two fluorescent tags (GFP and DsRed) compatible with molecular interactions of the two tagged proteins.

One of the fundamental features of nuclear organization is the compartmentation of the machineries dedicated to RNA synthesis and processing ***(8)***. During mitosis, redistribution or inactivation of the nuclear machineries that will be later involved in building nuclear functions in interphase occurs. Consequently, the recruitment of dedicated machineries and formation of discrete nuclear domains are crucial events at the beginning of interphase. To better understand the rebuilding of nuclear functions after mitosis, we investigate nucleolar assembly in real time in living cells. The nucleolus is the ribosome factory of the cell ***(9, 10)***, and its functions depend on the activation and recruitment of the nucleolar machineries involved in transcription of the ribosomal genes (rDNA) and processing of the ribosomal RNAs (rRNAs). The rRNA processing machineries are distributed around the chromosomes during mitosis, and when rDNA transcription is activated during telophase, they are targeted to sites of rRNA synthesis. Along the translocation pathway between the chromosomes periphery and the sites of transcription, prenucleolar bodies (PNBs) are formed ***(11)***. To investigate the role of PNBs in the establishment of nucleolar functions, we have analyzed the dynamics and the possible interactions between processing proteins along the assembly pathway in living cells ***(2)***.

2 Materials

2.1 Cells

1. Permanent human HeLa cell line (ATCC, CCL-2).
2. Culture medium: Eagle's minimum essential medium (MEM) without antibiotics stored at 4°C, supplemented with 10% fetal calf serum (stored at −20°C), 1% non-essential amino acids, and 2 m*M* L-glutamine. Trypsin–ethylene-diamine tetra-acetic acid (EDTA) to detach the cells (all from Invitrogen, Cergy Pontoise, France).
3. Live cell culture and imaging chamber (Ludin observation chamber; Life Imaging Services, Reinach, Switzerland) using round glass cover slips of 32-mm diameter (Menzel-Glaser, Bioblock, France).

2.2 Overexpression of Tagged Proteins

1. Cells are transfected at 60% confluency using Superfect reagent (QIAGEN, Valencia, CA, USA), following the instructions of the manufacturer (MEM without serum during transfection).
2. Nucleolar proteins were inserted into the vector pEGFP-C2 or pDsRed2-C1 (both from BD Biosciences Clontech, Palo Alto, CA, USA). In all cases, GFP and DsRed were fused to the NH_2 terminus of the proteins ***(2)***.
3. Stably transformed cell lines were established expressing GFP-Nop52, GFP-fibrillarin, GFP-B23, GFP-Bop1 ***(12)***, and DsRed-B23. Doubly transfected cells were generated from stably transformed cells transiently transfected with DsRed-B23, DsRed-Nop52, or GFP-Nop52 ***(2)***.

2.3 Time-Lapse Microscopy

1. Microscope: inverted wide-field microscope (Leica DM IRBE; Leica Microsystèmes, Rueil-Malmaison, France). The stage plate is motorized to move in the *x* and *y* directions and movement in the *z* direction is controlled by a piezo-driven microscope objective nanofocusing/scanning device (PIFOC; Physik Instrumente, Karlsruhe, Germany) placed at the base of the objective.
2. Objective: ×100 PlanApo 1.4 numerical aperture (NA) oil (Leica).
3. CCD camera: 5 MHz Micromax 872Y interline (Roper Scientific, Evry, France).
4. Microscope incubator (Life Imaging Services).
5. Lamp: 175 W Xenon housed in a DG4 illuminator (Sutter Instruments, Novato, CA, USA) linked to the microscope by an optical fiber.

2.4 Imaging Software

1. For deconvolution, we use a custom-made software package (Sibarita, 2005).
2. ImageJ, a public-domain Java image-processing program inspired by NIH Image, downloadable from the internet site: http://rsb.info.nih.gov/ij/. Documentation about the application is available on this website.
3. Metamorph (Molecular Devices Corporation, Sunnyvale, CA, USA).

2.5 Time Domain Fluorescence Lifetime Imaging Microscopy (tdFLIM) for FRET

1. A 480 nm excitation wavelength using a picosecond pulsed laser at a 4 MHz repetition rate (Titanium sapphire laser Millenia 5 W/Tsunami 3960-M3BBUPG; Spectra-Physics, Les Ulis, France) is used. Pulse picker (3980–39; Spectra Physics).

2. Wide-field laser illumination under the inverted wide-field microscope (**Sects. 2.3.1** and **2.3.2**) equipped with a dichroic beam splitter, an emission filter for GFP fluorescence (505DRLP and 535AF45, Omega; Optophotonics, Eaubonne, France), and a microscope incubator for temperature and CO_2/air control (Pecon, Erbach, Germany).
3. Time- and space-correlated single photon counting (TSCSPC) detector (Quadrant-Anode detector; Europhoton, Berlin, Germany) at the camera optical port of the microscope for fluorescence decay image acquisition.
4. QA analysis software (Europhoton, Berlin, Germany), then Globals Unlimited image analysis software (University of California, Irvine, CA, USA) to analyze fluorescence decays coming from selected regions of interest.

3 Methods

The dynamics and interactions of nucleolar processing proteins at the time of nucleolar assembly were analyzed. Along the assembly pathway between the chromosome periphery and the nucleolus, PNBs are formed. Our objectives were to compare the traffic of early and late processing proteins in PNBs by time-lapse microscopy and to question the possible formation of complexes in PNBs using FRET. Nucleolar assembly lasted about 1 h 30 min from telophase to early G1, and a previous study indicated a short time window (~15 min) for the recruitment of early processing proteins ***(12)***. Indeed, the open question was whether two types of PNBs, short- and long-lived PNBs, exist or if differential sorting from the same PNBs occurs. Only fast analysis of the traffic of two types of protein in the same cells can answer these questions.

3.1 Time-Lapse Microscopy

3.1.1 Cells

1. The glass cover slip supporting the cells is mounted in a Ludin observation chamber. Typically, 12×10^4 HeLa cells are seeded on a cover slip of 32-mm diameter, 24 h before observation. The number of cells should be adapted to the experiment and the cell line. It is recommended to use exponentially growing cells, to have the best proportion of cycling cells and because they are better for image acquisition (*see* **Note 1**).
2. To maintain the pH of the culture medium without CO_2, Hepes buffer (pH 7.4) is used at a final concentration of 10 m*M*. It is necessary to first test the viability of the cells under these incubation conditions (*see* **Note 2**). The temperature of the cells is maintained at 37°C by placing the microscope in a heated box with controlled temperature (*see* **Note 3**).

3.1.2 Observations

1. The DG4 illuminator was chosen to study assembly of the nucleolus at the end of mitosis *(2)* because since the excitation wavelength is selected by the illuminator, there is no need to change filters through the fluorescence module. Dual-pass filter cubes are used to filter the emission wavelength. With this system, it is possible to alternate the wavelength of excitation almost instantaneously and hence to follow fast kinetics of two fluorescent probes in the same cell (*see* **Notes 4 and 5**).
2. The recruitment into the nucleolus of GFP-fibrillarin and DsRed-B23, or GFP-Nop52 and DsRed-B23, from telophase to the G1 phase was followed. During this period, these proteins are either localized at the periphery of the chromosomes, in PNBs, or in the nucleolus and therefore a large part of the cell volume should be imaged, for example a surface of ~10 to 20 μm^2 at each z-step of ~0.3 µm. The frequency of acquisition of the *z* series was every 30 sec and in some cases every 10 sec. Two images were acquired for each *z*-step, the first corresponding to the GFP protein and the second corresponding to the DsRed protein. There is generally a choice between resolution and sensitivity, and analysis of PNB dynamics were made on a high-resolution camera (5 MHz Micromax) because of the small size of the PNBs (~0.1–0.5 µm) (*see* **Note 6**).

3.1.3 Parameters To Be Defined

1. Exposure time. One of the most interesting characteristics of this method is the speed of acquisition; exposure time is about a few hundred milliseconds so that time-lapse microscopy is convenient to follow rapid events and fast kinetics. The longer the sample is exposed, the larger is the level of grey recorded, but increasing the exposure time bleaches the sample, so it is necessary to find a compromise between good sampling of grey levels without bleaching.
2. The number of optical sections and number of time points. It is necessary to determine the top and the bottom of the sample and therefore to consider the total exposure time necessary to register all the optical sections of the volume for each time point. Considering an exposure time of 100 msec for each of 10 sections, the total exposure time will be 1 sec at each time point. Then, the total number and the frequency of time points should be defined based on the kinetics of the biological movements to be registered.
3. Binning of pixels. Binning presents the advantage of summing the intensity of the coupled pixels, allowing increased intensity without increasing the time of exposure and the danger of bleaching. Binning must be chosen considering the sampling, as follows: pixel size/magnification, and the Nyquist criterion. The latter recommends that sampling should be equal to d/2 where d is the optical resolution calculated as $d = (0.61 \times \lambda)/NA$; λ is emission wavelength and NA the numerical aperture of the objective. We worked with a ×100, 1.4 NA oil objective and GFP-proteins, and therefore d = 220 nm. Considering the Nyquist criterion, the sampling should be 110 nm. Using the Micromax camera, sampling corresponds

to 65 nm. In this condition, images would be oversampled and we therefore chose a camera setting at 2×2 binning so that the sampling was 130 nm.

3.1.4 Deconvolution of Images

Deconvolution is a mathematical process in which computations for the acquired stacks reassign diffracted light to its original location ***(13)***. During its formation, the image suffers optical distortion in the microscope, mostly due to optical blur and noise. This can be written as $i = o \otimes h + n$, where i, o, h, and n represent respectively the acquisition, the object we computed, the point spread function (PSF), and the noise; and $\otimes$ represents the convolution product (***(12)*** and references therein). The PSF describes the response of the microscope for each point of the object imaged, and most deconvolution algorithms require this information. The PSF may be calculated theoretically knowing the microscope setup and using a theoretical PSF generator, or measured empirically by the imaging of fluorescent beads. In our case, the PSF was extracted from 3D images of fluorescent beads 0.1 µm in diameter (Molecular Probes; Invitrogen) collected at each wavelength. The automated batch deconvolution of each *z*-series was then computed using the PSF measured with a custom-made software package ***(13)***. We chose the Richardson-Lucy Deconvolution algorithm.

3.1.5 How to Prepare a Movie with ImageJ

We describe here the successive steps to be applied to make a movie with the free downloadable software ImageJ (Fig. 9.1):

1. The deconvoluted images are assembled in stacks.
2. Stacks are projected along the *z*-axis. This step makes it possible to obtain one *x*, *y* image per time point. The *Maximum Intensity* projection was chosen. Each pixel of the output image contains the maximum value over all images in the stack at the corresponding coordinates pixel (*see* **Note 7**).
3. Maximum intensity *z* projection images are converted to a stack.
4. The stack of *z* projections is converted into a movie by using the Quick Time movie writer plug-in. Using the dialog box, the type of compression (codec), the quality, and the frame rate of the movie are chosen (*see* **Note 8**). We currently use the Cinepack codec, the best quality, and eight images per second (*see* **Note 9**).

3.1.6 Traffic of Processing Proteins During Nucleolar Assembly Observed in Living Cells

The kinetics of recruitment of processing proteins to the sites of rDNA transcription are rapid (10–15 min) for early processing proteins, and take longer (60–80 min) for

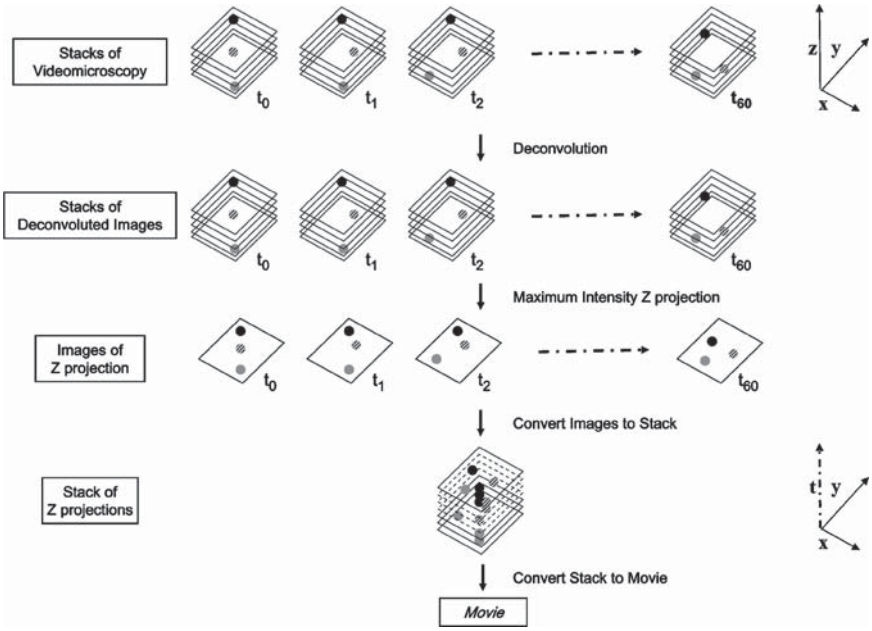

Fig. 9.1 Scheme of the different steps necessary to produce a movie. One time-lapse microscopy stack is represented by a stack of rectangles for each time point (*t*) according to the three directions in space (*x*,*y*,*z*). One rectangle represents a (*x*,*y*) focal plane. The three beads (*black*, *hatched*, and *grey*) indicate objects acquired on different focal planes. Time-lapse microscopy stacks are deconvoluted. Each stack is projected along the *z*-axis to obtain one (*x*,*y*) plane containing the maximum intensities as represented by the presence of the three beads in one rectangle. The *z* projection images are converted to one stack that is converted to a movie

the late-processing proteins ***(12)***. These short times make it necessary to compare the kinetics of two proteins in the same cell. When comparing the kinetics of GFP-fibrillarin with DsRed-B23 (early and late proteins, respectively) in the same cells, we observed the presence of both proteins in the same PNBs for a short time ***(2)***. The quantification of the concentration of both proteins in the same PNBs confirms this observation. For quantification, it was necessary to sum three slices because of the *z* movements of the PNBs. In addition, the real intensity contained in the pixels should be conserved. Because of these two conditions, the *Sum Slices* projection was used. The kinetics and quantification indicate that early and late-processing proteins shared the same PNBs. When comparing the relative kinetics of two late-processing proteins (B23 and Nop52), similar dynamics were observed as well as synchronized departure from the same PNBs (Fig. 9.2), which could indicate a similar mechanism of release, or the possibility that proteins of the same machinery are forming complexes. This result prompted us to develop FRET to analyze complex formation during the recruitment of processing proteins into the nucleolus (*see* **Section 3.2**, FRET).

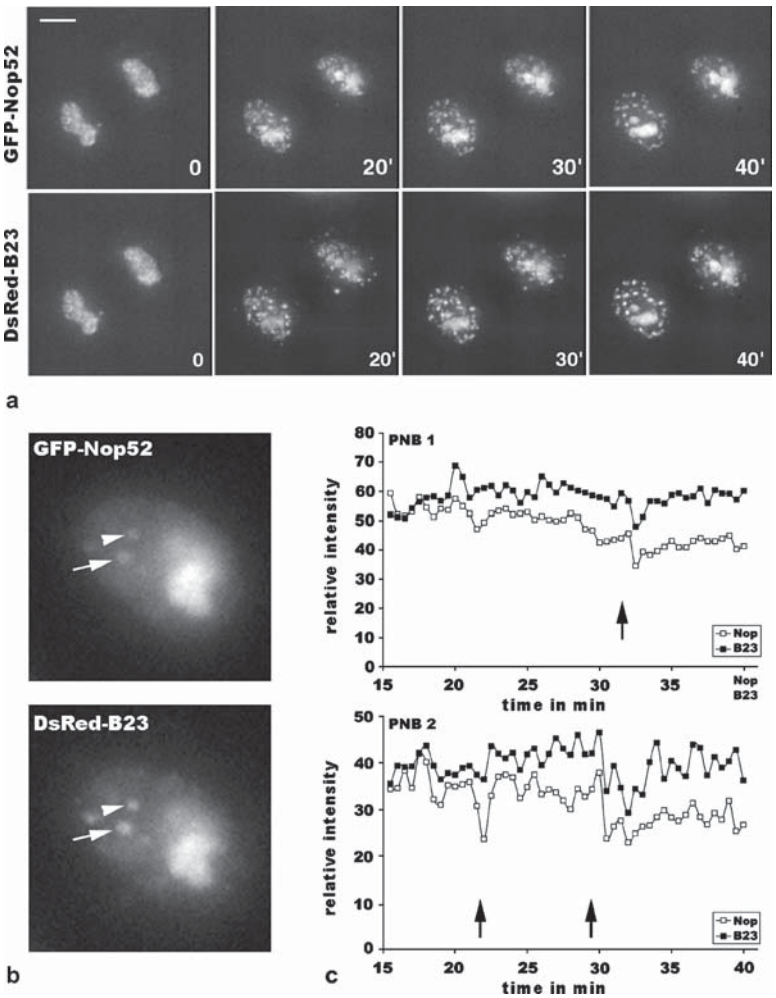

Fig. 9.2 Comparison of the dynamics of the nucleolar proteins Nop52 and B23. **a** Time-lapse sequences from telophase to early G1 of GFP-Nop52 and DsRed-B23. At time 0 (20 min after the beginning of anaphase), these proteins show the same dynamics during the formation of PNBs as well as during their recruitment and accumulation in nucleoli. In the same focal plane, images of GFP and DsRed are exactly superimposable. **b** Enlargement of a nucleus to show the PNBs in three consecutive merged optical sections that were analyzed (*arrow* PNB 1 and *arrowhead* PNB 2). **c** Relative fluorescence intensity from 15 to 40 min. The *open squares* correspond to GFP-Nop52 and the *dark squares* to DsRed-B23. The *arrows* indicate similar fluctuations of both proteins, suggesting simultaneous release (reproduced from **ref**. ***(2)*** with permission)

3.2 FRET

3.2.1 Biological Material

1. Stably transformed HeLa cells were grown on glass cover slips 32 mm in diameter; 75×10^3 cells were seeded 72 h before the experiment.
2. Cells were transfected 48 h before the experiment using the Superfect reagent (Qiagen) and following the manufacturer's instructions. Doubly transfected cells were generated by transient transfection of stably transformed cells.
3. Observation chamber (Lacon, Ulm, Germany).
4. During FRET acquisition, cells were in culture medium without phenol red and supplemented with 1% non-essential amino acids, 1% L-glutamine and 0.5% fetal calf serum.
5. Paraffin oil (1 mL) was gently dispersed on the surface of the culture medium to avoid evaporation during image acquisition.

3.2.2 Analysis of FRET in Nucleoli and PNBs

To determine whether Nop52 associates with B23 along the PNB pathway, FRET between GFP-Nop52 (donor) and DsRed-B23 (acceptor) was first evaluated in the nucleolus. As illustrated in Fig. 9.3Ab, the lifetime of GFP decreased in the nucleolus when the cells were cotransfected with the acceptor. This decrease was not observed with the pair GFP-fibrillarin and DsRed-B23 (Fig. 9.3Ad). The Gaussian distribution of the lifetime of the donor alone (green curves) or in the presence of an acceptor (red curves) is similar to that of the donor alone when there is no interaction (red curve f′). On the contrary, the decay of the lifetime of the donor is visible in the presence of the acceptor (red curve e′) when there is interaction between the partners. By measuring the lifetime in the nucleolus, it was established that positive FRET occurs when the reduction in the position of the center of the fluorescence lifetime distribution of the GFP-tagged protein is superior or equal to 200 psec. We further used such a value to estimate the FRET on region of interests (ROI) that we identified on recorded sequences. For example, we recognized the nucleoli and the PNBs on the time-lapse sequences; they were manually delineated and the lifetime of GFP in these ROI was analyzed over time. FRET was not detected during anaphase at the chromosome periphery, whereas it was seen in 20% of PNBs at the beginning of telophase, in 40% at the end of telophase, and in 55% in early G1. Thus, interaction between GFP-Nop52 and DsRed-B23 in PNBs was established progressively, indicating that PNBs are assembly platforms of processing complexes at the time of nucleolar assembly.

3.2.3 Analysis of FRET in Granular Masses Induced by Drugs

If nucleolar functions are inhibited, the nucleolus becomes disorganized and new structures are formed. When cells are treated with 5,6 dichloro-1-ribofuranosyl

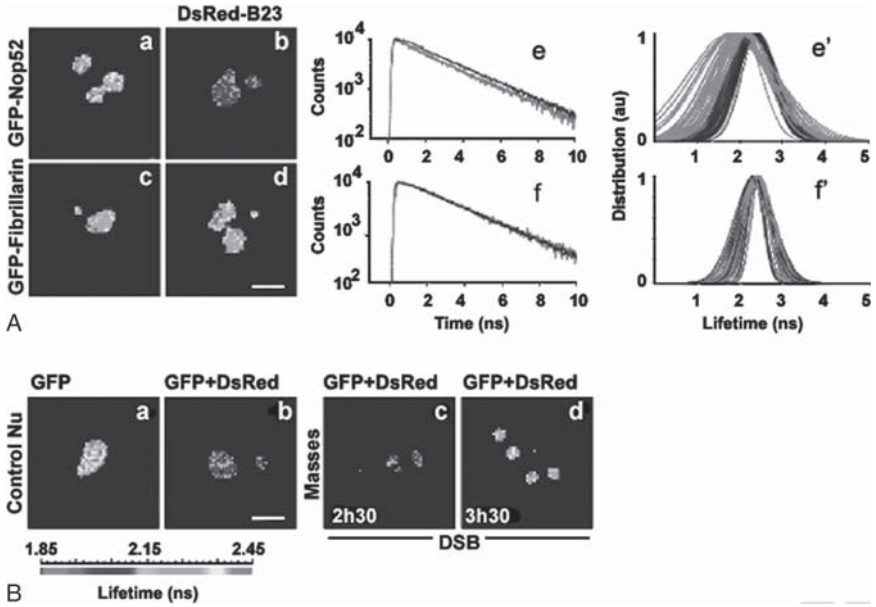

Fig. 9.3 **A** Nop52 and B23 interact in the nucleolus of living cells. tdFLIM-FRET measurements were carried out by acquiring fluorescence decay images of the GFP donor in cell lines permanently expressing GFP-Nop52 (*a*, *b*) or GFP-fibrillarin (*c*, *d*) either alone (*a*, *c*, and *green curves* in *e* and *f*) or in the presence of the DsRed acceptor after transfection with DsRed-B23 (*b*, *d*, and *red curves*). The tdFLIM images were obtained by analyzing pixel-by-pixel the fluorescence decays with a single lifetime and are displayed as pseudocolored fluorescence lifetime maps (*a–d*). Lifetimes between 2.45 nsec and 1.85 nsec are indicated by colors shown in the scale. The nucleolus-associated fluorescence decay of GFP-tagged proteins is visible (*b*), and is compared in (*a*) and (*c*) with donor alone (*green curves*; GFP-Nop52 and GFP-fibrillarin, respectively) and with donor with acceptor. Fits of these fluorescence decays were carried out using a Gaussian distribution lifetime model and the complete results are plotted in (*e*) for GFP-Nop52 alone (*green curves,* n = 53) or in the presence of DsRed-B23 (*red curves,* n = 35) and in (*f*) for GFP-fibrillarin alone (*green curves,* n = 22) or in the presence of DsRed-B23 (*red curves,* n = 21). Bar, 10 µm. (reproduced from **ref.** ***(2)*** with permission). **B** FRET analysis in DRB-induced masses. Fluorescence decays are represented by pseudocolored maps expressing the fluorescence lifetimes of the GFP donor (*a–d*). *a* Control nucleolus (*Nu*) of a permanent cell line expressing only the donor GFP-Nop52; no FRET is detectable as represented in *yellow* on the pseudocolored map. *b* FRET is detectable between GFP-Nop52 and DsRed-B23 in a nucleolus represented in *blue* on the pseudocolored map. *c* FRET is detectable (2 h 30 min) in DRB-induced masses as represented in *blue. d* At 3 h 30 min in DRB-induced masses, FRET is not detectable, as represented by their *yellow* color. To view this figure in color, see COLOR PLATE 2

benzimidazole (DRB), processing proteins form masses at a distance from transcription sites ***(14, 15)***. The question is how these masses are formed and maintained without processing activity, and we propose that their formation could be explained by protein–protein interactions. To verify this hypothesis, interactions between GFP-Nop52 and DsRed-B23 in masses were analyzed by FRET during DRB treatment. We describe here the successive steps necessary for this analysis. First, before acquisition it is necessary to select cells expressing GFP-Nop52 and

DsRed-B23 at similar and low levels to exclude aggregates of DsRed. After acquisition of the data, it is necessary to select those that are exploitable.

During image analysis of fluorescence decays, several successive selections occur and many ROI are excluded from the analysis at different steps. As an example, during one FRET analysis, the number of exploitable ROIs selected were:

- 277 ROI selected on CCD images of masses containing GFP-Nop52 and DsRed-B23.
- 159 decay-retained through soft QA analysis (Decay extraction software) because the measurement of decay was not clear in the other ROI.
- 71 curves retained after analyses using Globals Software for Fluorescence Dynamics.

This analysis permitted us to observe FRET in a few cases (4/11 cases) after 2 h 20 min of DRB treatment (Fig. 9.3Bc), but after 3 h 20 min (Fig. 9.3Bd), the majority of the data indicates no FRET (15/18 cases). These observations are compatible with the fact that when DRB treatment exceeds 4 h, the masses begin to disperse throughout the nucleoplasm. We focused our analysis on 3 h of DRB treatment to be able to analyze the maximum masses without exceeding 4 h to avoid their dispersal. After these preliminary results, we propose that it would be interesting to analyze the time-lapse FRET during the DRB treatment and more precisely at the beginning of mass formation.

3.3 Conclusions and Perspectives

It was discovered using time-lapse microscopy that all processing proteins pass through the same PNBs. This conclusion was unexpected, and it opens the question of the sequential release of the proteins. Further investigation should be carried out to understand the mechanism controlling the order of recruitment on transcription sites. In addition, we demonstrated that complexes of processing proteins were assembled in PNBs. The presence of stable pre-rRNAs in PNBs could favor the formation of these complexes ***(16)***. However, in the granular masses induced by DRB without processing activity ***(15)***, FRET between processing proteins can be detected at the beginning of the formation of the masses. These data could indicate that complexes between processing proteins either depend on rRNAs and then the complexes are stabilized, or that the complexes can be formed independently of the rRNAs under the control of binding affinity sites.

4 Notes

1. HeLa cells grow on glass cover slips, but in the case of cells that only grow on coated cover slips it is necessary to check the effect of the coating agent on the fluorescent background; for example poly-L-lysine produces a fluorescent background.

2. The pH of the culture medium can be maintained during imaging by saturating it with CO_2 and completely filling the incubation chamber, or alternatively the incubation chamber can receive a flow of CO_2; the choice depends on the duration of observation.
3. If the entire microscope cannot be heated in an adequate box, the cells are maintained at 37°C in an incubation chamber adapted to the stage of the microscope. The objective should also be heated to ensure homogeneity of the temperature on both sides of the cover slip; we observed a difference of about 4°C in the zone in contact with the objective at room temperature.
4. The standard system to illuminate samples is a mercury lamp whose light passes through an excitation filter to select wavelengths corresponding to the different fluorescent molecules, and emitted fluorescence is filtered via an emission filter. This pair of excitation/emission filters is mounted on dichroic cubes. To acquire DsRed and GFP signals, cubes corresponding to the wavelength of these two fluorochromes are selected. To permit automatic acquisition, the microscope is equipped with an automatically commanded motorized fluorescence module. However, this system is not recommended for fast acquisition, because it is slow compared with the DG4 illuminator.
5. Fluorescence crosstalk must be verified and avoided.
6. To follow weak signals, a 5-MHz Pentamax intensified camera coupled to a Gen IV intensifier (both from Princeton Instruments, Trenton, NJ, USA) that amplifies the signal was chosen.
7. *Average Intensity* projection outputs an image wherein each pixel stores average intensity over all images in a stack at the corresponding location. *Standard Deviation* creates a real image containing the standard deviation of the slices. *Sum Slices* creates a real image that is the sum of all the slices in the stack (ImageJ Documentation).
8. For PC users, a plug-in permits stacks to be saved as uncompressed AVI files, which can be opened by Macintosh users through the QuickTime movie player.
9. Different codecs exist such as Cinepack, Sorenson (supported by QuickTime and highly compressive), and Sorenson 3. Even though the Cinepack codec is obsolete, it is very convenient because it is supported by many players.

References

1. Lippincott-Schwartz, J., Snapp, E., and Kenworthy, A. (2001) Studying protein dynamics in living cells. *Nat. Rev. Mol. Cell Biol*. **2**, 444–456.
2. Angelier, N., Tramier, M., Louvet, E., Coppey-Moisan, M., Savino, T. M., De Mey, J. R., and Hernandez-Verdun, D. D. (2005) Tracking the interactions of rRNA processing proteins during nucleolar assembly in living cells. *Mol. Biol. Cell* **16**, 2862–2871.
3. Bubulya, P. A., Prasanth, K. V., Deerinck, T. J., Gerlich, D., Beaudouin, J., Ellisman, M. H., Ellenberg, J., and Spector, D. L. (2004) Hypophosphorylated SR splicing factors transiently

localize around active nucleolar organizing regions in telophase daughter nuclei. *J. Cell Biol*. **167**, 51–63.
4. Dundr, M., Misteli, T., and Olson, M. O. J. (2000) The dynamics of postmitotic reassembly of the nucleolus. *J. Cell Biol*. **150**, 433–446.
5. Leung, A. K., Gerlich, D., Miller, G., Lyon, C., Lam, Y. W., Lleres, D., Daigle, N., Zomerdijk, J., Ellenberg, J., and Lamond, A. I. (2004) Quantitative kinetic analysis of nucleolar breakdown and reassembly during mitosis in live human cells. *J. Cell Biol*. **166**, 787–800.
6. Savino, T. M., Bastos, R., Jansen, E., and Hernandez-Verdun, D. (1999) The nucleolar antigen Nop52, the human homologue of the yeast ribosomal RNA processing RRP1, is recruited at late stages of nucleologenesis. *J. Cell Sci*. **112**, 1889–1900.
7. Emiliani, V., Sanvitto, D., Tramier, M., Piolot, T., Petrasek, Z., Kemnitz, K., Durieux, C., and Coppey-Moisan, M. (2003) Low-intensity two-dimensional imaging of fluorescence lifetimes in living cells. *Appl. Phys. Lett*. **83**, 2471–2473.
8. Spector, D. L. (2001) Nuclear domains. *J. Cell Sci*. **114**, 2891–2893.
9. Leung, A. K., Andersen, J. S., Mann, M., and Lamond, A. I. (2003) Bioinformatic analysis of the nucleolus. *Biochem. J*. **376**, 553–569.
10. Mélèse, T. and Xue, Z. (1995) The nucleolus: an organelle formed by the act of building a ribosome. *Curr. Opin. Cell Biol*. **7**, 319–324.
11. Hernandez-Verdun, D., Roussel, P., and Gébranne-Younès, J. (2002) Emerging concepts of nucleolar assembly. *J. Cell Sci*. **115**, 2265–2270.
12. Savino, T. M., Gébrane-Younès, J., De Mey, J., Sibarita, J-B., and Hernandez-Verdun, D. (2001) Nucleolar assembly of the rRNA processing machinery in living cells. *J. Cell Biol*. **153**, 1097–1110.
13. Sibarita, J. B. (2005) Deconvolution microscopy. *Adv. Biochem. Eng. Biotechnol*. **95**, 201–243.
14. Louvet, E., Junera, H. R., Le Panse, S., and Hernandez-Verdun, D. (2005) Dynamics and compartmentation of the nucleolar processing machinery. *Exp. Cell Res*. **304**, 457–470.
15. Louvet, E., Junera, H. R., Berthuy, I., and Hernandez-Verdun, D. (2006) Compartmentation of the nucleolar processing proteins in the granular component is a CK2-driven process. *Mol. Biol. Cell* **17**, 2537–2546.
16. Dousset, T., Wang, C., Verheggen, C., Chen, D.,Hernandez-Verdun, D., and Huang, S. (2000) Initiation of nucleolar assembly is independent of RNA polymerase I transcription. *Mol. Biol. Cell* **11**, 2705–2717.

Chapter 10
Three-Dimensional Reconstruction of Nucleolar Components by Electron Microscope Tomography

Pavel Tchelidze, Hervé Kaplan, Adrien Beorchia, Marie-Françoise O'Donohue, Hélène Bobichon, Nathalie Lalun, Laurence Wortham, and Dominique Ploton

Keywords Nucleolus; Electron tomography; Nanogold; RNA polymerase I

Abstract The nucleus is a complex volume constituted of numerous subcompartments in which specific functions take place due to a specific spatial organization of their molecular components. To understand how these molecules are spatially organized within these machineries, it is necessary to investigate their three-dimensional organization at high resolution. To reach this goal, electron tomography appears to be a method of choice; it can generate tomograms with a resolution of a few nanometers by using multiple projections of a tilted section several hundred to several thousand nanometers in thickness imaged by transmission electron microscopy (TEM).

Specific identification of molecules of interest contained within such thick sections requires their specific immunocytochemical labelling using electron-dense markers. We recently demonstrated that electron tomography of proteins immunostained with nanogold particles before embedding, and subsequently amplified with silver, was very fruitful due to the inherently high spatial resolution of the medium-voltage scanning and transmission electron microscope (STEM). Here we describe this approach, which is very efficient for tracing the 3D organization of proteins within complex machineries by using antibodies raised against one of the proteins, or against GFP to analyse GFP-tagged proteins.

1 Introduction

The stepwise molecular events related to ribosome biogenesis are spatially highly organized within nucleolar subcompartments where ribosomal gene (r-gene) transcription, pre-ribosomal RNA (rRNA) processing, and pre-ribosome assembling are carried out. These functional territories are assembled from a plethora

R. Hancock (ed.) *The Nucleus: Volume 1: Nuclei and Subnuclear Components*,

of structural proteins, enzymes, and transcription factors integrated within the framework of extremely compacted ribosomal deoxynucleoprotein (rDNP) templates distinguished as ribosomal chromatin ***(1–9)***. Spatial visualization of the corresponding protein–ribosomal gene DNA (rDNA) interactions as well as protein–protein interactions is crucial for the structural and molecular modelling of the rRNA synthesis and maturation machineries.

At the same time, the complex molecular construction and highly dynamic nature of these machineries dramatically restricts the role of conventional 2D-electron microscopy in the depiction of r-gene complexes, and recognizing the functional arrangements during rDNP compaction imposes a 3D imaging approach. The possibility of precisely analyzing supramolecular organization at the spatial resolution afforded by TEM arose with the development of high-voltage electron microscopy (EM) tomography ***(10–17)***. The EM tomographic technique employs digital 3D reconstruction of serial planes imaged and recorded by tilting 0.5- to 1-μm-thick sections from −60° to +60° within a STEM working at 250 kV.

The identification of molecules by EM tomography requires extra-small electron-dense markers such as streptavidin-FluoroNanogold conjugates (FNG) ***(14, 18–20)***. These are composed of a fluorochrome molecule (e.g. FITC, Alexa) coupled with gold atoms grouped into 1.4-nm clusters. Nanogold particles penetrate the cell volume more efficiently, providing fast and homogenous dispersion within the nucleus and nucleolus that facilitates their access to antigens. When amplified by a silver-enhancing procedure, they become readily visible while the diameters of the nanoparticles increase up to 10 nm. This enhanced intensity of labelling throughout the whole cellular volume allows the ubiquitous use of pre-embedding immunolabelling methodology ***(20)***. Moreover, these advantages of FNG allow the simultaneous localization of an antigen in the same cell by light and electron microscopy ***(21, 22)***.

The complex molecular machinery of r-gene transcription is guided by RNA polymerase I (RNAP I), an enzyme complex dedicated solely to this task ***(5, 15, 23–27)***. Because RNAP I displays a strictly defined position within the r-gene transcription unit, it appears as a primary candidate to start 3D mapping of proteins involved in the initiation complex and in rDNA compaction. Recently, the volume distribution of RNAP I within nucleolar fibrillar centres (FCs) was determined using this technique and was used to propose a model of the 3D organization of r-genes ***(9, 15, 27–29)*** (*see* Figs. 10.1 and 10.2).

Fig. 10.2 (continued) **b–d** Different projections of the tomogram calculated after reconstruction of the cluster framed in (**a**). At +15° (**d**), five 60-nm coils are evident as indicated by brackets (*1* to *5*). The *large circle* shows the area where the coils are fused together. The *arrows* point to twines, 20 nm in thickness. **e** A stereopair of the tomogram presented in the same orientation as in (**d**) was calculated using a surface-rendering mode. **f–i** Four successive 30 nm-thick sections with a coronal orientation within the tomogram shown in (**d**). *Asterisks* in **g** and **h** indicate the internal part of the cluster, devoid of labelling; and *arrows* in **g–i** refer to twines. Bar, 200 nm (**a**) or 100 nm (**b–i**). Reproduced from (***7***) with permission

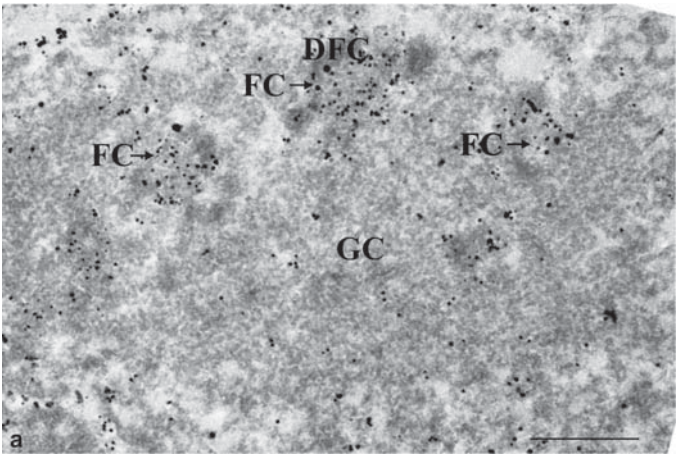

Fig. 10.1 Ultrastructural localization of RNA polymerase I (RP1) in A549 cells. Anti-RPI antibodies were revealed with FluoroNanogold followed by silver enhancement. After embedding, ultrathin sections (80 nm) were counterstained and observed in the electron microscope at 100 kV. The main nucleolar components are identified (FC, Fibrillar Component; DFC, Dense Fibrillar Component; GC, Granular Component). A high density of gold particles is observed within the fibrillar components of the nucleolus. Bar, 0.5 µm. Reproduced from (*7*) with permission

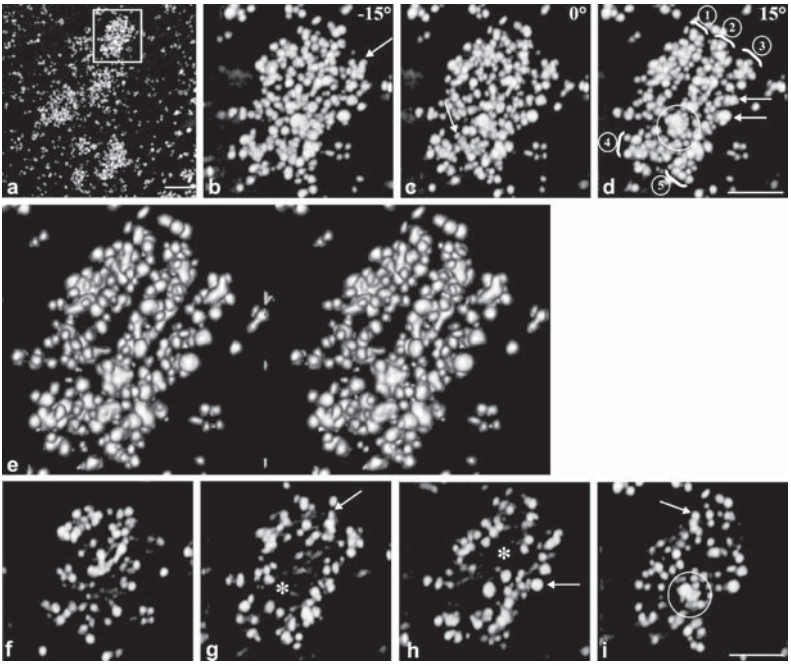

Fig. 10.2 A tomographic study of A549 cells immunolabelled with anti-RNA polymerase I antibodies. The contrast was inverted so that silver particles appear white. A 500-nm-thick section observed using a STEM at 250 kV is shown; several independent clusters, 270 nm in diameter, are seen (**a**).

In this chapter, we describe easily reproducible techniques for the reliable detection of RNAP I with subsequent selection of cells of interest for EM or tomographic reconstruction. Other proteins linked to the rDNA template would probably show a supramolecular organization similar to that observed for RNAP I. Having sampled the organization of RNAP I, it is now easy to overlap the 3D map of any other rDNA-specific protein with the spatial structure of r-genes. There is thus good reason to extend our protocol to examine other key r-gene transcription factors, in particular, upstream binding factor (UBF).

2 Materials

All chemicals and reagents should be chemically pure or EM grade, and solutions should be prepared using ultra-pure water. The results presented here were obtained using the following materials and recipes.

2.1 Reagents, Chemicals, and Solutions

1. Cell culture medium: HAM F-12 (Gibco; Invitrogen, Cergy Pontoise, France) with 10% fetal calf serum (FCS), 100 U/mL of penicillin, 100 µg/mL of streptomycin, and 2 m*M* L-glutamine (all Sigma-Aldrich, Saint-Quentin Fallavier, France).
2. Trypsin solution: 0.05% w/v containing 0.53 m*M* Na_4EDTA (Gibco).
3. Dulbecco's phosphate-buffered saline (D-PBS) without $CaCl_2$ and $MgCl_2$ (Gibco) or PBS powder (bioMérieux, Marcy l'Etoile, France).
4. Bovine serum albumin (BSA) solution: 30% w/v BSA (Sigma-Aldrich) in 0.85% w/v NaCl.
5. Citifluor AF1 antifade solution (Agar Scientific, Stansted, UK).
6. Glutaraldehyde and paraformaldehyde (EMS, Hatfield, PA, USA).
7. EMbed 812 Kit including: Epon812, DDSA, MNA, DMP-30 (EMS).
8. HQ SILVER Enhancement kit (Nanoprobes, Yaphank, NY, USA).
9. 100% acetone and 100% ethanol (EMS).
10. Triton X-100 (Sigma-Aldrich).
11. Uranyl acetate solution: 5% w/v uranyl acetate solution in 70% ethanol.
12. Sodium thiosulphate solution: 5% w/v in dH_2O.
13. Lead citrate solution: dissolve 1.33 g of $Pb(NO_3)_2$ in 30 mL of dH_2O, add 1.76 g of $Na_3C_6H_5O_7{\cdot}2H_2O$, shake vigorously for 1 min and intermittently for 30 min. Add 8 mL of freshly made 1 N NaOH and invert slowly; the cloudy solution should become clear. Adjust to 50 mL with dH_2O and invert slowly. Stable for several months at 4°C in the dark.

2.2 Cell Culture Plastic and Glassware

1. Glass-bottom microwell dishes, 35-mm diameter with 14-mm diameter cover glass (MatTek, Ashland, MA, USA).

2. 40-mm coverslips for cell culture (Bioptech, Butler, PA, USA).
3. Delta surface cell culture dishes and flasks (Nunclon, Roskilde, Denmark).

2.3 Antibodies

1. Rabbit polyclonal antibody to RNAP I (courtesy of Dr. K. M. Rose, Department of Pharmacology, University of Texas Medical School, Houston, TX, USA).
2. Biotinylated anti-rabbit secondary antibody (Sigma-Aldrich).
3. FluoroNanogold fluorescein–gold–streptavidin conjugate (Nanoprobes).
4. Streptavidin–Texas Red conjugate (Amersham; GE Healthcare, Piscataway, NJ, USA).

2.4 Equipment

1. Laser-scanning confocal microscope (MRC-1024ES; Bio-Rad, Hercules, CA, USA) mounted on an IX70 Inverted Fluorescent Microscope (Olympus, France).
2. CK2 inverted microscope with a ULWC DO30 phase contrast device (Olympus).
3. CM30 electron microscope with a eucentric goniometer stage and 250 kV STEM mode (Philips, Eindhoven, The Netherlands).
4. 200 CX transmission electron microscope (JEOL, Croissy-sur-Seine, France).
5. Reichert-Young Ultracut ultramicrotome (Reichert, Vienna, Austria).
6. TEM Turbo carbon coater (Oxford Instruments SAS, Saclay, France).
7. SuperFrost glass slides (Menzel-Gläser, Braunschweig, Germany).
8. Beam-type 8-mm capsules or plastic molds to prepare epoxy resin cylinders (EMS).
9. Gelatin capsules (Agar Scientific).
10. EM forceps, pick-up loop ("Magic Loop"), eyelashes, razor blades, dental wax (EMS).
11. EM grids: London Finder 200-mesh copper, Maxtaform 200-mesh, and slot grids with formvar supporting film (EMS).

2.5 Software

1. ORION software system (ELI sprl, Court-St-Etienne, Belgium).
2. Laser Sharp 3.2 software (Bio-Rad).
3. Analyze software (Mayo BIR, CN Software, UK).
4. Amira software (TGS, Bordeaux, France).

3 Methods

The whole procedure covers several stages: 1) immunolabelling of fixed cells using polyclonal anti-RNAP I antibodies; 2) initial examination of labeled structures in a laser confocal microscope (LCM); 3) preparation of cells for EM (TEM and STEM),

including silver enhancement and embedding; 4) sectioning and identification of a properly stained cell in 0.5-μm (500-nm) resin slices; 5) capture of STEM images and 3D reconstruction; and 6) TEM analysis. The final result is largely dependent on the sensitive detection protocol combined with the correct choice of cell line, as well as with the complementary 3D reconstruction and image treatment technologies. Correspondingly, all steps and manipulations should be executed meticulously.

These protocols were elaborated for cells of the human A549 line, which were chosen due to the small size of their FCs, which allows them to be fully included within the section thickness ***(15, 29)***.

3.1 Preparation of Cells for LCM and Immuno-EM

Classic post-embedding labelling on EM grids is spatially limited to the surface of ultrathin sections, making 3D studies impossible. Here we use pre-embedding immunolabelling to enhance antigen detection in thick sections, which is critical for tomographic studies. The technique includes treatment with detergents to facilitate antibody penetration, which could deform or loosen the nuclear structure of permeabilized cells for both photonic microscopy and EM. Satisfactory preservation of cell organelles has usually been considered as the main obstacle in pre-embedding labelling, and by following the protocol proposed here, one can achieve conditions when adequate preservation of structure is combined with optimal accessibility of antigens. Importantly, a feature of thick-sectioned cells embedded in epoxy resin is that they maintain good 3D-distribution of proteins in situ in the course of tilting and image acquisition. This protocol designed for medium-voltage STEM reconstruction is also useful for conventional TEM observations, since the nuclear ultrastructure after permeabilization remains adequately stable, allowing precise detection of antigens on counterstained ultrathin sections.

Basically, immuno-EM and immunofluorescence are done at room temperature (approximately +20°C). After labelling with FNG, all the procedures of silver enhancement are carried out using a light-tight box, and reduced illumination is required to prevent photobleaching of fluorochromes and photoprecipitation of metallic silver.

3.1.1 Cell Culture

1. Maintain stock cultures of A549 cells in 40-mL plastic flasks, and reseed in new media as soon as the monolayer reaches confluence (2–3 times per week).
2. Three to 5 h before passage of cells, change the medium on a stock culture which has just reached confluence. Wash the cells 3× 1 min with PBS, cover them with 1 mL of trypsin solution, and incubate at 37°C for 1 min. Dilute the cells to the desired concentration, resuspending them carefully with a 5-mL plastic pipette to obtain proper dispersion.

3. For immunolabelling, cells are grown for 48–72 h on 40-mm-diameter Bioptech glass coverslips which have been washed in 70% v/v ethanol and placed in 50-mm plastic tissue culture dishes. After evaporation of the alcohol, cover the dishes with the lid. Plate 4–5 mL of cell suspension into each dish. To obtain excellent dispersion and spreading, hold the lid with your finger and agitate the suspension by gently sliding the dish in different directions during ~5 min.
4. Check the growth rate each morning until ~50–60% confluence to define the time of fixation as well as the subsequent immunostaining time. Replace the medium after 24–36 h of incubation and at least 3–5 h before fixation.
5. For immunolabelling for combined light and electron microscopy (CLEM), cells are cultivated in 35-mm MatTek dishes with glass-bottom microwells. Use a cell concentration two to four times lower than for Bioptech coverslips. Plate 2 mL of carefully dispersed suspension and mix gently to obtain good spreading of the cells. Control their dispersion in a phase contrast microscope, and if necessary select the best samples; proper dispersion facilitates the localization of the cell of interest in the next steps of preparation. Replace the medium after 24 h of incubation and 3–5 h before fixation.
6. Check the cell growth accurately to define a suitable time of fixation and subsequent immunolabelling. A sparsely growing culture facilitates localization of the cell of interest (*see* **Note 1**).

3.1.2 Fixing (Prefixing) Cells

Paraformaldehyde is toxic and volatile: use a fume hood and gloves!

1. Prepare a fresh solution of 4% w/v paraformaldehyde (PAF) in PBS in a glass flask, cover with aluminum foil, heat and stir using a magnetic stirrer. Add 2–3 drops of 0.1 *M* NaOH to dissolve the PAF completely, cool, and adjust the pH to 7.2–7.4.
2. Rinse the cells briefly 3× with 5 mL of PBS and add 3–5 mL of PAF solution. Leave the cells in fixative for 10–30 min.
3. Wash the cells 3× 5 min with 3–5 mL of PBS.

3.1.3 Immunolabeling Cells

1. Permeabilize the cells with 0.3% v/v Triton X-100 in PBS for 2 min. Use EM forceps to transfer the glass coverslip.
2. Drain the Triton X-100 solution rapidly. Cover the glass with 3 mL of PBS, rinse the cells, then wash extensively with PBS (3× 5 min) using a 5-mL automatic pipette.
3. Cover the cells with 3% w/v BSA solution and incubate for 30 min to quench nonspecific immunolabelling.
4. Prepare the necessary volume of all the antibodies required by dilution in PBS, store in the refrigerator and do not freeze. To properly cover one 40-mm coverslip, ~500 µL of diluted antibody is necessary, and ~250 µL to fill a 14-mm

glass-bottom microwell of one MatTek dish for CLEM. The dilution of the primary antibody depends on the antibody type; generally, for TEM and STEM the concentration should be five to ten times greater than that used for immunofluorescence.
5. Incubate the cells for 4 h with rabbit polyclonal primary antibody against the large subunit of RNAP I diluted 1:400 in PBS.
6. Wash the cells 3× 5 min with PBS using a 5-mL automatic pipette.
7. Incubate the cells for 30 min with biotinylated goat anti-rabbit secondary antibody diluted 1:100 in PBS.
8. Wash the cells thoroughly 3× 5 min with PBS.
9. Expose the cells for 15 min to streptavidin–FNG conjugate diluted 1:20.
10. Wash the cells 3× 5 min with PBS.

3.1.4 Observing the Cells in the LCM

1. Prepare two (or more) SuperFrost slides and put a drop of Citifluor F1 on each.
2. Drain PBS from the coverslip onto filter paper. With a diamond pencil, very gently scratch a line across the centre, avoiding extensive damage, and bend the coverslip carefully with the fingers to break it into two similar halves.
3. Plate both halves cell-side down onto the slides with Citifluor and seal with transparent nail varnish. Dry for 30–60 min in a light-tight box and keep in a plastic histological container in the refrigerator.
4. In the LCM, record a Z-series containing 20–30 optical sections per cell with an 0.2 µm Z step for subsequent 3D reconstruction with Amira software.

3.2 Preparing Cells for Conventional TEM and STEM Reconstruction

1. After the fixation steps (**Section 3.1.2**), stabilize the cell structure by postfixation in 1.6% w/v glutaraldehyde for 10–30 min under the fume hood.
2. Wash the cells thoroughly (3× 5 min) to remove residual glutaraldehyde completely.

3.3 Preparing Cells for CLEM Analysis

1. After steps 9 and 10 (exposing the cells to streptavidin-FNG conjugate and washing with PBS) in **Section 3.1.3**, place the MatTek dish under the LCM.
2. Select and localize a properly labelled cell and record its position relative to the grid coordinates etched on the cover glass.
3. Record a Z-series for the following 3D reconstruction.

3.4 Enhancing Labelling for Immuno-EM by HQ Silver

The quality of silver staining is strongly temperature and time dependent. Thus to extend the time of silver enhancement, part of the material is treated at room temperature and part at 4°C in a cold room.

3.4.1 Enhancement at Room Temperature

1. Place a flask of deionized water at −20°C for 15–20 min to prepare an ice-cold bath to block the silver staining reaction immediately. Use only freshly prepared deionized water (*see* **Note 2**).
2. Prepare the HQ Silver mixture using equal amounts of the three reagents. Mix eight drops of each component to properly cover the surface of one 40-mm glass coverslip, and three to four drops of each to fill a 14-mm glass-bottom microwell of a MatTek dish. Dispense the initiator (solution A, red cap) into a clean microcentrifuge tube, add the moderator (B, white cap), close the lid tightly, and mix thoroughly using a Vortex-type mixer at the highest speed for 1 min. Add the activator (C, blue cap), close the lid tightly, and again mix thoroughly for 1 min. Leave the mixture in the light-tight box for 1 min before use.
3. Cover the coverslips with HQ Silver reagent mixture and leave to develop for 7–10 min. Different development times should be tested first to determine the optimal time for your experiment. Usually, a newly purchased HQ Silver kit produces satisfactory results after between 7.45 and 8.5 min of development.
4. Because of the high viscosity of the mixture, do not drain the reagent off to obtain the exact development time, but immerse the coverslip very rapidly 10–20 times in the ice-cold deionized water bath to avoid excessive background staining and a coarse silver precipitate.
5. Wash the cells thoroughly (6× 2 min) with deionized water.
6. Complete the silver enhancement procedure by incubating the coverslip for 10 min in a 5% w/v aqueous solution of sodium thiosulphate that quenches residual metallic silver.
7. Immerse the coverslips in fresh deionized water in a new 50-mm-diameter plastic Petri dish. For CLEM, replace the sodium thiosulphate solution by fresh deionized water, cover the MatTek dish with a lid, and store in the refrigerator.

3.4.2 Enhancement at 4°C

1. Prepare HQ Silver reagent according to **Section 3.4.1**, but in the cold room. Wait 2–3 min after the final mixing and before developing the specimens.
2. Develop the specimen by covering the coverslip with reagent mixture during 15–25 min in the cold room. A newly purchased HQ Silver kit should give good

results at 4°C within 18–19 min. However, a series of different staining times must be tried to define the time appropriate for your particular case.
3. Eliminate **step 4** of **Section 3.4.1** and carry out **steps 5** and **6** of **Section 3.4.1** at room temperature.
4. Replace the sodium thiosulphate solution with fresh deionized water, cover the dish with a lid, and store the stained cells in the refrigerator.

3.5 Collecting the Cells

1. Place the Petri dish under an inverted microscope, remove the RS40 diaphragm, and check the labelling quality at 40×10 magnification with reduced light. In properly stained interphase cells, RNAP I-positive nucleolar sites are clearly recognizable as dark brown, folded, bead-like chains in sharp contrast to the pale yellow nucleoplasm. In metaphase cells, the RNAP I signal can be found redistributed, eventually becoming concentrated in relatively big, distinct spots.
2. Prepare a glass with 20 mL of deionized water, add two to three drops of 30% BSA solution, and stir thoroughly. The BSA solution efficiently reduces sticking of HQ Silver-treated cells to plastic surfaces (Petri dish lids, scrapers, pipette tips).
3. Take the Petri dish lid, invert it, and place the wet coverslip on the inner surface. Shift the coverslip to the border of the lid with EM forceps and press it with the forceps to stick it tightly to the plastic.
4. Rinse the inner surface of a 1-mL automatic pipette tip with BSA solution to avoid massive sticking of cells to the plastic. Do not change this tip.
5. Cover the cells with 400 µL of BSA solution to prevent massive loss of cells during collection. Scrap the cell layer meticulously, tilt the Petri dish lid, and drain the floating cells to the dish border. Continue scraping cells from all over the glass surface and collect as many as possible in the drop streaming down to the lid border.
6. Take 400 µL of the cell suspension using the same tip and transfer into a 0.5-mL microcentrifuge tube. Take 100 µL of BSA solution and drain it onto the cells remaining on the coverslip (do not change the tip). Scrap the cells thoroughly again and add them to the suspension in the microcentrifuge tube using the same tip.
7. Centrifuge the suspension at 200×*g* for 10 min. Remove the supernatant and refill the tube with 200 µL of 30% BSA solution, and resuspend the cell pellet meticulously by passage through a needle for injection. Centrifuge again at 200×*g* for 10 min and remove the supernatant.
8. *Use the fume hood and latex gloves to avoid contact of glutaraldehyde with the skin*. Add two to three drops of 25% glutaraldehyde to the cell pellet. After 15–20 min, extract the jellified cell pellet from the tube using EM forceps or an injection needle; extraction can be facilitated by carefully cutting off the bottom of the tube with a razor blade.

9. Cut the cell pellet (or parts of it) into ~0.5–1 mm^3 pieces and transfer them to deionized water in 30-mm-diameter plastic Petri dishes. Change the water and store the samples overnight in the refrigerator.

3.6 Embedding the Cells in Epoxy Resin

All manipulations with the EMbed 812 kit should be performed at room temperature under the fume hood using latex gloves!

1. Store the EMbed 812 kit (Epon 812, DDSA hardener, MNA hardener, and DMP-30 accelerator) at 4°C. Before use, warm all the components at 60°C during 1 h to decrease their viscosity.
2. Using the instructions enclosed with the kit, determine the proportion and volume of each component to reach the necessary hardness of the EM blocks as well as the amount of embedding mixture. For excellent sectioning, use the extra-hard/hard embedding protocols. To prepare the embedding mixture, use a 50-mL beaker on a magnetic stirrer and a 5-mL automatic pipette with a new tip for each component; allow the pipette to drain meticulously because of the viscosity of the components. Pipette first Epon 812, then DDSA, then MNA, and add the necessary volume of DMP-30 accelerator with a 100-µL automatic pipette. Mix thoroughly with a magnetic stirrer for 30–60 min at a moderate speed to avoid formation of air bubbles. Cover tightly with aluminum foil. The embedding mixture is usable during 2–3 days.
3. Immerse the samples of jellified cells in 500 µL of 50% acetone in a 1-mL plastic centrifuge tube for 10–30 min, then in the same amount of 70% acetone for 10–30 min or overnight, then in 80% (10–30 min), 90% (10–30 min), 95% (10–30 min), and 100% acetone (3× 20–30 min).
4. Impregnate the cells in 500 µL of 2:1 (v/v) acetone/epoxy resin mixture for 1 to 2 h, then overnight in the same volume of 1:1 v/v acetone/epoxy resin, then in 1:2 acetone/epoxy resin, then finally in pure epoxy resin for 2–4 h (*see* **Note 3**). Transfer the samples into gelatin capsules filled with pure epoxy resin and polymerize the resin at 60°C during 24–48 h.
5. For MatTek samples for CLEM, use only ethanol for dehydration/impregnation, *NOT* acetone or propylene oxide; perform dehydration steps and impregnation using the corresponding series of ethanol/epoxy resin mixtures and finally fill the bottom microwell of the MatTek dish with pure epoxy resin and incubate for 2 h at room temperature. Polymerize the resin during 12 h (or overnight) at 60°C. Put a droplet of epoxy resin on the block over the location of the cell of interest, and on this area stick the flat bottom of a resin cylinder previously prepared in an 8-mm flat-bottom Beam type capsules or mold. Return the block to 60°C for additional polymerization during 16–36 h. Remove the polymerized resin from the etched cover glass by gentle bending and then lifting of the block.

3.7 Preparing Thick Sections

1. Prepare 200-mesh London Finder grids in advance, and coat them with a formvar supporting film if desired (*see* **Note 4**).
2. Under low magnification of the ultramicrotome stereomicroscope, trim the epoxy resin block with razor blades to obtain an ~1×1 mm pyramid completely positioned within the jellified sample material.
3. Put a specimen holder into the ultramicrotome arm and polish the top surface of the pyramid with a fresh glass knife.
4. Remove the specimen and correct the lateral borders of the pyramid using a fresh razor blade.
5. Align the bottom (longer) border of the pyramid parallel to the opposite (shorter) side and return the specimen holder into the ultramicrotome and replace the glass knife with the diamond one (*see* **Note** 5). Switch on the specimen rotation/cutting automatic stage. When the top surface of the pyramid is fully cut, switch on the automatic feed stage in the 500-nm position and then slow down the cutting speed to 3–5 mm/sec. Sections of 500-nm thickness should be pink. If the pyramid top is trimmed nicely, when the diamond knife cuts properly the sections become smooth without scratches, folding, holes or other damage and with strictly outlined borders. If the orientation between the knife and the pyramid has been performed correctly, the sections will stick to each other and form a long ribbon.
6. Stop the motor after a number of suitable sections have accumulated in the bath. Take the eyelash and clean its tip by immersion in 96% alcohol, dry, and use it to isolate sections under the stereomicroscope: gently touch the border of the section or ribbon with the eyelash tip to float or divide the band ribbon into pieces. Isolate a group of two to four closely located or adhering sections. Take the pick-up loop and rinse its working surface in 96% alcohol, dry it, and use it to pick up sections under the microscope. Bring the central area of the loop over the group of sections, gently touch the water surface, and then raise the loop. In this way, all the sections should be collected in the drop attached to the loop.
7. Plate the sections floating in the drop on the surface of a clean slide. Dry the slide, and in the phase contrast microscope make sure that properly labelled cells are in the plane of the sections.
8. Take a washed 200-mesh London Finder grid and dry it on filter paper. These grids contain letters, figures, and symbols that facilitate the orientation and search for the cell of interest in the EM. Using the pick-up loop, lift the drop with two to four floating sections and gently touch the grid on filter paper. Dry the grid and check the attachment of the sections in the stereomicroscope or phase contrast microscope. To pick up sections without a loop, take the grid with the forceps and gently touch a group of two to four sections floating in the knife bath. The sizes of the sections should fit inside the inner circle of the grid (*see* **Note 6**).
9. For blocks dedicated to CLEM, identify the location of the cell of interest under the stereomicroscope of the ultramicrotome. Trim the resin block with a razor blade to obtain a small pyramid with the cell of interest located in the central

area (do not touch the top surface of the specimen with the razor blade). Fix the glass knife in the holder and feed the knife as close as possible to the pyramid. Do not polish the top of the pyramid. Align the knife edge to the top surface and the bottom border of the pyramid. Rotate the knife and the specimen holder to trim a pyramid as small as possible with the cell of interest in its center. Replace the glass knife with a diamond knife and adjust the vertical position of the pyramid to the knife edge. Under the highest magnification of the stereomicroscope, feed the diamond knife as close to the specimen as possible and prepare 500 nm-thick sections. Pick them up using slot grids with a formvar supporting film: take the forceps with a slot grid in your left hand, and then carefully immerse 2/3 of the slot into the knife bath. Float a ribbon of sections to the slot with the eyelash in your right hand, then gently touch the supporting film with the sections. Lift the forceps with the grid carefully, then dry and check the sections and the supporting film under a microscope (*see* **Note 7**).

3.8 Selecting Cells of Interest in Thick Resin Sections

1. Place the grid with thick sections in the middle of a clean slide and examine it under 40×10 magnification using the RS40 phase contrast diaphragm. Usually, properly stained cells are the same color as the sections you have collected (cells show a pink color in 500-nm-thick sections). They must also be clean without background staining and reveal heavy labelling in the nucleolar area. An experienced person should readily recognize the nuclear/nucleolar contours. Examine the cells with a labelled nucleolus using a phase contrast diaphragm, and select the best samples.
2. Remove the phase contrast diaphragm and reduce the illumination to verify the intensity of labelling. Without the diaphragm, in properly stained cells the labelled nucleolar sites form dark brown bead-like chains or distinct spots.
3. Find cells with a suitable position for tilting according to the scheme in Fig. 10.3. Cells situated in the centre or close to the central area of the mesh are most convenient (Fig. 10.3a). Note the location of the selected cells on the map of the London Finder grid, and mark the grid's orientation in the EM holder if necessary (Fig. 10.3b–d).

3.9 Preparing Thick Sections for Tilting

1. Before use, stabilize the sections by covering them with 10 nm of carbon evaporated from a braided carbon fibre with the TEM Turbo carbon coater (*see* **Note 8**).
2. Insert the grid in the EM holder and orient it if desired.
3. Introduce the holder into the column of the EM and find the cells of interest according to the grid map, using TEM mode.

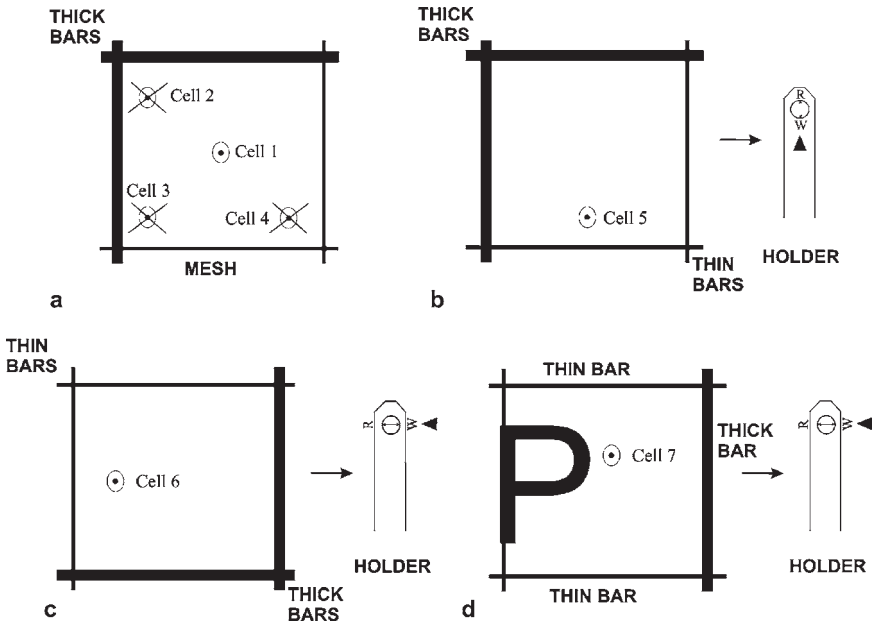

Fig. 10.3 Scheme of the orientation of the grid in the EM holder according to the localization of the cells of interest within the grid mesh. **a** Cell 1 positioned in the central area of the grid mesh is the most convenient for tilting. The orientation of this cell does not matter. It is impossible to tilt the peripherally located *cells 2*, *3*, and *4*. **b** An example of a peripherally located cell (*cell 5*) that can be successfully tilted by positioning the central line on the grid (identified with letters *R*, *W*, and a *pike*) parallel to the long axis of the EM holder. **c** Tilting of the peripherally located *cell 6* is possible by orientation of the central line perpendicular to the long axis of the EM holder. **d** *Cell 7* could be tilted by orientation of the central line perpendicular to the long axis of the EM holder

3.10 Ultrathin Sections for Immuno-TEM Analysis

3.10.1 Preparation

1. Wash and prepare 200-mesh Maxtaform grids in advance; these contain four large central holes that are very useful to observe a large area of the section. Coat with a formvar supporting film and then with carbon for 5 min if desired.
2. Carry out steps 2–4 of **Section 3.7**. Finally trim a pyramid big enough (0.5×0.5 mm to 0.7×0.7 mm) to be sure that one section will cover all four central holes of the grid. Using a diamond knife dedicated to ultrathin sectioning, cut 60–100-nm-thick sections (silver and pale gold color).
3. Pick up the sections on grids using the techniques described above (step 8 of **Section 3.7**). Take the grid with forceps and bring it over an isolated ribbon of sections, and, under the stereomicroscope, superpose the grid and the section band so that one middle section covers all four central meshes. Touch the sections gently with the grid surface. If you use a formvar-carbon-coated supporting film,

mark the side to which the sections are attached for the following staining. The Maxtaform grid has red and grey sides; always use only one of these to pick up the sections.

3.10.2 Staining Sections

CAUTION: uranium and lead salts as well as their solutions are toxic and dangerous for your health. Lead citrate easily penetrates the skin; use of latex gloves is obligatory.

1. Put a few drops of 5% uranyl acetate solution on dental wax. Float the grids, sections down, on the drop surface and stain for 10–20 min in the light-tight box at room temperature. Wash the sections extensively with deionized water and dry.
2. To stain with lead citrate, cover the bottom of a 50-mm plastic Petri dish with a piece of Parafilm and put two granules of NaOH into the dish. Put no more than two drops of the lead stain and float the sections on the surface; close the dish and expose the sections to lead citrate for 3–5 min at room temperature. Wash the sections thoroughly with deionized water, dry, and store in a specimen box.

3.11 Imaging

3.11.1 Laser Confocal Microscopy

Preparations selected for LCM are observed with a Bio-Rad MRC-1024ES confocal microscope combined with an Olympus IX70 inverted fluorescent microscope. Cells are imaged with a PlanApo/×63/1.40 oil objective.

1. Observe the cells mounted in Citifluor AF1 in phase contrast.
2. Excite the fluorescein within FluoroNanogold at 488 nm with the mercury lamp, and observe fluorescence at 510 nm to localize the label within the cell compartments.
3. Switch on the Kr/Ar laser and induce fluorescence using 3–10% of laser power. Adjust the gain and black level to position 2.0 of the diaphragm.
4. Visualize simultaneously the phase contrast and fluorescence images in the low scanning speed mode. Use Kalman (×3) digital filtering at zoom ×4, corresponding to a pixel size of 0.088 µm.

3.11.2 Electron Tomography

After orientation (if desired) of the cell within the specimen holder, the specimen should be stabilized to diminish anisotropic deformations of the resin section during image acquisition, by exposure of the area of interest under the electron beam at a dose of $100e^{-}/(Å^2 \times \text{sec})$ for 5–10 min. The tilting and digitalization are

performed at 250 kV in the STEM mode in the Philips CM30 electron microscope using a eucentric goniometer stage, tilting each section by successive 2-degree steps from −60 to +60 degrees. The cell of interest is directly imaged at ×50,000 magnification using a 5.6-nm electron beam. Final images are recorded in slow scanning mode (4 nsec/pixel) by the photo detector and then sampled in binary (512×512 pixel) format using the Orion software system. The contrast and the brightness of these images are adjusted by means of ImageJ free software.

To perform the image acquisition and the tomographic 3D reconstruction successfully, the following steps should be carried out:

1. Remove the objective diaphragm and at low magnification find the previously identified cell according to the grid map, using TEM mode.
2. Turn the EM to the STEM mode. Before the acquisition of a tilt series of images, stabilize the area of interest by exposure of the sections under the electron beam for 5–10 min.
3. Center the goniometer stage. To exclude rotation shift due to movement of the goniometer stage, align the object of interest along the *y* axis using the *y*-rotation mode of the EM. After this correction, the object must move as parallel to the *y* axis as can be adjusted.
4. Record an image of the global view of the cell at low magnification at a 0-degree angle. It is possible to digitalize the cell using higher-speed mode (10 nsec/pixel).
5. Magnify the cell at ×50,000 and adjust the scanning beam to the appropriate spot size. Bring the object to the center of the screen.
6. Tilt and record images. Before final recording, adjust the focus and contrast of each image in high-speed mode. During the tilting, keep the object of interest in the central area of the screen by moving along the *y* axis.

3.12 3D Image Reconstruction

Before 3D reconstruction, the contrast of the individual binary images is reversed and then they are precisely aligned. To increase the precision of the alignment and consequently the final quality of the reconstructed 3D image, two methods should be applied: first, coarse alignment of the projections according to the reference point, and second, refined alignment of the projections using sinograms ***(30, 31)***. The programs to generate and visualize sinograms were developed in our laboratory on a Linux workstation and the sinograms are displayed using ImageJ software. The quality of the coarse and refined alignments was finally controlled by visualizing an ImageJ movie composed of the successively aligned projections of the different angles of tilting ***(32, 33)***.

An extended field-additive unconstrained algebraic reconstruction technique (ART) was used to compute a 512×512×512 cube from the 60 recorded projections ***(12, 33, 34)***. The primary reconstructed volumes were visualized and extensively investigated using the Maximum Intensity Projection mode by using the Analyze

software. The region of interest of the primary reconstructed cubes were extracted and then submitted to further image treatment such as filtering, deconvolution, etc. Finally, processed cubes were visualized in the Amira software by using the method of surface and volume rendering (Isosurface rendering and Voltex mode, respectively). The interior organization of the cube was investigated by using ortho and oblique slices options, while the area of interest was extracted from the interior of the definitive cube using Volume Edit mode.

1. Import the series of binary images into ImageJ software and invert their contrast.
2. To perform coarse alignment:
   (a) Select within or close to the central area of the image a point that is clearly visible in all recorded projections. Use this point as a reference to determine the correct tilt axis.
   (b) Record the coordinates of the reference point for each angle of tilting.
   (c) Perform centering of the projections according to the reference point by translating each of them in the *x* and *y* directions.
   (d) Use all recorded projections to create a movie for the control of the alignment quality.
3. To perform refined alignment:
   (a) Visualize a horizontal sinogram and identify the stack of the central lines of each *x*,*z* projection. In the case of misalignments in the centered marker line, identify the corresponding projections.
   (b) Shift all misaligned projection along the *x* axis. Visualize the sinogram again to rebuild and correct the central line until any breaks are eliminated. The more the central line is straight, the more precise is the alignment.
   (c) Select the central *x*,*y* lines and stack them to build the vertical sinogram. Identify misaligned projections.
   (d) Shift the projection along the *y* axis to rebuild and correct the sinogram.
4. Submit the finally aligned projections to further postreconstruction image treatment, because the more precisely the projections are aligned (in both *y* and *x* directions) the better is the quality of the reconstruction.

3.13 Postreconstruction Image Treatment

Due to the missing wedge phenomenon (restriction of the possible tilt angles of the specimen leads to a missing wedge of data), silver-amplified FNG particles regularly show characteristic deformation along the electron beam axis (*x*, *z* projections). Here we propose improving the quality of the reconstructed cubes by techniques based on image restoration and volume deblurring that were developed, extensively tested, and used in our laboratory. The initial step implies computing a point spread function (PSF) for each reconstructed volume, and its use to deblur the reconstructed cube

plane by plane using the Richardson–Lucy algorithm implemented in Matlab software. This algorithm is preferred because it maximizes the likelihood function by the Poisson noise case, which applies to the tomograms ***(33, 35)***.

To improve the quality of the final image by the deblurring technique, the following operations with the reconstructed cube should be executed:

1. Determine the specific PSF for the projections of the tilted object as well as for the retro-projection process. To do this:
   (a) Separate the smallest (10–15 nm) single and well-defined silver/gold particles within all the *x,y* planes.
   (b) Cut at least 20 regions of interest containing a single particle from the tomogram.
   (c) Perform centering and averaging of all selected particles to obtain a reconstructed particle that corresponds to the PSF of the whole projection/reconstruction system.
2. Submit the volume of interest to the image restoration and volume deblurring procedures. To do this:
   (a) Evaluate the image restoration efficiency after 5, 10, 20, 50, and 100 iterations. Check the evolution of the deblurring process according to the shape of single particles along the *x*,*z* axis.
   (b) Using the Maximum Intensity Projection mode, visualize the *y*,*x* and the *z*,*x* planes of the processed volume.
   (c) Compare the improvement of the quality of the final 3D image before and after deblurring of the same tomogram. After such a treatment the particles that were partly blurred and elongated according to the *z* axis before deblurring should become well defined without elongations in the *z* direction and sharply outlined (*see* **Note 9**).

3.14 Conclusion and Prospects

There is a plethora of reports dedicated to the molecular organization of the nucleolar compartments. However, the functional role of rDNA transcription factors in the spatial packaging of r-gene chromatin, as well as in the structural organization of the whole nucleolus, is still far from clear. At the molecular level, the r-gene transcription machinery is visualized on unraveled ribosomal chromatin where active tandem genes are linearly arranged along the rDNA axis. Working genes are recognizable by laterally growing chains of nascent rRNA in the form of "Christmas trees" ***(36–38)***. This very long, continuous molecular complex represents the structural–functional basis of the nucleolus. However, within the nucleolus, all the structural constituents become tightly compressed, making it impossible to distinguish their relations in situ. Therefore, very little is known about how such a giant chain, easily reaching micrometers in length, is functionally organized at the structural level.

Obviously, due to the molecular resolution of EM tomography, there is an acute need for further theoretical and experimental concentration in the area of the nucleolus. Other proteins linked to the rDNA template would probably show a supramolecular organization similar to that obtained for RNAP I. Thus, new experimental evidence is required to link structure–function relationships between transcription factors and rDNA. Having sampled the organization of RNAP I, it is now easy to overlap the 3D map of any rDNA-specific protein with the spatial structure of the r-genes. One important target for this task is the transcription factor, upstream binding factor (UBF). Interestingly, an important relationship is proposed between UBF and RNAP I, while polymerase-associated factor PAF53 may bind to UBF ***(5, 39)***. The goal now could be to disclose the coordinate action of RNAP I together with UBF to determine how their interactions with rDNA are integrated into the structural framework of r-gene chromatin. The extensive binding of UBF along the full length of the repeated gene unit suggests a possible structural function, featuring as an architectural transcription factor ***(40, 41)***. UBF may present an especially interesting link between its competence to induce rDNA folding and its possible role in the structural organization of active r-gene chromatin fibers. There is thus good reason to extend our protocol for the discrimination of other key r-gene transcription factors, UBF in particular.

In the field of EM-tomographic approaches, there is clearly great interest in developing a technique that allows comparison of the structural distribution of specific proteins within the nucleolus of living cells expressing GFP constructs with supramolecular data obtained using anti-GFP–FNG labelling. Furthermore, due to the flexible organization of the nucleolus, a number of different inhibitors or activators of rRNA synthesis is ordinarily used as an appropriate tool to investigate nucleolar architecture regarding the functions of the nucleolus-specific proteins ***(2, 42–44)***. Correspondingly, the cooperative behavior of RNAP I, UBF, or other transcription factors in response to inhibitors is foreseen to yield intriguing results. All the above-mentioned topics are now in progress in our laboratory.

4 Notes

1. Forty-millimeter-diameter coverslips are very useful to scrape, collect, and then embed a sufficient amount of properly labelled cells to prepare a number of thick sections. On the other hand, the cover glasses attached to the bottom of MatTek dishes contain an etched grid with coordinates that allow the localization of cells.
2. To reduce the background, rinse the cells 3× 5 min with 0.02 *M* sodium citrate buffer, pH 7.0.
3. To obtain better penetration of epoxy resin, after 100% acetone use pure propylene oxide for dehydration and propylene oxide/epoxy resin mixtures (2:1, 1:1, and 1:2 v/v respectively) for impregnation.

4. To properly acquire the STEM image series, thick sections must be tightly stretched around the area of interest, and as a rule, the sticking of the sections is very good if you use formvar-coated London Finder grids. It is easier to enhance the sticking of sections to uncoated grids by "tempering"; just before the collection of sections take a new (not washed) grid by the forceps and pass it very rapidly through the flame of alcohol lamp (do not melt the grid!). If you prefer uncoated grids, to obtain excellent sticking of sections to the grid bars it is necessary to wash the grids in a 10% v/v solution of HCl and then store them in 100% acetone. To wash take ~50 new (or once used) grids and drop in a 25-mL plastic centrifuge tube with a conical bottom. Add 10 ml of 10% HCl solution and stir at the highest speed of a Vortex-type stirrer for 1–3 min. Rinse the grids 10× with ultra-pure water, then dry on filter paper and keep them in 100% acetone in a tightly sealed flask.
5. To yield excellent 500-nm sections, use an old but defect-free diamond knife to prevent scratches as well as other damage usually produced by a glass knife.
6. To pick up the sections with a new but not washed grid take it with the forceps, pass very rapidly through the flame of an alcohol lamp, and then gently touch two to four sections. Dry the grid and control the sticking of the sections.
7. There is an easier way to pick up the sections with a slot grid. Take the forceps with the formvar-coated slot grid in your right hand, bring it over the isolated ribbon of sections, and touch the sections gently with the formvar-coated side of the slot. Lift the sections and dry the slot grid. Caution is necessary because as a rule this causes folds on the supporting film and the sections that may damage the cell of interest, so microscopical control is obligatory.
8. To obtain a better stability of the supporting film, coat the other side of the slot grid with carbon; if you prefer to work with grids not covered with formvar, especially safe tilting can be performed when both sides of the sections are coated by carbon.
9. All procedures related to the image restoration and the deblurring processes were executed using a Linux workstation and Analyze software. The centering and averaging procedure was done on a Linux workstation by means of software developed in our laboratory ***(33)***.

Acknowledgments The financial support for this work was received from the Association pour la Recherche sur le Cancer (contract N° 4497) and the Ligue contre le Cancer (Departements de l'Aube, de la Marne, et des Ardennes). A long-term grant for invited scientists was obtained from the Région Champagne-Ardenne for Prof. P. Tchelidze.

References

1. Olson, M.O. (1990) The role of proteins in nucleolar structure and function, in *The Eucaryotic Nucleus* (Strauss, P.R., Wilson S.H. eds.), Telford Press, pp. 519–559.
2. Thiry, M. and Goessens, G. (1996) The nucleolus during the cell cycle, in *Molecular Biology Intelligence Unit* (Landes R.G, ed.). Springer-Verlag, Heidelberg, pp. 1–144.

3. O'Brien, T.P., Bult, C.J., Cremer, C., Grunze, M., Knowles, B.B., Langowski, J., McNally, J., Pederson, T., Politz, J.C., Pombo, A., Schmahl, G., and Spatz, J.P. (2003) Genome function and nucleolar architecture: from gene expression to nanoscience. *Genome Res*. **13**, 1029–1041.
4. Mosgoeller, W. (2003) Nucleolar ultrastructure in vertebrates, in *The Nucleolus* (Olson, M.O., ed.), Plenum Publishers, pp. 1–11.
5. Cavanaugh, A., Hirchler-Laszkiewicz, I., and Rothblum, L. (2003) Ribosomal DNA transcription in mammals, in *The Nucleolus* (Olson, M.O., ed.), Plenum Publishers, pp. 89–129.
6. Andersen, J.S., Lyon C.E., Fox A.H., Leung, A.K.L., Lam, Y.W., Steen, H., Mann, M., and Lamond, A. (2002) Directed proteomic analysis of the human nucleolus. *Curr. Biol*. **12**, 1–11.
7. Thiry, M. and Lafontaine, D.L. (2005) Birth of a nucleolus: The evolution of nucleolar compartments. *Trends Cell Biol*. **54**, 194–199.
8. Misteli, T. (2005) Concepts in nucleolar architecture. *BioEssays* **27**, 477–487.
9. Derenzini, M., Pasquinelli, G., O'Donohue M.-F., Ploton, D., and Thiry, M. (2006) Structural and functional organization of ribosomal genes within the mammalian cell nucleolus. *J. Histochem. Cytochem*. **54**, 131–145.
10. Crowther, R.A. and Klug, A. (1971) ART and science or Cconditions for 3D reconstruction from electron microscope images. *J. Theor. Biol*. **32**, 199–203.
11. Beorchia, A., Heliot, L., Menager, M., Kaplan H., and Ploton, D. (1993) Application of medium-voltage STEM for the 3-D study of organelles within very thick sections. *J. Microsc*. **170**, 247–258.
12. Heliot, L., Kaplan H., Lucas L., Klein C., Beorchia, A., Doco-Fenzy, M., Menager, M., Thiry, M., O'Donohue, M.F., and Ploton, D. (1997) Electron tomography of metaphase nucleolar organizers regions: Evidence for a twisted-loop organization. *Mol. Biol. Cell*. **8**, 2199–2216.
13. Baumeister, W., Grimm, R., and Walz, J. (1999) Electron tomography of molecules and cells. *Trends Cell Biol*. **9**, 81–85.
14. McEwen, B.F. and Marko, M. (2001) The emergence of electron tomography as an important tool for investigating cellular ultrastructure. *J. Histochem. Cytochem*. **49**, 553–563.
15. Cheutin, Th., O'Donohue, M.-F., Beorchia, A., Vandelaer, M., Kaplan, H., Defever, B., Ploton, D., and Thiry, M. (2002) Three-dimensional organization of active rRNA genes within the nucleolus. *J. Cell Sci*. **115**, 3297–3307.
16. McIntosh, R., Nicastro, D., and Mastronarde, D. (2004) New views of cells in 3D: An introduction to electron tomography. *Trends Cell Biol*. **15**, 43–51.
17. Baumeister, W. (2005) A voyage to the inner space of cells. *Protein Sci*. **14**, 257–269.
18. Robinson, J. M. and Vandre, D.D. (1997) Efficient immunocytochemical labelling of leukocyte microtubules with FluoroNanogold: an important tool for correlative microscopy. *J. Histochem. Cytochem*. **45**, 631–642.
19. Robinson, J.M., Takizawa, T., and Vandre, D.D. (2000) Enchanced labelling efficiency using ultrasmall immunogold probes: immunocytochemistry. *J. Microsc*. **199**, 163–179.
20. Yi, H., Leunissen, J.L.M., Shi, G.M., Gutekunst, C.A., and Hersh, S.M. (2001) A novel procedure for pre-embeding double immunogold-silver labelling at the ultrastructural level. *J.Histochem. Cytochem*. **49**, 279–283.
21. Powell, R.D., Halsey, C.M., and Hainfeld, J.F. (1998) Combined fluorescent and gold immunoprobes: Reagents and methods for correlative light and electron microscopy. *Microsc. Res. Tech*. **42**, 2–12.
22. Polishchuk R.S. and Mironov A.A. (2001) Correlative video light/electron microscopy. *Current Protocols in Cell Biology*. **11**, 4.8.1–4.8.9.
23. Gilbert, N., Lucas, L., Klein, C., Menager, M., Bonnet, N., and Ploton, D. (1995) Three-dimensional co-location of RNA polymerase I and DNA during interphase and mitosis by confocal microscopy. *J. Cell Sci*. **108**, 115–125.
24. Moss, T. and Stefanovsky, V.Y. (1995) Promotion and regulation of ribosomal transcription in eukaryotes by RNA polymerase I. *Progr. Nucleic Acids Res*. **50**, 25–66.
25. Grummt, I. (1999) Regulation of mammalian ribosomal gene transcription by RNA polymerase I. *Progr. Nucleic Acid Res. Mol. Biol*. 62, 109–154.

26. Grummt, I. (2003) Life on a planet of its own: Regulation of RNA polymerase I transcription in the nucleolus. *Genes & Dev*. **17**, 1691–1702.
27. Cheutin, Th., Misteli, T., and Dundr, M. (2003) Dynamics of nucleolar components, in *The Nucleolus* (Olson, M.O., ed.), Plenum Publishers, pp. 44–57.
28. Cheutin, T., Sauvage C., Tchelidze P., O'Donohue M.-F., Kaplan H., Beorchia, A., and Ploton, D. (2007) Visualizing macromolecules with FluoroNanogold: from photon microscopy to electron tomography. *Methods Cell Biol*. **79**, 559–574.
29. Ploton, D., O'Donohue, M.-F., Cheutin, T., and Thiry, M. (2004) Three-dimensional organization of rDNA and transcription, in *The Nucleolus* (Olson, M.O., ed.), Landes Bioscience, pp. 154–169.
30. Yau, S.F. and Du, M.H. (1998) Sinogram extrapolation for limited angle and time-varying object tomography. *Acta Electronica Sinica*. **26**, 86–90.
31. Liu, Z. and Yau S.F. (1998) A sinogram restoration technique for the hollow projections problem in computer tomography, in *Proc. 20th Annual Int. Conf. of IEEE Engineering in Medicine & Biology Soc*. **20**, pp. 656–659.
32. Abramoff, M.D., Magelhaes, P.J., and Ram, S.J. (2004) Image processing with Image J. *Biophotonics Int*. **11**, 36–42.
33. Tchelidze, P., Sauvage, C., Bonnet, N., Kilian, L., Beorchia, a., O'Donohue, M.-F., Ploton, D., and Kaplan, H. (2006) Electron tomography of amplified nanogold immunolabelling: Improvement of quality based on aligment of projections with sinograms and use of post-reconstruction deconvolution. *J. Struct. Biol*. **156**, 421–431.
34. Gordon, R., Bender, R., and Herman, G.T. (1970) Algebraic reconstruction techniques (ART) for 3D electron microscopy and X-ray photography. *J. Theor. Biol*. **29**, 471–481.
35. Richardson, W.H. (1972) Bayesian-based iterative method of image restoration. *J. Opt. Soc. Am*. **62**, 55–59.
36. Miller, O.L. and Beatty, B. (1969) Visualization of nucleolar genes. *Science* **164**, 995–957.
37. Miller, O.L. and Bakken, A.H. (1972) Morphological studies of transcription. *Acta Endocrinol. Suppl. (Copenh.)*. **168**, 155–177.
38. Trendelenburg, M. and Puvion-Dutilleul, F. (1987) in *Electron microscopy in molecular biology, a practical approach* (J. Sommerville and U. Scheer eds.), IRL Press, pp. 104–146.
39. Hanada, K., Song, C.Z., Yamamoto, K., Yano, K., Maeda, Y., Yamaguchi, K., and Muramatsu, M. (1996) RNA polymerase I associated factor 53 binds to the nucleolar transcription factor UBF and functions in specific rDNA transcription. *EMBO J*. **15**, 2217–2226.
40. O'Sullivan, A. C., Sullivan, G. J., and McStay, B. (2002) UBF binding in vivo is not restricted to regulatory sequences within the vertebrate ribosomal DNA repeat. *Mol. Cell Biol*. **22**, 657–668.
41. Mais, C., Wright, Jane E., Prieto, J.L., Raggett S. L., and McStay, B. (2005) UBF-binding site arrays form pseudo-NORs and sequester the RNA polymerase I transcription machinery. *Genes & Dev*. **19**, 1–15.
42. Hadjiolov, A. (1985) The nucleolus and ribosome biogenesis, in *Cell Biology Monographs* (Alfert, M., Beerman, W. and Goldstein, L. eds.), Springer-Verlag, Wien, New York, pp. 1–263.
43. Sheer, U. and Weisenberger, D. (1994) The nucleolus. *Curr. Opin. Cell Biol*. **6**, 354–359.
44. Scheer, U. and Hock, R. (1999) Structure and function of the nucleolus. *Curr. Opin. Cell Biol*. **11**, 385–390.

Chapter 11
The Perinucleolar Compartment (PNC): Detection by Immunohistochemistry

Alicja Slusarczyk and Sui Huang

Keywords Perinucleolar compartment; PNC; PNC prevalence; Nuclear structure; Tumor marker; Immunohistochemistry

Abstract The perinucleolar compartment (PNC) is a dynamic, irregularly shaped, and electron-dense nuclear structure that is physically associated with the nucleolus ***(1)***. It is found predominantly in transformed cells and various cancer tissues, and rarely in normal cells ***(1)***. The components of the PNC described to date include several small RNAs transcribed by RNA polymerase (pol) III, and several RNA binding proteins of which some are primarily implicated in pre-messenger RNA (mRNA) processing ***(2)***. The current working model suggests that the PNC is a dynamic functional organelle involved in the metabolism and trafficking of a subset of newly synthesized pol III RNAs in transformed cells. The PNC can be localized and visualized in tissue sections by a immunohistochemical technique using the mouse monoclonal antibody SH54 ***(3)***, which specifically recognizes the RNA binding protein PTB (polypyrimidine tract binding protein), which is highly concentrated in the PNC and is used as a marker for PNC detection.

The prevalence of PNCs has been found to be correlated with disease progression in breast cancer ***(3)*** and in tumors from other tissues, including prostate, colon, ovary, and endometrium (our unpublished studies). PNC prevalence increases with the degree of malignancy and reaches nearly 100% in distant metastases. A high PNC prevalence is associated with poor prognosis (our unpublished studies) ***(3)***. In this chapter, we describe methods, which are still under development, for PNC detection and PNC prevalence scoring. Due to the intrinsic limitations of immunocytochemistry using peroxidase assays, the signal intensity can vary from experiment to experiment. Studies are underway to optimize an automated protocol to increase its reproducibility and accuracy.

R. Hancock (ed.) *The Nucleus: Volume 1: Nuclei and Subnuclear Components*,

1 Introduction

The structural and functional organization of the nucleus is considerably changed during malignant transformation. Features correlated with malignant transformation include nuclear enlargement, alterations in nuclear shape, and changes in several specific nuclear domains. The alterations observed in nuclear structures and molecular components are currently at the experimental stage of validation of their potentials as tumor markers. They may provide a comprehensive picture of a malignant process, since they are often the outcome of the collective changes during transformation and its final manifestations. The nucleolus, PNC, Cajal Bodies, promyelocytic leukemia (PML) nuclear bodies, and heterogeneous ribonucleoproteins are currently being investigated as promising tumor markers ***(1)***.

The PNC is a nuclear substructure associated with malignancy. PNC prevalence (the percentage of cells that contain at least one PNC) is highly heterogeneous in a broad range of cancer cell lines and in primary tumors. It increases substantially in lymph node metastases of breast cancer and reaches nearly 100% in distant metastasis ***(3)***. Furthermore, PNC prevalence is correlated positively with progression of breast and colon cancer with respect to staging, grading, and lymph node involvement, and is correlated negatively with patient outcome ***(3)***. These observations support a model in which the formation of the PNC is a consequence of malignant transformation and may represent milestone changes of molecular and cellular events during transformation that confer metastatic capacity ***(4)***. Therefore, PNC prevalence could be potentially a useful tumor marker providing prognostic information for individual patients.

PNC prevalence can be scored in cultured cells or tissue samples using immunohistochemical labeling with the anti-polypyrimidine tract binding protein (PTB) monoclonal antibody SH54 developed by our laboratory to specifically recognize the key PNC-associated protein PTB ***(1)***. This method employs a streptavidin-biotin detection system that relies on the high binding affinity of streptavidin to biotin and provides very specific detection and amplification of the antigen–antibody binding event. It can be performed on paraffin-embedded tissue sections and is routinely applied to PNC detection and localization studies (Fig. 11.1).

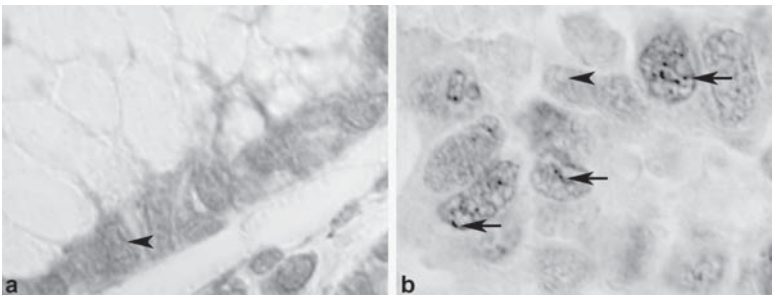

Fig. 11.1 Immunohistochemical staining of paraffin-embedded normal (**a**) and malignant (**b**) colorectal tissue samples to detect PNCs using the monoclonal antibody SH54. High-magnification images allow for visualization of PNC-containing cells (**b**, *arrows*) versus cells without the presence of a PNC (**a**, *arrowhead*)

2 Materials

2.1 Tissue Sample Preparation

Sections 4- to 5-μm thick of paraffin-embedded tissue can be used for the analysis. The sections are attached to slides by drying in an oven at 60°C for 10 to 20 min. It is to be cautioned that the fixation should be pH neutral for a minimal amount of time, and that the block should be heated at the lowest possible temperature for the shortest time. Most standard practices work well for the preservation of the antigen in tissue sections. With each group of samples, a positive control sample (e.g., HeLa cells) and a negative control sample (e.g., normal colorectal or breast tissue from the US National Cancer Institute's Cooperative Human Tissue Network (http://www-chtn.ims.nci.nih.gov/) should be included to verify proper labeling. Hematoxylin–eosin stained histological sections that are adjacent to the sections examined for PNCs have been used to examine the conformation of the tumor tissue and the most active areas of the tumor (highest grading).

2.2 Reagents

1. Neutral-buffered formalin fixing solution: 100 mL of 37 % (w/w) formaldehyde solution, 4.0 g of NaH_2PO_4, 6.5 g of Na_2HPO_4, and 900 mL of distilled H_2O (pH 6.8); available commercially (e.g., Sigma-Aldrich, St. Louis, MO, USA).
2. Xylene (Fisher Scientific, Fair Lawn, NJ, USA).
3. Ethanol (VWR International, West Chester, PA, USA): 100%, 95%, and 75% (v/v) solutions, make fresh and keep covered.
4. Methanol 100% (VWR).
5. H_2O_2 (Sigma-Aldrich): prepare a fresh 10% (v/v) solution, store covered at 4°C.
6. 10 m*M* citrate buffer: dissolve 1.92 g of anhydrous citric acid (Sigma-Aldrich) in 1,000 mL of H_2O, adjust to pH 6.0 if necessary with 1 N NaOH. Autoclave, store at room temperature for 3 months or at 4°C for a longer time.
7. Phosphate-buffered saline (PBS): prepare a 10× stock solution with 80 g of NaCl, 2 g of KCl, 11.5 g of $Na_2HPO_4.7H_2O$, and 2 g of KH_2PO_4 in 1,000 mL of H_2O, adjust to pH 7.4 with NaOH if necessary, and autoclave before storage at room temperature. Prepare the working solution of PBS by diluting one part of 10× PBS with nine parts of H_2O.
8. Blocking solution: normal horse serum (Atlanta Biologicals, Lawrenceville, GA, USA), store in single-use aliquots at −80°C. Prepare a working solution by diluting 1:10 in PBS, 0.05% Tween-20 (Fisher).
9. Primary antibody: monoclonal antibody SH54 that specifically recognizes the PNC-associated protein, PTB ***(1)*** (Santa Cruz Biotechnology, Santa Cruz, CA, USA). Store at 4°C. A working solution is prepared by diluting 1:200 in PBS, 0.05% Tween-20 (*see* **Note 1**).

10. Secondary antibody: biotinylated anti-mouse IgG (Vector Laboratories, Burlingame, CA, USA). Store at 4°C. Prepare a working solution by diluting 1:200 in PBS, 0.05% Tween-20 (*see* **Note 2**).
11. Streptavidin-conjugated horseradish peroxidase (BioGenex, San Ramon, CA, USA). Store at 2–8°C. Prepare a working solution by diluting 1:200 in PBS, 0.05% Tween-20 (*see* **Note 2**).
12. Chromogen: 3,3′-diaminobenzidine (DAB) (SigmaFast DAB tablet set; Sigma-Aldrich). Store at −80°C. Dissolve one DAB tablet and one urea hydrogen peroxide tablet in 5 mL of ultrapure H_2O, giving 0.7 mg/mL of DAB and 2 mg/mL of Urea Hydrogen Peroxide (H_2O_2 equivalence 0.7 mg/mL). Prepare freshly before labeling, keep covered in the dark. *DAB is a potential carcinogen and must be used with proper care and precautions!*
13. Mounting medium (Fisher) and cover glasses (VWR).

2.3 Equipment

1. Water-repelling pencil (Vector Laboratories) to circumscribe sections on slides.
2. Humid chambers: petri dishes with moistened paper inside and fully covered with the lid.
3. Optical microscope: we use a Nikon Eclipse E800 microscope with a ×60 objective and a monochromatic SenSys CCD camera (Photometrics, Tucscon, AZ, USA) that is controlled by the Metamorph Image Acquisition System (Universal Imaging, West Chester, PA, USA).

3 Methods

The PNC can be detected by a standard indirect immunohistochemistry detection protocol using the streptavidin-biotin detection system. This involves the binding of primary antibody to the protein PTB, which is highly enriched in PNCs, followed by a signal amplification step with a secondary antibody conjugated with streptavidin, and finally detection of the binding by a colorimetric reaction. The signal is developed by applying the chromogen DAB, which reacts with streptavidin-conjugated horseradish peroxidase (HRP) to yield a permanent brown-colored end product.

3.1 Sample Fixation

Tissue samples are generally fixed for a period ranging from 2 h to overnight in 10% neutral buffered formalin, a widely used fixing agent for pathologic histology. HeLa cells that were fixed either for 2 h or overnight did not show a significant difference in their PNC prevalence, demonstrating that the antigen-retrieval labeling method is not obviously affected by the length of fixation. Most samples are

put in fixative for a period ranging from less than 1 h up to several hours after discontinuing the blood supply, and those that were not fixed immediately are temporarily stored at 4°C. Samples with deteriorated cellular morphology should not be selected for PNC detection.

3.2 Immunohistochemistry

3.2.1 Deparaffinization and Rehydration

1. Using the water-repelling pencil, circumscribe 4- to 5-μm-thick paraffin-embedded tissue sections on slides.
2. Deparaffinize in two changes of xylene for 5 min each at room temperature.
3. Incubate the samples in 100% ethanol, two changes for 2 min each.
4. To block endogenous peroxidase activity, wash in freshly prepared 10% v/v H_2O_2 in 100% methanol for 10 min at room temperature.
5. Hydrate the samples in 95% ethanol, two changes for 1 min each.
6. Hydrate the samples in 75% ethanol, two changes for 1 min each.
7. Wash with PBS for 5 min.

3.2.2 Antigen Retrieval

1. Incubate slides in freshly prepared 10 m*M* citrate, pH 6.0, in a microwave oven for 10 min (*see* **Note 1**), using high microwave power for 2 min until the liquid is boiling and then low power for the remaining time. Add distilled H_2O as needed to keep the slides covered.
2. Allow the slides to cool down to room temperature for 30 min. It is important not to cool samples for too long (30–40 min), otherwise the citric acid may destroy the tissue.
3. Rise the slides 2× in distilled H_2O, agitating up and down.
4. Rinse in 1× PBS, 0.05% Tween-20 for 5 min.

3.2.3 Blocking

1. To minimize nonspecific binding of antibodies, incubate the samples in blocking solution for 15 min in a humid chamber at room temperature.

3.2.4 Labeling with Primary Antibody

1. Decant the blocking solution and apply 200 μL of the diluted SH54 primary antibody. Incubate overnight at 4°C in a humid chamber (*see* **Notes 2** and **3**).
2. Wash completely 2× with PBS, 0.05% Tween-20 for 10 min total.

3.2.5 Labeling with Secondary Antibody

1. Apply 200 µL of the diluted secondary antibody and incubate for 60 min at room temperature in a humid chamber (*see* **Note 2**).
2. Wash completely 2× with PBS, 0.05% Tween-20 for 10 min total.

3.2.6 Labeling with Streptavidin-HRP

1. Apply the diluted streptavidin-peroxidase conjugate and incubate at room temperature for 60 min in a humid chamber (*see* **Note 2**).
2. Wash completely 2× with PBS, 0.05% Tween-20 for 10 min total.
3. Wash with distilled H_2O for 5 min.

3.2.7 Applying the Substrate DAB

DAB is a potential carcinogen and must be used with proper care and precautions!

1. Apply the DAB solution and incubate for 20 min at room temperature until color is developed (*see* **Note 3**).
2. Rinse 2× in distilled H_2O to stop the reaction.

3.2.8 Mounting Samples

1. Dehydrate samples in 75% ethanol (2× 1 min) followed by 95% ethanol (2× 1 min) and 100% ethanol (2× 1 min).
2. Clear samples in 50% xylene/50% ethanol for 1 min and in 100% xylene for 2× 5 min each, at room temperature.
3. Mount the samples in mounting medium under a cover glass (*see* **Note 4**).

3.3 Examining slides by microscopy

Signals are visualized using an optical microscope and images are captured sing the Metamorph Image Acquisition System, whose densitometry software is used to determine the labeling intensity. PTB is diffusely distributed in cells that do not show detectable PNCs, and although fixation and paraffinization slightly distort nuclear structure resulting in an uneven labeling of nuclei, the heterogeneity of the nuclear labeling in PNC-negative cells usually does not reach a twofold difference in intensity. Nuclear PTB aggregates that are at least twofold higher in intensity than the diffuse nucleoplasmic labeling and that are near a nucleolus are scored as

PNC-positive. Nucleoli are often negatively stained by the antibody and appear as lighter areas but they may be above or below the plane of the section or too small to be evident, in which case these cells should either be disqualified or the PNC association should be examined in the adjacent sections.

At least 500 epithelial cells within the most aggressive diseased (histologically high grade) areas are evaluated and scored for PNC prevalence. The scoring is performed in a blind manner such that examiners are unaware of the patient information including the tumor size, nodal status, and patient outcome. Paraffin-embedded HeLa cells, whose average PNC prevalence is 90%, are used as a positive control and normal colorectal or breast tissue as a negative control for each round of labeling and scoring. In addition, the fact that the scoring is based on the ratio of the highest PTB labeling intensity in the nucleus to the diffuse nuclear labeling largely eliminates the effect of intercellular variability when the overall labeling is within a linear range.

4 Notes

1. The amount of diluted primary antibody solution to prepare depends on the number of samples. The normal dilution is 1:200 but in some cases, depending on the intensity of staining, it has been increased to 1:100. Diluted primary antibody can be stored at 4°C for subsequent experiments.
2. The eluted secondary antibody and streptavidin conjugate can be saved for several months at 4°C for subsequent experiments.
3. Twenty minutes are allowed for color development; however, in some experiments the time was decreased to 15 min due to undesirable background staining.
4. The sections are not counterstained.

Acknowledgments We thank Dr. A. Thor (University of Colorado, Health Science Center) and her group for developing the protocol and long term collaboration. This work was supported by a grant from the National Cancer Institute (NCI) (R33 CA097761-02) and by funds from The Robert H. Luria Comprehensive Cancer Center.

References

1. Huang, S., Deerinck, T. J., Ellisman, M. H., and Spector, D. L. (1997) The dynamic organization of the perinucleolar compartment in the cell nucleus. *J. Cell Biol*. **137,** 965–974.
2. Huang, S., Deerinck, T. J., Ellisman, M. H., and Spector, D. L. (1998) The perinucleolar compartment and transcription. *J. Cell Biol*. **143**, 35–47.
3. Kamath, R. V., Thor, A. D., Wang, C., Edgerton, S. M., Slusarczyk, A., Leary, D. J., Wang, J., Wiley, E. L., and Huang, S., et al (2005) Perinucleolar compartment prevalence has an independent prognostic value for breast cancer. *Cancer Res*. **65,** 246–253.
4. Kopp, K., and Huang, S. (2005) Perinucleolar compartment and transformation. *J. Cell Biochem*. **95,** 217–225.

Chapter 12
Isolation of the Constitutive Heterochromatin from Mouse Liver Nuclei

Olga V. Zatsepina, Oxana O. Zharskaya, and Andrei N. Prusov

Keywords Constitutive heterochromatin; Chromocenter; Isolation; Mouse liver

Abstract A method for isolation of constitutive heterochromatin (chromocenters) from nuclei of mouse liver cells is described. This method is based on the higher resistance of chromocenters to low ionic strength treatment as compared with that of nucleoli and euchromatin. The method allows separation of chromocenters that are essentially free of nucleoli and other nuclear contaminants. In contrast to nuclei and nucleoli, isolated chromocenters are characterized by a simpler protein composition and contain a smaller number of proteins (especially of high molecular weight proteins). They possess telomeric DNA and telomerase activity that suggests a tight association of chromocenters with the telomerase complex in mouse hepatocyte nuclei.

1 Introduction

The interphase nucleus is a highly organized structure that consists of numerous structural domains such as nucleoli, heterochromatin, euchromatin, clusters of interchromatin granules (speckles), Cajal bodies, and others ***(1)***. These compartments are involved in the cooperative functioning of various regions of chromosomes in interphase including gene transcription, processing, and modification of nascent RNA transcripts, assembly or degradation of transcription complexes, metabolic exchanges between the nucleus and cytoplasm, etc. Nevertheless, it is thought that approximately 90% of the chromosomal genetic material is in a transcriptionally inert state. In mammalian cells of various species, including the mouse *Mus musculus*, a significant portion of inactive chromatin exists as constitutive heterochromatin. In contrast to actively transcribed euchromatin, constitutive heterochromatin is characterized by a high packing density in interphase, a later replication in S-phase, and a lower content of structural genes ***(2, 3)***. Another remarkable feature of constitutive heterochromatin is its spatial association with the nucleolus, nuclear envelope, and pre-kinetochores ***(4–6)***. In mouse cells, constitutive heterochromatin is organized in

R. Hancock (ed.) *The Nucleus: Volume 1: Nuclei and Subnuclear Components*,

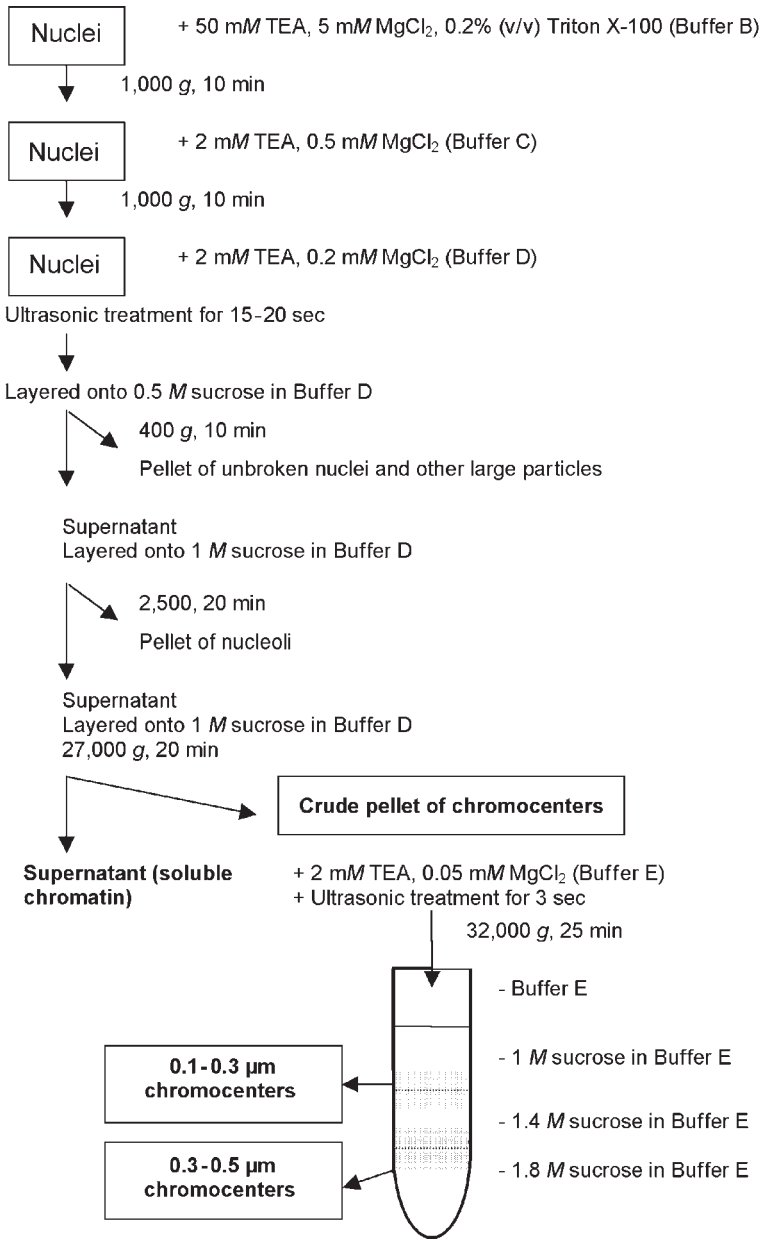

Fig. 12.1 The general protocol for chromocenter isolation

particularly large (up to 0.5 µm in size) and numerous (up to 20 per nucleus) chromatin blocks called chromocenters *(7)*. At the light microscopy level, chromocenters can be viewed by staining nuclei with AT-rich DNA- binding dyes such as DAPI or Hoechst 33258 (Fig. 12.2a). On ultrathin electron microscopy sections, they can be identified

among other nuclear regions due to a particularly tight and rather uniform structure ***(8, 9)***. In mouse interphase nuclei, the chromocenters include the centromeric regions of mitotic chromosomes ***(10)***, and in line with this idea, several proteins including CEN-proteins (CENPs) have been localized both in the centromeric region of chromosomes during mitosis and in association with chromocenters at interphase ***(4)***. Recently, telomeric DNA and telomerase activity have also been found associated with isolated mouse chromocenters, thus arguing in favor of the idea that in mouse cells the chromocenters include not only the centromeric but also the telomeric regions of mitotic chromosomes ***(11)***. However, the general molecular composition of chromocenters (constitutive heterochromatin) remains uncertain.

During the last decade, remarkable progress has been achieved toward the elaboration of methods for biochemical fractionation of nuclear structural domains including speckles ***(12)***, Cajal bodies ***(13)***, and nucleoli ***(14–17)***. These approaches have been applied to large-scale analyses of nuclear substructures in terms of their evolution ***(18)***, protein dynamics, and functional implications ***(16, 19, 20)***. In the present chapter, we describe a novel method for isolation of constitutive heterochromatin (chromocenters) from mouse hepatocytes (Fig. 12.1). This method is based on the higher resistance of the chromocenter material to dispersion in low ionic strength buffers as compared with that of nucleoli and euchromatin. We also employ differential centrifugation of a crude chromocenter fraction in a sucrose step gradient for further separation of chromocenters from nucleoli and soluble chromatin fragments. By this procedure, two fractions of chromocenters of different size can be obtained. Both fractions are essentially free of other nuclear or cellular contaminants and are similar in their total protein repertoire. The purity of the isolated fractions is sufficient for mass spectroscopic analysis of chromocenter proteins. This material could also be applied for immunization of animals in order to raise antibodies against chromocenter-bound proteins.

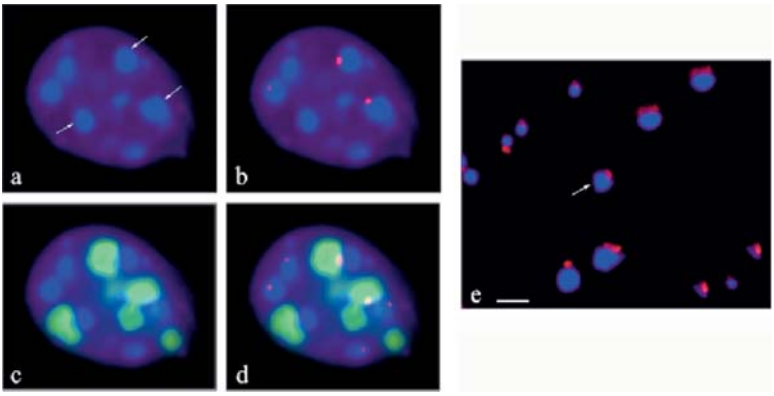

Fig. 12.2 General views of an isolated nucleus (**a–d**) and isolated chromocenters (**e**) after staining with the DNA stain DAPI (*blue*) and immunolabeling for CENP-A (*red*) and for the nucleolar protein B23 (*green*). Note the spatial association of the chromocenters (*arrows*) with nucleoli (in *green*) and pre-kinetochore (*in red*). Bar, 0.5 µm. To view this figure in color, see COLOR PLATE 3

2 Materials

2.1 Isolation of Nuclei

1. Triethanolamine-HCl (TEA) (Sigma-Aldrich, St. Louis, MO, USA): prepare a 1 *M* solution in water (*see* **Note 1**) and adjust to pH 7.6 with 1 *M* HCl with moderate stirring. Aliquot and store at −20°C.
2. KCl: 3 *M* stock solution in water; store at room temperature.
3. $MgCl_2$: 2 *M* stock in water, store at 4°C.
4. Phenylmethylsulfonyl fluoride (PMSF), a serine protease inhibitor (Sigma-Aldrich): prepare a 100 m*M* stock in absolute ethanol (or methanol or 2-propanol). The stock solution is stable for months at 4°C. Use at a final concentration of 0.1 m*M*.
5. Aprotinin (a serine protease inhibitor) (Sigma-Aldrich) in water at 10 mg/mL and stored at −20°C in aliquots. Use at a final concentration of 1 μg/mL.
6. Leupeptin (a serine and cysteine protease inhibitor) (Sigma-Aldrich) in water at 10 mg/mL and stored at −20°C in aliquots. Use at a final concentration of 1 μg/mL.
7. Pepstatin A (a potent inhibitor of acid proteases) (Sigma-Aldrich) in absolute ethanol at 1 mg/mL and stored at −20°C in aliquots. Use at a final concentration of 1 μg/mL.
8. Dithiothreitol (dTT) (Sigma-Aldrich): prepare a 1 *M* stock in water and store at −20°C in aliquots (1 mL). Use at a final concentration of 1 m*M*.
9. Buffer A: 20 m*M* TEA, 30 m*M* KCl, 10 m*M* $MgCl_2$ in water (do not adjust the pH); stable for up to 2 days at 4°C.
10. 2.5 *M* sucrose (Sigma-Aldrich) in Buffer A: dissolve sucrose by stirring on a heating plate at 80°C. Can be stored for up to 1 month at 4°C. Add dTT and protease inhibitors before use.
11. Prepare 0.25 *M* sucrose by diluting one part of 2.5 *M* sucrose with nine parts of Buffer A. Can be stored for 2 days at 4°C. Add dTT and protease inhibitors before use.
12. Potter homogenizer (45 mL, glass with glass pestle) (Sigma-Aldrich; cat. P7859EA1).
13. Tweezers, scissors, filter paper.
14. Three mice of any laboratory strain (e.g., Balb/c) 4 to 6 weeks old (weight ~20 g).

2.2 Isolation of Chromocenters

1. Triton X-100 (Sigma-Aldrich): prepare a 10% (w/v) stock solution in water; store at 4°C for up to a few months.
2. Buffer B: 50 m*M* TEA, 5 m*M* $MgCl_2$, 0.2% Triton X-100 in water (do not adjust the pH).
3. Buffer C: 2 m*M* TEA, 0.5 m*M* $MgCl_2$ in water (do not adjust pH).

4. Buffer D: 2 m*M* TEA, 0.2 m*M* $MgCl_2$ in water (do not adjust pH).
5. Buffer E: 2 m*M* TEA, 0.05 m*M* $MgCl_2$ in water (do not adjust pH).
6. 2.5 M sucrose in water: dissolve by stirring on a heater plate at 80°C. Store at −20°C. Heat up to room temperature, and add DTT and protease inhibitors before use.
7. 0.5 *M* sucrose in Buffer D (16.9 g/L): dissolve by stirring at room temperature. Store at −20°C. Warm to room temperature, add dTT and protease inhibitors before use.
8. 1 *M* sucrose in Buffer D (33.8 g/L): dissolve by stirring at room temperature. Store at −20°C. Warm to room temperature, add dTT and protease inhibitors.
9. 1 *M* sucrose in Buffer E (33.8 g/L): dissolve by stirring on a heating plate at 80°C. Store at −20°C. Warm to room temperature, add dTT and protease inhibitors.
10. 1.4 *M* sucrose in Buffer E (47.1 g/L): dissolve by stirring on a heating plate at 80°C. Store at −20°C. Warm to room temperature, add dTT and protease inhibitors.
11. 1.8 *M* sucrose in Buffer E (61.5 g/L): dissolve by stirring on a heating plate at 80°C. Store at −20°C. Warm to room temperature, add dTT and protease inhibitors.
12. Sucrose step gradient: layer successively 10 mL each of 1.8 *M*, 1.4 *M*, and 1 *M* sucrose solutions in Buffer E into a glass tube for the Beckman SW28 ultracentrifuge rotor.

2.3 Phase Contrast Microscopy (see Note 2)

1. Microscope slides and coverslips (e.g., 18 × 18 mm).

2.4 Fluorescence and Immunofluorescence Microscopy (see Note 3)

1. Phosphate-buffered saline (PBS) (stock): 140 m*M* NaCl, 2.7 m*M* KCl, 8.1 m*M* Na_2HPO_4, 1.5 m*M* KH_2PO_4 (adjust to pH 7.2–7.4 with HCl if necessary); can be stored for up to 1 week at 4°C.
2. Paraformaldehyde (ICN Chemicals, Irvine, CA, USA): prepare a 2% (w/v) solution in PBS by heating at 60–80°C on a stirring hotplate in a fume hood to completely dissolve (do not allow boiling) and then cool to room temperature before use.
3. 4′,6-diamidino-2-phenylindole (DAPI): 100 µg/mL in water, store at 4°C in the dark (light sensitive). Prepare a 0.3 µg/mL working solution in an appropriate buffer immediately before use.
4. Mounting medium: Vectashield (Vector, Peterborough, UK; cat. H-1000)
5. Primary antibody: human anti-CENP-A autoimmune serum (*see* **Note 4**).
6. Secondary antibody: goat anti-human IgG conjugated with Cy3 (Jackson ImmunoResearch, West Grove, PA, USA; cat. 109-165-003).
7. Poly-L-lysine-coated glass slides: Poly-Prep slides (Sigma-Aldrich; cat. P0425).

2.5 Electron Microscopy (see Notes 5 and 6)

1. 0.15 *M* Sørensen phosphate buffer: prepare two solutions: (a) dissolve 11.87 g of $Na_2HPO_4 \cdot 2H_2O$ in 1 L water, and (b) dissolve 9.07 g of KH_2PO_4 in 1 L water; both solutions can be stored for weeks at 4°C. Mix seven parts of solution (1) and three parts of solution (2). Adjust to pH 7.2 if necessary. Use fresh.
2. 25% glutaraldehyde (electron microscopy grade; Sigma-Aldrich; cat. 49626). Store at 4°C for routine use; for long-time storage follow the recommendations of the supplier). *Glutaraldehyde is toxic, handle with care!*
3. Neutral 25% glutaraldehyde: take an aliquot (1–2 mL) of 25% glutaraldehyde and adjust to pH 7.0 with 1 *M* NaOH. Do not use a pH meter, but indicator pH paper for the adjustment. Store at 4°C (*see* **Note 7**).
4. Osmium tetroxide (OsO_4, electron microscopy grade; Sigma-Aldrich; cat. 75633-1EA): 2% (w/v) in water. Light sensitive and *highly toxic*; should be stored in a tightly closed dish at 4°C. Stable for up to several months.
5. Uranyl acetate: 2% (w/v) solution in 70% ethanol. Light sensitive and *radioactive*. Should be stored at 4°C; stable for up to 1 year.
6. 30%, 50%, 70%, 96%, and 100% ethanol in water, store at room temperature.
7. 100% (absolute) acetone, store at room temperature.
8. Epoxy embedding medium kit (Sigma-Aldrich; cat. 45359). Prepare the resin following the manufacture's recommendations. Epoxy compounds should be stored at room temperature; *they are toxic and should be handled with care*.
9. Lead citrate for staining ultrathin sections ***(21)*** requires solutions prepared in glassware. Dissolve 1.33 g of $Pb(NO_3)_2$ (ACS reagent quality; Electron Microscopy Sciences, Hatfield, PA, USA; cat. 17900) in 30 mL of water, and add 1.76 g of $Na_3C_6H_5O_7 \cdot 2H_2O$ (Electron Microscopy Sciences; cat. 21140). Shake vigorously for 1 min and intermittently for 30 min. The solution will appear cloudy. Add 8 mL of freshly made 1 N NaOH (2 g/50 mL) in water, and invert slowly. The solution should now appear clear. Adjust to 50 mL with water, and invert slowly once. The stain is stable for several months at 4°C in the dark; it should be discarded if it becomes cloudy.

3 Methods

3.1 Isolation of Nuclei

All procedures should be carried out at 4°C.

1. Sacrifice mice by cervical dislocation, remove the livers, and place the livers into a homogenizer with 30 mL of 0.25 *M* sucrose in Buffer A.
2. Homogenize the livers by 30–40 strokes.
3. Transfer the homogenate to a 50-mL centrifuge tube and centrifuge at 1,000×*g* for 10 min. Discard the supernatant.

4. Measure the approximate volume of the resulting pellet and add 2.5 *M* sucrose (Section 2.1., item 10) to a final sucrose concentration of 2.1 *M* (e.g., add 20 mL to a ~4 mL pellet). Resuspend the pellet by intense shaking.
5. Transfer the suspension to an appropriate centrifuge tube and centrifuge at 50,000×g_{av} for 10 min (*see* **Note 8**). Discard the supernatant.
6. Add to the pellet a few drops of 0.25 *M* sucrose solution and stir with a glass rod (~10 mm in diameter). Repeat this procedure several times to resuspend the pellet. Add 8–10 mL of 0.25 *M* sucrose.
7. Centrifuge the suspension at 1,000×*g* for 10 min. Discard the supernatant. The pellet contains the isolated nuclei.
8. Facultative: monitor the purity of the nuclear fraction by microscopy; place a drop (10–20 µL) of the suspension on a microscope slide, cover with a coverslip, and view with a phase contrast microscope using a dry lens (*see* **Note 2**).

3.2 Isolation of Chromocenters

All procedures should be carried out at 4°C. The general scheme of chromocenter isolation is shown in Fig. 12.1.

1. Resuspend the isolated nuclei in 10 mL of Buffer B, incubate for 5 min to dissolve the nuclear membranes, and centrifuge at 1,000×*g* for 10 min. Discard the supernatant.
2. Resuspend the pellet in 10 mL of Buffer C and centrifuge at 1,000×*g* for 10 min. Discard the supernatant.
3. Resuspend the pellet in 12–15 mL of Buffer D and transfer to a glass tube (a centrifuge or sonicator tube of an appropriate volume are suitable).
4. Sonicate the suspension with an ultrasonic disintegrator (*see* **Note 9**) at an amplitude of 16 µ for 15–20 sec. Monitor the integrity of the nuclei by phase contrast microscopy.
5. Transfer the suspension to a 50-mL centrifuge tube and then gently underlay 5 mL of 0.5 *M* sucrose in Buffer D with a pipette. Centrifuge at 400×*g* for 10 min to sediment unbroken nuclei and other large particles.
6. Transfer the supernatant (the pellet can be discarded) to a 50-mL centrifuge tube and then gently underlay 5 mL of 1 *M* sucrose in Buffer D with a pipette. Centrifuge at 2,500×*g* for 20 min to sediment nucleoli.
7. Transfer the supernatant (the pellet can be discarded) to a SW28 centrifuge tube (volume ~37 mL). Gently underlay 5 mL of 1 *M* sucrose in Buffer D with a pipette, and then overlay 10–15 mL of Buffer D above the sample.
8. Centrifuge at 27,000×g_{av} for 20 min (*see* **Note 8**). Discard the supernatant. The resulting pellet is the crude chromocenter fraction.
9. Resuspend the pellet in 5 mL of Buffer E to induce further unravelling of non-chromocenter chromatin and nucleolar remnants (note that chromocenters remain compact in these conditions). Transfer the suspension to a glass tube for the following sonication.

10. Sonicate the suspension as above for 3 sec, add ~1.5 mL of 2.5 *M* sucrose in water to give a final sucrose concentration of 0.5 *M*, and mix by moderate shaking. The total volume of the resulting suspension is ~6 mL.
11. Prepare two SW28 centrifuge tubes with sucrose step gradients. Overlay 3 mL of the suspension onto the gradients, and then gently add exactly 10 mL of Buffer E to each tube above the suspension.
12. Centrifuge the tubes at 32,000×g_{av} for 25 min (*see* **Note 8**). The layer at the interface between 1 *M* and 1.4 *M* sucrose contains chromocenters 0.1–0.3 µm in size, and the layer between 1.4 *M* and 1.8 *M* sucrose contains chromocenters 0.3–0.5 µm in size (*see* **Note 10**).

3.3 Phase Contrast Microscopy (see Note 2)

1. Deposit 10–20 µL of fractions on slides and cover by a coverslip. View immediately under a phase contrast microscope using a dry objective lens.

3.4 Fluorescence and Immunofluorescence (see Note 3)

All procedures are carried out at room temperature.

1. Prepare a humid chamber: place a filter paper into a Petri dish of 100 mm (or more) diameter, dampen the paper with water, and cover the dish with a piece of Parafilm.
2. Put a poly-L-lysine-coated slide into the dish and place an aliquot of the suspension (50–100 µL) onto the slide, cover the dish with a lid, and leave for 15 min. Nuclei and chromocenters attach to the slide.
3. Fix the sample with 2% paraformaldehyde in PBS for 15 min and wash 3× 10 min with PBS.
4. Remove the PBS and replace it with an anti-CENP-A antibody (diluted 1:100 in PBS) for 30 min (*see* **Note 4**).
5. Remove the primary antibody and wash the slide 3× 10 min with PBS.
6. Remove the PBS and incubate the slide with secondary antibody (anti-human IgG conjugated with Cy3, 1:300 in PBS) for 20–30 min in the dark.
7. Remove the secondary antibody and wash the slide 3× 5 min with PBS.
8. Stain DNA with 0.3 µg/mL DAPI for 10 min.
9. Remove the DAPI and wash 3× 5 min with PBS.
10. Mount in Vectashield, add a coverslip, and seal with nail vanish. The slide can be viewed immediately under an epifluorescence microscope (*see* **Note 3**). Slides can generally be stored in the dark at 4°C for up to a month.
11. Excitation at 543 nm induces Cy3 fluorescence (red emission) for the CENP-A, and excitation at 364 nm induces DAPI fluorescence (blue emission) for DNA. AdobePhotoshop software can be used to overlay the two

fluorescence images. Examples of overlaid signals for DAPI and CENP-A are shown in Fig. 12.2a, b.

3.5 Electron Microscopy (see Notes 5 and 6)

All procedures are carried out in a 2-mL Eppendorf tube at room temperature unless indicated otherwise. If the pellet formed after fixation becomes dispersed, it should be spun at 5,000×*g* for 5–10 min in a table-top centrifuge.

1. To the suspension of chromocenters, add neutral 25% glutaraldehyde (**Section 2.5.,** item 3) to a final concentration of 2.5% and fix for 1 h. Alternatively, store the sample in fixative overnight at 4°C. *Glutaraldehyde is toxic, work with care!*
2. Rinse 3× 30 min with Sørensen buffer.
3. Fix in 1% OsO_4 (freshly diluted 2% OsO_4 (**Section 2.5.,** item 4) with Sørensen buffer, 1:1) for 1 h in the dark. *OsO_4 is toxic, work with care!*
4. Rinse 3× 30 min with Sørensen buffer.
5. Dehydrate the sample in 30% ethanol and then with 50% ethanol, 30 min each.
6. Contrast the sample with 2% uranyl acetate in 70% ethanol overnight at 4°C in the dark. *Uranyl acetate is radioactive, work with care!*
7. Dehydrate the sample in 96% ethanol (once) and then absolute ethanol (twice) for 30 min.
8. Incubate in absolute acetone for 30 min.
9. Incubate in a mixture of one volume of Epoxy resin and three volumes of absolute acetone for 30 min. *Epoxy resin is toxic, work with care in this and following steps!*
10. Incubate in a mixture of one volume of Epoxy resin and one volume of absolute acetone for 1 h.
11. Incubate in a mixture of three volumes of Epoxy resin and one volume of absolute acetone for 1 h.
12. Add pure Epoxy resin and polymerize for 1 day at 37°C and then for 2 days at 60°C.
13. Remove the block from the tube and cut ultrathin sections.
14. Stain the sections with lead citrate solution, carefully rinse with water, dry at room temperature and view under an electron microscope at 70 kV.

4 Notes

1. Unless stated otherwise, all solutions should be prepared in water that has a resistivity of 18.2 MΩ.cm, referred to as “water” in this text. We use a Direct-Q device (Millipore) to obtain water of the required quality.

2. Phase contrast microscopy is the simplest approach to control the efficiency of the isolation procedure. We use an Axiovert 200 microscope with a Plan-Neofluor ×40/0.75 dry lens (Carl Zeiss, Germany).
3. Staining of isolated fractions with the DNA dye DAPI and/or immunolabeling with antibodies to centromere protein markers (e.g., anti-CENP-A) are appropriate controls for the structural integrity of nuclei and chromocenters. We use the microscope described in Note 2 and also a Plan-Neofluor ×100/1.3 oil-immersion lens (Carl Zeiss) to view fluorescent signals (Fig. 12.2).
4. We use human anti-CENP autoimmune sera from patients with the CREST form of scleroderma, because in our hands commercial antibodies do not react with mouse centromeres by immunolabeling in situ.
5. The most reliable approach to evaluate the purity of isolated chromocenters is electron microscopy, although this method is laborious and requires training. It is recommended to refer to an electron microscopy service department or to a specialist for consultation concerning these methods.
6. *Glutaraldehyde, osmium tetroxide, and Epoxy resin compounds are toxic, allergenic, or both and uranyl acetate is radioactive. Particular care should be taken not to risk exposure*. Use gloves and work in a fume hood. In case of an accident, remove the reagent immediately by rinsing copiously with tap water.
7. Commercial solutions of glutaraldehyde have an acidic pH. The low ionic strength of TEA buffers is not sufficient to maintain a physiological pH (7.2–7.4) throughout the fixation procedure, and we therefore neutralize commercial glutaraldehyde with NaOH before use.

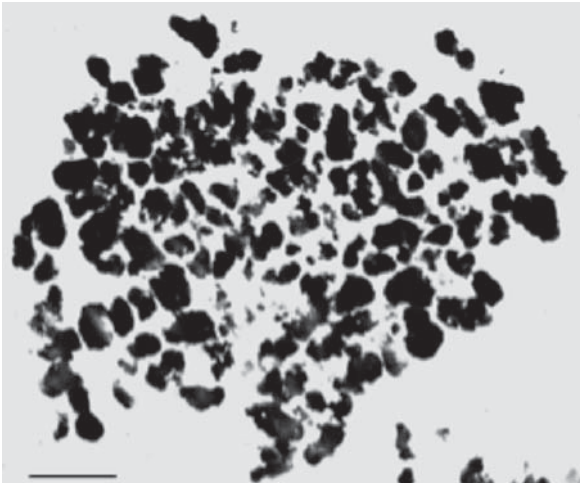

Fig. 12.3 A general view of chromocenters from the interface layer between 1.4 *M* and 1.8 *M* sucrose seen on ultrathin sections by electron microscopy. Note the tight compaction of the chromocenter material. Bar, 0.5 μm

8. We use an L8 ultracentrifuge with an SW28 rotor (Beckman-Coulter, Fullerton, USA). The rotor and the centrifuge are prechilled to 4°C before use.
9. Sonicate nuclei for the minimal time required to disrupt them but to maintain chromocenters and nucleoli intact, otherwise nucleolar fragments of size comparable to chromocenters will co-sediment with the chromocenters. We use an MSE sonifier (MSE, Crawley, UK) with a ~10-mm steel horn, but other appropriate ultrasonic disintegrators (e.g., Branson ultrasonifier 250) can be used.
10. Examples of typical isolated nuclei and chromocenters stained with DAPI and immunolabelled with a human anti-CENP-A autoimmune serum and a mouse monoclonal antibody recognizing the protein B23 (Sigma; cat. B0556) as observed by fluorescence microscopy are shown in Fig. 12.2. In Fig. 12.3, an ultrathin section of the chromocenter fraction from the interface layer between 1.4 M and 1.8 M sucrose is demonstrated.

Acknowledgments This work was partially supported by the Russian Foundation for Fundamental Research (Grant 06-04-49392).

References

1. Spector, D.L. (2001) Nuclear domains. *J. Cell Sci*. **114**, 2891–2893.
2. Craig, J.M. (2005) Heterochromatin—many flavours, common themes. *Bioessays* **27**, 17–28.
3. Dimitri, P., Corradini, N., Rossi, F., and Verni, F. (2005) The paradox of functional heterochromatin. *Bioessays* **27**, 29–41.
4. Pudenko, A.S., Kudryavtsev, I.S., Zatsepina, O.V., and Chentsov, Yu.S. (1997) Spatial association of prekinetochores and chromocentres in the interphase nuclei of mouse cultured fibroblasts. *Membr. Cell Biol*. **11**, 449–461.
5. Barsukova, A.S., Artemenko, E.G., Kalaidzidis, A.L., and Zatsepina, O.V. (2001) Stability of spatial interactions between chromocenters and pre-kinetochores in the interphase murine cells. *Tsitologiia* **43**, 46–51 (in Russian).
6. Prusov, A.N. and Zatsepina, O.V. (2002) Isolation of the chromocenter fraction from mouse liver nuclei. *Biochemistry* (Moscow) **67**, 423–431.
7. Cerda, M.C., Berrios, S., Fernandez-Donoso, R., Garagna, S., and Redi, C. (1999) Organisation of complex nuclear domains in somatic mouse cells. *Biol. Cell* **91**, 55–65.
8. Stephanova, E., Russanova, V., Chentsov, Y., and Pashev, I. (1988) Mouse centromeric heterochromatin: isolation and some characteristics. *Exp. Cell Res*. **179**, 545–553.
9. Frolova, E.I., Zatsepina, O.V., Poliakov, V.Iu., and Chentsov, Iu.S. (1989) Features of structural organization of mouse centrometric heterochromatin, detected during differential decondensation of chromosomes. *Tsitologiia* **31**, 380–385 (in Russian).
10. Kuznetsova, I.S., Prusov, A.N., Enukashvily, N.I., and Podgornaya, O.I. (2005) New types of mouse centromeric satellite DNAs. *Chromosome Res*. **13**, 9–25.
11. Dmitriev, P.V., Prusov, A.N., Petrov, A.V., Dontsova, O.A., Zatsepina, O.V., and Bogdanov, A.A. (2002) Mouse chromocenters contain associated telomeric DNA and telomerase activity. *Dokl. Biol. Sci*. **383**,171–174.
12. Mintz, P.J., Patterson, S.D., Neuwald, A.F., Spahr, C.S., and Spector, D.L. (1999) Purification and biochemical characterization of interchromatin granule clusters. *EMBO J*. **18**, 4308–4320.
13. Lam, Y.W., Lyon, C.E., and Lamond, A.I. (2002) Large-scale isolation of Cajal bodies from HeLa cells. *Mol. Biol. Cell* **13**, 2461–2473.

14. Andersen, J.S., Lyon, C.E., Fox, A.H., Leung, A.K., Lam, Y.W., Steen, H., Mann, M., and Lamond, A.I. (2002) Directed proteomic analysis of the human nucleolus. *Curr. Biol*. **12**, 1–11.
15. Scherl, A., Coute, Y., Deon, C., Calle, A., Kindbeiter, K., Sanchez, J.C., Greco, A., Hochstrasser, D., and Diaz, J.J. (2002) Functional proteomic analysis of human nucleolus. *Mol. Biol. Cell* **13**, 4100–4109.
16. Andersen, J.S., Lam, Y.W., Leung, A.K., Ong, S.E., Lyon, C.E., Lamond, A.I., and Mann, M. (2005) Nucleolar proteome dynamics. *Nature* **433**, 77–83.
17. Brown, J.W., Shaw, P.J., Shaw, P., and Marshall, D.F. (2005) Arabidopsis nucleolar protein database (AtNoPDB). *Nucleic Acids Res*. **33**, D633–D636.
18. Staub, E., Fiziev, P., Rosenthal, A., and Hinzmann, B. (2004) Insights into the evolution of the nucleolus by an analysis of its protein domain repertoire. *Bioessays* **26**, 567–581.
19. Coute, Y., Burgess, J.A., Diaz, J.J., Chichester, C., Lisacek, F., Greco, A., and Sanchez, J.C. (2006) Deciphering the human nucleolar proteome. *Mass Spectrom. Rev*. **25**, 215–234.
20. Leung, A.K., Trinkle-Mulcahy, L., Lam, Y.W., Andersen, J.S., Mann, M., and Lamond, A.I. (2006) NOPdb: Nucleolar Proteome Database. *Nucleic Acids Res*. **34**, D218–D220.
21. Reynolds, E.S. (1963) The use of lead citrate at high pH as an electron-opaque stain in electron microscopy. *J. Cell Biol*. **17**, 208–212.

Chapter 13
Isolation of Pathology-Associated Intranuclear Inclusions

Christine Iwahashi and Paul J. Hagerman

Keywords Flow cytometry; Immunochemistry; Fragile X syndrome; Parkinson; Fragile X-associated tremor/ataxia syndrome; FXTAS; dementia; Huntington; Ataxia; Ubiquitin; Crystallin

Abstract An emerging theme in neurodegenerative diseases is the aggregation of proteins as inclusions in neural cells. Their presence is a useful tool in the differential diagnosis of the particular illness, although in no instance is the specific role of the inclusions in disease pathogenesis understood at present. However, apart from their role in the disease mechanism, the inclusions themselves may contain important molecular clues as to the mechanism(s) behind the specific inclusion-associated disease. Thus, isolation and analysis of the composition of the inclusions is likely to yield biochemical evidence of the cellular pathways that are involved in the disease process.

1 Introduction

Intracellular inclusions are common pathogenic hallmarks for a number of neurodegenerative diseases ***(1)***. For some disorders such as Huntington's disease (Online Mendelian Inheritance in Man (OMIM)#143100), several of the spinocerebellar ataxias (SCAs), e.g., SCA3 (OMIM#109150), or fragile X-associated tremor/ataxia syndrome (FXTAS) (OMIM#300623), inclusions are found principally or exclusively in the nucleus. For other diseases, such as Parkinson disease (OMIM#168600) or multiple system atrophy ***(2)***, the associated inclusions are found in the cytoplasm. Although this chapter focuses on the isolation and purification of intranuclear inclusions, several of the principles involved with inclusion purification should be applicable to the isolation of inclusions in other locations.

Intranuclear inclusions/aggregates are typically ubiquitinated and are thought to accrete misfolded proteins due to the malfunction or overloading of the ATP-dependent ubiquitin proteasome system ***(3)***, although in most cases the relationship

R. Hancock (ed.) *The Nucleus: Volume 1: Nuclei and Subnuclear Components*,

between the presence of ubiquitinated proteins in the inclusions and the pathogenic mechanism is unclear ***(4, 5)***. However, apart from being a distinguishing morphological feature of neurodegenerative diseases, inclusions may provide clues both to their own genesis as well as to the broader pathogenic mechanisms of the inclusion-associated disease.

To analyze the composition of the intranuclear inclusions associated with FXTAS, we have developed a two-phase protocol that rapidly yields highly purified intranuclear inclusions from postmortem brain cortical tissue. The first phase of the purification strategy, isolation of intact nuclei, serves several purposes. First, removal of the cytoplasm and cytoplasmic proteases reduces the rate of degradation of inclusion-associated proteins; second, in isolating inclusions from postmortem tissue, an intact nucleus provides a means of selection for cells that have not undergone extensive autolysis; third, the intact nuclear membrane provides some degree of protection against possible mechanical disruption during the initial phase of the purification.

The second phase of the protocol is the purification of inclusions from the isolated nuclei. The central strategy in this phase is the fractionation, by automated flow-based methods, of the inclusions based on their size and the presence of specific proteins (e.g., ubiquitin) that can be immunofluorescently tagged as a flow-selection marker. Purification using fluorescence-activated flow cytometric particle (inclusion) sorting is based on a strategy that is widely used for the separation of cells, based on specific surface markers. Similar strategies employing fluorescent staining have been used for the purification of Lewy bodies ***(6, 7)***, and polyglutamine aggregates from transfected mouse neuroblastoma cells ***(8)***. We have successfully applied this protocol to the purification of intranuclear inclusions from postmortem brain tissue of FXTAS patients and have applied several proteomic methods to characterize their protein complement ***(9)***.

2 Materials

2.1 Initial Characterization of Intranuclear Inclusions

1. SuperFrost Plus microscope slides (Fisher Scientific, Pittsburgh, PA, USA).
2. Phosphate-buffered saline containing Tween 20 (PBS-T): 137 m*M* NaCl, 2.7 m*M* KCl, 4.3 m*M* Na_2HPO_4, 1.4 m*M* KH_2PO_4, pH 7.4, and 0.1% (v:v) Tween 20 (Sigma-Aldrich, St. Louis, MO, USA).
3. Antigen retrieval solution: 50 m*M* Tris-HCl, pH 9.5.
4. Parafilm "M" (Pechiney Plastic Packaging, Chicago, IL, USA).
5. Blocking solution: serum of the secondary antibody host species (e.g., rabbit, goat) diluted 1:10 (v/v) in PBS-T.

6. Fluorescent-labeled secondary antibodies: should be pre-absorbed against human proteins (assuming that the tissue of interest is of human origin). Jackson ImmunoResearch (West Grove, PA, USA) and Invitrogen (Molecular Probes, Carlsbad, CA, USA) supply secondary antibodies for staining and flow cytometry.
7. 4′,6-diamidino-2-(phenylindole) di-lactate (DAPI) (Sigma-Aldrich): 2 μ*M* in H_2O.
8. Mounting and anti-fading solution: ProLong Gold (Invitrogen Molecular Probes).
9. Immunohistochemical staining kit: VECTASTAIN ABC system (Vector Laboratories, Burlingame, CA, USA).

2.2 Isolation of Nuclei from Tissue

1. Dounce homogenizer (15 mL) with loose pestle.
2. Homogenizing buffer (HB-Complete): 0.32 *M* sucrose, 50 m*M* Tris-HCl, 5 m*M* EDTA, 17 μg/mL of phenylmethanesulfonyl fluoride, pH 7.4, and 1 tablet/50 mL of Complete protease inhibitors (Roche, Indianapolis, IN, USA).
3. Nylon mesh (500 μm and 100 μm) (Small Parts Inc., Miami Lakes, FL, USA).
4. BC-Complete solution: 20 m*M* 4-(2-hydroxyethyl)piperazine-1-ethanesulfonic acid (HEPES), 400 m*M* NaCl, 1 m*M* dithiothreitol, 1 m*M* EDTA, 1 m*M* ethylene glycol-bis(2-aminoethylether)-*N*,*N*,*N*′,*N*′ tetraacetic acid (EGTA), with 1 tablet of Complete protease inhibitors (Roche)/50 mL.

2.3 Isolation of Crude Inclusions from Nuclei

1. BD-Complete solution: 40 m*M* Tris-HCl, 10 m*M* NaCl, 10 m*M* $CaCl_2$, 5 m*M* $MgCl_2$, pH 7.9, with 1 tablet of Complete protease inhibitors (Roche)/50 mL.
2. DNase I.
3. Nonidet P-40 (Sigma-Aldrich).
4. Dounce homogenizer (7 mL) with tightly fitting pestle.

2.4 Purification of Inclusions

1. Nylon mesh cell strainer, 40-μm pore size (BD Falcon, Bedford, MA, USA).
2. Fluorescent flow cytometer size reference beads of a size approximating that of the inclusions (PeakFlowTM; Invitrogen Molecular Probes).
3. Cell sorter: MoFlo (DakoCytomation, Fort Collins, CO, USA).
4. Cytocentrifuge: Shandon Cytospin (Thermo Scientific, Waltham, MA, USA).

3 Methods

3.1 Initial Characterization of Intranuclear Inclusions

Identification of at least two inclusion-associated proteins by immunostaining in situ is essential for the success of the current inclusion isolation protocol. Many inclusions stain positively for the presence of ubiquitin, a posttranslational modification associated with proteins destined for degradation or translocation within the cell. However, given the widespread distribution of ubiquitin, this is not sufficiently specific as a fractionation tag for inclusions. Therefore, it is necessary to identify at least one additional inclusion protein, colocalizing in a specific manner with the ubiquitin-positive inclusions, to provide adequate specificity of the separation method. Because many disease-associated inclusions likely contain misfolded proteins, a probable candidate for a second protein tag is one of the chaperone proteins (e.g., small or large heat shock-related proteins (HSPs)). Colocalization of protein candidates in the inclusions must be established by immunofluorescent staining. Additionally, immunofluorescent staining should be confirmed by use of chromogen substrates, because particle autofluorescence can be misleading in the interpretation of fluorescence staining. Further important information that can be gleaned from these initial studies includes the size of the inclusions, the fraction of nuclei that contain inclusions, and how much starting material is necessary to yield sufficient material for downstream analysis.

1. Prepare formalin-fixed, paraffin-embedded tissue sections (~5 μm) on SuperFrost plus slides for in situ staining (*see* **Note 1**).
2. Deparaffinize and rehydrate the sections by heating the slides at 60°C for 10–20 min.
3. Transfer the slides immediately to xylene and incubate at room temperature for 3–5 min.
4. Transfer the slides to 100% ethanol for 5 min, repeat once, then to 95% ethanol for 5 min, repeat once, then to 90% ethanol for 3 min, to 85% ethanol for 3 min, and then to PBS-T.
5. To perform antigen retrieval, submerge a Coplin-style jar containing antigen retrieval solution in a water bath at room temperature and heat the water bath to ~95°C.
6. Place the slides in the jar, cover with a loose-fitting lid, and place the jar in the water bath for 20–30 min. Carefully remove the jar from the water bath and allow the slides to cool gradually in the jar.
7. Transfer the slides to PBS-T and wash them by exchanging the PBS-T solution, repeat for a total of three washes.
8. Block the slides against nonspecific binding of secondary antibodies. Line a tray with a strip of Parafilm "M." Carefully place ~250–300 μL of blocking solution on the Parafilm. Flip the slide over, tissue side down, onto the blocking solution. Repeat for the remaining slides and incubate them at room temperature for 1–2 h.

9. Incubate the slides with primary antibodies, diluted in blocking solution according to the vendor's specifications. For immunofluorescent staining, the slides can be incubated with both antibodies together, but these must be generated in different host species. For immunocytochemistry with chromogen substrates, the antibodies must be evaluated individually (*see* **Note 2**). Flip the slides over, as for the blocking step, onto an aliquot of primary antibodies. Incubation times and temperatures depend on the affinity and specificity of the antibodies; generally, overnight incubation at 4°C is sufficient.
10. Wash the slides in PBS-T for 5 min, repeat four times more.
11. Incubate the slides for 1–2 h with labeled secondary antibodies diluted in blocking solution. Generally, dilutions of 1/1,000 (v/v) for fluorescent staining and 1/200 for chromogen staining are adequate. Again, for fluorescent staining the fluorophore-labeled secondary antibodies can be combined (*see* **Note 3**).
12. Wash the slides in PBS-T for 5 min, repeat four times more.
13. For fluorescence microscopy, counterstain the slides in DAPI solution for 5 min. Place a drop of ProLong mounting media on the slides and then a coverslip.
14. For chromogen staining, ready-to-use kits such as the VECTASTAIN ABC system are convenient and provide good-quality staining for immunocytochemistry. Counterstain the slides with hematoxylin and add a coverslip with a compatible mounting medium such as Crystal/Mount (Biomeda, Foster City, CA, USA).
15. Evaluate microscopically the specificity of the staining and the colocalization of the antibodies on inclusions, the distribution of inclusions in the tissue, and the size of inclusions. Minimally, a pair of antibodies (Ab I and Ab II) with high specificity for inclusion-associated proteins (protein I and protein II) must be established for subsequent isolation and purification of the inclusions.

3.2 Isolation of Nuclei from Tissue

The separation of nuclei from tissue can, in principle, be accomplished through one of several methods. However, we found that methods employing isopycnic banding in iso-osmotic media were not useful for the efficient isolation of inclusion-bearing nuclei, for reasons that were not explored further. Gentle methods of tissue homogenization prior to the isolation of intact nuclei generally yield acceptable quantities of intact inclusions; however, harsher disruption methods such as sonication or motorized homogenizers appear to fracture the inclusions into smaller aggregates and significantly complicate their further purification.

1. Cut ~1–2 g of tissue into ~1 mm^3 pieces and suspend in four volumes of HB-Complete (*see* **Note 4**).
2. Homogenize the tissue on ice in a Dounce homogenizer (*see* **Note 5**) fitted with a loose pestle. Ten to 15 downward strokes are usually adequate.
3. Filter the homogenate successively through 500-μm and 100-μm nylon mesh. Rinse the homogenizer and the mesh with 2 mL of HB-Complete and pool the wash with the homogenate.

4. Centrifuge the filtered homogenate at 1,500×*g* for 10 min at 4°C.
5. Wash the pelleted nuclei 3× in HB-Complete and resuspend the pellet in BC-Complete such that final volume is 1.5–2.0 mL.
6. Make slides with nuclear smears for future staining experiments: apply ~1–2 µL of resuspended nuclei to a SuperFrost Plus slide and smear across the surface using another slide. Prepare 20–40 slides and fix them in 70% v/v methanol for 15 min, allow to dry, and store at −20°C.

3.3 Isolation of Crude Inclusions from Nuclei

The inclusions are released by disruption of the nuclear membrane and are easily pelleted from the resulting solution. However, despite several washes the inclusions may remain associated with DNA, making them prone to clumping and difficult to purify. A step involving mild DNase digestion removes extrinsic DNA, although a caveat with such treatment is that it may also affect proteins that are loosely associated with the inclusions.

1. To the suspension of nuclei, add Nonidet P-40 to a final concentration of 0.25% v/v (*see* **Note 6**).
2. Rotate the suspension on an end-over-end tube mixer for 15 min at 4°C.
3. Transfer the nuclei to a Dounce homogenizer (*see* **Note 7**) and homogenize on ice with 8–12 downward strokes of a tightly fitting pestle.
4. Pellet the crude inclusions by centrifuging at 2,000×*g* for 5 min at 5°C.
5. Wash the pellet 2× in BC-Complete and resuspend in 200–500 µL of BD-Complete.
6. Add DNase I to a final concentration of 500 U/mL and incubate on a rotator at 20°C for 30 min.
7. Centrifuge at 2,000×*g* for 5 min at 5°C.
8. Resuspend the pellet of crude inclusions in BC-Complete using 1.0 mL of BC-Complete per gram of original tissue, aliquot, and store at −80°C.

3.4 Purification of Inclusions

The second phase of the inclusion purification process uses fluorescence-activated flow cytometric particle sorting. As noted in the Introduction, similar strategies have been applied to the separation of cells based on fluorescent tagging of cell surface markers, and for the purification of Lewy bodies and polyglutamine inclusions. Based on estimates of the range of inclusion diameters (for particle size fractionation) and immunospecific fluorescent staining, inclusions can be preparatively sorted and collected. Visual examination by immunofluorescence microscopy is necessary to confirm that the sorting has been successful and that the morphology of the inclusions has not substantially changed during the purification process.

1. Pellet the crude inclusions by centrifugation at 2,000×*g* for 5 min at 5°C.
2. Prepare an appropriate blocking solution containing 5% v/v serum of the secondary antibody host species in PBS-T. Resuspend the crude inclusions in 500 µL of this blocking solution.
3. Incubate with rotation at 4°C for 2 h (*see* **Note 8**).
4. Pellet the inclusions at 2,000×*g* for 5 min at 4°C.
5. Resuspend the crude inclusions in between 200 and 400 µL of the appropriate primary antibody diluted in blocking buffer. Initially, antibody combinations and controls must be run to establish gates for sorting the inclusions (Table 13.1).
6. Rotate the crude inclusions overnight at 4°C and spin at 2,000×*g* to pellet them.
7. Resuspend the pelleted inclusions in ~1.0 mL of PBS-T and spin at 2,000×*g* to pellet them. Repeat four times more.
8. Prepare the secondary antibodies and incubate the pelleted inclusions in between 200 and 400 µL of the secondary antibody solutions for 2 h at 4°C with rotation; protect from light.
9. Centrifuge the inclusions at 2,000×*g*, resuspend the pellet in ~1.0 mL of PBS-T, spin at 2,000×*g* to pellet, and repeat four times more.
10. Resuspend the inclusions in ~1.0 mL of PBS-T and pass through a 40-µm-pore size nylon mesh cell strainer sieve. Wash the tube and sieve with a second aliquot of PBS-T and pool the wash with the sieved inclusions. Keep the samples on ice for sorting.
11. Fit the MoFlo cell sorter with a 70-µm nozzle tip.
12. Determine the excitation wavelengths and detection filters (bandpass) for fluorescent antibody probe I and fluorescent antibody probe II.
13. Estimate the size and complexity of the inclusions by assessing forward and side scatter of unlabeled inclusions (*see* **Note 9**).
14. Set the initial gate to exclude very small particles (<1.0 µm) and large debris (>10 µm).
15. Examine unlabeled inclusions and determine their distribution on each axis (forward and side scatter).
16. Examine inclusions incubated with Ab I and fluorescent probe I.
17. Examine inclusions incubated with Ab II and fluorescent probe II.
18. Set compensation for detection of signals from both fluorescent probe I and fluorescent probe II.
19. Examine inclusions incubated with fluorescently labeled secondary antibodies in the absence of primary antibodies (*see* **Note 10**).
20. Examine inclusions labeled with both antibodies and both probes, set gates and collect particles that are highly positive for both fluorescent probes (*see* **Note 11**). Sort the particles at ~19,000 events/sec with a coincidence rate at or below 9%.
21. Re-examine a small sample of the sorted population that is double positive for fluorescent probes I and II, using intensity versus forward scatter to verify positive staining (*see* **Note 12**).
22. Collect double-positive particles in PBS-T Complete at 4°C.
23. Dilute a small sample of the double-positive inclusions/particles ~1:20 in PBS-T, and cytospin onto slides for microscopic evaluation. Purification of FXTAS-related inclusions by flow cytometry is shown in Fig. 13.1 and immunofluorescence staining at various steps of their purification in Fig. 13.2.

Table 13.1 Antibody controls essential for flow cytometry

Antibody/Serum	Secondary	Purpose
Pair of primary antibodies, Ab I and Ab II (established in **Section 3.1** to be inclusion specific) in blocking serum	Labeled with fluorescent probe I and fluorescent probe II and specific for the hosts of Ab I and Ab II	Identify particles/ inclusions containing protein I and protein II
Ab I in blocking serum	Labeled with fluorescent probe I, specific for host of Ab I	Identify particles containing protein I
Ab II in blocking serum	Labeled with fluorescent probe II, specific for host of Ab II	Identify particles containing protein II
Non- or pre-immune serum from host of antibodies diluted comparably to antibodies in blocking serum	Labeled with fluorescent probe I and fluorescent probe II, specific for host of Ab I and Ab II	Negative control for primary antibodies
Blocking serum only	Labeled with fluorescent probe I and fluorescent probe II, specific for host of Ab I and Ab II	Negative control for secondary antibodies
Blocking serum	No secondaries	Size and complexity of inclusions, check for autofluorescence of inclusions

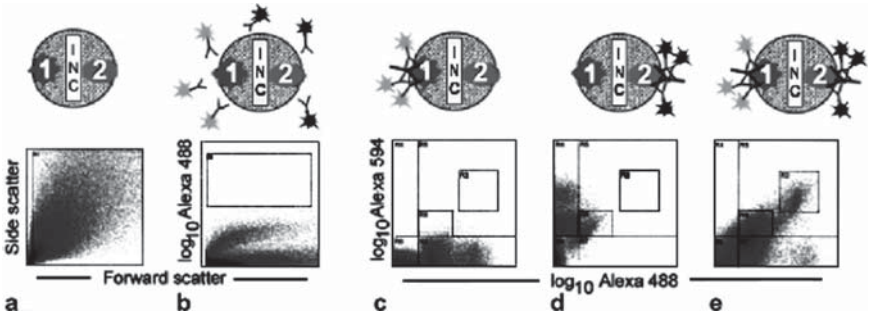

Fig. 13.1 Purification of FXTAS-related intranuclear inclusions (*INC*) by flow cytometry. **a** Forward scatter (FSC) versus side scatter (SSC) assessment of unlabeled crude inclusions (no primary or secondary antibodies) for the determination of size gating. **b** Secondary antibodies only, FSC versus fluorescence. **c** Immunolabeled with rabbit anti-ubiquitin and Alexa 488 goat anti-rabbit. **d** Immunolabeled with mouse anti-αB-crystallin and Alexa 594 goat anti-mouse IgG. **e** Immunolabeled with rabbit anti-ubiquitin/Alexa 488 goat anti-rabbit IgG, and mouse anti-αB-crystallin/Alexa 594 goat anti-mouse IgG

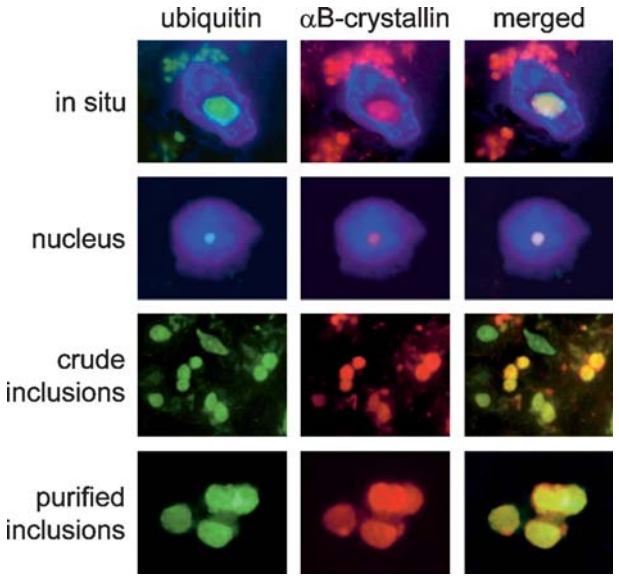

Fig. 13.2 Immunofluorescence staining of inclusions at various steps in their isolation and purification. FXTAS-related inclusions were processed for immunostaining with polyclonal rabbit antibody to ubiquitin and mouse monoclonal antibody to αB-crystallin. Secondary antibodies (Alexa 488 goat anti-rabbit and Alexa 555 goat anti-mouse) were visualized by fluorescence microscopy and nuclei were counterstained with DAPI. Merged images demonstrate the presence of both ubiquitin and crystallin in the inclusions. Purified nuclei contain ubiquitin- and crystallin-positive inclusions; no staining of the inclusions was observed with antibodies to nucleolar-related proteins. Staining of nonsorted, crude inclusions demonstrates the additive specificity of the two antibodies and improves the identification of the inclusions in the pool of nuclear material. Immunofluorescent staining of inclusions is an important tool in monitoring the progress of the isolation and purification process. To view this figure in color, see COLOR PLATE 4

4 Notes

1. Specimens from various regions of the tissue of interest will provide information on the distribution of inclusions, particularly the best region for the collection of the greatest numbers of inclusions.
2. Antibody controls must be tested, including non- or pre-immune sera and secondary antibodies without primary antibodies.
3. Use fluorophores with minimal overlap of excitation/emission wavelengths.
4. Control, non-inclusion bearing tissue should be processed in the same fashion to confirm the specificity of the isolation protocol.
5. A 15-mL-size homogenizer nicely handles the resuspension and the displacement of the tissue sample during the homogenizing process.
6. Because NP-40 is very viscous, an intermediate dilution (10% v/v) in BC-Complete allows for more accurate addition to achieve the desired final concentration.

7. We recommend a 7-mL-size homogenizer for this step.
8. Following this incubation, it is advisable to plan ahead as to how many antibody permutations must be evaluated. Prepare and parcel aliquots according to these conditions and proceed to the next step.
9. Size approximation is based on fluorescent reference beads. The size of the beads should approximate the size of the inclusions.
10. These inclusions should appear similar to unlabeled crude inclusions. If strong fluorescence is observed for either probe in the absence of primary antibody, more rigorous washing or further dilution of the secondary antibody may be necessary to eliminate nonspecific binding.
11. An intermediate population, slightly less positive for both fluorescent probes but likely far more abundant, can be collected and is useful for testing downstream analytical/proteomic methods.
12. The intensity of fluorescence may be reduced due to bleaching from the first round of sorting.

References

1. Ross, C. A. and Poirier, M. A. (2004) Protein aggregation and neurodegenerative disease. *Nat. Med.* **10 Suppl,** S10–17.
2. Ozawa, T. (2006) Pathology and genetics of multiple system atrophy: an approach to determining genetic susceptibility spectrum. *Acta Neuropathol. (Berl)* **112,** 531–538.
3. Olanow, C. W. and McNaught, K. S. (2006) Ubiquitin-proteasome system and Parkinson's disease. *Mov. Disord.* **21,** 1806–1823.
4. Lee, H. G., Petersen, R. B., Zhu, X., Honda, K., Aliev, G., Smith, M. A., and Perry, G. (2003) Will preventing protein aggregates live up to its promise as prophylaxis against neurodegenerative diseases? *Brain Pathol.* **13,** 630–638.
5. Slow, E. J., Graham, R. K., Osmand, A. P., Devon, R. S., Lu, G., Deng, Y., Pearson, J., Vaid, K., Bissada, N., Wetzel, R., Leavitt, B. R., and Hayden, M. R. (2005) Absence of behavioral abnormalities and neurodegeneration in vivo despite widespread neuronal huntingtin inclusions. *Proc. Natl. Acad. Sci. USA* **102,** 11402–11407.
6. Iwatsubo, T., Yamaguchi, H., Fujimuro, M., Yokosawa, H., Ihara, Y., Trojanowski, J. Q., and Lee, V. M. (1996) Lewy bodies: purification from diffuse Lewy body disease brains. *Ann. NY. Acad. Sci.* **786,** 195–205.
7. Iwatsubo, T., Yamaguchi, H., Fujimuro, M., Yokosawa, H., Ihara, Y., Trojanowski, J. Q., and Lee, V. M. (1996) Purification and characterization of Lewy bodies from the brains of patients with diffuse Lewy body disease. *Am. J. Pathol.* **148,** 1517–1529.
8. Hazeki, N., Tsukamoto, T., Yazawa, I., Koyama, M., Hattori, S., Someki, I., Iwatsubo, T., Nakamura, K., Goto, J., and Kanazawa, I. (2002) Ultrastructure of nuclear aggregates formed by expressing an expanded polyglutamine. *Biochem. Biophys. Res. Commun.* **294,** 429–440.
9. Iwahashi, C. K., Yasui, D. H., An, H. J., Greco, C. M., Tassone, F., Nannen, K., Babineau, B., Lebrilla, C. B., Hagerman, R. J., and Hagerman, P. J. (2006) Protein composition of the intranuclear inclusions of FXTAS. *Brain* **129,** 256–271.

Chapter 14
The Nuclear Ubiquitin–Proteasome System: Visualization of Proteasomes, Protein Aggregates, and Proteolysis in the Cell Nucleus

Anna von Mikecz, Min Chen, Thomas Rockel, and Andrea Scharf

Keywords Cell nucleus; Proteasomes; Protein aggregation; Proteolysis; Ubiquitin; Nanoparticles; Confocal microscopy; Immunocytochemistry; Quality control

Abstract The 20S proteasome is part of a larger complex, the 26S proteasome, that is implicated in the ATP-dependent degradation of multiubiquitin-conjugated proteins ***(1)***. About 80% of intracellular protein breakdown occurs via the ubiquitin-proteasome system (UPS). Key proteins such as transcription factors, nuclear receptors, cyclins, cyclin-dependent kinase inhibitors, p53, and NF-κB are regulated by this pathway. Thus, the UPS has been implicated to play a role in multiple cellular events including the cell cycle, signal transduction, antigen presentation, and DNA repair and transcription ***(2, 3)***. In 1984 Varshavsky and co-workers discovered that ubiquitin-dependent pathways play a role in cell cycle control, and suggested that protein degradation is instrumental in regulation of gene expression ***(4)***. Consistent with this idea, Franke and colleagues had shown that proteasomes localize to the nuclei of *Xenopus laevis* oocytes and HeLa cells ***(5, 6)***. Subsequent work confirmed that (i) all components of the UPS that are required for protein degradation indeed reside in the cell nucleus ***(7)***; (ii) nuclear proteins are substrates for proteasomal degradation ***(8)***; and (iii) proteasome-dependent proteolysis occurs in distinct nucleoplasmic foci ***(9)***. The intricate balance between nuclear function and quality control through proteolysis is exemplified by reports that show a correlation of aberrant nuclear protein aggregates with inhibition of transcription in neurodegenerative diseases such as Huntington's chorea and animal and cell culture models of polyglutamine repeat disorders ***(10, 11)***.

Considering the central role of the UPS in nuclear processes, a detailed knowledge of the time and place at which a substrate is ubiquitinylated and degraded will be essential to our understanding of the cellular mechanisms that orchestrate the expression of thousands of genes or development of subnuclear pathologies. Here, we describe fluorescence-based localization methods for proteasomes, protein aggregates, and proteasomal proteolysis in the cell nucleus that may aid to analyse the UPS in housekeeping and disease conditions.

R. Hancock (ed.) *The Nucleus: Volume 1: Nuclei and Subnuclear Components*,

1 Introduction

1.1 Visualization of Proteasomes

Nuclear proteasomes can be localized in great detail by a combination of indirect immunofluorescence and confocal microscopy. HEp-2 cells constitute a human epithelial cell line that is very well established for detection of nuclear proteins ***(12)***. To ensure that the intracellular distribution of endogenous proteasomes is studied in a fashion that reflects the in vivo situation, we suggest application of a panel of different fixation procedures. Formaldehyde fixes cells through weak cross linking, and, thus, is traditionally used to study the localization of nuclear proteins; however, it tends to mask antibody-binding sites (epitopes) under certain conditions. In contrast, methanol is a fixative that precipitates macromolecules and extracts the soluble pool of proteins, which may conceal an insoluble protein fraction. Despite such different modes of action, most nuclear proteins show the same distribution pattern with either formaldehyde- or methanol-based fixation procedures ***(13)***. Proteasomes, however, belong to a group of proteins that apparently change their subnuclear localization dependent on the fixation and permeabilization method. 20S Proteasomes distribute throughout the nucleoplasm in reticulated speckles, distinct foci, and in a diffuse localization pattern ***(9, 13, 14)***. Depending on the fixation procedure and the antibodies used, a more or less reticulated speckled and focal distribution can be observed (Table 14.1).

1.2 Induction of Nuclear Protein Aggregates

Aggresomes and neuronal intranuclear inclusions have been observed in a variety of protein aggregation diseases ***(15–17)***. Protein aggregates and inclusions containing huntingtin protein, superoxide dismutase (SOD1), or Aβ-peptide are hallmarks of expanded glutamine repeat (polyQ) neurodegenerative disorders such as Huntington's disease. Aggregates of these proteins are dynamically associated with cellular proteins such as ubiquitin, and components of the UPS ***(18)***. The availability of commercial antibodies to signature proteins of nuclear protein aggregates

Table 14.1 Distribution pattern of nuclear proteasomes after different fixation methods, detected by confocal immunofluorescence

Fixation	I	II	III	IV	V	VI
Pattern	npl, h, sp, f	npl, h, sp, f	npl, h	npl, f	npl, h	npl, h, sp

Subconfluent HEp-2 cells were subjected to different fixation/permeabilization procedures (I, methanol; II, methanol/acetone; III, 4% formaldehyde; IV, 0.4% formaldehyde; V, 4%/8% formaldehyde; VI, 4%/8% formaldehyde + pre-extraction; as detailed in the Materials and Methods sections) and immunolabelled with rabbit polyclonal antibody to the 20S core of the proteasome. The distribution patterns indicate foci (f); diffuse homogeneous (h); nucleoplasmic (npl); and speckles (sp)

such as ubiquitin, huntingtin, and polyglutamine enables intracellular detection of protein aggregation by means of immunocytochemical techniques. In cell culture, nano-SiO_2 particles induce abnormal nucleoplasmic protein clusters that rather resemble those seen in polyQ diseases and share a similar protein composition of protein aggregates ***(11)***. By confocal immunofluorescence detection, we showed that such nano-SiO_2-induced protein aggregates are (i) localized throughout the nucleoplasm, but not in nucleoli or the nuclear envelope region; (ii) grow over time; and (iii) can be prevented by inhibitors such as Congo red and trehalose.

1.3 Localizing Protein Degradation in the Nucleus of Eukaryotic Cells

To study the regulatory role of the UPS in gene expression, it is important to localize areas of proteolytic activity within the context of the functional architecture of the cell nucleus. The method shown here is based on injecting an ectopic protein (ovalbumin or bovine serum albumin) that is heavily labelled with the dye BODIPY FL (Molecular Probes, Carlsbad, CA, USA) in such a manner that the dye's fluorescence is quenched due to steric obstruction. Upon proteolytic digestion, the protein is degraded to peptides that have a 100-fold brighter fluorescence signal, thereby illuminating locations of protein cleavage. Cells microinjected with such substrates show distinct focal areas of high proteolytic activity (proteolytic foci) in the nucleus (Fig. 14.3c). This method works well in cell lines (HEp-2, # CCL-2A; ATCC, Middlesex, UK) and in primary cells (human dermal fibroblasts). The proteolytic foci can be visualized in living or in fixed cells ***(9)***.

2 Materials

2.1 Culture and Preparation of Cells

1. RPMI 1640 (PAA Laboratories, Pasching, Austria) supplemented with 10% bovine growth serum (HyClone, Logan, UT, USA) and 5% supplement complex: 2 m*M* L-glutamine, 1 m*M* sodium pyruvate, 1% non-essential amino acids, 10 U/mL penicillin, and 10 µg/mL streptomycin, 0.25 µ*M* 2-mercaptoethanol (Gibco, Invitrogen, Karlsruhe, Germany).
2. Trypsin-EDTA (1×), 0.05% trypsin, 0.53 m*M* Na_4EDTA (Gibco).
3. 100% absolute ethanol, analytical grade.
4. 22×22-mm No. 1.5 glass coverslips (Erie Scientific Co., Portsmouth, NH, USA) (*see* **Note 1**)
5. Six-well plates (Greiner, Solingen-Wald, Germany)
6. 35-mm tissue culture dishes (Becton Dickinson, Franklin Lakes, NJ, USA).

2.2 Silica Nanoparticles

1. Plain (unlabelled) and FITC-labelled silica particles (SiO_2) of size 50 nm (Kisker, Steinfurt, Germany) and 70 nm (Postnova, Landsberg/Lech, Germany).
2. 50-nm unlabelled silica microspheres (Polysciences, Warrington, PA, USA).

2.3 Microinjection

1. Substrates: DQ ovalbumin (DQ OVA, D-12053; Molecular Probes) or DQ bovine serum albumin (DQ BSA, De-12050; Molecular Probes)
2. Injection chamber: Attofluor cell chamber (A-7816; Molecular Probes)
3. Round coverslips: 25-mm circular microscope cover glasses (1001/0025; Hecht-Assistant, Sondheim, Germany)
4. Microinjection tips: Femtotips I or II (5242 952.008 and 5242 957.000; Eppendorf, Hamburg, Germany)
5. Microinjection apparatus: InjectMan NI2 (Eppendorf, Hamburg, Germany).

2.4 Fixation and Permeabilization

1. Methanol, extra pure grade (Merck, Darmstadt, Germany).
2. Acetone, synthesis grade (Merck).
3. Formaldehyde 10% ultrapure (methanol-free), EM grade (Polysciences, Warrington, PA, USA). Prepare a 4% and a 0.4% formaldehyde solution in PBS fresh for each experiment (use in **Sections 3.2.3** and **3.2.4**).
4. Paraformaldehyde (Sigma-Aldrich, München, Germany). Prepare 400 mL of a 16% formaldehyde stock solution. Heat ~300 mL distilled water to 60°C and add 64 g of paraformaldehyde (*see* **Note 2**). After stirring for 1 to 2 h add a few drops of 1 N NaOH to depolymerise the paraformaldehyde until the solution becomes clear. Cool to room temperature and adjust to pH 7.4–7.6. Adjust the volume to 400 mL and filter through a 0.2-µm filter. For the preparation of 8% formaldehyde/250 m*M* HEPES, add 50 mL of 500 m*M* HEPES stock solution to 50 mL of 16% formaldehyde. For 4% formaldehyde/250 m*M* HEPES add 25 mL of 16% formaldehyde solution to 50 mL of 500 m*M* HEPES stock solution and 25 mL distilled water. Aliquots are frozen at −20°C and only thawed once. Add 0.1% (v/v) Triton X-100 to 4% formaldehyde/250 m*M* HEPES solution for each experiment (use in **Sections 3.2.5** and **3.2.6;** prepare freshly and do not store the solution).
5. HEPES (Sigma). Prepare a 500 m*M* HEPES stock solution with distilled water and adjust to pH 7.4 to 7.5.
6. Triton X-100, molecular biology grade (Sigma). Prepare 0.5 and 0.25% (v/v) Triton X-100 solutions in PBS at least 30 min before use.

7. Phosphate buffered saline (PBS): prepare a 10× stock solution with 1.37 *M* NaCl, 27 m*M* KCl, 43 m*M* Na_2HPO_4, and 14 mM KH_2PO_4. Prepare working solution by dilution of one part 10× PBS with nine parts distilled water.
8. Coplin jars (Thomas Scientific, Swedesboro, NJ, USA).

2.5 Immunofluorescent Labelling

1. Primary antibodies: polyclonal rabbit antibody PW 8155 against the proteasome 20S core subunit and monoclonal mouse antibody PW8195 (clone MCP231) against the α-subunit (Biotrend, Köln, Germany). Rabbit anti-ubiquitin antibody from Santa Cruz Biotechnology (Santa Cruz, CA, USA) and mouse monoclonal antibodies against huntingtin and polyglutamine from Chemicon (Temecula, CA, USA).
2. Secondary antibodies: goat anti-mouse conjugated to fluorescein (FITC), goat anti-rabbit conjugated to fluorescein (FITC), goat anti-rabbit or anti-mouse IgG conjugated to rhodamine (Jackson Laboratories, Maine, USA).
3. Vectashield mounting medium (Vector Laboratories, Burlingame, CA, USA).
4. Nail varnish.
5. Microscope slides SuperFrost®Plus (Menzel-Gläser, Braunschweig, Germany).
6. Humidified chamber.

3 Methods

3.1 Cell Culture and Cell Preparation

HEp-2 cells are passaged when approaching 70% confluence with trypsin-EDTA to provide new maintenance cultures in 75-cm^2 culture flasks and experimental cultures on coverslips in 6-well plates. Subconfluence of cells on coverslips should be reached within 36–48 h of culture time, so that their subcellular structures can be observed under conditions of exponential growth and individual cells are clearly visible in immunofluorescence.

1. Sterilize square glass coverslips by dipping them into 100% ethanol for some seconds. Flame the coverslips by passing through the flame of a Bunsen burner (ethanol is inflammable: be careful with the burner) and place them in 6-well plates (*see* **Notes 3** and **7**).
2. Add 4 mL of medium per well, avoiding air bubbles between the plate and the coverslip.
3. Carefully add 1 droplet of HEp-2 cells (1×10^6 cells/mL) onto the coverslips.
4. Grow cells for 2 days at 37°C in 5% CO_2 until the culture is subconfluent.
5. For studies of nuclear protein aggregation induced by silica nanoparticles, the culture medium is replaced with fresh medium containing 25–50 µg/mL silica nanoparticles for 4 to 24 h.

3.2 Fixation and Permeabilization

3.2.1 Methanol Fixation

1. Remove the coverslips from wells with forceps and rinse by placing in small Coplin jars containing PBS (*see* **Notes 4** and **8**).
2. Pour off the PBS and add ice cold (−20°C) 100% methanol and incubate the coverslips for 20 min at −20°C (freezer).
3. Rinse fixed coverslips 6× quickly in PBS, afterwards wash them 3× 5 minutes each in PBS on a shaker (*see* **Note 5**).

3.2.2 Methanol/Acetone Fixation

1. Remove the coverslips from wells with forceps and rinse by placing in small Coplin jars containing PBS (*see* **Notes 4** and **8**).
2. Pour off the PBS and add ice cold (−20°C) 100% methanol and incubate the coverslips for 5 min in a −20°C freezer.
3. Permeabilize with ice cold (−20°C) acetone for 2 min in a −20°C freezer (*see* **Notes 5** and **6**).
4. Rinse fixed coverslips 6× quickly with PBS, then rinse 3× 5 minutes in PBS on a shaker.

3.2.3 4% Formaldehyde Fixation

1. Remove the coverslips from wells with forceps and rinse by placing in small Coplin jars containing PBS (*see* **Notes 4** and **8**).
2. Quickly exchange the PBS for 4% formaldehyde in PBS (diluted from 10% formaldehyde) and incubate the coverslips for 10 min at room temperature (*see* **Note 5**).
3. Permeabilize with 0.25% Triton X-100 in PBS for 3 min at room temperature.
4. Rinse fixed coverslips 6× quickly with PBS, then rinse 3× 5 minutes in PBS with gentle rocking on a shaker.

3.2.4 0.4% Formaldehyde Fixation

1. Remove the medium and rinse the coverslip quickly in PBS in the 6-well plate (*see* **Notes 4, 7,** and **8**).
2. Remove the PBS and fix the cells with 0.4% formaldehyde in PBS (diluted from 10% formaldehyde) for 10 min at room temperature (*see* **Note 5**).
3. Remove the formaldehyde and permeabilize with 0.25% Triton X-100 in PBS for 3 min at room temperature.

4. Remove the Triton X-100 solution and rinse fixed coverslips 6× quickly with PBS, then rinse 3× 5 min in PBS on a shaker.

3.2.5 4%/8% Formaldehyde Fixation *(19)*

1. Remove the coverslips from wells with forceps and rinse by placing in small Coplin jars containing PBS (*see* **Notes 4** and **8**).
2. Fix the cells in freshly prepared 4% formaldehyde in 250 m*M* HEPES, pH 7.6, for 10 min at 4°C (*see* **Note 5**).
3. Refix the cells in freshly prepared 8% formaldehyde in 250 m*M* HEPES, pH 7.6, for 50 min at 4°C (*see* **Note 5**).
4. Permeabilize the cells in 0.5% Triton X-100 in PBS for 30 min with gentle rocking on a shaker at room temperature.
5. Rinse fixed coverslips 6× quickly with PBS, then rinse 3× 5 minutes in PBS with gentle rocking on a shaker.

3.2.6 4%/8% Formaldehyde Fixation Combined with a Pre-extraction Step *(19)*

1. Remove the coverslips from wells with forceps and rinse by placing in small Coplin jars containing PBS (*see* **Notes 4** and **8**).
2. Fix/permeabilize the cells in 0.1% Triton X-100 in freshly prepared 4% formaldehyde in 250 m*M* HEPES, pH 7.6, for 10 min at 4°C (*see* **Note 5**).
3. Refix the cells in freshly prepared 8% formaldehyde in 250 m*M* HEPES, pH 7.6, for 50 min at 4°C (*see* **Note 5**).
4. Permeabilize the cells in 0.5% Triton X-100 in PBS for 30 min with gentle rocking on a shaker at room temperature.
5. Rinse fixed coverslips 6× quickly with PBS, then rinse 3× 5 minutes in PBS with gentle rocking on a shaker.

3.2.7 Methanol Fixation for Studies of Nuclear Protein Aggregates

1. The cells are rinsed rapidly once by placing the coverslips with forceps into small Coplin jars with PBS, keeping the cell side forward (*see* **Notes 4** and **8**).
2. Prechilled (−20°C) pure methanol solution is added into the Coplin jars to fix the cells for 5 min at −20°C in a freezer.
3. The methanol is discarded into a hazardous waste container and the cells are permeabilized with −20°C pure acetone for 2 min at −20°C in a freezer.
4. The acetone is discarded into a container for flammable waste and the cells are washed 4× with PBS (*see* **Note 5**).

3.3 Immunolabelling and Confocal Immunofluorescence Microscopy

1. Prepare a humidified chamber and a microscope slide for each coverslip (*see* **Note 9**).
2. Prepare the antibody at the appropriate concentration in PBS: antibody against the proteasome 20S core (dilution 1:50); proteasome α-subunits (1:40); ubiquitin (1:10), huntingtin (1:100), or polyglutamine (1:100).
3. Excess PBS is drained off (*see* **Notes 8** and **10**). Place 33 µL of diluted antibody on the side of the coverslip with the cell layer and invert it (cell face down) onto a microscope slide, followed by incubation for 1 h in a moist chamber at room temperature (*see* **Note 11**).
4. By gently floating the coverslips off the slides with PBS, they are returned to Coplin jars and washed 3× 10 min with PBS.
5. The secondary antibody is diluted 1:100 in PBS and added to the cells as described above (**Step 3**) for 45 min in a moist chamber at room temperature. To avoid photobleaching of the fluorophore, keep the coverslips in the dark (for example, cover the chamber with foil).
6. After three washes with PBS, the coverslip is carefully inverted onto a drop of mounting medium on a labelled microscope slide (avoid air bubbles) and sealed with nail varnish (*see* **Note 11**). The cells can either be viewed immediately after the varnish is *completely* dry or stored at 4°C in the dark for up to a month.
7. Examine the slides with epifluorescence or confocal microscopy. Excitation at 488 nm induces FITC fluorescence (green), excitation at 568 nm for rhodamine. Phase or differential interference contrast is helpful for analysis of the cell morphology. Software such as the Metamorph image analysis package (Universal Imaging, West Chester, PA, USA) can be used for further analyses of fluorescent signals (e.g. quantification of fluorescence). Representative micrographs of proteasome immunolabelling are shown in Fig. 14.1 and of protein aggregation in Fig. 14.2 (*see* **Note 12**).

3.4 Microinjection of Proteolysis Substrates into the Cell Nucleus

1. The cells should be grown on 25-mm round coverslips. Seed the cells into a well or dish containing the coverslip at a density providing a 70% confluent culture on the day of injection. Prior to the injection procedure the coverslip is clamped into an Attofluor cell chamber. Although cells can be microinjected in plastic dishes, a glass coverslip provides better visibility for the experimenter which is important for a high yield of efficiently microinjected cells.

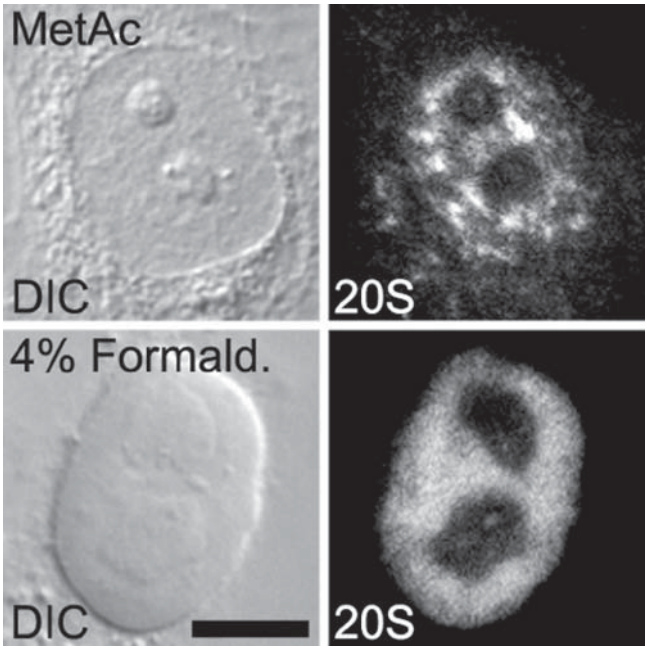

Fig. 14.1 Nuclear localization of 20S proteasomes. Subconfluent HEp-2 cells in interphase were fixed with methanol/acetone (*MetAc*) or 4% formaldehyde/0.25% Triton X-100 (*4% Formald.*) and immunolabelled with a rabbit polyclonal antibody to the 20S core protein of the proteasome. Representative cells were imaged by confocal microscopy (*right*) and the corresponding cell morphology was obtained by differential interference contrast (*DIC*, *left*). Bar, 5 µm

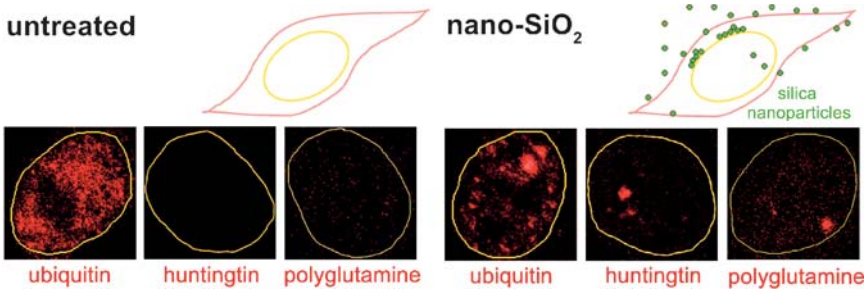

Fig. 14.2 Induction of protein aggregation by silica nanoparticles. HEp-2 cells were untreated (*left panel*) or treated for 4 h with 25 µg/mL silica nanoparticles (*nano-SiO_2*; *right panel*) and processed for immunofluorescence of protein aggregates containing ubiquitin, huntingtin, or polyglutamine. In the confocal images, the intracellular distributions of ubiquitin, huntingtin, and polyglutamine are shown in *red*. The nuclear region is delineated by the nuclear envelope (drawn in *yellow*). Note that in untreated cells, ubiquitin is distributed throughout the nucleoplasm without aggregates and neither huntingtin nor polyglutamine are detectable. However, nuclear aggregates of ubiquitin, huntingtin, and polyglutamine are formed after incubation with SiO_2 nanoparticles. To view this figure in color, see COLOR PLATE 5

2. Prepare the protein (DQ OVA or DQ BSA) for microinjection by diluting it to 0.2 mg/mL with sterile PBS.
3. Clear the protein solution from particles or aggregates by centrifugation (1 min, 20,000×*g*).
4. Transfer 5 µL of the suspension into the microinjection Femtotip.
5. To avoid clogging of the Femtotip by dried protein solution, immediately connect it to the Injectman and pressurize the system (e.g. 2,500 hPa). Immerse the tip into a dish or chamber filled with culture medium, focus on the tip and adjust the pressure to allow a constant low-level outflow (between 100 and 2,000 hPa).
6. Inject cells with the protein solution. A perfect injection (~5% of the cell volume) can be achieved if a small bulge is seen during injection, without destroying the integrity of the nuclear envelope or the cytoplasmic membrane.
7. After microinjection, the cells are incubated in culture conditions to allow physiological degradation of the exogenous protein. Incubation for 1 h prior to examination yields best results (Fig. 14.3).

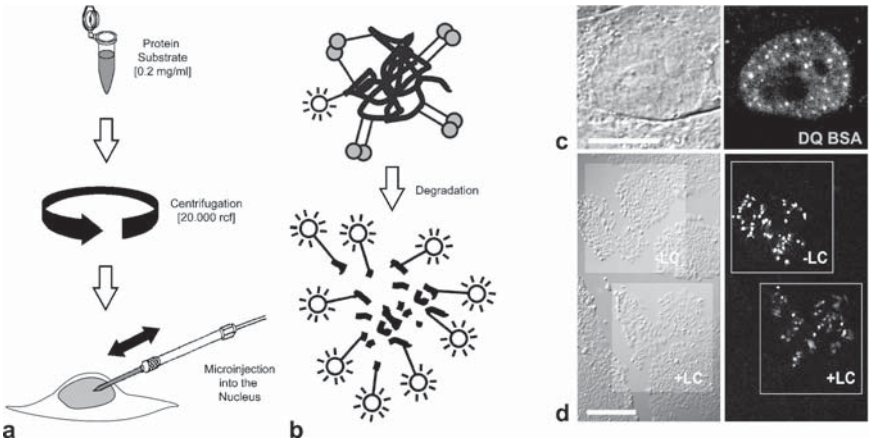

Fig. 14.3 **a** Rapid clogging of the injection tip is a serious problem for microinjection experiments. The diluted protein solution must be cleared from particles or aggregates by centrifugation and the injection procedure started immediately. **b** Mechanism of dequenching of the fluorescent precursor. The intact protein emits only ~3% of its fluorogenic potential, but upon digestion to peptides, quenching of the fluorochrome is released, resulting in a strong increase of fluorescence. **c** A HEp-2 cell was injected with DQ BSA, incubated for 1 h, and subjected to fluorescence microscopy. Areas of bright fluorescence show locations of protein degradation in the nucleus (proteolytic foci) Bar, 5 µm. **d** These foci cannot be detected in cells treated with the specific proteasome inhibitor lactacystin (*LC*). Cells were injected with DQ OVA (*upper square* labelled *–LC*) alone or additionally with LC (*lower square* labelled *+LC*). The cells treated with the proteasome inhibitor show only background fluorescence from the quenched protein substrate. Bar, 100 µm

4 Notes

1. No. 1.5-mm coverslips are better to handle than 1-mm coverslips, which are more likely to break during fixation and permeabilization procedures and tend to flex under the microscope.
2. Never heat above 60°C during preparation. Be careful: protect yourself because paraformaldehyde is toxic and volatile. Use a fume hood, gloves, safety goggles, and face mask.
3. The coverslips also fit in 35-mm petri dishes.
4. Changes of buffer and transfers of coverslips should be done carefully but *quickly* to avoid drying of the cells. Do not allow the cells to dry out during any step of fixation/permeabilization and indirect immunofluorescence, because this will increase background signal and induce nonspecific binding of the antibodies.
5. Methanol, acetone, and formaldehyde must be discarded into a hazardous waste container.
6. Methanol must be removed quickly and totally before adding acetone, otherwise the cells may show aberrant morphologies.
7. It is easy to lose the cells during low-percentage formaldehyde fixation. It is better to keep the coverslips in the 6-well plates or in Petri dishes without shaking and to remove and add the solutions carefully. Another possibility is to grow the cells on coverslips that have been coated with poly-L-lysine.
8. After removing the coverslip from the 6-well plate, be aware on which side the cells are located. Mark the Coplin jars accordingly. If you have forgotten the orientation of your coverslip, take it with forceps and scratch with a scalpel on one side; if the cells are located on this side you will see the scratch on the cell layer.
9. A humidified chamber is easily constructed: place moistened filter paper into a plastic box or a Petri dish.
10. Before you add the antibody, carefully drain off excess PBS from the coverslip. This step should be performed quickly, because the cells are very easily air-dried and at no time should they be allowed to become dry. Apply the antibodies onto one edge of the coverslip and transfer it face down on the slide quickly.
11. Air bubbles should be avoided during incubations with antibodies and the mounting procedure.
12. Controls should be performed in order to confirm the specificity of fluorochrome-conjugated antibodies for their respective Igs.

References

1. Driscoll, J. and Goldberg, A.L. (1990) The proteasome (multicatalytic protease) is a component of the 1500 kDa proteolytic complex which degrades ubiquitin-conjugated proteins. *J. Biol. Chem*. **265**, 4789–4792.
2. Kirschner, M. (1999) Intracellular proteolysis. *Trends Cell Biol*. **9**, M42–M45.
3. Muratani, M. and Tansey, W.P. (2003) How the ubiquitin-proteasome system controls transcription. *Nat. Rev. Mol. Cell Biol*. **4**, 192–201.

4. Finley, D., Ciechanover, A., and Varshavsky, A. (1984) Thermolability of ubiquitin-activating enzyme from the mammalian cell cycle mutant ts85. *Cell* **37**, 43–55.
5. Hugle, B., Kleinschmidt, J.A., and Franke, W.W. (1983) The 22S cylinder particles of Xenopus laevis. II. Immunological characterization and localization of their proteins in tissues and cultured cells. *Eur. J. Cell Biol*. **32**, 157–163.
6. Kleinschmidt, J.A., Hugle, B., Grund, C., and Franke, W.W. (1983) The 22S cylinder particles of Xenopus laevis. I. Biochemical and electron microscopic characterization. *Eur. J. Cell Biol*. **32**, 143–156.
7. Pines, J. and Lindon, C. (2005) Proteolysis: anytime, any place, anywhere? *Nat. Cell Biol*. **7**, 731–735.
8. Lee, D.H. and Goldberg, A.L. (1998) Proteasome inhibitors: valuable tools for cell biologists. *Trends Cell Biol*. **8**, 397–403.
9. Rockel, T.D., Stuhlmann, D., and von Mikecz, A. (2005) Proteasomes degrade proteins in focal subdomains of the human cell nucleus. *J. Cell Sci*. **118**, 5231–5242.
10. Nucifora, F.C., Sasaki, M., Peters, M.F., Huang, H., Cooper, J.K., Yamada, M., Takahashi, H., Tsuji, S., Troncoso, J., Dawson, V.L., Dawson, T.M., and Ross, C.A. (2001) Interference by huntingtin and atrophin-1 with CBP-mediated transcription leading to cellular toxicity. *Science* **291**, 2423–2428.
11. Chen, M. and von Mikecz A. (2005) Formation of nucleoplasmic protein aggregates impairs nuclear function in response to SiO_2 nanoparticles. *Exp. Cell Res*. **305**, 51–62.
12. von Mikecz, A., Konstantinov, K., Buchwald, D., Gerace, L., and Tan, E.M. (1997) High frequency of autoantibodies to insoluble cellular antigens in chronic fatigue syndrome. *Arthritis and Rheum*. **40**, 295–305.
13. Scharf, A., Rockel, T.D., and von Mikecz, A. (2007). Localization of proteasomes and proteasomal proteolysis in the mammalian interphase cell nucleus by systematic application of immunocytochemistry. *Histochem. Cell Biol*. **127**, 591–601.
14. Rockel, T.D. and von Mikecz, A. (2002) Proteasome-dependent processing of nuclear proteins is correlated with their subnuclear localization. *J. Struct. Biol*. **140**, 189–199.
15. Sisodia, S. (1998) Nuclear inclusions in glutamine repeat disorders: are they pernicious, coincidental or beneficial? *Cell* **95,** 1–4.
16. Ross, C.A. (2002) Emergence of unifying mechanisms of Huntington's disease and related disorders. *Neuron* **35,** 819–822.
17. Taylor, J. P., Hardy, J., and Fischbeck, K. H. (2002) Toxic proteins in neurodegenerative diseases. *Science* **296,** 1991–1995.
18. Kim, S., Nollen, E. A. A., Kitegawa, K., Bindokas, V. P., and Morimoto, R. I. (2002) Polyglutamine protein aggregates are dynamic. *Nat. Cell Biol*. **4,** 826–831.
19. Guillot, PV., Xie, SQ., Hollinshead, M., and Pombo A. (2004) Fixation-induced redistribution of hyperphosphorylated RNA polymerase II in the nucleus of human cells. *Exp. Cell Res*. **295**, 460–468.

Chapter 15
Multicolor 3D Fluorescence In Situ Hybridization for Imaging Interphase Chromosomes

Marion Cremer, Florian Grasser, Christian Lanctôt, Stefan Müller, Michaela Neusser, Roman Zinner, Irina Solovei, and Thomas Cremer

Keywords Multicolor 3D-FISH; Interphase Chromosomes; Imaging

Abstract Fluorescence in situ hybridization (FISH) of specific DNA probes has become a widely used technique mostly for chromosome analysis and for studies of the chromosomal location of specific DNA segments in metaphase preparations as well as in interphase nuclei. FISH on 3D-preserved nuclei (3D-FISH) in combination with 3D-microscopy and image reconstruction is an efficient tool to analyze the *spatial* arrangement of targeted DNA sequences in the nucleus. Recent developments of a "new generation" of confocal microscopes that allow the distinct visualization of at least five different fluorochromes within one experiment opened the way for multicolor 3D-FISH experiments. Thus, numerous differently labeled nuclear targets can be delineated simultaneously and their spatial interrelationships can be analyzed on the level of individual nuclei.

In this chapter, we provide protocols for the preparation of complex DNA-probe sets suitable for 3D-FISH with up to six different fluorochromes, for 3D-FISH on cultured mammalian cells (growing in suspension or adherently) as well as on tissue sections, and for 3D immuno-FISH.

In comparison with FISH on metaphase chromosomes and conventional interphase cytogenetics, FISH on 3D-preserved nuclei requires special demands with regard to probe quality, fixation, and pretreatment steps of cells in order to achieve the two goals, namely the best possible preservation of the nuclear structure and at the same time an efficient probe accessibility.

1 Introduction

Fluorescence in situ hybridization (FISH) provides the most direct way to map the chromosomal location of DNA sequences and has become a widely used technique to detect numerical aberrations and structural chromosomal rearrangements both in metaphase chromosomes as well as in interphase nuclei. FISH on 3D-preserved nuclei (3D-FISH) in combination with 3D-microscopy and image reconstruction has become an efficient tool to analyze the *spatial* arrangement and nuclear architecture of distinct

R. Hancock (ed.) *The Nucleus: Volume 1: Nuclei and Subnuclear Components*,

targets such as entire chromosome territories (CTs), chromosomal subregions, or individual gene loci on the single cell level using appropriate DNA probes. There is increasing evidence that nonrandom and evolutionary conserved higher-order chromatin arrangements contribute to the different epigenetic mechanisms that interact in complex ways and at several hierarchical levels to secure gene expression patterns and other nuclear functions of a given cell type (for recent reviews *see* **refs.** ***(1–4)***).

Recent developments of confocal microscopy and other comparable microscopic systems allow the distinct visualization of at least five different fluorochromes within one experiment (for review *see* **ref.** ***(5)***). Such multicolor approaches opened the way for the simultaneous delineation of numerous differently labeled nuclear target sequences and the analysis of their spatial interrelationships on the level of individual nuclei.

(Multicolor) 3D-FISH and 3D immuno-FISH on fixed nuclei should be considered as complementary approaches to biochemical and biophysical assays for the assessment of specific DNA and protein location and their interactions (for a recent review *see* **ref.** ***(6)***). Compared with fluorescence microscopy, biochemical assays such as chromatin immunoprecipitation (ChIP) or chromosome conformation capture (3C) technologies ***(7–9)*** provide a higher resolution. However, information on the spatial arrangement on the single-cell level requires fluorescence microscopy as an indispensable tool. Although first approximations on the spatial arrangement of specific DNA segments can be obtained by FISH and wide-field epifluorescence microscopy of 2D specimens, a quantitative assessment requires state-of-the-art techniques for 3D preservation of nuclei, 3D imaging, and eventually voxel-based algorithms for data evaluation. For readers who are interested in the technique of 3D imaging and quantitative assessments in more detail we refer to recent publications ***(5, 10, 11)***.

In this chapter, we provide protocols for the preparation of complex DNA–probe sets suitable for 3D-FISH with up to six different fluorochromes (**Section 3.1**), for 3D-FISH on cultured mammalian cells (growing in suspension or adherently) including the option for 3D immuno-FISH (a combination of 3D-FISH and immunodetection of specific nuclear proteins) (**Section 3.2**), and for 3D-FISH on tissue sections (**Section 3.3**).

2 Materials

For reasons of clarity, in the following **Sections 2.1** to **2.3,** chemicals and solutions are listed separately according to each method.

2.1 Generation, Labeling, and Setup of Complex DNA Probes for Multicolor 3D-FISH

We strongly suggest the use of chemicals of high purity, normally labeled as "p.A." grade. Chemicals should be stored according to the manufacturer's instructions. For solutions used for primary polymerase chain reactions (PCR), DNA- and DNAse-free reagents should be used. Water used for solutions should have a resistivity of 18.2 MΩ/cm, referred to here as ddH_2O. See Tables 15.1, 15.2, and 15.3.

Table 15.1 Sources of reagents

Chemical	Company, distributor
Aminoallyl-dUTP	Sigma-Aldrich, Deisenhofen, Germany
Biotin succinimidyl ester (bio)	Molecular Probes (Invitrogen), Karlsruhe, Germany
Cot-1 DNA	Invitrogen
Cy3 mono NHS ester (Cy3)	Amersham Biosciences, Freiburg, Germany
Cy5 mono NHS ester (Cy5)	Amersham Biosciences
Dextran sulphate	Amersham Biosciences
Digoxigenin succinimidyl ester (dig)	Molecular Probes
Dinitrophenyl aminohexanoid acid succinimidyl ester (dnp)	Molecular Probes
FITC succinimidyl ester (FITC)	Molecular Probes
Glycine	Amersham Biosciences
$NaHCO_3$	Sigma-Aldrich
Salmon sperm DNA	Invitrogen
TAMRA succinimidyl ester (TAMRA)	Molecular Probes
Texas Red succinimidyl ester (Texas Red)	Molecular Probes
Tris-HCl	Sigma-Aldrich
W1 (Polyoxyethylene ether W1)	Sigma-Aldrich

All other chemicals are from Merck, Darmstadt, Germany

Table 15.2 Enzymes, buffers, and kits (if not stated otherwise, store at −20°C)

Enzymes, buffers, and kits	Company, distributor
DNA polymerase I (Kornberg polymerase)	Roche, Mannheim, Germany
DNase I	Roche
GeneAmp PCR buffer 10×	Applied Biosystems, Darmstadt, Germany
GenomiPhi DNA Amplification Kit (store at −80°C)	GE Healthcare, Munich, Germany
$MgCl_2$ solution (25 m*M*) PCR	Perkin Elmer, Wellesley, MA, USA
Nick translation buffer (10×)	Roche
PCR buffer D (5×)	Invitrogen
PCR buffer I (10×) without $MgCl_2$	Perkin Elmer, Jügesheim, Germany
Proteinase K	Roche
Taq polymerase	GE Healthcare

2.2 Fixation, Pretreatment Steps, and Setup of Multicolor FISH in 3D-Preserved Cultured Mammalian Cells

See Tables 15.4, 15.5, and 15.6.

2.3 3D-FISH on Histological Sections

See Table 15.7.

Table 15.3 Solutions

Solution	Constituents	Annotations
4× SSC/Tween	0.2% Tween 20 in 4× SSC	2 mL of Tween 20 in 1,000 mL of 4× SSC; store at room temperature
ACG-Mix for label DOP-PCR	2 m*M* dATP, dCTP and dGTP	10 µL of dATP, dCTP, dGTP (100 m*M*) each + 470 µL of ddH_2O (autoclaved); store at −20°C
ACGT-Mix for human pancentromere and mouse major satellite PCR	2 m*M* dATP, dTTP, dCTP, and dGTP	10 µL of dATP, dTTP, dCTP, dGTP (100 m*M*) each + 460 µL of ddH_2O (autoclaved); store at −20°C
Aminoallyl-dUTP (20 m*M*)	20 m*M* aminoallyl-dUTP in bicarbonate buffer	Dissolve 1 mg of aminoallyl-dUTP in 95.60 µL of bicarbonate buffer; store at −20°C
Bicarbonate buffer, 0.2 *M*	0.2 *M* $NaHCO_3$	16.798 g of $NaHCO_3$ in 1,000 mL ddH_2O, store at −20°C
dNTP-mix (for primary and secondary DOP)	2.5 m*M* dATP, dCTP, dGTP, and dTTP	25 µL of dATP, dCTP, dGTP, dTTP (100 m*M*) each + 900 µL of ddH_2O (autoclaved); store at −20°C
dNTP-mix for NT	0.5 m*M* dATP, dCTP, dGTP; 0.1 m*M* dTTP	5 µL of dATP, dCTP, dGTP (100 m*M*) each + 1 µL of dTTP (100 m*M*) + 984 µL of ddH_2O (autoclaved); store at −20°C
dTTP for label DOP-PCR	1 m*M* dTTP	10 µL of dTTP + 990 µL of ddH_2O (autoclaved); store at −20°C
EDTA (0.5 *M*)	EDTA (0.5 *M*)	Dissolve 186.12 g of EDTA in 200 mL of ddH_2O, adjust pH to 8.0 with NaOH, make to 1,000 mL of ddH_2O; store at room temperature
HCl (0.1 *M*)		50 mL of HCl (1 *M*) + 450 mL of ddH_2O; store at room temperature
Hybridization mastermix	20% Dextran sulphate in 2× SSC	Dissolve 8 g dextran sulfate in 40 mL of 2× SSC, vortex, filter using 0.45-µm filter and aliquot. Store at −20°C
Pepsinization solution	0.005% pepsin in 0.01 *M* HCl	50 µL of pepsin (10%) + 10 mL of 0.1 *M* HCl, make to 100 mL using ddH_2O and warm up to 37°C; store at −20°C
SSC-buffer, pH 7.0	150 m*M* NaCl, 15 m*M* Na citrate	20× SSC: 175.3 g of NaCl + 88.2 g of Na citrate, make to 1,000 mL with ddH_2O, adjust pH to 7.0 with NaOH. Dilute to 4×, 2×, or 0.1× SSC with ddH_2O; store at room temperature
β-mercaptoethanol (100 m*M*)	0.1 *M* β-mercaptoethanol	0.1 mL of β-mercaptoethanol + 14.4 mL of ddH_2O; store at −20°C

Table 15.4 Chemicals

Chemicals	Company, distributor
Bovine serum albumin (fraction V)	ICN Biomedicals, Eschwege, Germany
Glycerol	Merck, Darmstadt, Germany
Paraformaldehyde	Merck
Pepsin	Sigma-Aldrich, Deisenhofen, Germany
Poly-L-lysine hydrobromide	Sigma-Aldrich
Propidium iodide (PI)	Sigma-Aldrich
Triton X-100	Merck
Vectashield mounting medium	Vector, Burlingame, CA, USA

Other chemicals are as in Table 15.1

Table 15.5 Solutions

Solution	Constituents	Annotations
4× SSC/Tween	0.2% (v/v) Tween 20 in 4× SSC	2 mL of Tween 20 in 1,000 mL of 4× SSC
Blocking solution	4% (w/v) BSA in 4× SSC/Tween	2 g of BSA in 50 mL of 4× SSC/Tween
Formamide/2× SSC (storing and denaturation solution)	50% formamide in 2× SSC	50 mL of 20× SSC + 350 mL of formamide + 100 mL of ddH_2O, adjust to pH 7.0 with 1 *M* HCl, store at −20°C
Glycerol (20% v/v)	20% glycerol in 1× PBS	100 mL of glycerol + 400 mL of 1× PBS
HCl (0.1 *M*)		50 mL of HCl (1 *M*) + 450 mL of ddH_2O; store at room temperature
Paraformaldehyde (4%)	4% paraformaldehyde in 1× PBS or 0.3× PBS	4 g of paraformaldehyde to 100 mL in 1× PBS (or 0.3× PBS), dissolve by heating and stirring, adjust pH to 7.4. Avoid boiling. Can be kept at −20°C
Pepsinization solution	10% pepsin in ddH_2O (stock solution)	Dissolve 10 g of pepsin in 100 mL of ddH_2O; store at −20°C
Pepsinization solution	0.005% pepsin in 0.01 *M* HCl (working solution)	50 µL of pepsin (10%) + 10 mL of 0.1 *M* HCl, make to 100 mL using ddH_2O, warm up to 37°C
PBS-buffer, pH 7.4, 20×	140 m*M* NaCl, 2.7 m*M* KCl, 6.5 m*M* Na_2HPO_4, 1.5 m*M* KH_2PO_4	160 g NaCl, 4 g KCl, 36 g $Na_2HPO_4.2\ H_2O$, 4.8 g KH_2PO_4, make to 1 L ddH_2O. Adjust pH to 7.4 with 1 *M* HCl, dilute to 1× PBS
PBST, pH 7.4, 1×	0.2% (v/v) Tween 20 in 1× PBS	2 mL of Tween 20 in 1,000 mL of 1× PBS
Poly-lysine stock solution	10 mg/mL poly-lysine in ddH_2O	Dissolve poly-lysine in ddH_2O, stir, and make 1-mL aliquots. Keep at −20°C. Dilute to 1 mg/mL in ddH_2O before use
SSC-buffer, pH 7.0 0.1–20×	150 m*M* NaCl, 15 m*M* Na citrate	175.3 g of NaCl + 88.2 g of Na citrate to 1,000 mL with ddH_2O. Adjust pH to 7.0 with NaOH, dilute to 4×, 2×, or 0.1× SSC with ddH_2O
Triton X-100 permeabilization solution	0.5% Triton X-100	0.5 mL of Triton X-100 to 100 mL in 1× PBS, dissolve by stirring

Table 15.6 DNA staining solutions (stored at –20°C)

Stain	Constituents	Annotations
4′,6-Diamidino-2-phenylindole (DAPI) (Sigma-Aldrich)	0.05 µg/mL in 2× SSC	Prepare freshly from a stock solution (5 µg/mL in ddH_2O)
Propidium iodide (PI) (Sigma-Aldrich)	25 µg/mL in 2× SSC	Prepare freshly from a stock solution (500 µg/mL in ddH_2O)
TO-PRO-3 (Invitrogen)	1 µ*M* in 2× SSC	Prepare freshly from stock solution (1 m*M* in DMSO)

Table 15.7 Chemicals, enzymes, DNA stains, and antifade solution

Chemicals, enzymes, DNA stains, antifade solution	Company, distributor
Acetone	Merck
Saponin	SERVA, Heidelberg, Germany
Sodium azide	Merck
Sodium isothiocyanate	Sigma-Aldrich
Sodium monophosphate dihydrate	Merck
Xylene	Merck
Pepsin	Sigma-Aldrich
Proteinase K	Roche
Vectashield mounting medium	Vector, Burlingame, CA, USA

Other chemicals are as in Tables 15.1 and 15.4

3 Methods

3.1 Generation, Labeling, and Setup of Complex DNA Probes

Although a large number of labeled DNA probes are commercially available, we strongly encourage generating tailored probes in the laboratory. This approach is cost efficient and ensures higher flexibility in designing experiments. An official source to obtain chromosome-specific DNA probes is currently provided by the University of Bari (M. Rocchi, http://www.biologia.uniba.it/rmc/).

High quality of labeled DNA probes is crucial for efficient 3D-FISH experiments. Several factors such as probe complexity, amount of probe available, the hapten used, and others will influence the decision of which labeling method to use for probe labeling. Direct labeling by incorporation of fluorochrome-conjugated nucleotides (FITC-dUTP, Texas Red-dUTP or others) has been very successful following our protocols and can be considered equally efficient in comparison to hapten-labeled probes such as biotin, digoxigenin, and dinitrophenol.

DNA probes used for FISH can be generated and labeled by various methods. Although repetitive sequences can be readily amplified from genomic DNA using appropriate primer pairs, specific genomic loci are usually assessed by choosing the

respective cloned sequences from DNA libraries (at present mostly from bacterial artificial chromosome [BAC] libraries). Additionally, more complex probes for the visualization of large chromosomal regions can be obtained by microdissection or, if whole chromosomes are to be visualized, by flow sorting. Due to the small amount of source DNA for the latter probes, they have to be amplified prior to labeling.

Several possibilities exist regarding the labeling of probes, normally achieved by incorporating nucleotides carrying a hapten or fluorophore (dUTP-conjugates). Nick translation is the traditional and a very reliable method, still widely used for labeling of all kinds of source material. The nick translation reaction incorporates tagged nucleotides by introducing nicks into the probe via DNAse I, which serve as starting points for DNA polymerase I (Kornberg polymerase) which elongates the 3′-OH ends generated and removes the old strand by its 5′-3′ exonuclease activity. During elongation, labeled nucleotides are incorporated. Nick translation generates labeled DNA in equivalent amounts to the input probe, and therefore requires relatively large amounts of source material.

Most DNA probes may also be efficiently labeled by PCR amplification techniques with universal primers such as the degenerate oligonucleotide-primed (DOP) primer ***(12)***, which saves time and material. In contrast to nick translation, PCR labeling has the great advantage of increasing the amount of probe during labeling. It should however be noted that DOP-PCR is prone to loss of probe complexity during the amplification step.

A relatively new approach used as an alternative to DOP-PCR for the amplification of complex probe sets is based on an isothermal, multiple displacement amplification (MDA) reaction ***(13)***. This method uses a phage polymerase and random hexamer primers and is commercially available as the GenomiPhi DNA amplification Kit (GE Healthcare, Munich, Germany). This method yields excellent DNA probes from small amounts of source DNA with a highly uniform representation of the amplified and labeled product across the genome.

The following is restricted to protocols describing the labeling of a given DNA probe with a single hapten or fluorochrome. In this context, we note that the term M-FISH was initially used as an abbreviation for multiplex FISH (not multicolor FISH), a technique that implements combinatorial labeling of one probe with different, usually two or three fluorochromes/haptens for the delineation of all chromosomes of a species. Although this approach has been widely used as a tool for the analysis of metaphase chromosomes, its successful application for 3D-FISH on 3D-preserved nuclei has been shown only in a few studies (see, e.g., **ref. *(14)***) mainly due to the fact that analysis of confocal image stacks containing combinatorially labeled probes is difficult to perform. For special aspects regarding the generation of DNA probes for 3D-FISH by combinatorial labeling, please *see* **refs. *(14, 15)***.

In the following, we provide protocols for the conjugation of dUTPs with haptens or fluorochromes and for generation and labeling of DNA probes starting from genomic DNA of flow-sorted chromosomes, from BAC or cosmid DNA, and from specific genomic sequences. Different labeling procedures for probes and advice

for the setup of complex probe pools, for example large sets of BAC pools, are described. Finally, a protocol is provided for probe precipitation and setup in a hybridization mix ready to be used for 3D-FISH experiments.

3.1.1 Conjugation of dUTPs with Hapten or Fluorochrome (Time ~5 h)

A variety of fluorochrome- or hapten-conjugated nucleotides (dUTPs) required for probe labeling are commercially available. However, we strongly encourage conjugation of dUTPs with haptens or fluorochromes. We provide a simplified protocol initially described in **ref.** ***(16)*** for haptens and fluorochromes that have been routinely used in our lab for conjugation reactions.

1. Dilute the hapten or fluorochrome in DMSO for subsequent conjugation reactions according to Table 15.8 (dilutions may be stored at −20°C up to several months).
2. For conjugation of dUTP with different haptens/fluorochromes yielding a 1 m*M* solution of the respective conjugated dUTP, mix the following reagents:

   For Dig-, dnp-, and TexasRed-dUTP labeling: mix 10 µL of 20 m*M* dUTP (aminoallyl-dUTP), 15 µL of ddH_2O, 10 µL of 0.2 *M* bicarbonate buffer, 10 µL of DMSO, and 10 µL of dissolved hapten/fluorochrome, total 55 µL.

   For Bio-dUTP labeling: mix 10 µL of 20 m*M* dUTP, 15 µL of ddH_2O, 10 µL of 0.2 *M* bicarbonate buffer, and 10 µL of 40 m*M* Bio, total 45 µL.

   For Cy3-, FITC-, and Cy5-dUTP labeling: mix 10 µL of 20 m*M* dUTP, 10 µL of ddH_2O, 10 µL of 0.2 *M* bicarbonate buffer, and 10 µL of dissolved fluorochrome, total 40 µL.

   For TAMRA-dUTP labeling: mix 10 µL of 20 m*M* dUTP, 10 µL of ddH_2O, 10 µL of 0.2 *M* bicarbonate buffer, and 20 µL of 10 m*M* TAMRA, total 50 µL.

3. Incubate at 30°C for 3–4 h.
4. Add 2 µL of 2 *M* glycine, pH 8.0 to stop the reaction, 4 µL of 1 *M* Tris-HCl, pH 7.75 to stabilize the nucleotides, and ddH_2O to adjust the total volume to 200 µL.

Table 15.8 Dilution of fluorochromes/haptens in DMSO

Hapten/fluorochrome	Quantity delivered in commercial product	DMSO to be added (µL)	Final concentration
Biotin succinimidyl ester (bio)	100 mg	4,401	40 m*M*
Digoxigenin succinimidyl ester (dig)	5 mg	213	40 m*M*
Dinitrophenyl amino-hexanoid acid succinimidyl ester (dnp)	25 mg	1,562	40 m*M*
Cy3 mono NHS ester	1 mg	66	20 m*M*
TAMRA succinimidyl ester	10 mg	1,560	10 m*M*
Texas Red succinimidyl ester	5 mg	612	10 m*M*
FITC succinimidyl ester	10 mg	417	40 m*M*
Cy5 mono NHS ester	1 mg	62	20 m*M*

5. Aliquot the labeled dUTPs (e.g., 20 µL) and store at −20°C (with the exception of dnp-dUTP, store at +4°C). Aliquots can be stored up to several years.

3.1.2 Labeling of DNA by Nick-Translation (Time ~3 h)

Nick-translation (NT) can be used for all kinds of source DNA (dissolved in either H_2O or 10 m*M* Tris-Cl, pH 8.0) provided that sufficient starting material is available. This method yields excellent labeling quality but does not involve DNA amplification. The following protocol provides the setup for a standard NT reaction yielding 50 µL of labeled probe with a concentration of 20 ng/µL (*see* **Note 1**).

1. Prepare a water bath at 15°C.
2. Dilute DNAse I stock solution (2,000 U/mL) 1:250 in ice-cold water and keep on ice.
3. Mix the reagents listed in Table 15.9 in a 1 mL tube. Keep all reagents on ice.
4. Incubate the reaction at 15°C for 90 min (*see* **Note 2**).
5. Check the length of the resulting DNA fragments with an aliquot of 5 µL on a 1% agarose gel with appropriate size markers (e.g., a *Hind*III lambda DNA digest). Keep the remaining solution at −20°C. A perfect NT should yield a smear of DNA fragments ranging from ~300–1,000 bp. If further digestion is necessary (e.g., in case a considerable fraction of DNA is >1.5 kb), add 1 µL of diluted DNase I for 5–10 min at 20°C and check the DNA fragment size again on an agarose gel.
6. Add 1 µL of 0.5 *M* EDTA when the desired fragment size is obtained to stop the reaction.
7. Store the NT product at −20°C (up to several years) or proceed immediately for probe preparation (*see* **Section 3.1.9**).

Table 15.9 Setup of nick-translation

Reagent	Amount	Final concentration
1 µg DNA (*see* **Note 1**)	× µL	
NT-buffer 10×	5 µL	50 m*M* Tris-HCl, pH 7.5, 5 m*M* $MgCl_2$, 50 µg/mL BSA
β-mercaptoethanol (100 m*M*)	5 µL	10 m*M*
dNTP-mix (0.5 m*M* dATP, dCTP, dGTP; 0.1 m*M* dTTP)	5 µL	50 µ*M* each dATP, dCTP, dGTP, and 10 µ*M* dTTP
Modified dUTP 1 m*M* (e.g., dig-dUTP or fluoro-dUTP)	2.5 µL (5 µL)	20 µ*M;* 40 µ*M* for fluorochrome-labeled nucleotide
ddH_2O	to 50 µL	—
DNase I (2,000 U/mL) (*see* **Note 2**)	1 µL	0.008 U in 50 µL reaction
Polymerase I	1 µL	0.1 U/µL

3.1.3 Generation of DNA-Probes by DOP-PCR Using the 6MW-Primer (Primary Amplification) (Time ~6 h)

FISH experiments with complex DNA probes require comparably large amounts of probe DNA. A widely used method for DNA amplification from small amounts of starting material is DOP-PCR ***(12)*** using the primer 6MW. A "primary" DOP-PCR can be performed with a minimal amount of source material (in the picogram to nanogram range) and works well for most template DNAs, including total genomic DNA and BAC clones. DOP-PCR is of particular use for the amplification of so-called chromosome painting probes, which are usually generated from flow-sorted chromosomes and may be obtained from genome project resource centers or commercial sources. Typically, 500 flow-sorted chromosomes (~50 pg, depending on the chromosome size) are delivered in ~30 µL of ddH_2O. DOP-PCR is however not recommended for cosmids or plasmids due to low insert complexity. For these kinds of probes, we suggest NT of genomic DNA (*see* **Section 3.1.2**) or an initial isothermal, MDA (*see* **Section 3.1.7**).

Before the "primary" amplification of BAC DNA, RNAse treatment should be performed and the concentration adjusted to ~50–100 ng/µL. DNA should be dissolved in H_2O or 10 m*M* Tris-Cl, pH 8.0.

1. For a standard reaction for primary DOP-PCR amplification, mix the reagents listed in Table 15.10 in a 0.6-mL tube (DNAse free) (*see* **Note 3**).
2. Perform primary amplification in a thermocycler according to Table 15.11 (time ~4 h 15 min).
3. Check 2 µL of amplification product on a 1% agarose gel with appropriate size markers. The product should yield a visible smear between ~200 bp and 1.5 kb. Primary amplification normally yields a few micrograms of DNA, depending on the amount of template DNA. For example, with 50 ng of template DNA, the expected yield of a 50-µL primary DOP-PCR would be 1.5–10 µg DNA (30–200 ng/µL).
4. Store the amplified DNA at −20°C (up to several years) or proceed immediately with the secondary DOP-PCR (*see* **Section 3.1.4**).

Table 15.10 Setup of primary DOP-PCR

Reagent	Amount	Final concentration
Flow-sorted chromosomes in ddH_2O or genomic DNA	Variable	~500 chromosomes or 1–100 ng DNA
Buffer D (5×)	10 µL	1×
6MW primer* (100 µ*M*)	1 µL	2 µ*M*
Detergent W1 (1%)	5 µL	0.1%
dNTP mix (2.5 m*M* each)	4 µL	200 µ*M*
Adjust with ddH_2O	to 50 µL	—
Taq polymerase	0.5-1 µL	2.5–5 U

*6 MW primer sequence: CCGACTCGAGNNNNNNATGTGG

Table 15.11 Conditions for primary DOP-PCR using the 6MW primer

Number of cycles	Reaction	Temperature, time
1	Initial denaturation	96°C 3'00"
8	Denaturation	94°C 1'00"
(Low stringency cycles)	Annealing	30°C 1'30"
	Extension	3'00" ramp (14°C/min) followed by 72°C 2'00"
35	Denaturation	94°C 1'00"
(High stringency)	Annealing	56°C 1'00"
	Extension	72°C 2'00"
1	Final extension	72°C 5'00"

3.1.4 Reamplification of primary DOP-PCR products using the 6MW primer (time ~5 h)

The "primary" amplification product can be reamplified by up to four rounds of DOP-PCR in the presence of the same primer, in order to further increase the amount of DNA probe. Only after the fourth round of DOP-PCR reamplification is the probe quality considerably reduced. We suggest reamplification of the primary DOP-PCR product to increase the amount of DNA and suggest using this further reamplified DOP-PCR product as template for labeling of DNA (*see* **Section 3.1.5**). The composition of secondary and subsequent amplification reactions are the same as that described for primary amplification, but the PCR conditions differ. For frequent reamplification reactions using the 6MW primer, we recommend preparation of a mastermix (MM) as described below, containing all reagents except DNA and Taq polymerase, which can be stored at −20°C for several years.

1. For MM sufficient for 20×50 µL amplification reactions, mix the reagents listed in Table 15.12 in a 1-mL tube.
2. For a standard reaction for (re-)amplification in a single DOP-PCR reaction, mix in a 0.6-mL PCR tube: 48.5 µL of MM, 1 µL of DOP-PCR-amplified DNA (usually corresponds to 30–200 ng) (*see* **Note 4**), and 0.5 µL of TAQ polymerase (5 U/µL).
3. Perform (re-)amplification in a thermocycler according to Table 15.13.
4. Run 2 µL of amplification product on a 1% agarose gel with appropriate size markers. It should yield a visible smear ranging between ~200 bp and 1.5 kb.

Using 50 ng of template DNA, the expected yield of a 50-µL primary DOP-PCR would be 1.5–10 µg DNA (30–200 ng/µL). Store the amplified DNA at −20°C (up to several years) or proceed immediately with the subsequent labeling by DOP-PCR (*see* **Section 3.1.5**).

3.1.5 Probe Labeling by DOP-PCR Using the 6MW Primer (Time ~3 h)

For frequent reamplification reactions, it is possible to prepare a mastermix (MM) containing all reagents except DNA and TAQ polymerase that can be stored at −20°C for several years.

Table 15.12 Master-mix (MM) for secondary DOP-PCR reactions

Reagent	Amount	Final concentration
Buffer D 5×	200 µL	1×
6MW primer* (100 µ*M*)	20 µL	2 µ*M*
Detergent W1 (1%)	100 µL	0.1%
dNTP mix (2.5 m*M* each)	80 µL	200 µ*M*
ddH_2O	570 µL	—

*6MW primer sequence: CCGACTCGAGNNNNNNATGTGG

Table 15.13 Conditions for secondary (and subsequent) DOP-PCR reactions using the 6MW primer (time ~3 h)

Number of cycles	Reaction	Temperature
1	Initial denaturation	96°C 3'00"
35	Denaturation	94°C 1'00"
(High stringency)	Annealing	56°C 1'00"
	Extension	72°C 2'00"
1	Final extension	72°C 5'00"

1. For setup of the label-MM sufficient for 20×50 µL amplification reactions, mix the reagents listed in Table 15.14 in a 1-mL tube.
2. For a standard 50-µL single-label DOP-PCR reaction, mix together in a 0.6-mL PCR tube, 48 µL of label-MM, 1–2 µL of DOP-PCR-amplified DNA (usually corresponds to 30–200 ng) (*see* **Note 5**), and 0.5 µL of TAQ-polymerase (5 U/µL).
3. Perform PCR in a thermocycler according to Table 15.15 (time ~1 h 15 min).
4. With 50 ng of template DNA, the expected yield of a 50-µL label DOP-PCR would be 1.5–10 µg DNA (30–200 ng/µL).
5. Run 2 µL of amplification product on a 1% agarose gel with appropriate size markers. The amplification product should yield a visible smear ranging between ~200 bp and 1.5 kb.
6. Store the labeled DNA at −20°C (up to several years) or proceed immediately to **Section 3.1.9** for probe preparation. In the case of fluorochrome-labeled probes, protect the probes from light while handling.

3.1.6 Amplification by MDA (Time ~18 h)

Presently, our recommended method for efficient DNA probe amplification from small amounts of total genomic DNA or from BAC and cosmid DNA is a recently developed technique based on an isothermal, MDA of DNA by Phi29 polymerase and subsequent nick-translation (*see* **Section 3.1.2**). This approach provides a highly uniform representation of the amplified and hence of the subsequently labeled product across the genome. A commercial product (GenomiPhi DNA Amplification Kit; GE Healthcare) works very well in our hands. Genomic DNA from BACs, cosmids,

Table 15.14 Mastermix for DOP-PCR labeling (label-MM) using the 6MW-primer

Reagent	Amount	Final concentration
GeneAmp PCR buffer 10×	100 µL	50 m*M* KCl, 10 m*M* Tris, pH 8.3
$MgCl_2$ (25 m*M*)	80 µL	2 m*M*
6MW primer*(100 µ*M*)	20 µL	2 µ*M*
ACG mix (each 2 m*M*)	50 µL	100 µ*M*
dTTP (1 m*M*)	80 µL	80 µ*M*
Bio (or DIG or DNP)-dUTP or fluor-dUTP (e.g., FITC-dUTP) (1 m*M*)	20 µL (40–60 µL for fluor-dUTPs)	20–60 µ*M*
ddH_2O adjust to	970 µL	—

*6MW primer sequence: CCGACTCGAGNNNNNNATGTGG

Table 15.15 Amplification conditions for label DOP-PCR using the 6MW primer

Number of cycles	Reaction	Temperature
1	Initial denaturation	94°C 3'00"
	Denaturation	94°C 1'00"
20–25	Annealing	56°C 1'00"
	Extension	72°C 0'30"
1	Final extension	72°C 5'00"

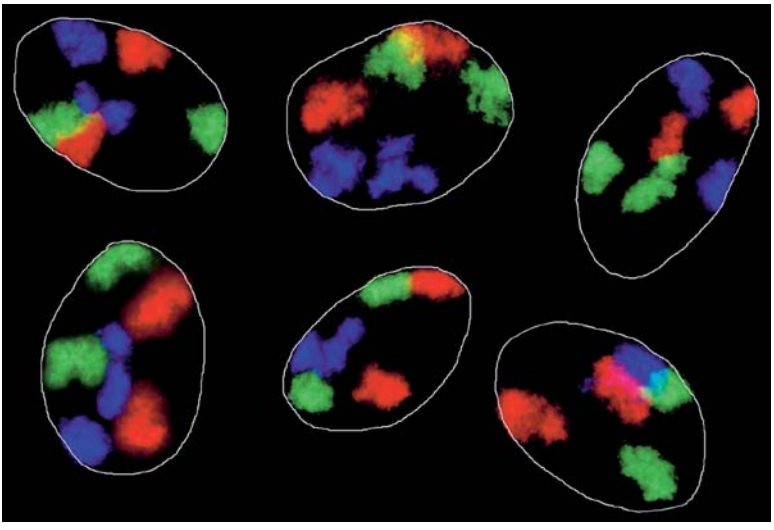

Fig. 15.1 Three-color 3D-FISH on nuclei of normal diploid human fibroblasts. Maximum intensity projections of confocal serial sections are shown. Chromosome territories (CTs) 3 are in *green* (labeled with dinitrophenol, detected with FITC), CTs 5 are in *blue* (labeled with digoxigenin, detected with Cy3), and CTs 11 are in *red* (labeled with biotin, detected with Cy5). Each paint yields a strong signal with little unspecific background. This and all other figures are reproduced from "Cold Spring Harbor Protocols" (www.cshprotocols.org) with the kind permission of the Cold Spring Harbor Laboratory Press (2007). To view this figure in color, see COLOR PLATE 6

plamids, etc. can be obtained by any conventional DNA extraction method. Prior to amplification, the DNA concentration should be adjusted to ~50–100 ng/μL. For a single standard MDA reaction using the GenomiPhi kit, proceed as follows (keep all reagents on ice):

1. Pipet 9 μL of sample buffer into a 0.6-mL tube.
2. Add 1 μL of template DNA (minimum 5 ng, recommended >10 ng), mix (*see* **Note 6**).
3. Denature at 95°C for 3 min.
4. Add 9 μL of reaction buffer and 1 μL of enzyme mix.
5. Incubate at 30°C for 16 h (maximum 24 h).
6. Heat inactivate the enzyme at 65°C for 10 min.
7. Check 1 μL of product on a 1% agarose gel with appropriate size markers. The reaction should yield 6–12 μg of DNA with a size from ~2 to 12 kb.
8. Store amplified DNA at −20°C (up to several years) or proceed immediately for subsequent nick-translation (*see* **Section 3.1.2**).

3.1.7 DNA probe Labeling by MDA (Time ~18 h)

A modified MDA protocol (*compare* **Section 3.1.6**) allows for simultaneous DNA probe amplification and labeling with hapten-dUTPs (bio-dUTP, dig-dUTP, dnp-dUTP), thus making subsequent labeling of the amplified DNA product by nick-translation redundant. Currently, in our hands, this protocol is only applicable for labeling with hapten-dUTPs but not with fluorochrome-coupled dUTPs (e.g., FITC-dUTP or Cy3-dUTP).

Proceed for a single standard reaction for labeling MDA using the GenomiPhi DNA Amplification kit as follows (keep reagents on ice):

1. Pipet 9 μL of sample buffer into a 0.6-mL tube.
2. Add 1 μL of template DNA (minimum 5 ng, recommended >10 ng), mix.
3. Denature at 95°C for 3 min.
4. Lyophilize 5 μL of 1 m*M* hapten-dUTP in a Speedvac.
5. Dissolve hapten-dUTP in 9 μL of reaction buffer.
6. Add 1 μL of enzyme mix; mix.
7. Mix 10 μL of sample buffer/DNA and 10 μL of reaction buffer/hapten-dUTP.
8. Incubate at 30°C for 16 h.
9. Heat inactivate at 65°C for 10 min.
10. Check 1 μL of product on a 1% agarose gel with appropriate size markers. The reaction should yield 6–12 μg with a size ranging from 2 to 12 kb.
11. Digest with 1 μL of DNAse 1 (2,000 U/mL stock solution diluted 1:250 in ddH_2O) per 20 μL of MDA product for 6 min at room temperature (RT) to an appropriate fragment size of 300–1,000 bp.
12. Store probe at −20°C (up to several years) or proceed immediately with probe preparation (*see* **Section 3.1.9**).

3.1.8 Generation of Human Pancentromeric and Mouse Major Satellite FISH Probes (Time ~3 h)

Centromere-specific probes are widely used in 3D-FISH experiments. We provide protocols yielding excellent quality human and mouse centromere-specific FISH probes. To generate human pancentromeric (**steps 1** and **2**) and mouse major satellite (**steps 3** and **4**) probes, we recommend first amplifying the repetitive sequences by specific primer sequences, and then labeling the primary amplified DNA by nick-translation *(see* **Section 3.1.2**).

1. For a standard 100-µL amplification reaction for a human pancentromeric probe, mix the reagents listed in Table 15.16 in a 0.6-mL tube.
2. Perform PCR in a thermocycler according to Table 15.17 (time ~2 h).
3. For a standard 100-µL amplification reaction for mouse major satellite DNA probe, mix the reagents listed in Table 15.18 in a 0.6-mL tube.
4. Perform PCR in a thermocycler according to Table 15.19.
5. Check the DNA concentration on a gel or photometrically and use 2 µg for nick translation according to **Section 3.1.2**.

3.1.9 Probe Preparation, Precipitation, and Setup (Minimum Time ~2 h)

We recommend using 1–10 ng of DNA per microliter of hybridization solution for repetitive probes and 20–100 ng/µL for nonrepetitive probes. Because exact measurement of DNA concentration may be somewhat tedious, as a rule of thumb, we recommend using 2 µL of labeled PCR product per 1 µL of hybridization solution for chromosome painting or locus-specific probes. It may be helpful to increase the concentration for small nonrepetitive probes, e.g., plasmids. The concentration of unlabeled competitor DNA (e.g., Cot-1 DNA) added for suppression of nonspecific hybridization depends on the frequency of repetitive sequences in the probe, and should be around 10- to 50-fold the concentration of probe DNA. However, in the case of complex probe mixtures, it is assumed that probes suppress each other

Table 15.16 Setup for specific amplification of a human pancentromeric probe

Reagent	Amount (µL)	Final concentration
GeneAmp PCR buffer 10×	10	1× (50 m*M* KCl, 10 m*M* Tris, pH 8.3)
$MgCl_2$ (25 m*M*)	8	2 m*M*
α27 Primer* (100 µ*M*)	2	2 µ*M*
α30 Primer** (100 µ*M*)	2	2 µ*M*
Genomic DNA (100 ng/µL)	2	2 ng/µL
ACGT mix (each 2 m*M*)	5	100 µ*M*
ddH_2O	70	—
Taq polymerase (5 U/µL)	0.8	

*5′-CAT CAC AAA GAA GTT TCT GAG GCT TC
**5′-TGC ATT CAACTC ACA GAG TTG AAC CTT CC

Table 15.17 Amplification conditions for human pancentromeric DNA probe

Number of cycles	Reaction	Temperature	
1	Initial denaturation	94°C	3'00"
	Denaturation	94°C	0'45"
35	Annealing	62°C	1'20"
	Extension	72°C	1'20"
1	Final extension	72°C	5'00"

Table 15.18 Setup of PCR for mouse major satellite DNA

Reagent	Amount (µL)	Final concentration
GeneAmp PCR buffer 10×	10	1× (50 m*M* KCl, 10 m*M* Tris-Cl)
$MgCl_2$ (25 m*M*)	8	2 m*M*
Forward primer* (25 µ*M*)	4	1 µ*M*
Reverse primer** (25 µ*M*)	4	1 µ*M*
Genomic DNA (10 ng/µL)	10	1 ng/µL
ACGT-mix (each 2 m*M*)	5	100 µ*M*
ddH_2O	58	—
Taq polymerase	0.8	

*5′-GCG AGA AAA CTG AAA ATC AC
**5′-TCA AGT CGT CAA GTG GAT G

Table 15.19 Amplification conditions for mouse major satellite DNA

Number of cycles	Reaction	Temperature	
1	Initial denaturation	94°C	3'00"
	Denaturation	94°C	1'00"
35	Annealing	56°C	1'00"
	Extension	72°C	2'00"
1	Final extension	72°C	5'00"

and the amount of Cot-1 DNA can be reduced to around fivefold. A hybridization area covered by a 18×18-mm coverslip requires 5–8 µL of hybridization mixture. For smaller or larger hybridization areas, the amount should be adjusted accordingly.

1. In a 1.5-mL tube, mix all the labeled DNA probes that will be hybridized together, unlabeled competitor DNA, e.g., Cot-1 DNA with 5-, 10-, or 50-fold (***see above***) the concentration of probe DNA (*see* **Note 7**), and 20 µg of unlabeled salmon sperm DNA for efficient precipitation (especially important for small amounts of DNA).
2. Mix the probe DNA with ice-cold 100% EtOH (2.5× volumes) for at least 30 min, preferably overnight at −20°C or at −80°C.
3. Spin down at 15,000×*g* for 20 min.
4. Discard the supernatant and dry the pellet (using a vacuum centrifuge if available).
5. Resuspend the pellet in 50% formamide/2× SSC/10% dextran sulfate as follows: dissolve the pellet in the appropriate amount of 100% formamide, shake at 37°C

(can take up to a few hours) and then add an equal volume of 4× SSC/20% dextran sulfate. Briefly mix and incubate at 37°C for 10 min (*see* **Note 8**).
6. Hybridization probes can be stored at −20°C for up to several years or immediately used for hybridization (*see* **Section 3.2.4**).

3.1.10 Troubleshooting

The quality of a DNA probe to be used in FISH experiments can only be reliably determined by a trial FISH experiment. Troubleshooting at the stage of probe generation and labeling is therefore questionable. We recommend checking the DNA amount and fragment size of the labeled probe, but also refer the reader to the troubleshooting section, **Section 3.2.7**.

1. Problem: Weak signal.
   Solution: Increasing the amount of probe may help, but weak signals can be due to different factors. Check the probe size according to the instructions given here. In case of a poor incorporation of labeled nucleotides (recognizable by a large amount of nucleotides in the gel), repeat the reaction.
2. Problem: Strong background.
   Solution: Fragments that are too long may cause some unspecific background: try DNAse I treatment. If the probe was not completely dissolved in formamide: dissolve again.

3.2 Cell Fixation, Pretreatment Steps, and Setup of Multicolor FISH in 3D-Preserved Cultured Mammalian Cells

The following protocols focus on fixation, pretreatments, hybridization on cultured mammalian cells (growing adherently or in suspension), and detection of hybridized probes. An efficient hybridization requires a number of permeabilization steps and the denaturation of cell DNA. These steps have to be carefully balanced, in order to maintain the best possible nuclear morphology on one hand and making chromatin accessible for probe penetration on the other hand. Minor deviations or experimental mistakes can easily change the quality of the experimental outcome. Paraformaldehyde (PFA) is likely to be the most gentle of current fixatives, appropriate for subsequent FISH. Previously, we could demonstrate that structural preservation of chromatin was maintained throughout the whole 3D-FISH procedure down to preservation of individual replication foci ***(17, 18)*** that likely represent ~1 Mb chromatin domains ***(1)***. These observations indicate that measurements performed after 3D-FISH reasonably well reflect the situation in vivo down to putative ~1 Mb chromatin domains. Electron microscopic investigations, however, showed major alterations in the ultrastructure of the nucleus caused mainly by the heat denaturation step. These changes indicate a caveat for interpretations of 3D-FISH experiments at nanometer scales.

3.2.1 Fixation and 3D-FISH Pretreatment of Adherently Growing Cells (Time ~2.5 h)

For fixation of cells growing in suspension, *see* **Section 3.2.2**. This protocol can be applied to all types of adherently growing cells. The pretreatment steps listed below work well for a variety of cell types, such as fibroblasts, primary epithelial cells, or tumor cell lines. However, pretreatment steps should be adjusted to the cell type and requirements of hybridization probes in order to get an optimal balance between the preservation of the nuclear morphology and hybridization efficiency. Treatment with the detergent Triton X-100 and repeated freezing in liquid nitrogen after incubation in glycerol helps to make nuclear DNA accessible for FISH probes without strongly affecting the 3D chromatin architecture. These two steps are generally sufficient for hybridization of highly repetitive sequences, e.g., centromeric regions.

Additional deproteinization steps are necessary when single-copy DNA sequences are targeted. There are two methods of deproteinization, incubation in HCl and digestion with pepsin. Depending on the DNA probes and (to a lesser extent) to the cell type used for hybridization, these pretreatments may be combined or used separately. Normally, incubation in 0.1 N HCl makes nuclear DNA sufficiently accessible for centromere specific probes. Pepsin incubation (*see* **Section 3.2.3**) is necessary for cells with voluminous cytoplasm. This step should be monitored under the microscope because the duration of pepsin treatment finally affects the preservation of the nuclear morphology and may cause detaching of cells from slides.

1. Briefly rinse the slide or coverslip (*see* **Note 9**) with cells grown to subconfluency in two or three changes of 1× PBS at 37°C (*see* **Note 10**).
2. Fix in 4% PFA in 1× PBS (freshly made, pH 7.0) at RT for 10 min. During the last minute, a few drops of 0.5% Triton X-100/PBS should be added (5 drops/100 mL fixation solution using a plastic Pasteur pipette).
3. Wash in 1× PBS with 0.01% Triton X-100 at RT for 3× 3 min.
4. Incubate in 0.5% Triton X-100/1× PBS at RT for 5–15 min.
5. Incubate in 20% glycerol in 1× PBS at RT for a minimum of 60 min (preferably overnight).
6. Freeze by dipping the slide into liquid nitrogen (~30 sec) and thaw on a piece of paper towel. As soon as the frozen layer disappears, put the coverslip back into 20% glycerol/PBS and repeat four times.
7. Wash in 1× PBS for 3× 10 min.
8. Incubate in 0.1 N HCl for 5 min at RT (*see* **Note 11**).
9. Incubate in 2× SSC for 2× 3 min.
10. Incubate in 50% formamide (pH = 7.0)/2× SSC for at least 1 h at RT (preferably overnight) before proceeding with hybridization or optional pepsin digestion. For pepsinization, proceed to **Section 3.2.3**; if not required, proceed to **Section 3.2.4**.
11. Slides may be stored for at least 3–4 months in 50% formamide/2× SSC at +4°C. Longer storage may result in deterioration of nuclear morphology after denaturation for 3D-FISH.

3.2.2 Fixation and 3D-FISH Pretreatment of Cells Growing in Suspension (Time Until Storage in Formamide ~4–5 h)

This protocol can be applied to all types of cells growing in suspension, such as lymphoblastoid cells or cells directly isolated from peripheral blood, such as lymphocytes or granulocytes. Prior to fixation, cells have to be made adherent on a polylysine-coated glass surface. Lymphocytes and related cells are especially prone to shrinking during the fixation process, which can be compensated by a brief incubation in 0.3× PBS prior to fixation.

1. For the preparation of polylysine-coated slides, use a dry coverslip (*see* **Note 12**) (stored in 80% EtOH) and incubate it for 1 h with ~150 µL of polylysine hydrobromide (1 mg/mL). We recommend putting the drop of polylysine on a piece of Parafilm or in a petri dish, and placing the coverslip on the drop.
2. Rinse the coverslips carefully in ddH_2O and air-dry.
3. For seeding cells, we recommend applying ~1 mL of culture medium containing ~1×10^5 to 1×10^6 cells per 20×20-mm coverslip.
4. Alternatively, for peripheral blood cells, isolate the desired cell type according to the appropriate method. Cells obtained from 1 mL of peripheral blood seeded on a 20×20-mm area should yield a sufficient cell density for hybridization.
5. Spin the suspension of cells at ~200×*g* for 10 min.
6. Discard the supernatant and resuspend the pellet in RPMI/50%FCS. This step is thought to improve the adherence of cells to the glass surface. In order to increase cell density on the slide, about one quarter of the initial volume should be used for resuspension.
7. Place ~200 µL of cell suspension on a polylysine-coated coverslip and incubate at 37°C in an incubator containing 5% CO_2 for 1 h.
8. Check attachment of the cells under the microscope, briefly drain off the medium (*see* **Note 10**).
9. Incubate in 0.3× PBS for 40 sec (this step prevents the shrinkage of spherically shaped cells that are otherwise prone to collapse during the following fixation. However, keep this time strictly, otherwise the nuclei will increase in size).
10. Fix cells in 4% PFA/0.3× PBS for 10 min at RT.
11. Wash in 1× PBS at RT for 3× 5 min.
12. Incubate in 0.5% Triton X100/1× PBS at RT for 20 min.
13. Transfer to 20% glycerol/1× PBS and incubate at RT for at least 30 min.
14. Freeze cells by dipping the slide into liquid nitrogen (~30 sec) and thaw on a piece of paper towel. As soon as the frozen layer disappears, put back into 20% glycerol/PBS. Repeat the freezing/thawing step four times.
15. Wash in 0.05% Triton X-100/1× PBS for 3× 5 min.
16. Incubate in 0.1 N HCl for 5 min (*see* **Note 11**).
17. Wash in 2× SSC for 2× 1 min.
18. Incubate in 50% formamide (pH 7.0)/2× SSC at RT for at least 1 h (better overnight) before proceeding with hybridization or optional pepsin digestion. For pepsinization, proceed to **Section 3.2.3**, if not required, proceed to **Section 3.2.4**.

19. Slides may be stored for at least 3–4 months in 50% formamide/2× SSC at +4°C. Longer storage may result in deterioration of nuclear morphology after denaturation for 3D-FISH.

3.2.3 Optional Treatment with Pepsin (Time ~45 min)

For efficient hybridization, pepsin incubation is required for most cell types with a voluminous cytoplasm and/or in cultures with a high cell density. The pepsin step is critical with regard to nuclear morphology, we therefore suggest first testing a hybridization without pepsin treatment and including this step only in the case of insufficient probe penetration. Pepsinization should be monitored under the microscope, because its duration critically affects the preservation of the nuclear morphology and may cause detachment of cells from slides. Pepsin incubation should be stopped as soon as reduction of cytoplasm becomes visible under the microscope.

1. Equilibrate slides (kept in 50% formamide/2× SSC) in 2× SSC at RT for 2 min.
2. Equilibrate slides in 1× PBS at RT for 3 min.
3. Incubate in pepsin (0.005% in 0.01 N HCl): warm 0.01 N HCl to 37°C in a bottle and add pepsin (30–50 µL of 10% stock solution) just before use, shake well, and pour into a Coplin jar. Incubate in pepsin for 3–5 min.
4. Incubate in 1× PBS/50 m*M* $MgCl_2$ to inactivate pepsin, RT for 2× 5 min.
5. Postfix in 1% paraformaldehyde/1× PBS, RT for 10 min.
6. Wash in 1× PBS, RT for 5 min.
7. Wash in 2× SSC for 2× 5 min, then return slides to 50% formamide/2× SSC for at least 1 h before hybridization.

3.2.4 Probe Denaturation and Setup Of Hybridization (Time ~1 h)

The time for setup strongly depends on the number of slides; the time required for hybridization is ~2–3 days.

We recommend simultaneous denaturation of nuclear and probe DNA, even in the case of probes that require a high excess of Cot1-DNA. Simultaneous denaturation is quick, simple, and optimal for retention of 3D morphology.

1. Place the hybridization mixture with dissolved probe on a coverslip (e.g., 6–8 µL per 18×18-mm coverslip).
2. Take a slide with cells out of the 50% formamide/2× SSC and quickly drain the excess of fluid off the slide (*see* **Note 13**).
3. Cover the target area of the slide by the coverslip with probe.
4. Wipe off the excess fluid around the coverslip and seal with rubber cement; let the rubber cement dry completely (protect from light during drying in case of fluorochrome-labeled probes).

5. Place slides on a hot block at 75°C to denature cellular and probe DNA for 2 min. Keep this time and temperature strictly.
6. Perform hybridization in a metal box floating in a 37°C water bath for at least overnight or preferably for 2–3 days.

3.2.5 Washing Steps and Detection (Time ~1–5 h)

The time depends on the number of layers used for detection. The choice of the detection scheme depends on several factors: (i) the number of haptens and fluorochromes used for probe labeling; (ii) the number of antibody layers required to obtain a sufficiently strong signal; (iii) the color of nuclear counterstain; and (iv) most importantly, the microscopic setup available. One should also carefully plan the scheme used for the detection of different haptens in order to avoid cross-reactions between antibodies. In our laboratory, different combinations of up to six different fluorochromes are successfully applied with regard to efficient signal intensities, signal/noise ratios and distinct color separation using a Leica SP2 confocal microscope for visualization. For a five-color detection scheme, we obtained best results by combining Alexa 488 (or FITC), Cy3 (or TAMRA), Texas Red, Cy5, and DAPI as the DNA counterstain. One or two more fluorochromes can be added to this basic set up, e.g., Alexa 514 and/or Alexa 633. In such case, a linear unmixing (also known as "spectral unmixing") of fluorochromes is required after acquisition of image stacks in order to separate images of FITC–Alexa 514–Cy3 or Texas red–Alexa 633–Cy5 ***(5)***. This fluorochrome combination is achieved by using directly labeled probes for Cy3 and TexasRed (optionally, for FITC) while Alexa 514, Alexa 633, and Cy5 are detected using the respective antibody conjugates against hapten-labeled probes (e.g., bio-dUTP, dig-dUTP, or dnp-dUTP). In our experience, all commercially available fluorochrome-conjugated antibodies from the established companies work well. However, one should be aware that the quality of an antibody may sometimes vary depending on the batch provided.

1. After hybridization, peel off the rubber cement, gently remove the coverslip, and transfer the cells to 2× SSC. In case the coverslip cannot be stripped off easily, incubate briefly in 2× SSC and try again. Take care that all subsequent steps are performed under light protection.
2. Wash in 2× SSC at 37°C, shaking for 3× 5 min.
3. Wash in 0.1× SSC at 60°C (stringent washes), shaking for 3× 5 min (*see* **Note 14**).
4. Rinse briefly in 4× SSC/0.2%Tween.
5. Block in 4× SSC/0.2%Tween + 4% BSA at 37°C for 10–15 min.
6. Dilute the required antibodies or avidin-conjugates to the appropriate working concentration in 4× SSC/0.2%Tween + 1% BSA.
7. Incubate with primary antibody (first layer) in a dark moist chamber at 37°C for 45 min.
8. Wash in 4× SSC/0.2%Tween, shaking for 3× 3 min.

9. Incubate with the appropriate concentration of secondary antibody (second layer) in a dark moist chamber at 37°C for 45 min.
10. Wash in 4× SSC/0.2%Tween, shaking for 3× 3 min.
11. Optional further layers accordingly.
12. For DNA counterstaining use, e.g., DAPI (0.05 µg/mL) for 2–5 min (longer staining is OK), TOPRO-3 (1 µ*M*) for 5–10 min (longer incubation may lead to strong overstaining), or PI (25 µg/mL) (*see* **Note 15**) for 2–5 min, all at RT.
13. Wash briefly in 4× SSC/0.2%Tween.
14. Mount hybridized areas in antifade (Vectashield).
15. Seal coverslips with colorless nail polish.
16. Store in dark at 4°C. FISH signals should be stable for at least 1 year, however.

The detection scheme in Table 15.20 shows an example for the combined utilization of six different fluorochromes that works well in our hands (Fig. 15.2). When performing five-color experiments, we recommend omitting Alexa 514, in three-color experiments, Alexa 514 and TexasRed. In case your confocal microscope is not equipped with a UV laser, counterstain your slide with TOPRO-3 or PI. Since PI emits partially in the same spectral range as Cy3 and TexasRed, the choice of fluorochromes used to label the probes needs to be selected accordingly.

3.2.6 Multicolor 3D Immuno-FISH

3D-immuno-FISH is a somewhat delicate method, since the pretreatment steps (especially HCl and heat denaturation) necessary for DNA probe access can result in protein degradation and loss of the epitope for a given antibody. Although some proteins such as lamins or the cell cycle-related protein pKi67 tolerate these steps and can easily be detected after FISH, others are more prone to degradation. Depending on the protein of interest, different approaches for immuno-FISH have been described (see, e.g., **refs.** ***(19–21)***), including sequential staining, which is however labor intensive since it requires superimposition of images after immunostaining and FISH. With regard to the preservation of a variety of different epitopes

Table 15.20 Labeling scheme for six different fluorochromes

Labeling	Fluorochrome	Detection
(none)	DAPI (blue)	Stain with 0.05 µg/mL DAPI in 4× SSC/0.2% Tween for 5 min
		layer 1: avidin conjugated to Alexa 488
bio-dUTP	FITC (green)	layer 2: goat anti-avidin conjugated to FITC
		layer 1: rabbit anti-dnp
dnp-dUTP	Alexa 514 (yellow)	layer 2: goat anti-rabbit conjugated to Alexa 514
Cy3-dUTP	Cy3 (orange)	Cy3-dUTP
TexasRed-dUTP	TexasRed (red)	TexasRed-dUTP
		layer1: mouse anti-DIG conjugated to Cy5
DIG-dUTP	Cy5 (far red)	layer 2: goat anti-mouse conjugated to Cy5

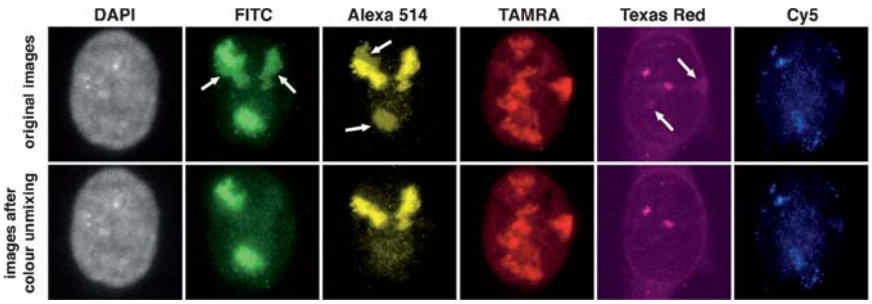

Fig. 15.2 Six-color 3D-FISH on nuclei of human fibroblasts. Maximum intensity projection of a confocal image stack with six color channels are shown as original images (*upper row*) and after linear color unmixing (*bottom row*) using the software of the Leica SP2 confocal microscope. The FITC channel delineates the territories of chromosome 12, Alexa514 the territories of chromosomes 11, and TAMRA the territories of chromosomes 17, 19, and 20. Texas Red delineates a BAC contig of chromosome 11 and Cy5 a BAC pool covering different regions of chromosome 12. *White arrows* point at the image regions generated due to "leakage" of some fluorochromes into the neighboring channels, e.g., Alexa514 into the FITC channel (and vice versa), or TAMRA into the Texas Red channel. To view this figure in color, see COLOR PLATE 7

recognized by specific antibodies, we obtained the best results by binding an epitope with the first specific antibody followed by a second biotin-conjugated antibody and stabilizing this complex by a postfixation step before proceeding with pretreatment and denaturation. We consider this step as essential, since biotin is relatively heat resistant and thus is not prone to destruction by heat denaturation before FISH ***(18)***. By this approach we obtained FISH signals together with immunodetection signals for proteins of interest (e.g., methylated histones) that were qualitatively not distinguishable from those obtained after immunodetection alone.

1. Fix cells (grown to ~50% confluency) in 4% PFA for 10 min.
2. Permeabilize cells in 0.5% Triton for 15 min.
3. Block in 4% BSA/PBST for 10 min.
4. Incubate with first antibody in a humid chamber at 37°C for 1 h.
5. Wash in PBST for 2× 5 min.
6. Incubate with the second biotinylated antibody (e.g., biotin-conjugated goat anti-rabbit) at 37°C for 45 min.
7. Wash in PBST for 2× 5 min.
8. Postfix cells in 1% PFA for 10 min.
9. Incubate in 0.1 N HCl for 7–10 min.
10. Permeabilize again with 0.5% Triton for 5 min.
11. Incubate in 20% glycerol for 45 min.
12. Freeze cells by dipping the slide into liquid nitrogen (~30 sec) and thaw on a piece of paper towel. As soon as the frozen layer disappears, put the coverslip back into 20% glycerol/PBS. Repeat the freezing/thawing step four times.
13. Wash in 2× SSC for 5 min.
14. Store coverslips in 50% formamide/2× SSC for at least 24 h.

15. Perform optional pepsin treatment if necessary, as described in **Section 3.2.3**.
16. Perform hybridization as described in **Section 3.2.4**.
17. Perform posthybridization washings and detection of FISH signals according to **Section 3.2.5**. The detection of the biotinylated antibody by a (strept)-avidin-conjugated fluorochrome for immunostaining should be performed together with the last antibody (antibodies) for FISH detection for optimal results (Fig. 15.3).

3.2.7 Troubleshooting

1. Problem: Nuclei are shrunken or frayed after hybridization.
   Solution: Avoid drying up of cells, reduce denaturation time and/or temperature, reduce or skip pepsin treatment.
2. Problem: Weak hybridization efficiency of probes.
   Solution: First test your probe on a metaphase slide. In case of weak hybridization signals on metaphase chromosomes, check detection scheme and probe quality with regard to the appropriate probe length and amount of probe (*see* **Section 3.1** on DNA probe preparation). If hybridization on metaphases gives good results, add or increase pepsin pretreatment of 3D-preserved cells.
3. Problem: Strong unspecific background.
   Solution: Increase Cot-1 DNA concentration, check concentration of antibodies used in detection, check probe length.

3.3 FISH on Histological Sections

The protocols presented here describe the techniques of pretreatment, 3D-FISH, and detection of DNA probes on histological sections. These protocols have

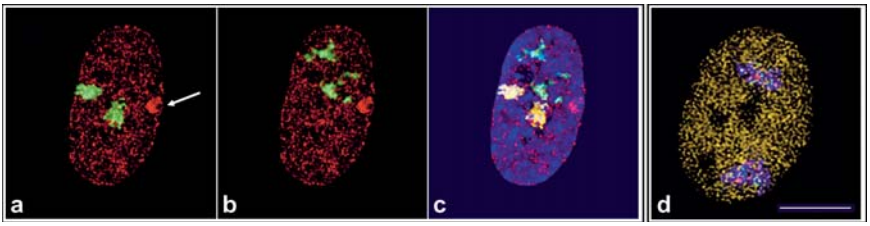

Fig. 15.3 Four-color 3D Immuno-FISH on single optical sections of human fibroblast nuclei. **a–c** Painted CTs #18 (*green* in **a**) and CTs #19 (*green* in **b**) together with the typical immunostaining pattern of histone H3 trimethylated at lysines 27. The histone modification is visualized in *red* in *(a–c)*. The focal cluster in (**a**) and (**b**) marks the region of the inactive X (*arrow*), which is strongly decorated by this histone modification. The merged image in (**c**) shows, in addition, the nuclear counterstain (*blue*), CTs #18 are shown here in *yellow*. **d** Immuno-FISH of pools of BAC clones representing either gene-poor (red) or gene-dense (green) segments of chromosome #12 (CTs #12 visualized in blue) together with the typical immunostaining pattern of histone H3 trimethylated at lysines 4 (visualized in golden). Bar, 5 μm. To view this figure in color, see COLOR PLATE 8

been successfully used in our hands for hybridization on paraffin, vibratome, and frozen sections. Pretreatment of tissue sections with heat or protease is necessary to allow unmasking of the target DNA and efficient penetration of reagents into the nuclei. Since the goal of the technique is to obtain data on the native 3D structure of the genome, close attention is paid to the preservation of nuclear morphology.

Routine sections of paraffin-embedded tissues are usually 5–10 µm in thickness, and thus most nuclei on the section will have to be discarded during analysis because they have been cut one way or another. The use of thick cryosections (20 µm) yields a relatively high proportion of intact nuclei, thereby facilitating the acquisition of data at the microscope. However, it should be noted that the use of thick sections can also lead to the appearance of a signal gradient from top to bottom due to poor antibody penetration. To remedy this problem, we have suggested adding non-ionic detergents to the solutions used in the detection of hapten-labeled probes.

Our experience with fluorophore-labeled probes indicates that accessibility of probes is generally not a significant problem, whereas efficient accessibility of larger antibody molecules is more difficult to achieve. Therefore, our protocol includes an "unmasking" step to partially free DNA from cross-linking proteins, which we have found is crucial to the success of the experiment and depends on the tissue as well as the fixative and embedding medium used during processing of the sample. Below we provide protocols for PFA-fixed tissue embedded in paraffin and sectioned using a microtome (*see* **Section 3.3.1**) or embedded in agar or freezing medium and sectioned using a vibratome or a cryotome, respectively (*see* **Section 3.3.2**).

Paraffin embedding causes notable deformation of nuclei, but still remains the most common method for human pathological material and other histological applications. We have found it difficult to obtain high-quality FISH signals on paraffin sections of adult human tissues, especially in the case of large diffuse signals typical of chromosome paint probes. In our hands, good results were consistently obtained only using fluorophore-labeled probes against repetitive sequences (e.g., alpha-satellites for pericentromeric regions of human chromosomes, Fig. 15.4). It should be noted however that we have obtained decent signals with hapten-labeled probes using the following protocol (proteinase K pretreatment) on mouse embryonic tissues, which are much less fibrous and compact than adult tissues. Vibratome sections and cryosections afford good preservation of nuclear morphology and, therefore, are preferable for nuclear architecture studies (Figs. 15.5 and 15.6). In our experience, vibratome sections are more permeable than paraffin sections and cryosections are superior to both.

One of the characteristics of some tissues, particularly at embryonic stages, is a very tight packing of nuclei. Due to this high density of nuclei, some image analysis algorithms, e.g., to measure radial distribution of signals, may require that individual nuclei be isolated from the image stack. This "segmentation" can be accomplished using Amira software (v4.0; Mercury Computing Systems, Dusseldorf, Germany) as shown in Fig. 15.7.

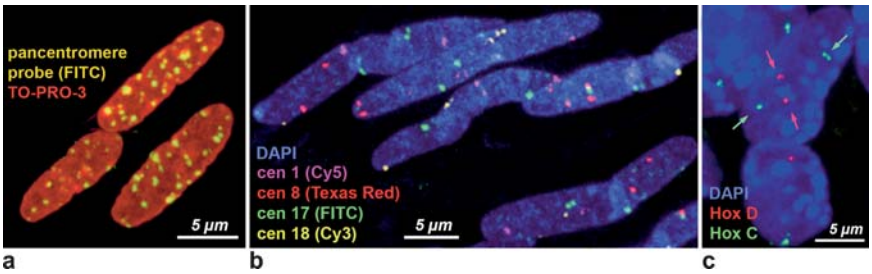

Fig. 15.4 FISH on sections of paraffin-embedded tissues. **a** Nuclei of human skeletal muscle myotubes counterstained with TO-PRO-3 (*red*) after hybridization with a probe against human centromeric sequences (labeled with FITC-dUTP; *green*). Projection of a confocal image stack (~10 µm). **b** Nuclei of human smooth muscle cells counterstained with DAPI (*blue*) after hybridization with a probe directed against chromosome-specific alphoid DNA and directly labeled with different fluorochromes. Projection of 42 optical sections of a confocal image stack (~12.5 µm). **c** Nuclei of mouse embryonic mesenchymal cells after hybridization with hapten-labeled BAC clones comprising the *HoxD* gene cluster (*red*) or *HoxC* gene cluster (*green*). Sections were counterstained with DAPI (*blue*). *Arrows* point to the two pairs of BAC signals corresponding to *Hox* genes inside a single ovoid-shaped nucleus. Note that one of the *HoxC* signal is a doublet (*upper right*), indicative of DNA replication. Projection of confocal images (~6 µm). To view this figure in color, see COLOR PLATE 9

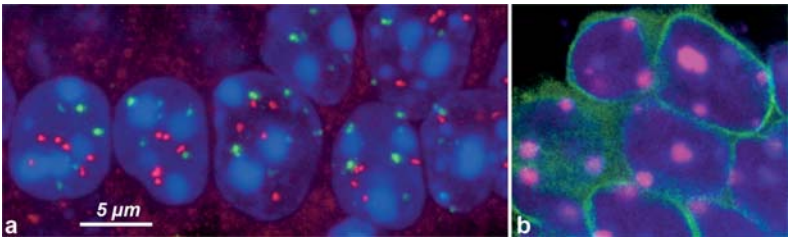

Fig. 15.5 FISH on vibratome sections. **a** Nuclei of ganglion cells of mouse retina counterstained with TO-PRO-3 (blue) after hybridization with a pool of differentially labeled BAC clones comprising either transcriptionally active or inactive genes. BAC DNA was labeled with biotin-dUTP (*green*) or digoxigenin-dUTP (*red*). Projection of part of a confocal image stack (~5 µm). **b** Nuclei of bipolar cells of mouse retina counterstained with TO-PRO-3 (*blue*) after lamin B immunostaining (*green*) and FISH with a mouse major satellite repeat probe directly labeled with Cy3-dUTP (*red*). Projection of part of a confocal image stack (~1 µm). To view this figure in color, see COLOR PLATE 10

Fig. 15.7 Segmentation of individual nuclei in image stacks of tissue sections. **a** Single optical section of a confocal image stack of mouse embryonic brain showing densely packed neuronal cells. **b** In this tissue, counterstained nuclei cannot be segmented by straightforward intensity thresholding. **c–f** Individual nuclei can be outlined using the Amira software. The contour of the nucleus must be outlined by the user on a few optical sections in the *xy*, *yz*, and *xz* planes (**c**, **d**, and **e**, respectively). Based on this input, the program automatically outlines the surface of the nucleus. This data can be used for 3D rendering (**f**) or submitted to other programs for quantitative evaluations

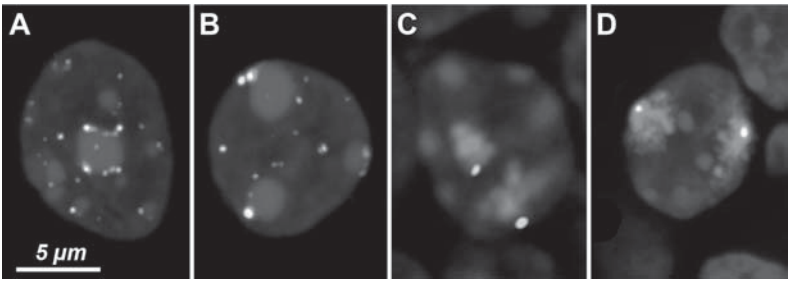

Fig. 15.6 FISH on cryosections. **A**, **B** Nuclei of ganglion (**a**) and bipolar (**b**) cell of mouse retina counterstained with TO-PRO-3 (*blue*) after hybridization with a mouse minor satellite probe that recognizes centromeres of mouse chromosomes (directly labeled with Cy3-dUTP, *red*) and with a probe recognizing telomeres (labeled with biotin-dUTP, *green*). Projection of a confocal image stack (~4 µm). **C** Nuclei of mouse embryonic neurons after hybridization with a paint probe for mouse chromosome 14 (*red*) and a labeled BAC DNA (*green*) from the same chromosome. Probes were labeled with different haptens and the nucleus was counterstained with DAPI (*blue*). Projection of part of a confocal image stack (~3 µm). **d** Nuclei of chicken embryonic neurons after hybridization with a paint probe for chicken chromosome 1 (*red*) and labeled BAC DNA (*green*) from the same chromosome. Probes were labeled with different haptens and the nucleus was counterstained with DAPI (*blue*). Projection of part of a confocal image stack (~2 µm). To view this figure in color, see COLOR PLATE 11

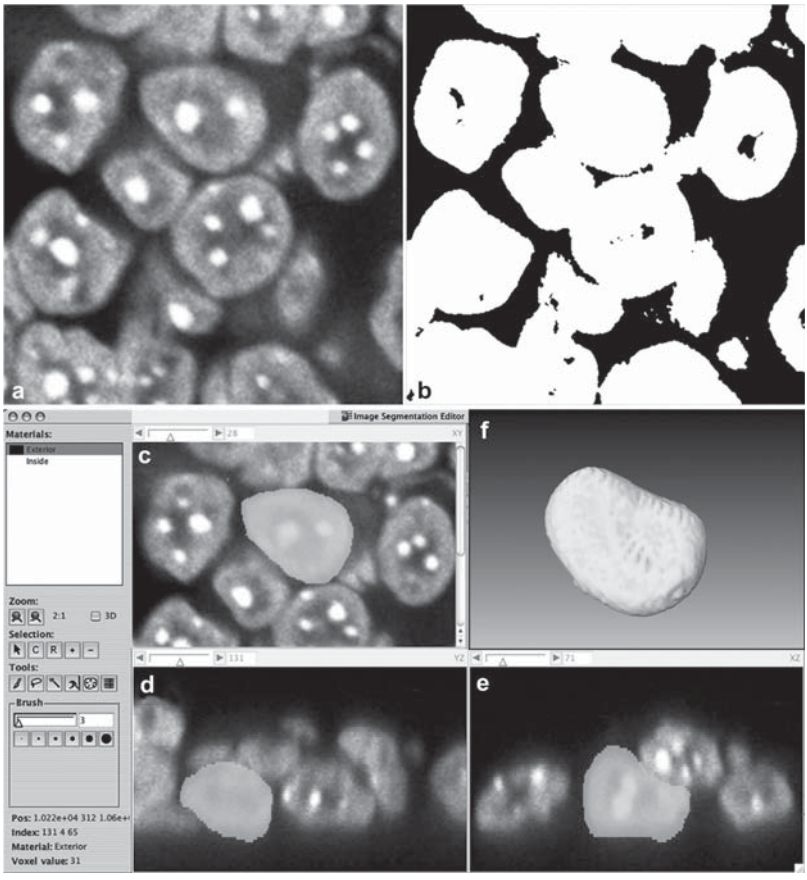

3.3.1 FISH on Paraffin-Embedded Tissue Sections (Including Washing and Detection)

Time required: ~6–7 h until hybridization setup; 2–3 days for hybridization; and 1 to several hours, depending on the number of layers, for detection.

1. Deparaffinize sections (*see* **Note 16**) in 100% xylene for 3× 10 min at 45°C
2. Rehydrate in an ethanol series: 100% ethanol for 2× 15 min, 95% ethanol for 1× 5 min, 70% ethanol for 1× 5 min, 50% ethanol for 1× 5 min, ddH_2O for 5 min.
3. Unmask DNA: sections are treated either with a denaturing chemical and pepsin (**step 4**) or with proteinase K (**step 5**). The choice and duration of treatment should be determined empirically.
4. *EITHER*:
   (a) Permeabilize the tissue with 1 *M* sodium isothiocyanate (freshly prepared solution) at 80°C (in water bath) for 30 min and rinse briefly in ddH_2O.
   (b) Treat sections with pepsin (14 mg/mL in 0.01 N HCl) at 37°C for 30 min, rinse in ddH_2O.
   (c) Dehydrate slides in 70% ethanol for 1× 10 min (*see* **Note 17**) and 100% ethanol for 2× 10 min, air-dry at RT. Continue with **step 6**.
5. *OR*:
   (a) Equilibrate slides in 25 m*M* Tris-Cl, pH 7.4/5 m*M* EDTA for 5 min at RT.
   (b) Digest with 100 µg proteinase K/mL in 25 m*M* Tris-Cl, pH 7.4/5 m*M* EDTA for 10 min at RT, rinse in 1× PBS.
   (c) Refix in 4% PFA in PBS 1× for 10 min at RT. Wash with PBS 1× for 2× 5 min.
6. Equilibrate slides in 50% formamide/2× SSC for at least 4 h (*see* **Note 18**).
7. Mount the probe dissolved in hybridization mixture (*see* **Section 3.1.9**) on the section (*see* **Note 19**), cover the probe with a coverslip (avoid making air bubbles), seal with rubber cement, and leave to completely dry at RT.
8. Prehybridize: incubate slides with mounted probe to allow infiltration of the section with the probe at 37°C for 1–2 h (*see* **Note 20**).
9. Simultaneously denature cellular DNA and probe (*see* **Note 21**): incubate slides with mounted probe on a hot block set at 85°C for 5 min.
10. Hybridize: incubate slides at 37°C in humid dark chambers (e.g., metal boxes floating in a water bath) for 2–3 days.
11. Posthybridization wash: peel off rubber cement, flick off the coverslip and quickly transfer slides into 2× SSC buffer, wash in 2× SSC buffer (preferably with shaking) at 37°C for 3× 10 min; if appropriate, wash at high stringency in 0.1× SSC at 60°C for 1× 10 min.
12. If fluorophore-labeled probes were used, proceed directly to **step 13**. In the case of hapten-labeled probes, perform detection as follows:
    (a) Incubate slides in blocking solution for 15 min.

(b) Dilute primary and secondary antibodies (and/or conjugated avidin) in blocking solution.
(c) Incubate sections with antibodies (and/or conjugated avidin) under coverslips in dark humid containers at 37°C for 1 h.
(d) After each incubation with antibody (and/or conjugated avidin), wash with 4× SSC/0.2% Tween warmed up to 37°C for 3× 5 min.

13. Counterstain: incubate in 0.05 µg DAPI/mL in 4× SSC/0.2% Tween for 10 min (*see* **Note 22**).
14. Briefly rinse in 2× SSC and mount in antifade medium: place a drop of Vectashield on the top of section and cover with coverslip (avoid making air bubbles), gently remove excess Vectashield with soft tissue and seal with nail varnish.
15. When the nail varnish has dried, the preparation is ready for examination under the microscope.

3.3.2 FISH on Vibratome Sections and Cryosections (Including Washing and Detection)

Time required: for **steps 1–12** (until hybridization) 8–9 h; for **step 13** (hybridization) 2–3 days; for **steps 14–17**, 1 to several hours (depending on the number of layers chosen for detection).

After cutting, vibratome sections (50-µm thick) are stored in PBS containing 0.04% sodium azide at 4°C. Sections are dried on slides by incubation in ddH_2O for 5 min followed by dehydration in an ethanol series: 30% and 50%, each 10 min, and then 2× in 70% for 30 min each. Sections are transferred to SuperFrost Plus slides in a drop of 70% ethanol, spread with thin brushes, and air dried at RT for 1–2 days.

Cryosections (15–30-µm thick) are placed on SuperFrost Plus slides, immediately frozen on dry ice, and stored at −80°C. The day before setting up hybridization, thaw slides at RT and leave to dry overnight.

1. Rehydrate sections in 1× PBS for 15 min.
2. (Optional) To increase probe/antibody penetration in very dense tissues, permeabilize in 1× PBS/0.5% Triton X-100 at RT for 20 min.
3. Put slides in a plastic slide holder and place this in a microwave-safe plastic container filled with 200 mL of 10 m*M* sodium citrate buffer, pH 6.0. Slides should be completely covered with liquid. Equilibrate slides at RT for 10 min.
4. DNA unmasking (*see* **Note 23**): put container in a microwave oven set at 700 W and heat for 2.5 min or until the first signs of boiling (*see* **Note 24**), cool for 2 min, resume heating for 15–25 sec until the first signs of boiling, and repeat the heating and cooling steps seven times.
5. Transfer slides to 2× SSC.
6. (Optional) To increase probe/antibody penetration in dense tissues, incubate slides in prechilled 100% acetone at −20°C for 5 min and wash with 2× SSC at RT for 3× 5 min.

7. If desired, immunostaining of cellular components can be performed at this point. **Step 4** can be then considered also as the antigen retrieval treatment and adjusted according to the antibody that is being used. After immunostaining, postfix sections with 2% PFA in 1× PBS at RT for 10 min.
8. Equilibrate slides in 50% formamide/2× SSC solution for at least 4 h. Slides can be stored in this solution for up to 2–4 months at 4°C.
9. Probe can be mounted under coverslips or, preferably, under small glass chambers specifically designed for DNA hybridization on relatively thick tissue sections (**step 10**, see Fig. 15.8 for preparation of glass chambers).
10. *EITHER*: using coverslips:

    (a) Take slides out of the 50% formamide/2× SSC, remove excess liquid around the section using soft paper.
    (b) Load the probe dissolved in hybridization mixture (*see* **Section 3.1.9**) (*see* **Note 19**).
    (c) Cover probe with coverslip (avoid making air bubbles) and seal with rubber cement and leave to completely dry at RT.
    (d) Continue with **step 11**.

    OR: using glass chambers (*see* Fig. 15.8):

    (a) Take slides out of the 50% formamide/2× SSC, remove excess liquid around section using soft paper.
    (b) Cover section with the glass chamber.
    (c) Fill glass chamber with probe by capillarity (*see* **Note 19**).
    (d) Seal the chamber with rubber cement and leave to completely dry at RT.

11. Prehybridize slides with mounted probe at 37°C for 1–2 h (*see* **Note 20**) to allow infiltration of the section with the probe.
12. Simultaneous denaturation of cellular DNA and probe: incubate slides with mounted probe on a hot block at 80°C for 5 min.
13. Hybridization: incubate slides at 37°C in humid dark chambers (e.g., metal boxes floating in a water bath) for 2–3 days.

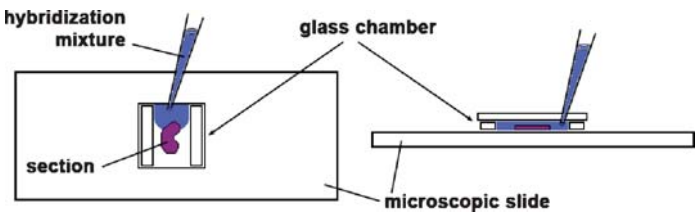

Fig. 15.8 Schematic representation of a glass chamber used for hybridization. To prepare glass chambers, cut glass strips from a coverslip (0.17-mm thick) using a diamond cutter and glue them parallel on two borders of an intact coverslip (e.g., 12×12 mm) using nail polish. Note that the section (*purple*) should first be covered by the glass chamber before filling it with hybridization mixture (*blue*) from one of the open sides

14. Posthybridization washings: peel off rubber cement, transfer slides to 2× SSC, and let coverslips or glass chambers detach by themselves. Wash in 2× SSC (preferably with shaking) at 37°C for 3× 5 min (if appropriate, wash at high stringency in 0.1× SSC at 60°C for 3× 5 min).
15. If fluorophore-labeled probes were used, proceed directly to **step 16**. In the case of hapten-labeled probes, perform detection as follows (*see* **Note 25**):
    (a) Incubate slides in blocking solution for 15 min.
    (b) Dilute primary and secondary antibodies (and/or conjugated avidin) in blocking solution.
    (c) Incubate sections with antibodies (and/or conjugated avidin) under coverslips in dark humid containers at 37°C for 1 h.
    (d) After each incubation with antibody (and/or conjugated avidin), wash with 4× SSC/0.2% Tween warmed up to 37°C for 3× 5 min.
    (e) Counterstain and mount in antifade medium as described in **Section 3.3.1**, **steps 13–15** (*see* **Note 26**).

3.3.3 Troubleshooting

1. Problem: Loss of tissue.
   Solution: Decrease concentration and/or length of incubation with protease.
2. Problem: Hybridization signal is weak or absent (paraffin sections).
   Solutions: Increase length of deparaffinization in xylene up to 1 h; increase concentration and/or length of incubation with protease; increase probe concentration; check the temperature of the hot block used for denaturation.
3. Problem: Hybridization signal is weak or absent (cryosections and vibratome sections).
   Solutions: Increase the number and/or duration of heating pulses during the DNA unmasking step; increase length of the permeabilization step with acetone; increase probe concentration; check the temperature of the hot block used for denaturation.
4. Problem: Poor preservation of nuclear morphology (paraffin sections).
   Solutions: Decrease temperature and/or length of incubation with 1 *M* sodium isothiocyanate; decrease concentration and/or length of incubation with protease.
5. Problem: Poor preservation of nuclear morphology.
   Solutions: Shorten the heating pulses during the DNA unmasking step; make sure that the sodium citrate solution does not boil.

4 Notes

1. A standard NT reaction of 50 µL may be set up for labeling 500 ng to 3 µg of DNA. For higher DNA amounts to be labeled, increase the volume of the reaction accordingly.

2. The activity of DNase I appears to be variable and may also depend on the DNA source, purity, and storage buffer. Therefore, the amount of DNase I added and/or the incubation time has to be titrated in order to obtain the appropriate size of DNA fragments. In our experience for example, plasmids may be more sensitive to DNAse I compared to BAC clones. This may require higher dilution (1:750 to 1:1,000) and/or reduction of incubation time for plasmids.
3. To avoid contamination with foreign DNA, setup of primary amplifications should be performed with a fresh set of filter tips, using pipettes that have not previously been used for handling DOP-PCR amplified products. Ideally, primary DOP-PCR reactions should be performed in a separate room with reagents exclusively used for these reactions.
4. In the case of simultaneous amplification of several painting probes or BAC clones, prepare a "pre-pool" of these components containing primary DOP-PCR-amplified DNA from each component in equal amounts (in our hands pre-pools containing DNA from up to 20 BACs or a large number of chromosome painting probes worked well). Usually 1 µL of the pre-pooled DNA is sufficient as template for subsequent secondary DOP-PCR, but it is possible to increase the amount up to 3 µL for a standard DOP-PCR reamplification reaction. "Balancing" of pre-pools may be necessary after performing a trial FISH experiment to metaphase preparations, by adding DNA from underrepresented BACs to the pre-pool in order to ensure that each member of the pool shows equal hybridization signal intensity.
5. In the case of simultaneous labeling of several probes (chromosome specific painting probes or BACs) with the same hapten or fluorochrome, prepare a pre-pool containing several DNA probes as described in **Note 4** and use 1–2 µL of template DNA for the DOP-PCR labeling.
6. When generating complex probe sets, e.g., BAC or cosmid pools containing DNA from several clones, we suggest the following procedure: in order to simultaneously label multiple DNAs in a single label reaction, prepare a pre-pool containing DNA from each BAC clone (in our hands pre-pools containing DNA from up to 20 BACs or 10 cosmids, respectively, worked well). Ensure that the pre-pool contains equal amounts of each BAC DNA and that 1 µL of a pre-pool contains >10 ng of each BAC DNA. Amplify the pre-pool by MDA and label the amplification product by nick-translation (*see* **Section 3.1.2**). Balancing of pre-pools may be necessary after performing a trial FISH experiment to metaphase preparations, by adding DNA from underrepresented BACs to the pre-pool to ensure that each member of the pool shows equal hybridization signal intensity.
7. When genomic DNA probes (i.e. chromosome paints, BAC clones) are hybridized together with repetitive DNA probes, Cot-1 DNA can reduce the intensity of the hybridization signal of highly repetitive sequences. This can be compensated by using higher amounts of repetitive probes.
8. Probes containing segments with partial homology to other chromosomes may require higher concentrations of formamide (e.g., 70%) in the hybridization mix

in order to reduce unspecific hybridization. As an example, cross hybridization to other chromosomes of centromeric probes that essentially bind to one chromosome can be prevented by hybridization in 70% formamide.

9. Cells may be grown on microscopic slides or on thin coverslips of variable size. Thin coverslips provide better image quality for confocal microscopy; they are a bit more delicate to handle but endure all pretreatment steps including freezing and thawing in liquid nitrogen. Seeding cells on small coverslips (e.g., 15×15 mm) has the advantage that they can be directly placed on a microscopic slide for the hybridization setup.
10. To avoid any drying up of cells during the procedure, we recommend that all steps such as washings, changing incubation media, etc. are performed by quickly transferring the slides from one Coplin jar (or six-well plastic dish for small coverslips) to the next.
11. Incubation in 0.1 N HCl may be extended up to 10 min for slides or coverslips with densely grown cells and/or nuclei embedded in a voluminous cytoplasm. The appropriate time has to be adjusted to these requirements, but we recommend only varying the incubation time and not the concentration.
12. Cells may also be attached to conventional microscope slides. In this case, place ~200 µL of poly-lysine on the slide to cover an area 20×20 mm and mark this field. Coverslips of variable size can be used. Thin coverslips provide better image quality after confocal microscopy.
13. In case cells are grown on a small coverslip (e.g., 15×15 mm or 18×18 mm), one can place the drop of hybridization mix directly on a microscopic slide and then cover this drop with the coverslip with the cells facing the drop. It is also possible to cut the coverslip with the cells (without drying them up!) to the appropriate size prior to hybridization.
14. In case you have only directly fluorochrome-labeled probes, immediately proceed to DNA counterstaining (**step 12**) after the washing steps.
15. There are more DNA counterstains available, such as SYTO16, YOYO, Hoechst dye, and others, which may be used, but we do not have extended experience with these for 3D-FISH experiments.
16. If the slides have been stored at 4°C, make sure that they are dry before immersing in xylene in order to prevent condensed water from contaminating the xylene solution. If needed, incubate the slides for 30 min in a dry oven (37°C) after removal from storage.
17. For long storage, slides can be kept after this step in 70% ethanol at +4°C.
18. Slides can be stored in this solution for up to 2–4 months at 4°C.
19. If fluorophore-labeled probes are used, protect the slides from light throughout the remainder of the protocol in order to avoid probe bleaching.
20. Incubation time can be extended to 12–20 h with no noticeable increase in background.
21. These steps should be performed quickly in order to prevent sections from drying. If fluorophore-labeled probes are used, protect the slide from light throughout the remainder of the protocol in order to avoid bleaching of the probe.

22. Alternatively, nuclei can be counterstained with 1 µ*M* TO-PRO-3 for 5 min (far red fluorescence) or with 25 µg/mL propidium iodide (PI) for 15 min (red fluorescence), both in 4× SSC/0.2%Tween. Note that PI also stains RNA.
23. This is the single most critical step of the protocol. The optimal number and duration of heating pulses should be determined empirically for each tissue and probe set. The parameters given here are those that we have used for the hybridization of BAC probes to 20-µm cryosections of mid-gestation mouse embryos fixed for 16–20 h using 4% PFA.
24. The temperature of the citrate solution varies between ~70°C (cooling period) and ~90°C (microwave heating). In order to preserve nuclear morphology, care should be taken not to let the solution boil.
25. We have found that adding saponin and Triton X-100 at a final concentration of 0.1% to all solutions used during the detection of hapten-labeled probes can lead to better penetration of reagents in thick sections, as well as decreasing background.
26. The sections become fragile after the FISH procedure. Avoid applying strong pressure on the coverslip.

Acknowledgments These protocols were developed as part of our ongoing studies supported by grants from the Deutsche Forschungsgemeinschaft (Cr 59/20-1-3, Cr 59-26-1/2 and Mu 1850/2-1), the Bundesministerium für Bildung und Forschung NGFN II-EP (0313377A), the Wilhelm-Sanderstiftung (2001.079.2), and the EU 3D-Genome Project (ESF FP6-503441).

References

1. Cremer, T., Cremer, M., Dietzel, S., Muller, S., Solovei, I., and Fakan, S. (2006) Chromosome territories-a functional nuclear landscape. *Curr. Opin. Cell Biol*. **18**, 307–316.
2. Foster, H. A. and Bridger, J. M. (2005) The genome and the nucleus: a marriage made by evolution. Genome organisation and nuclear architecture. *Chromosoma* **114**, 212–229.
3. Kosak, S. T. and Groudine, M. (2004) Form follows function: The genomic organization of cellular differentiation. *Genes Dev*. **18**, 1371–1384.
4. Parada, L. A., Sotiriou, S., and Misteli, T. (2004) Spatial genome organization. *Exp. Cell Res*. **296**, 64–70.
5. Walter, J., Joffe, B., Bolzer, A., Albiez, H., Benedetti, P., Müller, S., Speicher, M., Cremer, T., Cremer, M., and Solovei, I. (2006) Towards many colors in FISH on 3D-preserved interphase nuclei. *Cytogenet. Genome Res*. **114**, 367–378.
6. Giepmans, B. N., Adams, S. R., Ellisman, M. H., and Tsien, R. Y. (2006) The fluorescent toolbox for assessing protein location and function. *Science* **312**, 217–224.
7. Simonis, M., Klous, P., Splinter, E., Moshkin, Y., Willemsen, R., de Wit, E., van Steensel, B., and de Laat, W. (2006) Nuclear organization of active and inactive chromatin domains uncovered by chromosome conformation capture-on-chip (4C). *Nat. Genet*. **38**, 1348–1354.
8. Spilianakis, C. G., Lalioti, M. D., Town, T., Lee, G. R., and Flavell, R. A. (2005) Interchromosomal associations between alternatively expressed loci. *Nature* **435**, 637–645.
9. Wurtele, H. and Chartrand, P. (2006) Genome-wide scanning of HoxB1-associated loci in mouse ES cells using an open-ended chromosome conformation capture methodology. *Chromosome Res*. **14**, 477–495.

10. Conchello, J. A. and Lichtman, J. W. (2005) Optical sectioning microscopy. *Nat. Methods* **2**, 920–931.
11. Pawley, J. B. (ed.) (2006) *Handbook of biological confocal microscopy*. Springer, Berlin.
12. Telenius, H., Carter, N. P., Bebb, C. E., Nordenskjold, M., Ponder, B. A., and Tunnacliffe, A. (1992) Degenerate oligonucleotide-primed PCR: general amplification of target DNA by a single degenerate primer. *Genomics*. **13**, 718–725.
13. Dean, F. B., Nelson, J. R., Giesler, T. L., and Lasken, R. S. (2001) Rapid amplification of plasmid and phage DNA using Phi 29 DNA polymerase and multiply-primed rolling circle amplification. *Genome Res*. **11**, 1095–1099.
14. Bolzer, A., Kreth, G., Solovei, I., Koehler, D., Saracoglu, K., Fauth, C., Muller, S., Eils, R., Cremer, C., Speicher, M. R., and Cremer, T. (2005) Three-dimensional maps of all chromosomes in human male fibroblast nuclei and prometaphase rosettes. *PLoS Biol*. **3**, e157.
15. Fauth, C. and Speicher, M. R. (2001) Classifying by colors: FISH-based genome analysis. *Cytogenet. Cell Genet*. **93**, 1–10.
16. Henegariu, O., Bray-Ward, P., and Ward, D. C. (2000) Custom fluorescent-nucleotide synthesis as an alternative method for nucleic acid labeling. *Nat. Biotechnol*. **18**, 345–348.
17. Solovei, I., Cavallo, A., Schermelleh, L., Jaunin, F., Scasselati, C., Cmarko, D., Cremer, C., Fakan, S., and Cremer, T. (2002b) Spatial preservation of nuclear chromatin architecture during three-dimensional fluorescence in situ hybridization (3D-FISH). *Exp. Cell Res*. **276**, 10–23.
18. Solovei, I., Walter, J., Cremer, M., Habermann, F., Schermelleh, L., and Cremer, T. (2002a). In: *FISH: a practical approach* (Squire, J., Beatty, B., and Mai, S., eds.), pp. 119–157, Oxford University Press, Oxford.
19. Brown, K. (2002) Visualizing nuclear proteins together with transcribed and inactive genes in structurally preserved cells. *Methods* **26**, 10–18.
20. Grimaud, C., Bantignies, F., and Cavalli, G. (2005) *Epigenome network of excellence: protocols* (http://www.epigenome-noe.net/researchtools/protocol.php?protid=23).
21. Lavrov, S., Déjardin, J., and Cavalli, G. (2004) Combined immunostaining and FISH analysis of polytene chromosomes. *Methods Mol. Biol*. **247**, 289–303.

Chapter 16
Fluorescent Transgenes to Study Interphase Chromosomes in Living Plants

Antonius J.M. Matzke, Bruno Huettel, Johannes van der Winden, and Marjori Matzke

Keywords Live cell imaging; Interphase chromosomes; Fluorescent proteins; *lac* operator/repressor; *tet* operator/repressor; *Agrobacterium tumefaciens*; Binary vectors; *Arabidopsis thaliana*

Abstract Fluorescence tagging of genomic sites through the use of bacterial operator/repressor systems combined with fluorescent proteins permits high-resolution analysis of interphase chromosomes in living cells. This technique has been used to study interphase chromosome arrangement and dynamics in yeast, Drosophila, and mammalian cells, but is only beginning to be exploited in plant systems. In this chapter, we describe methods for producing and identifying *Arabidopsis thaliana* plants harbouring fluorescence-tagged transgenes. The use of these plants to analyze various aspects of interphase chromosome organization and dynamics in living cells using 3D wide-field fluorescence microscopy is discussed. Potential problems encountered when utilizing this technology in plants are considered.

1 Introduction

It is widely acknowledged that the three-dimensional arrangement of interphase chromosomes influences eukaryotic genome function and expression ***(1)***. However, the rules that govern interphase chromosome arrangement in distinct cell types, and the degree to which these rules vary among different organisms, remain largely unknown. A related issue concerns interphase chromatin dynamics ***(2)***; in particular, whether interphase chromosomes or individual chromosome sites move over short or long distances in the nucleus and if so, whether movement occurs in a random or directed manner. Although fluorescence in situ hybridization (FISH) has provided important insights into interphase chromosome arrangement, the technique is limited because of requirements for fixation and hybridization procedures, which can distort nuclear size and chromosome structure, and for visualization of static, non-living material. FISH is not suitable for analyzing interphase chromosome dynamics in real time.

R. Hancock (ed.) *The Nucleus: Volume 1: Nuclei and Subnuclear Components*,

An alternate method to FISH involves live cell imaging of unfixed interphase chromosomes that are marked at specific sites by genome-encoded fluorescence tags. This approach exploits bacterial operator/repressor systems combined with fluorescent proteins. The desired operator repeats are integrated into the host genome as a transgene array, which then specifically binds the respective nuclear-localized repressor protein that is translationally fused to a fluorescent protein such as green fluorescent protein (GFP). The tagged loci appear as bright fluorescent dots when viewed with appropriate filters under the fluorescence microscope (Fig. 16.1). Using a fluorescence microscope equipped with a motorized *z* axis and image-processing software, it is possible to make optical sections through nuclei and reconstruct them in three dimensions to determine spatial relationships among fluorescence-tagged loci that are present at known sites in the genome. This technique has been employed in yeast, *Drosophila*, and mammalian cells to analyze interphase chromosome organization and dynamics ***(2, 3)*** and is being used increasingly in plants to study various aspects of interphase chromosomes in living cells in real time ***(4–6)***.

We have recently adapted both the *tet* and *lac* operator/repressor systems for use in *Arabidopsis thaliana*. We have tagged 16 distinct sites distributed throughout the *Arabidopsis* genome with arrays of either *tet* or *lac* operator repeats (Fig. 16.2). We have fused the respective Tet and Lac repressor proteins to enhanced yellow fluorescent protein (YFP), enhanced GFP, or dsRed. The repressor protein–fluorescent protein (RP-FP) fusion proteins are under the control of the nominally constitutive 35S promoter of cauliflower mosaic virus, so that no inducing treatments, which

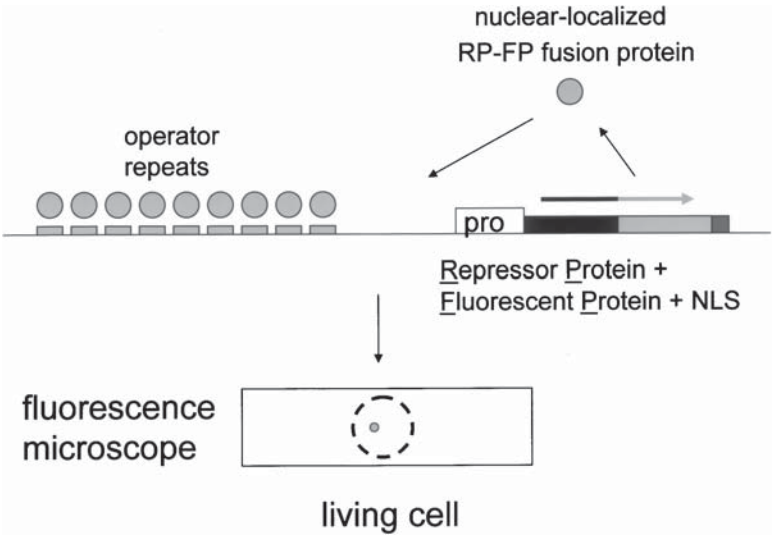

Fig. 16.1 The principle of fluorescent tagging using bacterial operator/repressor systems. A translational fusion between a repressor protein and a fluorescent protein is modified by a nuclear localization signal (*NLS*). The resulting RP-FP fusion protein can bind to arrays of the respective operator repeats integrated into the plant genome. The tagged locus in living cells is visualized under the fluorescence microscope as a bright fluorescent dot. *Pro*, promoter

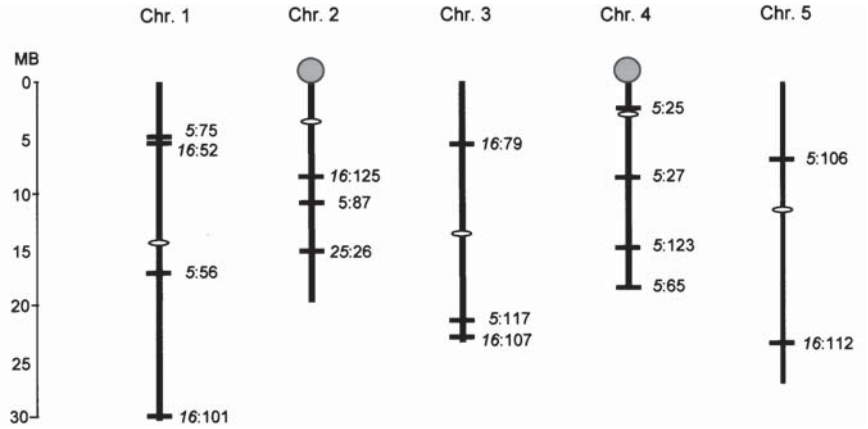

Fig. 16.2 Chromosomal sites of fluorescence-tagged transgenes in *Arabidopsis thaliana*. Using the BV4 plant transformation vectors containing the constructs shown in Fig. 16.3, 16 transgenic *Arabidopsis* lines have been produced to date. With the exception of the short arm of chromosome (*Chr*) 2, all chromosome arms are tagged at least once and, with the exception of chromosome 4, all chromosomes have at least one enhanced YFP (construct 5) and one dsRed (construct 16) insert. Only one enhanced GFP insert (construct 25) has been identified so far. The precise insertion sites are known so that the transgenes can be detected by PCR analysis *(7)*. *White ovals*, centromeres; *gray spheres*, nucleolar organizing regions

might disrupt nuclear organization, are required for expression. These lines have been used to study various quantitative features of interphase chromosomes in root nuclei of living plants *(7)*.

In this chapter, we describe plant transformation vectors that encode different RP-FP fusion proteins and contain *tet* or *lac* operator repeat arrays, and present methods for transforming *Arabidopsis* with these vectors. Ways to screen transgenic plants by visualizing fluorescence-tagged inserts in ovules of unfixed carpel tissue and in roots of living seedlings are presented. We discuss the quantitative analysis of interphase chromatin three-dimensional (3D) arrangement and dynamics using live cell imaging, and highlight potential problems of using this technology in plant systems.

2 Materials

2.1 Floral Dip Transformation of A. thaliana var. Columbia

2.1.1 Growth of Plants

1. *Arabidopsis* seed-sowing medium: put 0.1 g of Phytoblend Tissue Culture Grade Agar (Caisson Labs., North Logan, UT, USA; cat. PTC001) in a 500 mL Erlenmyer flask, add 100 mL of ddH_2O, and heat in a microwave oven until a

homogeneous suspension is obtained (bring to a boil several times and swirl the flask regularly).
2. Plastic 50-mL tubes with screw-on caps.
3. Square plastic bedding plant containers (EJP1201, 3 1/2×5 1/4×2 5/16 inches, ≈9×13×6 cm; McConkey, Sumner, WA, USA).
4. Araflats (ASN04), aratrays (ASN05), and arabaskets (ASN06) for growing *Arabidopsis* on soil (Betatech, Gent, Belgium).
5. Soil: mix commercial soil for young plants and Vermiculite in a 2:1 ratio in bedding plant containers. Spray with a 1% (v/v) solution of Agritox (Kwizda; Hasitschka, Deutsch Wagram, Austria) until soaked to prevent black fly infestation. Fill the bottom of the tray with H_2O, let sit overnight and next day pour off excess H_2O.

2.1.2 Introduction of the BV4 Vector into *A. tumefaciens*

1. L-broth: dissolve 5 g of Tryptone (BACTO 211705), 2.5 g of Bacto Yeast Extract (BACTO 212750), and 5 g of NaCl in H_2O and make to 500 mL, pH 7.0. For L-agar plates add 7.5 g of Select Agar (Gibco BRL; Invitrogen, Lofer, Austria, USA; cat. 30391-023), autoclave for 20 min, cool to ~55°C in a water bath, and pour plates in a sterile hood.
2. *Agrobacterium tumefaciens* strain ASE containing a disarmed tumor-inducing (Ti) plasmid in which the transferred DNA (T-DNA) region is replaced by a neomycin phosphotransferase gene; this allows selection of bacteria on kanamycin-containing medium ***(8)***. The *A. tumefaciens* genome encodes rifampicin resistance. This strain can be obtained from Detlef Weigel, Max Planck Institute for Developmental Biology, Tübingen, Germany (weigel@weigelworld.org).
3. *E. coli* strain mm294 containing plasmid pRK2013, which encodes resistance to kanamycin and has mobilizing functions for wide host-range plasmids ***(9)***, available from the German Resource for Biological Material DSMZ, Braunschweig, Germany or from A. J. M. Matzke (antonius.matzke@gmi.oeaw.ac.at).
4. Glass tubes: 15 mL with metal caps, sterilize in a 150°C baking oven overnight.
5. MAX Efficiency Stbl2 Compentent Cells for cloning unstable inserts such as direct repeats (Invitrogen; cat. 10268-019).
6. Plastic Petri dishes: 94 mm diameter, 15 mm deep (round) and 120×120×17-mm square (cat. 632190 and Nr. 688102, respectively; Greiner Bio-one, Kremsmünster, Austria).
7. Nutrient broth agar: for 500 mL, 4 g of Nutrient broth powder (BACTO 234000), 7.5 g of Select agar (Gibco BRL; cat. 30391-023), no pH adjustment necessary. Add 15 mg/L of rifampicin, 30 mg/L of gentamicin, and 100 mg/L of kanamycin.
8. Antibiotic solutions: kanamycin (50 mg/mL in H_2O); gentamicin (100 mg/mL in H_2O), and rifampicin (10 mg/mL in methanol).
9. Bent glass rod ("hockey stick") for spreading bacteria.

2.1.3 Preparation of *A. tumefaciens* Containing the BV4 Vector for Plant Transformation

1. YEP liquid medium: for 2 L, 20 g of Yeast extract (BACTO 212750), 20 g of Bacto Peptone (BACTO 211677), 10 g of NaCl, no pH adjustment required.
2. Sucrose solution: 5% w/v in ddH_2O.
3. Plastic container (~11.5×8 cm, 5 cm deep).

2.1.4 Floral Dip Transformation

1. Silwet L-77 (Lehle Seeds, Road Rock, TX, USA; cat. VIS-02).

2.2 Analyses for the Presence of Operator Repeats in A. tumefaciens Used for Transformation

2.2.1 Isolation of *A. tumefaciens* DNA

1. TE: 1 mL of Tris-HCl, pH 8.0, 200 µL of 0.5 *M* EDTA, and 98.8 mL of ddH_2O.
2. *N*-lauryl sarcosine solution: dissolve 2.5 g of *N*-lauryl sarcosine in 50 mL of TE.
3. Pronase solution: 2.5 mg pronase (nuclease-free; Calbiochem, Darmstadt, Germany) in 1 mL of TE.
4. Equilibrated phenol: distill phenol, p.A. grade, in standard organic chemistry apparatus, with air cooling only, in a chemical fume hood (boiling temperature is 182°C). *Avoid skin contact!* Equilibrate with 3% w/v NaCl solution and add 100 mg of 8-hydroxyquinone (Sigma) for 100 mL. Store at 4°C in a dark bottle.
5. Chloroform:isoamyl alcohol: 24:1 mixture, both p.A. grade.
6. NaCl solution, 5% w/v.
7. Ethanol, p.A. grade, 100% and 70% v/v.
8. Sterile double-distilled water (ddH_2O).

2.2.2 Digestion with Restriction Enzymes, Gel Electrophoresis, and Southern Blotting

1. Restriction enzymes: *Sal*I (New England Biolabs, Bad Homburg, Germany). *Hin*dIII (Roche, Vienna, Austria) each with 10× reaction buffer.
2. RNase A solution: RNase A (Sigma; cat. R-5500) 10 mg/mL in H_2O, heat to 95°C for 10 min, store at −20°C.
3. Agarose Type V (Sigma; cat. A-3768).

4. TBE: prepare a 10× solution with 108 g of Tris-HCl, 55 g of boric acid, and 9.3 g of Na_2EDTA to 1 L in deionized H_2O.
5. DNA size markers: *Hin*dIII digest of phage λ DNA.
6. Ethidium bromide gel stain: 10 mg/mL stock solution, dilute 20 µL in 100 mL of H_2O.
7. Sample loading buffer: 7 mL of 20% SDS, 6 mL of glycerol, 40 mg of bromphenol blue, 0.7 mL of 1 *M* Tris-HCl, and 6.3 mL of sterile ddH_2O, pH 7.9.
8. Gel denaturing solution: 20 g of NaOH and 87.7 g of NaCl in 1 L deionized H_2O.
9. Gel neutralization solution: 175.3 g of NaCl and 245 g of Tris-base in 1.8 L of deionized H_2O, adjust pH to 7.5 with concentrated HCl (~100 mL), make to 2 L.
10. Whatman filter paper, types 1 and 3 MM.
11. Nitrocellulose transfer membrane: 300 mm × 3 m, 0.45-µm pore size (Whatman Protran BA85 or Schleicher & Schuell; Whatman, Dassel, Germany).
12. 20× SSC solution: 175.32 g of NaCl, 88.23 g of sodium citrate in 1 L of H_2O.
13. Oligonucleotides to prepare probes corresponding to either the *lac* or the *tet* operator (op) sequence as appropriate:

    tet op top: 5′- gat ctt tta cca ctc cct atc agt gat aga gaa aag tga aag-3′
    tet op bottom: 5′- gat cct ttc act ttt ctc tat cac tga tag gga gtg gta aaa-3′
    lac op top: 5′- gat ccc aca aat tgt tat ccg ctc aca att cca cat gtg gc -3′
    lac op bottom: 5′- gat cgc cac atg tgg aat tgt gag cgg ata aca att tgt gg –3′

14. T4 DNA ligase and ligation buffer.
15. (α^{32}P)dATP and Megaprime DNA probe synthesis kit (GE Healthcare, Freiburg, Germany).
16. Plastic syringes, 1 mL.
17. Glass wool.
18. Sephadex G50 Medium: equilibrate in 10 m*M* Tris-HCl, pH 8.0, 0.1% w/v SDS.
19. Denhart's solution: solution A: 0.8 g of Ficoll (Sigma), 0.8 g of polyvinylpyrrolidone (Nr. PVP-360; Sigma), 0.8 g of bovine serum albumin (BSA), and 120 mL of 20× SSC in 400 mL; solution B: 16 mL of 1 *M* Tris-HCl, pH 7.5, 4 mL of 20% w/v SDS, 16 mL of denatured calf thymus DNA (1 mg/mL) in 400 mL. Store solutions A and B at 4°C, mix in a 1:1 ratio just before use.
20. Hybridisation membrane washing solution: mix 150 mL of 20× SSC, 10 mL of 20% SDS, 10 mL of 0.5 *M* EDTA, and deionized H_2O to 1 L.
21. X-ray film and cassettes (e.g. Kodak BioMax MS with Intensifying Screen).

2.3 Selection of Transformed Plants and Screening for Fluorescent Dots

2.3.1 Selection of Transformed Plants

1. Ethanol 70% v/v, Triton X-100 0.01% v/v.
2. Murashige Skoog (MS) medium with cefotaxim for seedlings: 2.3 g of MS salt mix (Duchefa Biochemie, Haarlem, NL), 15 g of sucrose, 50 mg of

myo-inositol (Sigma), 250 mg of methane-ethane sulfonate (MES) (Sigma), 1 mL of thiamine solution (15 mg of thiamine (Sigma) in 40 mL of ddH_2O), 4.5 g of Phytoblend, make to 500 mL with ddH_2O. Adjust pH to 5.7 with 1 N KOH, sterilize (sanitize) by heating under pressure to 120°C, and cool in a water bath to 55°C. Add 625 µL of a 20% w/v solution of cefotaxim (Calbiochem) and pour plates in a sterile hood (final cefotaxim concentration is 250 mg/L).

3. Kanamycin selection plates for transformed plants: to 500 mL of MS medium with cefotaxim, add 40 mg of kanamycin/L.

2.3.2 Screening Transformants for YFP Fluorescent Dots in Carpels

1. Glass microscope slides (2.6×7.6 cm) and cover slips (2.4×4 cm).
2. Rubber cement (FixoGum; Marabu Werke, Tamm, Germany).

2.3.3 Screening Transformants for DsRed Fluorescent Dots in Roots

1. Glass microscope slides with an indentation (2.6×7.6 cm with a cavity of 15–18 mm, 0.6–0.8 mm depth) (Assistent, Sondheim, Germany; cat. 2410) and cover slips (2.4×4 cm).
2. Forceps, electron microscope grade.
3. Absorbing paper book for absorption of excess liquid on microscope slides.

2.4 Detecting Operator Repeats in Plants by Southern Blot Hybridization

1. Plant DNA mini or maxi preparation kit (Qiagen, Hilden, Germany).

2.5 Equipment

2.5.1 General Equipment

1. Air-conditioned plant growth room with lighted shelves (62 cm between shelves and 5× 58-W fluorescent light rods, creating a light intensity of 5,000 lux at the bottom of the shelf) with cycles of 16 h light, 8 h dark, at 22–25°C.
2. Rotary shakers at 28°C and 37°C.
3. Incubators at 25°C, 28°C, 37°C, and 64°C.
4. Oven that can be heated up to 150°C overnight for baking and sterilizing glassware.

5. Sorvall high-speed centrifuge with Type GS3 rotor.
6. Eppendorf centrifuges at room temperature and in a cold room at 4°C (or Heraeus Biofuges with cooling capability).
7. Spectrophotometers: NovaSpecII (GE Healthcare, Freiburg, Germany) and NanoDrop ND-1000 (PEQLAB Biotechnologie, Erlangen, Germany).
8. Heating block for 1.5-mL tubes (Eppendorf ThermoStat plus; Eppendorf, Hamburg, Germany).
9. Vacuum oven at 80°C.
10. Gel electrophoresis apparatus with trays, combs, and power supply.
11. UV transilluminator and gel documentation camera.

2.5.2 Live Cell Imaging

1. Lab-Tek chambered #1 borosilicate cover glass with cover system (sterile vessels with coverslip bottoms, 1 chamber) (Nunc, Wiesbaden, Germany; cat. 155361).
2. Stereomicroscope for dissecting and mounting carpels and seedlings.
3. Leica MZFLIII Fluorescence Stereomicroscope with CoolView colour camera (Photonic Science, Robertsbridge, UK).
4. Leica Fluo Combi III Fluorescence Stereomicroscope MZ16FA with DFC300FX camera (Leica, Vienna, Austria).
5. Zeiss Axioplan2 with motorized Z-axis, Quantix camera (Kodak 1400 chip, 6.8×6.8-µm pixels; Photometrix, Tucson, AZ, USA).
6. Zeiss Axiovert 200 MOT, Pursuit Spot camera (chip 6.45-µm pixel).
7. Axioplan AF filters for cubes DsRed: HQ 585/30, Q 585 LP, HQ 620/60; YFP: HQ 500/20, Q 515 LP, HQ 535/30; CFP: D 436/20, 455 DCLP, D480/40.
8. Axiovert filter wheel: Excitation/Emission DsRed 580/630, YFP 492/535, CFP 436/465.
9. Image-Pro Plus software for Colour CoolView camera (Media Cybernetics, Silver Spring, MD, USA).
10. MetaMorph software (Visitron Systems, Puchheim, Germany). Make sure your package includes the "Multidimensional Acquisition Tool," a user-friendly system that can be adjusted to any wavelength, exposure time, stacks, and time lapse.
11. AutoDeblur software (Visitron Systems).

3 Methods

In this section, we describe how to use existing plant transformation vectors to produce *Arabidopsis thaliana* lines containing fluorescent transgenes. Three constructs containing either *tet* or *lac* operator repeats and genes encoding the respective repressor protein–fluorescence protein (RP-FP) fusion protein have been introduced

into the plant transformation vector BV4 ***(10)***, which also encodes resistance to kanamycin for selection of transformed plant cells (Fig. 16.3).

These vectors, which have been assembled step-wise from several modules (Fig. 16.4), can be used for *Agrobacterium tumefaciens*-mediated transformation of *A. thaliana*. The procedures are designed to enhance the probability that the operator repeats, which tend to be unstable in bacteria, will be successfully transferred into the host plant genome (*see* **Note 1**). In these vectors, the nominally constitutive 35S promoter of cauliflower mosaic virus drives expression of the gene encoding the RP-FP fusion protein. This promoter can be exchanged with other promoters (for example, tissue-specific or inducible promoters) by digesting with *Xho*I and *Nhe*I at the pBC stage of vector construction (Fig. 16.4b) and inserting an *Xho*I–*Nhe*I fragment containing the promoter of choice ***(11)***. Alternatively, the RP-FP fusion protein, under the control of the promoter of choice, can be supplied in *trans* from a second transgene construct that lacks the operator repeats. The second transgene construct, which encodes an RP-FP fusion protein and resistance to phosphinotricin for selection of transformed plants (Fig. 16.3), can be introduced into existing transgenic lines that contain operator repeat arrays at distinct chromosome sites (Fig. 16.2).

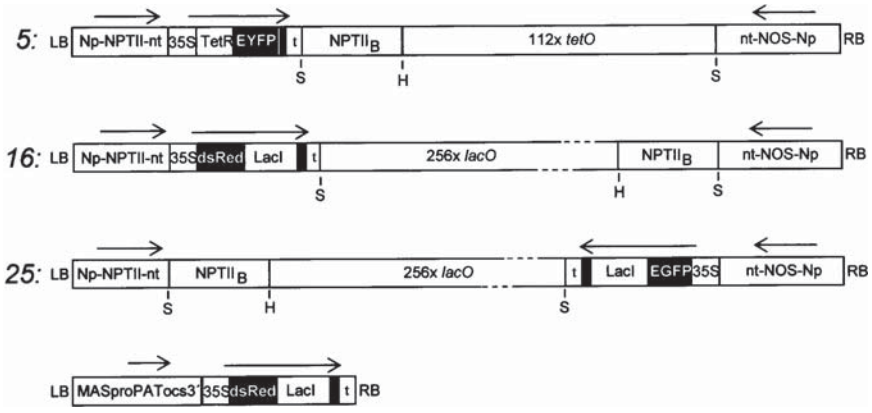

Fig. 16.3 Three constructs containing genes encoding RP-FP fusion proteins and operator repeat arrays. Construct 5: enhanced YFP and tet repressor/operator system; construct 16: dsRed and lac repressor/operator system; construct 25: enhanced GFP and lac repressor/operator system. The constructs were assembled step-wise from the three components illustrated in Fig. 16.4. In addition, an example of an operator repeat-free construct for supplying the RP-FP fusion protein in *trans* is shown (*bottom*). Abbreviations: *S*, *Sal*I; *H*, *Hin*dIII (only sites shown for understanding the DNA blots in Figs. 16.6 and 16.8); *MASpro*, mannopine synthase promoter; *PAT*, gene encoding resistance to phosphinotricin; *ocs3*, octopine synthase terminator region ***(26)***. Additional abbreviations are given in the legend of Fig. 16.4. *Arrows* indicate the direction of transcription

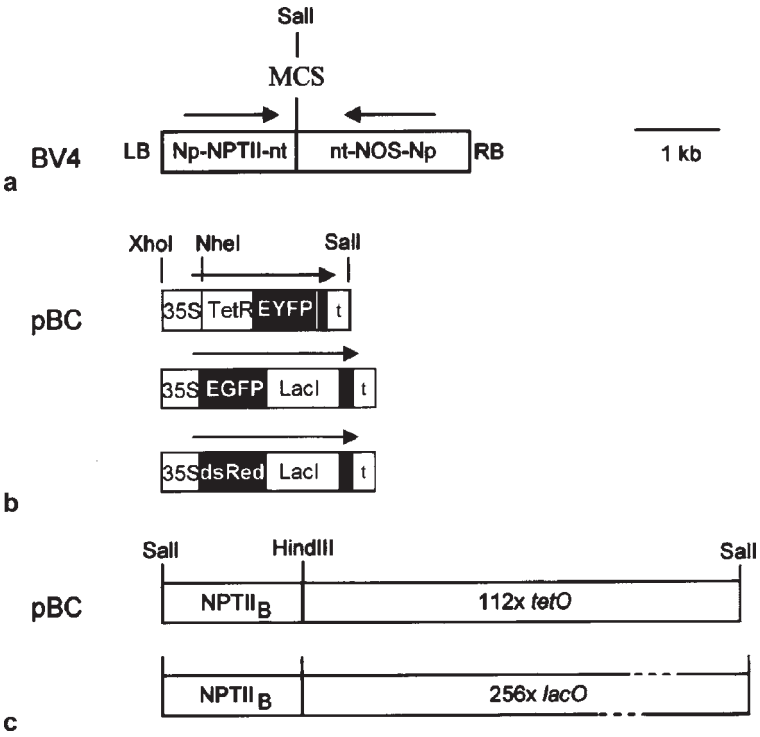

Fig. 16.4 System components. Three components are used in vector construction. At this stage, they can still be manipulated individually to obtain the desired features before assembling into the final plant transformation vectors (Fig. 16.3). **a** The binary vector BV4 can be cultivated in both *Escherichia coli* and *Agrobacterium tumefaciens*. DNA sequences positioned between the left and right transferred DNA (T-DNA) borders (*LB* and *RB*, respectively) are integrated into the plant genome during *Agrobacterium*-mediated transformation of plant cells. BV4 has an RSF1010 backbone, which contains bacterial selection markers for gentamicin and streptomycin (not shown) ***(10)***. The multiple cloning site (*MCS*) contains, from left to right, recognition sites for *Eco*RI, *Kpn*I, *Sma*I, *Bgl*II, *Xba*I, *Sal*I, and *Hind*III. A plant selection marker, neomycin phosphotransferase (*NPTII*), allows selection of transformed plant cells on kanamycin-containing medium. An intact nopaline synthase (*NOS*) gene provides a biochemical screening marker for transformed plant cells. Both genes are under the control of the nopaline synthase promoter (*Np*) and terminator (*nt*), which function in plant cells. **b** Genes encoding repressor protein–fluorescent protein (RP-FP) fusion proteins are positioned between the *Xho*I and *Sal*I sites of the multiple cloning site of pBC (Stratagene): T7 *Kpn*I, *Apa*I, *Xho*I–*Sal*I, *Cla*I, *Hin*dIII, *Eco*RV, *Eco*RI, *Pst*I, *Sma*I, *Bam*HI, *Spe*I, *Xba*I, *Not*I, *Sac*II, and *Sac*I T3. The genes encoding the RP-FP fusion proteins are under the control of the nominally constitutive 35S promoter (*35S*) and 35S terminator (*t*) of cauliflower mosaic virus ***(27)***. At this stage, the 35S promoter can be exchanged for other promoters by digesting with *Xho*I and *Nhe*I and inserting the promoter of choice on an *Xho*I/*Nhe*I fragment. **c** *tet* operators or *lac* operators in combination with a bacterial kanamycin selection marker ($NPTII_B$) are positioned between *Sal*I and *Hin*dIII sites of a multiple cloning site of pBC: T7 *Kpn*I, *Apa*I, *Xho*I, *Sa*II ($NPTII_B$) *Hin*dIII (operators) *Sal*I, *Hin*dIII, *Eco*RV, *Eco*RI, *Pst*I, *Sma*I, *Bam*HI, *Spe*I, *Xba*I, *Not*I, *Sac*II, and *Sac*I T3. The operators together with $NPTII_B$ can be released as a single fragment by digesting with *Sal*I. The $NPTII_B$ allows selection of the operator repeat cluster. The *tet* operator array is ~4.7 kb (112 copies of a 19-bp *tet*O monomer plus an additional 23-bp linker sequence); the *lac* operator array is ~9.2 kb (256 copies of a 24-bp *lac*O monomer plus a 12-bp linker sequence)

3.1 Floral Dip Transformation of A. thaliana var. Columbia

This method (adapted from **ref.** ***(12)***) has been used in our laboratory to successfully transfer BV4 vectors containing operator repeat arrays into the *A. thaliana* genome by *A. tumefaciens*-mediated transformation. To prevent loss of the operator repeats, it is advisable to introduce the vector into *A. tumefaciens* and then to proceed immediately to the plant transformation steps.

3.1.1 Growth of Plants

Begin this procedure about 8 weeks before carrying out the transformation; it ensures that *Arabidopsis* plants are growing evenly at an optimal density for achieving a high transformation efficiency.

1. Prepare 100 mL of seed-sowing medium (*see* **Section 2.1.1**), cool to room temperature, swirl to obtain a smooth thick suspension, and pour into a plastic 50-mL tube with a screw-on cap. Add 12.5 mg of *Arabidopsis* seeds, screw on the cap and shake hard up and down. The seeds should be evenly distributed throughout the thick suspension. Put the tube in the cold room for 3 days to stratify (*see* **Note 2**).
2. After stratification, spread 10 mL of seed suspension evenly with a plastic pipette onto soil in a plastic bedding plant container on Araflats. Cover the trays with plastic wrap to keep the soil moist.
3. When the seeds germinate and small green seedlings are visible, remove the plastic wrap and grow the plants under standard conditions.
4. After the plants start flowering (7–8 weeks) and about a week before the floral dip transformation procedure, the plants are cut back ("clipped") to produce more flowers within a week (*see* **Note 3**).

3.1.2 Introduction of the BV4 Vector into *A. tumefaciens* Using the Triparental Mating Procedure *(9)*

1. On day 1, start a 1.5-mL L-broth culture of *A. tumefaciens* strain ASE in a sterile 15-mL glass tube and grow at 28°C for 2 days in a rotary shaker at 200 rpm.
2. On day 2, start 1.5-mL L-broth cultures of *E. coli* strain mm294 containing pRK2013. Also start a 1.5-mL L-broth culture of the desired BV4 construct (described in **ref.** ***(11)***) in MAX Efficiency Stbl2 Competent cells. Incubate at 28°C overnight in a rotary shaker at 200 rpm (*see* **Note 4**).
3. On day 3, mix together 500 µL of each of the three bacterial cultures by pipetting up and down in a sterile 15-mL glass tube. Place 500 µL of the mixture on an L-agar plate but do not spread. Incubate the plate right-side up, without disturbance, at 25°C overnight in the dark.

4. On day 4, the bacterial droplet will have absorbed onto the L-agar. Pipette 5 mL of fresh L-broth on the plate, which will fill the plate with a thin layer of liquid, and resuspend the bacteria by mixing with a "hockey stick."
5. Transfer a drop of this suspension (adhering to the tip of the hockey stick) to a Nutrient broth agar plate supplemented with 15 mg/L of rifampicin, 30 mg/L of gentamicin, and 100 mg/L of kanamycin. Repeat three times. Spread the bacteria evenly on the surface of the medium with the hockey stick.
6. Incubate the plate upside down for 3 days at 25°C in the dark. After this time, single bacterial colonies should appear. Allow the colonies to reach ~1–2 mm in diameter and proceed immediately to the next step.

3.1.3 Preparation of *A. tumefaciens* Containing the BV4 Vector for Plant Transformation

1. On day 1, use the bacterial colonies obtained in the previous step to inoculate a 20-mL YEP culture in a 100-mL sterile Erlenmeyer flask supplemented with kanamycin, gentamicin, and rifampicin. Shake at 200 rpm in a rotary shaker at 28°C for 2 days.
2. On day 3, transfer 2.5 mL of this suspension to 250 mL fresh YEP medium (supplemented with 250 µL kanamycin solution; 125 µL gentamicin solution, and 400 µL rifampicin solution; *see* **Section 2.1.2**) in a sterile 1-L Erlenmeyer flask and shake at 200 rpm at 28°C for 24 h. Save 1 mL of the bacterial suspension in an Eppendorf tube at −20°C for later analysis of operator repeats (**Section 3.2**).
3. On day 4, centrifuge the bacteria in 500-mL bottles using a GS3 rotor in a Sorvall high-speed centrifuge at 4,000×*g* at 15°C for 1 h. Add 100 mL of 5% (w/v) sucrose solution to the bacterial pellet and resuspend completely by vortexing.
4. Add 200 mL of 5% (w/v) sucrose solution and measure the optical density at 600 nm (OD_{600}). The optimum OD_{600} for transformation is 0.9 to 1.0. To obtain this value, it might be necessary to dilute with an additional 100 mL of 5% sucrose solution (total volume should be ~400 mL).
5. To reduce the surface tension of the liquid so that the bacteria can adhere to the surface of the plant, add 200 µL of Silwet to the 400 mL of bacterial suspension and pour into a plastic container (11.5×8 cm, 5-cm deep), which should now be filled nearly to the top. Use immediately for floral dip transformation of *Arabidopsis*.

3.1.4 Floral Dip Transformation

1. Take the box containing the flowering *Arabidopsis* plants (clipped one week previously) and dip upside down into the suspension of *A. tumefaciens* containing the BV4 vector. Leave the plants in that position for ~20 sec.

2. Remove the plants, cover with plastic wrap to maintain a moist environment, and place in the dark at room temperature overnight.
3. After ~15 h remove the plastic wrap and move to the *Arabidopsis* growth room. Allow the plants to self-fertilize and set seeds (6–8 weeks); harvest seeds and proceed with selection of transformants after confirming the presence of operator repeats in the bacteria used for transformation.

3.2 Analyses for the Presence of Operator Repeats in A. tumefaciens Used for Transformation

This procedure (modified from **ref. *(13)***) uses Southern blotting to detect operator repeats in DNA of the *A. tumefaciens* used for transformation. This is the preferred method, since PCR-based detection techniques are difficult to interpret for repetitive sequences. Positive detection of the repeats in the bacterial DNA from this analysis justifies further screening of transformed plants for fluorescent dots.

3.2.1 Isolation of *A. tumefaciens* DNA

1. Thaw the 1 mL of *A. tumefaciens* suspension kept at −20°C for this analysis (**Section 3.1.3**) and centrifuge in an Eppendorf centrifuge at ~15,000×*g* for 5 min.
2. Resuspend the pellet in 300 µL of TE by vortexing and add 100 µL of 5% *N*-lauroyl-sarcosine solution and 100 µL of Pronase solution. Mix by agitating the tube and incubate at 37°C until cleared (~1–2 h).
3. Add 300 µL of equilibrated phenol and, with a Pasteur pipette pressed against the tube bottom, pipet up and down (usually around seven times) to shear the DNA and facilitate extraction until a white homogenous suspension is obtained. Shake vigorously, then centrifuge in an Eppendorf centrifuge at ~15,000×*g* for 2–5 min to separate the phases. Transfer the top layer (avoiding the interface as much as possible) to a new Eppendorf tube containing 200 µL of chloroform: isoamyl alcohol (24:1), shake vigorously, and centrifuge for 2–5 min. Transfer the top layer (avoid the interface as much as possible) to a new tube with 100 µL of chloroform:isoamyl alcohol (24:1). Shake and centrifuge at ~15,000×*g* for 2–5 min. Transfer 190 µL of supernatant to a tube containing 10 µL of 5 *M* sodium chloride, mix, add 400 µL ethanol stored at −20°C and mix until the DNA precipitates. Leave for complete precipitation at least 1 h at −20°C or 10 min at −80°C.
4. Pellet DNA at ~15,000×*g* in a refrigerated Eppendorf centrifuge for 5–10 min. Wash the DNA pellet by pipetting on 150 µL of 70% ethanol and quickly removing it, and dry the pellet in a desiccator under vacuum for 5 min. Dissolve the DNA in 100 µL of sterile ddH_2O, mix by agitating the tube, and store at −20°C.

3.2.2 Digestion with Restriction Enzymes, Gel Electrophoresis, and Southern Blotting

1. To 20 µL of the above DNA solution, add 2.5 µL of 10× reaction buffer, 1 µL of RNase A solution, 1 µL of *Sal*I, and 1 µL of *Hin*dIII to release the operator repeat array (Fig. 16.3): incubate at 37°C overnight.
2. Prepare a 1.5% (w/v) agarose gel in 1× TBE and submerge it in 1× TBE.
3. Load the samples, and electrophorese at 50 mA (~75 mV).
4. Transfer the gel to denaturing solution on a shaking platform for 1 h, then to neutralization solution and agitate for 2 h. Cut Whatman 3 MM filter paper and nitrocellulose membrane to the size of the gels, prewet in H_2O, and transfer to the neutralization solution containing the gel. Prepare stacks of Kimwipe tissues (76×144 mm, 1 package for each gel). Put the nitrocellulose on top of the Whatmann 3 MM and float the gel on top of the nitrocellulose, then lift the assembly and position on a stack of Kimwipes. Wrap crosswise with several layers of plastic wrap and let capillary blotting take place overnight.
5. Cut the membrane out of the plastic wrap with a sharp razor blade, separate gel and paper from the membrane and wash the membrane in 6× SSC (remove gel particles by rubbing firmly with gloved fingers), air dry on paper towels, label with a pencil, and bake for 2 h in a vacuum oven at 80°C. Keep at room temperature until hybridization.
6. Prepare a probe consisting of oligonucleotides of either the *lac* operator or the *tet* operator sequence as appropriate: dissolve the oligonucleotides (*see* **Section 2.2.2**) in ddH_2O, mix 1:1, heat to 95°C for 5 min, cool to room temperature, add 10× ligation buffer to obtain 1× final concentration, 0.5 µL (2.5 U) of T4 DNA ligase, and incubate overnight at 15°C. Denature the ligation products at 95°C for 10 min, transfer to ice, and let stand 5 min.
7. Set up Megaprime DNA-labelling reactions for ^{32}P-labelled probes: mix 9.5 µL of sterile ddH_2O, 1 µL of denatured DNA probe, 6 µL of dNTP mix (dG, dC, dT), 2.5 µL of buffer, 2.5 µL of primer, 2.5 µL of ($\alpha^{32}P$)ATP, and 1 µL of Klenow enzyme (total volume 25 µL). Incubate at room temperature for 1–15 h and add 75 µL sterile ddH_2O.
8. Prepare a spin column to remove unincorporated ($\alpha^{32}P$)ATP (modified from **ref. *(14)***, p. 566). Stuff a small piece of glass wool in the bottom of a 1-mL plastic syringe, mount it in a glass centrifuge tube, and fill the syringe with Sephadex G-50 and spin at 1,000×*g* for 5 min; add more Sephadex until the syringe is stably filled to the 0.9-mL mark after centrifugation. Add 100 µL of Sephadex equilibration buffer, spin, repeat once, and transfer the column to a new glass tube with a lid-less Eppendorf tube at the bottom. Load 100 µL of a labelling reaction, centrifuge for 5 min, and transfer the eluate, which contains the radioactively labeled probe, to a new Eppendorf tube.
9. Heat the eluate from the spin column in a heating block at 95°C for 5 min to denature, transfer to ice, and pipette the denatured ^{32}P-labelled probe into 50 mL Denhardt's solution in a plastic container with a lid. Prewet the nitrocellulose filters in H_2O, submerge in this solution, and hybridize at 64°C overnight.

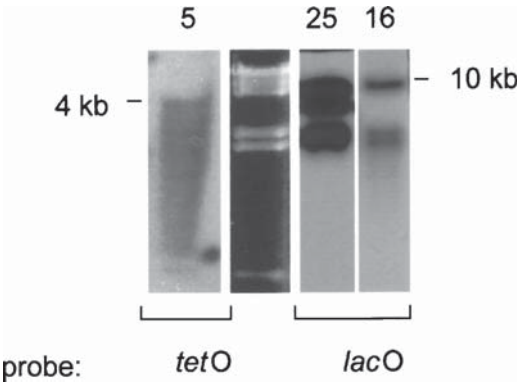

Fig. 16.5 Southern blot analysis of operator repeat arrays in *Agrobacterium tumefaciens* cells used for plant transformation. One successful example for each transformation construct (***5, 25*** and ***16***; Fig. 16.3) is shown. Size markers correspond to a *Hin*dIII digest of phage λ DNA (ethidium bromide-stained gel in lane 2)

10. Wash the membrane 3× 20 min in hybridisation washing solution, air dry, expose to X-ray film for a few hours and develop.
11. The operator repeats usually appear as a smear or as several bands deviating from the expected sizes of ~4.7 kb for the *tet* operator block and ~9.2 kb for the *lac* operator block (Fig. 16.5).

3.3 Selection of Transformed Plants and Screening for Fluorescent Dots

In this procedure, seeds harvested from self-fertilized *Arabidopsis* plants transformed by the floral dip method are sterilized and plated onto solid Murashige and Skoog (MS) medium that contains kanamycin to select for transformed plants (T0 generation), and cefotaxim to kill remaining *A. tumefaciens*. Obtaining kanamycin-resistant T0 plants does not guarantee that these will also be suitable for observing fluorescent transgenes. Expression of the RP-FP fusion protein alone is not adequate unless a sufficient number of operator repeats have integrated into the host genome to provide binding sites for the RP-FP fusion protein. We have found that many (up to 150) kanamycin-resistant plants must be screened to find ones in which the fusion protein is expressed at an appropriate, intermediate level, and fluorescent dots are visible against a background of low or no nucleoplasmic fluorescence (Fig. 16.6b,c).

It is not advisable to screen T0 seedlings that have been selected on kanamycin-containing MS medium, since they often have residual bacteria. In addition, they are sometimes weakened by the antibiotic, making them more prone to damage

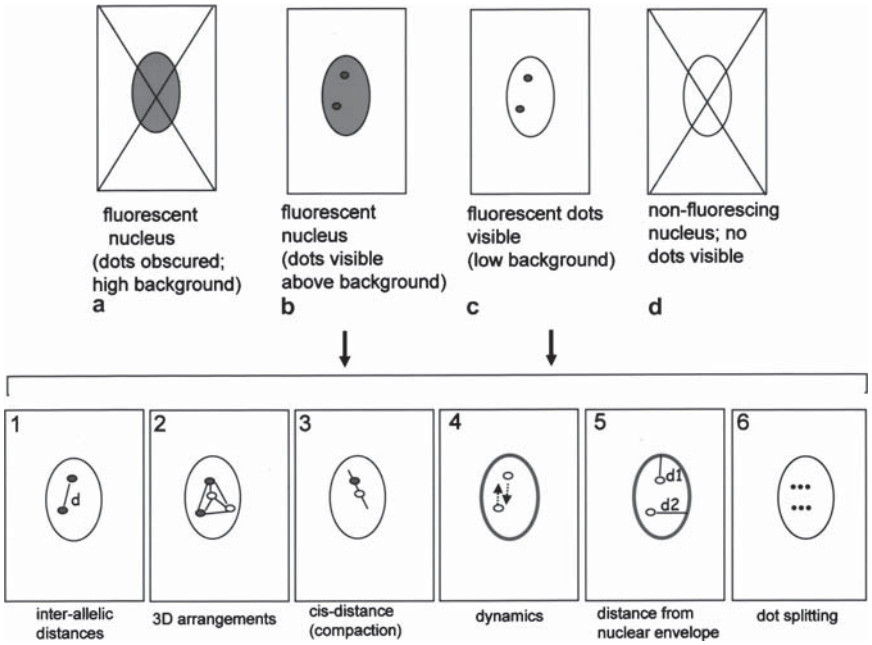

Fig. 16.6 **a** and **d** depict nuclei that are unsuitable for analyzing fluorescent dots. Only nuclei appearing as in (**b**) and (**c**) are suitable for further analysis. *1–6*, examples of high-resolution, quantitative measurements that are possible with this technology. *d*, distance

during microscopic observation and less likely to survive when replaced on the medium. Therefore, we screen either adult T0 plants or T1 seedlings (obtained by self-fertilization of T0 plants) grown on nonselective MS medium. We have found it convenient to screen ovules present in carpels (the female floral organ) of adult T0 plants for expression of the genes encoding enhanced YFP- and enhanced GFP-based fusion proteins and for the presence of operator repeats (yielding fluorescent dots). Ovules can be less suitable for observing dsRed-based RP-FP fusion proteins because of high autofluorescence, and for these fusion proteins, the roots of T1 seedlings provide a good screening material with low background.

T0 plants that are hemizygous for one tagged transgene locus will have one fluorescent dot per nucleus; two (or more) fluorescent dots in nuclei of T0 plants indicates two (or more) unlinked transgene loci. Note that transgenic plants cannot be homozygous for a transgene insert until the T1 generation.

3.3.1 Selection of Transformed Plants

1. Place ~300 µL *Arabidopsis* seeds from self-fertilized "dipped" plants in an Eppendorf tube, add 1 mL of 70% ethanol–0.01% Triton X-100, and agitate for 20 min on a shaking platform.

2. Centrifuge for 1 min in an Eppendorf centrifuge at ~15,000×*g*, remove the supernatant, and add 1 mL of absolute ethanol. Using a sterile 1-mL micropipet with the tip cut off, pipet the seeds onto sterile filter paper in a sterile hood.
3. After the ethanol has evaporated, sprinkle seeds by hand from the filter paper onto selection plates containing MS medium supplemented with kanamycin. Wrap the plates tightly with Parafilm and stratify for 3 days at 4°C (*see* **Note 2**) before transferring to the light incubator.
4. After 1–2 weeks, transformed T0 plants are easily identified as dark green seedlings against a background of pale and dying untransformed seedlings. Remove transformed seedlings from the plates and transfer to a new plate of MS medium (without kanamycin but still containing cefotaxim to kill remaining bacteria).

3.3.2 Screening Carpels for Expression of YFP and GFP Fluorescent Dots

Carpels, which are the female floral organ housing ovules, can be used to screen for the expression of the genes encoding enhanced YFP- and enhanced GFP-based fusion proteins and the presence of operator repeats (yielding fluorescent dots) in adult T0 plants.

1. Under a stereo microscope, dissect carpels from flower buds into a drop of water on a slide. Cover with a cover slip, place between two sheets of a booklet of absorbing paper for microscope slides, and squash by pressing hard with the thumb. Fix a cover slip in place with rubber cement.
2. Observe using the YFP filter set at ×630 magnification (*see* **Note 5**). In transformants that harbor one fluorescence-tagged transgene (in the hemizygous state), nuclei in ovule cells will show one bright dot (Fig. 16.7).
3. YFP- or GFP-positive plants are allowed to self-fertilize and the T1 progeny are screened for resistance to kanamycin. Lines that segregate 3:1 for kanamycin resistance, indicating a single active transgene locus, can be maintained for future work.
4. Kanamycin-resistant T1 plants that are homozygous for the transgene locus can be identified by screening for ones that show two dots/ovule nucleus (Fig. 16.7).

3.3.3 Screening for Fluorescent DsRed Dots in Roots

Roots have low background fluorescence for dsRed and hence are suitable to use for screening of fluorescent dots, which indicate both the appropriate expression of the RP-FP fusion protein and the presence of operator repeats. The mounting protocol for living seedlings is designed to allow optimal root imaging while minimizing damage and stress to the seedling. This is important for live cell imaging studies and for recovery of the seedling after microscopy so that it can be observed again at another time and/or saved for eventual seed collection and propagation.

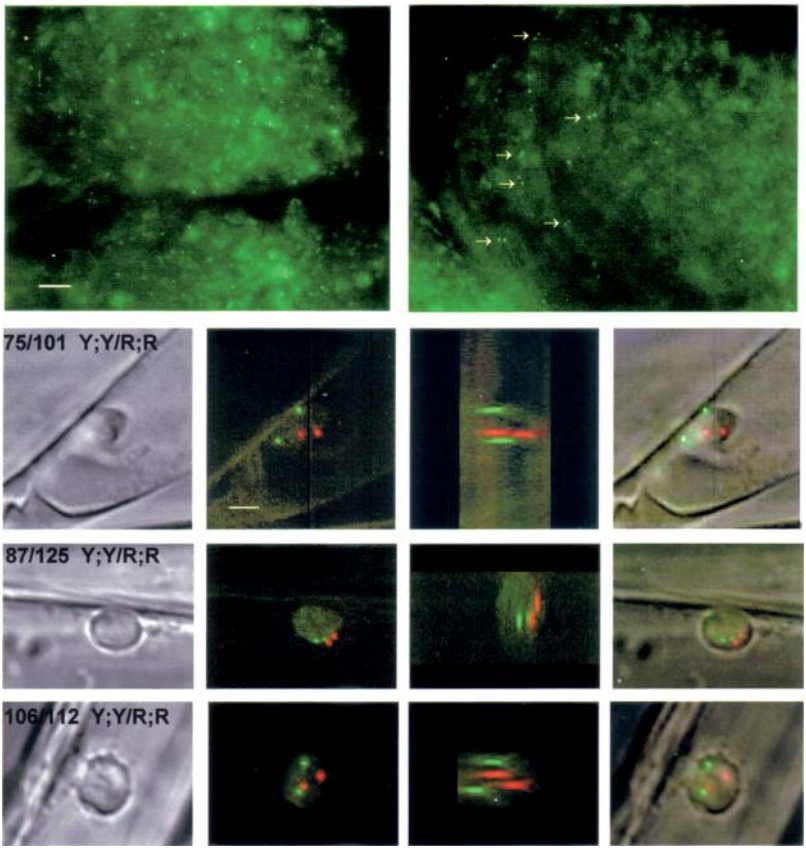

Fig. 16.7 *Top row*, examples of images of YFP fluorescent dots in nuclei of ovules in carpels (hemizygous plant, *left*; homozygous plant, *right*). *White arrows* point to nuclei with two visible dots. *Bottom three rows*, examples of images of fluorescent dots in nuclei of roots of living seedlings that are doubly homozygous for YFP (*Y*;*Y*) and dsRed (*R*;*R*) inserts. Three *Y*;*Y/R*;*R* lines are shown, 75/101; 87/125; and 106/112. From *left* to *right*, light microscope image; top view; side view (rotated 90 degrees); overlay of light image and top view. Bar, 5 µm. *See* Fig. 16.2 for chromosome insertion sites in individual lines. To view this figure in color, see COLOR PLATE 12

1. Grow T0 kanamycin-resistant transformants and allow to self-fertilize to generate T1 seeds. Sterilize and germinate the T1 seeds on nonselective MS medium and grow in the light incubator until roots are ~1.5 cm in length (~10–14 days).
2. In the sterile hood, use ethanol to clean a glass slide (2.6×7.6 cm) that has an indentation in the middle. Place a drop of tap water at the edge of the indentation.
3. Using sterile forceps (electron microscope grade), transfer a T1 seedling from the MS plate to the water droplet on the slide: loosen up the agar around the root before pulling the seedling out, otherwise the root might tear. Place the seedling

on the slide so that the leaves are free to expand into the indented area. Using the forceps, gently stretch the root horizontally along the surface of the slide.

4. Clean a 2.4×4-cm cover slip with ethanol and place it gently on the seedling; remove air bubbles by holding the cover slip at one end with your fingers and moving it up and down until they dissipate, then let go of the cover slip. This will distribute the water evenly under the cover slip and leave the leaves of the seedling in an almost water-free indentation.
5. Seal the cover slip with rubber cement and air dry for a few minutes before starting with fluorescence microscopy. Observations are made using the dsRed filter at ×630 magnification. Bear in mind that the seedling will not survive prolonged illumination and extended periods under the cover slip, which can lead to anoxia. The optimal times or observation need to be determined for each microscope setup (*see* **Note 6**).

3.4 Detecting Operator Repeats in Plants by Southern Blot Hybridization

In addition to analyzing *A. tumefaciens* for the presence of operator repeats (**Section 3.2**), it is advisable to perform a similar analysis on transgenic plants in which fluorescent dots have been detected. These results can give an indication of the approximate copy number and integrity of the operator repeat arrays, which in our experience integrate as multiple fragments that deviate from the expected size (~4.2 kb for *tet*O arrays and ~9.7 kb for *lac*O arrays) (Fig. 16.8).

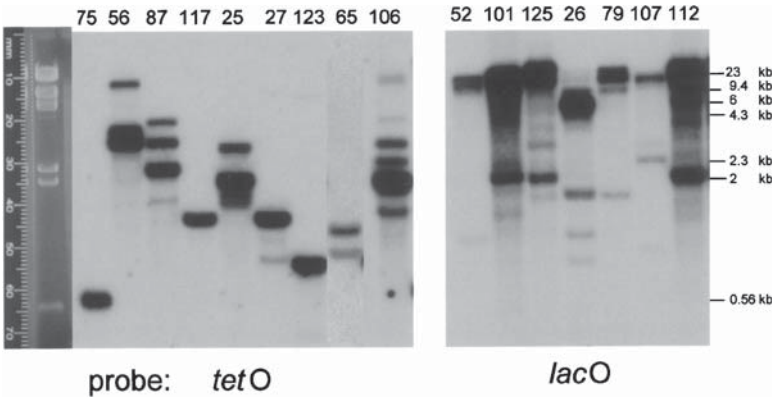

Fig. 16.8 Southern blot analysis of operator repeat arrays in transgenic *Arabidopsis thaliana* lines. Size markers correspond to a *Hin*dIII digest of phage λ DNA (ethidium bromide-stained gel on left). Numbering of lanes is as in Fig. 16.2

1. Isolate plant DNA using a Qiagen plant DNA isolation kit.
2. As described for *A. tumefaciens* DNA (**Section 3.2**), digest the DNA with *Sal*I and *Hin*dIII, electrophoresis on an agarose gel, blot onto nitrocellulose, and probe with ^{32}P-labelled oligonucleotides.

3.5 Live Cell Imaging Using 3D Wide-Field Microscopy

Since each laboratory will have their own microscope, computers and software, we do not provide a common protocol that can be used in all cases. In our laboratory, we use the equipment described in **Section 2.7**.

1. For viewing fluorescent dots in root cells, which have the lowest background fluorescence for YFP, GFP, and dsRed, we mount and observe living seedlings as described in **Section 3.3.3**. When dots are visualized in a nucleus, an image stack (optical sections) is made, collecting 41 planes in a distance of 0.2 µm around the starting position of acquisition. Exposure times vary between 100 and 1,000 msec depending on the strength of the signal (normally ~1 min/stack/color). Approximately 3–10 stacks can be made for an individual seedling on a microscope slide before potentially harming the seedling. For making multiple stacks on a single seedling over a longer time period (e.g. one stack every 15 min for 6 h) seedlings can be immobilized in a Lab-Tek sterile chamber.
2. Auto Deblur deconvolution software removes out-of-focus haze and sharpens the image. Pseudocolouring and 3D reconstruction are performed in Auto Deblur or in Metamorph, and measurements in 3D in Metamorph using the "Measure XYZ tool" under "Apps." Fig. 16.7 shows the types of images that can be obtained using this setup.

3.6 Perspectives

3.6.1 Uses of this Technology in Plants

The availability of fluorescence-tagged lines and the appropriate microscope and image processing tools permit a number of parameters of interphase chromosome behaviour to be assessed in living cells of intact seedlings. With the two-color system based on either *tet* or *lac* repressors/operators, it is possible to intercross different tagged lines and obtain ones that are doubly homozygous for enhanced YFP and dsRed-tagged transgenes. The single homozygous and doubly homozygous lines can be used for high-resolution measurements of interphase chromosomes (Fig. 16.6) *(7)*. To ensure a low fluorescence background for all three of the RP-FP fusion proteins (enhanced YFP, enhanced GFP, and dsRed), we routinely carry out 3D measurements on root nuclei of living, untreated 10–20-day old seedlings that

are grown under sterile conditions and mounted in water on microscope slides. Various aspects of interphase chromosomes can be quantitatively assessed (Fig. 16.6, 1–6):

1. Inter-allelic distances can be measured to test hypotheses invoking allelic pairing. Although it is not yet clear exactly how pairing will be assessed using this technique, it has been shown in budding yeast that two GFP dots separated by less than 300 nm cannot be resolved ***(15)***. In nuclei of *Arabidopsis* root cells, we usually observe inter-allelic distances greater than or equal to 0.5 µm. This distance, which allows easy resolution of two fluorescent dots, suggests that stable inter-allelic pairing does not occur in these cells. The inter-allelic distance appears to accommodate increases in nuclear diameter, with generally greater distances being observed in larger nuclei ***(7)***. However, a report using a transgenic line that contains two GFP-tagged loci separated by 4.2 Mb on chromosome 3 suggests that alleles of the fluorescence-tagged loci pair frequently, perhaps via the operator repeat arrays ***(16)***. Interestingly, pairing is reduced in mutants that reduce global levels of DNA methylation ***(17)***, suggesting the involvement of epigenetic modifications in interphase chromosome associations in plants. Whether enhanced pairing is typical of other tagged loci in *Arabidopsis* remains to be determined. Data on this point from other systems are mixed: whereas operator repeats have been shown to pair frequently in budding yeast ***(18)***, they do not appear to do so in *Drosophila* ***(19)***. If operator repeat arrays regularly induce unnatural allelic pairing or other chromosome associations, the value of the fluorescence-tagging technique for analyzing interphase chromosome arrangement needs to be reassessed. Using a combination of fluorescence technology and FISH to analyze many fluorescence-tagged lines will help to resolve this issue.
2. 3D arrangements can be studied in lines that are doubly homozygous for two transgene inserts of different colors (e.g. enhanced YFP and dsRed) (Fig. 16.6). We have found considerable variability in the 3D arrangement in root nuclei of individual seedlings, suggesting that the arrangement of interphase chromosomes in these nuclei is essentially random ***(7)***. This conclusion is in agreement with results from FISH analyses ***(20)*** and chromosome painting in *Arabidopsis* ***(21)***.
3. Another interesting parameter to assess is the distance between two fluorescent dots on the same chromatin chain (*cis*-distance). This arrangement can be obtained by backcrossing a plant that is homozygous for two fluorescent transgene inserts on the same chromosome to nontransgenic plants, thus producing progeny that contain two fluorescent tags on the same homolog. This value provides an indication of the degree of chromatin compaction or folding. With the tagged lines currently available in our collection (Fig. 16.2), the shortest *cis*-distance is 2.4 Mb (enhanced YFP and dsRed inserts on the bottom arm of chromosome 2). Two dots are still visible, which indicates that 2.4 Mb is still above the minimum resolvable *cis*-distance. Interestingly, the calculated fold-compaction across this distance was 380-fold ***(7)***, which is about ten times higher than observed for two fluorescent dots on the same chromatin fiber in budding yeast (40-fold; **ref.** ***(15)***). This result suggests that plant chromatin in predominantly euchromatic chromosome arms is considerably more compacted than chromatin in budding yeast.

4. A strength of the fluorescence-tagging technique is that it allows measurements of interphase chromatin dynamics in living cells. In budding yeast, *Drosophila*, and mammalian cells, interphase chromatin appears to undergo constrained diffusion within a rather confined area. The movement is thought to be due to Brownian motion since it is insensitive to metabolic poisons. One recent report, however, has shown that upon transcription factor binding, a genomic site relocates from the nuclear periphery to a more internal region, a distance of 1–5 μm at a speed ranging from 0.1–0.9 μm/min ***(22)***. One study in plants using the GFP-tagged line EL702C is generally consistent with constrained diffusion, but also indicated differences depending on the ploidy of a given nucleus: chromatin movement in endoreduplicated pavement cell nuclei had a lower diffusion coefficient but a six-fold larger confinement area than in diploid guard cells ***(23)***. We have found little change in the inter-allelic distance at a fluorescence-tagged locus in root nuclei over time, suggesting that interphase chromosome sites are generally static under normal growth conditions ***(7)***. However, it will be interesting to study additional tagged sites under various stress or inducing conditions to determine whether directed movement occurs in plant interphase nuclei.
5. The distance from the nuclear envelope can be measured if this membrane system is tagged with a fluorescence marker. Given that proximity to the envelope has been considered a factor in regulating gene expression ***(1)***, the fluorescence-tagging technology could help to study this possibility in plants.
6. In root nuclei, we have found that fluorescent dots at some locations in the genome can split frequently into multiple, smaller dots. This is probably due to separation of chromatids in polytene nuclei of many root cells. Factors influencing the frequency of splitting can be studied using this approach.

3.6.2 Special Problems in Plants

Although the fluorescence-tagging technique basically works in plants, there are problems that presently limit the usefulness of this technology in plant systems. We describe in the Methods section (**Section 3**) the rather laborious screening process that is required to identify transgenic lines suitable for microscopical observation and analysis. The key is to find lines expressing RP-FP fusion proteins at an intermediate level that allows visualization of fluorescent dots superimposed on low or no background fluorescence in the nucleoplasm. With the lines obtained with our vectors (Fig. 16.3), the situation is complicated by the presently inexplicable non-uniform activity of the nominally constitutive 35S promoter, which can lead to over- or under-expression from cell to cell within a given tissue or organ (Fig. 16.6a, d). Therefore, this might not be the optimal promoter to drive expression of RP-FP fusion protein and others should be tested in the future. We have also encountered significant problems with gene silencing, in which there is no expression of the RP-FP fusion protein at all (Fig. 16.6d). One possibility is that the operator repeats, which are present on the same transgene complex as the gene encoding the RP-FP fusion protein, can potentially trigger repeat-induced gene silencing. Particularly in

roots, we have observed silencing of the gene encoding the RP-FP fusion protein in a large proportion of cells. If the operator repeats are indeed inducing silencing, a possible solution is to supply the RP-FP fusion protein in *trans* by super-transforming the tagged lines with a second transgene complex that lacks the operator repeat array (Fig. 16.3). This strategy is currently being tested in our lab and appears to considerably increase the percentage of root nuclei expressing the RP-FP fusion protein, which can then bind to the resident operator repeats. We are also crossing the tagged lines with mutants defective in various types of epigenetic gene silencing to determine the basis of silencing.

Another potential difficulty in using fluorescent tagged transgenes in plants is that many plant tissues, particularly those that are photosynthetic, have a high background fluorescence at the excitation wavelengths of commonly used fluorescent proteins. This can be overcome using a confocal microscope with spectral imaging capabilities (emission fingerprinting) but remains a limitation when using a standard fluorescence microscope.

Studying interphase chromosome dynamics can be problematic in roots, where nuclei are highly mobile over time periods of minutes to hours (***(24)***; A. Matzke, unpublished results). Fluorescent markers for nuclear envelope fluorescence should help to control for movement of nuclei (Fig. 16.6, example 4). In addition, root nuclei show large variations in size and shape and sometimes appear almost amoeboid if observed over time (***(24)***; A. Matzke, unpublished results). Plant nuclei appear to lack nuclear lamin proteins ***(25)***, which might make them more structurally pliable than animal nuclei. Whether the lack of a classic nuclear lamina in plant nuclei influences interphase chromosome organization in a manner unique to the plant kingdom is not yet known. A thought to keep in mind is that plants might have different organizing principles for interphase chromosomes than those found in other eukaryotic organisms.

One consideration in using *Agrobacterium*-mediated transformation is that the integration of the transgene complex (the so-called T-DNA for transferred DNA) can potentially cause chromosomal rearrangements. For example, GFP-tagged line EL702C is associated with a chromosomal inversion comprising the two tagged loci on chromosome 3 ***(16)***. Such disruptions in chromosome structure can confound subsequent assessments of interphase chromosomes. To detect rearrangements, FISH analysis using BAC probes flanking the transgene insert is useful ***(15)***.

In summary, the use of fluorescence-tagged transgenes to study interphase chromosomes in living plants is at a very early stage of development. Although it is clear that meaningful results on interphase chromosome arrangement and dynamics in living cells can be obtained, there are nevertheless a number of important problems that remain to be resolved before this technology can be used routinely in plant systems. A complete picture of interphase chromosome arrangement in plants will require a combination of approaches including both FISH and fluorescence-tagging technology. Despite the current problems, the potential pay-off from using fluorescent transgenes to study interphase chromosomes in living plants in real time under a variety of inducing and stress conditions is substantial, thus justifying continued efforts to optimize this technology for plant systems.

4 Notes

1. It should be possible to use these vectors to introduce the fluorescent-tagging constructs into other plant species that are susceptible to *Agrobacterium*-mediated transformation.
2. Stratification of seeds leads to more uniform germination.
3. Clipping a week before the floral dip transformation procedure will lead to copious production of more flowers, which will be at the optimal stage for high efficiency transformation.
4. The instructions from Invitrogen suggest growth of Stbl2 cells at 30°C, but we have found that 28°C is better for stability of operator repeats.
5. We use the YFP filter for visualizing both enhanced YFP and enhanced GFP. Use of the GFP filter leads to high background fluorescence.
6. After microscopy, the seedlings can be replaced on MS plates for recovery before further observation or transfer to soil. To immobilize them for longer periods (more than 2 h) for time-lapse studies, use a sterile scalpel to cut out a piece of solid medium in which a seedling has penetrated the agar to the bottom of the dish. Transfer the agar cube into a Lab Tek sterile vessel with a cover slip bottom and mount on an inverted microscope.

Acknowledgments This work was supported by the Austrian Fonds zur Förderung der Wissenschaftlichen Forschung (grant no. P 16545-B12).

References

1. Misteli, T. (2004) Spatial positioning: a new dimension in genome function. *Cell* **119**, 153–156.
2. Gasser, S. (2002) Visualizing chromatin dynamics in interphase nuclei. *Science* **296**, 1412–1416.
3. Spector, D.L. (2003) The dynamics of chromosome organization and gene regulation. *Annu. Rev. Biochem*. **72**, 573–608.
4. Kato, N. and Lam, E. (2001) Detection of chromosomes tagged with green fluorescent protein in live *Arabidopsis* plants. *Genome Biol* **2**, research0045.
5. Esch, J.J., Chen, M., Sanders, M., Hillestad, M., Ndkium, S., Idelkope, B., Neizer, J., and Marks, M.D. (2003) A contradictory GLABRA3 allele helps define gene interactions controlling trichome development in *Arabidopsis. Development* **130**, 5885–5894.
6. Lam, E., Kato, N., and Watanabe, K. (2004) Visualizing chromosome structure/ organization. *Annu. Rev. Plant Biol*. **55**, 537–554.
7. Matzke, A.J.M., Huettel, B., van der Winden, J., and Matzke, M. (2005) Use of two color fluorescently-tagged transgenes to study interphase chromosomes in living plants. *Plant Physiol*. **139**, 1586–1596.
8. Hood, E.E., Nilsson, O., Wu, E., Wolfe, D.S., and Weigel, D. (1998) Genetic ablation of flowers in transgenic *Arabidopsis. Plant J*. **15,** 799–804.
9. Matzke, A.J.M. and Matzke, M.A. (1986) A set of novel Ti plasmid-derived vectors for the production of transgenic plants. *Plant Mol. Biol*. **7**, 357–365.
10. Matzke, A.J.M., Stöger, E.M., Schernthaner, J.P., and Matzke, M.A. (1990) Deletion analysis of a zein gene promoter in transgenic tobacco plants. *Plant Mol. Biol*. **14**, 323–332.

11. Matzke, A.J.M., van der Winden, J., and Matzke, M. (2003) Tetracycline operator/ repressor system to visualize fluorescence-tagged T-DNAs in interphase nuclei of *Arabidopsis. Plant Mol. Biol. Rep*. **21**, 9–19.
12. Clough, S.J. and Bent, A. (1998) Floral dip: A simplified method for *Agrobacterium*-mediated transformation of *Arabidopsis thaliana. Plant J*. **16**, 735–743.
13. Dhaese, P., De Greve, H., Decraemer, H., Schell, J., and Van Montagu, M. (1979) Rapid mapping of transposon insertion and deletion mutations in the large Ti plasmids of Agrobacterium tumefaciens. *Nucleic Acids Res*. **7**, 1837–1849.
14. Maniatis, T. Fritsch, E.F., and Sambrook, J. (eds.) (1982) *Molecular cloning, a laboratory manual*. Cold Spring Harbor Laboratory, NY.
15. Bystricky, K., Heun, P., Gehlen, L., Langowski, J., and Gasser, S.M. (2004) Long-range compaction and flexibility of interphase chromatin in budding yeast analyzed by high resolution imaging techniques. *Proc. Natl. Acad. Sci. USA* **101**, 16495–16500.
16. Pecinka, A., Kato, N., Meister, A., Probst, A.V., Schubert, I., and Lam, E. (2005) Tandem repetitive transgenes and fluorescent chromatin tags alter local interphase chromosome arrangement in Arabidopsis thaliana. *J. Cell Sci*. **118**, 3751–3758.
17. Watanabe, K., Pecinka, A., Meister, A., Schubert, I., and Lam, E. (2005) DNA hypomethylation reduces homologous pairing of inserted tandem repeat arrays in somatic nuclei of *Arabidopsis thaliana*. *Plant J*. **44**, 531–540.
18. Fuchs, J., Lorenz, A., and Loidl, J. (2002) Chromosome associations in budding yeast caused by integrated tandemly repeated transgenes. *J. Cell Sci*. **15**, 1213–1220.
19. Vasquez, J., Belmont, A.S., and Sedat, J.W. (2002) The dynamics of homologous chromosome pairing in male *Drosophila* meiosis. *Curr. Biol*. **12**, 1473–1483.
20. Fransz, P., de Jong, J.H., Lysak, M., Castiglione, M.R., and Schubert, I. (2002) Interphase chromosomes in *Arabidopsis* are organized as well defined chromocenters from which euchromatin loops emanate. *Proc. Natl. Acad. Sci. USA* **99**, 14584–14589.
21. Pecinka, A., Schubert, V., Meister, A., Kreth, G., Klatte, M., Lysak, M.A., Fuchs, J., and Schubert, I. (2004) Chromosome territory arrangement and homologous pairing in nuclei of *Arabidopsis thaliana* are predominantly random except of NOR-bearing chromosomes. *Chromosoma* **113**, 258–269.
22. Chuang, C.H., Carpenter, A.E., Fuchsova, B., Johnson, T., de Lanerolle, P., and Belmont, A.S. (2006) Long-range directional movement of an interphase chromosome site. *Curr. Biol*. **16**, 825–831.
23. Kato, N. and Lam, E. (2003) Chromatin of endoreduplicated pavement cells has greater range of movement than that of diploid guard cells in *Arabidopsis thaliana*. *J. Cell Sci*. **116**, 2195–2201.
24. Chytilova, E., Macas, J., Sliwinska, E., Rafelski, S.M., Lambert, G.M., and Galbraith, D.W. (2008) Nuclear dynamics in *Arabidopsis thaliana*. *Mol. Biol. Cell* **11**, 2733–2741.
25. Meier, I. (2007) Composition of the plant nuclear envelope: theme and variations. *J. Exp. Bot*. **58**, 27–34.
26. Aufsatz, W. Mette, M.F., van der Winden, J., Matzke, M., and Matzke, A.J.M. (2002) HDA6, a putative histone deacetylase needed to enhance DNA methylation induced by double stranded RNA. *EMBO J*. **21**, 6832–6841.
27. Pietrzak, M., Shillito, R.D., Hohn, T., and Potrykus, I. (1986) Expression in plants of two bacterial antibiotic resistance genes after protoplast transformation with a new plant expression vector. *Nucleic Acids Res*. **14**, 5857–5868.

Chapter 17
Analysis of Telomeres and Telomerase

Jiří Fajkus, Martina Dvořáčková, and Eva Sýkorová

Keywords Telomeres; Telomere sequence; Telomere length; Telomerase activity; BAL31 digestion; Terminal restriction fragments; Telomere repeat amplification protocol; TRAP assay; Real-time TRAP; In situ analysis

Abstract The terminal chromatin structures at the ends of eukaryotic chromosomes, the telomeres, are a focus of intensive research due to their importance for the maintenance of chromosome integrity. Their shortening due to incomplete replication functions as a molecular clock counting the number of cell divisions, and ultimately results in cell-cycle arrest and cellular senescence. Telomere shortening can be compensated by the nucleoprotein enzyme complex called telomerase, which is able to extend shortened telomeres. In humans, only embryonic and germ cells show telomerase activity that is sufficient for telomere length stability and cellular immortality. Unfortunately, telomerase is activated in cancer cells, which, thus, achieve unlimited growth and a malignant phenotype. Even if there were no any other links of telomere biology to other essential processes in the cell nucleus such as DNA repair, chromosome positioning, and nuclear architecture in mitosis and meiosis, the close connection of telomere biology to aging and cancer makes telomeres and techniques for their analysis important enough from the point of view of us, mortal and disease-prone people. In this chapter, we describe the most common types of analyses used in telomere biology: screening for typical and variant telomeric sequences, determination of telomere lengths, and measurement of telomerase activity.

1 Introduction

Well before the composition of chromosome termini, telomeres, started to be revealed, telomeres were defined functionally as structures that form and protect chromosome ends and distinguish them from unrepaired chromosome breaks ***(1, 2)***. From the structural point of view, telomeres can be regarded as specific chromatin domains composed of telomere DNA and various associated proteins. The DNA

R. Hancock (ed.) *The Nucleus: Volume 1: Nuclei and Subnuclear Components*,

component is usually composed of repeated minisatellite sequences of asymmetric G/C content between complementary strands, for example $(TTAGGG)_n$ in vertebrates including humans ***(3)*** and $(TTTAGGG)_n$ or $(TTAGGG)_n$ in plants (reviewed in **ref.** ***(4)***). In some exceptions, chromosome ends are formed by retrotransposons, as in *Drosophila* ***(5)***, or by satellite DNA repeats, as in *Chironomus* ***(6)***.

Telomeres based on minisatellite sequences form a single-stranded overhang at their very extremity, which can be elongated by the specialized reverse transcriptase, telomerase ***(7, 8)***. Telomerase is composed of at least two core components, the protein (catalytic) subunit with reverse transcriptase activity and the RNA subunit, which bears a short domain serving as the template for elongation of telomeric DNA by addition of telomeric repeat units. In this way, telomerase can compensate for incomplete replication of chromosome ends, which otherwise would lead to telomere shortening. Shortening results finally in dysfunctional telomeres, which prevent cell-cycle progression and function as a molecular clock of the cell's proliferative lifespan (Hayflick's limit). In humans, telomerase activity sufficient for stable telomere maintenance is present only in embryonic tissues, germ cells, and most cancer cells. It can therefore be used as the most universal tumor marker, as well as a target of antitumor therapy (reviewed in **ref.** ***(9)***).

It becomes more and more evident, however, that it is not the DNA alone that determines telomere properties but rather the functional nucleoprotein structure that is formed on the DNA platform. Proteins participating in telomere structure include those that specifically bind single- or double-stranded DNA, others that associate with these proteins, and also more general chromatin proteins or their specific variants. In contrast to previous expectations, most proteins originally described as DNA repair factors are also indispensable for normal telomere composition and function ***(10, 11)***.

This chapter focuses on the characteristics of telomeres that are most frequently used in diagnostic and research applications, including DNA sequence composition, length, and telomerase activity. The composition of a telomere sequence is important in cases in which alternative, telomerase-independent mechanisms for telomere lengthening (ALT) are found, for example, in rare cases of human tumors, as well as in studying new species. Measurement of telomere length is frequently used to examine telomere shortening caused by cellular aging or by mutations in telomerase or other telomere-associated factors, and can also be useful for detection of the extremely heterogeneous profiles of telomere lengths typical for cells using ALT ***(12)***. The presence of a putative telomeric sequence can be screened by slot-blot hybridization, but if a positive result is obtained, it remains necessary to demonstrate that the sequence is localized at telomeres. Classically, this can be done in two ways. In the first approach, high molecular weight DNA is digested by nuclease BAL31 to progressively degrade DNA from the ends at double-strand breaks. The DNA is then digested with one or more restriction enzymes that cannot cleave within telomeric repeats, and the fragments are separated by gel electrophoresis. After blotting, membranes are probed with either a terminal marker sequence or a telomeric sequence. If the sequence is telomeric, there should be a progressive

shortening in length of terminal restriction fragments (TRF) with increasing BAL31 digestion time. The TRF pattern at zero BAL31 digestion time then indicates the approximate telomere length. The second approach to measure telomere length and to confirm the telomeric location of a sequence at low resolution is fluorescence in situ hybridization (FISH) or primed in situ labeling (PRINS). PRINS is particularly amenable for telomeric localization, because telomeric minisatellite sequences usually contain only two or three of the four possible nucleotides in each DNA strand (e.g., 5′-TTAGGG-3′ in vertebrates). Thus, the dideoxy-PRINS variant of the technique can be used ***(13)***. Here DNA polymerase I extends one of the DNA strands and the nucleotide that is not found in the extended strand is provided in the dideoxy-form (ddNTP), which terminates the PRINS reaction if it gets incorporated. Therefore, any telomeric primer that hybridizes to nontelomeric sites will not be extended and the reaction will not label this DNA.

Measurement of telomerase activity is primarily important in the molecular diagnostics of human tumors, because telomerase is present in the vast majority of all major types of cancer ***(14)***. Further, it is a relevant marker for monitoring the action of telomerase inhibitors in basic research and in cancer therapy. Finally, telomerase activity is also recognized as an essential factor in cellular immortality, whose expression can be used in cell and tissue engineering or for rejuvenation of cells for transplantation purposes ***(15)***. Compared with other characteristics of telomere metabolism (for example, the expression of the catalytic and RNA subunits of telomerase), the activity reflects the functional status of telomerase as determined by the different regulatory steps in the pathway of expression of its components. The most widespread assay to detect and measure telomerase activity is the telomere repeat amplification protocol (TRAP) assay, first described in **ref.** ***(16)*** and modified to achieve maximum reliability and convenience (*see* **ref.** ***(17)*** for a review).

Human and mouse cells represent the most frequently used material for telomere and telomerase analysis, and the protocols described here are optimized for these cells unless otherwise stated. The chapter is divided into sections that respectively describe methods to detect variant telomere sequences, to determine their length and position, to visualize telomeres and measure their length in situ, and to measure telomerase activity.

2 Materials

2.1 Screening Genomic DNA for Variant Telomere Sequences

1. Genomic DNA: 1 µg per species or sample to be analyzed (*see* **Note 1**).
2. Control genomic DNA: 1 µg of human genomic DNA, and optionally, a set of genomic DNAs from model species representing different type of telomeric sequences (e.g., *Arabidopsis*, *Bombyx*, *Tetrahymena*).

3. Control telomere concatemers prepared by template-free PCR using oligonucleotide primers corresponding to both strands of the sequence, e.g., for human-type sequence, the primers G-$(TTAGGG)_5$ and C-$(TAACCC)_5$; for the PCR reaction, Taq DNA polymerase, PCR buffer, and dNTP mix (*see* **Section 3.1.1**).
4. 20× SSC: stock solution 175.3 g of NaCl, 88.2 g of sodium citrate in 900 mL of distilled H_2O (dH_2O), adjust pH to 7.0 with drops of 10 N NaOH, add dH_2O to 1 L, and sterilize by autoclaving; for blotting procedures you need this stock diluted to 6× SSC and 2× SSC.
5. Sodium hydroxide: 0.4 *M* NaOH.
6. End-labeling of probes: T4 polynucleotide kinase (PNK) (Takara Bio Inc., Japan), buffer for T4 PNK, gamma [^{32}P]ATP (~6,000 Ci/mmol), 10 µ*M* oligonucleotide (*see* **step 3**). For concatenated probes, *see* **Note 2**.
7. Nylon membranes, positively charged, e.g., Hybond XL (Amersham Bioscience, Little Chalfont, UK).
8. Hybridization buffer: 0.5 *M* phosphate buffer, pH 7.5, with 10 m*M* EDTA and 7% (w/v) sodium dodecyl sulphate (SDS).
9. Washing buffer I (low stringency): 2× SSC, 0.1% SDS; mix 100 mL of 20× SSC, 10 mL of 10% SDS, and 890 mL of dH_2O.
10. Washing buffer II (higher stringency): 0.5× SSC, 0.1% SDS; mix 25 mL of 20× SSC, 10 mL of 10% SDS, and 965 mL of dH_2O.
11. PCR cycler: Twin Tower (MJ Research, Waltham, MA, USA).
12. Slot-blot apparatus (e.g., BioDot SF, Bio-Rad Laboratories, Prague, Czech Republic).
13. Vacuum pump (a water jet pump is sufficient), hybridization oven.

2.2 Length and Chromosome Position of Putative Telomeric Repeat Tracts

2.2.1 Preparation of High-Molecular Weight DNA in Agarose Plugs

1. 1–10×10^6 cells (10^6 human or mouse cells contain ~6 µg of genomic DNA).
2. Phosphate-buffered saline (PBS): for 10× PBS, dissolve 80 g of NaCl, 2 g of KCl, 14.4 g of Na_2HPO_4, and 2.4 g of KH_2HPO_4 in 800 mL of dH_2O. Add dH_2O to 1 L and adjust the pH to 7.4 with HCl. Dispense into aliquots and sterilize, store at room temperature (RT).
3. Cell lysis buffer (TES): 0.5 *M* EDTA, pH 8.0, 10 m*M* Tris-HCl, pH 8.0, and 1.0% (w/v) *N*-lauroylsarcosine (Sigma-Aldrich, Prague, Czech Republic).
4. Low melting-point agarose: for 10 mL of 1.6% gel, boil 0.16 g of LMP agarose in 10 mL of 1× PBS in a loosely closed 15-mL Falcon tube. The gel may be stored at 4°C for repeated use.
5. Proteinase K: 20 mg/mL proteinase K (Roche Applied Science) in dH_2O, store in 200 µL aliquots at −20°C and minimize the number of freeze-thaw cycles.
6. TE buffer: 10 m*M* Tris-HCl, 1 m*M* EDTA, pH 8.

7. Phenylmethylsulfonyl fluoride (PMSF): 100 m*M* stock solution prepared by dissolving 17.4 mg of PMSF in 1 mL of dry isopropanol.

2.2.2 BAL31 Nuclease Digestion

1. BAL31 nuclease (New England Biolabs, Frankfurt, Germany).
2. BAL31 nuclease buffer: 600 m*M* NaCl, 20 m*M* Tris-HCl, pH 8.0, 1 m*M* EDTA, 12 m*M* $MgCl_2$, 12 m*M* $CaCl_2$ (can be purchased from New England Biolabs).
3. Thermomixer (Eppendorf, Hamburg, Germany).
4. Phenol:chloroform mixture (1:1 v/v) saturated with TE buffer.

2.2.3 Restriction Enzyme Digestion

1. Restriction enzymes: the set recommended is *Alu*I, *Bst*NI, *Hae*III, *Hinf*I, and *Rsa*I (New England Biolabs); reaction buffers are supplied by the manufacturer.
2. 100× bovine serum albumin (BSA) solution (New England Biolabs).

2.2.4 Electrophoretic Separation and Southern Hybridization

1. Pulsed-field gel electrophoresis (PFGE) instrument (e.g., Bio-Rad or Amersham Biosciences).
2. TBE buffer: for 5× solution mix 108 g of Tris-base, 55 g of boric acid, and 9.3 g of Na_4EDTA in 1.8 L of dH_2O; after dissolving, bring up to 2 L. The pH is 8.3 and requires no adjustment. Working concentration is 0.5×TBE.
3. Agarose for PFGE: from, e.g., Serva (Heidelberg, Germany) or Sigma-Aldrich. Electroendosmosis ($-m_r$) <0.13 allows for increased voltages and more rapid DNA migration.
4. Solutions for blotting and hybridization:

   Depurination solution: 0.25 *M* HCl.
   Denaturation and alkali blotting solution: 0.4 N NaOH.
   Hybridization solution: **Section 2.1.8**.
   Washing solutions: **Sections 2.1.9** and **2.1.10**.

2.3 Visualization of Telomeres and Measurement of Their Length In Situ

2.3.1 Preparation of Cell Nuclei on Slides for FISH

1. Microscope slides.
2. 0.075 *M* KCl preheated to 37°C.
3. Freshly prepared ice-cold Carnoy's fixative: glacial acetic acid:methanol 1:3 (v/v).

4. Water bath or thermostat.
5. Poly-L-lysine solution (Sigma-Aldrich) diluted 1:10 (v/v) in sterile dH_2O.
6. STE buffer: 0.5% w/v SDS, 5 m*M* EDTA, 100 m*M* Tris-HCl, pH 7.4.
7. 70% and 95% (v/v) solutions of ethanol in dH_2O.

2.3.2 Labeling Probes by Nick-Translation

1. Sterile PCR tubes, PCR machine.
2. A nick-translation kit (Roche, Prague, Czech Republic) containing a labeled nucleotide (digoxigenin-11-dUTP or biotin-16-dUTP), unlabeled nucleotide mix, enzymes, and reaction buffer. Alternatively, a self-made mix can be used containing:

   10× nick-translation buffer (500 m*M* Tris-Cl, pH 7.8, 50 m*M* $MgCl_2$, 5 mg/mL of purified BSA).
   Labeled nucleotide mix in 100 m*M* Tris-Cl, pH 7.5.
   Digoxigenin mix: 0.2 m*M* digoxigenin-11-dUTP (Roche) and 0.4 m*M* TTP (Roche).
   Biotin mix: 0.4 m*M* biotin-16-dUTP (Roche) and 0.2 m*M* TTP.
   Direct labels: 0.3 m*M* of fluorescently labeled nucleotide (e.g., fluorescein-dUTP, rhodamine-dUTP, e.g., Roche) and 0.3 m*M* TTP.
3. Unlabeled nucleotide mix containing 0.5 m*M* dCTP, dATP, and dGTP in 100 m*M* Tris-Cl, pH 7.5 (prepared by diluting of 0.5 µL of each 100 m*M* stock solution (Roche Applied Science) into 100 µl of Tris-Cl).
4. 100 m*M* dithiothreitol (DTT): 77 mg in 5 mL of dH_2O, make aliquots and store at −20°C.
5. DNA polymerase I/DNAse I solution (Invitrogen, Prague, Czech Republic) 0.5 U of polymerase I and 0.4 mU of DNase I/µL, store at −20°C.
6. 500 m*M* EDTA, pH 8.0.
7. DNA to be labeled: 1 µg (~70 ng/µL).

2.3.3 Labeling Probes by PCR

1. Primers (10 µ*M*) specific to the sequence of interest, or universal primers for a vector.
2. DNA polymerase (2 U DyNAzyme II/µL; Finnzymes, Espoo, Finland) supplied with 10× reaction buffer.
3. 25 m*M* nucleotide mix (mix equal volume of each from 100 m*M* stock solutions).
4. 1 m*M* solution of labeled nucleotide (Roche) (*see* **Note 3**).
5. 1% agarose in Tris-acetate buffer (TAE): for 1 L of 50× TAE, add 242 g of Tris-base, 57.1 mL of glacial acetic acid, and 100 mL of 0.5 *M* EDTA; final pH 8.
6. Ethidium bromide: 0.5 mg/mL, store at 4°C in the dark.
7. DNA precipitation solutions: 3 *M* NaAc, 70% and 90% (v/v) ethanol, 10 mg/mL salmon sperm DNA (Invitrogen).
8. HB50 solution: 2× SSC, 50 m*M* sodium phosphate, 50% (v/v) deionized formamide, pH 7 (Sigma-Aldrich), freshly prepared or stored at −20°C.
9. 20× SSC: *see* **Section 2.1.4**.

2.3.4 Hybridization and Detection

1. Coplin jars, humid chamber, water bath or thermostat, twin tower for PCR machine (optional), diamond pencil (optional).
2. 20% (w/v) dextran sulphate (Sigma-Aldrich): dissolve 2 g of dextran sulphate in 10 mL of HB50 solution (*see* **Section 2.3.3.8**), adjust pH to 7, sterilize, aliquot, and store at −20°C.
3. Ribonuclease A (Sigma-Aldrich): 10 mg/mL in sterile water, aliquot, and store at −20°C. Working concentration is 100 µg/mL in 2× SSC.
4. 2× SSC: dilute from 20× SSC stock solution.
5. 0.01 *M* HCl.
6. Pepsin (Sigma-Aldrich): 500 mg/mL in dH_2O, aliquot and store at −20°C. Working concentration is 500 µg/mL in 0.01 *M* HCl.
7. Washing solution (SF50): 2× SSC, 50% (v/v) formamide, pH 7.
8. PBS: *see* **Section 2.2.2**.
9. 1% formaldehyde: prepare freshly by mixing 1 mL of 37% formaldehyde (Sigma-Aldrich) with 3.7 mL of 10× PBS and add dH_2O to 37 mL. *Caution: formaldehyde is toxic!*
10. Washing buffer: 0.2% (v/v) Tween-20 (Sigma-Aldrich) in 1× PBS.
11. 4′,6,diamidino-2-phenylindole (DAPI): 2 µg/mL in Vectashield mounting medium (Vector Laboratories, Peterborough, UK), store at 4°C in the dark.
12. Fluorescent antibody enhancer set for DIG detection (Roche) containing 10× blocking solution and set of antibodies for digoxigenin signal detection and amplification (monoclonal anti-DIG antibody, anti mouse-Ig-DIG, anti-DIG-fluorescein—all of them have to be diluted 1:25 in blocking buffer, which is prepared from 10× stock solution by 1:9 dilution in PBS).
13. Fluorolink Cy3-labeled streptavidin (Amersham): working dilution 1:800 to 1:1,000 in blocking buffer.
14. Biotinylated anti-streptavidin (Vector Laboratories): working dilution 1:500 to 1:1,000 in blocking buffer.

2.3.5 Primed In Situ Labeling (PRINS)

1. Labeled nucleotide mix: digoxigenin-, biotin-, fluorescein-, or rhodamine-dUTP (Roche) is used depending on the label preferred. *See* **Section 2.3.2**, **step 2**.
2. 10× dNTP mix: 1 m*M* dATP, 1 m*M* dideoxy(dd)GTP (Roche), 1 m*M* dCTP (diluted from 100 m*M* stock solutions, Roche), 100 µ*M* labeled-dUTP (diluted from 1 m*M*, Roche), in 50% v/v glycerol.
3. Stop buffer: 10 mL of 500 m*M* EDTA, 1 mL of 5 *M* NaCl, and 85 mL of dH_2O.
4. Wash buffer: 100 mL of 20× SSC, 1.25 mL of stock solution of Tween-20 (100%; Sigma P7949), and 400 mL of dH_2O.

5. 0.5–1 µg of telomeric primer $(CCCTAA)_7$ (*see* **Note 4**).
6. Blocking solution: 3% (w/v) milk powder or BSA in wash buffer.
7. Tth DNA polymerase 5 U/µL (Roche).
8. 5× Tth buffer: dilute 10× Tth buffer supplied with Tth polymerase 1:1 with glycerol.
9. Fluorolink Cy3-labeled streptavidin (Amersham): working concentration is 1:800–1:1,000 in blocking solution; alternatively, use anti DIG-fluorescein or anti DIG-rhodamine (Roche); dissolve the lyophilized antibody with 100 µL of sterile dH_2O to a concentration of 2 mg/mL, working dilution is 1:800–1:1,000 in blocking solution.

2.3.6 Imaging and Analysis

1. Fluorescence microscope with an appropriate filter set and a CCD camera.
2. Software for measuring telomere length: Telo.TFL ***(18)***, free on request at (http://www.flintbox.com/technology.asp?sID=1209F02AF866451DB693098C0E38FB00&page=FB535FB).
3. ISIS imaging system (MetaSystems, Altlussheim, Germany).

2.4 Measurement of Telomerase Activity by the TRAP Assay

2.4.1 Preparation of Cell or Tissue Extracts

1. Microtubes certified DNase- and RNase-free, 0.5-mL PCR tubes (e.g., ABgene, Epsom, UK), barrier tips (e.g., Denville Scientific, Westbourne, UK).
2. DEPC-treated (RNase-free) water.
3. 10^5 cultured cells or ~50 mg of tissue sample (fresh or frozen at −80°C).
4. RNase-free disposable PELLET PESTLES (Kimble Kontes, Vineland, NJ, USA).
5. Cell lysis and extraction buffer (LE):10 m*M* Tris-HCl, pH 8.0, 1 m*M* $MgCl_2$, 1 m*M* EDTA, 1% (v/v) Nonidet P-40, 0.25 m*M* sodium deoxycholate, 10% (v/v) glycerol, 150 m*M* NaCl, 5 m*M* 2-mercaptoethanol, 0.1 m*M* 4-(2-aminoethyl)-benzenesulfonyl fluoride (AEBSF). Make in RNase-free water, filter-sterilize, and store at −20°C in 1-mL aliquots.
6. Bench-top refrigerated centrifuge providing ≥18,000×*g*.
7. Liquid nitrogen.
8. Reagents and equipment for determination of protein concentration, e.g., BCA protein assay kit (Pierce, Rockford, IL, USA) and spectrophotometer.

2.4.2 TRAP Assays

1. TRAP reaction buffer (5×): 100 m*M* Tris-HCl, pH 8.3, 7.5 m*M* $MgCl_2$, 300 m*M* KCl, 0.25% (v/v) Tween-20, 5 m*M* EGTA. Make in RNase-free water, filter-sterilize and store at −20°C in 1 mL aliquots.

2. dNTP mix: 50× mix contains 2.5 m*M* each of dATP, dTTP, dGTP, and dCTP in RNase-free water.
3. TS primer (5′-AATCCGTCGAGCAGAGTT-3′): 20 nmol/mL.
4. Primer mix:
   (i) Reverse primer (ACX) (5′-GCGCGGCTTACCCTTACCCTTACCCTAACC-3′), final concentration 10 nmol/mL.
   (ii) Reverse primer for the internal standard (NT) (5′-ATCGCTTCTCGGCC TTTT-3′), final concentration 20 nmol/mL.
   (iii) Substrate oligonucleotide for the 36-bp internal standard (TSNT) (5′-AAT CCGTCGAGCAGAGTTAAAAGGCCGAGAAGCGAT-3′), final concentration 0.01 amol/mL.

   The stock solution of TSNT and its dilutions are performed separately from other solutions to avoid cross-contamination of other reaction components used in TRAP. Use of barrier tips, a specific set of pipettes, a separate biohazard box, and siliconized tubes is recommended. TSNT solution is added as the last component to the primer mix, which is then divided into 25-µL aliquots and stored at –20°C.
5. DyNAzyme DNA polymerase (Finnzymes).
6. Thermal cycler.
7. Ultrapure BSA, 50 mg/mL (Ambion-Applied Biosystems, Prague, Czech Republic).

2.4.3 Analysis of TRAP Products

1. Reagents and equipment for non-denaturing polyacrylamide gel electrophoresis.
2. Gel-loading buffer: 0.25% (w/v) each of bromophenol blue and xylene cyanol in 50% (v/v) glycerol, 50 m*M* EDTA, pH 8.0. Store at 4°C.
3. SYBR Green I (Sigma-Aldrich, supplied as 10,000× concentrated stock solution in DMSO).
4. CCD camera documentation system or fluorescence scanner (e.g., Storm or Typhoon; GE Healthcare, Vienna, Austria; or FLA7000; Fujifilm, Stamford, CT, USA) with evaluation software.

2.5 Measurement of Telomerase Activity by Dual Color Real-time TRAP Assays

2.5.1 Preparation of Samples

1. 10^5 cultured cells or ~50 mg of tissue (fresh or frozen at –80°C).
2. RNase-free disposable PELLET PESTLES (Kimble Kontes).
3. Reagents and equipment for determining protein concentration (e.g., BCA protein assay kit, Pierce) and spectrophotometer.

2.5.2 Dual-Color Real-time TRAP and Its Evaluation

1. Optically clear tubes for real-time PCR (e.g., ABgene) and barrier tips certified RNase- and DNase-free (e.g., Denville).
2. Real-time PCR thermocycler able to measure fluorescein and rhodamine fluorescence in two independent channels (excitation/emission 470/510 nm and 585/610 nm, respectively) (e.g., Rotor-Gene 3000 or later version; Corbett Research, Sydney, Australia).
3. Thermo-Start Taq DNA polymerase (5 U/μL (ABgene) (*see* **Note 5**).
4. RNase inhibitor (New England Biolabs).
5. TRAPeze XL telomerase detection kit (Chemicon, Chandlers Ford, Hampshire, UK) contains the following components:
   (i) Lysis/extraction buffer (CHAPS lysis buffer).
   (ii) 5× TRAPEZE XL reaction mix containing TS primer, RP Amplifluor primer (analog of ACX), K2 Amplifluor primer (analog of NT), TSK2 template (analog of TSNT), dA, dC, dG, and dTTP, in 100 m*M* Tris-HCl, pH 8.3, 7.5 m*M* $MgCl_2$, 315 m*M* KCl, 0.25% Tween-20, 5 m*M* EGTA, and 0.5 mg/mL BSA.
   (iii) PCR-grade water, protease-, DNase-, and RNase-free, deionized (8.2 mL).
   (iv) TSR8* (control template) (45 μL, 0.2 amole/μL), an oligonucleotide with a sequence identical to the TS primer extended with eight telomeric repeats $AG(GGTTAG)_7$. This standard permits construction of calibration curves for quantitative evaluation; 0.1 amol of TSR corresponds to 100 TPG (total product generated) units.
   (v) Control cell pellet: 10^6 telomerase-positive cells, store at −80°C.

3 Methods

3.1 Screening Genomic DNA for Variant Telomere Sequences

This method can be used for testing large sample collections, for example, for screening members of certain taxonomic groups. In the absence of a telomeric sequence that is expected for the organism with respect to its taxonomic classification (e.g., due to mutation in a gene coding for the RNA or protein subunits of telomerase), the test can reveal the kind of variant telomeric repeat that has substituted the original sequence. Genomic DNA is transferred onto a nylon membrane and hybridized with telomeric probes, and comparison of signals between membranes is enabled by using control DNA concatemers and preferably also control genomic DNAs. Control concatemers of known concentration also serve as a normalizing standard between membranes hybridized with different telomeric probes. When comparing the strength of signals among samples, be aware of differences of their genome size (1C value), which may vary from 0.1 pg to 20 pg of DNA in plants.

The standard procedure uses 1 µg of genomic DNA loaded onto a membrane, which is equivalent to different numbers of "whole genomes" in different samples. Another influence on the signal strength may come from differences of telomere length in organisms with the same chromosome number (and therefore the same number of telomeres) or from the inverse, a different chromosome number among species with the same telomere length.

Different kinds of telomeric probes can serve for hybridization with comparable results, and we recommend using a method that is common in your lab. The easiest way is to use a radioactive end-labeled oligonucleotide, but cloned fragment of telomeric DNA or in vitro-concatenated telomeric oligonucleotides can also be used as probes. For labeling of concatemers or cloned telomeric sequences, we recommend nick-translation rather than random primer-based labeling with Klenow enzyme. Probes can also be labeled by PCR using a radioactive dNTP in the PCR mix. Here we describe the most common procedure using alkali blotting of genomic DNA on a nylon membrane with labeled oligonucleotides as probes.

3.1.1 Preparation of Control Concatemers

1. Mix for a template-free PCR reaction (final concentrations): 0.3 µ*M* primers G and C (*see* **Section 2.1.3**), 0.2–0.25 m*M* dNTPs, 1× PCR buffer with 1.5 m*M* $MgCl_2$, and Taq DNA polymerase (optimum concentrations of $MgCl_2$, dNTP, and polymerase may vary according to the manufacturer's description).
2. Run the PCR reaction in the following conditions: initial denaturation at 94°C for 2 min, 10 cycles of 94°C/30 sec, 55°C/30 sec, 72°C/20 sec with 10 sec extension per cycle, then 25 cycles of 94°C/30 sec, 55°C/30 sec, 72°C/2 min, and final extension at 72°C for 7 min.
3. Check the products by electrophoresis on a 1% agarose gel; they should form a smear ranging from 0.5 to 2 kb.
4. Purify the concatemers by phenol/chloroform extraction and ethanol precipitation, or using a commercial PCR purification kit (e.g., Qiagen, Hilden, Germany).
5. Measure the DNA concentration by spectrophotometry.

3.1.2 Slot-Blot Procedure

1. Set the volume of your genomic DNA samples (and also of the control genomic DNA) at 50 µL by diluting 1 µg with sterile water.
2. Prepare two concentrations of concatemers, 100 pg and 500 pg in 50 µL.
3. Add 200 µL of 0.4 *M* NaOH to each sample and mix.
4. Incubate for 15 min at 37°C.

5. Prepare a slot-blot sandwich of two or three sheets of filter paper and a nylon membrane soaked with 2× SSC on the slot-blot apparatus and seal the lid with the screws.
6. Connect the apparatus to a vacuum and load sterile water in a chessboard arrangement to check the sealing of neighboring wells. Sealing is very important.
7. Load 500 µL of 0.4 *M* NaOH into each well to equilibrate the membrane.
8. Load the DNA samples from **step 4** into the wells
9. Load 500 µL of 0.4 *M* NaOH to wash the wells.
10. Wash the wells with 500 µL of 6× SSC, repeat twice.
11. Under vacuum, unscrew the lid and place the membrane on filter paper to dry.
12. Fix the DNA onto the membrane by heating at 80°C for 1 h or by UV-crosslinking.

3.1.3 End-labeling of Oligonucleotide Probes and Hybridization

Day 1:

1. Prehybridize the membranes in hybridization buffer for 1 h at 55°C in slowly rolling cylinders in a hybridization oven.
2. Mix the end-labeling reaction: 2 µL of 10 µ*M* primer G (*see* **Section 2.1.3**), 3 µL of 10× buffer for PNK, 30 U of T4 polynucleotide kinase, 50 µCi of gamma [^{32}P]-ATP in a 30-µL final volume.
3. Incubate at 37°C for 30 min, inactivate at 70°C for 10 min.
4. Denature any secondary structure in the probe by boiling for 2 min and add it into the hybridization buffer of **step 1**.
5. Hybridize at 55°C overnight (at least 16 h) in the hybridization oven.

Day 2:

6. Preheat washing solutions I and II at 55°C.
7. Pour the radioactive probe solution to the radioactive waste vessel, add washing solution I, and incubate in the hybridization oven for 15 min at 55°C.
8. Discard washing solution I and add washing solution II, incubate for 20 min at 55°C.
9. Repeat **step 8** twice more.
10. Discard washing solution II and cover the membrane with Saran wrap (*see* **Note 6**).
11. Expose the membrane to X-ray film or a phosphoimager screen.

3.2 Length and Chromosome Position of Putative Telomeric Repeat Tracts

The presence of a putative telomeric repeat sequence in genomic DNA does not necessarily mean that it is positioned at the terminus of a chromosome. To test the terminal position of the sequence, digestion with BAL31 nuclease is commonly used

(*see* **Introduction**). To obtain accurate and reproducible data, integrity of the starting DNA is essential and to avoid shearing during preparation and consequent artificial initiation of BAL31 digestion at breakpoints, preparation of DNA in agarose plugs as commonly used for pulsed-field gel electrophoresis (PFGE) is recommended.

Telomere lengths differ not only among species, but also among individual chromosome ends within a single cell and among cell types. The average distribution of telomere lengths in a sample can be obtained indirectly from analysis of terminal restriction fragments (TRFs). This technique relies on the fact that repeated minisatellite telomeric units do not contain target sites for restriction enzymes. Consequently, telomeres together with the associated subtelomere segment, whose size depends on the position of the first restriction enzyme site, remain in relatively long fragments (TRFs), whereas the genomic DNA is digested into short pieces. The protocol below includes embedding cells in agarose plugs, preparation of high molecular weight DNA within the plugs, serial digestion of the DNA with BAL31, extraction of DNA from the agarose, restriction enzyme digestion, electrophoretic separation of fragments, and Southern hybridization.

3.2.1 Preparation of High-Molecular Weight DNA in Agarose Plugs

1. Melt an aliquot of 1.6% (w/v) low-melting point agarose in PBS in a boiling water bath and place at 40°C in a water bath.
2. Wash the cell pellet (~10^7 cells) twice with PBS at RT.
3. Resuspend the pellet in a minimal volume of PBS (100–200 µL) and assess the approximate total volume with a micropipette with a wide-bore tip.
4. Incubate the cell suspension briefly at 40°C and add 1 volume of molten agarose. Mix by careful pipetting up and down using a wide-bore pipette, avoiding formation of bubbles.
5. Transfer the mixture to a sample mold provided with the PFGE instrument.
6. Place the sample mold in the refrigerator for 20 min to let the agarose blocks solidify.
7. Transfer the blocks to a Petri dish using a thin spatula, cut into aliquots corresponding to ~10^6 cells with a scalpel, and place them in 15-mL Falcon tubes with 2 mL of lysis buffer. Incubate for 20 min at RT.
8. Remove the lysis buffer and replace it with 1 mL of the same buffer. Add 25 µL of proteinase K (20 mg/mL) and incubate at 50°C for 24 h. Optionally, repeat the deproteinization step.
9. Wash the blocks for at least 3× 20 min with 10 mL of TE buffer, then 2× 30 min with 2 mL of TE containing 0.2 m*M* PMSF to remove all remaining protease activity. Finally, wash the blocks with 10 mL of 0.1× TE to remove PMSF and its hydrolysis products.

3.2.2 BAL31 Nuclease Digestion

1. Take six or more sample blocks, depending on the number of digestion times planned, place each in a 2-mL round-bottom Eppendorf tube, and equilibrate

them in 300 µL of BAL31 nuclease buffer for 30 min. During this period, label the tubes with the planned digestion time, e.g., 0, 10, 20, 40, 60, and 90 min.
2. Replace the BAL31 buffer with 300 µL of the same buffer and put the tubes into a Thermomixer set to 30°C. Add 3 U of BAL31 nuclease to all but the zero-time sample and digest for the required time.
3. Stop the reaction by removing the buffer and adding 500 µL of 50 m*M* EGTA, pH 8.0.
4. Inactivate BAL31 nuclease irreversibly by incubation at 58°C for 15 min.
5. Replace the EGTA solution with 1 mL of TE buffer and incubate at 72°C until the agarose melts (10–30 min) (*see* **Note 7** for analysis of telomeres longer than 15 kb).
6. Extract DNA with phenol-chloroform (2×) and chloroform (1×) and precipitate with ethanol.
7. Dissolve the DNA in 20 µL of 0.1× TE buffer.

3.2.3 Restriction Enzyme Digestion

1. Choose a set of frequently cutting restriction enzymes that cleave under similar reaction conditions (buffer, temperature optimum), show relatively long survival in a reaction, and are not sensitive to cytosine methylation. The example used here is *Alu*I, *Bst*NI, *Hae*III, *Hinf*I, and *Rsa*I.
2. Dilute 3 µL of 100× concentrated BSA solution with 27 µL of sterile dH_2O and add 2.8 µL of this mixture to 20 µL of DNA solution in all samples.
3. Add 2.8 µL of 10× NEB buffer 2 to all samples.
4. Prepare 20 µL of the mixture of restriction enzymes (4 µL of each at 10 U/µL before mixing, 2 U/µL each after mixing). Keep the mixture at −20°C.
5. Add 2 µL of the restriction enzyme mixture to each reaction and incubate for 2 h at 37°C.
6. Add 1 µL of the restriction enzyme mixture to each reaction. Incubate for the next 4–6 h, optionally overnight, at 37°C.
7. Terminate the reactions by adding 2 µL of 10× STOP-gel loading buffer.

3.2.4 Electrophoretic Separation and Southern Hybridization

1. To achieve optimal resolution of terminal restriction fragments, use a PFGE system with hexagonal electrodes (e.g., CHEF DR, Bio-Rad or Gene Navigator, Amersham).
2. Prepare a 1% agarose PFGE gel in 0.5× TBE. Pour 0.5× TBE into the PFGE unit and precool to 14°C.
3. Set the electrophoresis parameters; for a size range between 1 and 200 kb, suitable values are 14°C, 6 V/cm, switch time ramped from 1 to 12 sec for 15 h.

4. Load the samples into the gel wells and switch on the power source and pulser. For liquid samples, keep the buffer circulation off until the samples migrate into the gel (20 min) and only then switch on the buffer circulation.
5. After separation, transfer the DNA by capillary or vacuum alkali blotting and hybridize with end-labeled telomeric oligonucleotide probes (*see* **Section 3.1.3** and **Note 8**).

3.3 Visualization of Telomeres and Measurement of Their Length In Situ

Two techniques are available for microscopic visualization of telomeres, fluorescence in situ hybridization (FISH) and primed in situ labeling (PRINS). FISH can be used either for single-copy genes or for repetitive sequences, because a labeled gene-specific DNA probe is used for hybridization. In contrast, in PRINS, an unlabeled oligonucleotide anneals to its target DNA and is elongated by polymerase in the presence of labeled nucleotides; the oligonucleotide anneals simultaneously to many random targets in repetitive sequences, so these are visualized much more easily than single-copy genes. For telomeres such as those of vertebrates or plants that lack one or more nucleotide in one strand of their repetitive unit, PRINS can be performed as a dideoxy-reaction where the lacking nucleotide is added as the dideoxy form ***(19)***; the PRINS reaction is then stopped at nonspecific sites and very strong signals without background noise are obtained.

The most commonly used quantitative in situ method is quantitative FISH (Q-FISH), which is based on peptide–nucleic acid (PNA) probes (*see* Fig. 17.1), which

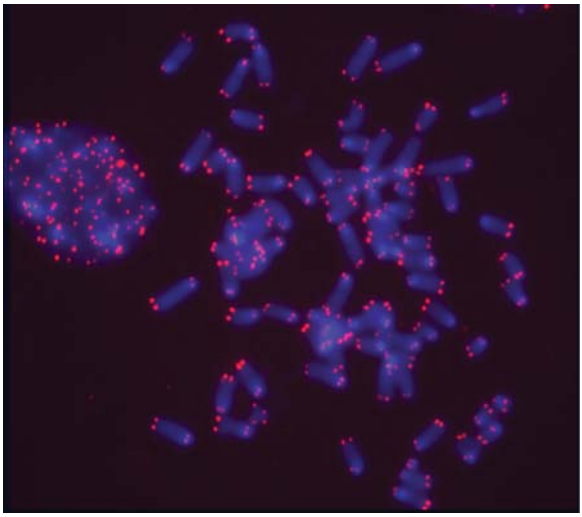

Fig. 17.1 Fluorescence in situ hybridization on mouse MEF chromosome spreads. A Cy3-labeled PNA telomeric probe $(TTAGGG)_n$ was used (*red*), chromosomes are stained with DAPI (*blue*). To view this figure in color, see COLOR PLATE 13

can be short due to the higher stability of PNA-DNA hybrids. Because PNA probes are synthetic and contain a known number of fluorescence-labeled nucleotides, signal intensities correlate with telomere length.

FISH on extended DNA fibers, termed fiber-FISH, is a high-resolution method with a resolution of 1–2 kb. Its major limitation is the length of the sequence that can be detected, which theoretically is (10 kb so that each signal spot should correspond to 1–2 kb. This limit can vary with the degree of stretching of the fibres. Fiber-FISH can be used for approximate quantification of telomere length using a standard to calibrate the number of spots per length of sequence.

3.3.1 Preparation of Cell Nuclei on Slides for FISH

1. Collect cells from an appropriate culture medium (~10^6 cells/mL), use at least 20 mL (*see* **Note 9**).
2. Spin the cells down for 5–10 min at 800×*g* and remove the medium gently.
3. Without adding any solutions, resuspend the cell pellet by gently shaking the tube and slowly pour in 10 mL of 0.075 KCl at 37°C, mix gently, and incubate for 20 min at 37°C. The hypotonic KCl solution causes swelling of the cells and release of nuclei.
4. Spin the cells down for 5–10 min at 800×*g* and remove the supernatant completely.
5. Fix the nuclei by adding, drop-wise, 10 mL of ice-cold Carnoy's fixative; mix slowly. *Use gloves, methanol is highly toxic*.
6. Wash the nuclei by five to six repetitions of steps 4 and 5.
7. Resuspend the pellet in an appropriate amount of fixative (has to be determined empirically) and store at −20°C if necessary.
8. Drop 10–20 µL of suspension of nuclei onto a clean slide (*see* **Note 10**) and leave it to dry for a couple of minutes.
9. For FISH, bake the slides in the Twin Tower block or on a hot plate at 60°C for 30 min, or store for 1 week at RT before use; for PRINS, use freshly prepared slides.

3.3.2 Extending DNA Fibers on Slides for Fiber-FISH

1. Pour 70 mL of STE buffer into a clean Coplin jar.
2. Drop 10–20 µL of nuclei (*see* **Section 3.3.1**) onto a poly-L-lysine coated slide (*see* **Note 11**) and put immediately into STE lysis buffer, leave for 6–10 min (*see* **Note 12**).
3. Add 70 mL of 95% ethanol, the first portion drop-wise, and incubate for more than 10 min.
4. Remove the slides gently and slowly and place them in 70% ethanol for 30 min.

5. Air-dry the slides.
6. Bake the slides at 60°C for 30 min in the Twin Tower block of a PCR machine or on a hot plate.

3.3.3 Labeling of FISH Probes

The best method depends on the length of the probe; PCR labeling can be used for probes 100–500 bp in length but nick-translation is necessary for longer probes. Cloned telomere fragments or fragments generated by self-annealing of telomeric oligonucleotides can be used as probes (*see* **Section 3.1.1**).

3.3.3.1 Probe Labeling by Nick-Translation

Either a commercially available kit or a self-made mix (*see* **Note 13**) can be used. When using a kit:

1. Mix 1 µg of DNA and 4 µL of kit master mix, and add sterile water to 20 µL.
2. Incubate at 15°C for 2 h using a PCR machine or a water bath.
3. Stop the reaction by adding 0.5 µL of 500 m*M* EDTA and incubate at 60°C for 10 min (*see* **Note 14**).
4. Add 10 µg of salmon sperm DNA as carrier and competitor, to decrease background noise and increase the recovery of the probe.
5. Precipitate DNA by adding 0.1 volumes of 3 *M* NaAc and 3 volumes of 95% ethanol.
6. Centrifuge the precipitated probe at 15,000×*g*, add 70% ethanol, spin again, remove the supernatant, and air-dry the pellet.
7. Dissolve the probe in 20 µL of HB50.

3.3.3.2 Probe Labeling by PCR

1. Perform a PCR reaction in 50 µL containing:

   2 µL of forward primer (10 µ*M*).
   2 µL of reverse primer (10 µ*M*).
   1 µL of 25 m*M* unlabeled nucleotide mix.
   1 µL of 1 m*M* labeled nucleotide (dig-, bio-, fluorescein-, or rhodamine-dUTP).
   1–10 ng of template DNA.
   5 µL of 10× reaction buffer.
   2 U of DyNAzyme II polymerase.
   Sterile H_2O to 50 µL.

Program your thermal cycler as follows:

(i) 93°C for 2 min.
(ii) 94°C for 30 sec.

(iii) 56°C for 30 sec.
(iv) 72°C for 1 min.
(v) repeat (i)–(iv) 30×.
(vi) 72°C for 7 min.
(vii) End.

Verify that synthesis of the PCR product was successful by electrophoresing an aliquot of the reaction mix on a 1% agarose gel and staining with ethidium bromide.

Follow steps 4–6 in the nick-translation protocol (**Section 3.3.3.1**).

3.3.4 Hybridization and Detection

The protocol described below can be generally used; it is based on that performed at an EMBO workshop (Advanced Molecular and Immuno-Cytogenetics on Chromosomes and Nuclei of Plants, Wageningen, Netherlands, October 2003) with further modifications. For fiber-FISH, start with **step 11**.

1. Pipet 100 µL of RNase A (*see* **Section 2.3.4.3**) onto the slide and cover it with a 24×50-mm cover slip. To avoid air bubbles, pipetting on the cover slip and covering it with the slide is better.
2. Incubate at 37°C for 1 h.
3. Rinse in 2× SSC at RT for 3× 5 min.
4. Rinse in 0.01 *M* HCl for 10 min.
5. Incubate in pepsin working solution (*see* **Section 2.3.4.6**) at 37°C for 10 min.
6. Rinse once in 1× PBS for 5 min.
7. Fix in 1% formaldehyde for 10 min at RT.
8. Rinse in 1× PBS for 2× 5 min.
9. Dehydrate the slides through an ice-cold ethanol series (70%, 90%, 100% v/v), each for 3 min.
10. Air dry.
11. Prepare the hybridization mix (20 µL/slide) (*see* **Note 15**): 10 µL of 20% dextran sulfate in HB50, x µL of probe (containing 20–50 ng of DNA) in HB50, supplement with HB50 to a total volume of 20 µL.
12. Pipet the hybridization mix onto the slide, cover with a 24×24-mm coverslip (*see* **Note 16**).
13. Denature the sample in a PCR machine (Twin Tower) or on a hot plate at 80°C for 2 min.
14. Hybridize in a moist chamber at 37°C overnight (*see* **Note 17**).
15. (Optional) Mark the area covered by the cover slip with a diamond pencil.
16. Wash the slides in a Coplin jar in washing solution SF50 at 42°C, 3× 10 min. Use a waterbath (*see* **Note 18**).
17. Wash the slides 2× 5 min in 2× SSC.
18. Wash the slides 10 min with washing buffer.
19. Pipet 100 µL of blocking solution on each slide and incubate at RT for 30 min (*see* **Note 19**).

20. Pipet 50 µL of primary antibody (monoclonal anti-DIG antibody or fluorolink Cy3-labeled streptavidin or both, depending on the hapten used).
21. Incubate at 37°C for 1 h.
22. Wash briefly 3× in washing buffer.
23. Pipet 50 µL of secondary antibody (*see* **Note 20**) (anti mouse-Ig-DIG or biotinylated anti-streptavidin, or both).
24. Incubate at 37°C for 1 h.
25. Wash briefly 3× in washing buffer.
26. Pipet 50 µL of tertiary antibody (anti DIG-fluorescein or fluorolink Cy3-labeled streptavidin, or both) (*see* **Note 20**).
27. Wash briefly 3× in washing buffer.
28. Stain with DAPI.

3.3.5 Primed In Situ Labeling (PRINS)

The protocol of Koch (1995) ***(19)*** is described. Slides are prepared as for FISH, but in this case, they have to be fresh.

1. Prepare a master mix for the appropriate number of slides. Mix for one slide consists of 4 µL of 5× reaction buffer, 2 µL of 10× dNTPs, 0.4 µL of oligonucleotide, 1 U of Tth polymerase, and 13.6 µL of sterile water.
2. Pipet 20 µL of master mix on the slide, cover with a 24×24-mm cover slip, fix with glue or nail polish to avoid drying (*see* **Note 21**).
3. Put slides in the Twin Tower and set the PCR machine as follows:

   (i) 94°C for 3 min.
   (ii) 57°C for 50 min (*see* **Notes 22** and **23**).

4. Carefully remove the cover slip using a razor blade or scalpel, and incubate the slide for 1 min in stop buffer preheated to 55°C.
5. Wash slides 3× 5 min in wash buffer.
6. For direct labeling (fluorescein or rhodamine), stain with DAPI. For indirect labeling (Dig or Bio) carry on with **step 7**.
7. Pipet 100 µL of blocking solution on each slide and incubate at RT for 30 min.
8. Pipet 50 µL of antibody (anti DIG-fluorescein or fluorolink Cy3-labeled streptavidin).
9. Wash 3× 5 min in wash buffer.
10. Stain with DAPI.

3.3.6 Imaging and Analysis

A fluorescence microscope with an appropriate filter set and a CCD camera is needed for imaging. When Q-FISH is performed, a fixed exposure time has to be set. To determine absolute telomere length in kilobases, a length standard has to

be used and cloned telomere fragments of different length are used for calibration, as described in ***(20)***. Without calibration, only differences between samples can be studied, but this is sufficient for most purposes.

Several software tools for measuring telomere length are available. Telo.TFL developed in the laboratory of Peter Lansdorp ***(18)***, is based on single signal intensity measurements and each telomere is evaluated separately; the acquired values are processed by Excel to make a graph. Telo.TFL is compatible with the ISIS imaging system (MetaSystems), in which the karyotype of human samples can be visualized, enabling real single telomere measurement including information on chromosome arm identity.

In mouse samples, karyotyping is difficult because all chromosomes are acrocentric and because the differences in telomere lengths are very large (tens of kilobases), putting all the data together makes the interpretation of results more difficult.

Quantification of telomere length by Fiber-FISH is also possible by counting the number of signals, each corresponding to 1.5–3.0 kb depending on the degree of extension. This technique is simple, but a large set of samples and standards has to be analyzed for reliable calibration. Quantification of this type is suitable in species with long telomeres (e.g., mouse, tobacco, or tomato) but is not applicable for short telomeres (e.g., the shortest human telomeres are ~5 kb, which is near the detection limit).

3.4 Analysis of Telomerase Activity by the TRAP Assay

The principle of the TRAP assay is the extension by the telomerase complex of a substrate oligonucleotide (TS) with a nontelomeric sequence. This primary product is then PCR-amplified using excess TS primer molecules and the reverse primer (complementary to the G-telomeric strand synthesized by telomerase). The reverse primer ACX ***(21)*** has been modified by mismatches in the telomere sequence to suppress PCR artifacts such as formation of primer-dimers, and by a GC-rich 5′-end anchor which promotes keeping the original size distribution of primary telomerase products. The PCR products are then analyzed using nondenaturing polyacrylamide gel electrophoresis. The technique as originally described ***(16)*** used a [^{32}P]-end-labeled TS primer, but the optimized reaction is sufficiently sensitive when using fluorescein-labeled substrate primers or only conventional in-gel staining of the products by SYBR Green. Here we describe the latter protocol, using a technique and reagents that roughly correspond to a commercially available telomerase detection kit (TRAPeze; Chemicon).

3.4.1 Preparation of Cell or Tissue Extracts

1. Pellet (10^5 cells in a DNase- and RNase-free 0.5-mL microcentrifuge tube at 3,000×*g* for 5 min at RT. The pellet can be used immediately or snap-frozen in liquid nitrogen and stored at −80°C until use.

2. Add 100 µL of ice-cold LE buffer to the cell pellet (1 µL per 1,000 cells), resuspend, and incubate for 30 min on ice. If tissues are to be used, homogenize 50–100 mg with RNase-free disposable PELLET PESTLES in a 0.5-mL microcentrifuge tube on ice and incubate for 30 min on ice.
3. Centrifuge the extract at ≥18,000×*g* for 20 min at 4°C and transfer the supernatant to new 0.5-mL tubes in 20-µL aliquots (*see* **Note 24**). Also take two 2-µL aliquots for determination of protein concentration. Centrifugation is only necessary for tissue extracts, whereas cell extracts may be used as whole lysates without centrifugation.
4. Snap-freeze the lysates in liquid nitrogen and store at −80°C until the TRAP assay.
5. Determine protein concentration using the Bradford assay ***(22)*** or another standard method (e.g., BCA protein assay kit; Pierce).

3.4.2 TRAP Assays

1. Dilute aliquots of cell extracts with LE buffer to a concentration corresponding to 100–1,000 cells/µL (the initial concentration is 1,000 cells/µL) or to 1 µg protein/µL for tissue extracts (*see* **Note 25**).
2. Prepare negative controls by heat-inactivating 1 µL of cell or tissue extract diluted with 2 µL of RNase-free water (to compensate for evaporation) in a thermal cycler at 85°C for 10 min.
3. Prepare a reaction mix for the desired number of 50 µL reactions and controls, plus two additional reactions to compensate for possible pipetting mistakes. Remember that each sample should be analyzed in two parallel reactions. Mix for one reaction contains:

   1 µL of 50× dNTP mix (50 µ*M* final concentration).
   10 µL of 5× TRAP reaction buffer.
   1 µL of TS primer (20 nmol/mL).
   1 µL of primer mix.
   34.6 µL RNase-free water.
   0.4 µL of 50 mg/mL ultrapure BSA.
   1 µL of DyNAzyme II DNA polymerase (2 U/µL).

   Prepare the reaction mix immediately before the assay and aliquot 49 µL into individual 0.5-mL PCR tubes (prelabeled with sample numbers) on ice.
4. To prevent contamination, reactions should be set up in a separate room from that in which PCR and TRAP-product analyses are to be performed (use of a flow box, barrier tips, and a different set of pipettes is highly recommended).

   Add 1 µL of an extract to be analyzed to a 49-µL aliquot of reaction mix on ice. Include also the negative controls (**step 2**) and another kind of negative control in which the extract is replaced by LE buffer. Whereas the former control is to check for telomerase-independent artifacts of the TRAP assay (e.g.,

formation of primer-dimers), the latter is to check for the presence of contaminants (e.g., telomerase products from previous assays) in the LE buffer and other reaction mix components.

5. Place all the reactions into the thermocycler and start the following program:
   (i) 30°C for 30 min, extension of TS primer by telomerase with variant numbers of telomere repeats.
   (ii) 94°C for 3 min, termination of telomerase-extension step and heat inactivation of telomerase.
   (iii) 94°C for 30 sec, PCR denaturation step.
   (iv) 59°C for 30 sec, primer annealing.
   (v) 72°C for 30 sec, extension.

   Repeat steps (iii) to (v) 27–30 times.

3.4.3 Analysis of TRAP Products

1. Prepare a 1.0–1.5 mm-thick, 16 cm-long 12.5% polyacrylamide gel in 0.5× TBE.
2. Add 4 μL of gel-loading buffer to 16 μL of TRAP reaction products and load on the gel.
3. Run the gel in 0.5× TBE at 60 V for 15 min and then at 250 V until the bromophenol blue dye runs out of the gel.
4. Stain the gel for 15 min with SYBR Green I diluted 1:10,000 with 0.5× TBE.
5. Destain the gel for 10 min in 0.5× TBE.
6. Visualize the pattern of TRAP products using a CCD camera documentation system or a fluorescence scanner.
7. Using the evaluation software, sum the intensities of the bands in the TRAP ladders. The values obtained in the heat-inactivated controls should be subtracted from the corresponding sample values. Divide the result by the intensity of the internal standard band (36 bp, in front of the shortest TRAP product) to calculate relative TRAP activities (the synthesis of TRAP products and internal standard is semicompetitive with respect to TS primer usage) (*see* **Notes 25** and **26**).

3.5 Measurement of Telomerase Activity by Dual Color Real-time TRAP Assays

For a more convenient and precise quantitation of telomerase activity, we recommend the TRAPezeXL telomerase detection kit (Chemicon), which uses a modified version of the TRAPeze telomerase detection kit and the same reaction scheme as that described above. The modification lies in the use of differentially labeled energy transfer (Amplifluor) primers, which consist of a 3′ end sequence

complementary to the target sequence and a 5′ end hairpin structure. The fluorophore (energy donor) and the quencher dabsyl (4-dimethyl-aminobenzene-4′-sulfonyl) are in close proximity within the 5′ hairpin. When the primer is incorporated into a double-stranded PCR product, the hairpin is unfolded by the activity of the polymerase. In this extended conformation, the distance between the fluorophore and quencher is increased and a fluorescence signal is generated. In the TRAPezeXL kit, amplified telomerase products are labeled with fluorescein, and an internal standard control labeled with sulforhodamine serves to monitor the PCR amplification and aid the quantitation of telomerase activity, using end-point fluorescence values without the need for electrophoretic separation of samples. Moreover, using the TRAPezeXL kit in a real-time mode [23, 24] instead of end-point fluorescence measurement greatly improves quantification of telomerase activity and maximizes the convenience of the assay. The general advantage of the real-time technique is that the basic value used for evaluation is not the total product generated by PCR, but rather a threshold cycle that always occurs in the exponential phase of the amplification; thus, quantification is not affected by any reaction component becoming limiting in the plateau phase, which would result in a systematic bias against the more abundant template and make quantification based on measurements of overall product yield intrinsically unreliable. The RQ-mode gives the opportunity not only to evaluate telomerase activity but also to recognize false-positive results directly from the reaction kinetics, thus avoiding time-consuming postamplification analysis. False-negative results can be detected in the rhodamine channel for all samples, including the nontemplate control.

3.5.1 Preparation of Samples

1. Follow the procedure described for conventional TRAP assays (*see* **Section 3.4.2**) or the manufacturer's instructions if using a lysis/extraction solution provided in a kit. Extracts prepared with either of the lysis/extraction buffers are compatible with dual-color real-time TRAP.
2. Prepare a telomerase-positive control extract (control 1) using 200 µL of CHAPS lysis buffer and the control cell pellet (10^6 cells) provided in the kit, or any other telomerase-positive cells relevant to the material to be tested. Divide the extract into 10-µL aliquots and snap-freeze in liquid nitrogen. Dilute the extract to 1,000 cells/µL before use.
3. Prepare dilutions of the control template TSR8* (0.1, 0.05, 0.025, and 0.010 amol/µL) separately from other pipetting work.
4. Prepare the other controls:
   (a) Minus-telomerase control (control 2): the extract is replaced with extraction buffer. Only an increase in sulforhodamine fluorescence should be observed, indicating the PCR amplification efficiency of the internal control (*see* **Note 27**). Detection of an increase in fluorescein emission in this reaction suggests either the presence of primer-dimer artifacts due to

suboptimal PCR conditions; the presence of PCR contamination (amplified TRAPEZE XL products) carried over from another assay; or the contamination of an assay component with telomerase-positive cell extract.

(b) Minus-*Taq* polymerase control (control 3): an assay excluding *Taq* polymerase. No increase of fluorescence signal should occur in either the sulforhodamine or the fluorescein channel; an increase may indicate undesirable polymerization-independent events, for example degradation of primers.

5. Prepare heat-inactivated parallels to all samples as controls reflecting telomerase-independent events. Heat 1 µL of cell or tissue extract diluted with 2 µL of RNase-free water (to compensate for evaporation) at 85°C for 10 min in 0.5 mL RNase- and DNase-free PCR tubes compatible with your real-time thermal cycler.
6. Thaw the 5× TRAPEZE XL Reaction Mix and make 200–300 µL aliquots to limit the number of freeze-thaw cycles and possible contamination of the whole reaction mix.
7. Prepare a master mix of all reagents (except for the extract). We suggest performing each real-time reaction in two parallel 25-µL samples consisting of 5.0 µL of 5× TRAPEZE XL Reaction Mix, 1.0 µL of 25 m*M* $MgCl_2$, and 17.8 µL of dH_2O.
8. At this stage, before addition of polymerase, aliquot 2× 23.8 µL of the mix for the minus-Taq polymerase control.
9. To the remainder of the mix, add 0.2 µL of Thermo-Start Taq DNA polymerase (5 U/µL) for each reaction aliquot, corresponding to 24µL final volume of the mix.
10. Aliquot 24 µL of the master mix into RNase-, DNase-free PCR tubes compatible with a real-time thermocycler. The number of aliquots should be sufficient for two parallel reactions of the following: samples, telomerase positive control extract, four dilutions of TSR8* control template, and minus-telomerase control (CHAPS buffer). For heat-inactivated controls, add the master mix directly to the tubes with the samples.
11. Add samples or remaining controls to prelabeled reaction tubes with the master mix.

3.5.2 Dual-Color Real-time TRAP and its Evaluation

The following description concerns the Rotor-Gene thermocycler type 3000 or 6000 (Corbett Research) for which the technique has been optimized. However, other instruments compatible with the excitation/emission parameters for fluorescein (495 nm/516 nm) and sulforhodamine (600 nm/620 nm) can be used.

1. Place all the reaction tubes in the real-time thermocycler. Set up the parameters for real-time TRAP:

   (i) Telomerase extension step at 30°C for 30 min.

(ii) Heat-inactivation of telomerase and activation of hot-start *Taq* DNA polymerase at 95°C for 15 min.
(iii) 40–45 cycles of denaturation at 94°C for 30 sec, annealing at 59°C for 30 sec (fluorescence is acquired in FAM (470/510) and ROX (585/610) channels in this step).
(iv) Extension at 72°C for 60 sec.
(v) Final extension step at 72°C for 3 min.

2. Run the program.

3.5.3 Evaluation of Results of Dual-Color Real-time TRAP

It is possible to perform either comparative or absolute quantification of fluorescence curves using the take-off or threshold cycle values (Ct) evaluated by the Rotor-Gene 3000 software (Fig. 17.2). As a basis for quantification, either a calibration curve calculated using TSR8* dilutions can be used (0.1 amol of TSR8* corresponds to 100 TPG units) (*see* Fig. 17.2, inserted window), or activity can be related to that observed in the extract from 1,000 control positive cells.

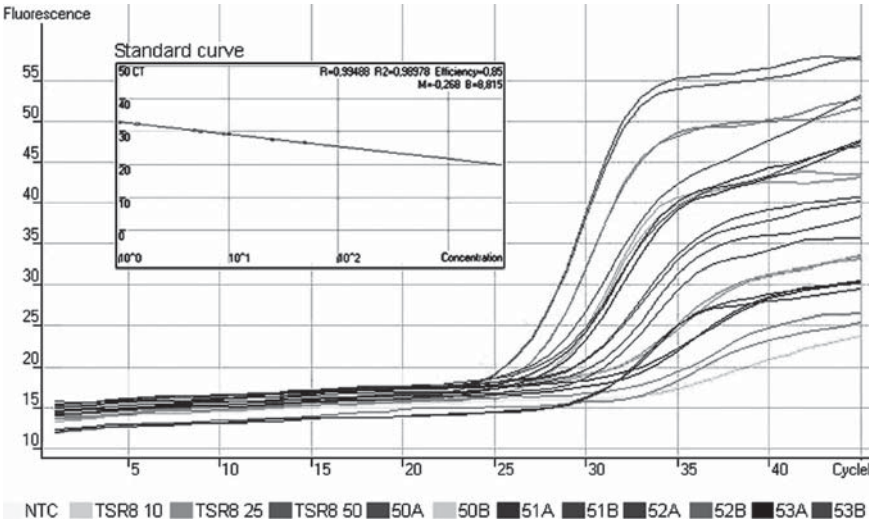

Fig. 17.2 An example of results of dual-color real-time TRAP. Fluorescence curves of standards (dilutions of TSR8 control template) and of samples are recorded in the FAM channel. *NTC*, nontemplate control; *TSR8 10*, 0.010 amol of TSR8; *TSR8 25*, 0.025 amol of TSR8; *TSR8 50*, 0.050 amol of TSR8; *50A–53B*, = samples, each analyzed in two parallel reactions. A calibration curve (*inserted window*) is used for evaluation. To view this figure in color, see COLOR PLATE 14

Whereas Ct data in the FAM channel are used for quantification, those from the ROX channel (reflecting amplification of the internal control) should be invariable in the absence of PCR inhibition and need not be included in the calculation. However, it is necessary to check for amplification in the ROX channel of all samples, including the nontemplate control, to check for possible false-negative results. Further, the end-point fluorescence values in both channels should display an inverse relationship arising from semicompetitive amplification of the telomerase products and internal standard (*see* **Notes 28** and **29** for more comments on evaluation).

4 Notes

1. To obtain enough DNA, you may need to try different isolation methods; the yield often depends on the tissue and is also species dependent.
2. Concatemer telomeric probes (as used for controls in **Section 3.1**) can be used instead of oligonucleotide probes. They should be labeled by nick-translation with incorporation of, e.g., alpha-[^{32}P] dATP using a commercially available kit (e.g., Amersham Biosciences), which can also be used for nonradioactive labeling, or by a simple protocol ***(25)*** based on protocols used for labeling FISH probes: the total 25-µL reaction mixture contains 1 µg of concatemer DNA, a dNTP mix (final concentrations 20 µ*M* dATP, 46 µ*M* each of dCTP, dGTP, and dTTP), 50 µCi of alpha-[^{32}P] dATP (6,000 Ci/mmol), 2.5 µL of 0.1 *M* DTT and 10× nick translation buffer (0.5 *M* Tris-Cl, pH 7.8, 50 m*M* $MgCl_2$, 0.5 mg/mL BSA), then 10 U of DNA polymerase I (New England Biolabs) and 1,000× diluted RQ/DNase I (1 U/µL; Promega) are added. The DNase concentration and labeling time at 16°C are optimized in a parallel nonradioactive reaction whose products are checked by electrophoresis on an agarose gel, so that an optimal fragment length of 300–500 bp is reached. During this electrophoresis, the reaction mixtures are kept on ice; the reactions can be restarted by reincubation at 16°C to achieve an optimal fragment length. Finally, the reaction products are deproteinized with phenol/chloroform, precipitated, and dissolved in sterile water.
3. For indirect labeling, biotin and digoxigenin are commonly used and are detected by antibodies conjugated to a fluorochrome, providing visualization of the signal. Nucleotides can also be labeled directly by fluorochromes, e.g., tetramethylrhodamine-5-dUTP or fluorescein-12-dUTP (Roche) and are detected directly.
4. A primer with the sequence CCCTAA has been found to provide better results than TTAGGG ***(13)***.
5. Of six hot-start Taq DNA polymerases tested, this shows the best compatibility with the reaction mixtures and TRAP conditions.
6. When using double-stranded DNA probes (concatemers or cloned DNA fragments), an additional higher-stringency washing step (0.2× SSC, 0.1% SDS) is recommended.

7. For analysis of telomeres longer than 15 kb, as is the case in mouse cells or in many model plants (e.g., tomato, tobacco, wheat, or barley), DNA is not extracted from agarose blocks but restriction enzyme digestion is performed directly in the blocks, which are then loaded onto the PFGE gel (*see* **Section 3.2.4**).
8. Instead of Southern hybridization, some laboratories prefer in-gel hybridization, which is especially suitable if information on single-strand G-overhangs is required. In this technique ***(26)***, the gel is dried in a vacuum dryer on filter paper for 1 h at 50°C, prehybridized for 1 h at 55°C, and hybridized with an end-labeled oligonucleotide probe for the C-strand sequence (3 h at 55°C). Gels are then washed 3× 20 min in 4× SSC at room temperature and 3× for 20 min in 4× SSC, 0.1% SDS at 57°C. Following native gel hybridization (or directly, if the result of the native hybridization is not required), dried gels are alkali denatured in 0.6 *M* NaCl, 0.2 *M* NaOH for 1 h, neutralized in 1.5 *M* NaCl, 0.5 *M* Tris-Cl, pH 7.4, rinsed in dH_2O for 30 min, and reprobed. While the native hybridization generates signals only on telomeric G-overhangs (and their intensity reflects the overhang length), the following reprobing represents the hybridization signal of all telomeric sequences irrespectively of their secondary structure or presence of an overhang.
9. The number of metaphase cells depends on the sample. For best results, their number can be increased by adding colcemid (0.01%) to the culture several hours before collecting the cells.
10. Another method is to make the slide a little wet by the steam coming from a warm water bath or by breathing on it, before dropping the cells, but we find that this is not necessary. For cytogenetics, nuclei fixed in acetic acid:methanol (1:3) are commonly used; the concentration should be determined empirically to get a monolayer of well-spread nuclei after dropping 10 µL on the slide. Several types of slides are commercially available, some precleaned, but it is better to clean them in ethanol before use.
11. Coating is performed by dipping slides in diluted poly-L-lysine solution (*see* **Section 2.3.1**) for 10 min, washing 3× in sterile water, and air-drying; they can be stored in the refrigerator. It is better to use slides coated at least 1 day before to avoid the poly-lysine film peeling off.
12. For nuclei of human cells, 8 min incubation in STE is sufficient, whereas mouse cells need a longer time. Usually it is necessary to determine the optimal time empirically.
13. When using a self-made master mix, perform nick translation reactions in 50 µL consisting of 2.5 µL of unlabeled nucleotide mix, 1 µL of labeled nucleotide (dig-, bio-, fluorescein-, or rhodamine-dUTP), 1 µL of DTT, 5 µL of 10× reaction buffer, 1 µg of DNA, and 5 µL of enzyme mix (DNaseI/polymerase I) made to 50 µL with sterile water. Continue the procedure in paragraph **Section 3.3.3.1** from **step 2**.
14. **Step 3** is not necessary when precipitation is done immediately; incubation on ice is sufficient. Labeling efficiency can be checked on an agarose gel, where DNA fragments of 100–500 bp should be visible. Probes can be tested by dot

blots, but results can be ambiguous and probes that give no signal on a dot-blot may hybridize properly in FISH; it is easier to test a probe directly by FISH.

15. Usually 20 µL of hybridization mix are used, but the volume can be varied depending on the area to be hybridized. More than one probe may be included in the mix, but dextran sulphate solution has to compose 50% of the volume. For repetitive sequences, 20–50 ng of probe is sufficient.
16. For fibre-FISH, 24×32-mm cover slips can be used because unlike metaphase chromosomes, fibers usually cover the whole area of the slide.
17. When using the DAKO PNA kit for Q-FISH, follow the instructions in the manual, which indicate that 2 h are sufficient for hybridization. The time for the procedure is reduced to one quarter, but this advantage has to be weighed against the price of the kit.
18. The stringency of washing can be regulated by:

    (i) Concentration of formamide; an increase increases stringency, but do not use a concentration >50%.
    (ii) Concentration of SSC; a decrease increases stringency.
    (iii) Temperature; an increase increases stringency.

    For PNA probes, high stringency can be used, which decreases background noise. For telomeric DNA probes, 45°C and 2× SSC, 50% formamide is optimal.
19. BSA or milk powder (3% w/v) can be used to block unspecific sites that could be recognized by antibodies.
20. Three-step antibody detection is necessary for fiber-FISH, but is optional for metaphase FISH. Generally, more detection steps increase signal intensity but also background noise. For directly labeled probes, skip **steps 18–27** and continue with DAPI staining.
21. Optionally, put wet cellulose into the Twin Tower in front of the shelves where the slides are located, instead of sealing the slides, which can sometimes produce dirt.
22. When signals are weak and amplification is needed, cycling PRINS based on PCR rather than on primer extension ***(27)*** can be used. Several cycles of denaturation, annealing, and extension are performed; for human and mouse telomeres, one step is sufficient.
23. For PRINS on mouse samples, different conditions (62.5°C for annealing and 65°C for elongation) have been used, and elongation time was only 10 min ***(28)***.
24. In particular cell or tissue types, the optimal protein concentration per assay may differ by up to ±one order of magnitude. When a new cell or tissue type is to be analyzed, it is suggested to carry out preliminary pilot reactions using two or three different concentrations to find an optimum ratio between telomerase and contingent TRAP-interfering compounds present in lysates.
25. For practical use, the relative TRAP activity of a given sample is further related to the TRAP activity of a positive control that is run on the same gel. This positive control may be an extract corresponding to a defined number of previously char-

acterized telomerase-positive cells (e.g., HeLa cells) and activity is then expressed in percentage of activity of these cells. Alternatively, a defined number of molecules of a quantitation standard (a linear DNA fragment with a TS primer-complementary sequence at one end and three to four telomeric repeats at the other, so that it can be amplified using the same primers as the primary products of telomerase-extended TS primer). In the TRAPeze kit (Chemicon), a standard of this kind is provided (TSR8*, *see* **Section 2.5.2**). Here, the amount of PCR product generated with 0.1 amol of TSR8* corresponds to 100 TPG units and activity in all samples is then expressed in TPG units.

26. Only the internal standard and a low background smear should be visible in both types of negative control, the heat inactivated sample, and the LE-only sample. The presence of ladders in negative controls may show cross-contamination of reactions, contamination of some reaction component with TRAP products, or PCR artifacts.
27. A PCR amplification control (internal control) is included in every assay by default. It is generated by amplification of a TSK2 template with a TS primer and a K2 Amplifluor primer (sulforhodamine-labeled). Amplification of this control (56 bp) is detected as an increase in sulforhodamine fluorescence in the ROX channel, and indicates that an eventual negative result is not only a false-negative due to inhibition of *Taq* polymerase.
28. Although performing TRAPezeXL reactions in real-time mode avoids postamplification procedures and provides more precise results, it is also possible to use the end-point fluorescence data from the fluorescence curves to evaluate results following the manufacturer's instructions, or to analyze TRAP products using PAGE (*see* **Section 3.4.3**).
29. An increase of fluorescence starting after the 35th cycle is a suspected artifact, and if the sample is to be included in evaluation, it should be checked by PAGE.

References

1. Muller, H. J. (1938) The re-making of chromosomes. *Collecting Net, Woods Hole* **13,** 182–198.
2. McClintock, B. (1941) The stability of broken ends of chromosomes in Zea mays. *Genetics* **26,** 234–282.
3. Moyzis, R. K., Buckingham, J. M., Cram, L. S., Dani, M., Deaven, L. L., Jones, M. D., Meyne, J., Ratliff, R. L., and Wu, J. R. (1988) A highly conserved repetitive DNA sequence, (TTAGGG)n, present at the telomeres of human chromosomes. *Proc. Natl. Acad. Sci. USA* **85,** 6622–6626.
4. Fajkus, J., Sykorova, E., and Leitch, A. R. (2005) Telomeres in evolution and evolution of telomeres. *Chromosome Res*. **13,** 469–479.
5. Levis, R. W., Ganesan, R., Houtchens, K., Tolar, L. A., and Sheen, F. M. (1993) Transposons in place of telomeric repeats at a Drosophila telomere. *Cell* **75,** 1083–1093.
6. Kamnert, I., Lopez, C. C., Rosen, M., and Edstrom, J. E. (1997) Telomeres terminating with long complex tandem repeats. *Hereditas* **127,** 175–180.

7. Greider, C. W. and Blackburn, E. H. (1985) Identification of a specific telomere terminal transferase activity in Tetrahymena extracts. *Cell* **43,** 405–413.
8. Greider, C. W. and Blackburn, E. H. (1987) The telomere terminal transferase of Tetrahymena is a ribonucleoprotein enzyme with two kinds of primer specificity. *Cell* **51,** 887–898.
9. Fajkus, J., Simickova, M., and Malaska, J. (2002) Tiptoeing to chromosome tips: facts, promises and perils of today's human telomere biology. Philos. Trans. R. Soc. Lond. B Biol. Sci. 357, 545–562.
10. d'Adda di Fagagna, F., Teo, S. H., and Jackson, S. P. (2004) Functional links between telomeres and proteins of the DNA-damage response. Genes Dev. 18, 1781–1799.
11. Smogorzewska, A. and de Lange, T. (2004) Regulation of telomerase by telomeric proteins. *Annu. Rev. Biochem*. **73,** 177–208.
12. Bryan, T. M., Marusic, L., Bacchetti, S., Namba, M., and Reddel, R. R. (1997) The telomere lengthening mechanism in telomerase-negative immortal human cells does not involve the telomerase RNA subunit. *Hum. Mol. Genet*. **6,** 921–926.
13. Krejci, K. and Koch, J. (1999) An in situ study of variant telomeric repeats in human chromosomes. *Genomics* **58,** 202–206.
14. Shay, J. W. and Bacchetti, S. (1997) A survey of telomerase in human cancer. *Eur. J. Cancer* **33,** 787–791.
15. Bodnar, A. G., Ouellette, M., Frolkis, M., Holt, S. E., Chiu, C. P., Morin, G. B., Harley, C. B., Shay, J. W., Lichtsteiner, S., and Wright, W. E. (1998) Extension of life-span by introduction of telomerase into normal human cells. *Science* **279,** 349–352.
16. Kim, N. W., Piatyszek, M. A., Prowse, K. R., Harley, C. B., West, M. D., Ho, P. L., Coviello, G. M., Wright, W. E., Weinrich, S. L., and Shay, J. W. (1994) Specific association of human telomerase activity with immortal cells and cancer. *Science* **266,** 2011–2015.
17. Fajkus, J. (2006) Detection of telomerase activity by the TRAP assay and its variants and alternatives. *Clin. Chim. Acta* **371,** 25–31.
18. Poon, S. S., Martens, U. M., Ward, R. K., and Lansdorp, P. M. (1999) Telomere length measurements using digital fluorescence microscopy. *Cytometry* **36,** 267–278.
19. Koch, J., Hindkjaer, J., Kolvraa, S., and Bolund, L. (1995) Construction of a panel of chromosome-specific oligonucleotide probes (PRINS-primers) useful for the identification of individual human chromosomes in situ. *Cytogenet. Cell Genet*. **71**,142–147.
20. Martens, U. M., Zijlmans, J. M., Poon, S. S., Dragowska, W., Yui, J., Chavez, E. A., Ward, R. K., and Lansdorp, P. M. (1998) Short telomeres on human chromosome 17p. *Nat. Genet*., **18**, 76–80.
21. Kim, N. W. and Wu, F. (1997) Advances in quantification and characterization of telomerase activity by the telomeric repeat amplification protocol (TRAP). *Nucleic Acids Res*. **25,** 2595–2597.
22. Bradford, M. M. (1976) A rapid and sensitive method for the quantitation of microgram quantities utilizing the principle of protein dye binding. *Anal. Biochem*. **72,** 248–254.
23. Elmore, L. W., Forsythe, H. L., Ferreira-Gonzalez, A., Garrett, C. T., Clark, G. M., and Holt, S. E. (2002) Real-time quantitative analysis of telomerase activity in breast tumor specimens using a highly specific and sensitive fluorescent-based assay. *Diagn. Mol. Pathol*. **11,** 177–185.
24. Fajkus, J., Koppova, K., and Kunicka, Z. (2003) Dual-color real-time telomeric repeat amplification protocol. *Biotechniques* **35,** 912–914.
25. Neplechova, K, Sykorova, E., and Fajkus, J. (2005) Comparison of different kinds of probes used for analysis of variant telomeric sequences. *Biophys. Chem*. **117,** 225–231.
26. Hemann, M. T. and Greider, C. W. (1999) G-strand overhangs on telomeres in telomerase deficient mouse cells. *Nucleic Acids Res*. **27,** 3964–3969.
27. Musio, A. and Rainaldi, G. (1997) Cycling-PRINS. A method to improve the accuracy of telomeric sequence detection in mammalian chromosomes. *Mutat. Res*. **390,** 1–4.
28. Lavoie, J., Bronsard, M., Lebel, M., and Drouin, R. (2003) Mouse telomere analysis using an optimized primed in situ (PRINS) labeling technique. *Chromosoma* **111,** 438–444.

Chapter 18
Combined Immunofluorescence, RNA Fluorescent In Situ Hybridization, and DNA Fluorescent In Situ Hybridization to Study Chromatin Changes, Transcriptional Activity, Nuclear Organization, and X-Chromosome Inactivation

Julie Chaumeil, Sandrine Augui, Jennifer C. Chow, and Edith Heard

Keywords Immunofluorescence; Fluorescent in situ hybridization; RNA FISH; DNA FISH; Nuclear organization; X inactivation

Abstract Epigenetic mechanisms lead to the stable regulation of gene expression without alteration of DNA and trigger initiation and/or maintenance of cell-type-specific transcriptional profiles. Indeed, modulation of chromatin structure and the global 3D organization of the genome and nuclear architecture participate in the precise control of transcription. Thus, dissection of these epigenetic mechanisms is essential for our understanding of gene regulation. In this chapter, we describe challenging combinations of immunofluorescence, and RNA and DNA fluorescent in situ hybridization and their application to our studies of a remarkable example of epigenetic control of gene expression in female mammals, the process of X chromosome inactivation.

1 Introduction

The extraordinary diversity of cell lineages that form a multicellular organism requires the establishment and the maintenance of complex gene expression pathways and epigenetic mechanisms (heritable modification of gene expression without alteration of DNA sequence) are clearly at the heart of these processes ***(1, 2)***. First, chromatin modulation itself can define active or repressive functional genomic regions. On a larger scale, global 3D organization of the genome and nuclear architecture also participate in the precise control of transcription. In this context, cell biology techniques such as immunofluorescence (IF), and RNA and DNA fluorescent in situ hybridization (FISH) represent powerful tools for dissection of epigenetic mechanisms and, thus, for our understanding of the creation of specific transcription patterns. Immunofluorescence allows the visualization of nuclear

R. Hancock (ed.) *The Nucleus: Volume 1: Nuclei and Subnuclear Components*,

proteins (histone variants or modified histones, specific nuclear compartments, etc.); DNA FISH enables the labeling of gene loci and chromosome territories; nuclear RNA FISH permits the detection of noncoding RNAs and primary transcripts at gene loci (to assay for the transcriptional status of a gene ***(3)***). Such techniques have been used to investigate: 1) the specific 3D organization of chromosomes in the nucleus, with respect to chromosome size, gene density, tissue-specificity ***(2, 4)***, 2) the role of the gene location with respect to a chromosome territory and/or specific nuclear compartments in their transcriptional regulation ***(2, 5, 6)***, 3) the impact of chromatin modulation (post-translational histone modifications, incorporation of histone variants, chromatin remodelling complexes, non-coding RNAs and DNA methylation) on gene expression ***(1, 7, 8)***.

Our laboratory works on X-chromosome inactivation, a developmental process that involves the silencing of one of the two X chromosomes in female mammals, and enables dosage compensation between XY males and XX females for X-linked gene products. X inactivation represents a powerful model system for the investigation of the formation of facultative heterochromatin. Over the past decades, many lines of evidence have shown that non-coding RNAs, chromatin modifications, and nuclear organization are involved in X inactivation ***(9)***. The initiation of this process is dependent on the non-coding Xist RNA, which coats the future inactive X chromosome in cis (*see* Fig. 18.1) and induces its silencing. Xist RNA also leads to the recruitment of a number of epigenetic features involved in the maintenance of this inactive state (*see* Figs. 18.2 and 18.3). We have used extensively IF, RNA FISH, and DNA FISH as tools for defining the kinetics of these events and their potential causal relationships. Female embryonic stem (ES) cells provide a useful tissue culture system for studying X inactivation, because X inactivation can be recapitulated during their in vitro differentiation. In undifferentiated female ES cells, both X chromosomes are active and the two Xist alleles are expressed at low levels. This is detectable by RNA FISH as two punctate signals (or "pinpoints") at their sites of transcription (Fig. 18.1). At the onset of X inactivation, the Xist allele on the chromosome that will be inactivated is up-regulated, and the RNA accumulates in cis over the territory of the X chromosome in interphase nuclei. This "coating" can be detected by RNA FISH as a domain covering ~70% of the X chromosome territory, whereas the Xist allele on the other X chromosome is progressively silenced (Fig. 18.1) ***(10)***. Xist RNA coating is followed (1–2 days later) by transcriptional silencing of X-linked genes, based on the disappearance of primary transcript signals detected by RNA FISH at the Xist RNA domain (*see* Fig. 18.4).

In this chapter, we outline protocols for combinations of IF, RNA FISH, and DNA FISH that we have applied and developed for our studies of the changes associated with the X-inactivation process and the epigenetic and nuclear changes at the same time as transcriptional status, at the single-cell level, during ES cell differentiation. The main challenge of a combined IF and FISH analysis is, on the one hand, to preserve nuclear organization and the epitope detected by the antibody (IF) as far as possible but, on the other hand, to allow the penetration of the FISH probe for detection of nuclear primary transcripts (RNA FISH), gene loci, or chromosome territories (DNA FISH). As the optimal conditions for each technique are often

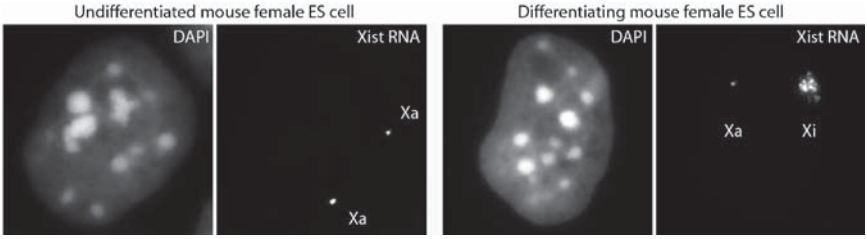

Fig. 18.1 Xist RNA FISH in mouse female ES cells. In undifferentiated cells, Xist primary transcripts are detectable as two pinpoints at their sites of transcription on the two active X chromosomes (*left panel*). During differentiation, Xist RNA coating of the X chromosome undergoing inactivation is detected as a domain covering the majority of the X chromosome territory, whereas the other Xist allele is progressively silenced (*right panel*). DAPI is shown in *gray. Xa*, active X chromosome; *Xi*, inactive X chromosome. Bar, 5 μm

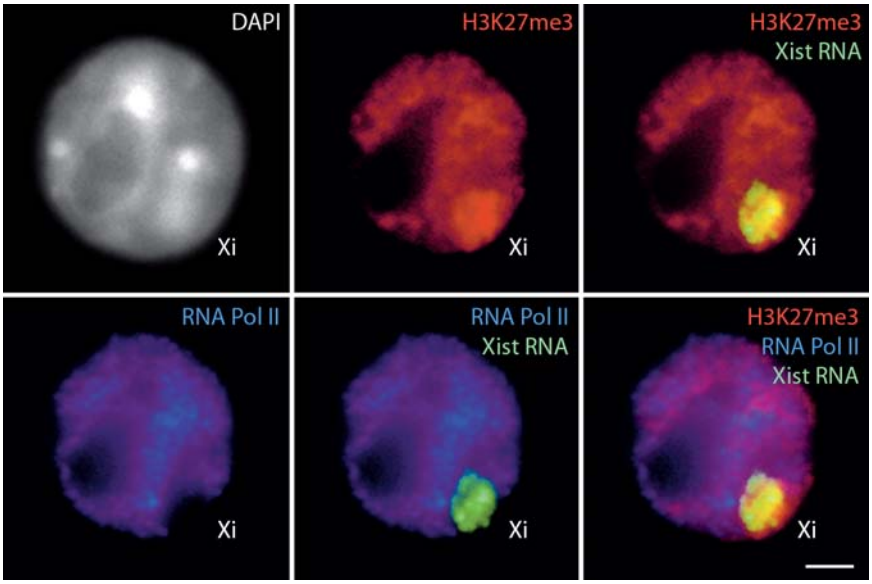

Fig. 18.2 Dual immunofluorescence combined with RNA FISH in differentiated mouse female ES cells. RNA FISH detects Xist RNA coating of the X chromosome undergoing inactivation (*green*), combined with dual IF showing the specific enrichment in histone H3 tri-methylated on lysine 27 (H3K27me3) (*red*) and the exclusion of RNA polymerase II (Pol II; blue) on the inactive X chromosome. DAPI is shown in gray. Bar, 5 μm. To view this figure in color, see COLOR PLATE 15

poorly compatible with each other, we have tested various methods. Here we describe protocols that we find optimal for the detection of nuclear proteins combined with RNA or DNA FISH, as well as combined RNA and DNA FISH on mouse fibroblasts or embryonic stem cells. The reader is also referred to **refs.** ***(10–12)***.

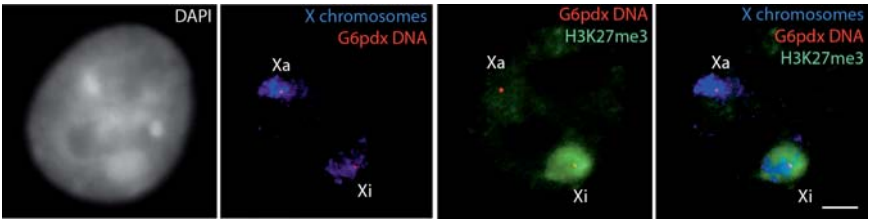

Fig. 18.3 Immunofluorescence combined with dual DNA FISH in differentiated female mouse ES cells. Dual DNA FISH detecting both X chromosomes (*blue*) and the two alleles of the X-linked G6pdx gene (*red*), combined with an IF showing the specific enrichment in H3K27me3 on the inactive X chromosome (*green*). DAPI is shown in *grey Xa*, active X chromosome; *Xi*, inactive X chromosome. Bar, 5 µm. To view this figure in color, see COLOR PLATE 16

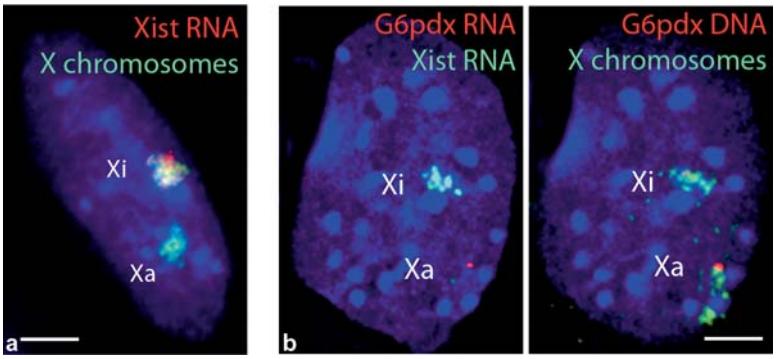

Fig. 18.4 Examples of combined RNA and DNA FISH in differentiated female mouse ES cells. **a** Simultaneous RNA–DNA FISH. Xist RNA FISH (*red*) is combined with X chromosome DNA FISH (*green*). DAPI is shown in *blue*. **b** Sequential RNA–DNA FISH. The dual RNA FISH detects Xist RNA (*green*) and G6pdx primary transcript (*red*) (*left panel*). The absence of G6pdx RNA signal on the Xist RNA-coated X chromosome confirms its silencing on the inactive X chromosome. The subsequent DNA FISH detects X chromosomes (*green*) and G6pdx alleles (*right panel*). DAPI is shown in *blue. Xa*, active X chromosome; *Xi*, inactive X chromosome. Bars, 5 µm. To view this figure in color, see COLOR PLATE 17

Part of this protocol was first published by the European Network of Excellence "The Epigenome" in open access format (http://www.epigenome-noe.net) ***(13)***.

2 Materials

2.1 Cell Culture on Slides or Coverslips

Culture cells for at least 24–48 h on SuperFrost slides (Menzel Gläser; Bioblock, Illkirch, France) or coverslips (18×18 mm, ESCO; VWR, Fontenay, France) coated with gelatin (Merck, Fontenay-sous-Bois, France).

2.2 Fixation and Permeabilization

1. Fresh PBS: We use 10× PBS diluted in water for cell culture (both Sigma-Aldrich, Saint-Quentin Fallavier, France or St. Louis, USA).
2. Fixation solution: filter-sterilised 3% paraformaldehyde (PFA) in PBS, freshly made or store aliquots at −20°C.
3. Fresh permeabilization solution: PBS or CSK buffer, 0.5% v/v Triton X-100 (ICN, Orsay, France). Add an RNase inhibitor, 2 m*M* Ribonucleoside Vanadyl Complex (RVC) (New England Biolabs; OZYME, Saint Quentin Yvelines, France) in case of subsequent RNA FISH.
4. Cytoskeletal buffer (CSK): 100 m*M* NaCl, 300 m*M* sucrose, 3 m*M* $MgCl_2$, 10 m*M* PIPES, pH 6.8. Filter, sterilise, and store in aliquots at −20°C.

2.3 Immunofluorescence

1. Fresh blocking solution: 1% w/v BSA (Gibco; Invitrogen, Cergy Pontoise, France) in PBS. Store aliquots at −20°C.
2. Fresh antibody dilution buffer: use blocking solution, with an RNase inhibitor (0.4 U/mL RNAguard, Amersham; GE Healthcare, Orsay, France) in case of a subsequent RNA FISH.
3. Secondary antibodies: Alexa-conjugated fluorescent secondary antibodies (green (488), red (568), and infra-red (680) (Molecular Probes; Invitrogen).

2.4 FISH Probes

1. We label DNA probes by nick translation using fluorescent nucleotides (SpectrumGreen- and SpectrumRed-dUTP (Vysis; Abbott, Rungis, France) or Cy5-dUTP (Amersham)).
2. Formamide for probes: Once opened, store sterile formamide (Sigma-Aldrich) in 1-mL aliquots at −20°C.
3. 2× hybridization buffer: 4× SSC prepared from a stock solution of 20× SSC (Sigma-Aldrich), 40% w/v dextran sulfate (Sigma-Aldrich), 2 mg/mL BSA (Biolabs), and 400 m*M* RVC.

2.5 RNA and DNA FISH

1. Fresh 2× SSC diluted from 20× SSC (Sigma-Aldrich), water for cell culture (Sigma-Aldrich).
2. Formamide for washes: once opened, store sterile formamide (Sigma-Aldrich) in 50-mL aliquots at −20°C.

2.6 DNA Counterstaining and Mounting

1. Fresh DNA staining solution: 4′,6-diamidino-2-phenylindole dihydrochloride (DAPI) (Sigma-Aldrich), 0.2 mg/mL in PBS.
2. Mounting medium (*see* **step 14**): 90% v/v glycerol (Sigma-Aldrich), PBS, 0.1% w/v p-phenylenediamine (Sigma-Aldrich), pH 9. Should be "straw" colored; if it veers to purple or yellow, discard. Store at −20°C; always keep in the dark and on ice when aliquoting.

3 Methods

3.1 Immunofluorescence

Numerous methods involving a variety of fixation and permeabilization techniques can be used for IF applications, and the choice depends on cell type, epitope, and antibody being used ***(14)***. The following protocol is optimized for the detection of nuclear proteins in ES cells and mouse embryonic fibroblasts (MEFs).

1. Briefly rinse cells cultured on coverslips in freshly prepared PBS.
2. Fix in freshly made, filter-sterilised 3% PFA for 10 min at RT or 4°C.
3. Wash three times in PBS for 5 min each.
4. Permeabilize with freshly made PBS, 0.5% v/v Triton X-100 (in the case of subsequent RNA-FISH, add an RNase inhibitor, 2 m*M* RVC) on ice for 3–5 min. The exact time of permeabilization depends on the cell type and antibody, but a shorter time usually results in less efficient FISH.
5. Wash three times in PBS for 5 min each.
6. Block in 1% w/v BSA for 15 min at RT.
7. Incubate with primary antibody diluted in 1% BSA (containing 0.4 U/mL RNAGuard in the case of a subsequent RNA-FISH) for 45 min at RT in a dark and humid chamber. The temperature and length of incubation can vary between antibodies, as can the blocking agent (*see* **Note 1**).
8. Wash at least three times in PBS for 5 min each.
9. Incubate with secondary antibody (diluted in the same solution as in **step 7**) for 40 min at room temperature in a dark and humid chamber (*see* **Note 2**).
10. Wash at least three times in PBS for 5 min each.
11. Counterstain DNA with DAPI for 10 min.
12. Wash twice in PBS.
13. Mount the coverslip on a slide and fix it in place with a minimal amount of nail varnish.

3.2 Preparation of Probes for RNA FISH

To detect the primary transcripts of genes, genomic probes several kilobases long should be used. Probes spanning introns and exons will detect both the processed messenger RNA (mRNA) and the primary transcript. Oligonucleotides within intronic sequences will be specific for the primary transcript (*see* Robert Singer's web site for more details on the use of oligos as probes: http://singerlab.aecom.yu.edu/). For the detection of Xist RNA coating of the X chromosome in cis, or of primary transcripts of X-linked genes, we have used several genomic DNA probes spanning a minimum of 3 kb, labelled by nick translation or random priming, with success.

1. Genomic probes (plasmids, lambda clones, or BACs) to be used for RNA or DNA FISH are labeled by nick translation using 1–2 µg DNA per 50 µL reaction and following the manufacturer's instructions.
2. Approximately 0.1 µg of probe (usually 5 µL of a standard nick translation reaction of 50 µL) is ethanol precipitated together with 10 µg of salmon sperm DNA (molecular biology grade; Boehringer, Meylan, France) (sufficient for hybridization on an 18×18-mm coverslip).
3. The precipitated DNA is washed twice in 70% v/v ethanol and then air-dried.
4. The pellet is resuspended thoroughly in formamide (5 µL per coverslip), by pipetting and incubating at 37°C if necessary.
5. The probe is denatured for 7 min at 75°C.
6. 5 µL of 2× hybridization buffer are added to the denatured probe (for one coverslip). The probe solution is mixed well, and can be kept on ice for up to 30 min while coverslips are being prepared for the hybridization step.

3.3 RNA FISH

For a general description and discussion of RNA FISH protocols, the reader is referred to **ref.** ***(14)***. Conditions for detection of cytoplasmic versus nuclear RNAs are different, and here we focus only on the detection of nuclear transcripts.

1. Briefly rinse cells cultured on slides or coverslips in freshly prepared, RNase-free PBS: we use sterile cell culture 10× PBS and water, or stocks must be autoclaved.
2. Permeabilize in freshly made CSK buffer, 0.5% v/v Triton X-100 containing 2 m*M* RVC on ice for 5–7 min. Permeabilization in PBS, 0.5% v/v Triton X-100 can also be used, especially for IF combined with FISH, but CSK buffer is best suited for optimal nuclear RNA detection.
3. Fix in freshly made, filter-sterilised 3% PFA for 10 min at room temperature. The fixation step can also be done before permeabilization, especially for IF combined with FISH, but it may affect the quality of the detection of transcripts and increase the background.

4. Wash twice in 70% v/v ethanol for 5 min each. Slides or coverslips can be stored in 70% ethanol at −20°C for several months prior to use.
5. Prior to FISH, dehydrate the cells in 80%, 95%, and 100% v/v ethanol for 3 min each.
6. Air dry.
7. Deposit the denatured probe onto an RNase-free glass slide (fresh SuperFrost slides are RNase-free, and we keep boxes only for this purpose) and then place the coverslip onto the drop cell-side down, avoiding the formation of air bubbles. Once the coverslip has made contact with the probe solution, it should not be moved, to avoid damaging the cells.
8. Hybridize overnight at 37°C in a dark and humid chamber (made using paper tissues soaked in 50% v/v formamide in 2× SSC).
9. Remove the coverslips carefully with forceps and wash them three times in freshly made 50% formamide, 2× SSC (adjusted to pH 7.2) for 5 min each at 42°C.
10. Wash three times in 2× SSC for 5 min each at 42°C.
11. Counterstain DNA with DAPI.
12. Wash twice in 2× SSC for 5 min each.
13. Mount the coverslips on a slide and fix in place with a minimal amount of nail varnish.

3.4 Preparation of Probes for DNA FISH

1. Prepare the nick translation probe (*see* **Section 3.2**).
2. Precipitate 0.1 µg of probe with 10 µg of salmon sperm DNA, and 1–5 µg of Cot-1 DNA (Gibco; Invitrogen) if competition of repetitive sequences is required, per 18×18-mm coverslip.
3. Wash the pellet twice in 70% ethanol and air dry.
4. Resuspend the pellet in 5 µL of formamide per coverslip at 37°C.
5. Denature for 7 min at 75°C.
6. Add 5 µL of hybridisation buffer per coverslip (*see* stock solutions in **Section 2**).
7. Incubate to compete for 30 min to 1 h at 37°C.
8. For chromosome paint probes (Cambio, Cambridge, UK), we follow the supplier's recommendations for conditions of denaturation and competition.

3.5 DNA FISH on Coverslips

For a general description and discussion of DNA FISH protocols, the reader is referred to **ref.** ***(14)***.

1. Briefly rinse the cells cultured on coverslips in freshly made PBS.
2. Fix in filter-sterilised, freshly made 3% PFA for 10 min at RT.

3. Wash twice in PBS for 5 min each.
4. Permeabilize in freshly made PBS, 0.5% Triton X-100 on ice for 5–7 min.
5. Wash twice in 70% ethanol for 5 min each. Coverslips can be stored in 70% ethanol at −20°C for several months prior to use.
6. Dehydrate the slides in 80%, 95%, and 100% v/v ethanol for 3 min each.
7. Air dry.
8. Note that you can perform an RNase treatment at this stage in order to remove primary transcripts at the locus of the gene of interest (10 U/mL RNase A in 2× SSC, 1 h at 37°C).
9. Denature in 50% formamide, 2× SSC (adjusted to pH 7.2) for 30–45 min at 80°C. The exact time of denaturation is highly variable depending on cell type and differentiation status.
10. Wash three times in ice-cold 2× SSC or dehydrate the slides in cold ethanol.
11. Place the coverslip cell-side down onto the drop of probe (*see* **Section 3.3**, **step 7**).
12. Hybridize with the probe overnight at 42°C in a dark and humid chamber (paper tissues soaked in 50% formamide, 2× SSC).
13. Remove the coverslips carefully with forceps and wash them three times in 50% formamide, 2× SSC (adjusted to pH 7.2) for 5 min each at 42°C.
14. Wash three times in 2× SSC for 5 min each at 42°C.
15. If a biotin-labelled probe (e.g. a chromosome paint) is used, a detection step has to be included: block in 4× SSC, 0.1% v/v Tween 20, 5% w/v BSA (Gibco; Invitrogen) for 15 min at room temperature and incubate in fluorescently labelled streptavidin or avidin diluted in blocking buffer for 40 min at RT in humid chamber.
16. Wash three times in 2× SSC.
17. Counterstain DNA with DAPI.
18. Wash twice in 2× SSC for 5 min each.
19. Mount the coverslip and fix in place with a minimal amount of nail varnish.

3.6 DNA FISH on Slides

1. Follow the first seven steps described in **Section 3.5**.
2. Denature in 70% formamide, 2× SSC (adjusted to pH 7.2) for 2–4 min at 75°C. The time of denaturation can vary between cell types; we usually use 3 min.
3. Follow steps 10 to 19 in **Section 3.5**.

3.7 Combination of Immunofluorescence and RNA FISH (Fig. 18.2)

When IF and FISH are to be combined, we prefer to perform IF (under RNAse-free conditions) prior to FISH, because the formamide treatment during the FISH procedure is sometimes incompatible with preservation of the epitopes detected by some antibodies.

1. For the preparation of the RNA FISH probe, follow **Section 3.2**.
2. Follow **Section 3.1** up to **step 10**.
3. Post-fix in freshly made 3% PFA for 10 min at room temperature.
4. Wash twice in 2× SSC (freshly made from a sterile 20× stock) for 5 min.
5. Follow **steps 7** to **13** of **Section 3.3**.

3.8 Combination of Immunofluorescence and DNA FISH (Fig. 18.3)

The detection of DNA requires a DNA denaturation step, which can destroy the immunofluorescence signal in some cases. Therefore, if a microscope enabling the tracking of the coordinates of nuclei is available, IF images should ideally be recorded prior to performing DNA FISH using slides instead of coverslips, and without post-fixation between the two steps.

1. For preparation of the DNA FISH probe, follow **Section 3.4**.
2. Follow **Section 3.1** up to **step 10**.
3. Post-fix in freshly made 3% PFA for 10 min at room temperature.
4. Wash twice in 2× SSC (freshly made from a sterile 20× stock) for 5 min.
5. Permeabilize in freshly made 0.1 *M* HCl, 0.7% Triton X-100 for 10 min on ice.
6. Wash twice in 2× SSC for 5 min each.
7. Denature in 50% formamide, 2× SSC (adjusted to pH 7.2) for 30 min at 80°C. The exact time of this denaturation step is highly variable depending on cell type and differentiation status, as well as on the degree of fixation and the IF step that preceded denaturation. Different conditions should therefore be tested to ensure that the best compromise is made between denaturation and detectability of DNA on the one hand, and conservation of nuclear structure on the other.
8. Wash several times in ice-cold 2× SSC.
9. Follow **steps 10** to **19** of **Section 3.5**.

3.9 Combination of RNA FISH and DNA FISH (Fig. 18.4)

3.9.1 Simultaneous RNA–DNA FISH on Coverslips (Fig. 18.4a)

1. For preparation of the FISH probes, follow **Sects. 3.2** and **3.4** (*see* **Note 4**).
2. Follow **Section 3.5**. The time of denaturation is highly variable (also *see* **Section 3.5**), and different conditions should be tested in order to determine the best compromise between the detectability of DNA and preservation of the RNA signal. Note that the temperature of the overnight hybridization depends on the samples and probes: 42°C or higher is usually best for DNA FISH, but can lead to loss of the RNA FISH signal; in this case, use 37°C.

3.9.2 Sequential RNA–DNA FISH on Slides (Fig. 18.4b)

The detection of DNA requires a DNA denaturation step, which can destroy the RNA FISH signal in some cases. Furthermore, simultaneous RNA–DNA FISH to detect both the primary transcript of a gene and the locus itself is not feasible. In these cases, post-fixation (3% PFA in PBS for 10 min at room temperature) of the RNA signal prior to the DNA FISH should be used, although this dramatically affects the efficiency of DNA denaturation. Therefore, if a microscope enabling tracking of the coordinates of nuclei is available, RNA FISH images should be recorded prior to the DNA FISH.

1. For the preparation of the FISH probes, follow **Sects. 3.2** and **3.4.**
2. For RNA FISH, follow **Section 3.3**.
3. Record images and coordinates of nuclei on an appropriate microscope.
4. Scratch off the nail varnish.
5. Wash off the mounting medium in 4× SSC, 0.2% Tween-20, three times at 42°C.
6. Samples are incubated with 1 U/mL RNase A (Fermentas; EUROMEDEX, Mundolsheim, France) and 10 U/mL RNase X (New England Biolabs) in 2× SSC for 1 h at 37°C.
7. Follow **Section 3.6**.

4 Notes

1. The coverslips are placed cell-side down, avoiding the formation of air bubbles, onto a drop of antibody solution on a sterile glass slide. The volume depends on the size of coverslip used (we routinely use 18×18-mm coverslips and 40 µL of antibody solution). Following incubation, the coverslips are carefully removed with forceps and put back into PBS for washing. If resistance is encountered when removing the coverslip, it should be flooded with PBS so that it floats, in order to avoid damaging the cells.
2. For combined IF and RNA or DNA FISH, the choice of fluorochrome to which the secondary antibody is conjugated will depend on the fluorochrome with which the FISH probe is labelled, and on the filter sets available on the microscope. In the case of a double IF experiment, high-affinity purified secondary antibodies should be used (e.g. Molecular Probes, highly cross-absorbed antibodies) to minimise cross-species reactivity. Even then, appropriate controls (e.g. each primary with both secondary antibodies) should be performed systematically to confirm specificity.
3. We also sometimes label probes by random priming, particularly if the quantity of template DNA is limiting, or with fluorescently tagged oligonucleotides. The latter avoid the labelling step and also enable discrimination between sense or antisense transcripts (double-stranded DNA probes will of course detect both), but is costly. When nick translation is used for labelling, the size-range of the

labelled DNA must be checked by electrophoresis on a 1% agarose gel. The optimal size range for a FISH probe is between 50 and 200 bp, short enough to enter the nucleus but long enough to be specific. Fluorescently labelled probes of this kind can be stored at −20°C for a few weeks.

4. Note that RNA FISH and DNA FISH probes are precipitated separately and each is resuspended in half the volume used for a simple RNA or DNA FISH (e.g. 2.5 µL per coverslip). A competition is performed for the DNA FISH probe, and the two probes are mixed just prior to the overnight hybridization.

Acknowledgments We thank the EU Network of Excellence "The Epigenome" for permission to republish these procedures. Funding sources for this work were the Human Frontiers Science Program, EU FP6 Integrated Project HEROIC (LSHG-CT-2005-018883), the Schlumberger Foundation for Research, and the EU FP6 Network of Excellence "The Epigenome" (LSHG-CT-2004-503433). JC was funded by the French "Ligue Nationale contre le Cancer" and the HEROIC IP; SA was funded by the French "Centre National de la Recherche Scientifique"; JCC was funded by the HEROIC IP.

References

1. Fischle, W., Wang, Y., and Allis, C.D. (2003) Histone and chromatin cross-talk. *Curr. Opin. Cell Biol*. **15**, 172–183.
2. Dillon, N. (2006) Gene regulation and large-scale chromatin organization in the nucleus. *Chrom. Res*. **14**, 117–126.
3. Lawrence, J.B. and Singer, R.H. (1985) Quantitative analysis of in situ hybridization methods for the detection of actin gene expression. *Nucleic Acids Res*. **13**, 1777–1799.
4. Foster, H.A. and Bridger, J.M. (2005) The genome and the nucleus: a marriage made by evolution. Genome organization and nuclear structure. *Chromosoma* **114**, 212–219.
5. Baxter, J., Merkenschlager, M., and Fisher, A.G. (2002) Nuclear organization and gene expression. *Curr. Opin. Cell Biol*. **14**, 372–376.
6. Chambeyron, S. and Bickmore, W.A. (2004) Does looping and clustering in the nucleus regulate gene expression? *Curr. Opin. Cell Biol*. **16**, 256–262.
7. Nightingale, K.P., O'Neill, L.P., and Turner, B.M. (2006) Histone modifications: Signalling receptors and potential elements of a heritable epigenetic code. *Curr. Opin. Gen. Dev*. **16**, 125–136.
8. Mattick, J.S. and Makunin, I.V. (2006) Non-coding RNA. *Hum. Mol. Genet*. **15**, 17–29.
9. Heard, E. and Disteche, C.M. (2006) Dosage compensation in mammals: fine-tuning the expression of the X chromosome. *Genes Dev*. **20**, 1848–1867.
10. Chaumeil, J., Le Baccon, P., Wutz, A., and Heard, E. (2006) A novel role for Xist RNA in the formation of a repressive nuclear compartment into which genes are recruited when silenced. *Genes Dev*. **20**, 2223–2237.
11. Chaumeil, J., Okamoto, I., Guggiari, M., and Heard, E. (2002) Integrated kinetics of X-chromosome inactivation in differentiating embryonic stem cells. *Cytogen. Gen. Res*. **99**, 75–84.
12. Chaumeil, J., Okamoto, I., and Heard, E. (2004) X-inactivation in mouse embryonic stem cells: Analysis of histone modifications and transcriptional activity using immunofluorescence and FISH. *Methods Enzymol*. **376**, 405–419.
13. Chaumeil, J. (2005) Immunofluorescence–fluorescent in situ hybridization. Protocol for the Epigenome Network of Excellence (http://www.epigenome-noe.net).
14. Spector, D.L., Goldman, R.D., and Leinwand, L.A. (1998) *Cells: a laboratory manual*. Cold Spring Harbor Laboratory Press: Cold Spring Harbor, NY.

Chapter 19
Analysis of the Mobility of DNA Double-Strand Break-Containing Chromosome Domains in Living Mammalian Cells

Przemek M. Krawczyk, Jan Stap, Ron A. Hoebe, Carel H. van Oven, Roland Kanaar, and Jacob A. Aten

Keywords DNA double-strand breaks; Chromosome domain mobility; Live cells

Abstract DNA double-strand breaks (DSBs) are among the most dangerous types of DNA damage. Unrepaired, DSBs may lead to cell death, and when misrejoined, they can result in potentially carcinogenic chromosome rearrangements. The induction of DSBs and their repair take place in a chromatin microenvironment. Therefore, understanding and describing the dynamics of DSB-containing chromatin is of crucial importance for understanding interactions among DSBs and their repair. Recent developments have made it possible to study ionizing radiation-induced foci of DSB repair proteins in vivo. In this chapter, we describe techniques that can be applied to visualize and analyze the spatio-temporal dynamics of DSB-containing chromatin domains in mammalian cell nuclei. Analogous procedures may also be applied to the analysis of mobility of other intranuclear structures in living cells.

1 Introduction

Ionizing radiation is known to induce multiple types of DNA modifications. These include base adducts and pyrimidine dimers, single-strand breaks (SSBs), and double-strand breaks (DSBs) ***(1)***. Of these, DSBs are among the most dangerous. If unrepaired, or joined incorrectly, they may cause cell death or chromosome rearrangements that can lead to cancer ***(2–4)***. Living organisms are equipped with efficient surveillance and repair mechanisms that are responsible for keeping genetic information intact ***(5, 6)***. In mammalian cells, the majority of two-ended breaks, such as those caused by ionizing radiation, are repaired by the members of the nonhomologous end joining pathway, including the Ku70/Ku80 complex, the DNA-PK catalytic subunit, DNA ligase IV, and XRCC4. This repair pathway is active throughout the cell cycle, but it is error prone ***(7, 8)***. An alternative DNA repair system, homologous recombination, is active mainly in the S/G_2 phases of the cell cycle, at postreplicative chromatin, where duplicated DNA can serve as a template to accurately restore the damaged DNA to its original state. Proteins

R. Hancock (ed.) *The Nucleus: Volume 1: Nuclei and Subnuclear Components*,

involved in homologous recombination include Rad51, Rad54, the Rad51 paralogs, and the breast cancer-associated protein, BRCA2 ***(9)***.

DSB repair-related processes have been studied in great detail using biochemical and genetic methods ***(5)***. Recently, fluorescent protein technology has opened up the field of the DSB repair to living cell microscopy. Many DSB repair-related proteins have been reported to accumulate at microscopically discernible ionizing radiation-induced foci (IRIFs) at sites of DSBs ***(10)***. IRIFs may vary in size, accumulation, and lifetime. It is speculated that IRIFs might provide increased local protein concentrations needed for efficient DSB processing. IRIFs most probably mark a physiological chromatin microenvironment, suitable for DNA repair activities. Therefore, details on mobility, dynamics, and lifetime of the IRIFs are important to understand processing of DSBs at the chromatin and nuclear levels. Moreover, they can serve to resolve long-standing controversies concerning interactions between DSBs contained in the separate IRIFs and the formation of chromosome translocations ***(11–15)***.

Time-lapse imaging and analysis of processes in living cells requires meticulous DNA cloning and cell culture procedures as well as robust microscopy and image processing techniques ***(16)***. First, vectors expressing proteins of interest fused to fluorescent tags (usually GFP variants) are generated. The expression vectors must then be transferred into the DNA of mammalian cells. Cell lines expressing the proper amount of the fluorescently tagged protein of interest may then be used for imaging of cellular processes on which the tagged protein reports. Direct analysis of dynamics of intracellular structures is hindered by the mobility of the cell itself. Objects under analysis move relative to the coordinate system of the cell nucleus but, at the same time, this coordinate system rotates and translates as the cell moves. Therefore, to unify the coordinate system across the entire time series, the cell nuclei must be transformed back to the reference coordinate system of the nucleus at time point 0. This operation, further called alignment, can be achieved by various methods. To calculate the rotational and translational components of the cell movement, analysis of the density gradient of a fluorescence signal covering the entire cell nucleus can be used ***(17)***. Other methods are based on maximizing correlation functions ***[18, 19]*** and require extraction of features from the images followed by establishment of spatial correspondences between objects at subsequent time points.

In this chapter, we describe analysis of the dynamics of DSB-containing IRIFs labeled with 53BP1-GFP, a fluorescently tagged protein involved in the cellular response to DSBs ***(20)***. First, we describe the transfection of mammalian U2OS (osteosarcoma) cells with the expression vector and the isolation of stably transfected clones. Construction of the fusion protein expression vector is described elsewhere ***(21)***. We then provide a description of the microscopy technique used to capture 3D time-lapse images of gamma-radiation-induced IRIFs in living cells (*see* Fig. 19.1a). Next, cell translation and rotation during the imaging is eliminated using a data alignment approach based on the Iterative Closest Point (ICP) algorithm in Matlab scripting language ***(22)***. This method requires extraction of

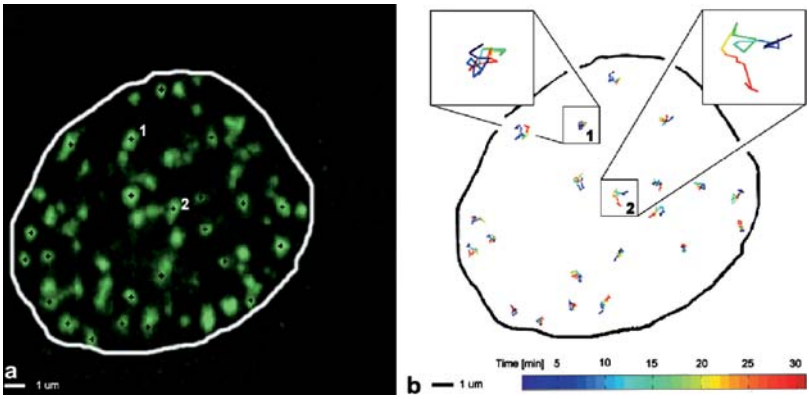

Fig. 19.1 Visualization and tracking of 53BP1-GFP IRIFs in a U2OS cell. **a** Maximum intensity projection of a reconstructed 3D image, 20 min after exposure to 4 Gy of gamma-radiation. The mobility of the IRIFs marked by *black crosses* was analyzed (*see* **b** and Fig. 19.2). **b** Visualization of trajectories of IRIFs. *Inlays* show magnified trajectories of two spots; the *color* of the trajectories indicates time. To view this figure in color, see COLOR PLATE 18

IRIF's positions from the pictures using image thresholding ***(23)***, followed by calculation of the individual centers of gravity (the most stable description of their position). To correct for the movement of the nucleus between time point 0 and a given time point, the coordinates of all centers of gravity at a given time point are aligned with the coordinates at time point 0 using ICP. The aligned coordinate sets are then checked for IRIFs that, within a single time interval, moved over a distance exceeding a preset value. This can be a consequence of optical merging or disappearance of objects leading to false nearest neighbor correspondence assignment. Such false-assigned events are removed from the coordinate sets and excluded from the analysis. Following alignment, the spatio-temporal properties of the IRIFs in the cell nucleus can be analyzed. The data on IRIF's dynamics are presented as the mean squared displacement (MSD) and an average of displacements of all IRIFs in the analyzed cell per time step (*see* Figs. 19.2a–c). The slope of the initial part of the MSD versus time can be used to calculate the diffusion coefficient of the IRIFs. The shape of the MSD curve can be used to obtain information on the type of process (unrestricted diffusion, restricted diffusion, or directed motion) that governs the dynamics of the IRIFs.

The procedure described here has been used by the authors to analyze the mobility of other nuclear structures, e.g., intranuclear aggregates of ataxin1-GFP (***24***), centromeres labeled by CENPB-GFP, fluorescently labeled nucleotides incorporated into DNA, and telomeres labeled by TRF2-GFP (data not shown). Depending on the research question, the live-cell imaging, image processing and data analysis procedures described here can be adapted to individual needs.

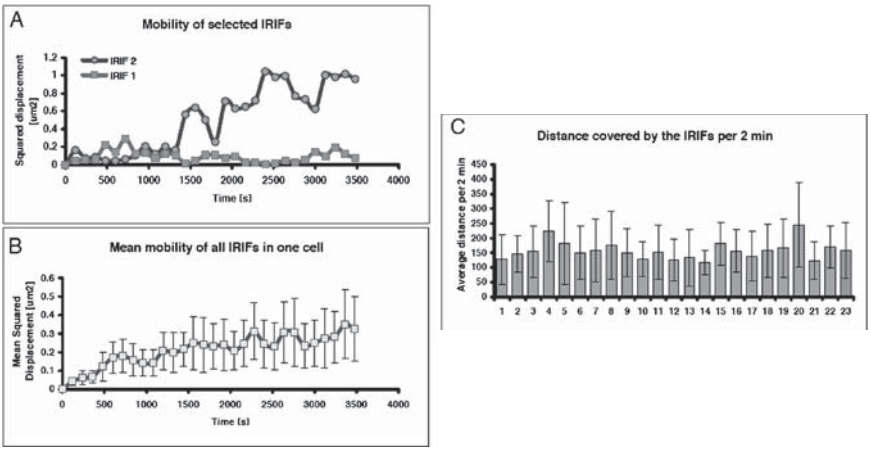

Fig. 19.2 Analysis of the mobility of 53BP1-GFP IRIFs. **a** Squared displacement of two IRIFs (magnified in Fig. 19.1b) from their positions at time 0 as a function of time. **b** Mean squared displacement (MSD) of all IRIFs from their positions at time 0 as a function of time. **c** Mean displacement per time step (2 min) of the individual IRIFs (*bars 1–22*) and of all IRIFs in the analyzed cell (*bar 23*). Error bars indicate standard deviation

2 Materials

2.1 Microscopy

1. Inverted wide-field fluorescence, phase contrast microscope (e.g., Leica IR-BE; Leica Microsystems, Wetzlar, Germany; or other inverted fluorescence microscope with a Z-motor drive, *see* **Note 1**).
2. Incubator enclosing the microscope, maintaining an atmosphere of 10% CO_2 at 37°C (custom-made or other microscope incubator).
3. Motorized microscope stage (Märzhäuser, Wetzlar, Germany), allows for simultaneous imaging of multiple fields in one experiment.
4. Light source for fluorescence imaging: mercury or metal halide lamp (e.g., metal-halide EL6000; Leica). Metal-halide lamps, although more expensive, provide longer lifetime. Also, their intensity can be manually adjusted.
5. A filter cube for GFP imaging (Leica C1, excitation 450–490 nm, emission 500–550 nm).
6. Cooled CCD camera (KX85; Apogee Instruments, Auburn, CA, USA).
7. A Plan apo ×63/1.40 oil objective (Leica).
8. Glass-bottom cell culture dishes (Fluorodish FD35; World Precision Instruments, Stevenage, Hertfordshire, England).

9. Custom-made fixture for the glass-bottom cell culture dishes on the microscope table.
10. Image Pro Plus (IPP) software (Media Cybernetics, Bethesda, MD, USA).
11. Time-lapse image acquisition plug-in with auto-focusing routine, custom-written for IPP or other time-lapse, 3D image acquisition software.

2.2 Cell Culture and Transfection

1. U2OS osteosarcoma cell line.
2. 37°C incubator, 10% CO_2.
3. Dulbecco's Modified Eagle's Medium (DMEM) (Gibco; Invitrogen, Carlsbad, CA, USA) supplemented with 10% fetal bovine serum.
4. Solution of trypsin (0.25% w/v) and 1 m*M* ethylenediamine tetraacetic acid (EDTA) (Gibco).
5. 35-mm and 10-cm cell culture-treated plastic Petri dishes.
6. pEGFP-N1 mammalian expression vector containing full-length 53BP1 insert ***(21)***.
7. Fugene 6 transfection reagent (Roche Diagnostics, Indianapolis, IN, USA).
8. DMEM for transfection without fetal bovine serum (Gibco).
9. Puromycin (BD Biosciences, Erembodegem, Belgium).
10. Inverted phase contrast, cell-culture microscope with ×10 objective.

2.3 Ionizing Radiation Source

1. A cesium (^{137}Cs) gamma-radiation source.

2.4 Image Processing

1. Huygens Pro image deconvolution software (Scientific Volume Imaging, Hilversum, The Netherlands).
2. Matlab programming environment (Mathworks, Natick, MA, USA).
3. DipImage image processing toolbox for Matlab (Quantitative Imaging Group, Delft University of Technology, Delft, The Netherlands).
4. Iterative Closest Point (ICP) alignment algorithm ***(22)***, implementation custom-written in Matlab scripting language.
5. Semi-automatic image alignment routine based on ICP, custom-written in Matlab programming language.

3 Methods

3.1 *Transfection and Isolation of a Stable Cell Line Expressing 53BP1-GFP*

This section describes transfection of cells with the 53BP1-GFP expression vector and isolation of stably transfected clones.

1. Maintain the U2OS cells in DMEM supplemented with 10% FCS and antibiotics in an atmosphere containing 10% CO_2.
2. 24 h prior to transfection, plate 5×10^6 cells into a 10-cm Petri dish.
3. Mix 6 µg of expression-plasmid DNA with 1 mL of serum-free DMEM, add 20 µL of Fugene 6, and incubate 15 min at room temperature. Adjust the DNA/Fugene ratio according to the Fugene 6 product manual if transfection efficiency is low.
4. Add the mixed reagents to the Petri dish, incubate for 24 h.
5. Add puromycin to the culture medium to a final concentration of 1 µg/mL. After this step, maintain cells in culture medium supplemented with puromycin (*see* **Note 2**).
6. Incubate cells for 5–7 days, refreshing the medium every 2–3 days.
7. Trypsinize the cells; use a 5-mL syringe with a 21-gauge needle to obtain a single-cell suspension. Count and plate the cells into four new dishes at concentrations of 10^5, 10^4, 10^3, and 10^2 cells per dish. Incubate for 6–7 days until single colonies consisting of at least 100 cells are formed.
8. Observe the dishes with colonies using an inverted fluorescence microscope with a ×10 objective. Using a felt-tip pen, mark (on the bottom side of the culture dish) the positions of 20–30 colonies of cells containing green nuclei (*see* **Note 3**).
9. Install an inverted cell culture microscope equipped with a ×10 objective in a laminar flow cabinet to avoid contamination. Trypsinize the cells in the 10-cm dish while carefully observing them under the microscope. Carefully add 10 mL of medium when the cells round up, but are still attached to the bottom. Transfer the dish onto the microscope. Use a 100-µL micropipette cleaned with 70% ethanol and sterile tips to carefully suck up the cells while scratching the marked green colonies with the tip. Take care not to mix two or more colonies. Transfer each collected colony into a 35-mm culture dish and incubate until the cultures are 20–50% confluent, then check the cells in each dish for GFP expression. Subculture dishes containing a high percentage of stably expressing cells into 75-cm^2 flasks.
10. Test the selected cell lines for the presence of 53BP1-GFP protein by immunoblotting using antibodies against both 53BP1 and GFP. Cell lines expressing truncated protein products should be excluded. Screen for cell lines displaying equal expression levels of endogenous and GFP-tagged 53BP1. Freeze suitable cells in liquid nitrogen for extended storage.

3.2 Irradiation of Cells and Time-Lapse Microscopy

In this section, we describe cell culture conditions and irradiation, followed by time-lapse 3D microscopy of the IRIFs in living cells (*see* also **ref. 25**).

1. Plate 7.5×10^5 cells into a glass-bottom dish, 24 h prior to the experiment (*see* **Note 4**).
2. Irradiate the cells with the required dose. Typically, 4–5 Gy should yield a number of IRIFs sufficient for analysis. Keep the dish with cells on a 25-cm^2 culture flask filled with 37°C water during irradiation to minimize cooling of the cells.
3. Put a drop of immersion oil on the ×63/1.4 objective. Mount the dish onto the microscope stage. Wait 5–10 min until the temperature inside the incubation chamber is stabilized.
4. Pick cells for imaging. Select multiple imaging fields if a motorized XY microscope stage is available.
5. Image cells for the required length of time, using auto-focusing if available. Illuminate cells as short as possible to minimize phototoxicity (*see* **Note 5**). Acquire 5–10 optical sections, with 300–500 nm Z interval (*see* **Note 5**). Save images as single-channel, gray-scale 3D stacks in ICS 1.0 format (*see* **Note 6**).

3.3 Image Processing and Object Extraction

This section provides step-by-step instructions for the image processing required for extraction of IRIF coordinates from captured 3D images using Matlab and DipImage. The dynamic behavior of cells on a coverslip poses a serious problem for the analysis of dynamics of objects inside living cells because nuclei of living cells undergo constant morphological changes and they move. Correction for the mobility of the cell nucleus is performed using the coordinates of IRIFs extracted from the images after thresholding. Each subsequent operation is illustrated in the example Matlab code. Where applicable, the numbers in parenthesis identify the lines where the described operation is executed in the example code. The line numbers refer to the position in the file "IRIFtracking.m" when it is opened in Matlab. The "IRIFtracking.m" file and files containing the ICP algorithm code as well as installation instructions can be downloaded from http://www.amc.nl/cmo.

1. Process 3D images with Huygens 2 software (*see* Fig. 19.1a). Use the classic iterative MLE deconvolution algorithm.
2. Compare the shape of the analyzed nucleus in the first and the last image of the time series. Exclude nuclei that undergo extensive morphological changes from the analysis (*see* **Note 7**).
3. Perform gaussian filtering of the image with large sigma (code line 51, also *see* **Note 8**).

4. Segment the gaussian-filtered image using isodata thresholding to find pixels that belong to the cell nucleus (code line 52, also *see* **Note 9**).
5. Process the original image using the median filter with a sigma comparable to the size of the IRIFs (code line 53, also *see* **Note 10**).
6. From the median-filtered image, isolate pixels that were detected as belonging to the cell nucleus (code line 54).
7. Detect the IRIFs by isodata thresholding of the nuclear part of the median-filtered image (code lines 55–56).
8. Calculate the coordinates of the gravity centers of the detected IRIFs (code line 57).

3.4 Data Alignment and Analysis

After image processing and extraction of the IRIF's coordinates from all images forming a time series, the 3D data clouds must be corrected for the movement of the cell nuclei. The movement of the cell nucleus is treated here as rigid body transformation, consisting of translational and rotational components in the *x*-*y* plane. The ICP algorithm is used here to align the clouds of IRIF coordinates ***(23)***. To describe the dynamics of IRIFs in living cell nuclei, the mean square displacement (MSD), average distance covered by the IRIFs per time step, and their average diffusion coefficient are calculated.

1. For all time steps, calculate the shift between the image at time point t_i and t_{i-1} (code lines 79–86, *see* **Note 11**).
2. For all time steps, shift coordinates from the time point t_i to prealign them with the coordinates at time point t_{i-1} (code lines 88–89).
3. For all time steps, find the indices of the nearest neighbor of each object from the coordinate set at time t_{i-1}, in the coordinate set from the subsequent time point t_i (code line 91–92).
4. Find and remove multiple-assigned nearest neighbors (code line 94–101, also *see* **Note 12**).
5. Apply the ICP algorithm to the coordinate set from the first (t_0) time point and coordinate sets from all subsequent ($t_{1,2,3,\ldots n}$) time points to calculate the rotation and translation between the first and all subsequent time points (code line 111).
6. Apply the rotation and translation to the data sets (code line 113).
7. Find and remove objects that in a single time step moved further than the allowed distance (code lines 119–125, also *see* **Note 13**).
8. Perform definitive ICP alignment of the first (t_0) and subsequent ($t_{1,2,3,\ldots n}$) coordinate sets to calculate the rotation and translation matrices (code line 134).
9. Apply the rotation and translation to the data sets (code line 135). At this time, the data can be plotted to visualize the trajectories of IRIFs (*see* Fig. 19.1b).

10. Using the calculated rotation and translation, align all images from the time series to the first image. Create maximum intensity projections (MIPs) of aligned images. Mark the MIPs by black crosses at the coordinates of the gravity centers of the IRIFs for visualization purposes (code lines 141 and 216–245, also *see* Fig. 19.1a).
11. Check images visually for objects that may have been assigned incorrectly, exclude these from further analysis (*see* **Note 14**).
12. For each IRIF, calculate the squares of the distances between the positions of the IRIF at time point t_0 and at time points $t_{1,2,3,...n}$. Calculate the mean of the distances of all IRIFs after each time point (code lines 145–153, also *see* Figs. 19.2a, b).
13. Calculate the mean displacement of all objects in the cell per time step (code line 154, also *see* Fig. 19.2c).

4 Notes

1. Here we describe the use of a conventional wide-field fluorescence microscope; a confocal microscope is also suitable and has the advantage of a better resolution in the *z*-direction. A disadvantage is that, compared with excitation under a conventional fluorescence microscope, more phototoxicity is induced by the laser scanning of a confocal microscope. However, recent findings demonstrate reduced phototoxicity and bleaching using a modified confocal microscope ***(26)***. When using a nonconfocal system, it should be equipped with a motorized Z-drive, which enables 3D imaging.
2. The cells may be FACS-sorted after this step to enrich the GFP-expressing population. Puromycin is an antibiotic toxic for mammalian cells; the pEGFP-N1 vector contains a puromycin-resistance gene and incubation of pEGFP-N1–transfected cells in medium complemented with puromycin selects for cells stably expressing the construct. It is recommended, but not always necessary, to maintain stable cell lines in the presence of the antibiotic.
3. Expression levels within the transfected cell population can vary to a high degree. The amount of expressed GFP fusion protein should be comparable to the level of endogenous protein. Therefore, colonies of cells with medium-low to medium levels of GFP in the nucleus and low levels in the nucleoli and cytoplasm should be selected.
4. To limit movement of cells, which is convenient for the processing of images, cells should be >90% confluent at the time of experiment. Avoid overconfluency; nuclei of cells in overconfluent cultures may be rounded-up and require collecting more optical sections to capture the entire *z*-depth of the nucleus.
5. Prolonged exposure of cells to fluorescent light is toxic due to free radical production and resulting protein and DNA damage. The fluorescence intensity of GFP fusion proteins varies between clones and cells. The exposure time should therefore be adjusted for each cell individually. As a rule, the minimal exposure

time necessary to obtain images sufficiently exposed should always be used. Note that an image that looks very noisy frequently contains enough information for the image deconvolution software. The number of optical sections per time point should also be limited; between 5 and 10 sections at 300–500-nm intervals is enough to image most of the cell nucleus of flat, adherent cells. More sections may be required for cells with less flat nuclei and for cells in overconfluent cultures.

6. If the image capturing software does not support the ICS file format, the images may be saved in another format and later converted using DipImage.
7. Chromatin is tightly connected to the nuclear membrane. Therefore, changes of the nuclear morphology result in apparent motion of the IRIFs that are located close to the membrane. This motion can lead to overestimation of the IRIF's mobility. Therefore it is suggested that cell nuclei undergoing morphological changes be excluded from the analysis.
8. Filtering the image with a gaussian filter with large sigma reduces noise and enhances large objects (such as the cell nucleus).
9. Isodata thresholding is based on the intensity histograms of the entire image. In an image of a 53BP1-GFP-expressing cell, the intensity of areas outside of the cell nucleus is low. The nucleus, with the exception of nucleoli, is uniformly green. On top of the nuclear staining, there are more intensely green IRIFs. Isodata thresholding of the entire image would therefore detect the low-intensity areas outside the cell nucleus as the background and the entire nucleus as an object. Therefore, to detect the IRIFs, only the pixels belonging to the cell nucleus must be thresholded. Then, the uniform nuclear staining is detected as background and the IRIFs as objects.
10. A median filter with small sigma reduces the noise in the image and enhances the detection of the IRIFs.
11. This initial shift is later used to establish correspondences between objects from images taken at two subsequent time points; it does not include rotation of the cell.
12. Tracked IRIFs frequently vanish from the image (due to limited z-axis imaging or actual disappearance of the IRIFs) or merge. As a consequence, an IRIF could be assigned to more than one nearest-neighbor pair. Therefore, multiple-assigned neighbors should be removed from the analysis.
13. Vanishing or merging of IRIFs during imaging causes false nearest-neighbor assignments, leading to overestimation of an IRIF's mobility. A remedy is to exclude IRIFs that move over a distance larger than a maximum, user-defined distance in a single time step. This distance should be approximately two times larger than average distance covered by the tracked objects between two subsequent time points. In our experimental conditions, the maximum allowed distance was 800 nm per 2 min. If images are collected at longer time intervals, the maximum allowed distance might be proportionally increased.
14. Randomly localized IRIFs are frequently positioned close to one another. Such close localization results in optical merging of objects and their tracking during the entire experiment fails. However, such events can be usually detected by an observer, because the human brain is highly skilled in pattern recognition.

Wrongly tracked IRIFs might strongly influence the mobility measurements and should be excluded from the analysis.

References

1. Cadet, J., Bellon, S., Douki, T., Frelon, S., Gasparutto, D., Muller, E., Pouget, J. P., Ravanat, J. L., Romieu, A., and Sauvaigo, S. (2004) Radiation-induced DNA damage: formation, measurement, and biochemical features. *J. Environ. Pathol. Toxicol. Oncol*. **23**, 33–43.
2. Agarwal, S., Tafel, A. A., and Kanaar, R. (2006) DNA double-strand break repair and chromosome translocations. *DNA Repair (Amst)* **5**, 1075–1081.
3. Suzuki, K., Ojima, M., Kodama, S., and Watanabe, M. (2003) Radiation-induced DNA damage and delayed induced genomic instability. *Oncogene* **22**, 6988–6993.
4. Weinstock, D. M., Richardson, C. A., Elliott, B., and Jasin, M. (2006) Modeling oncogenic translocations: distinct roles for double-strand break repair pathways in translocation formation in mammalian cells. *DNA Repair (Amst)* **5**, 1065–1074.
5. Wyman, C. and Kanaar, R. (2006) DNA double-strand break repair: all's well that ends well. *Annu. Rev. Genet*. **40**, 363–383.
6. Bartek, J. and Lukas, J. (2007) DNA damage checkpoints: from initiation to recovery or adaptation. *Curr. Opin. Cell Biol*. **19**, 238–245.
7. Burma, S., Chen, B. P., and Chen, D. J. (2006) Role of non-homologous end joining (NHEJ) in maintaining genomic integrity. *DNA Repair (Amst)* **5**, 1042–1048.
8. Sonoda, E., Hochegger, H., Saberi, A., Taniguchi, Y., and Takeda, S. (2006) Differential usage of non-homologous end-joining and homologous recombination in double strand break repair. *DNA Repair (Amst)* **5**, 1021–1029.
9. Wyman, C., Ristic, D., and Kanaar, R. (2004) Homologous recombination-mediated double-strand break repair. *DNA Repair (Amst)* **3**, 827–833.
10. Bekker-Jensen, S., Lukas, C., Kitagawa, R., Melander, F., Kastan, M. B., Bartek, J., and Lukas, J. (2006) Spatial organization of the mammalian genome surveillance machinery in response to DNA strand breaks. *J. Cell Biol*. **173**, 195–206.
11. Aten, J. A. and Kanaar, R. (2006) Chromosomal organization: mingling with the neighbors. *PLoS. Biol*. **4**, e155.
12. Savage, J. R. (1993) Interchange and intra-nuclear architecture. *Environ. Mol. Mutagen*. **22**, 234–244.
13. Aten, J. A., Stap, J., Krawczyk, P. M., van Oven, C. H., Hoebe, R. A., Essers, J., and Kanaar, R. (2004) Dynamics of DNA double-strand breaks revealed by clustering of damaged chromosome domains. *Science* **303**, 92–95.
14. Savage, J. R. (2000) Cancer. Proximity matters. *Science* **290**, 62–63.
15. Lisby, M., Mortensen, U. H., and Rothstein, R. (2003) Colocalization of multiple DNA double-strand breaks at a single Rad52 repair centre. *Nat. Cell Biol*. **5**, 572–577.
16. Essers, J., Houtsmuller, A. B., and Kanaar, R. (2006) Analysis of DNA recombination and repair proteins in living cells by photobleaching microscopy. *Methods Enzymol*. **408**, 463–485.
17. Rieger, B., Molenaar, C., Dirks, R. W., and Van Vliet, L. J. (2004) Alignment of the cell nucleus from labeled proteins only for 4D in vivo imaging. *Microsc. Res. Tech*. **64**, 142–150.
18. Bornfleth, H., Edelmann, P., Zink, D., Cremer, T., and Cremer, C. (1999) Quantitative motion analysis of subchromosomal foci in living cells using four-dimensional microscopy. *Biophys. J*. **77**, 2871–2886.
19. Wilson, C. A. and Theriot, J. A. (2006) A correlation-based approach to calculate rotation and translation of moving cells. *IEEE Trans. Image Process* **15**, 1939–1951.

20. Anderson, L., Henderson, C., and Adachi, Y. (2001) Phosphorylation and rapid relocalization of 53BP1 to nuclear foci upon DNA damage. *Mol. Cell Biol*. **21**, 1719–1729.
21. Jullien, D., Vagnarelli, P., Earnshaw, W. C., and Adachi, Y. (2002) Kinetochore localisation of the DNA damage response component 53BP1 during mitosis. *J. Cell Sci*. **115**, 71–79.
22. Besl, P. and McKay, N. (1992) A method for registration of 3-d shapes. *IEEE Transactions on Pattern Analysis and Machine Intelligence* **14**, 239–256.
23. Ridler T. W. and Calvard S. (1978) Picture thresholding using an iterative selection method. *IEEE Trans. System, Man and Cybernetics* **8**, 630–632.
24. Krol, H. A., Krawczyk, P. M., Bosch, K. S., Aten, J. A., Hol, E. M., and Reits, E. A. (2008) Polyglutamine expansion accelerates the dynamics of ataxin-1 and does not result in aggregate formation. *PLoS ONE* **3,** e1503.
25. Stap, J., Krawczyk, P. M., van Oven, C. H., Barendsen, G. W., Essers, J., Kanaar, R., and Aten, J. (2008) Induction of linear tracks of DNA double-strand breaks by alpha-particle irradiation of cells. *Nat. Methods* **5,** 261–266.
26. Hoebe, R. A., van Oven, C. H., Gadella, T. W., Jr., Dhonukshe, P. B., Van Noorden, C. J., and Manders, E. M. (2007) Controlled light-exposure microscopy reduces photobleaching and phototoxicity in fluorescence live-cell imaging. *Nat. Biotechnol*. **25**, 249–253.

Index

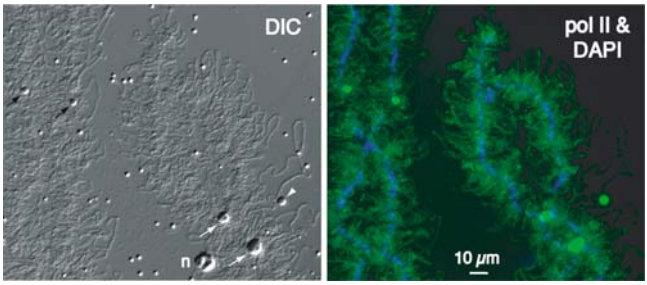

COLOR PLATE 1. **Fig. 4.3** Fixed and immunostained GV spread from an axolotl oocyte. *See* complete caption on p. 63

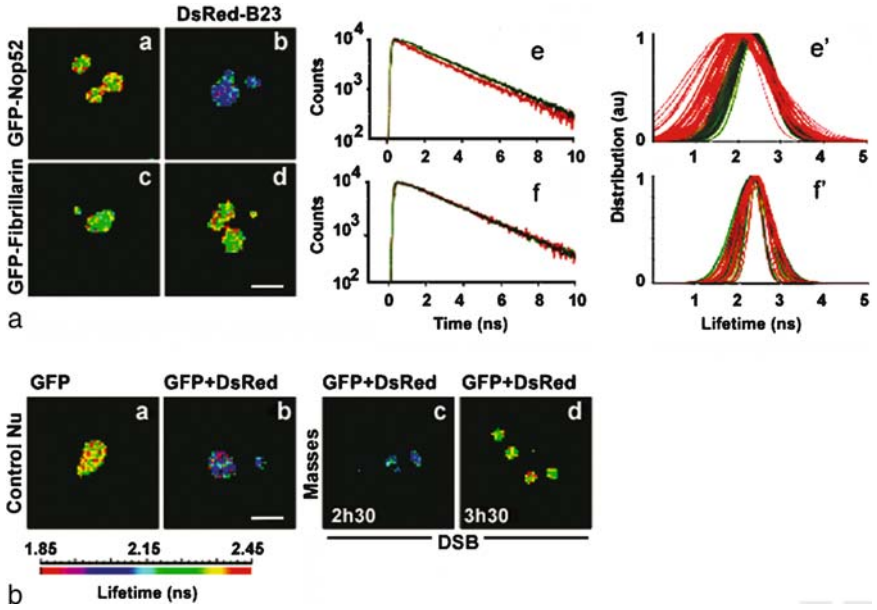

COLOR PLATE 2. **Fig. 9.3** Nop52 and B23 interact in the nucleolus of living cells. *See* complete caption on p. 132

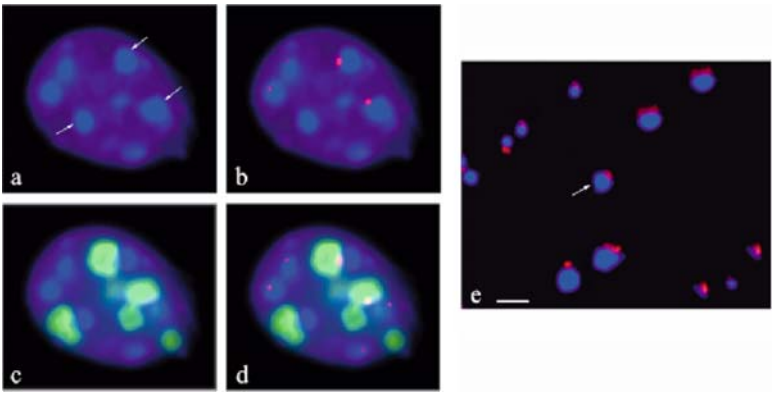

COLOR PLATE 3. **Fig. 12.2** General views of an isolated nucleus. *See* complete caption on p. 171

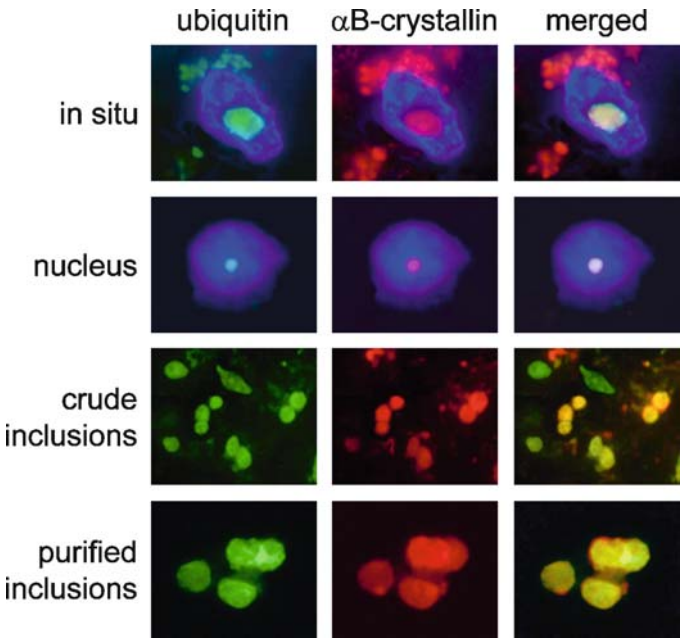

COLOR PLATE 4. **Fig. 13.2** Immunofluorescence staining of inclusions at various steps in their isolation and purification. *See* complete caption on p. 189

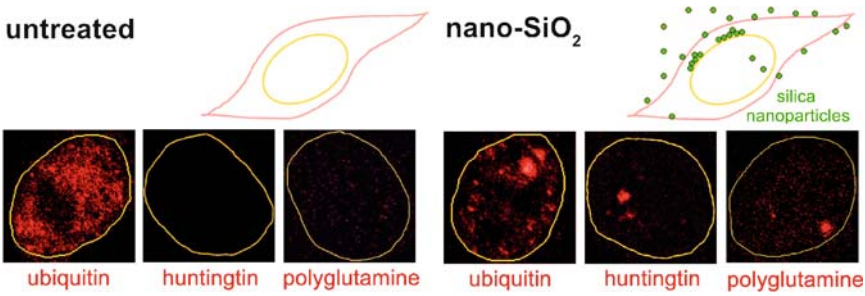

COLOR PLATE 5. **Fig. 14.2** Induction of protein aggregation by silica nanoparticles. *See* complete caption on p. 199

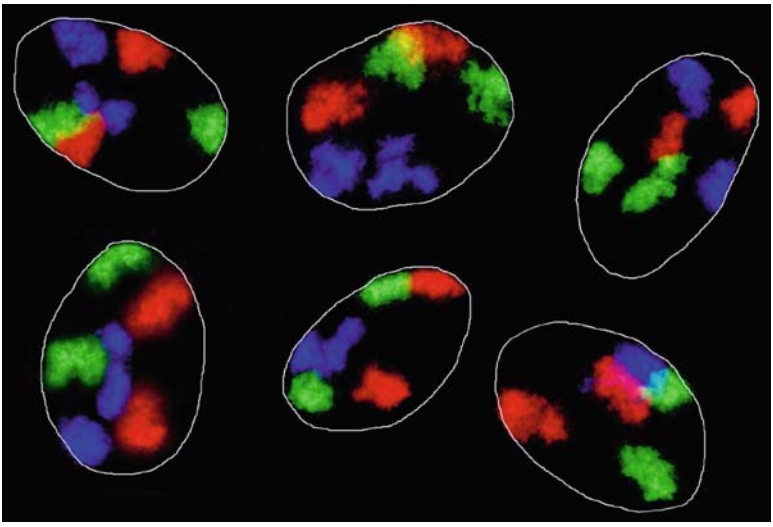

COLOR PLATE 6. **Fig. 15.1** Three-color 3D-FISH on nuclei of normal diploid human fibroblasts. *See* complete caption on p. 217

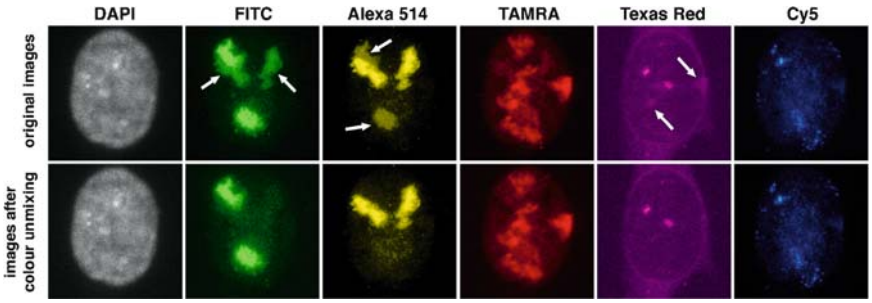

COLOR PLATE 7. **Fig. 15.2** Six-color 3D-FISH on nuclei of human fibroblasts. *See* complete caption on p. 227

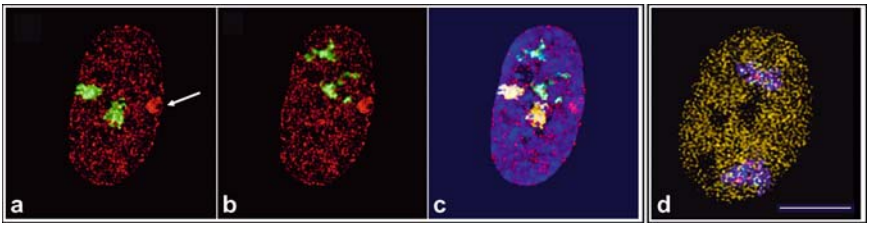

COLOR PLATE 8. **Fig. 15.3** Four-color 3D Immuno-FISH on single optical sections of human fibroblast nuclei. *See* complete caption on p. 228

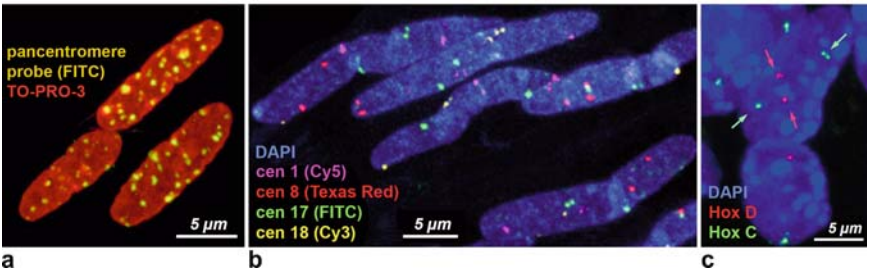

COLOR PLATE 9. **Fig. 15.4** FISH on sections of paraffin-embedded tissues. *See* complete caption on p. 230

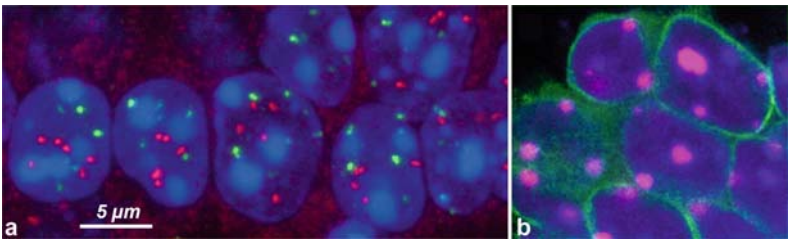

COLOR PLATE 10. **Fig. 15.5** FISH on vibratome sections. *See* complete caption on p. 230

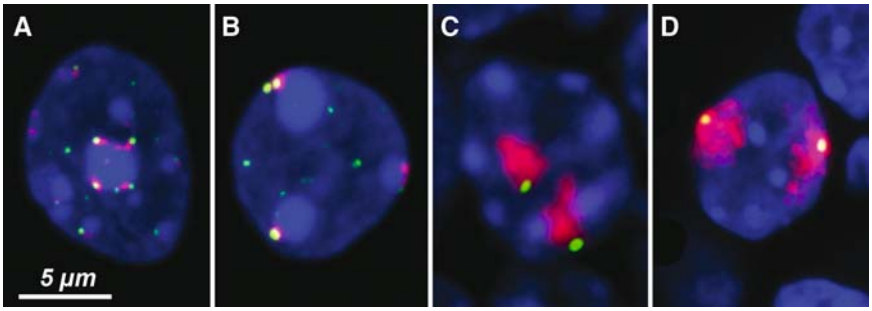

COLOR PLATE 11. **Fig. 15.6** FISH on cryosections. *See* complete caption on p. 231

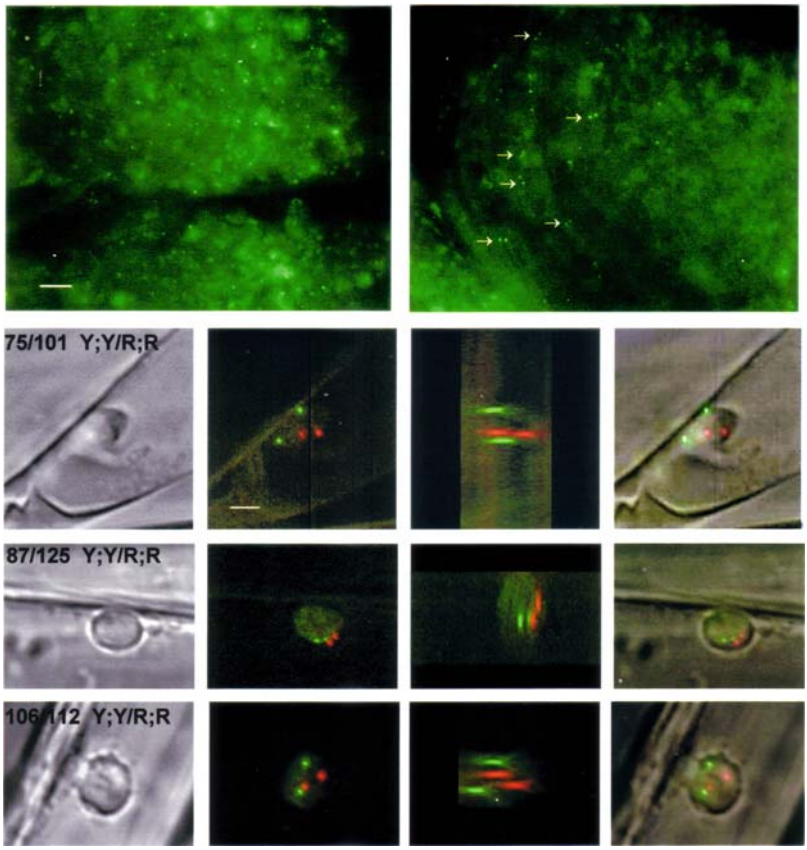

COLOR PLATE 12. **Fig. 16.7** *Top row*, examples of images of YFP fluorescent dots in nuclei of ovules in carpels (hemizygous plant, *left*; homozygous plant, *right*). *See* complete caption on p. 258

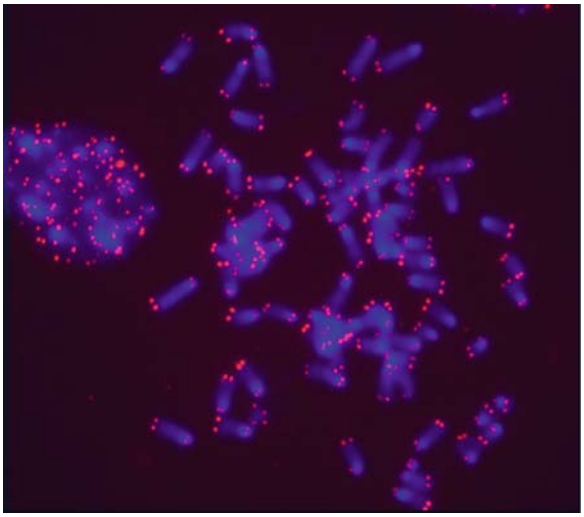

COLOR PLATE 13. **Fig. 17.1** Fluorescence in situ hybridization on mouse MEF chromosome spreads. *See* complete caption on p. 281

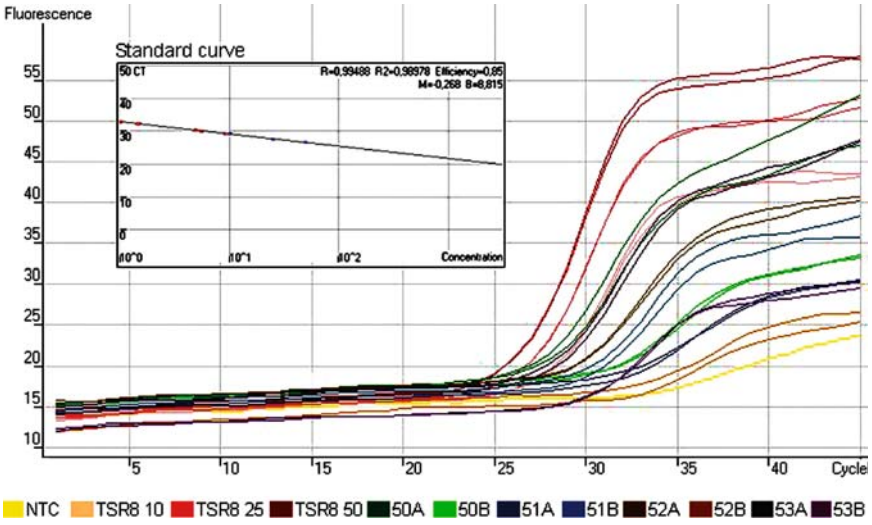

COLOR PLATE 14. **Fig. 17.2** An example of results of dual-color real-time TRAP. *See* complete caption on p. 291

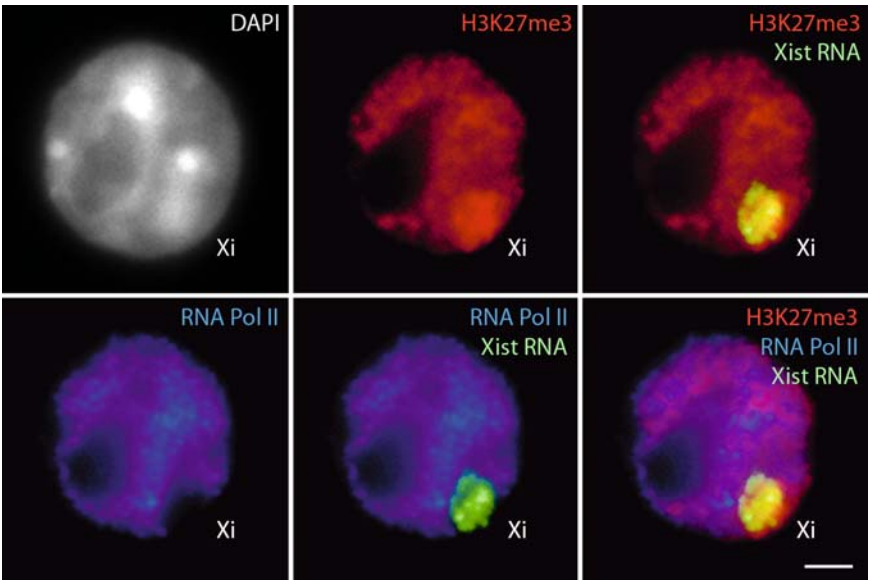

COLOR PLATE 15. **Fig. 18.2** Dual immunofluorescence combined with RNA FISH in differentiated mouse female ES cells. *See* complete caption on p. 299

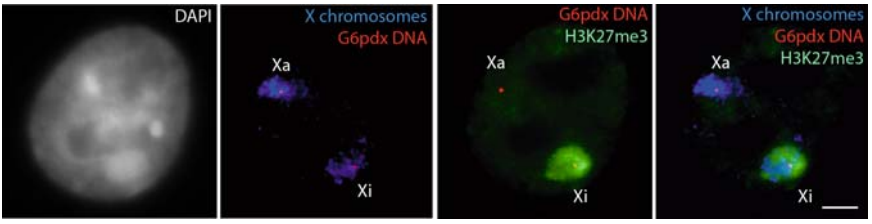

COLOR PLATE 16. **Fig. 18.3** Immunofluorescence combined with dual DNA FISH in differentiated female mouse ES cells. *See* complete caption on p. 300

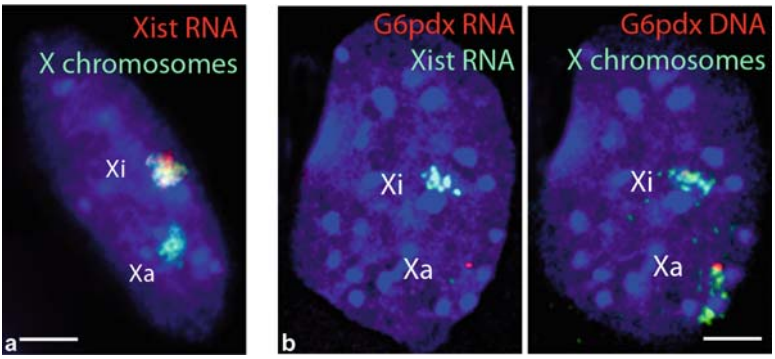

COLOR PLATE 17. **Fig. 18.4** Examples of combined RNA and DNA FISH in differentiated female mouse ES cells. *See* complete caption on p. 300

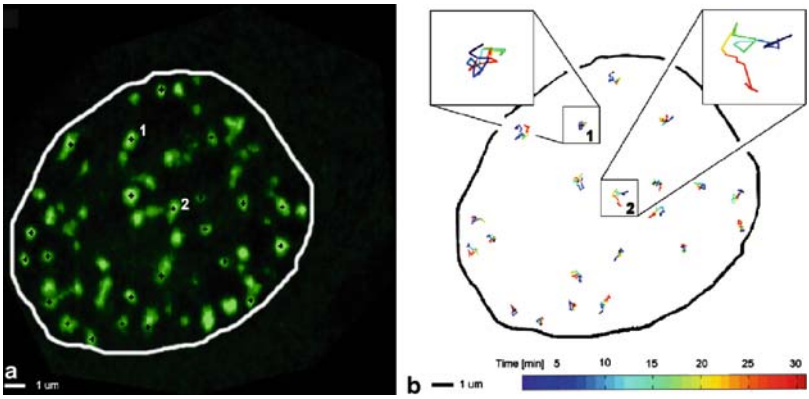

COLOR PLATE 18. **Fig. 19.1** Visualization and tracking of 53BP1-GFP IRIFs in a U2OS cell. *See* complete caption on p. 311